

Protein Physics

Protein Physics

Second, Updated and Extended Edition

Alexei V. Finkelstein

Oleg B. Ptitsyn*

Institute of Protein Research

Russian Academy of Sciences, Pushchino,
Moscow Region, Russian Federation



ELSEVIER

AMSTERDAM • BOSTON • HEIDELBERG • LONDON
NEW YORK • OXFORD • PARIS • SAN DIEGO
SAN FRANCISCO • SINGAPORE • SYDNEY • TOKYO

Academic Press is an imprint of Elsevier



* Deceased

Academic Press is an imprint of Elsevier
125 London Wall, London EC2Y 5AS, UK
525 B Street, Suite 1800, San Diego, CA 92101-4495, USA
50 Hampshire Street, 5th Floor, Cambridge, MA 02139, USA
The Boulevard, Langford Lane, Kidlington, Oxford OX5 1GB, UK

© 2016, 2002 Elsevier Ltd. All rights reserved.

No part of this publication may be reproduced or transmitted in any form or by any means, electronic or mechanical, including photocopying, recording, or any information storage and retrieval system, without permission in writing from the publisher. Details on how to seek permission, further information about the Publisher's permissions policies and our arrangements with organizations such as the Copyright Clearance Center and the Copyright Licensing Agency, can be found at our website: www.elsevier.com/permissions.

This book and the individual contributions contained in it are protected under copyright by the Publisher (other than as may be noted herein).

Notices

Knowledge and best practice in this field are constantly changing. As new research and experience broaden our understanding, changes in research methods, professional practices, or medical treatment may become necessary.

Practitioners and researchers must always rely on their own experience and knowledge in evaluating and using any information, methods, compounds, or experiments described herein. In using such information or methods they should be mindful of their own safety and the safety of others, including parties for whom they have a professional responsibility.

To the fullest extent of the law, neither the Publisher nor the authors, contributors, or editors, assume any liability for any injury and/or damage to persons or property as a matter of products liability, negligence or otherwise, or from any use or operation of any methods, products, instructions, or ideas contained in the material herein.

Library of Congress Cataloging-in-Publication Data

A catalog record for this book is available from the Library of Congress

British Library Cataloguing-in-Publication Data

A catalogue record for this book is available from the British Library

ISBN 978-0-12-809676-5

For information on all Academic Press publications
visit our website at <https://www.elsevier.com/>



Working together
to grow libraries in
developing countries

www.elsevier.com • www.bookaid.org

Publisher: John Fedor

Acquisition Editor: Anita Koch

Editorial Project Manager: Sarah Watson

Production Project Manager: Anitha Sivaraj

Cover Designer: Vicky Pearson Esser

Typeset by Spi Global, India

Contents

Foreword to the First English Edition	xiii
Preface	xv
Acknowledgements	xix
Part I	
Introduction	1
Lecture 1	3
Main functions of proteins. Amino acid sequence determines the three-dimensional structure, and the structure determines the function. The reverse is not true. Fibrous, membrane, and globular proteins. Primary, secondary, tertiary, and quaternary structures of proteins. Domains. Co-factors. Active sites and protein globules. Protein biosynthesis; protein folding in vivo and in vitro. Post-translational modifications.	
Recommended additional reading	12
Part II	
Elementary Interactions in and Around Proteins	15
Lecture 2	17
Amino acid residues in proteins. Backbone and side chains. Stereochemistry of natural L-amino acids. Peptide bonds. Covalent interactions and quantum mechanics. Heisenberg's principle of uncertainty. Covalent bonds and angles between them. Their vibrations. Dihedral angles. Rotation around the covalent bonds. Potential barriers for rotations. Peptide group: why is it flat and rigid? <i>Trans-</i> and <i>cis</i> -prolines.	
References	25
Lecture 3	27
Quantum mechanics, Pauli Exclusion Principle, and non-covalent interactions. Van der Waals interaction: attraction at long distances, repulsion at short distances. Potential of the van der Waals interaction. Typical radii of atoms. Why <i>cis</i> -conformations of peptide bonds are rare. Allowed conformations of amino acid residues. Ramachandran plots for glycine, alanine, valine, proline.	
References	37

Lecture 4	39
Influence of water environment. Hydrogen bonds. Their electrostatic origin. Their energy. Their geometry in crystals. Ice. Hydrogen bonds in water are distorted. Notes on entropy and free energy. Hydrogen bonds in the protein chain replace the same bonds of this chain to water; as a result, the hydrogen bonds in proteins—in an aqueous environment—are entropy-driven bonds.	
References	50
Lecture 5	51
Water, hydrophobicity, and proteins. Boltzmann distribution. Elements of thermodynamics. Free energy and chemical potential. Hydrophobic interactions: entropic forces. Their connection with the necessity to saturate hydrogen bonds in water. Origin of hydrophobic interactions. The strength of hydrophobic interactions depends on temperature. Hydrophobic effect is responsible for formation of compact globules. Water-accessible surface of amino acids and their hydrophobicity.	
References	65
Lecture 6	67
Influence of an aqueous environment on electrostatic interactions. Electric field near the surface and inside the protein globule. Permittivity. Electrostatic interactions and corpuscular structure of the medium. Debye-Hückel effect: shielding of charges in saline solutions. Measuring of electric fields in proteins by protein engineering. Electrostatics in water is entropic. Disulfide bonds. Coordinate bonds. Entropic forces—again.	
References	81
Part III	
Secondary Structures of Polypeptide Chains	83
Lecture 7	85
Secondary structure of polypeptides. Chirality of helices. Helices: 2_7 , 3_{10} , α , π , poly(Pro)II. The main secondary structures: hydrogen bonds and Ramachandran maps of allowed and disallowed conformations of amino acid residues. Antiparallel and parallel β -structure. Small secondary structures: β -turns, β -bulges. What is the “coil”? Methods of experimental identification of secondary structure.	
References	99
Lecture 8	101
Elements of statistical mechanics. Temperature; its connection with the change of entropy with the energy increase. Probability of states with different	

energy (Boltzmann-Gibbs distribution). Partition function and its connection with the free energy. Conformational changes. The first-order (“all-or-none” in small systems) phase transitions, the second-order phase transitions, and non-phase transitions. Kinetics of free-energy barrier overcoming during “all-or-none” conformational changes: what it looks like at the level of a molecule and at the level of an ensemble of molecules. The transition-state theory of reaction rates. Parallel and sequential processes. Typical times of diffusion processes. The mean free path of molecules in water.	
References	121
Lecture 9	123
Free energy of initiation and elongation of α -helices in a homopolyptide. Landau’s theorem and the non-phase character of the helix-coil transition. The size of the cooperative region at the helix-coil transition. α -Helix stability in water. α -Helix and β -sheet boundaries. β -Structure stability in water. Rate of α -helix, β -hairpin, and β -sheet formation.	
References	136
Lecture 10	139
20+2+1 gene-coded amino acids in proteins. Properties of amino acid side chains. Amino acids in secondary structures. Alanine, glycine, proline, valine. Branched side chains. Non-polar, short polar, and long polar side chains. Capping of α -helices. Charged side chains; pH dependence of their charges. Hydrophobic surfaces on protein secondary structures.	
References	146
Part IV	
Protein Structures	149
Lecture 11	151
Fibrous proteins, their functions, their regular primary and secondary structures; α -keratin, silk β -fibroin, collagen. Packing of secondary structures. α -Helical coiled coils. Collagen triple helix. Assisted folding of collagen. Packing of long α -helices and large β -sheets. Matrix-forming proteins; elastin. Genetic defects of protein structures and diseases. Amyloids. Kinetics of their formation.	
References	161
Lecture 12	165
Membrane proteins; peculiarities of their structure and function. Transmembrane α -helices, transmembrane β -barrels. High cost of hydrogen bonds in a lipid environment. Bacteriorhodopsin; receptors and G-proteins; porin;	

photosynthetic reaction center. Transmitting channels. Selective permeability of membrane pores. The photosynthetic reaction center at work. Tunneling. Electron-conformational interaction. Assisted and spontaneous folding of membrane proteins.	
References	179
Lecture 13	181
Water-soluble globular proteins. Is the protein structure the same both in crystals and in solution? Simplified presentation of protein globules. Structural classes, architectures, topologies, folding patterns. Structure of β -proteins: β -sheets, their aligned and orthogonal packing. Meanders, Greek keys, jellyrolls, blades, prisms. β -Structure in β -proteins is mainly antiparallel. Topology of β -proteins.	
References	196
Lecture 14	199
Structure of α -proteins. Bundles and layers of helices. Model of the quasi-spherical α -helical globule. Close packing of α -helices. Structure of α/β -proteins: parallel β -sheet covered with α -helices, α/β -barrel. Topology of $\beta\text{-}\alpha\text{-}\beta$ subunits. Structure of $\alpha+\beta$ proteins. The absence of direct connection between overall protein architecture and its function, though the active site position is often determined by the overall protein architecture.	
References	212
Lecture 15	215
Classification of protein folds. The absence of observable “macroevolution” of protein folds and the presence of observable “microevolution” of their detailed structures. Gene duplication and protein specialization. Evolution by reconnection of domains. “Standard” protein folds. Typicality of “quasi-random” patterns of amino acid sequences in primary structures of globular proteins in contrast to periodic sequences of fibrous proteins and blocks in the sequences of membrane proteins. Physical principles of architectures of protein globules. The main features observed in protein globules: separate α - and β -layers; rare over-crossing of loops; rare parallel contacts of secondary structures adjacent in the chain; rare left-handedness of $\beta\text{-}\alpha\text{-}\beta$ superhelices. “Energy-” and “entropy-defects” of rarely observed structures and connection between these “defects” and rarity of the amino acid sequences capable of stabilizing the “defective” structures. Natural selection of protein folds. “Multitude principle.”	
References	229

Lecture 16 233

What secondary structure can be expected for random and quasi-random amino acid sequences? Domain construction of the folds formed by long quasi-random sequences. Quasi-Boltzmann statistics of the elements of protein structures. These statistics originate from the physical selection of stable protein structures. Influence of element stability on selection of sequences supporting the fold of a globular protein; or, why some protein structures occur frequently while others are rare. What structure— α or β —should be usually expected in the center of a large globule? Connection between “entropy-defects” and “energy-defects.” Do globular proteins emerge as “selected” random polypeptides? Selection of “protein-like” sequences in protein engineering experiments.

References 249

Part V
Cooperative Transitions in Protein Molecules 251

Lecture 17 253

“Well-folded” and “natively disordered” (or “intrinsically disordered”) proteins. Protein denaturation. Cooperative transitions. Reversibility of protein denaturation. Denaturation of globular protein is a cooperative “all-or-none” transition. Van’t Hoff criterion for the “all-or-none” transition. Heat and cold denaturation. Phase diagram for states of a protein molecule. What does denatured protein look like? The coil and the molten globule. Large-scale inhomogeneity of some “natively disordered” proteins. The absence of “all-or-none” phase transition during swelling of “normal” polymer globules.

References 271

Lecture 18 275

Denaturation of globular protein: why is it an “all-or-none” transition? Decay of closely packed protein core and liberation of side chains. Penetration of solvent into denatured protein; decay of the molten globule, subsequent gradual unfolding of the protein chain with increasing solvent strength. Energy gap between the native protein fold and all other globular folds of the chain. The main physical difference between a protein chain and random heteropolymers. The difference in melting between “selected” chains (with energy gap) and random heteropolymers.

References 286

Lecture 19 289

Protein folding *in vivo* and *in vitro*. Co-translational folding. Auxiliary mechanisms for *in vivo* folding: chaperones, etc. Spontaneous folding is

possible in vitro. Aggregation, the main obstacle to in vitro protein folding, and crowding effects in vivo. The “Levinthal paradox.” Protein folding experiments in cell-free systems; on various understandings of the term “in vitro.” Stepwise mechanism of protein folding. Discovery of metastable (accumulating) folding intermediates for many proteins. The molten globule is a common (but not obligatory) intermediate in protein folding under “native” conditions. The simplest (“two-state”) folding of some proteins proceeds without any accumulating intermediates. Folding nucleus.	
References	304
Lecture 20	307
Two-state folding of small proteins: kinetic analog of the thermodynamic “all-or-none” transition. Two- and multi-state folding. Theory of transition states. Experimental identification and investigation of unstable transition states in protein folding. Φ -value analysis. Folding nucleus. Its experimental discovery by protein engineering methods. Nucleation mechanism of protein folding. Native and non-native interactions in the nucleus. Folding nucleus is less specific and less “invariant” than the native protein structure.	
References	320
Lecture 21	323
Solution of “Levinthal paradox”: a set of fast folding pathways (a “folding funnel” <i>with</i> phase separation) automatically leads to the most stable structure. It is necessary only to have a sufficient energy gap separating the most stable fold from others. Volume of conformational space at the level of secondary structure formation and assembly. Discussion of very slow folding of stable structure in some proteins: serpins. “Chameleon” proteins. Misfolding. Notes on “energy funnels” and “free-energy landscapes” of the folding protein chains. Consideration of the unfolding and folding sides of the free-energy barrier. The detailed balance law. Protein structures: physics of folding and natural selection of chains capable of folding.	
References	344
Part VI	
Prediction and Design of Protein Structure	347
Lecture 22	349
Protein structure prediction from amino acid sequences. Specific amino acid sequences of globular, membrane, fibrous, and intrinsically disordered proteins. Recognition of protein structures and their functions using homology of sequences. Key regions and functional sites in protein structures. Profiles for primary structures of protein families and multiple alignments. Detection	

of stable elements of protein structures. “Templates” of elements of protein structures. Predicted structures are unavoidably judged from only a part of interactions occurring in the chain. As a result, we have probabilistic predictions. Interactions that stabilize and destroy secondary structures of polypeptide chains. Calculation of secondary structures of non-globular polypeptides. Prediction of protein secondary structures.	
References	364
Lecture 23	367
Overview of approaches to prediction and recognition of tertiary structures of proteins from their amino acid sequences. Protein fold libraries. Recognition of protein folds by threading. Prediction of common fold for a set of remote homologs reduces uncertainty in fold recognition. Structural genomics and proteomics. Bioinformatics. Advances in modeling of protein folding. Protein engineering and design. Almost identical sequences can produce different folds with different functions. Advances in design of protein folds.	
References	381
Part VII	
Physical Background of Protein Functions	385
Lecture 24	387
Protein function and protein structure. Elementary functions. Binding proteins: natively disordered proteins, DNA-binding proteins, immunoglobulins. Enzymes. The active site as a “defect” of globular protein structure. Protein rigidity is crucial for elementary enzyme function. Catalytic and substrate-binding sites. Inhibitors. Mechanism of enzymatic catalysis; activation of enzymes. Example: serine proteases. Transition state theory and its confirmation by protein engineering. Abzymes. Specificity of catalysis. “Key-lock” recognition.	
References	406
Lecture 25	409
Combination of elementary functions. Transition of substrate from one active site to another. “Double sieve” increases specificity of function. Relative independence of protein folds from their elementary catalytic functions. Different catalytic sites can perform the same job. <i>Ser-proteases</i> and <i>metalloproteinases</i> . Multicharged ions. Visible connection between protein fold and protein environment. Combination of elementary protein functions and flexibility of protein structure. Induced fit. Mobility of protein domains. Shuffling of domains and protein evolution. Domain structure: kinases, dehydrogenases. Co-factors. Allostery: interaction of active sites.	

Allosteric regulation of protein function. Allostery and protein quaternary structure. Hemoglobin and myoglobin. Mechanochemical cycle. Kinesin: a bipedal protein. Mechanism of muscle contraction. Rotary motors.	
References	427
Appendices	429
Appendix A	
Theory of globule-coil transitions in homopolymers	431
References	435
Appendix B	
Theory of helix-coil transitions in homopolymers	436
References	439
Appendix C	
Statistical physics of one-dimensional systems and dynamic programming	440
References	446
Appendix D	
Random energy model and energy gap in the random energy model	448
References	452
Appendix E	
How to use stereo drawings	453
Problems with solutions and comments	457
Index	501

Foreword to the First English Edition

In June 1967, Oleg Ptitsyn became the Head of the Laboratory of Protein Physics at the new Institute of Protein Research at Pushchino. Three months later, he was joined by Alexei Finkelstein; first as a research student and then as a colleague. Their approach to the study of proteins was different from that common in the West, being strongly influenced by the Russian school of polymer physics. One of its most distinguished members, Michael Volkenstein, had been Ptitsyn's PhD supervisor. Together Ptitsyn and Finkelstein created, at Pushchino, one of the world's outstanding centers for the study of the physics and chemistry of proteins.

Certain areas of their work, particularly that on protein folding, have become well known in Europe, India and America, either directly through their papers or indirectly through the elaboration of their work by two of their former students: Eugene Shakhnovich, in America, and Alexei Murzin, in England. However, it became obvious when Finkelstein or Ptitsyn talked with colleagues, that the range of their work went far beyond what was commonly known in the West. We would find that fundamental questions that were our current concerns had already been considered by them and they had some elegant calculation that provided an answer. Usually, they had not got round to publishing this work. Now, to make their overall achievements available to more than just their friends and the students of Moscow University; Finkelstein has written this book on the basis of lectures he and Ptitsyn gave to these students.

In the breadth of its range, the rigor of its analysis and its intellectual coherence, this book is a *tour de force*. Of those concerned with the physics and chemistry of proteins, I doubt if there can be any, be they students or senior research workers, who will not find herein ideas, explanations and information that are new, useful and important.

Cyrus Chothia, FRC
MRC Laboratory of Molecular Biology
Cambridge, UK
2002

Preface

This book is devoted to protein *physics*, that is, to the overall topics of structure, self-organization and function of protein molecules. It is written as a course of lectures, which include a more-or-less conventional introduction to protein science (specifically, in the first and last parts of the book), as well as the story of in-depth protein science studies (in the middle of the book). Thus, the book is a kind of monograph embedded in the course of lectures, and it bridges the gap between introductory biophysical chemistry courses and research literature.

The course is based on lectures given by us (earlier by O.B.P. and later by A.V.F.), first at Moscow PhysTech Institute, then at Pushchino State University, and now at the Pushchino Branch of Lomonosov Moscow State University and at Biology and Bioengineering & Bioinformatics Departments of Lomonosov Moscow State University. Initially, our students were physicists, then mainly biologists with some chemists. That is why, by now, the lectures have not only been considerably up-dated (as research never stops) but also thoroughly revised to meet the requirements of the new audience.

Since what you will be reading has a form of a course of lectures, repetition is hardly avoidable (specifically, we have repeated some figures). Indeed, when delivering a lecture one cannot refer to “Figure 2 and Equation 3 of the previous lecture”; however, we have done our best to minimize repetition.

The following comments will help you to understand our approach and the way in which the material is presented:

On the “lecturer”. All lectures are presented here in the way they are delivered, that is, from the first person—the lecturer.

On the “inner voice”. The personality of the “lecturer” comprises both authors, O.B.P. and A.V.F., although this does not mean that no disagreement has ever occurred between us concerning the material presented! Moreover, sometimes each of us felt that the problem in question is disputable and subject to further studies. We made no attempt to smooth these disputes and contradictions over, so the “lecturer’s” narration is sometimes interrupted or questioned by the “inner voice.” Or the “inner voice” may simply articulate the frequently asked questions or elaborate the discussion. *Why “protein physics”?* Because we are amazed to see how strongly biological evolution enhances, secures and makes evident the consequences of the physical principles underlying molecular interactions in the protein. It is

also striking how much our understanding of biological systems, proteins in particular, has developed through the application of physical methods. We see this from mass spectrometry and single-molecule techniques to electron or atomic force microscopy, X-ray crystallography and NMR studies of proteins. There is hardly any other area of contemporary science in which the traditional boundaries between disciplines and philosophies have been so clearly breached to such great profit.

On the physics and biology presented in these lectures. In the course of lecturing, we shall take the opportunity to present physical ideas, such as some elements of statistical physics and quantum mechanics. These ideas, to our minds, are absolutely necessary not only for an understanding of protein structure and function but also for general scientific culture, but usually a “normal” biology graduate has either completely forgotten or never known them. On the other hand, among a myriad of protein functions, we will discuss only those absolutely necessary to demonstrate the role of spatial structures of proteins in their biological, or rather biochemical, activities.

On “in vivo” and “in vitro” experiments. The terms “in vivo” and “in vitro”, as applied to experiments, are often understood differently by physicists and biologists. Strictly speaking, between the pure “in vivo” and the pure “in vitro” there are a number of ambiguous intermediates. For example, protein folding in a cell-free system (with all its ribosomes, initiation factors, chaperones, crowding, etc.) is unequivocally an “in vivo” experiment in the physicist’s view (for a physicist, “in vitro” would be mostly a separate protein in solution; even the cell-free system contains too many biological details). But for a biologist, this is undoubtedly an “in vitro” experiment (since “in vivo” is referred to a living and preferably intact organism). However, structural studies of a separate protein in an organism are hardly possible. Therefore, reasonable people compromise by making biologically significant “in vivo” events accessible for experimental “in vitro” studies.

On experiment, physical theory and calculations. Experiment provides the basic facts underlying all our ideas of phenomena, as well as a lot of refining details. However, the experimental methods used in protein physics are only briefly described in this book, with references to excellent textbooks that describe them in detail. The same, and to an even greater extent, concern chemical and biochemical methods (such as those used in purification of proteins or genetic engineering), which are just barely mentioned in the book.

Theory allows us to understand the essence and interrelation of the phenomena and is helpful in planning informative experiments. Some basic physical theories—in a simplified form, naturally—are included in our lectures, not only because they permit us to put in order and comprehend from a common standpoint the vast experimental material, but also because they are elegant. Besides, we believe that knowledge of basic physical theories and models is essential to human culture.

Calculations connect theory with experiment and verify key points of the theory. However, not everything that can be calculated must be calculated; for example, it is easier just to measure water (or protein) density than to calculate it from first principles. And not only is this easier but it yields a more accurate result, since a detailed calculation requires many parameters that can hardly be accurately estimated.

*On physical models, rough estimates and computer (*in silico*) experiments.* In these lectures, we will often discuss simple models, that is, those drastically simplified compared with reality, and use rough estimates. And we want you, after reading these lectures, to be able to make such estimates and use simple models of the events in question. The use of simple models and rough estimates may seem to be quite old-fashioned. Indeed, it is often believed that with the powerful computers available now, one can enter “all as it is in reality”: water molecules, salt, coordinates of protein atoms, DNA, etc. fix the temperature, and obtain “the precise result.” As a matter of fact, this is a Utopian picture. The calculation—we mean a detailed one (often made using so-called molecular dynamics)—will take days and cover only some nano- or microseconds of the protein’s life, because you will have to follow the thermal motions of many thousands of interacting atoms. In any case, this calculation will not be absolutely accurate either, since all elementary interactions can be estimated only approximately. And the more detailed the description of a system is, the more elementary interactions are to be taken into account, and the more minor errors will find their way into the calculation (not to mention the increased computer time required). Eventually, you will obtain only a more-or-less precise estimate of the event instead of the desired absolutely accurate description of it—with days of a supercomputer’s time spent. Meanwhile, what really interests you may be a simple quick estimate such as whether it is possible to introduce a charge into the protein at a particular site without a risk of protein structure explosion. That is why one of our goals is to teach you how to make such estimates. However, this does not mean that we will simply ignore computer experiments. Such experiments yield a lot of useful information. But the computer experiment is a real experiment (although *in silico*, not *in vitro* or *in vivo*). It involves highly complex systems and yields facts requiring further interpretation, which, in turn, demands simplified but clear models and theories.

On equations. We are aware that mathematical equations can be a difficulty for biologists, so we have done our best to refrain from using them, and only those really unavoidable have survived (some very useful but more complicated equations are used in the Appendices and Problem sections). Our advice is: when reading these lectures, “test words by equations.” It is certainly easier for biologists to read words only, but they are often ambiguous, so word-verifying by equations and vice versa will help your understanding. To avoid going into insignificant (and unhelpful) detail, we shall often use

approximate calculations; therefore you will often see the symbols “ \approx ” (approximately equal to) and “ \sim ” (of the same order of magnitude as).

On references and figures. The references are included in the text, legends to figures and tables; the lists of references are positioned at the end of each Lecture or Appendix.

Protein structures are drawn using the programs MOLSCRIPT (Kraulis, P.J., J. Appl. Cryst. 24, 946–950); WHAT IF (Vriend, G., J. Mol. Graphics 8, 52–56); RASMOL (Sayle, R., Milnerwhite, E.J., Trends Biochem. Sci. 24, 374–376); Insight II (Molecular Simulations Inc., 1998); ViewerLite (Accelrys Inc., 2001); and coordinates taken from the Protein Data Bank (initially described in: Bernstein, F.C., Koetzle, T.F., Meyer, E.F., Jr., Brice, M.D., Kennard, O., Shimanouchi, T., Tasumi, T., J. Mol. Biol. 112, 535–542). Many figures are adapted from the literature, with appropriate references and permissions. Most of other figures are purposely schematic.

On tastes. These lectures, beyond doubt, reflect our personal tastes and predilections and are focused on the essence of things and events rather than on a thorough description of their details. In the main, they contain physical problems and theories, while only the necessary minimum of experimental facts are given and experimental techniques are barely mentioned. (Specifically, almost nothing will be said in these lectures about the techniques of X-ray crystallography and NMR spectroscopy that have provided the bulk of our knowledge of protein structure; we tried to compensate this by reference to excellent textbooks on experimental methods.)

Therefore, these lectures are by no means a substitute for regular fact-rich biophysical and biochemical courses on proteins. When referring to specific proteins, we merely give the most important (from our viewpoint) instances; only absolutely necessary data are tabulated; all values are approximate, etc.

On small print. This is used for helpful but not essential excursus, additions and explanations.

On the personal note in these lectures. We shall take the opportunity of noting our own contributions to protein science and those by our co-workers and colleagues from the Institute of Protein Research, Russian Academy of Sciences. This will certainly introduce a “personal note” into the lectures and perhaps make them a bit more vivid.

What is the difference between 1st and 2nd English editions of Protein Physics? To my (A.V.F.) surprise, the current revision of the book showed no need of any correction of the initial text. I have made only a few cuts there. But of course I have updated the book to include new fascinating material. Specifically, this concerns novel information on intrinsically disordered proteins, amyloid aggregation, protein folding *in vivo*, protein motors, misfolding, chameleon proteins, advances in protein engineering and design and advances in modelling of protein folding. Also, the revised version includes a Problems section (with solutions).

Acknowledgements

We are grateful to all co-authors of our works that we have used in this book.

We are grateful to our colleagues from the Institute of Protein Research, Russian Academy of Sciences, and especially to former and current co-workers from our Laboratory of Protein Physics: this book would never have been written without scientific and friendly human contact with them.

We thank our university students from different countries, participants of various summer schools and readers of all previous (English, Russian, Chinese) editions of this book for their questions and comments that helped us to clarify (primarily, to ourselves) some points of this course and were helpful for better presentation of the lectures.

We are most grateful to A.B. Chetverin, A.S. Spirin, V.A. Kolb, A.V. Efimov, D.I. Kharakoz, V.E. Bychkova, Yu.V. Mitin, M.A. Roytberg, V.V. Velkov, I.G. Ptitsyna, G.I. Gitelson, D.S. Rykunov, G.V. Semisotnov, A.V. Skugaryev, A.K. Tsaturyan, C.Y. Bershtsky, D.N. Ivankov, A.Ya. Badretdinov, S.O Garbuzynskiy, O.V. Galzitskaya, and A. Li for reading the manuscript, discussions and most useful comments, and to A.A. Vedenov, A.M. Dykhne, M.D. Frank-Kamenetskii, V.N. Uversky, V.E. Finkelstein, A.A. Klimov, D.A. Klimov, F.K. Gioeva, A.M. Gutin, A.G. Murzin, E.I. Shakhnovich, I.M. Gelfand, B.A. Reva, E.S. Nadezhina, E.N. Samatova-Baryshnikova, V.G. Sharapov, L.B. Pereyaslavets, C. Chothia, M. Levitt, M.S. Gelfand, A. Kister, A. Alexandrescu, C. Dobson, A. Fersht, G. Vriend, A. Tramontano, A. Lesk, K.W Plaxco and D. Baker for discussing various items touched upon in this book and supplying us with some additional materials or calculations.

Special thanks to D.S. Rykunov, G.A. Morozov, A.V. Skugaryev, D.N. Ivankov, M.Yu. Lobanov, N.Yu. Marchenko, N.S. Bogatyreva, M.G. Nikitina, V.G. Semisotnova I.V. Sokolovsky, A.A. Shumilin, M.G. Dashkevich, T.Yu. Salnikova, A.E. Zhumaev, A.A. Finkelstein and M.S. Vilner-Marmer for their valuable assistance in the preparation of the manuscript and figures, and to E.V. Serebrova for preparation of the English translation of the current and preceding editions of this book.

And, last but not least, we are grateful to the Russian Foundation for Basic Research, the “Molecular and Cell Biology” program of the Russian Academy of Sciences, the Moscow Grants, the Russian grants for Leading Scientific Schools and to the Howard Hughes Medical Institute (USA) for the financial support of our laboratory that enabled us to complete the previous editions of this book.

xx Acknowledgements

The preparation of the current edition is supported by a grant from the Russian Science Foundation.

To my deep sorrow, I (A.V.F.) had to complete the first edition and now to revise and update this new edition of the book alone: my teacher and co-author Oleg B. Ptitsyn passed away in 1999 ... Therefore, I am completely responsible for any deficiencies in this book, and I am indeed indebted to Oleg B. Ptitsyn for his contribution to the composition and initial editing of the book.

Alexei V. Finkelstein, 2016

Lecture 1

This lecture contains an introduction to the whole course—a brief overview of what is given (or omitted) in the following lectures. Therefore, unlike other lectures, this one is not supplied with specific references; instead, it contains a list of textbooks that may be recommended for additional reading.

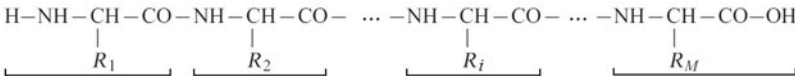
Proteins are molecular machines, building blocks, and arms of a living cell. Their major and almost sole function is enzymatic catalysis of chemical conversions in and around the cell. In addition, regulatory proteins control gene expression, and receptor proteins (which sit in the lipid membrane) accept inter-cellular signals that are often transmitted by hormones, which are proteins as well. Immunoproteins and the similar histocompatibility proteins recognize and bind “foe” molecules as well as “friend” cells, thereby helping the latter to be properly accommodated in the organism. Structural proteins form micro-filaments and microtubules, as well as fibrils, hair, silk, and other protective coverings; they reinforce membranes and maintain the structure of cells and tissues. Transfer proteins transfer (and storage ones store) other molecules. Proteins responsible for proton and electron transmembrane transfer provide for the entire bioenergetics, that is, light absorption, respiration, ATP production, etc. By ATP “firing” other proteins provide for mechanochemical activities—they work in muscles or move cell elements.

The enormous variety of protein functions is based on their high specificity for the molecules with which they interact, a relationship that resembles a key and lock (or rather, a somewhat flexible key and a somewhat flexible lock). This specific relationship demands a fairly rigid spatial structure of the protein—at least when the protein is “operating” (before and after that, some proteins are “natively unfolded”). That is why the biological functions of proteins (and other macromolecules of the utmost importance for life—DNA and RNA) are closely connected with the rigidity of their three-dimensional (3D) structures. Even a little damage to these structures, let alone their destruction, is often the reason for loss of, or dramatic changes in, protein activities.

A knowledge of the 3D structure of a protein is necessary to understand how it functions. Therefore, in these lectures, the physics of protein function will be discussed after protein structure, the nature of its stability and its ability to self-organize, that is, close to the end of this course.

Proteins are polymers; they are built up by amino acids that are linked into a peptide chain; this was discovered by E. Fischer as early as the beginning of the 20th century. In the early 1950s, F. Sanger showed that the sequence of amino acid residues (a “residue” is the portion of a free amino acid that remains after polymerization) is unique for each protein. The chain consists of a chemically regular backbone (main chain) from which various side chains

$(R_1, R_2, \dots, R_i, \dots, R_M)$ project (later on, we will consider certain deviations from the backbone, $-\text{NH}-\text{CH}-\text{CO}-$, regularity):



The number M of residues in protein chains ranges from a few dozens to many thousands. This number is gene-encoded.

There are 20 main (and a couple of accessory) species of amino acid residues. Their position in the protein chain is gene-encoded, too. However, subsequent protein modifications may contribute to the variety of amino acids.

Also, some proteins bind various small molecules, serving as cofactors.

In an “operating” protein, the chain is folded in a strictly specified structure. In the late 1950s, Perutz and Kendrew solved the first protein spatial structures and demonstrated their highly intricate and unique nature. However, it is noteworthy that the strict specificity of the 3D structure of protein molecules was first shown (as it became clear later) back in the 1860s, by Hoppe-Zeiler who obtained hemoglobin crystals—in a crystal each atom occupies a unique place.

The question whether the structure of a protein is the same in a crystal (where protein structures had been first established) and in a solution had been discussed for many years (when only indirect data were available) until the virtual identity of these (apart from small fluctuations) was demonstrated by nuclear magnetic resonance (NMR) spectroscopy.

Proteins “live” under various environmental conditions, which leave an obvious mark on their structures. The less water there is around, the more valuable the hydrogen bonds are (which reinforce the regular, periodic 3D structures of the protein backbone) and the more regular the stable protein structure ought to be.

According to their “environmental conditions” and general structure, proteins can be roughly divided into three classes:

1. Fibrous proteins form vast, usually water-deficient aggregates; their structure is usually highly hydrogen-bonded, highly regular, and maintained mainly by interactions between various chains.
2. Membrane proteins reside in a water-deficient membrane environment (although they partly project into water). Their intramembrane portions are highly regular (like fibrous proteins) and highly hydrogen-bonded, but restricted in size by the membrane thickness.
3. Water-soluble (residing in water) globular proteins are less regular (especially small ones). Their structure is maintained by interactions of the chain with itself (where an important role is played by interactions between

hydrocarbon—"hydrophobic"—groups that are far apart in the sequence but adjacent in space) and sometimes by chain interactions with cofactors.

Finally, there are some, mostly small or hydrocarbon group-poor or charged group-rich polypeptides, which do not have an inherent fixed structure in physiological conditions by themselves but obtain it by interacting with other molecules. They are usually called "natively" (or "intrinsically") disordered (or unfolded) proteins.

The above classification is extremely rough. Some proteins may comprise a fibrous "tail" and a globular "head" (eg, myosin), and so on.

To date, we know many millions of protein sequences (they are deposited at special computer databanks, eg, Swiss-Prot) and hundreds of thousands of protein spatial structures (they are compiled at the Protein Data Bank, or simply PDB). What we know about 3D protein structures mostly concerns water-soluble globular proteins. The solved spatial structures of membrane and fibrous proteins are relatively few. The reason is simple: water-soluble proteins are easily isolated as separate molecules, and their structure is relatively easily established by X-ray crystallography and by NMR studies in solution. That is why, when speaking about "protein structure" and "protein structure formation" one often actually means regularities shown for water-soluble globular proteins only. This must be kept in mind when reading books and papers on proteins, including these lectures. Moreover, it must be kept in mind that, for the same experimental reason, contemporary protein physics is mainly physics of small proteins, while the physics of large proteins is only starting to develop.

Noncovalent interactions maintaining 3D protein architecture are much weaker than chemical bonds fixing a sequence of monomers (amino acids) in the protein chain. This sequence—it is called "the primary structure of a protein" ([Fig. 1.1](#))—results from biochemical matrix synthesis according to a gene-coded "instruction."

Protein architectures, especially those of water-soluble globular proteins, are complex and of great diversity, unlike the universal double helix of DNA (the single-stranded RNAs appear to have an intermediate level of complexity). Nevertheless, certain "standard" motifs are detected in proteins as well, which will be discussed in detail in the last half of this course (note that the "standard" structures are, in fact, the same in all kingdoms of living matter).

In the first place, proteins have regular secondary structures, namely, the α -helices and β -sheets; α -helices are often represented by helical ribbons, and extended β -structural regions (which by sticking together form sheets) by arrows (see [Fig. 1.1](#)). Secondary structures are characterized by a regular periodic shape (conformation) of the main chain with side chains of a variety of conformations.

The packing of the secondary structures of one polypeptide chain into a globule is called the "tertiary structure," while several protein chains integrated into a "superglobule" form the "quaternary structure" of a protein. For instance

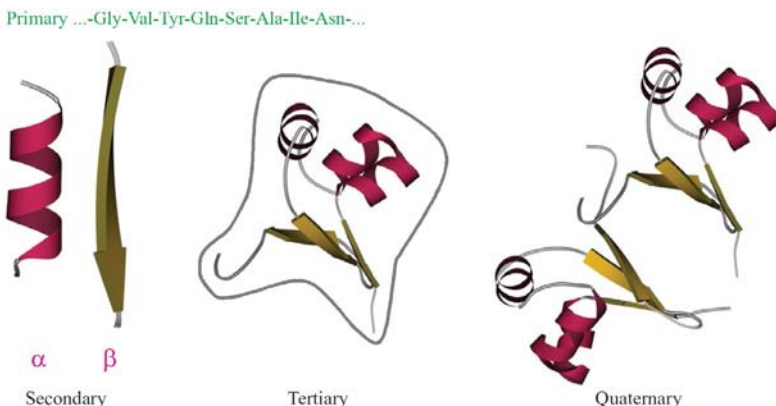


FIG. 1.1 Levels of protein structure organization: primary structure (amino acid sequence); regular secondary structures (α -helix and one strand of β -structure are shown); tertiary structure of a globule formed by one chain (the gray contour outlines the body of a dense globule); and quaternary structure of an oligomeric protein formed by several chains (here, dimeric *cro* repressor). This figure and most of the others show schemes of the backbone folds only; an all-atom presentation of a protein is given, eg, in Fig. 1.3.

(another example in addition to the dimeric *cro* repressor shown in Fig. 1.1), hemoglobin consists of two β - and two α -chains (this has *nothing to do* with α - and β -structures!). A quaternary structure formed by identical chains usually appears to be symmetrical (*cro* repressor and hemoglobin are no exception). Sometimes a quaternary structure comprises tens of protein chains. Specifically, virus coats can be regarded as such “superquaternary” structures (which are left unconsidered here).

Among tertiary structures, some can be distinguished as the most typical, and we will consider these later. They often envelop not the entire globular protein but only compact subglobules (so-called domains) within it (Fig. 1.2). A domain (like a small protein) usually consists of 100–200 amino acid residues, ie, of \sim 2000 atoms. Its diameter is about 30–40 Å.

The *in vivo* formation of the native (ie, biologically active) tertiary structure occurs during biosynthesis or immediately after. However, it is noteworthy that a 3D structure can result other than from biosynthesis: around 1960, Anfinsen showed that it could also be yielded by “renaturation,” ie, by *in vitro* refolding of a somehow unfolded protein chain and that the renaturation process goes spontaneously, unaided by the cellular machinery. This means that the spatial structure of a protein is determined by its amino acid sequence alone (provided water temperature, pH, and ionic strength are favorable), ie, the protein structure is capable of *self-organizing*. Later on we will consider certain exceptions.

Inner voice: Strictly speaking, this has been shown mainly for relatively small (up to 200–300 amino acid residues) water-soluble *globular* proteins.

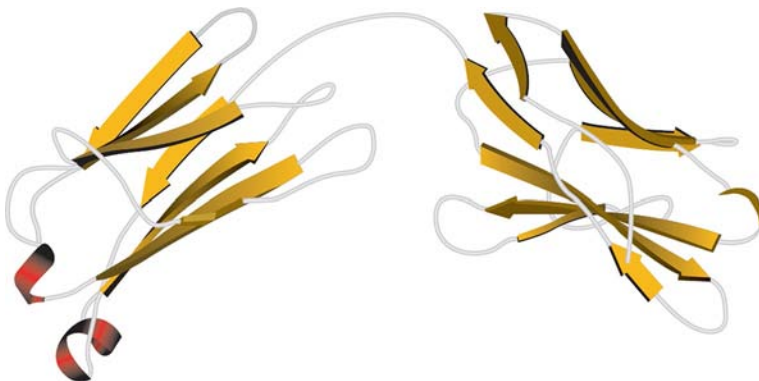


FIG. 1.2 The domain structure of a large protein is similar to the quaternary structure built up by small proteins. The only difference is that in large proteins, the compact subglobules (domains) pertain to the same chain, while the quaternary structure comprises several chains.

Concerning larger proteins, especially those of higher organisms, it is not that simple: far from all of them refold spontaneously...

Lecturer: Thanks for the refinement. Yes, it is not that simple with such proteins. Part of the reason is aggregation, part is posttranslational modification, especially when it comes to higher organisms, eukaryotes. Still less is known about spontaneous self-organization of membrane and fibrous proteins. In some proteins of this kind it happens, but mostly they do not refold. Therefore, let us agree right away that when speaking about protein physics, protein structure and its formation, I will actually discuss (if not specified otherwise) relatively small, single-domain globular proteins. This convention is quite common for biophysical literature, but the fact that it is insufficiently articulated causes frequent misunderstandings.

Anfinsen's experiments provided fundamental detachment of the physical process, that is, the spatial structure organization, from biochemical synthesis of the protein chain. They made clear that the structure of protein is determined by its own amino acid sequence alone and is not imposed by cellular machinery. It seems that the main task of this machinery is to protect the folding protein from unwanted contacts (among these are also contacts between remote regions of a very large protein chain), since *in vivo* folding occurs in a cellular soup with a vast variety of molecules to stick to. But *in diluted in vitro solution*, a protein, at least a small one, folds spontaneously by itself.

Strictly speaking, proteins are capable of spontaneous refolding provided they have undergone no strong posttranslational modification, ie, if their chemical structure has not been strongly affected after biosynthesis and initial folding. For example, insulin (which loses half of its chain after its *in vivo* folding has been accomplished) is unable to refold.

Posttranslational modifications (which are hardly considered in this book) are of a great variety. As a rule, chemical modifications are provided by special

enzymes rather than “self-organized” within protein. First of all, I should mention cleavage of the protein chain (proteolysis: it often assists conversion of zymogen, an inactive proenzyme, into the active enzyme; besides, it often divides a huge “polyprotein” chain into many separate globules). The cleavage is sometimes accompanied by excision of protein chain fragments (eg, when deriving insulin from proinsulin); by the way—the excised fragments are sometimes used as separate hormones. Also, one can observe modification of chain termini, acetylation, glycosylation, lipid binding to certain points of the chain, phosphorylation of certain side groups, and so on. Even “splicing” of protein chains (spontaneous excising of a chain fragment and sticking the loose ends together) has been reported. Spontaneous cyclization of protein chains or their certain portions is also occasionally observed.

Particular attention has to be given to formation of S—S bonds between sulfur-containing Cys residues: “proper” S—S bonds are capable (under favorable *in vitro* conditions) of spontaneous self-formation, although *in vivo* their formation is catalyzed by a special enzyme, disulfide isomerase. S—S-bonding is typical mostly of secreted proteins (there is no oxygen in the cell, and consequently, no favorable oxidizing potential for S—S-bonding). The S—S bonds, if properly paused, are not at all harmful but rather useful for protein renaturation.

In contrast, “improper” S—S bonds prevent protein renaturation. That is why, by the way, a boiled egg does not “unboil back” as the temperature decreases (although I should say that, in 2015, the “Improbable Nobel Prize” was awarded, see <http://www.improbable.com/ig/winners/>, for inventing a chemical recipe on how to partially unboil back an egg). The reason is that high temperature not only denatures the egg’s proteins but also initiates formation of additional S—S bonds between them (like in a gum). As the temperature is decreased, these new chemical bonds persist, thereby not allowing the egg’s proteins to regain their initial (native) state.

Thus, the amino acid sequence of a protein determines its native spatial structure, and this structure, in turn, determines its function, ie, with whom this protein interacts and what it does.

Here, I have to make some additional comments:

First, Fig. 1.1 apparently shows that there is ample empty space in the interior of the protein, and can create an impression that the protein is “soft.” In fact, this is not true. Protein is “hard”: its chain is packed tightly, atoms against atoms (Fig. 1.3A). However, the space-filling representation is inconvenient for studying protein anatomy, its skeleton, its interior; these can be seen using the wire model or some of the above-presented schemes with “transparent” atoms and a clear pathway of the protein chain (see Fig. 1.3B and especially Figs. 1.1 and 1.2 where the side chain atoms are stripped off and secondary structure elements stand out).

The space-filling model (Fig. 1.3A) gives no idea even of the polymeric nature of protein; it only shows the surface of a globule looking potato-like. However, this model is useful for studying protein function, since it is the physicochemical and geometrical properties of the globule surface, the “potato

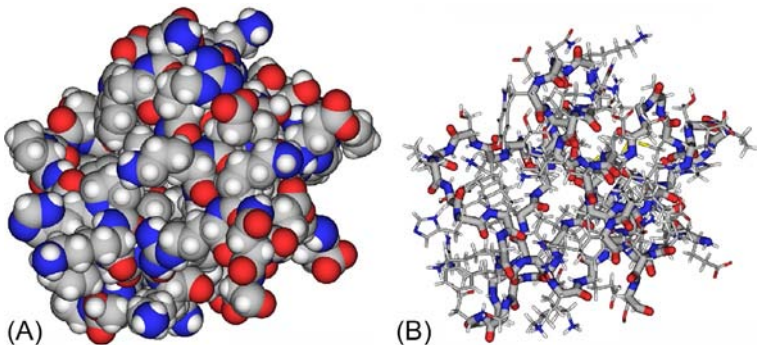


FIG. 1.3 Space-filling representation of a protein globule (A) and its wire model (B). In the wire model, side chains are shown as thin lines, the backbone as the thick line. Atoms are shown in colors: gray, C; white, H; red, O; blue, N.

skin,” that determine the specificity of the protein activity, whereas the protein skeleton is responsible for the creation and maintenance of this surface.

Second, apart from the polypeptide chain, proteins often contain *cofactors* (Fig. 1.4), such as small molecules, ions, sugars, nucleotides, fragments of nucleic acids, etc. These nonpeptide molecules are involved in protein functioning and sometimes in the formation of protein structure as well. The cofactors

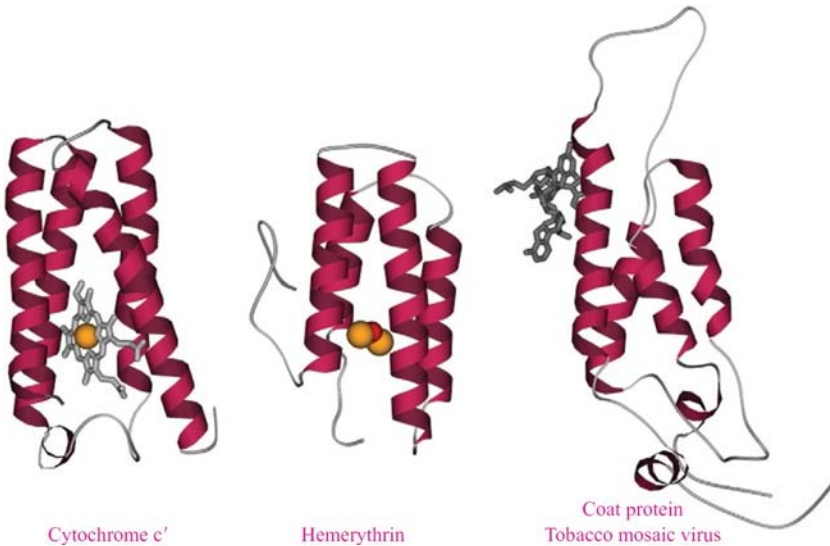


FIG. 1.4 Three α -helical proteins similar in overall architecture (comprising four α -helices each), but different in function: cytochrome c' , hemerythrin, and coat protein of Tobacco mosaic virus. Protein chain is shown as a ribbon; cofactors are shown as follows: wire models, heme (in cytochrome), and RNA fragment (in viral coat protein); orange balls, iron ions (in cytochrome heme and hemerythrin); a red ball, iron-bound oxygen (in hemerythrin).

can be linked by chemical bonds or just packed in cavities in a protein globule. Also, many water molecules (not shown in Fig. 1.4) are usually tightly bound to the protein surface.

Third, a solid protein (“aperiodic crystal” in Schrödinger’s wording) behaves exactly like a crystal under varying conditions (eg, at increasing temperature), that is, for some time it “stands firm” and then melts abruptly, unlike glass, which loses its shape and hardness gradually. This fundamental feature of proteins is closely allied to their functional reliability: as with a light bulb, proteins become inoperative in the “all-or-none” manner, not gradually (otherwise their action would be unreliable, eg, cause low specificity, etc. We will discuss this later on).

Finally, as concerns hardness, we have to distinguish between relatively small single-domain proteins that are really hard (they consist of one compact globule) and larger proteins that have either a multidomain (Fig. 1.2) or quaternary (Fig. 1.1) structure. The component subglobules of larger proteins can somewhat move about one another.

In addition, like a solid body, all globules can become deformed (but not completely reorganized) in the course of protein functioning.

Proteins with similar interior organization (anatomy) usually have the same related function.

For example, many (though not all) cytochromes look like the one shown in Fig. 1.4, and many (though again not all) serine proteases from different species (from bacteria to vertebrates) look like chymotrypsin, as shown in Fig. 1.5.

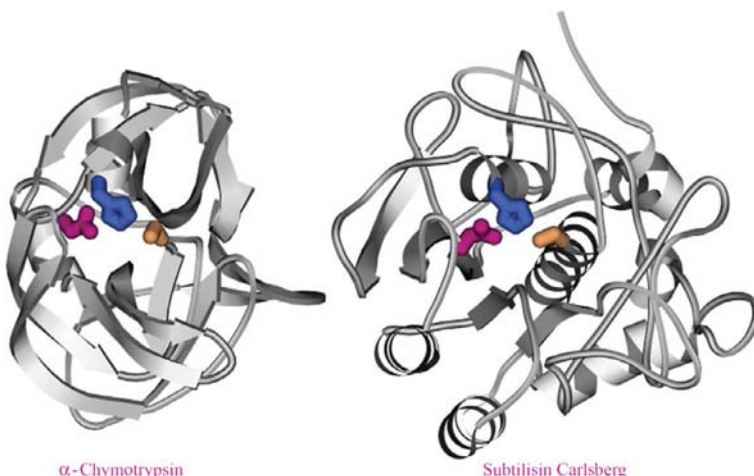


FIG. 1.5 Two proteins structurally different but almost identical in function (serine proteases): chymotrypsin, formed by β -structure, and subtilisin, formed by α -helices (some of which pertain to the active site) along with β -structure. In spite of drastically different chain folds, their catalytic sites comprise the same residues similarly positioned in space (but not in the amino acid sequence): Ser195 (orange), His57 (blue), and Asp102 (crimson) in chymotrypsin and Ser221 (orange), His64 (blue), and Asp32 (crimson) in subtilisin.

But sometimes very similar spatial structures may provide completely different functions. For example, cytochrome, one of the three proteins with similar spatial structures shown in Fig. 1.4, binds an electron, while hemerythrin, another protein of this shape, binds oxygen (these functions are somewhat alike, since they both are involved in the chain of oxidation reactions) and viral coat protein associates with much larger molecules, such as RNA and other coat proteins, and has nothing to do with oxidation.

We have already said that the structure of a protein determines its function. Is the reverse true? That is, does the function of a protein determine its structure?

Although some particular correlations of this kind have been reported, in general the influence of function on the structure has been detected mainly at a “rough” structural level, that is, the level connected with the “environmental conditions” of protein functions (eg, proteins controlling the structural function, like those building up hair or fibrils, are mostly fibrous proteins, receptors are membrane proteins, etc.). But most frequently, we see no influence of function on protein anatomy and architecture. For example, two serine proteases, chymotrypsin and subtilisin, have the same catalytic function and even similar specificity, whereas their interior organizations have nothing in common (see Fig. 1.5; their similarity is no greater than that between a seal and a diving beetle: only the proteins’ “flippers,” ie, their active sites including half a dozen of amino acid residues (from a couple of hundreds forming the globules), are structurally alike, while in every other respect they are completely different). Moreover, there exist structurally different active sites performing the same work (eg, those of serine proteases and metal proteases).

These, and many other examples, show that the function of a protein does not determine its 3D structure.

But, while saying this, account must be taken of size.

If the treated molecule (the molecule with which the protein interacts) is large, then a large portion of the protein may be involved in the interaction, and hence nearly the entire architecture of the protein is important for its functioning.

If the protein-treated molecule is small (which is more common, for enzymes in particular), then it is minor details of a small fraction of the protein surface that determine its function, while the rest of its “body” is responsible for fixing these crucial details. Hence, the main task of the bulk of the protein chain is to be hard and provide a solid foundation for the active site.

Inner voice: The nontrivial and piquant facts that one and the same function is performed by proteins of utterly different architectures, and different functions by architecturally similar proteins, should not overshadow the absolutely correct commonplace that architecturally close proteins are often homologous (genetically related) and have identical or similar functions...
Lecturer: This is true—but trivial. What I wanted to emphasize is the idea, important for protein physics (and protein engineering), that active sites may depend only slightly on the arrangement of the remaining protein body.

And the common feature of “the native protein body” is its hardness, since there is no other way to provide active-site specificity.

In time, we will consider the structures of proteins, their ability to self-organize and the reason for their hardness; we will discuss their functions and other aspects of interest for a biologist; but first we have to study amino acid residues and their elementary interactions with one another and the environment, as well as secondary structures of proteins that form their frameworks. These will be the subjects of the next several lectures.

RECOMMENDED ADDITIONAL READING

Below I give a list of books that can be useful when reading these lectures.

This list does not include basic books on physics, chemistry, and mathematics for undergraduates. Also, it comprises no monographs, advanced books and collections dedicated to experimental and computational techniques and other special aspects of protein science, such as chemistry of protein chains and their chemical modifications; gene manipulations; enzymology; mathematical backgrounds of bioinformatics or proteomics; and other subjects that are related, but not directly related to these lectures.

Biochemistry and molecular biology textbooks:

- Nelson, P., 2013. Biological Physics: With New Art by David Goodsell. W.H. Freeman & Co., New York.
- Nelson, D.L., Cox, M.M., 2012. Lehninger Principles of Biochemistry, sixth ed. W.H. Freeman & Co., New York.
- Stryer, L., 1995. Biochemistry, fourth ed. W.H. Freeman & Co., New York.
- Lehninger, A.L., Nelson, D.L., Cox, M.M., 1993. Principles of Biochemistry, second ed. Worth Publishers, New York.
- Cantor, C.R., Schimmel, P.R., 1980. Biophysical Chemistry. W.H. Freeman & Co., New York.

Books on protein physics and physical chemistry:

- Petsko, G.A., Ringe, D., 2003. Protein Structure and Function. Sinauer Associates, Sunderland, MA.
- Creighton, T.E., 1993. Proteins: Structures and Molecular Properties, second ed. W.H. Freeman & Co., New York.
- Schulz, G.E., Schirmer, R.H., 1979, 2013. Principles of Protein Structure. Springer, New York.
- Tanford, C., 1980. The Hydrophobic Effect, second ed. Wiley-Interscience, New York.

Books on physics applied to biomolecules:

- Frauenfelder, H., 2010. The Physics of Proteins. An Introduction to Biological Physics and Molecular Biophysics. Springer, New York.

- Dill, K.A., Bromberg, S., 2010. Molecular Driving Forces: Statistical Thermodynamics in Biology, Chemistry, Physics, and Nanoscience, second ed. Garland Science, New York.
- Grosberg, A.Yu., Khokhlov, A.R., 1994. Statistical Physics of Macromolecules. American Institute of Physics, New York.
- Volkenstein, M.V., 1977. Molecular Biophysics. Academic Press, New York.

Books on protein structures and bioinformatics:

- Lesk, A., 2010. Introduction to Protein Science: Architecture, Function, and Genomics, second ed. Oxford University Press, Oxford, NY.
- Tompa, P., 2010. Structure and Function of Intrinsically Disordered Proteins. Chapman & Hall/CRC Press, Taylor & Francis Group, Boca Raton, FL.
- Lesk, A., 2001. Introduction to Protein Architectures. Oxford University Press, Oxford, NY.
- Perutz, M.F., 1992. Protein Structure. W.H. Freeman & Co., New York.
- Branden, C., Tooze, J., 1991, 1999. Introduction to Protein Structure. Garland Science, New York.

Books on protein folding, function and engineering:

- Nöltig, B., 2010. Protein Folding Kinetics: Biophysical Methods. Springer, New York.
- Howard, J., 2000. Mechanics of Motor Proteins and the Cytoskeleton. Sinauer Associates, Sunderland, MA.
- Fersht, A., 1999. Structure and Mechanism in Protein Science: A Guide to Enzyme Catalysis and Protein Folding. W.H. Freeman & Co., New York.
- Fersht, A., 1985. Enzyme Structure and Mechanism, second ed. W.H. Freeman & Co., New York.

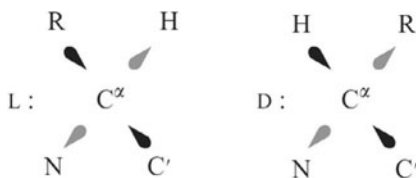
Books on experimental and computational methods in protein science:

- Schlick, T., 2010. Molecular Modeling and Simulation: An Interdisciplinary Guide, second ed. Springer, New York.
- Lesk, A.M., 2008. Introduction to Bioinformatics, third ed. Oxford University Press, Oxford.
- Serdyuk, I.N., Zaccai, N.R., Zaccai, J., 2007. Methods in Molecular Biophysics: Structure, Dynamics, Function. Cambridge University Press, Cambridge, NY.
- Durbin, R., Eddy, S., Krogh, A., Mitchison, G., 1998. Biological Sequence Analysis: Probabilistic Models of Proteins and Nucleic Acids. Cambridge University Press, Cambridge.

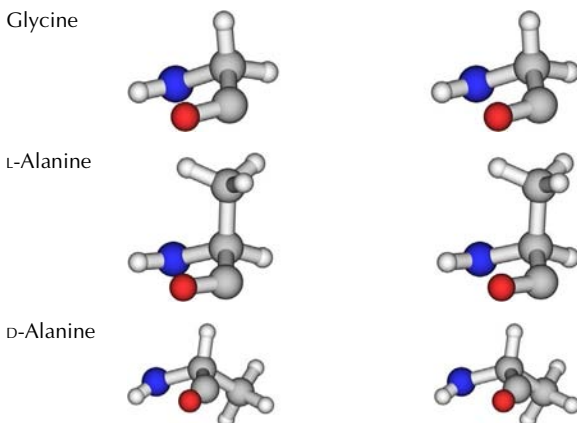
Lecture 2

The protein (polypeptide) chain consists of the main chain and side groups of amino acid residues (see Fig. 2.1) (Cantor and Schimmel, 1980; Schulz and Schirmer, 1979 & 2013; Nelson and Cox, 2012).

Amino acids that build up polypeptide chains (Figs. 2.1 and 2.2) can have either the L or the D steric form. The forms L and D are mirror-symmetric: the massive residue side chain (R) and the H-atom, both positioned at the α -carbon (C^α) of the amino acid, exchange places in these forms (arrows show atoms above and below the plane of the figure):



Glycine (Gly), with only a hydrogen atom as a side chain, shows no difference between the L- or D-form; for all other amino acids, the L- and D-forms have different shapes, as seen in the cross stereo drawings given here, for L-alanine and D-alanine:



(See How to use stereo drawings, in Appendix E.)

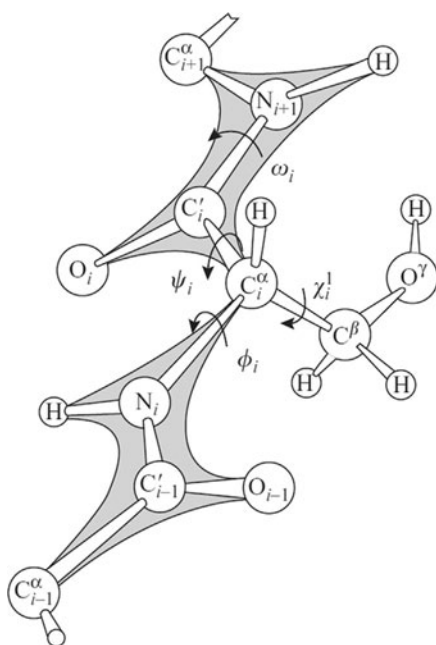
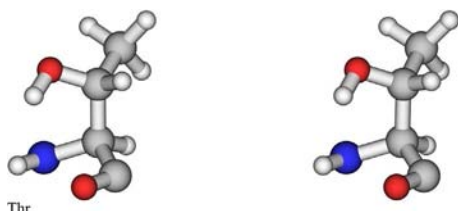


FIG. 2.1 Diagram showing a polypeptide chain with a side group (here: side group of Serine (Ser); ' i ' is its number in the chain). The peptide units are outlined. The main-chain angles of rotation (ϕ , ψ , ω) and that of the side chain (χ^1) are presented. Arrows show the direction of rotation of the part of the chain closest to the viewer about its remote part that increases the rotation angle. (Adapted from Schulz, G.E., Schirmer, R.H., 1979 & 2013. *Principles of Protein Structure*. Springer, New York, Chapter 2, with permission.)

Protein chains are built up only from L-residues. Only these are gene-coded. D-residues (sometimes observed in peptides) are not encoded during matrix protein synthesis but made by special enzymes. Spontaneous racemization (L \leftrightarrow D transition) is not observed in proteins. It never occurs during biosynthesis but often accompanies chemical synthesis of peptides, and then its elimination is highly laborious.

All side chains have no L- and D-forms, but for Ile and Thr, where C^γ atoms have covalent bonds to four non-equal neighbours:



Only one of these forms (shown in the stereo drawing as an example) is present in proteins.

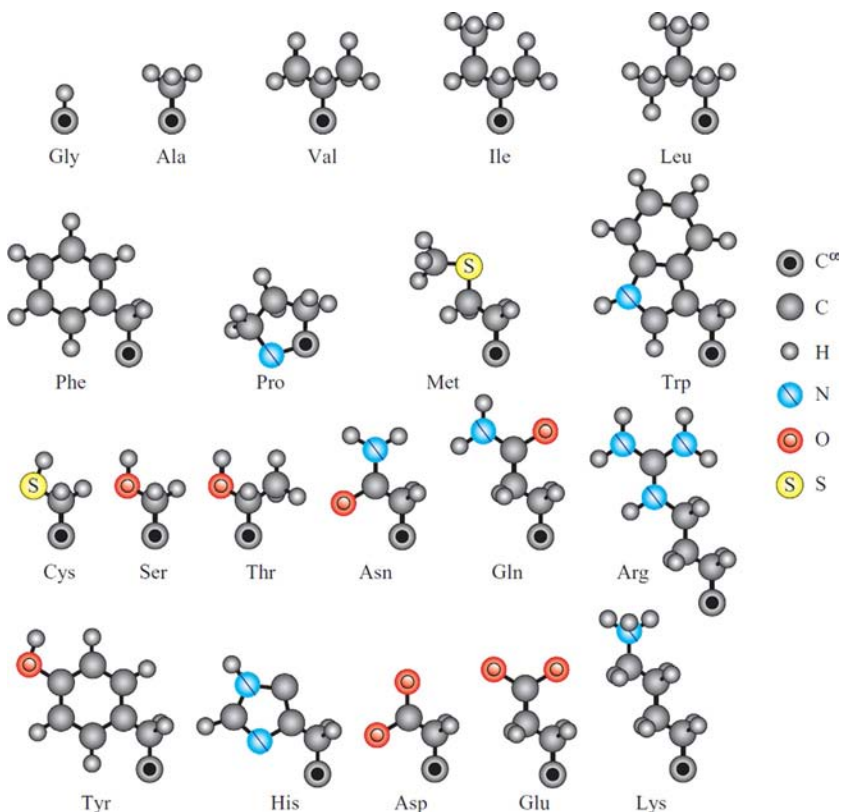
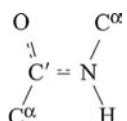


FIG. 2.2 The side chains of 20 standard amino acid residues (projecting from the main-chain C^α atoms). Atoms forming the amino acids are shown on the right. Apart from the 20 standard amino acid residues shown here, there are some rare non-standard ones, which are either produced by modification of a standard amino acid or (like selenocysteine) are coded by a RNA codon positioned in a special RNA context (Creighton, 1993).

In the protein chain, amino acids are linked by *peptide* bonds between C'- and N-atoms (Fig. 2.1). An important role is played by the planar rigid structure of the whole *peptide unit*:



Its planar character is provided by the so-called sp²-hybridization of electrons of the N- and C'-atoms. ‘Hybridization’ of electron orbitals is a purely quantum effect. sp²-Hybridization turns one spherical s-orbital and two ‘8-shaped’

p-orbitals into three extended (from the nucleus) sp^2 -orbitals. These three orbitals involve the atom in three covalent bonds pertaining to one plane ($\text{-}\bullet\langle$). A covalent bond is created by a ‘delocalized’ electron cloud covering the bound atoms.

The peptide group is rigid owing to an additional bond formed by p-electrons from the N- and C'-atoms uninvolved in sp^2 -hybridization. These electrons of N-, C'-, and O-atoms also bond and ‘delocalize’, thereby creating an electron cloud that envelops all these atoms (that is why the bonds $\text{C}=\text{N}$ and $\text{C}=\text{O}$ are drawn as ‘partial’ double bonds, $=\text{=}$). And since the ‘8-shaped’ p-orbitals are perpendicular to the plane of the sp^2 -orbitals ($\text{-}\bullet\langle$), the additional covalent bond of these perpendicular p-orbitals



blocks the rotation around the C'-N bond.

I would like to remind you that chemical bonds are caused mainly by ‘delocalization’ of electrons, ie, their permanent transition from one atom to another. This follows from Heisenberg’s *Principle of Uncertainty*:

$$\Delta p \Delta x \sim \hbar \quad (2.1)$$

(more rigorously: $\Delta p \Delta x \geq \hbar/2$; [Landau and Lifshitz, 1977](#)).

Here Δp is the uncertainty in impulse ($p=mv$) of the particle, Δx is the uncertainty in its coordinate, and the reduced Planck’s constant $\hbar \equiv h/2\pi$, where h is Planck’s constant. Since the direction of electron movement within the atom is unpredictable, $\Delta p \sim |p|=mv$, where v is the velocity and m is the mass of the particle. Hence,

$$|v| \sim \frac{\hbar}{m \Delta x} \quad (2.2)$$

At the same time, the kinetic energy of the particle $E = mv^2/2$, ie, (neglecting insignificant ‘2’):

$$E \sim \frac{\hbar^2}{m \Delta x^2} \quad (2.3)$$

Hence, owing to the delocalization, the energy of the particle decreases with increasing Δx , and thereby the particle adopts a more stable state. As seen, light particles (electrons) are those mostly affected. This is how electron delocalization causes chemical bonding ([Pauling, 1970](#)).

The length of a chemical bond is close to the van der Waals radius of atoms, ie, it amounts to $1\text{--}2 \text{ \AA}$ (to be more exact, it is 1 \AA for C-H, N-H and O-H bonds, about $1.2\text{--}1.3 \text{ \AA}$ for $\text{C}=\text{O}$, $\text{C}=\text{O}$, $\text{C}=\text{N}$ and $\text{C}=\text{C}$, 1.5 \AA for C-C and about 1.8 \AA for S-S).

Typical values of covalent angles are approximately 120° and 109° . The former are at sp^2 -hybridized atoms like $-\text{C}'<$, $-\text{N}<$, where three covalent bonds are directed from the center to the apexes of a planar triangle, and the latter are at sp^3 -hybridized atoms, like $>\text{C}^\alpha<$, where four bonds are directed from the center to the apexes of a tetrahedron, as well as at $\text{O}<$ or $\text{S}<$ atoms having two bonds each (Pauling, 1970; Schulz and Schirmer, 1979 & 2013).

Now let us consider typical values of vibrations, ie, thermal vibrations of covalent bonds and angles. These can contribute to the flexibility of the protein chain.

Vibrational frequencies manifest themselves in the infrared (IR) spectra of proteins. Typical frequencies are as follows (Schulz and Schirmer, 1979 & 2013): $v \sim 7 \times 10^{13} \text{ s}^{-1}$ for vibrations of the H atom (eg, in the bond C–H; the corresponding IR light wavelength $\lambda = c/v \sim 5 \mu\text{m}$, where c is the speed of light, $300,000 \text{ km s}^{-1}$). For vibrations of ‘heavy’ atoms and groups (eg, in the bond $\text{CH}_3\text{--CH}_3$), $v \sim 2 \times 10^{13} \text{ s}^{-1}$ (then $\lambda = c/v \sim 15 \mu\text{m}$).

Are these vibrations excited at room temperature?

To answer this question, we have to compare heat energy per degree of freedom (‘heat quantum’, kT) with vibration energy. Let us estimate kT at ‘normal’ temperature. Here, T is absolute temperature in Kelvin ($T=300 \text{ K}$ at 27°C , ie, at about ‘room’ temperature; K denotes Kelvin), and k (sometimes written as k_B) is the Boltzmann constant (equal to $\approx 2 \text{ cal mol}^{-1} \text{ K}^{-1}$, or $0.33 \times 10^{-23} \text{ cal K}^{-1}$ per particle, since one mole contains 6×10^{23} particles). Hence, at room temperature the ‘heat quantum’ $kT=600 \text{ cal mol}^{-1}$, or $(600 \text{ cal})/(6 \times 10^{23} \text{ particles})$, ie, 10^{-21} calories per particle.

The frequency ν_T corresponding to this heat quantum can be derived from the well-known equation $kT=h\nu_T$ (where Planck’s constant $h \equiv 2\pi\hbar=6.6 \times 10^{-34} \text{ J s} \equiv 1.6 \times 10^{-34} \text{ cal s}$; let me remind you that 1 calorie is equal to 4.2 joules, J). So, the characteristic frequency of thermal motions, ν_T , is equal to $7 \times 10^{12} \text{ s}^{-1}$ at $T=300 \text{ K}$, ie, at 27°C .

The ‘heat quantum’ cannot induce vibrations with a higher frequency than its own (Pauling, 1970; Schulz and Schirmer, 1979).

Thus, at room temperature, covalent bonds are ‘hard’ and do not vibrate: their vibrational frequency $v \sim 2 \times 10^{13} - 7 \times 10^{13} \text{ s}^{-1}$, ie, an order of magnitude higher than $\nu_T=7 \times 10^{12} \text{ s}^{-1}$.

However, vibrations of covalent bonds can be induced by IR light; this underlies the importance of IR spectroscopy of proteins (Creighton, 1993). It is IR spectroscopy that provides information about the vibrations of atoms, covalent bonds and covalent angles. The properties of these vibrations are first derived from experiments on small molecules and then used for protein investigations.

Covalent angles are less rigid than bond lengths, and therefore, they vibrate at room temperature; their vibrational frequency ranges from 10^{12} to 10^{13} s^{-1} . However, their typical amplitude amounts only to 5° (Schulz and Schirmer, 1979 & 2013).

Thus, covalent bond vibrations do not contribute to the flexibility of protein chain, and the contribution of vibrations of covalent angles is minor.

In fact, this flexibility (which implies the ability to fold into α -helices and globules) is provided by rotation (although not a completely free rotation—see later) *around* the covalent bonds. That is why the chain structure (configuration) is often described simply in terms of angles of rotation around covalent bonds—then it is called the ‘conformation’. It should be noted, that the terms ‘structure’, ‘configuration’ and ‘conformation’ are often used as synonyms.

The relative position of atomic groups linked by a covalent bond is described by a dihedral angle (that is formed by two planes: in Fig. 2.3, one includes points **a**, \mathbf{O}' , \mathbf{O}'' and the other \mathbf{O}' , \mathbf{O}'' , **c**).

Figs. 2.1 and 2.3 illustrate the measurement of this angle. The measurement is made as described in school trigonometry, if we assume that the covalent bond closest to the viewer is the ‘rotating arrow’, the far bond is the ‘coordinate axis’, and the central one is the ‘rotation axis’. As in trigonometry, the arrow’s turn in a counter-clockwise direction increases the angle of rotation, while its clockwise movement decreases this angle.

The major information on rotation of atomic groups around covalent bonds is also provided by IR spectroscopy; again, I will discuss only the basic results obtained.

Fig. 2.4 illustrates the typical variation of energy in the case of rotation around the bond between two sp^3 -hybridized atoms ($\text{H}_3\text{C}-\text{CH}_3$ and $\text{CH}_2\text{C}-\text{CH}_2\text{C}$ serve as examples). These bonds are typical of aliphatic side chains. Side-chain angles of rotation are called χ (‘chi’) angles (Fig. 2.1). The maximums of such triple (in accordance with symmetry of rotation about the sp^3-sp^3 bond) potentials (ie, potentials that have three maximums and three minimums within 360°) correspond to three eclipsed conformations (0° , 120° and 240°) that result in approach (and repulsion) of the electron clouds. The repulsion occurs because these electrons have been already involved in covalent bonding.

The resultant potential barriers of rotation around $\text{H}_3\text{C}-\text{CH}_3$ amount to about 3 kcal mol^{-1} , and the typical range of thermal fluctuations about these minimums (ie, deviations accompanied by energy increasing by kT) is $15-20^\circ$.

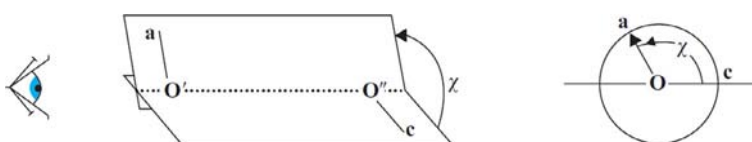


FIG. 2.3 Measurement of the dihedral angle (angle of rotation) shown in both axial (right) and transverse (left) views. The central bond $\mathbf{O}'-\mathbf{O}''$ serves as the ‘rotation axis’, the covalent bond $\mathbf{O}''-\mathbf{c}$ serves as the ‘coordinate circle axis’, and the closest (to the viewer) bond $\mathbf{O}'-\mathbf{a}$ serves as the ‘arrow on the coordinate circle’ in trigonometry. When the dihedral angle is measured in the chain, the atoms **a** and **c** belong to the heaviest atomic groups attached to the $\mathbf{O}'-\mathbf{O}''$ bond. (See IUPAC-IUB 1970, for more, sometimes rather tricky details of the dihedral angle nomenclature.)

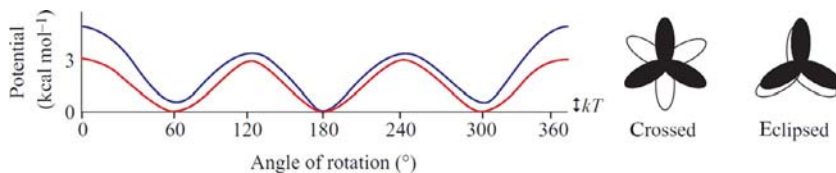


FIG. 2.4 Typical (see Halgren, 1995; Levitt et al., 1995; Jorgensen et al., 1996; Wang et al., 2004) potential of rotation around a single bond between two sp^3 -hybridized atoms: around $\text{H}_3\text{C}-\text{CH}_3$ (red curve) and $\text{CH}_2\text{C}-\text{CH}_2\text{C}$ (blue curve). The major energetic effect results from repulsion of electron clouds that is at a maximum in the ‘shaded’ conformations (at 0° , 120° and 240°) and at a minimum in the ‘crossed’ ones (at 60° , 180° and 300°). Repulsion of small H-atoms is negligible. However, repulsion of heavy C-atoms surrounded by large electron clouds occurring around 0° (in the chain $\text{C}-\text{C}-\text{C}-\text{C}$) yields an additional energetic effect that distinguishes rotation around the $(\text{C}-\text{CH}_2)-(\text{CH}_2-\text{C})$ bond from that around the $\text{H}_3\text{C}-\text{CH}_3$ bond. For comparison, \dagger shows the magnitude of the ‘heat quantum’ kT .

When more massive atoms are sp^3 -bonded instead of some H atoms, repulsion of these contributes to the barrier in the region where they become too close to one another. This is exemplified (see Fig. 2.4) by the rotation around the central bond in $(\text{C}-\text{CH}_2)-(\text{CH}_2-\text{C})$.

Fig. 2.5 illustrates the typical variation of energy in the case of rotation around a peptide bond between two sp^2 -hybridized atoms (C' and N). The angle of rotation around this bond is denoted as ω (Fig. 2.1). The potential is double (ie, it has two maxima and two minima within 360°) in accordance with the symmetry of rotation about the sp^2-sp^2 bond. The potential barriers are high owing to the involvement of additional p-electrons in the peptide bond (as discussed at the beginning of this lecture). The potential minima are at 0° and 180° (where the p-orbitals pulling together C' and N atoms are at their closest), and its maxima are at 90° and 270° (where these p-orbitals are farthest apart and, hence, least connected with one another). High barriers mean

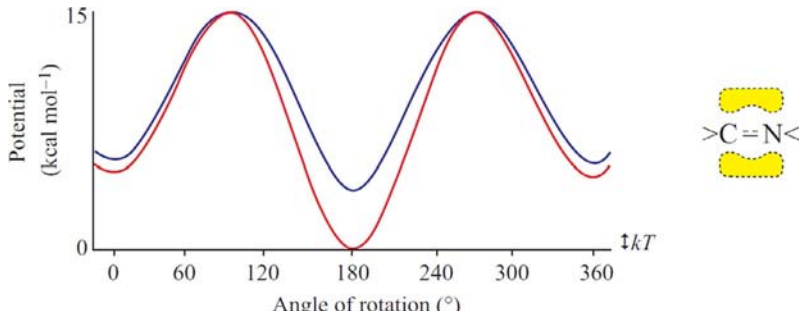
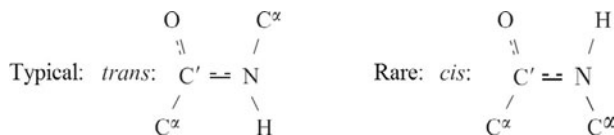


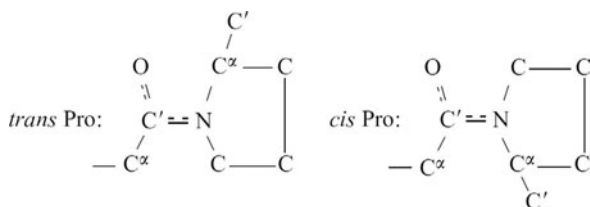
FIG. 2.5 Typical potential of rotation around a peptide bond between two sp^2 -hybridized atoms (C' and N): p-orbital-bonding at 0° (or 180°) is shown in yellow on the right. For all (except proline) peptide bonds, their energy (red curve) is higher at 0° than at 180° owing to the repulsion between massive C' -atoms at 0° . This difference in energy is small for the peptide bond preceding Pro (blue curve): Pro has not one but two C-atoms bonded to the N-atom. (See the text and the diagram illustrating the structural formula of proline.)

that the typical range of thermal fluctuations of the angle of rotation around such bonds is small (5–10°).

It is noteworthy that repulsion of massive C^α-atoms makes the *cis*-conformation ($\omega=0^\circ$) rather unfavourable energetically; therefore, in proteins, almost all peptide groups are in the *trans*-conformation ($\omega=180^\circ$).



An exception is the proline-preceding peptide bond. Pro is an *imino* but not an *amino* acid: its N atom has not two but three similar massive radicals (C', –C^αHC₂ and –CH₂C; see Fig. 2.2), and therefore its *trans*-conformation has only a minor advantage as compared with the *cis* one.



In both globular and unfolded (ie, fluctuating, lacking a fixed structure) peptides, there are about 90% of *trans*- and 10% of *cis*-prolines (Branden and Tooze, 1999).

I would like to draw your attention to this regularity—the more favourable some detail is in itself (individually), the more frequently this detail occurs in proteins. We will see it many times to come.

Finally, let us consider the potential of rotation around the bond between sp³-hybridized and sp²-hybridized atoms. Angles of rotation around such bonds are denoted as φ (rotation around N-C^α) and ψ (rotation around C^α-C') (Fig. 2.1).

This rotation yields a six-fold (six minimums and six maximums within 360°) potential with rather low barriers (<1 kcal mol⁻¹, see Fig. 2.6) that are

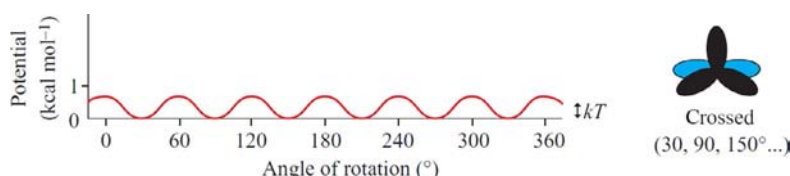


FIG. 2.6 Typical potential of rotation around a single bond between sp³- and sp²-hybridized atoms (exemplified by rotation around H₃C–C₆H₅). The sp²-hybridized (light-blue) and the sp³-hybridized (black) electron clouds are shown in the ‘crossed’ conformation.

of the same order as the energy of thermal fluctuations (which, as we remember, amounts to 0.6 kcal mol⁻¹ at room temperature). It is these nearly free rotations around such bonds (N–C^α and C^α–C') in the polypeptide main chain that ensure the flexibility of the polypeptide.

Concluding, I have to add that, although potentials of rotation around covalent bonds seem to be rather well established (Halgren, 1995; Levitt et al., 1995; Jorgensen et al., 1996; Wang et al., 2004), some correction of torsional potentials was necessary (Lindorff-Larsen et al., 2010) for the recently achieved progress in reproducing protein folding by molecular dynamics simulations (Shaw et al., 2010).

REFERENCES

- Branden, C., Tooze, J., 1999. Introduction to Protein Structure, second ed. Garland Science, New York (Chapter 6).
- Cantor, C.R., Schimmel, P.R., 1980. Biophysical Chemistry. W.H. Freeman & Co, New York (Part 1, Chapter 2).
- Creighton, T.E., 1993. Proteins: Structures and Molecular Properties, second ed. H. Freeman & Co., New York (Chapters 1, 2, 5).
- Halgren, T.A., 1995. Merck molecular force field. I. Basis, form, parameterization and performance of MMFF94. *J. Comput. Chem.* 17, 490–519.
- IUPAC-IUB, 1969. Commission on Biochemical Nomenclature. Abbreviations and symbols for the description of the conformation of polypeptide chains. Tentative rules (1969). *Biochemistry* 9, 3471–3479.
- Jorgensen, W.L., Maxwell, D.S., Tirado-Rives, J., 1996. Development and testing of the OPLS all-atom force field on conformational energetics and properties of organic liquids. *J. Am. Chem. Soc.* 118, 11225–11236.
- Landau, L.D., Lifshitz, E.M., 1977. Quantum Mechanics (Vol. 3 of A Course of Theoretical Physics). Pergamon Press, Oxford, New York (Section 16).
- Levitt, M., Hirshberg, M., Sharon, R., Daggett, V., 1995. Potential energy function and parameters for simulations of the molecular dynamics of proteins and nucleic acids in solution. *Comput. Phys. Commun.* 91, 215–231.
- Lindorff-Larsen, K., Piana, S., Palmo, K., Maragakis, P., Klepeis, J.L., Dror, R.O., Shaw, D.E., 2010. Improved side-chain torsion potentials for the Amber ff99SB protein force field. *Proteins* 78, 1950–1958.
- Nelson, D.L., Cox, M.M., 2012. Lehninger Principles of Biochemistry, sixth ed. W.H. Freeman & Co, New York (Chapter 3).
- Pauling, L., 1970. General Chemistry. W.H. Freeman & Co, New York (Chapters 3–6).
- Schulz, G.E., Schirmer, R.H., 1979 & 2013. Principles of Protein Structure. Springer, New York (Chapter 2).
- Shaw, D.E., Maragakis, P., Lindorff-Larsen, K., Piana, S., Dror, R.O., Eastwood, M.P., Bank, J.A., Jumper, J.M., Salmon, J.K., Shah, Y., Wriggers, W., 2010. Atom-level characterization of structural dynamics of proteins. *Science* 330, 341–346.
- Wang, J., Wolf, R.M., Caldwell, J.W., Kollman, P.A., Case, D.A., 2004. Development and testing of a general amber force field. *J. Comput. Chem.* 25, 1157–1174.

Lecture 3

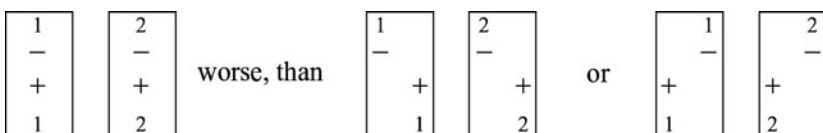
In this lecture, we shall focus on elementary noncovalent interactions between atoms.

First of all, let us recall in what circumstances no covalent bond is formed between approaching atoms. Let me remind you that chemical bonding basically results from delocalization of electrons, that is, their “transition” from one atom to another and back: these electrons are often said to share the same (common) orbital enveloping two or more atoms. However, according to the *Pauli Exclusion Principle* ([Landau and Lifshitz, 1977](#)), not more than two electrons can share the same orbital, and they can do this only when their spins (moments of rotation) are oppositely directed (then they are “paired electrons”). Pairing in a common orbital of electrons coming from two different atoms results in a tight covalent bond.

If orbitals of two mutually approaching atoms already bear a pair of electrons each, no covalent bond can emerge. Otherwise, there would be too many electrons in the common orbital—four. But, as stated by the *Pauli Exclusion Principle*, one orbital can bear no more than two electrons. Consequently, a “saturated” orbital with an electron pair on cannot accept extras. Therefore, atoms with saturated electron orbitals repel as they come near enough for their electron clouds to begin to overlap. Such atoms are impenetrable to one another at ordinary (though not at stellar) temperatures.

The same is observed when molecules with no vacant valency approach one another: they repel at a distance between their atoms as short as 2–3 Å.

However, at a greater distance (when electron clouds do not overlap) all atoms and molecules attract each other ([London, 1937](#); [Landau and Lifshitz, 1977](#); [Dill and Bromberg, 2010](#)), unless they are charged (we will discuss this later). This attraction is purely quantum in nature. It is connected with coordinated vibrations of electrons in both atoms. The thing is, the coordinated (in the same direction) shift of electrons results in attraction of the atoms (whereas atoms with nonshifted electrons do not attract or repel each other). This becomes clear from the following diagram showing two atoms, 1 and 2, with an electron “−” and nucleus “+” in each.



When considering this diagram, one must bear in mind that electric energy increases with decreasing distance r as $1/r$. The electron shift causes no change

in electron-electron and nucleus-nucleus interactions, but the increase in attraction between electron 1 and nucleus 2, which become close (see the extreme right of the diagram) is greater than the decrease in attraction between electron 2 and nucleus 1. Now recall that electrons are in constant vibration within an atom (they “orbit the nucleus” and cannot fall onto it because of Heisenberg’s quantum uncertainty). The above effect provokes a coordination of electron vibrations as the atoms come closer and hence causes attraction of these atoms.

At greater distances, the atomic interactions weaken. As a result, interaction energy decreases as a function of distance r between the centers of the two atoms; it can be shown that the energy decrease is proportional to $(1/r)^6$ (London, 1937; Landau and Lifshitz, 1977).

The total potential of atomic interaction (also called “the energy of van der Waals interaction”) is illustrated by Fig. 3.1 and approximately described by the Lennard-Jones potential of the form:

$$U_{\text{LJ}}(r) = E_0 \left[\left(\frac{r_0}{r}\right)^{12} - 2 \left(\frac{r_0}{r}\right)^6 \right] \quad (3.1)$$

Here r_0 (as can be easily proved by taking the U_{LJ} derivative over distance r) is the distance at which the energy U_{LJ} is at a minimum, and E_0 is the depth of the minimum. The last term that decreases as $(\text{const./distance})^6$ gives the attraction (minus “−” shows that the corresponding energy decreases with decreasing distance); the term of the 12th power gives the repulsion (it is positive, ie, the corresponding energy increases with decreasing distance).

Eq. (3.1) gives a precise description of the attraction at large distances (when $r \gg r_0$). The repulsion at small distances is described only qualitatively as “very strong and exceeding any attraction when r tends to zero.” The approximate character of Eq. (3.1) is demonstrated by the fact that atoms are implied to be spherical (since the described interaction is direction-independent), whereas actually, the atomic electron cloud is not spherical because of projecting p-electrons. In general, only quantum mechanics can provide the correct description of interactions between atoms, but it can strictly calculate only very simple systems like the He atom, H_2^+ ion, or H_2 molecule. All other systems have to be described using approximate “semiempirical” equations such as Eq. (3.1), the form of which is

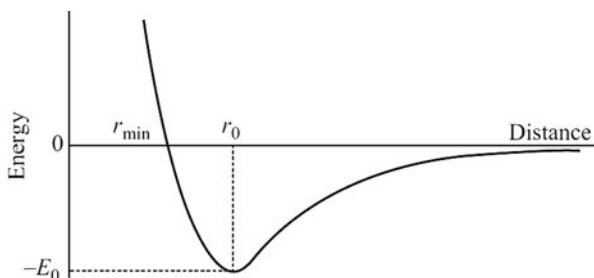


FIG. 3.1 Typical profile of the van der Waals interaction potential.

based on only semiquantitative physical considerations and parameters (in this case, E_0 and r_0) on experiment. Some basic data are given in [Table 3.1](#).

You should notice that [Table 3.1](#) presents not only values of the optimal distance r_0 but also those of the minimum distances r_{\min} that exist in the crystalline state. In [Fig. 3.1](#), r_{\min} approximately corresponds to the point where energy passes through 0 at a short distance between atoms. Values of r_{\min} are helpful in estimating the possibility of a particular chain conformation.

Inner voice: There are a lot of works on deriving potentials of atom-atom interactions (see, eg, [Halgren, 1995](#); [Levitt et al., 1995](#); [Jorgensen et al., 1996](#); [Wang et al., 2004](#)). Is not this indicative of the questionable precision of all these potentials?

Lecturer: As to the *form* of the potential ([Fig. 3.1](#)), there is no particular disagreement. The estimates of r_{\min} are also alike as they are directly measured in crystals. The difference in views concerns values of r_0 and especially E_0 . For example, many authors point out that the radius of H in polar N–H and O–H groups is much smaller than that in nonpolar C–H groups. The radii and energies are mainly derived from crystals as well, that is, from their structure (radii) and sublimation heat (energies). However, crystals usually consist of not atoms but molecules, for example, CH₄, C₂H₆... So, when calculating the energy, a question arises as to the contribution of interactions C···C, H···H, and C···H. Different authors answer it in different ways, so sometimes their potentials differ significantly. However, this difference is smoothed out as soon as they come back from atoms to molecules. But it

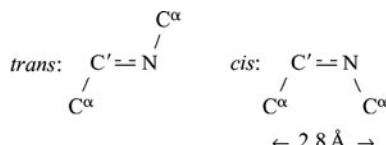
TABLE 3.1 Typical parameters of van der Waals interaction potentials.

Interaction	E_0 (kcal mol ⁻¹)	r_0 (Å)	r_{\min} (Å)	Minimum van der Waals radius of atom (Å)
H···H	0.12	2.4	2.0	H: 1.0
H···C	0.11	2.9	2.4	
C···C	0.12	3.4	3.0	C: 1.5
O···O	0.23	3.0	2.7	O: 1.35
N···N	0.20	3.1	2.7	N: 1.35
CH ₂ ···CH ₂	≈0.5	≈4.0	≈3.0	CH ₂ : ≈1.5

E_0 and r_0 values for interactions between atoms are from [Scott and Scheraga \(1966\)](#); r_{\min} values from [Ramachandran and Sasisekharan \(1968\)](#). These values provided the basis for estimating CH₂···CH₂ interaction parameters. The interaction CH₂···CH₂ depends on the relative orientation of these groups; therefore, the tabulated results are approximate. Nevertheless, they are often used to calculate interactions in proteins when H-atoms are “invisible” to X-rays.

is important to remember that when calculating molecular structures, the source of one parameter (say, the energy of the C···C interaction) should not differ from the source of the others (eg, the H···H interaction energy): here, the principle “all-or-none” must be followed to avoid mistakes.

The tabulated values are helpful for understanding why the *trans*-conformation (180 degree) of the C'≡N bond is allowed and its *cis*-conformation (0 degree) is disallowed (for all amino acid residues, except Pro, as mentioned earlier): for the C'≡N *trans*-conformation, the distance between C^α atoms is 3.8 Å, while for its *cis*-conformations (when these atoms are at their closest), it is only 2.8 Å, ie, less than the minimum distance $r_{\min}=3.0$ Å allowed for the C···C pair.



Inner voice: According to Eq. (3.1), the van der Waals interaction is pairwise. Is it really independent of the environment?

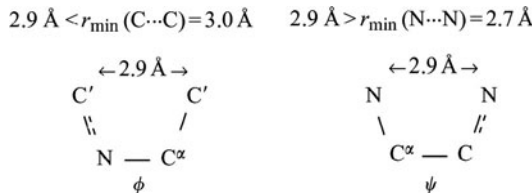
Lecturer: The repulsive part of this interaction is independent because it is due to overlapping of electron clouds of two atoms. The attractive term ($\sim(r_0/r)^6$ in Eq. (3.1)) depends on electrostatic interactions of vibrating electrons; therefore, on average, it decreases (but not very much) with an increase of that component of dielectric permittivity of the media which corresponds to the frequency of these vibrations (Finkelstein, 2007). Actually, the mutual attraction of atoms “1” and “2” can be increased or decreased, depending on the position of atom “3,” which is close to them in space (Axilrod and Teller, 1943); the most important in this respect is atom “3” covalently bound to either atom “1” or “2” (Finkelstein, 2007).

Here, it is worth making a comment. Considering the interactions of proteins and other molecules surrounded by water, people often prefer to consider water *implicitly*, as something that has no molecular structure but only changes the value of interaction between the molecules (the use of the medium dielectric constant is the most famous example of this kind). The same is applicable to van der Waals interactions. The approaching of atom “1” to “2” displaces waters (w) from these atoms (and these displaced waters start to interact between themselves). The resulting energy of this approach in water can be presented as $\Delta E_{12}=E_{12}+E_{ww}-(E_{1w}+E_{2w})$, where E_{12} , etc., are approach energies of the corresponding particles in vacuum. The values ΔE for interactions in *implicitly* considered water can be obtained from the crystal dissociation in water in the same way as the in-vacuum energies E are usually obtained from the crystal sublimation (Pereyaslavets and Finkelstein, 2012).

C^α atoms of the sequence-neighboring amino acids are rather far apart in space owing to the rigid *trans*-form of the $C' \equiv N$ bond. This provides an opportunity for these neighboring residues to change their conformations almost independently of each other. But inside a residue, rotations over ϕ and ψ angles are interconnected. The “allowed” and “disallowed” conformations of a residue plotted in the (ϕ, ψ) coordinates are called *Ramachandran plots* ([Ramachandran and Sasisekharan, 1968](#)) or, to be more exact, Sasisekharan-Ramakrishnan-Ramachandran plots.

Prior to drawing these maps, let us see what conformations are allowed (and what are not) in the case of ϕ (about $N-C^\alpha$) and ψ (about $C^\alpha-C'$) rotations separately.

As we already know, rotation around these bonds (between the sp^3 -hybridized C^α atom and sp^2 -hybridized N or C') is nearly free. However, in *cis*-conformations (at $\phi=0$ degree or $\psi=0$ degree), atoms rotating around these bonds (C'_{i-1} and C'_i for ϕ_i , and N_i and N_{i-1} for ψ_i ; see [Fig. 3.2](#); $i-1, i, i+1$ are numbers of consecutive residues in the chain) come close to each other, and, because of their repulsion, this conformation may be disallowed, or in other words, sterically prohibited.



The above scheme shows that minimum distances between the atoms C'_{i-1} and C'_i (ϕ_i angle) and between N_i and N_{i-1} (ψ_i angle) are the same, 2.9 Å.

The 2.9 Å is a bit *less* than $r_{\min}=3.0$ Å (see [Table 3.1](#)) for the C···C interaction (so the *cis*-conformation over ϕ_i is disallowed) and a bit *more* than $r_{\min}=2.7$ Å (but less than the optimal $r_0=3.1$ Å) for the N···N interaction (so the *cis*-conformation over ψ_i is not prohibited, though strained; however, as it can be shown, even the minor ($\approx \pm 5$ degree) flexibility of the covalent angle N-C $^\alpha$ -C' is sufficient to relieve the strain considerably). If we only had to consider these C'···C' and N···N interactions, Ramachandran plots of the prohibited, strained, and allowed conformations would look as shown in [Fig. 3.2](#).

Inner voice: You speak about “prohibited,” “strained,” and “allowed” conformations. OK, but what does this mean in the energy terms? And how can we understand whether this or that energy effect is significant for a protein or not?

Lecturer: When speaking of significance of energy effects in general, it is useful to remember the following. For an *individual* element (eg, for the above shown turn about a covalent bond or for an amino acid residue),

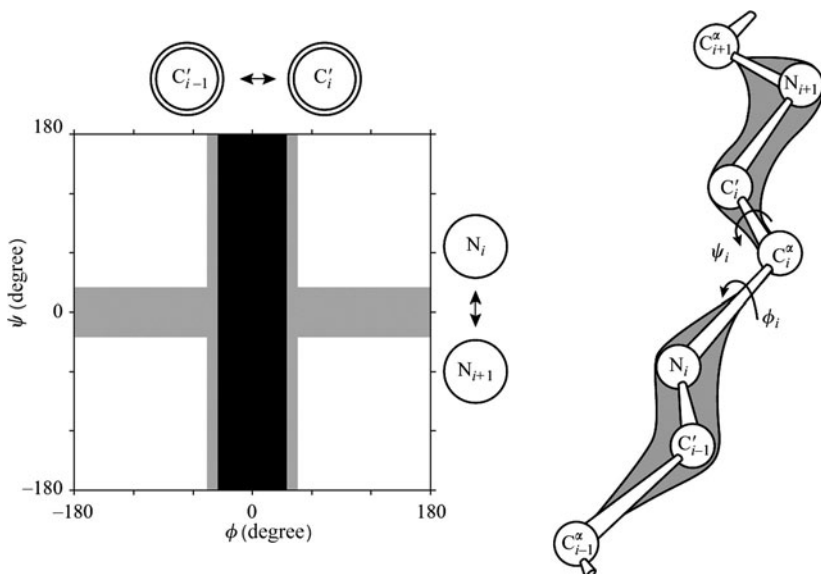


FIG. 3.2 This is how Ramachandran plots of the disallowed ■, somewhat strained □, and fully allowed □(ϕ, ψ) conformations of the fragment $C''C'N-C^\alpha-C'NC^\alpha$ would look, provided all these atoms had no other atoms attached (right) and atoms of residues $i-1$ and $i+1$ had no interactions between themselves.

the impact of energy below “heat quantum” kT is hardly significant: it is “washed out” by thermal fluctuations. Thus, $kT \approx 0.6$ kcal/mol (at room temperature) is the first threshold worth remembering.

When speaking of significance of the *individual* energy effects for proteins, it is useful also to know that a characteristic structural “reserve of stability” (the difference between free energies of the native and denatured form of a protein) is about 5–10 kcal/mol (as we will see later on). The protein can be “exploded” by an energy “defect” that exceeds 5–10 kcal/mol. Therefore, such “defects” are strongly prohibited, as we will see when discussing statistics of protein structures.

Inner voice: This reminds me of the saying “what’s good for General Motors is good for America”... Do you mean that one can say “what’s good for a protein’s detail is good for the whole protein, and what’s bad for a protein’s detail is bad for the whole protein”?

Lecturer: Exactly. A stable protein structure must be mostly built from stable elements! The impact of element’s energy on statistics of its occurrence in observed protein structures requires a careful analysis which will be done later on. Now, very roughly, I can say the following to conclude this discussion:

“fully allowed” are conformations whose energy exceeds the minimal one by less than one kT ;

- “strained” conformations are those whose energy exceeds the minimal one by about $kT \approx 0.6$ kcal/mol or a little more;
- “prohibited” conformations are those whose energy exceeds the minimal one by several kT (or kcal/mol); and
- “strongly prohibited” conformations are those whose energy exceeds the minimal one by many kcal/mol.

Turning back to the Ramachandran plots, we can state that with only $C' \cdots C'$ and $N \cdots N$ interactions considered, the ϕ, ψ regions for the prohibited, strained, and allowed conformations would look as shown in Fig. 3.2.

Fig. 3.2 shows that, in this case, the ϕ, ψ rotations would be completely independent of each other.

However, the C' atoms have, in addition, O atoms attached, and the N atoms are, in addition, bonded to H atoms (and in water this H atom is quite rigidly linked by a hydrogen bond to a water molecule, as we will soon see). As a result, the Ramachandran map, that is, plots of disallowed and allowed conformations of the smallest amino acid residue, glycine (with H as its side chain), looks as presented in Fig. 3.3.

Glycine has no massive side chain. All other amino acid residues do have such a chain, and its collision (or, rather, the collision of its C^β atom closest to the main

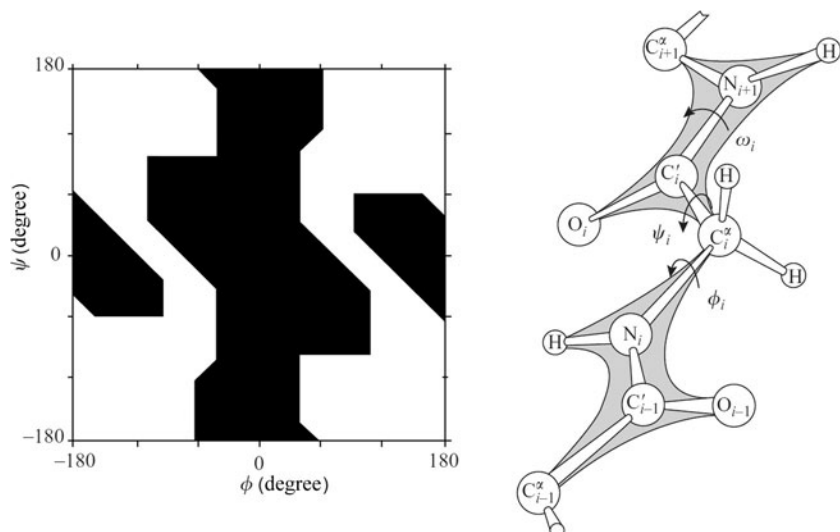


FIG. 3.3 The map of disallowed ■ and allowed □ ϕ, ψ conformations of glycine (Gly) in the protein chain. Angle $\omega = 180$ degree. The contour of allowed regions here, as well as in subsequent figures, is taken from (Finkelstein and Ptitsyn, 1977), where (unlike in Ramachandran and Sasisekharan, 1968) two additional physical factors are taken into account: (i) flexibility of covalent angles (the flexibility of $N-C^\alpha-C'$ is especially important) and that of the angle ω and (ii) hydrogen bonding of NH groups to waters (where the lines $N-H \cdots O_{\text{water}}$ are virtually straight). The contours were drawn using r_{\min} values listed in Table 3.1.

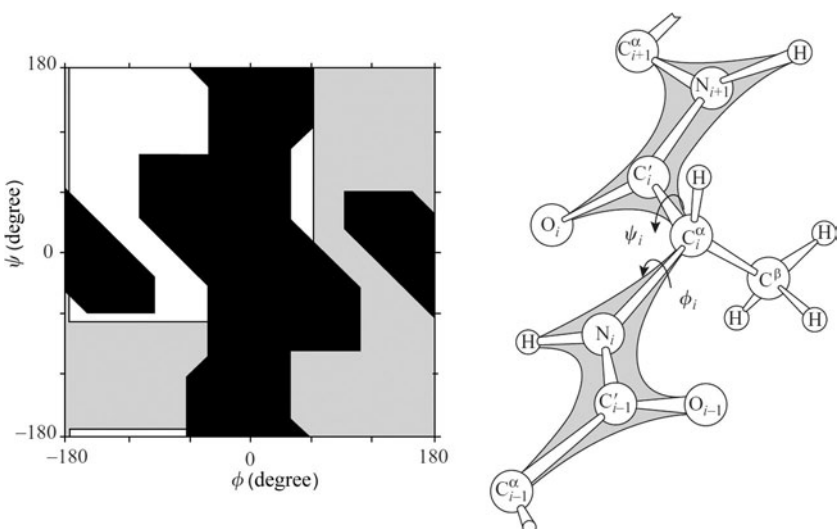


FIG. 3.4 The map of allowed $\square \phi, \psi$ conformations of alanine (Ala) in the protein chain; ■, regions allowed for Gly only; ▨, regions disallowed by main-chain interactions for all residues.

chain) with the C'_{i-1} -atom accounts for the disallowed ϕ region, while its collision with the N_{i+1} atom accounts for the disallowed ψ region (Fig. 3.4).

The map shown in Fig. 3.4 is for alanine that has a small side chain comprising the $C^\beta H_3$ group only. The side chains of all other amino acid residues are larger; they include one or two heavy γ atoms attached to the C^β atom. Since these “new” γ atoms (and the still more remote δ , ϵ , etc.) are far from the main chain, their effect on the Ramachandran map is only minor.

More precisely, in a small region (left white in Fig. 3.5), γ atoms have no collisions at all with the main chain, whereas in other conformations allowed for alanine there are such collisions for side chains with larger (C or S, but also O) γ atoms. These collisions between γ atoms and the main chain are most significant for valine, isoleucine, as well as threonine, which have two large γ atoms each. Therefore, these three residues must be somewhat strained (Leach et al., 1966) outside the white circle shown in Fig. 3.5.

Next, let us consider the Ramachandran plot for the imino acid proline, where the ϕ angle is nearly fixed at -70 degree with a ring built up by the Pro side group linked to the N-atom of its main chain, while rotation over ψ is similar to that of alanine. As a result, the allowed conformations of proline are accommodated by the white band in the Ala’s Ramachandran plot, Fig. 3.6.

The N atom-bound Pro ring also diminishes the region of allowed conformations of the residue preceding proline in the polypeptide chain (Fig. 3.7).

Finally, let us see whether all these theoretical considerations agree with the observed (by X-ray crystallography and NMR spectroscopy) conformations of amino acid residues in proteins. In Fig. 3.8, these observed conformations are

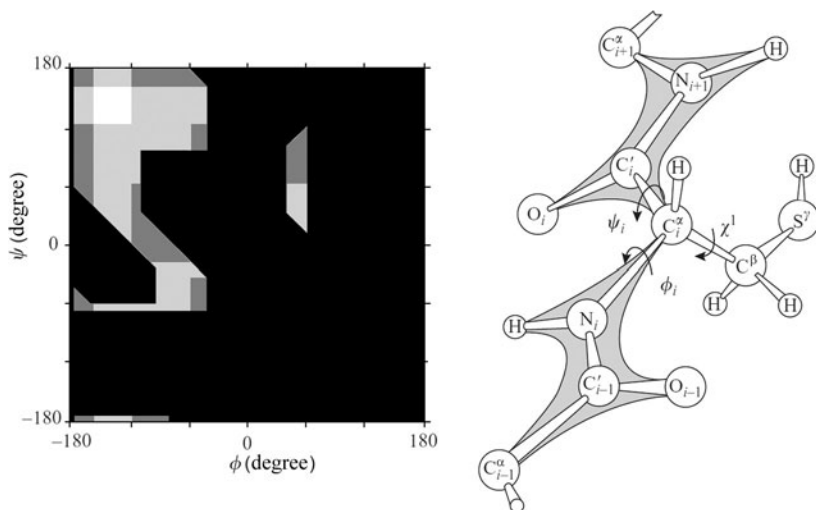


FIG. 3.5 The map of disallowed (■) and allowed (□, ▨, ■) ϕ , ψ conformations of larger residues in the protein chain. □, the region where all three χ^1 -rotamers of the side chain C^γ (or S^γ) atom are allowed; ▨, the region where two χ^1 -rotamers of the C^γ atom are allowed and one is disallowed; ■, the region where only one χ^1 -rotamer of the C^β atom is allowed and two others are disallowed. (Adapted from Finkelstein, A.V., Ptitsyn, O.B., 1977. Theory of protein molecule self-organization. I. Thermodynamic parameters of local secondary structures in the unfolded protein chains. Biopolymers 16, 469–495.)

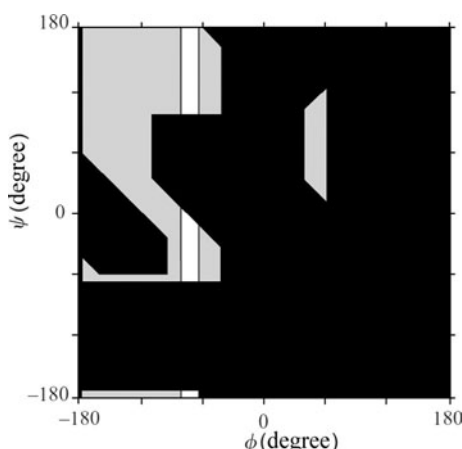


FIG. 3.6 The map of allowed □ Pro conformations plotted against allowed Ala conformations ■; ■, the region of disallowed conformations for both residues.

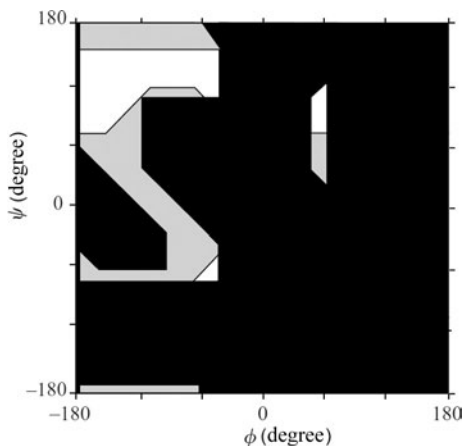


FIG. 3.7 The region of allowed \square conformations of an Ala residue that precedes Pro in the protein chain. If not the following Pro, ■ would also be included in the region of allowed Ala's conformations.

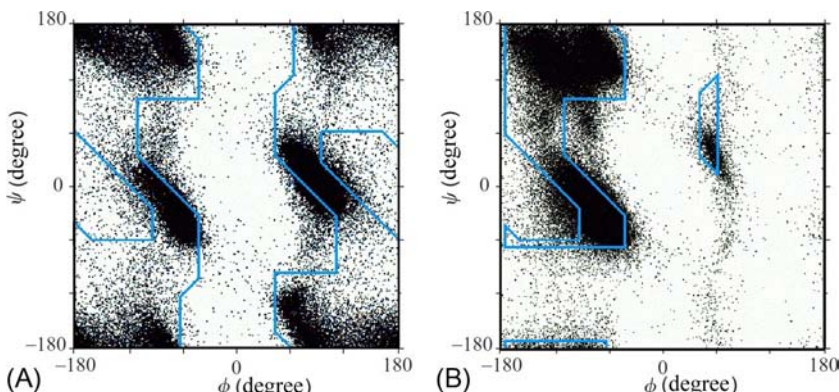


FIG. 3.8 Observed conformations (dots) of glycine (A) and of other amino acid residues (B) in nonhomological proteins taken from the Protein Data Bank (Berman et al., 2012). The sterically allowed regions are contoured.

plotted against the contours of regions theoretically allowed for glycine, on the one hand, and for alanine and all other residues, on the other hand. As seen, the agreement is quite good. We see that the “sterically allowed” regions accommodate the majority of the experimental points. Some parts of these regions are more populated than others. Later on, we will see that these parts are related to secondary structures. We also see that some points are in the “sterically prohibited” regions. This is not surprising, since the regions that we call “sterically prohibited” are those of high energy—not infinitely high, for sure, as that would

cause complete prohibition—but higher than the minimum conformational energy by, say, a couple of kilocalories per mole. In other words, a protein has to spend some energy to drive its residue into such a region. We see that it is able to do so, although it rarely does.

In the course of these lectures, we will learn the general rule: strained, high-energy elements are rare, though sometimes observed. This is not surprising since a stable protein must contain—mostly, but not exclusively—stable components.

REFERENCES

- Axilrod, B.M., Teller, E., 1943. Interaction of the van der Waals' type between three atoms. *J. Chem. Phys.* 11, 299–300.
- Berman, H.M., Kleywegt, G.J., Nakamura, H., Markley, J.L., 2012. The Protein Data Bank at 40: Reflecting on the past to prepare for the future. *Structure* 20, 391–396. <http://www.wwpdb.org/>.
- Dill, K.A., Bromberg, S., 2010. *Molecular Driving Forces: Statistical Thermodynamics in Biology, Chemistry, Physics, and Nanoscience*, second ed. Garland Science, New York (Chapter 24).
- Finkelstein, A.V., 2007. Average and extreme multi-atom van der Waals interactions: Strong coupling of multi-atom van der Waals interactions with covalent bonding. *Chem. Central J.* 1, 21.
- Finkelstein, A.V., Ptitsyn, O.B., 1977. Theory of protein molecule self-organization. I. Thermodynamic parameters of local secondary structures in the unfolded protein chains. *Biopolymers* 16, 469–495.
- Halgren, T.A., 1995. Merck molecular force field. I. Basis, form, parameterization and performance of MMFF94. *J. Comput. Chem.* 17, 490–519.
- Jorgensen, W.L., Maxwell, D.S., Tirado-Rives, J., 1996. Development and testing of the OPLS all-atom force field on conformational energetics and properties of organic liquids. *J. Am. Chem. Soc.* 118, 11225–11236.
- Landau, L.D., Lifshitz, E.M., 1977. *Quantum Mechanics. A Course of Theoretical Physics*, vol. 3 Pergamon Press, Oxford, New York (Sections 62, 89).
- Leach, S.J., Némethy, G., Scheraga, H.A., 1966. Computation of the sterically allowed conformations of peptides. *Biopolymers* 4, 369–407.
- Levitt, M., Hirshberg, M., Sharon, R., Daggett, V., 1995. Potential energy function and parameters for simulations of the molecular dynamics of proteins and nucleic acids in solution. *Comput. Phys. Commun.* 91, 215–231.
- London, F., 1937. The general theory of molecular forces. *Trans. Faraday Soc.* 33, 8–26.
- Pereyaslavets, L.B., Finkelstein, A.V., 2012. Development and testing of PFFsol_1, a new polarizable atomic force field for calculation of molecular interactions in implicit water environment. *J. Phys. Chem B* 116, 4646–4654.
- Ramachandran, G.N., Sasisekharan, V., 1968. Conformation of polypeptides and proteins. *Adv. Protein Chem.* 23, 283–438.
- Scott, R.A., Scheraga, H.A., 1966. Conformational analysis of macromolecules. III. Helical structures of poly-glycine and poly-L-alanine. *J. Chem. Phys.* 45, 2091–2101.
- Wang, J., Wolf, R.M., Caldwell, J.W., Kollman, P.A., Case, D., 2004. Development and testing of a general amber force field. *J. Comput. Chem.* 25, 1157–1174.

Lecture 4

So far we have not taken the aqueous environment of proteins into account. It's high time we bridged the gap.

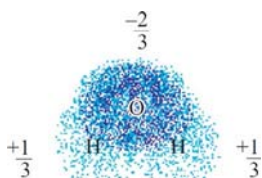
Water is a peculiar solvent. First, it boils and freezes at abnormally high temperatures compared with those typical for substances of similarly low molecular weight. Indeed, water (H_2O) boils at 373 K and freezes at 273 K, while O_2 boils at 90 K and freezes at 54 K; H_2 boils at as low a temperature as 20 K and freezes at 4 K; CH_4 boils at 114 K, etc. The fact that ice and water structures are heat-resistant suggests some strong bonding among water molecules.

The bond responsible for this effect is specifically that between O- and H-atoms of H_2O . This bond is called a *hydrogen bond*.

Hydrogen bonds are not only observed in water. They invariably occur when a hydrogen atom approaches some electronegative (ie, electron attracting) atom while being chemically bonded to another electronegative atom, as exemplified by the $\text{O}-\text{H}:\text{:O}$, $\text{N}-\text{H}:\text{:N}$ bonds. But, for instance, a C-H group is not involved in perceptible hydrogen bonding since the electronegativity of the C atom is insufficient.

The solvent properties of water are dominated by strong hydrogen bonds (Sokolov, 1955; Pauling, 1970). The hydrogen bonding between water molecules is nearly completely electrostatic in nature. It is connected with electrons and charges, but not with the nuclei of the hydrogen atoms (unlike $\text{F}-\text{H}:\text{:F}$ bonds involving atoms F that are much more electronegative than O (see Sokolov, 1955); as is shown by the close similarity of boiling and melting parameters of light (H_2O) and heavy (D_2O) waters in spite of a twofold difference in mass between D and H nuclei.

The water molecule is polar. This implies small ("partial") charges on its atoms: negative on O and positive on H. The distribution of charges and electron clouds at these atoms appears as follows:



Here, the density of dots reflects the density of the electron cloud, and numerals indicate the partial charges on the atoms. These are expressed in fractions of the proton charge which, naturally, in these units amounts to +1 while the electron charge is -1.

An electronegative oxygen draws the electron clouds off the neighboring hydrogens, thereby causing polarization of atoms. As a result, H atoms acquire partial positive charges, while there is a negative charge on O in the water molecule.

As you will remember, in a vacuum, the energy of interaction of charges q_1 and q_2 at distance r is

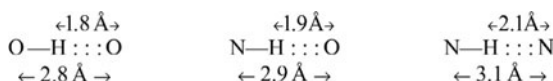
$$U = \frac{q_1 q_2}{r} \quad (4.1)$$

In a vacuum, interactions between charges are very strong. The energy of interaction of two single charges (ie, proton or electron charges) at a distance of 1 Å is nearly 330 kcal mol⁻¹ (keep this figure in mind: we will use it for different estimates later), while at a more realistic distance of 3 Å (with van der Waals repulsion of atoms taken into account) this energy is about 110 kcal mol⁻¹. The energy of single-charge interaction is the typical energy of a chemical bond; it is hundreds of times higher than the typical thermal energy kT or the typical energy of van der Waals interactions between atoms.

The partial charges of water molecules are still lower than unity, and therefore, their interaction is weaker: at a distance of 3 Å its energy is about 10 kcal mol⁻¹; however, this energy is sufficient to distort the electron envelopes of H-atoms by H to O attraction. Hydrogen atoms are most sensitive in this respect: their single-electron envelope is drawn towards O and therefore undergoes the distortion most easily. It takes much more energy to distort, say, the electron envelope of oxygen that has eight “own” electrons and a share of the single electron of both hydrogens of the water molecule.

It is the ease of distortion of the electron cloud of a hydrogen atom that turns a normal electrostatic interaction into a hydrogen bond. This is true for all hydrogen bonds, among which those of interest to us are: O—H:::O, N—H:::O, N—H:::N.

Thus, a hydrogen atom has the thinnest cloud, whose significant distortion results from attraction between the partial positive charge of hydrogen and the partial negative charge of oxygen (or nitrogen). This gives distances between H and O (or N) nuclei as small as 1.8–2.1 Å (reported for crystals of small molecules) instead of the 2.35–2.75 Å typical for van der Waals interactions discussed in the previous lecture. Therefore, it is accepted that the van der Waals radius of H in the O—H or N—H group is about 30% less than that of H in the C—H group (Levitt et al., 1995).

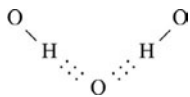


This close approach yields a *hydrogen bond* (or *H-bond*). The H atom (to be more exact, the O—H or N—H group) is called the *donor* of the hydrogen bond,

and the O or N atom towards which the hydrogen moves, is called the *acceptor* of the hydrogen bond.

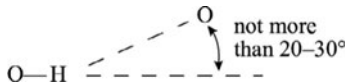
Note that in crystals, H-bonding occurs when the distance between O- and/or N-atoms of the donor and acceptor is about 3 Å (eg, in ice it is 2.8 Å). This is similar to the optimal van der Waals distance between O and/or N atoms, ie, the presence of the mediating H atom does not increase the distance between these atoms of the donor and acceptor, as it pushes them, not apart, but together.

Each H-bond has one donor and one acceptor. The hydrogen atom almost always acts as a donor of only one H-bond, while the oxygen atom may participate as an acceptor in two H-bonds simultaneously, thereby causing “fork-like” H-bonding:



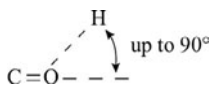
Since the “fork-like” H-bonding implies a short distance between two H atoms (with +1/3 charge on each), its total energy is less than double the energy of a single H-bond.

Unlike van der Waals interactions, H-bonding is rather orientation-sensitive, especially as concerns the orientation of the donor group ([Ramakrishnan and Prasad, 1971](#); [Finkel'shtein, 1976](#)). Usually, a valence bond of the donor is directed at the acceptor atom (O or N) to be involved in the hydrogen bond:



It seems that this effect is due to repulsion between O atoms and a very small radius of H atom, when H is in the O–H (or N–H) group.

Orientation of the acceptor group is of considerably less importance for the H-bond:



The H-bond energy is about 5 kcal mol⁻¹. This estimate results from comparison of experimental evaporation heats of similar compounds, some of which are capable of H-bonding, while others are not. For example, the evaporation heat of dimethyl ether, H₃C–O–CH₃, is about 5 kcal mol⁻¹, and that of ethanol, CH₃–CH₂–OH, is about 10 kcal mol⁻¹. These compounds consist of the same

atoms (ie, their van der Waals interactions are nearly the same), but ethanol is capable of H-bonding, while dimethyl ether is not (as it lacks the O–H group). Each O–H group can participate as donor in only one H-bond, and its O atom can accept this bond. Since each H-bond is supposed to have one donor and one acceptor, there is only one H-bond per ethanol molecule, that is, an H-bond “costs” about 10 kcal mol^{-1} (*ethanol*) – 5 kcal mol^{-1} (*ether*) = 5 kcal mol^{-1} .

The same estimate follows from the value of ice evaporation heat ($680 \text{ cal g}^{-1} = 680 \text{ cal (1/18 mol)}^{-1} = 12 \text{ kcal mol}^{-1}$). Here, a couple of kilocalories per mole are the share of van der Waals interactions, as seen from the evaporation heat of small molecules such methane (CH_4) or O_2 . The remaining 10 kcal mol^{-1} are for H-bonding. In ice, there are two H-bonds (Fig. 4.1) per molecule of H_2O , since its two O–H groups can serve as donors for two H-bonds (and as many can be accepted by its oxygen). Again, the “cost” of one H-bond appears to be about $(10 \text{ kcal mol}^{-1})/2 = 5 \text{ kcal mol}^{-1}$.

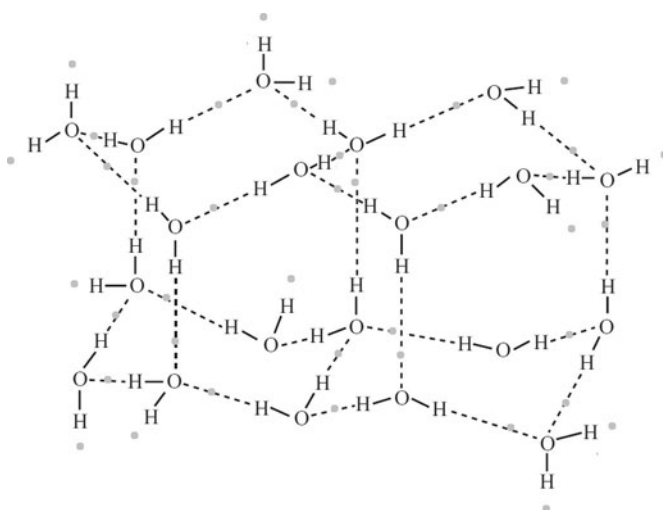


FIG. 4.1 Normal ice (“ice I_h ”; there are also other forms of ice, but they can be stable at very high pressure only). The *continuous lines* show covalent bonding, the *dashed lines* show H-bonding. As seen, the openwork structure of ice has small cavities surrounded by H_2O molecules. The drawing is adapted from Creighton, T.E., 1993. Proteins: Structures and Molecular Properties, second ed. W. H. Freeman & Co., New York (Chapter 4), with minor modifications. In this drawing, each H atom is unambiguously bound to one O atom. However, as shown by X-ray analysis (Madura, 1994), each H atom can occupy *two* positions with an equal probability of 50%: *either* close to an O atom with which it is covalently bound (as shown in the picture), *or* close to an O atom with which it forms an H-bond (the latter, alternative position of H atom, is shown by a small gray spot in the picture). Transition of an H atom from one O atom to another is relatively easy. In ice, this transition is connected with rearrangement of all covalent and H-bonds of these two O atoms and of all their neighbors. As a result, the entire network of covalent and H-bonds in the ice can fluctuate greatly, which leads to its abnormally high polarizability: its permittivity is 97 at 0°C , exceeding that of liquid water (88 at 0°C) (Lide, 2005).

The structure of normal ice is determined by H-bonds (Fig. 4.1): it is good for their geometry ($\text{O}-\text{H}$ is directed at O), although not so good for close van der Waals contacts between water molecules. In ice, water molecules envelop tiny (smaller than H_2O molecules) pores, thereby giving it an openwork structure. This results in two well-known phenomena: (1) ice is not as dense as water, it floats, and (2) under strong pressure (eg, caused by skate blades), ice melts. It is also the case that the abnormally high permittivity of ice is indicative of easy rearrangement of the H-bonds (and covalent bonds!) in it; this is illustrated by Fig. 4.1.

Inner voice: I can readily accept easy rearrangement of H-bonds. But “easy rearrangement of covalent bonds” sounds strange indeed ... Normally, covalent bonds are stable in the absence of a catalyst!

Lecturer: Easy rearrangement of bonds formed by hydrogens with electronegative atoms must not surprise you, because, from chemistry, you must be already familiar with easy transfer of H atoms from acids to water in the absence of any catalyst (except environment which consists of electronegative atoms and hydrogens bonded to them) ... Such an easy rearrangement of the covalent bonds relates also to coordinate bonds of electronegative atoms with certain metal ions, which we will consider soon.

The majority of H-bonds existing in ice (Fig. 4.1) persist in liquid water. This follows from the low melting heat of ice (80 cal g^{-1}) as compared with water boiling heat (600 cal g^{-1} at 0°C and 540 cal g^{-1} at 100°C). We might think that only as many as $80/(600+80)=12\%$ of all H-bonds existing in ice, break down in liquid water. However, this picture—with some H-bonds broken while others persist—is not quite true: rather, in liquid water all H-bonds exist but become slightly loose.

This is well illustrated by the experimental results shown in Fig. 4.2.

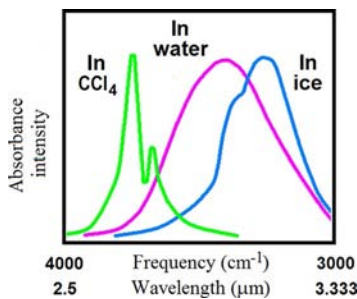


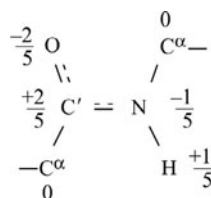
FIG. 4.2 Typical IR (infrared) absorption spectra for O-H groups in ice, CCl_4 solution and in liquid water. (Adapted from Greinacher, E., Lüttke, W., Mecke, R., 1955. Infrarotspektroskopische Untersuchungen an Wasser, gelöst in organischen Lösungsmitteln. Z. Electrochem. 59, 23–31; Zolotarev, V.M., 1970. Optical constants of ice I in a broad infrared spectrum. Opt. Spectrosc. (in Russian). 29, 1125–1128.)

Here, Curve “in ice” shows the maximum of the infrared (IR) absorption spectrum for O–H groups in ice (where all H-bonds are saturated); Curve “in CCl₄” illustrates this maximum for the O–H-groups of separate water molecules dissolved in CCl₄ (where no H-bonding occurs because of the extreme dilution); and Curve “in water” shows the absorption spectrum for liquid water. Suppose liquid water contained two types of O–H groups: those participating and those not participating in H-bonds. Then the former would vibrate with frequencies typical for ice (where they have been involved into H-bonding), while the latter would vibrate like those in water molecules dissolved in CCl₄ (where no H-bonding has occurred). Then the IR absorption spectrum for liquid water would be double-peaked to reflect the two types of O–H groups and their two typical frequencies, since the vibrational frequency of a group is equal to its light absorption frequency. However, no such “double-peaked” picture is actually observed. Instead, Curve “in water” presents one broad peak that goes from the peak on Curve “in ice” to that of Curve “in CCl₄. This means that in liquid water, all O–H groups are involved in H-bonding and all resulting H-bonds are loose but in different ways.

Strictly speaking then, the model with some H-bonds persisting in liquid water and others broken is incorrect. However, people often use it, owing to its simplicity and convenience in describing the thermodynamic properties of water—and we may use it as well, although its drawbacks must be kept in mind.

Now let us concentrate on interactions between the protein chain and water molecules.

As with water molecules, the backbone of a protein chain is polar. To be more exact, it is its peptide groups that are polar. The net charge of the protein chain backbone is 0, and the distribution of charges on its atoms (again, the charge on each atom is expressed in fractions of the proton charge) is as follows:

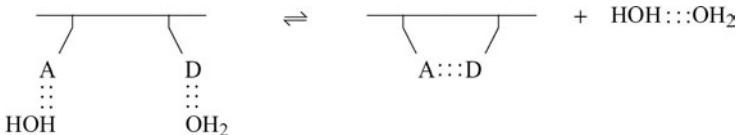


Partial charges are acquired by some side-groups too, eg, by that of Ser (its side-group, -CH₂-OH, is similar to ethanol). Charged amino acid residues are even more polarized: a charge of -1 is typical for the acidic side-groups of Asp and Glu when they are ionized (at about neutral pH), while +1 is characteristic of the ionized basic side-groups of Arg, Lys, and His.

Both main-chain peptide groups and polar side-groups participate as donors and acceptors in hydrogen bonds. They can be—and mostly are—involved in H-bonds formed among themselves or to water molecules: since the H-bond

energy (5 kcal mol^{-1}) is about an order of magnitude higher than that of thermal movement, H-bonds are mostly preserved by these movements.

When an H-bond between donor (D) and acceptor (A) is formed within a protein molecule in the aqueous environment, it replaces two hydrogen bonds between the protein and water molecules (that existed earlier, since an H-bond is too expensive to be neglected), and an additional bond between the two freed water molecules is formed (for the same reason):



The energy balance of this reaction is close to 0: two bonds yield two bonds. However, the *entropy* of the water molecules increases since they are no longer bonded to the protein chain but only mutually H-bonded and free to go anywhere (and the entropy results just from the freedom of movement). This entropy increase caused by the water dimer release is approximately equal to an entropy increase resulting from the molecule H₂O transition from ice to liquid water (in both cases one particle becomes free in its movements).

The entropy difference resulting from one molecule H₂O transition from ice to liquid water can be estimated as follows. At the melting-point (for ice, at 0°C, ie, 273 K), the increase in entropy caused by melting is known to fully compensate for the corresponding decrease in energy. And we know the value of this decrease—it is $80 \text{ cal g}^{-1} \times 18 \text{ g mol}^{-1} = 1440 \text{ cal mol}^{-1}$ (18 g mol^{-1} is the molecular weight of H₂O).

Thus, owing to this increase of water entropy, the free energy of the “protein in water” system decreases by about $1.5 \text{ kcal mol}^{-1}$ of emerging intra-protein hydrogen bonds D:::A.

This free energy released by waters may fully or partially compensate the free energy increase that results from decreasing conformational entropy of the chain during the D:::A bonding. As we will see later, a decrease in free energy of the water molecules nearly compensates for the entropy of fixation of the amino acid residue conformation required for H-bonding (N—H:::O) in secondary structures of the polypeptide chains (as a result, in water, the regular secondary structure of polypeptides is just at the edge of stability).

These awful words “entropy” and “free energy” have been articulated ... My experience shows that a biologist has normally knows about entropy (that it is a measure of the multitude of possible states, a measure of disorder) but is uncertain about what free energy is ... As we often appeal to the concept of free energy (which is a measure of stability), I would like to devote a few minutes to it just now, and later, when the need arises, to discuss it (and entropy too) in more detail.

Let us start with a simple example: suppose a molecule can have two states, “a” and “b”; “a,” when it is here, in this room, 200 m above sea level; “b,” when it is in the Dalai Lama’s monastery, in The Himalayas, 5 km above sea level. What is the relationship of the probabilities of these two states provided that (1) temperature T is the same in both places, and (2) we watch the molecule long enough for it to visit both places?

As stated by the well-remembered Boltzmann formula:

$$\text{Probability of being in the state of energy } E \propto \exp\left(\frac{-E}{kT}\right) \quad (4.2)$$

Physically, the sense of this formula is that the heat of the medium (ie, collisions with other molecules) excites our molecule to a certain extent (proportional to the medium temperature T , on average) and thereby enables it to enter the region of more or less high energies. (All this will be discussed later in more detail but at the moment, I am taking the liberty of believing that you remember this formula.) Still let me remind you that k is Boltzmann’s constant, and T is the absolute temperature in Kelvin (K) (counted from the “absolute zero,” so $OK = -273.15^\circ C$, and “ \propto ” means “is proportional to”).

However, it is better to deduce the Boltzmann formula and not rely on your memory! We will deduce it for at least the case that is of interest to us here, that is, for distribution of gas molecules over height, when their energy is described as $E(h) = mgh$, where m is mass of a gas molecule, g is acceleration of gravity, and h is height.

As stated by Clapeyron-Mendeleev law, the pressure of an ideal gas $P = nkT$, where n is the number of gas molecules per unit volume. If T remains unchanged at any h , then $dP/dh = (dn/dh)kT$. On the other hand, when considering a gas column of unit cross-section, we see that $dP = (mgn)(-dh)$, since the weight of the gas pressing down on the unit cross-section decreases by $(mgn)dh$ when the height grows by dh . Therefore, $dP/dh = (dn/dh)kT = -mgn$. Hence, $dn/dh = -(mg/kT)n$, or $d[\ln(n)]/dh = -mg/kT$, that is, $n \propto \exp(-mgh/kT) = \exp(-E(h)/kT)$.

Thus, as applied to the problem in question (What is the relationship of probabilities for a molecule to be at different heights?), the Boltzmann formula reduces to the barometrical relationship

$$\begin{aligned} & [\text{Probability of being at a height “b”}] \text{ relates to } [\text{Probability of} \\ & \text{being at a height “a”}] - \text{as } \exp\left(\frac{-E_b}{kT}\right) \text{ relates to } \exp\left(\frac{-E_a}{kT}\right) \quad (4.3) \end{aligned}$$

where E_a , energy of the molecule in the state “a” (ie, “here”); E_b , in the state “b” (“at a height of 5 km”); T , absolute temperature (for simplicity, as mentioned above, is assumed to be invariable with height).

Because of gravity, “here” the energy of the molecule is lower than “at a height of 5 km”; so, according to Boltzmann, the molecule will stay “at a height of 5 km” for a shorter time than “here” (the time will be 1.5–2 times shorter).

Make the calculations yourselves by taking $T = 300 \text{ K}$ and recalling that $E = mgh$, where $m = \text{average mass of an air molecule} (\approx 30 \text{ Da} = 30 \text{ g mol}^{-1})$, $g \approx 10 \text{ m s}^{-2}$ (gravitational acceleration), $h \approx 5 \text{ km}$ (height difference) and Boltzmann's constant $k = 1.38 \times 10^{-23} \text{ J degree}^{-1} \text{ particle}^{-1} = 0.33 \times 10^{-23} \text{ cal degree}^{-1} \text{ particle}^{-1}$ (since $J = \text{kg m}^2 \text{ s}^{-2} = 0.24 \text{ cal}$, ie, $\approx 2 \text{ cal degree}^{-1} \text{ mol}^{-1}$ (since $1 \text{ mol} = 6 \times 10^{23} \text{ particles}$). As you may remember, $R = 2 \text{ cal K}^{-1} \text{ mol}^{-1}$ is the "gas constant."

In other words, at a height of 5 km the molecules will be about two times less numerous than here. Or rather, this will be the case for *equal volumes*, for example, your lungs (as you may easily ascertain by breathing at different heights). However, *in total*, the molecules in the Dalai Lama's monastery are much more numerous than they are here just because the monastery is much larger than our room. That is, over there, the molecule may have more positions, since for a freely flying molecule the number of positions is proportional to the room volume. In this case, physicists would say that in the monastery the number of *microstates* of the molecule is far greater than in our room. So, the probability that our molecule is *somewhere* in the Dalai Lama's monastery relates to the probability that it is *somewhere* in this room as

$$\begin{aligned} & [\text{Probability of being somewhere in volume "b"}] \\ & : [\text{Probability of being somewhere in volume "a"}] = \left[V_b \exp\left(\frac{-E_b}{kT}\right) \right] \\ & : \left[V_a \exp\left(\frac{-E_a}{kT}\right) \right] \end{aligned} \tag{4.4}$$

where V_a is the volume of "a" ("our room") and V_b is the volume of "b" ("his monastery"). From elementary college maths you will remember that V can be presented as $\exp(\ln V)$, so the above formula can be written as

$$\begin{aligned} & [\text{Probability of being somewhere in volume "b"}] \\ & : [\text{Probability of being somewhere in volume "a"}] \\ & = \left[\exp\left(\frac{-E_b}{kT} + \ln V_b\right) \right] : \left[\exp\left(\frac{-E_a}{kT} + \ln V_a\right) \right] \\ & = \left[\exp\left(\frac{-(E_b - T \times k \ln V_b)}{kT}\right) \right] : \left[\exp\left(\frac{-(E_a - T \times k \ln V_a)}{kT}\right) \right] \end{aligned} \tag{4.5}$$

The last expression looks very much like Eq. (4.3), the Boltzmann equation, but it is applicable not to a volume *unit* but to the *total* volume of a system, and—note carefully—it has $E - T \times k \ln V$ instead of E .

It is the value $F = E - T \times k \ln V$ that is called *free energy* of our molecule of air in a given volume V at temperature T . And the value $S = k \ln V$ is called the *entropy* of our molecule in the volume V (which, in our case, is proportional to the "number of accessible states" of our molecule).

In the general case, entropy S is simply equal to $k \times [\logarithm of the number of accessible states]$. And free energy F relates to energy E , entropy S , and temperature T according to the general equation

$$F = E - TS \quad (4.6)$$

Of two states, the more stable (ie, more *probable*) is the one having a lower free energy:

$$\begin{aligned} & [\text{Probability of being somewhere in volume "b"}] \\ & : [\text{Probability of being somewhere in volume "a"}] \\ & = \exp\left(\frac{-F_b}{kT}\right) : \exp\left(\frac{-F_a}{kT}\right) = \exp\left[-\frac{(F_b - F_a)}{kT}\right] \end{aligned} \quad (4.7)$$

In other words, a more probable, that is, a *more* stable, state of the system is that with a lower F , and the *most* stable state of a system (at a given temperature and volume of this system) corresponds to the *minimum free energy* F .

Thus, the “free energy” is a natural generalization of the regular “energy” for the case when *the system exchanges heat* with the environment. Let me remind you that if a body is *not* excited by environmental heat, its stable state corresponds to its minimum energy (or simply, everything that can fall down—eventually falls down). When excited by environmental heat, molecules of the system start acquiring numerous states of a higher energy (ie, the entropy of this system, of its movements, increases), and as a result, air molecules fly and do not drop onto the ground.

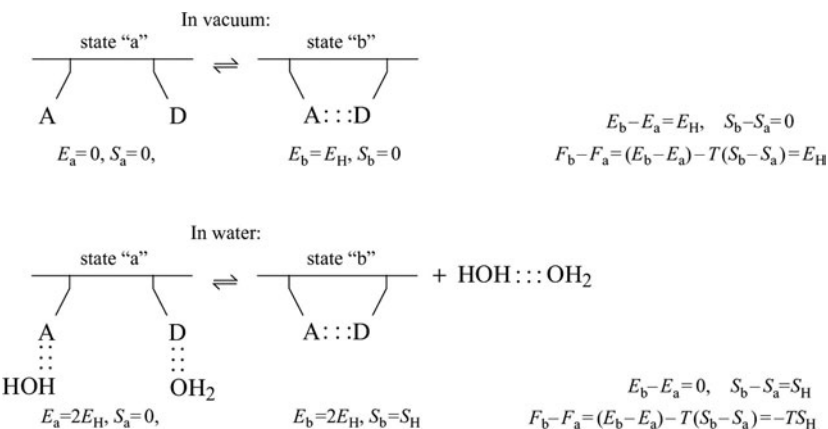
This can also be put as follows:

A change in the energy, $E_b - E_a$, is the work required to transfer a body from state “a” into state “b” when there is no heat exchange with the environment. And a change in the free energy $F_b - F_a$ is the work required to transfer a body from state “a” into state “b” *when the body keeps exchanging heat* with the environment.

Let us now descend from The Himalayas to proteins. So, what is the balance of energy, entropy and free energy in the previous example of H-bonding in the protein chain?

To visualize this, let us compare how the process goes under different conditions (see the scheme below). There, $E_H < 0$ is the H-bond energy, and $S_H > 0$ is the entropy of movements and rotation of a free body, ie, of the free dimer HOH::OH₂. The H-bonds—between water molecules or between water and protein molecules—are stable when $E_H < -TS_H < 0$ (and if $E_H > -TS_H$ the H-bonding is unstable, and what we deal with is not liquid water but water vapor).

A comparison of the diagrams given earlier shows that H-bonds within the protein chain surrounded by water display a lower stability than when in a vacuum. Indeed, in water, the H-bond free energy is $F_b - F_a = -TS_H$, ie, it is smaller in absolute value than in a vacuum, where $F_b - F_a = E_H$.



I would like to emphasize again that the reason for this decrease in the H-bond stability is that *in water* an H-bonding within the protein chain *replaces* the H-bonding between the chain and water. For the same reason, the hydrogen bonds that stabilize protein structure *in water* are entropic but not energetic in nature: the energies of the two states of the chain (with and without the intra-chain H-bond) are approximately equal, and of these two, the state with a higher entropy (with a greater number of microstates) is more stable. And a free water molecule has a greater number of microstates (ie, a greater number of positions in space) than a bound molecule.

I call your attention to the following: in the protein chain (surrounded by water molecules) hydrogen bonds are entropic and *not* energetic in nature just *because* the energy of H-bonding is extremely high! Consequently, donors and acceptors that are “free” of bonding *within the protein* are not really free of *any* bonding, as they participate in H-bonds to water molecules. The water molecules released from the protein during H-bonding inside the chain immediately bind to one another, thereby compensating for the energy, such that the free energy gain of intra-protein H-bonds occurs only because of the increasing number of possible microstates of the released water molecules. While it is true that to bond to one another, the water molecules have to sacrifice a part of their gained freedom (entropy), it is better to lose a small entropy than a large energy.

Two facts determine the behavior of water as a specific solvent: (1) water molecules are strongly H-bonded to one another; (2) this H-bonding occurs only at a certain mutual orientation of water molecules. A variety of interesting effects are thereby caused. These will be the subjects of Lectures 5 and 6.

REFERENCES

- Finkel'shtein, A.V., 1976. Stereochemical analysis of the polypeptide chains secondary structure by Courtauld space-filling models. II. Hydrogen and hydrophobic bonds. Mol. Biol. (Mosk) 10, 724–730.
- Levitt, M., Hirshberg, M., Sharon, R., Daggett, V., 1995. Potential energy function and parameters for simulations of the molecular dynamics of proteins and nucleic acids in solution. Comput. Phys. Commun. 91, 215–231.
- Lide, D.R., 2005. Section 6 “Fluid properties: permittivity”. Section 12 “Properties of solids: permittivity”. In: CRC Handbook of Chemistry and Physics on CD. CRC Press, Boca Raton, FL.
- Madura, J.D., 1994. Ice coordinates. http://www.ibib_lj.org/water/wsn_archive/msg00037.html.
- Pauling, L., 1970. General Chemistry. W.H. Freeman & Co, New York (Chapter 12).
- Ramakrishnan, C., Prasad, N., 1971. Study of hydrogen bonds in amino acids and peptides. Int. J. Pept. Protein Res. 3, 209–231.
- Sokolov, N.D., 1955. Hydrogen bond. Phys. Usp. (Adv. Phys. Sci., Moscow, in Russian) 57, 205–278.

Lecture 5

Hydrophobicity is a phenomenon that occurs only in an aqueous environment. It plays a very important role in formation and maintenance of protein structures (Bresler and Talmud, 1944; Kauzmann, 1959; Tanford, 1980; Cantor and Schimmel, 1980; Nelson and Cox, 2012).

However, before considering the hydrophobicity, in the initial part of this lecture, I would like to talk on *thermodynamics*. This will be useful for further consideration of water as a specific solvent. The focus of this consideration will be the free energy of immersing various molecules in water.

To study the free energy of immersion of a molecule in water, we take a closed tube, half of which is filled with water and the other half with vapor, and watch how introduced molecules are distributed between these phases.

As we have learned, the difference between free energies F defines a more favorable state of the system (in this case, a more favorable position of the studied molecule) according to the formula:

$$\begin{aligned} & [\text{Probability of being somewhere in "b"}] : \\ & [\text{Probability of being somewhere in "a"}] = \exp[-(F_b - F_a)/kT] \end{aligned} \quad (5.1)$$

The free energy $F = E - TS$ comprises the energy E and the entropy S . I believe you know what energy is. As to temperature, your knowledge, I think, is rather *intuitive*, so we will return to it again later. The problem of entropy is still more complex, so let us discuss it once again.

In the simplest case of a particle in the container (as we discussed in Lecture 4), $S = k \ln V$, where V is the volume accessible to the particle.

In what sense are we incorporating this entropy into the free energy in the form of $-TS$? When considering $\exp[-F/kT]$ irrespective of E , we have got $\exp[-(-TS)/kT] \exp[-(-Tk \ln V)/kT] \equiv V$, that is just the accessible volume defining the *number of accessible states* of the particle in space. The greater the entropy, the larger this number, and the higher the probability that the particle is somewhere in this volume.

In the general case (when the accessible states of the particles are limited not only by the walls surrounding the volume V but also by collisions between the particles), the entropy S is given by

$$S = k \times [\text{logarithm of the number of accessible states of the studied particle}] \quad (5.2)$$

In molecular physics, biology and chemistry not a single particle but a mole (6.022×10^{23}) of particles are usually considered (6.022×10^{23} is called the *Avogadro's number*). Then the entropy of a mole is given by

$$S = R \times [\text{logarithm of the number of accessible states of one particle}] \quad (5.3)$$

where $R = k \times (6.022 \times 10^{23} \text{ mol}^{-1})$. The only difference between k and R is that k refers to a single particle and R to a mole of particles.

Remark: In classical physics we have no “number of accessible states”; we only have “accessible volume of coordinates q and impulses p ”. However, this volume can be transferred into number of quantum states using the Heisenberg Uncertainty Principle ($\Delta q \Delta p \sim \hbar$, where Δq , Δp are the uncertainties in q and p , while \hbar , the Planck’s constant, is the elementary volume of the coordinate-impulse space) [Landau and Lifshitz, 1977, 1980].

Strictly speaking, the value:

$$F = E - TS \quad (5.4)$$

is known as the Helmholtz free energy. It is easy to describe and convenient to calculate this value, since it refers to a system that (like the molecule we have just discussed) is enclosed in some fixed volume.

However, a normal experiment deals not with a fixed volume V but with a constant pressure P (eg, atmospheric pressure). In this case, as you may remember, we measure not a change in the energy E of the studied body but a change in its *enthalpy* $H = E + PV$. The change in enthalpy H includes, apart from the change in energy (E), the work against the external pressure P in changing the body volume V .

The value of PV will be negligible for all objects considered in these lectures, since we will deal with liquids or solids (where the volume per molecule is small) at a rather low (eg, atmospheric) pressure. Under these conditions, the value of PV is many times less than the thermal energy of the body.

Indeed, even for a gas (where the volume per molecule is particularly large), $PV \approx RT \times [\text{number of moles}]$ (remember the Clapeyron-Mendeleev law?). So, per mole of gas, the correction $PV = 1RT \approx 0.55/0.75 \text{ kcal mol}^{-1}$ at temperatures ranging from 0 to 100°C, that is, at $T = 273$ to 373 K. In other words, even in gases this value is commonly low compared with the magnitudes of the effects of interest, which usually amount to a few kilocalories per mole. Under a pressure close to atmospheric, for liquids and solids, the effect on H of correcting for PV is still hundreds or thousands of times less: here the volume of one mole is a minor fraction of a liter [$\approx 1/55 \text{ L}$ for H_2O , $\approx 1/10 \text{ L}$ for $(\text{CH}_2)_6$, etc.], while for a gas at a pressure of 1 atmosphere and room temperature this volume amounts to about 25 L.

That is why, later I will neglect the difference between H and E and refer to them both simply as “energy.”

Similarly, there is little difference (for us) between *Helmholtz free energy* $F = E - TS$ and *Gibbs free energy*

$$G = H - TS = (E + PV) - TS = F + PV \quad (5.5)$$

Making no difference between G and F we will refer to them both simply as “free energy.” However, it is worth keeping in mind that for processes occurring

in a fixed volume, we should use E and F , while for processes occurring under constant pressure, we should use H and G letters.

Next, you should remember that at a given temperature ($T=\text{const.}$), any system adopts the equilibrium *stable* state at the minimum $F=E-TS$ if the *volume* is fixed, and at the minimum $G=H-TS$ if the *pressure* is constant. (The number of particles in the system is assumed to be fixed, unless the opposite is defined.)

With a minor change in the state of the system, its free energy varies as:

$$\begin{aligned} F \rightarrow F + dF &= F + dE - TdS - SdT \\ \text{or} \\ G \rightarrow G + dG &= G + dH - TdS - SdT \end{aligned} \quad (5.6)$$

This means that all possible rearrangements of the system about its stable state are described by the following equations characterizing the free energy minimum—as we know, a peculiarity of the point of minimum (and maximum) is that minor deviations from it result in almost no change in the function's value:

1. at $V = \text{const.}$, the stable state (at a given T) is gained with F at a minimum, where

$$dF|_{V=\text{const}} = dE|_{V=\text{const}} - TdS|_{V=\text{const}} = 0 \quad (5.7)$$

- (taking into account that $dT=0$ at $T=\text{const.}$, that is, $SdT=0$ in Eq. (5.6));
2. at $P=\text{const.}$, the stable state (at a given T) is gained with G at a minimum, where

$$dG|_{P=\text{const}} = dH|_{P=\text{const}} - TdS|_{P=\text{const}} = 0 \quad (5.8)$$

These equations yield *the thermodynamic definition of absolute temperature*:

$$T = \left[\frac{dE}{dS} \right]_{V=\text{const}} = \left[\frac{dH}{dS} \right]_{V=\text{const}} \quad (5.9)$$

I realize that this definition has been obtained rather formally, and its physical sense is not obvious. Therefore, I will return to it later.

Now let us consider the chemical potential. This quantity describes the thermodynamic characteristics of one molecule in a system, rather than those of the system as a whole.

If molecules are added to a system one by one *under constant pressure*, identical efforts are required for driving in each of them. (This is not so if we add particles one by one to a system having a constant volume—it takes more and more effort to drive more particles in: it is easy to inject one drop into a sealed bottle, but what about another? One more? Still more?) *Under constant pressure*, the volume will grow when we add particles, while the density of the

system and the intensity of interactions in its interior will remain unchanged. That is, *under constant pressure* H and G are proportional to N , the number of particles in the system (while at a constant volume, E and F are *not* proportional to N).

Thus, the thermodynamic state of a single molecule in a large homogeneous system is adequately described by the Gibbs free energy G divided by the number of molecules N ,

$$\mu = \frac{G}{N} \quad (5.10)$$

where μ is known as the *chemical potential*, which can be also defined as the work spent to add one more particle to the system: $\mu = (dG/dN)_{T,P=\text{const}} = (dF/dN)_{T,V=\text{const}}$ (Landau and Lifshitz, 1980) (and since in liquids or solids $F \approx G$ at low pressures, here $\mu \approx F/N$). However, $G = N\mu$ if the system consists of identical molecules. If there are different types of molecules ($i = 1, 2, \dots$) in the system, then $G = \sum_i N_i \mu_i$. Note: If N means not the number of molecules but, as usual in physical chemistry, the number of moles of molecules, then μ refers not to one molecule but to a mole of molecules.

The chemical potential, or, which is the same, the Gibbs free energy per molecule, will be of use later in this lecture for considering the distribution of molecules between phases. The thing is molecules pass from the phase where their chemical potential is higher to a phase where it is lower, thereby lowering the total free energy of the system and shifting it to equilibrium. And the equilibrium state is characterized by identical chemical potentials of molecules in both phases.

For further considerations, we will need two more equations.

First, the definition of heat capacity reflecting a temperature-dependent increase of energy:

$$C_P = \left[\frac{dH}{dT} \right]_{P=\text{const}} \quad (5.11)$$

(this is for a constant pressure; one can also calculate heat capacity at constant volume, but we do not need such details).

Second, the relationship between the entropy and the free energy:

$$S = - \left[\frac{dG}{dT} \right]_{P=\text{const}} = - \left[\frac{dF}{dT} \right]_{V=\text{const}} \quad (5.12)$$

Eq. (5.12) is one of the most important in thermodynamics. It results directly from the fact that the small increment of free energy $dG = d(H - TS) = dH - TdS - SdT$ (and $dF = d(E - TS) = dE - TdS - SdT$), whereas, in equilibrium, $dH - TdS = 0$ (and $dE - TdS = 0$) in accordance with the thermodynamic definition of temperature: $T = dH/dS = dE/dS$ (see Eq. 5.9).

Eq. (5.12) shows that the free energy has its minimum (or maximum) value at such temperature T , where $S(T) = 0$.

It is also useful to know that G/RT is at a minimum (maximum) when $H(T)=0$, since

$$\frac{d(G/RT)}{dT} = \frac{d(G/dT)}{RT} - \frac{G}{RT^2} = \frac{-S}{RT} - \frac{(H-TS)}{RT^2} = \frac{-H}{RT^2} \quad (5.13)$$

Remarks:

1. Using Eqs. (5.5) and (5.12), one can show that $H=G+TS=G-T(dG/dT)$, and therefore C_P (see Eq. 5.11) can be obtained in the form:

$$C_P = -T \left[\frac{d^2G}{dT^2} \right]_{P=\text{const}} \quad (5.14)$$

2. We are never interested in values of energy, entropy, and free energy themselves. We are interested only in *changes* of these values. Indeed, speaking on energy: we can count off the gravitational energy of particles from the sea level, from the floor level, from the center of the Earth, etc. The values will be all different, but this does not matter. The only important thing is the *difference* between gravitational energies of a particle in two states. Just the same, when we define the particle's entropy as $k \ln V$, we can measure the volume V in liters, in cubic feet, etc. The values will be all different, but this does not matter: the only important thing is the *difference* between particle's entropies in two volumes (V and V'). And this difference, $\Delta S = k \ln(V/V')$, is independent of the unit of measurements.

With this introduction, we can now go on to discuss hydrophobicity and water as a specific solvent that creates it.

First of all, let us consider the so-called *hydrophobic effect*.

“Hydrophobicity” is “fear of water.” Who is “afraid” of water?—all nonpolar molecules such as inert gases (argon, xenon), hydrogen, and all purely hydrocarbon molecules (methane, ethane, benzene, cyclohexane, etc.). We will focus on hydrocarbons in water, since proteins have many hydrocarbon side chains. It is these water-fearing and water-escaping side chains that form the *hydrophobic core of a protein globule* (Bresler and Talmud, 1944; Kauzmann, 1959).

So, what does hydrophobicity mean in terms of experiment?

Methane's (CH_4) concentration in water is about an order *lower* than in gas above this water at a temperature of 20–40°C (the exact value depends on temperature). For H_2 and for propane $\text{CH}_3\text{CH}_2\text{CH}_3$, the difference is nearly the same. All of them are water-fearing (phobic) molecules: they are *more numerous* in a vapor than in the water. In contrast, ethanol $\text{CH}_3\text{CH}_2\text{OH}$ and water are easily miscible, and as you know, their separation is quite laborious, but the ethanol molecule is polar (its polar O–H group is capable of H-bonding). As to the purely nonpolar molecules, they would prefer a vacuum (vapor is nearly a vacuum) rather than water. And this happens *in spite* of van der Waals attraction between *any* molecules, even H_2 or CH_4 and water.

Let us consider (using one example shown in Fig. 5.1) some typical thermodynamic effects for hydrocarbons in water. The thermodynamic parameters presented in Fig. 5.1 (free energies, energies, and entropies of transfer from one phase to another) resulted from experimental studies of the equilibrium distribution of molecules of cyclohexane, $(\text{CH}_2)_6$, among three phases: vapor, aqueous solution, and liquid cyclohexane.

If molecules can go from one phase to another, their chemical potentials μ , in equilibrium, are equal in all the phases; otherwise, molecules will start to leave the phase with a higher chemical potential and go to the phase with a lower chemical potential: this will decrease the free energy.

Chemical potential for a given type of molecules in a given phase (where they have concentration $X \equiv N/V$) may be presented as

$$m = G^{\text{int}} + RT \ln(X), \quad (5.15)$$

where G^{int} is the “mean force potential” acting upon these molecules in this phase (ie, the free energy of interactions of the molecules in question with their surrounding).

For equilibrium distribution of given molecules between two phases (nonpolar liquid and aqueous solution), $\mu_{\text{in liquid}} = \mu_{\text{in aqueous solution}}$. Thus, the

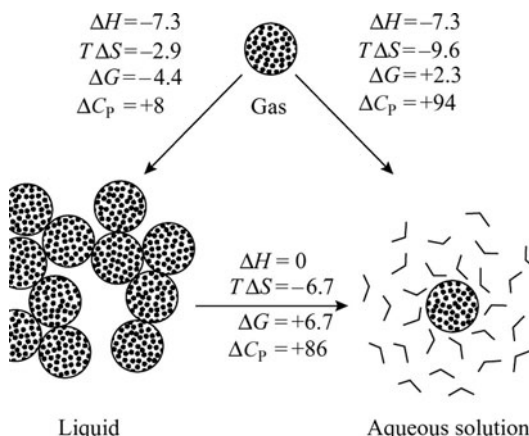


FIG. 5.1 The thermodynamics of transfer of a typical nonpolar molecule, cyclohexane ($\text{CH}_2)_6$, from vapor (top) to water (right), and from liquid cyclohexane (left) to water. The numerical values are for 25°C (ie, $T \approx 300 \text{ K}$, $RT \approx 0.6 \text{ kcal mol}^{-1}$). ΔH (as with energy, it is measured in “kilocalories per mole”) is the interaction enthalpy change per mole of molecules; ΔS is the corresponding interaction entropy change ($T\Delta S$, the contribution of the entropy change to the free energy, is also measured in kilocalories per mole); $\Delta G = \Delta H - T\Delta S$ (kcal mol^{-1}) is the change in Gibbs free energy of interactions per mole of transferred molecules; ΔC_p [$\text{cal mol}^{-1} \text{ K}^{-1}$] is the change in heat capacity per mole of transferred molecules. All values are recalculated using Eqs. (5.16)–(5.18) and experimental values from reference books. (Adapted from Creighton, T.E., 1993. *Proteins: Structures and Molecular Properties*, second ed. W. H. Freeman & Co., New York (Chapter 4).)

difference in the free energy of interactions upon transfer of a mole of molecules from the nonpolar liquid to water is defined as:

$$\Delta G_{\text{liquid} \rightarrow \text{aqueous solution}} \equiv G_{\text{in aqueous solution}}^{\text{int}} - G_{\text{in liquid}}^{\text{int}} = -RT \ln(X_{\text{aq}}/X_{\text{liq}}) \quad (5.16)$$

Here X_{aq} and X_{liq} are equilibrium concentrations of studied molecules in the aqueous solution and in the nonpolar liquid that contacts with the former.

The value $\Delta G_{\text{liquid} \rightarrow \text{aqueous solution}}$ is a difference between the mean force potentials affecting our molecule in water and in the nonpolar liquid. The mean force potential is created by all interactions of our molecule with its molecular surrounding; it includes both energy and entropy terms that arise from these interactions. Since concentration is the number of molecules in a given volume, Eq. (5.16) follows from the Boltzmann distribution over two phases with different values of the mean force potential.

At 25°C and low (~ 1 atm, or less) pressure of the air, $X_{\text{liq}} \approx 9.25 \text{ mol}^{-1}$ for pure liquid $(\text{CH}_2)_6$ and $X_{\text{aq}} \approx 0.0001 \text{ mol}^{-1}$ for its saturated solution in water. Accordingly, $\Delta G_{\text{liquid} \rightarrow \text{aqueous solution}} = +6.7 \text{ kcal mol}^{-1}$.

The free energy of transfer of our molecule from gas to the nonpolar liquid $(\text{CH}_2)_6$ and to the aqueous solution can be defined in the same way:

$$\Delta G_{\text{gas} \rightarrow \text{liquid}} = -RT \ln(X_{\text{liq}}/X_{\text{gas}}) \quad (5.17)$$

$$\Delta G_{\text{gas} \rightarrow \text{aqueous solution}} = -RT \ln(X_{\text{aq}}/X_{\text{gas}}), \quad (5.18)$$

where X_{gas} is the equilibrium concentration of our molecules in gas above the liquid(s). The pressure of the saturated $(\text{CH}_2)_6$ vapor at 25°C is about 0.05 atm, which means that $X_{\text{gas}} = 0.002 \text{ mol}^{-1}$ (ie, X_{gas} is 50 times higher than X_{aq}). The resulting ΔG values are presented in Fig. 5.1. Note: the experimentally measured value of $X_{\text{aq}}/X_{\text{gas}}$ at $X_{\text{gas}} \rightarrow 0$ is called “Henry’s law constant” ($k_{\text{H,cc}}$).

Since the mean force potential of interactions affecting a molecule in a rarefied gas ($G_{\text{in gas}}$) is virtually zero, $\Delta G_{\text{gas} \rightarrow \text{liquid}} = G_{\text{in liquid}} - G_{\text{in gas}}$ is very close to $G_{\text{in liquid}}$ that is the mean force potential of interactions of the molecule in the nonpolar liquid; and the mean force potentials of the molecule’s interactions in water, $G_{\text{in aqueous solution}}$, equals to $G_{\text{gas} \rightarrow \text{aqueous solution}}$.

When ΔG and its temperature dependence is known, the values of ΔS , ΔH , ΔC_P are derived from this dependence according to Eqs. (5.12)–(5.14).

Fig. 5.1 shows that the *energy* of attraction of $(\text{CH}_2)_6$ molecules to water is as high as that to liquid cyclohexane ($\Delta H = -7.3 \text{ kcal mol}^{-1}$), but $(\text{CH}_2)_6$ molecules do not want to go into water, though they go into liquid cyclohexane readily. As is clear from Fig. 5.1, it is entropy that causes this hydrophobicity; it becomes too low when a cyclohexane molecule comes into water.

Why are nonpolar molecules like CH_4 or $(\text{CH}_2)_6$ hydrophobic?

The reason is that, unlike water molecules, nonpolar H_2 or Ar , CH_4 or $(\text{CH}_2)_6$ are incapable of H-bonding. This is confirmed by the well-known fact that polar ethanol molecule, $\text{CH}_3\text{CH}_2\text{OH}$ (which consists mainly of

hydrocarbon groups, such as $(\text{CH}_2)_6$, but has a $-\text{OH}$ group and therefore is capable of H-bonding, like H_2O is not hydrophobic.

A naive suggestion could be made that upon coming into water, CH_4 or $(\text{CH}_2)_6$ molecules disrupt H-bonding in water. But it is not that simple. If it were so, the solution energy would have *increased* drastically with incoming $(\text{CH}_2)_6$, while in fact it actually *decreases* (see Fig. 5.1) by 8 kcal mol⁻¹ of incoming $(\text{CH}_2)_6$. Actually, instead of increasing energy, we have *decreasing entropy* (and this decrease is substantial: $T\Delta S = -9.6 \text{ kcal mol}^{-1}$).

This entropy decrease prevents cyclohexane from dissolving in water. The free energy $G = H - TS$ increases not only with increasing energy H but also with *decreasing* entropy S (S contributes to G in the form of $-TS$). Thus, a large decrease of the entropy S , even with a simultaneous decrease of energy H , results in increasing free energy G , and hence (see Eq. (5.1)) in a *decreasing probability* of molecules remaining in the current state (or more simply, in their decreasing concentration in this state).

Now the main physical question arises as to why the entropy of water molecules decreases as a result of their contact with a nonpolar surface.

It decreases because an H_2O molecule must not point at a hydrophobic surface with its H atom. Otherwise, its hydrogen bonds will be lost (see Fig. 5.2; as you may remember, H-bonds are orientation-dependent and emerge only when an O–H group is directed towards the O atom of another water molecule).

Let me remind you that H_2O molecules are almost fully hydrogen-bonded in water, so it is impossible to sacrifice some H-bonds without a great loss of the free energy. To avoid the loss of H-bonds (ie, to avoid O–H groups being directed towards the hydrophobic surface), water molecules seek favorable positions (see the upper molecule in Fig. 5.2) and partially freeze their thermal motions. Thereby, they preserve their valuable H-bonds at the expense of some

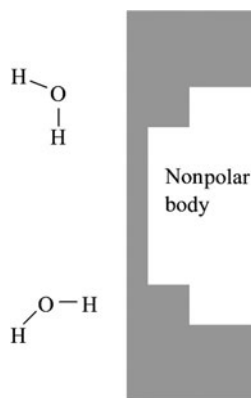


FIG. 5.2 Water molecules near the surface of a nonpolar body. The upper molecule can make all its H-bonds, but this “favorable” position about the body surface is restricted and therefore entropy-expensive. The lower molecule loses one energy-expensive H-bond to water because its O–H group is directed towards the nonpolar obstacle.

of their entropy. From the data presented in Fig. 5.1 and the number of waters surrounding $(\text{CH}_2)_6$, we can estimate that the entropy-driven loss of free energy is about 0.2 kcal per mole of mean-surface waters, which is an order of magnitude less than the price of lost H-bonds would be.

Low temperature (up to 20°C, and for some hydrocarbons, up to 60°C) even allows the hydrogen bonds near a hydrophobic surface (see Fig. 5.3) to gain a little energy (see Fig. 5.4; because now these bonds are less damaged by movements of half-frozen near-surface waters), but this gain does not fully compensate for the entropy loss resulting from freezing the near-surface waters.

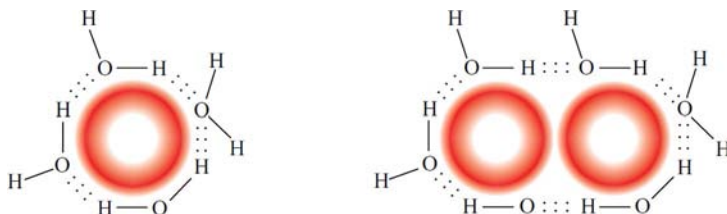


FIG. 5.3 Irregular packing of H-bonded waters around a nonpolar molecule (left) and around a pair of such molecules. A hydrophobic bond is formed in the latter case.

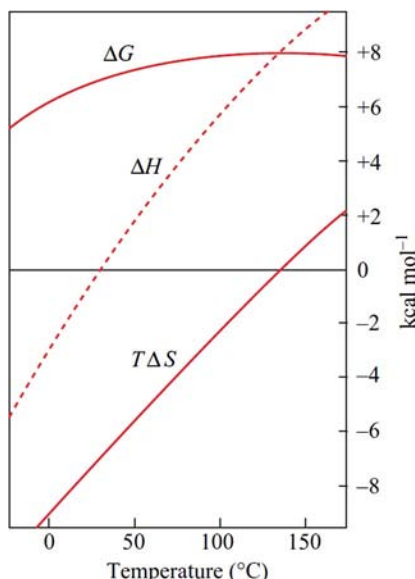


FIG. 5.4 The thermodynamics of transferring a typical nonpolar molecule, pentane C_5H_{12} , from liquid pentane to water at various temperatures. The transfer free energy, $\Delta G = \Delta H - T \Delta S$, and its enthalpic (ΔH) and entropic ($T \Delta S$) components are measured in kilocalories per mole of transferred molecules. ΔG is at a maximum when $\Delta S=0$; the proportion of pentane distribution between the water and the liquid pentane phases (which is proportional to $\exp(-\Delta G/RT)$) is at a minimum when $\Delta H=0$. (Adapted from Privalov, P.L., Gill, S.J., 1988. Stability of protein structure and hydrophobic interaction. *Adv. Protein Chem.* 39, 191–234.)

Note that again the net effect is entropic rather than energetic in nature *just because* the energy of H-bonds is extremely high: since it is so, waters would prefer to become frozen (although this is also thermodynamically bad) and sacrifice a part of their freedom (entropy) than to lose the large energy of a hydrogen bond.

I would like to emphasize that the resultant entropic effect on the free energy value is of *the same sign* as the energetic effect expected by naiveté, but *less* in magnitude.

The suggestion that waters close to a nonpolar surface are, in a way, frozen, is additionally supported by the anomalously high heat capacity of cyclohexane (and other hydrocarbons) in water. The excessive heat capacity of a $(\text{CH}_2)_6$ molecule in aqueous surrounding is 10 times as high as that amidst its fellow cyclohexanes. To be more exact, a high heat capacity in water is typical not of the hydrocarbon itself but of its ice-like water shell; with increasing temperature this “iceberg” tends to melt out, and this explains the anomalous heat capacity.

In considering frozen hydrogen-bonded surface waters, bear in mind that their relative orientation *differs* from that in normal ice. In ice, water molecules must have regular space positions because they have to form a huge three-dimensional crystal. At the surface they can adopt any position they like, provided that it is favorable for H-bonding. The water molecules do not observe translational symmetry of the three-dimensional lattice of ice because the resultant “microiceberg” is not going to grow infinitely: it only tends to coat the introduced hydrophobic molecule (Fig. 5.3) or a group of such molecules.

In the latter case, these hydrophobic molecules form a “hydrophobic bond.”

Inner voice: There is “hydrophobic bond” and there is “hydrogen bond.” Both bonds are hidden from water—so, what’s the difference between them?

Lecturer: Hydrogen bond is a bond between differently charged atoms of polar groups, say, $\text{N}^-\text{H}^+:::\text{O}^-\text{C}^+$, and its strength is *decreased* by water environment (as the strength of electrostatic bond, which will be considered in the next lecture); therefore, it is not called “hydrophobic.” Hydrophobic bond is a bond between nonpolar (“hydrophobic”) groups, say, $(\text{CH}_2)_6:::(\text{CH}_2)_6$ or $\text{CH}_4:::\text{C}_5\text{H}_{12}$, and its strength is provided by ordering of waters surrounding these groups. (That is, hydrophobic bond is stronger than a simple van der Waals bond between the same groups.)

The so-called *clathrates* represent an extreme ordering of waters caused by hydrophobic molecules. Clathrates are crystals built up by water and nonpolar molecules (Pauling, 1970).

From your chemistry course, you may know that they are far less stable than the crystalline hydrates built up by water and polar molecules. Clathrates emerge only at low temperatures (about 0°C or less) and high pressures, which cause many molecules of nonpolar gas to penetrate into water. In clathrates, as in ice, water molecules have their hydrogen bonds saturated, although their geometry is different from that in normal ice. In the resultant crystal, quasi-

ice keeps nonpolar molecules in its pores. Incidentally, clathrates are thought to contain more natural gas than ordinary gas fields, and gas production from clathrates (from a great depth where high pressure ensures their existence) is perhaps a project of tomorrow.

The hydrophobic effect is rather temperature-dependent ([Fig. 5.4](#)). The temperature affects ΔG , but even more, it affects the magnitude (and even sign) of its constituents, ΔH and ΔS .

As the temperature is increased, the surface hydrogen bonds tend to melt out. Up to $\approx 140^\circ\text{C}$, this is accompanied by an increasing hydrophobic effect, since the thermodynamically unfavorable ordering of surface waters persists, while favorable hydrogen bonds are destroyed.

While at low and room temperature the hydrophobic effect results from entropy only, at elevated temperatures, the energy of the lost near-surface hydrogen bonds becomes more and more important. But ΔG keeps increasing until $\Delta S < 0$, ie, up to $\approx 140^\circ\text{C}$ (see [Fig. 5.4](#)).

However, at still higher temperatures, there are too many disrupted H-bonds in water (which now remains liquid only under high pressure); as a result, the hydrophobic surface interferes with hydrogen bonding less and less, and the hydrophobic effect begins to diminish.

[Fig. 5.4](#) illustrates the transfer of a nonpolar molecule to water from a nonpolar solvent rather than from a vapor. This is done deliberately: we are going to consider the hydrophobic effect in proteins where amino acid residues are transferred from water to the protein core, which is similar to a nonpolar solvent rather than to a vapor.

The hydrophobicity of amino acids will be in focus later but now it would be useful to consider [Table 5.1](#); it contains some characteristics measured at room temperature for nonpolar groups similar to protein ones.

It is immediately apparent from [Table 5.1](#) that ΔG (unlike ΔH and ΔS) increases with increasing size of a hydrophobic molecule. How exactly does it increase? A more detailed analysis of a variety of nonpolar molecules shows that their hydrophobic free energy ΔG increases almost proportionally to the accessible surface area of the nonpolar molecules.

The physical sense and mode of construction of the accessible surface is demonstrated in [Fig. 5.5](#) (see also [Fig. 5.3](#)).

The hydrophobic free energy is about $+0.02 \rightarrow +0.025 \text{ kcal mol}^{-1} \text{ \AA}^{-2}$ for the accessible nonpolar area of a molecule transferred from a nonpolar solvent to water ([Chothia, 1974](#)). Specifically, for benzene, the accessible area is about 200 \AA^2 , and $\Delta G \approx 4.6 \text{ kcal mol}^{-1}$; for cyclohexane, the accessible area is about 300 \AA^2 , and $\Delta G \approx 6.7 \text{ kcal mol}^{-1}$.

The same regularity is observed ([Chothia, 1974](#)) for hydrophobic amino acid residues ([Fig. 5.6](#)).

The hydrophobicities of amino acids are derived experimentally from equilibrium distributions of amino acids between water and a nonpolar or slightly polar solvent; the latter is usually a high-molecular-weight alcohol (eg, octanol)

TABLE 5.1 Typical Thermodynamic Parameters of Hydrophobic Group Transfer from a Nonpolar Liquid to an Aqueous Solution at 25°C

Molecule	Transfer from → to	ΔG (kcal mol ⁻¹)	ΔH (kcal mol ⁻¹)	$T\Delta S$ (kcal mol ⁻¹)	C_P (kcal mol ⁻¹ K ⁻¹)
Ethane (CH ₃) ₂ (compare with Ala side group: -CH ₃)	Benzene → water	+3.6	-2.2	-5.8	+59
	CCl ₄ → water	+3.8	-1.8	-5.4	+59
Benzene C ₆ H ₆ (compare with Phe side group: C ₆ H ₅ -CH ₂ -)	Benzene → water	+4.6	+0.5	-4.1	+54
Toluene C ₆ H ₅ -CH ₃ (compare with Phe side group)	Toluene → water	+5.4	+0.4	-5.8	+63

Values taken from Tanford (1980).

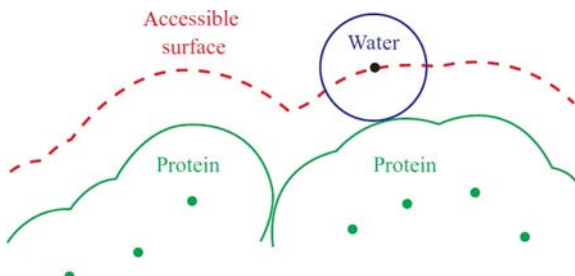


FIG. 5.5 The “accessible surface” of a molecule in water. Dots indicate the centers of the molecule’s atoms exposed to water; the solid line denotes their van der Waals envelopes. A water molecule is shown as a sphere of radius 1.4 Å. The “accessible” (to water) surface is defined as the area described by the center of a 1.4 Å sphere that rolls over the van der Waals envelope of the protein. (Adapted from Schulz, G.E., Schirmer, R.H., 1979. *Principles of Protein Structure*. Springer, New York (Chapter 1).)

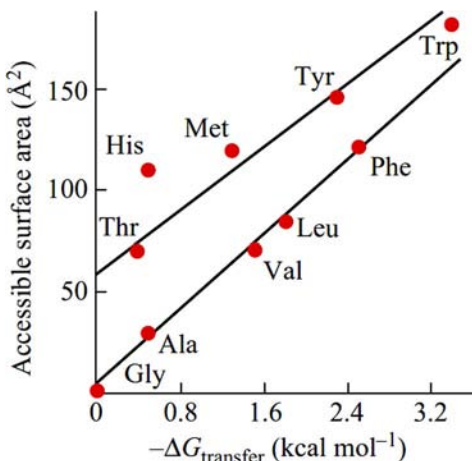


FIG. 5.6 The accessible surface area of amino acid side chains and their hydrophobicity. (The accessible surface of a side chain X is equal to the accessible surface of amino acid X minus that of Gly having no side chain; the hydrophobicity of a side chain X is equal to the experimentally measured hydrophobicity of amino acid X minus that of Gly.) The side chains of Ala, Val, Leu, Phe consist of hydrocarbons only. Those of Thr and Tyr additionally have one OH-group each, Met–SH-group, Trp–NH-group, and His–N-atom and NH-group; therefore, their accessible *non-polar* area is smaller than their total accessible surface. (Adapted from Schulz, G.E., Schirmer, R.H., 1979. *Principles of Protein Structure*. Springer, New York (Chapter 1), with minor modifications.)

or dioxane. These experiments are far from simple because some amino acids are hardly soluble in water, while others are hardly soluble in organic solvents (for instance, polar amino acids are virtually insoluble in purely nonpolar cyclohexane or benzene). Therefore, a nonpolar solvent is replaced by a specially selected slightly polar one (such as octanol, which is satisfactory for both strongly and weakly polar amino acids); other tricks are used too (Fauchére

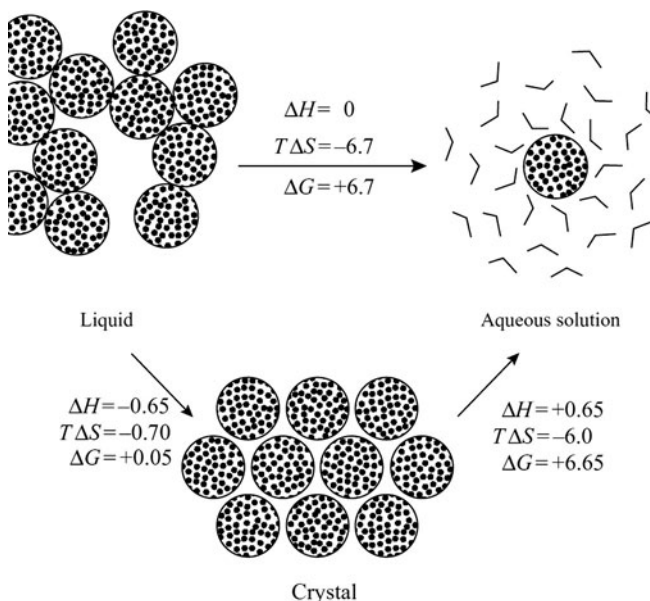


FIG. 5.7 The thermodynamics of transfer of a typical nonpolar molecule, cyclohexane, from the liquid to the solid phase and to aqueous solution. The numerical values are for 25°C. H , $T\Delta S$ and ΔG are measured in kilocalories per mole. All values are recalculated using Eqs. (5.16)–(5.18) and experimental data from reference books. (Adapted from Creighton, T.E., 1993. *Proteins: Structures and Molecular Properties*, second ed. W. H. Freeman & Co., New York (Chapter 4).)

and Pliska, 1983). According to the various solvents used, the results differ, specifically for charged and strongly polar amino acids. However, the qualitative agreement of these results is not bad.

The hydrophobic effect is smaller for the side chains with polar atoms than for completely nonpolar groups (provided their total accessible surface area is the same). However, if we consider only the nonpolar-atom-produced portion of their accessible surface area (ie, the total accessible surface area minus approximately 50 Å² for each polar atomic group), essentially the same surface dependence of hydrophobicity can be revealed for all the groups (see Fig. 5.6).

The hydrophobic effect is of major importance in maintaining the stability of the protein structure. It is this effect that is responsible for the compact globule formation of the protein chain (Bresler and Talmud, 1944; Kauzmann, 1959). As seen from Fig. 5.7, the free energy of transfer of a hydrophobic group from water to hydrophobic media is high and amounts to a few kilocalories per mole, while the free energy of hardening of the nonpolar liquid is close to zero at physiological temperatures. To be more accurate, I should say that the free energy of hardening of comparatively small hydrocarbons (see cyclohexane, shown in Fig. 5.7) is actually positive, which prevents their hardening at room temperature. The hardening is prevented by entropy of rotations and movements

of a molecule in the liquid, where each molecule is more or less free, in contrast to a solid in which the crystal lattice keeps the molecules fixed. However, the entropy of these motions of a molecule does not depend on its size, while the enthalpy of a molecule increases with increasing number of intermolecular contacts, that is, with the size of the molecular surface. In a side chain, the entropy of motions is lower, since amino acid residues are linked into a chain and cannot move freely, and this facilitates hardening.

However, even if the entire entropic component of cyclohexane crystallization, $\Delta G_{\text{liquid} \rightarrow \text{crystal}}$, was neglected (ie, if we assume that $\Delta G_{\text{liquid} \rightarrow \text{crystal}} \approx \Delta H_{\text{liquid} \rightarrow \text{crystal}} = -0.65 \text{ kcal mol}^{-1}$), the thermodynamic effect of crystallization would be much weaker than the hydrophobic effect condensing the water-dissolved cyclohexane molecules into a liquid drop ($\Delta G_{\text{aqueous solution} \rightarrow \text{liquid}} = -6.7 \text{ kcal mol}^{-1}$).

Thus, loosely speaking, the hydrophobic effect is responsible for approximately 90% of the effort required to make a compact globule. However, by itself it cannot provide a native solid protein. It creates only the molten globule that is yet to be discussed. The hardening of a protein, like that of all compounds, results from van der Waals interactions, as well as from hydrogen and ionic bonds, which are far more specific and more sensitive to peculiarities in the atomic structure than simple hydrophobicity (which is, actually, an effect operating in water). But what they perform is the final “polishing” of the native protein, whereas the bulk of the basic work is done by the hydrophobic effect.

REFERENCES

- Bresler, S.E., Talmud, D.L., 1944. On the nature of globular proteins. II. Some consequences of a new hypothesis. *Dokl. Akad. Nauk SSSR* (in Russian) 43, 326–330; 367–369.
- Cantor, C.R., Schimmel, P.R., 1980. *Biophysical chemistry*. W.H. Freeman & Co, New York (Part 1, Chapters 2, 5).
- Chothia, C., 1974. Hydrophobic bonding and accessible surface area in proteins. *Nature* 248, 338–339.
- Fauchére, J.L., Pliska, V., 1983. Hydrophobic parameters of amino acid side chains from the partitioning of N-acetyl-amino acid amides. *Eur. J. Med. Chem. Chim. Ther.* 18, 369–375.
- Kauzmann, W., 1959. Some factors in interpretation of protein denaturation. *Adv. Protein Chem.* 14, 1–63.
- Landau, L.D., Lifshitz, E.M., 1977. *Quantum Mechanics. A Course of Theoretical Physics*, vol. 3. Pergamon Press, Oxford, New York (Chapters 1, 2).
- Landau, L.D., Lifshitz, E.M., 1980. *Statistical Physics*, third ed. *A Course of Theoretical Physics*, vol. 5. Elsevier, Amsterdam–Boston–Heidelberg–London–New York–Oxford–Paris–San Diego–San Francisco–Singapore–Sydney–Tokyo Sections 7, 14, 15, 24.
- Nelson, D.L., Cox, M.M., 2012. *Lehninger Principles of Biochemistry*, sixth ed. W.H. Freeman & Co, New York (Chapter 2).
- Pauling, L., 1970. *General Chemistry*. W.H. Freeman & Co, New York (Chapters 10, 12).
- Tanford, C., 1980. *The Hydrophobic Effect*, second ed. Wiley-Interscience, New York.

Lecture 6

In this lecture, we discuss electrostatic interactions and, specifically, their features induced by the protein globule and its aqueous environment.

It may seem that there is nothing to discuss; undoubtedly, you remember that in a medium with permittivity (dielectric constant) ϵ the charge q_1 creates an electric field whose potential at the distance r is:

$$\varphi = \frac{q_1}{\epsilon r} \quad (6.1)$$

and q_1 interacts with the charge q_2 at this distance with the energy

$$U = \varphi q_2 = \frac{q_1 q_2}{\epsilon r} \quad (6.2)$$

You may also remember that in a vacuum (or air) $\epsilon = 1$, in water ϵ is close to 80, and in media such as plastics (and dry protein as well) ϵ is somewhere between 2 and 4.

Inner voice: All this is true, or, better to say, almost true. First, strictly speaking, U is not the energy but the *free* energy that tends to a minimum when our charges are in some medium instead of a vacuum; and U depends on permittivity ϵ of the medium and hence varies with temperature together with ϵ ; this means that U contains an entropic part.

Lecturer: This comment is absolutely right, but inasmuch as we are considering how charge interactions affect protein stability, these are minor items, a matter of purism. For the sake of simplicity, let me use the term “energy” for a while...

What is more important, Eq. (6.2) is valid only for homogeneous media. And when studying charge interactions in proteins, we are dealing with a most heterogeneous medium. The permittivity of a protein itself, as with that of plastics, is not high and amounts to about 2–4, while that of water is 80. And the charged groups of the protein are mostly located on its surface, close to the water (we will see why later). What value of ϵ then should be chosen to make estimates of electrostatic interactions in the protein? If we take $\epsilon \approx 80$, the energy of interaction between two elementary (proton) charges at a 3 Å distance will be approximately 1.5 kcal mol⁻¹; with $\epsilon \approx 3$, this energy will be about 40 kcal mol⁻¹. The difference is too large: the additional 40 kcal mol⁻¹ can destroy any protein structure. (It has been already mentioned that the typical “reserve of stability” of a protein structure—the difference in free energies between the native and denatured states of the protein—is about 10 kcal mol⁻¹; any effect exceeding this value causes an “explosion” of the structure.)

The other problem is as follows: Eqs. (6.1) and (6.2) are valid when the distance r between charges much exceeds the size of surrounding molecules.

However, in proteins, charges are often in immediate contact with as little as 3–4 Å distance between them, which does not allow even a water molecule, not to mention a side chain, to take an intervening position. How can we estimate electrostatic interactions in this case? Should we assume that $\epsilon = 1$, as in a vacuum? Or should we take $\epsilon = 80$? Or rather...?

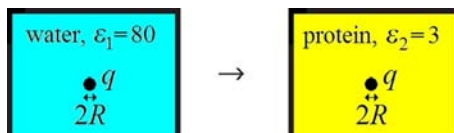
A brief philosophical digression. Why are these rough estimates wanted at all? Indeed, it is often believed that with the powerful computers available now, one can input “all as it is in reality”: water molecules, the coordinates of protein atoms including the coordinates of the charges, the temperature (ie, the energy of thermal motion) and obtain “the precise result.” As a matter of fact, this is a rather Utopian picture. The calculation—I mean the detailed one (made using the so-called “molecular dynamics”)—will take hours or days because you will have to follow both thermal motions and polarization of many thousands of interacting atoms (and, by the way, will not be absolutely accurate either; if nothing else, remember that atoms are “nonspherical” owing to their p-orbitals and other quantum effects; however, this fact is ignored by the interaction potentials (Levitt et al., 1995; Halgren, 1995; Jorgensen et al., 1996; MacKerell et al., 1998; Wang et al., 2004; Donchev et al., 2008; Pereyaslavets, Finkelstein) used in molecular dynamics and conformational analysis. And what really interests you is most likely a simple quick estimate, such as whether it is possible to introduce a charge into the protein at this or that site without a risk of protein explosion. My aim is to teach you how to make such estimates.

First of all, let us estimate the change in energy of a charge upon its transfer from water ($\epsilon \approx 80$) into the middle of the protein (where $\epsilon \approx 3$). For the time being, let us use classical electrostatics: consider water and protein as continuous media and disregard their corpuscular (ie, atomic) structures; or rather, let us postpone considering those details.

According to classical electrostatics, a sphere of charge q and radius R in a medium of permittivity ϵ has the energy:

$$U = \frac{q^2}{2\epsilon R} \quad (6.3)$$

This expression directly follows from Eq. (6.2): when we charge up the sphere (from zero to q_1) by bringing small charges dq onto its surface, each small charge dq increases the energy of the sphere by $dU = q dq/\epsilon R$ (according to Eq. (6.2)), and the integral of $q dq$ from 0 to q_1 is $q_1^2/2$.



$$\Delta U_{1 \rightarrow 2} = \frac{q^2}{2\epsilon_2 R} - \frac{q^2}{2\epsilon_1 R}$$

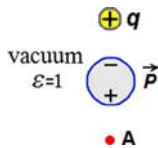
If the radius of the charged atom is about 1.5 Å, then its (free) energy is nearly 1.5 kcal mol⁻¹ at $\epsilon \approx 80$ (in water) and nearly 40 kcal mol⁻¹ at $\epsilon \approx 3$ (in protein). This great difference explains why inside the protein, in contrast to its surface, charged groups are virtually absent (it is easy to estimate that even immersion of a close pair of oppositely charged particles into the medium with $\epsilon \approx 3$ increases the free energy by about the same magnitude of 40 kcal mol⁻¹). Therefore, an ionizable group is virtually always uncharged when it is deeply involved in the protein globule (Nelson and Cox, 2012): that is, a positively charged side-group donates its surplus H⁺ to water, and a negatively charged side-group takes its missing H⁺ from water. True, this discharging costs some additional free energy—but “only” a few kcal mol⁻¹ (as you will see in Lecture 10), and not a few dozen kcal mol⁻¹. To be more exact, there are some charges in the interior of a protein; but these are almost always functional, and the protein has to put up with their presence just to keep functioning.

Now let us learn how to estimate the interaction of charges taking into account the interface between the protein ($\epsilon \approx 3$) and water ($\epsilon \approx 80$).

To begin with, let us consider a simple “problem of a charge and one dipole.”

It is well known that increased (as compared with a vacuum) permittivity ϵ of the medium is created by the medium molecules, that is, dipoles oriented or polarized by an electric field. As a result, the medium $\epsilon > 1$, and the field is *reduced* (see Eq. 6.1).

Suppose we have a charge $+q$, and our “medium” is a vacuum ($\epsilon = 1$), and only *one* dipole is situated between the charge and the point A where the field potential is measured:



(the dipole \vec{P} is naturally oriented along the field, that is, its “ $-$ ” looks at our charge $+q$).

Question: Is the field at the point A reduced or increased by the dipole as compared to the ‘vacuum case’?

Answer: However odd and counterintuitive it might seem, the dipole *increases* the field at the point A! (Counterintuitive—because the medium filled with many such dipoles *decreases* the field, while one, the central and thus seemingly the most important dipole, does just the *opposite!*)

However, the **answer** was obtained very simply: The dipole “minus” is directed at our charge $+q$, while its “plus” looks in the opposite direction, that is, towards the point A; and because this “plus” is closer to A than “minus,” its impact at the point A is *stronger* than that of the “minus,” thereby *increasing* the field created by our $+q$ at the point A.

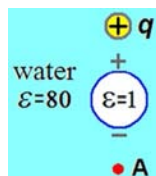
So, a single molecule located between the charge and the point where the field is measured reinforces the field, while the many molecules distributed over the entire space weaken the field! (Problem 6.1 shows that the field is reinforced by those molecules that are inside the sphere whose poles are the charge $+q$ and the observation point A, and weakened by molecules that are outside this sphere).

Note two important facts:

1. The same dipole \vec{P} that enhances the potential at the point A, weakens the potential near the charge $+q$.
2. Dipole \vec{P} is attracted to the charge $+q$, and *vice versa*.

We now consider a problem that is complementary to the first, and almost as simple: the “problem of a charge and a bubble.”

Suppose that the “medium” is water (with $\epsilon=80$), and a vacuum bubble is located between the charge $+q$ and the point A where the field is measured:



Question: Is the field at the point A reduced or increased by the bubble as compared with the “pure water case”? *It may seem* that the field in A should be strengthened, because it goes from $+q$ to A through a space with a lower (on average) permittivity than that of pure water. But in fact...

Answer: Oddly, the field in A is reduced! Since the vacuum bubble is *not* polarized, and water is polarized, waters turn their “minuses” towards $+q$, and their “pluses” away from $+q$ (see Fig. 6.1). As a result, a positive induced charge arises at that surface of the bubble which faces $+q$, and a negative induced charge arises on the opposite surface of the bubble facing the point A (the sum of these induced charges is zero, according to a theorem in electrostatics given, eg, in Landau et al., 1984). The induced “minus,” which is closer to A, weakens the potential created by $+q$ at the point A in pure water in the absence of a vacuum bubble.

Note two important effects opposed to those in the previous “problem of a charge and one dipole”:

1. The same bubble that weakens the potential at the point A enhances the potential near the charge $+q$.
2. The bubble is repelled by the charge $+q$, and the charge $+q$ by the bubble.

Similar is the behaviour of the field of the charge positioned in water near the surface of a protein (Fig. 6.1). Here, polarization of the protein (with $\epsilon \approx 3$) can be neglected, to the first approximation, as compared with that of water (with $\epsilon \approx 80$).

Fig. 6.1 shows how polar water molecules are oriented around the protein and the charge \oplus . They are oriented in conformity with the field: their “–” are directed mostly at “our” charge \oplus , while their “+” are directed oppositely. This results, first, in partial compensation of the charge \oplus by adjacent “–” of waters; this is trivial and simply causes a partial compensation of \oplus and, as a result, a large water permittivity ϵ_1 . But, second, this also produces the event that is of interest to us. Namely, the water “pluses,” trying to be directed away from \oplus , have to turn to the protein side facing the charge \oplus , and this polarization induces a positive charge at this side of the water/protein interface, while the water “minuses” come to the protein on the other side. This induces there an opposite (negative) polarized charge (as mentioned above, polarization of the protein itself can be neglected, since $\epsilon_{\text{protein}} \ll \epsilon_{\text{water}}$).

As a result, on the \oplus -facing protein side, the field potential becomes higher compared with what would have been in the absence of the protein: here, the induced “pluses” add to the potential of \oplus (and the induced “minuses” are far away and their effect is minor). That is why here $\epsilon_{\text{eff}} \approx 40$ (see Problems 6.2–6.5 for the simplest, and Landau et al. (1984) and Finkel'shtein (1977) for more complicated cases).

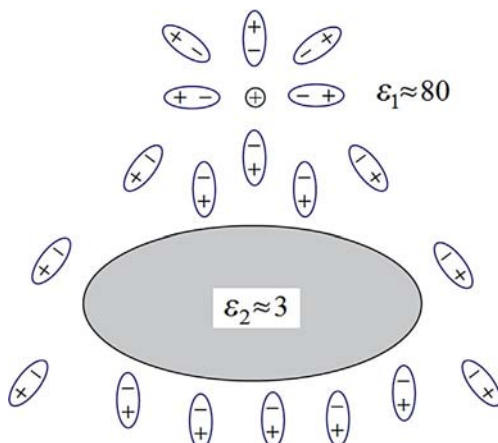


FIG. 6.1 The orientation of water molecules (shown as dipoles $(-+)$) around the protein (gray) and the charge \oplus (which is shown as positive for the sake of simplicity only).

At the same time, on the \oplus -opposite side of the protein, the field potential becomes *lower* than it would have been in the absence of the protein: here, the potential of the charge \oplus is diminished by the opposite in sign potential of “minuses” induced at this side of the protein/water interface (and the induced “pluses” are far away and their effect is minor). And since here (on the \oplus -opposite side of the protein), the field potential is *lower* than it would have been in the absence of the protein, ϵ_{eff} is *higher* than $\epsilon_1 = 80$ (the value in the absence of the protein; see Landau et al., 1984 and Finkel’shtain, 1977 for calculations).

The resulting distribution of numerical values of ϵ_{eff} “in and around the protein” for the field produced by the charge \oplus and the induced polarized charges looks as shown in Fig. 6.2A if \oplus is in water near the protein surface, and as in Fig. 6.2B if it is deep in the protein. Let me remind you that ϵ_{eff} is the effective value of permittivity for the point r to be used in the formula $\varphi(r) = q_1 / [\epsilon_{\text{eff}} |\mathbf{r} - \mathbf{r}_1|]$ to calculate the potential of the charge \oplus located at \mathbf{r}_1 .

It is useful to have in mind a simple expression describing interaction of two charges in a nonuniform media:

$$U \approx \frac{q_1}{\langle \epsilon \rangle_1} \times \frac{\langle \epsilon \rangle_{12}}{r} \times \frac{q_2}{\langle \epsilon \rangle_2} \quad (6.4)$$

where $\langle \epsilon \rangle_1$ is the average permittivity around charge q_1 (so that $\frac{q_1}{\langle \epsilon \rangle_1}$ is this charge partly screened by polarization of the medium), $\langle \epsilon \rangle_2$ is that for q_2 vicinity, and $\langle \epsilon \rangle_{12}$ is the average permittivity in-between and around charges q_1, q_2 . As seen, in a uniform medium (when $\langle \epsilon \rangle_1 = \langle \epsilon \rangle_2 = \langle \epsilon \rangle_{12} = \epsilon$), this expression is reduced to a conventional form given by Eq. (6.2).

It is worth considering one more consequence of the interface. This is the effect of the charge on itself: a charge located outside the protein is *repelled* from the protein surface, while a charge inside the protein is *strongly attracted* to the protein surface, that is, actually, to water. In both cases, the medium of higher permittivity attracts the charge, and that with a lower permittivity repels it. The values of these effects can be estimated (Finkel’shtain, 1977).

Let us consider some numerical examples. One can show that the energy of an ion (modelled as a conducting sphere with a charge q equal to the proton charge and radius $R = 1.5 \text{ \AA}$) is $q^2/[2\epsilon_1 R] \approx 1.4 \text{ kcal mol}^{-1}$ when it is in water

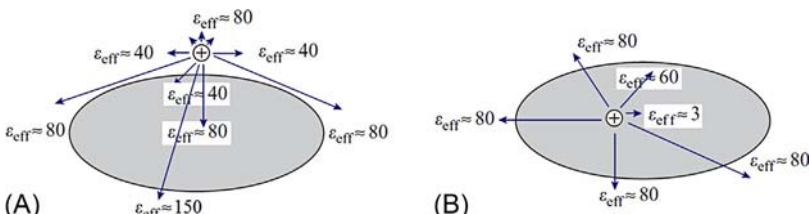


FIG. 6.2 Typical effective permittivity values ϵ_{eff} in various points for a potential produced by the charge \oplus located near the protein surface (A) and inside the protein (B). In both cases, the protein (with permittivity 3) is surrounded with water (with $\epsilon \approx 80$).

with permittivity $\epsilon_1 \approx 80$ and $q^2/[(\epsilon_1+\epsilon_2)R] \approx 2.7 \text{ kcal mol}^{-1}$ when it is half-immersed in the protein with permittivity $\epsilon_2 \approx 3$ (see Problem 6.5). Thus, the half-immersion-caused increase in energy is $\approx 1.3 \text{ kcal mol}^{-1}$. But when the same charge is placed between two proteins (or just deeply immersed in a protein), its energy is $q^2/[2\epsilon_2 R] \approx 36.9 \text{ kcal mol}^{-1}$. Thus, the full-immersion-caused increase in energy is $\approx 35.5 \text{ kcal mol}^{-1}$, which is nearly 30-fold energy of half-immersion. This illustrates a strong nonadditivity of electrostatic interactions in a nonuniform medium.

Now let us focus on the effects connected with the molecular structure of the medium. Polarization of the molecules determines the value of permittivity ϵ . If the medium consists of nonpolar molecules, an electric field only shifts electrons in the molecules, which is rather difficult; therefore, the polarization is small, and ϵ is low. If the medium consists of polar molecules (eg, of waters), an electric field turns these molecules, which is easier, and, hence, ϵ of such medium is high.

In both cases, with electrons shifted or molecules turned, polarization of the medium partially screens the immersed charges (\oplus and \ominus , see Fig. 6.3A) and thereby diminishes the electric field in the medium compared with what it would have been in a vacuum.

It would be only natural to expect that the polarized molecules must strongly affect the interaction of charges at short distances, since the classical equations, such as (6.1)–(6.3), are valid, strictly speaking, only when the charges are separated by many medium molecules. And if the charges are $3\text{--}4 \text{ \AA}$ apart (as often happens in proteins), no other atom can get between them to change their interaction.

In the case of such close contact, the permittivity might be believed to approach 1, even in the aqueous environment. This viewpoint, or rather this misapprehension, may still be encountered in the literature.

However, strange as it may seem, the medium's particulate nature makes no drastic changes in the "macroscopic" (ie, derived for large distances between the charges) permittivity, even if the distance is as short as 3 \AA . In other words, even at the smallest distances (when \oplus and \ominus are in a close contact), the value of water permittivity is much closer to 80 or 40 than to 1 or 3.

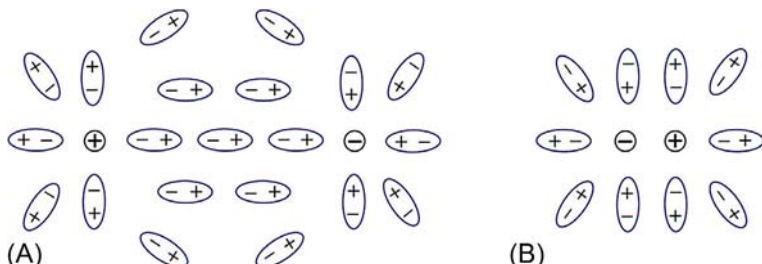
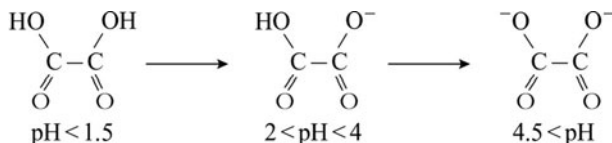


FIG. 6.3 Schematic drawing of orientation of water molecules surrounding charges \oplus and \ominus which are not in (A) or are in (B) a close contact.

This follows from the fact that salt easily dissolves in water, which is possible only with a weak attraction between counter-ions, even at very short distances of about 3 Å ([Finkel'shtein, 1977](#)).

Indeed, the distance between Na^+ and Cl^- ions is as short as 3 Å in a direct van der Waals contact. Then their free energy of attraction would amount to $-1.5 \text{ kcal mol}^{-1}$ at $\epsilon=80$, -3 kcal mol^{-1} at $\epsilon=40$, and -6 kcal mol^{-1} at $\epsilon=20$. The latter (6 kcal mol $^{-1}$) exceeds the energy of a hydrogen bond. Such an energy would make the counter-ions stick together more tightly than water molecules do, and then the concentration of a saturated salt solution would be about $10^{-4} \text{ mol L}^{-1}$, like the concentration of saturated water vapor. But this obviously cannot be true: it is no problem to dissolve one mole of NaCl (58 g) in 1 L of water (this will be an ordinary, perhaps a bit too salty brine). Consequently, water permittivity is considerably higher than 20, even at a distance of about 3 Å.

The value of ϵ at the closest distances inside the molecule can be estimated more precisely using the first and second constants of dissociation of dihydric acids in water. For example, dissociation of oxalic acid occurs as follows:



The second dissociation is shifted from the first one by approximately 2.5 pH units, that is, it occurs when the H^+ concentration is $10^{2.5} = e^{2.3 \times 2.5}$ times lower. This shows that the free energy of interaction of the first charge with the second one is $2.5 \times 2.3RT \approx 3.5 \text{ kcal mol}^{-1}$ when the distance between the charges is about 2.5–3 Å. This value of interaction energy corresponds to $\epsilon \approx 40$ at a distance of 2.5–3 Å. A similar result ($\epsilon \approx 30$ at a distance of about 2–2.5 Å) was obtained for dissociation of carbonic acid, $\text{H}_2\text{CO}_3 \rightarrow \text{HCO}_3^- \rightarrow \text{CO}_3^{2-}$, and of other dibasic acids and bases ([Birshtein et al., 1964](#)). It should be noted that a “correct” hydrogen bond energy is obtained at $\epsilon \approx 20$ at a distance of about 2 Å (and, of course, ϵ must approach 1 at a distance of ≈ 1 Å—otherwise energy of all covalent interactions would change drastically, which is not observed).

Hence, even a salt bridge between oppositely charged side-chains on the protein surface must “cost” 2–3 kcal mol $^{-1}$ only. In the interior of the protein, its “price” is higher, but immersion of charged side-chains into the protein would have been still more expensive, so it is no wonder that such bonds are rather rare in native proteins.

Thus, we conclude that the particulate nature makes no drastic changes in the “macroscopic” (derived for large distances between the charges) permittivity of water even at a distance of about 3 Å, which is too small for any other molecule to get between the interacting charges. The reason is suggested by the already considered case of “a charge and a dipole,” which suggests that a dipole located between charges increases rather than decreases their interaction, and thus this central dipole does not increase the value of permittivity. The permittivity is increased not by the central but by other dipoles. Thus, we can conclude that the charges are quite well shielded by solute molecules coming from other sides and from the flanks (Fig. 6.3B): these molecules become polarized (in the case of water, they simply turn), so that their “+”s shift towards the charge \ominus , and their “−”s towards the charge \oplus .

Here we see again (see also Fig. 6.2A and B) that the electrostatic interaction between the charges occurs mainly via the medium of a higher permittivity and nearly ignores the medium of weak polarization.

All our previous discussions referred to “micromolecular” systems. But are the conclusions drawn valid for proteins (where the particulate effects are coupled with the huge difference in permittivity between the water and the protein)?

Experiments reported by the research team headed by A. Fersht, the founder of protein engineering, show that the above estimates are valid for proteins (Russel and Fersht, 1987; Fersht, 1999).

The basis of these experiments is as follows. There are proteins (enzymes) that exhibit a particularly high activity at a certain value of pH (Nelson and Cox, 2012); they are said to have a pH-optimum. This pH-optimum can be shifted (Fig. 6.4) using a charged residue introduced to the protein by mutating its gene, and the electric field induced at the active site by the charge of the mutated residue can be estimated by the shift of the pH-optimum.

The pH-optimum is caused by the fact that, to keep the enzyme functioning, a group at its active site must have a certain charge that, in turn, depends on the concentration of hydrogen ions in the medium. The H^+ concentration (ie, $[H^+]$ mol L⁻¹) is equal to 10^{-pH} by definition, and the OH^- concentration in water is about 10^{-14+pH} .

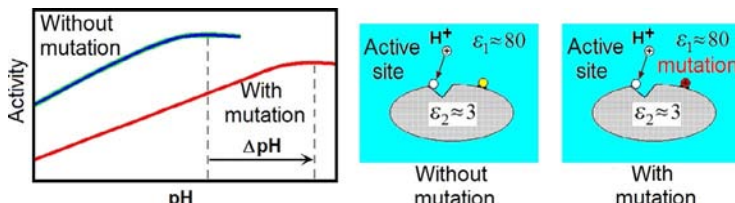


FIG. 6.4 A scheme of experiment on the mutation-caused shift of pH-optimum (after Russel and Fersht, 1987, with simplifications).

Let the active site (AS) accept the ion H^+ : $AS + H^+ = ASH^+$. Then, according to the active mass law, the ratio between these two forms of the active site (with and without H^+) is:

$$\frac{[ASH^+]}{[AS]} = \exp\left(-\frac{\Delta F_{ASH^+}}{RT}\right) \times [H^+] = \exp\left(-\frac{\Delta F_{ASH^+}}{RT}\right) \times 10^{-pH} \\ = \exp\left\{-\left(\frac{\Delta F_{ASH^+}}{RT} + 2.3 \times pH\right)\right\} \quad (6.5)$$

where ΔF_{ASH^+} is the free energy of H^+ binding (at $[H^+] = 1 \text{ mol L}^{-1}$) to the active site, and the symbol $[\cdot]$ denotes concentration.

If the mutation-introduced charge induces a potential φ at the protein active site, then ΔF_{ASH^+} changes as $\Delta F_{ASH^+}|_{\text{with mutation}} = \Delta F_{ASH^+}|_{\text{without mutation}} + \varphi \times e$, where e is the charge of H^+ . Since at the pH-optimum the magnitude of $\frac{[ASH^+]}{[AS]}$ (and the magnitude of $\frac{\Delta F_{ASH^+}}{RT} + 2.3 \times pH$) must remain the same both with and without the mutation, then

$$\frac{\frac{\Delta F_{ASH^+}|_{\text{without mutation}}}{RT} + 2.3 \times pH|_{\text{opt. without mutation}}}{\frac{\Delta F_{ASH^+}|_{\text{with mutation}}}{RT} + 2.3 \times pH|_{\text{opt. with mutation}}} \quad (6.6)$$

That is,

$$\varphi \times e = \Delta F_{ASH^+}|_{\text{with mutation}} - \Delta F_{ASH^+}|_{\text{without mutation}} \\ = 2.3RT \times (pH|_{\text{opt. without mutation}} - pH|_{\text{opt. with mutation}}) = 2.3RT \times (-\Delta pH) \quad (6.7)$$

Thus, having learned the shift of the pH-optimum, ΔpH , we can estimate the potential induced at the active site by the mutated protein residue. Then, using the known three-dimensional structure of the protein, and, hence, the distance r from the mutated residue to the active site, we can estimate the effective permittivity ϵ_{eff} (a term in the equation $\varphi = q/(\epsilon_{\text{eff}}r)$) for the interaction between the mutation-introduced charge q and the active site.

In Fersht's experiments, the mutations were performed at the surface of the protein in order not to damage its structure (as we have already learned, the energy of a charge deeply immersed in the protein is high and can literally explode the protein globule).

The experimental result reported: the effective permittivity ϵ_{eff} ranges from about 40 to 100, the former being typical of mutations at short distances from the active site, and the latter for remote (and shaded by the protein body) ones. The fact that ϵ_{eff} can reach a value of 100 appeared to be not a little surprising to those believing that ϵ_{eff} must lie between 3 (as inside the protein) and, at the

most, 80 (as in water). However, for us, these values are not surprising, since they are in good agreement with what follows from [Fig. 6.2A](#).

A brief digression on protein engineering. Its major advantage is that by changing a codon in a protein gene, we can perform a mutation at an exact site of the protein globule, since the gene in question, the amino acid sequence of the protein and the protein 3D structure are known. Besides, the mutation effect on the structure can also be monitored by X-ray analysis or NMR. Thus, the entire work is performed with one's eyes open.

In the experiments that we discussed earlier, the protein served as a microscopic (or rather, nanoscopic) electrometer. And protein engineering allows us to use such instruments as well as jumping from the physical theory to genetic manipulations, which is great fun!

Here, I would like to make some additions concerning electrostatic interactions.

First: So far, I have discussed only the interaction of separate charges. However, electrostatics also covers the interactions of dipoles (eg, the dipoles $\text{H}^{(+)}-\text{O}^{(-)}$ and $\text{H}^{(+)}-\text{N}^{(-)}$ involved in hydrogen bonding) as well as quadruples; the latter are present, for example, in aromatic rings ([Fig. 6.5](#)).

The reason for my considering interactions of ions is simply the strength of these interactions: even in immediate contact they are a few times stronger than interactions between dipoles (also, their decrease with increasing distance is slower), while interactions of dipoles are stronger than those between quadrupoles.

Second: With free charges (eg, salt) available in the water, the electrostatic interactions diminish with distance r as $(1/r) \times \exp(-r/D)$ rather than as $1/r$ [[Pauling, 1970](#)]. Here D , the Debye-Hückel radius, corresponds to the typical size of the counter-ion cloud around the charge. The value of D is independent of the charge itself but depends on the charges of the salt ions, on their concentration in the medium, on its permittivity and on temperature. In water, at room temperature:

$$D \approx \frac{3}{I^{1/2}} \text{\AA} \quad (6.8)$$

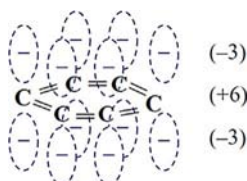


FIG. 6.5 The electric quadruple of an aromatic ring: the layer of “halves” of six p-electrons (charge -3)—the layer of cores (charge +6)—the layer of the last “halves” of p-electrons (charge -3).

where

$$I = \frac{1}{2} \sum_i c_i z_i^2 \quad (6.9)$$

is the *ionic strength* of the solution given in moles per liter. In Eq. (6.9), the sum is taken over all kinds of ions present in the solution, z_i is the charge (in proton charge units), c_i is the concentration (in moles/L) of ion i . Under ordinary physiological conditions (room temperature, $c_i \approx 0.1\text{--}0.15 \text{ mol L}^{-1}$ for ions with the charges +1 and -1, while the concentration of ions with the charge +2 is much lower), $I \approx 0.1\text{--}0.15 \text{ mol L}^{-1}$, and then $D \approx 8 \text{ \AA}$. However, some microorganisms live at $I \approx 1 \text{ mol L}^{-1}$ and more; then the persisting electrostatic interactions of the charged groups of the protein, though much weakened, are only those corresponding to “salt bridges”, that is, to the immediate contact of the charges.

In general, with an ionic atmosphere present in the solution, the energy of interaction of the two charges is

$$U = \frac{q_1 q_2}{\epsilon_{\text{eff}} r} \times \exp\left(-\frac{r}{D}\right) \quad (6.10)$$

Third: As seen from above, the electrostatic interaction is a striking example of the *non-pairwise* interaction of particles (unlike, for example, van der Waals interaction). It depends not only on the distance r between the charges q_1 and q_2 but also on the medium properties (those change both ϵ and D), and specifically, on the distance between the charges and other bodies and on the shape of these bodies (these affect ϵ_{eff}), as well as on the concentration of free ions with the charges +1 and -1 in the solution (which affects D). Nevertheless, the maths form for the resulting interaction is rather simple.

One more example of this kind: The energy of interaction of a charge q situated in a salt-free medium with permittivity ϵ_1 with a small noncharged body of volume V and permittivity ϵ_2 can be estimated (Finkel'shtein, 1977) as:

$$U \approx \frac{q^2 V}{8\pi r^4} \times \frac{\epsilon_1 - \epsilon_2}{\epsilon_1 \left(\frac{2\epsilon_1}{3} + \frac{\epsilon_2}{3} \right)} \quad (6.11)$$

And one more addition: So far, I have used the term “the energy of electrostatic interactions.” This was done for the sake of simplicity; as I mentioned at the beginning of this lecture, the strict term would be “free energy.” This is because we focused only on the attraction and repulsion of charges, without preventing the *heat exchange* with the environment. And with heat exchange allowed, what we dealt with is the free energy by definition.

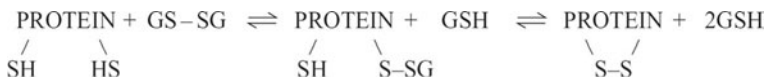
Moreover, the temperature dependence of electrostatic effects in aqueous environment may be used to show the predominance of the entropic constituent over the energetic (enthalpic) one; the latter, by the way, is close to zero. This

follows from the fact that water permittivity decreases from 88 to 55 (ie, the electrostatic interactions increase by 40%), with increasing absolute temperature T from 273 to 373 K (ie, by 35%). This means that the electrostatic interactions increase approximately proportionally to the absolute temperature. And the interaction increasing proportionally to the absolute temperature implies an exclusively entropic constituent (take a look at Problem 6.7). Hence, in water, the entire electrostatic effect is caused *not* by energy, but by the ordering of water molecules around the charges and by its variation with variation distance between the charges.

Hence, strange as it may seem, electrostatics in water originates *not* from energy but from entropy, just like hydrophobic interactions or hydrogen bonding in an aqueous environment.

In concluding this section on “Elementary interactions in and around proteins,” I would also like to mention disulfide and coordinate bonds. Although not as abundant in proteins as hydrogen bonds, these may often be of great importance ([Schulz and Schirmer, 1979, 2013; Creighton, 1993](#)).

Disulfide (S–S) bonds are formed by cysteine (Cys) amino acid residues (the Cys side-chain is $-\text{C}^\beta\text{H}_2-\text{SH}$). No direct oxidation of cysteines accompanied by hydrogen release (according to the scheme $-\text{CH}_2-\text{SH} + \text{HS}-\text{CH}_2 \rightarrow -\text{CH}_2-\text{S}-\text{CH}_2 + \text{H}_2$) occurs in proteins because at room temperature this process is too slow. However, in proteins, S–S-bonding can be rapid when assisted by thiol-disulfide exchange. In the cell, the exchange is thought to involve *glutathione* that has both the monomeric thiol (GSH) and dimeric disulfide (GSSG) form, and to follow the scheme



Both breakdown and formation of S–S-bonds can occur spontaneously *in vitro*, but in cells, these are catalysed (ie, accelerated but not directed) by a special enzyme, disulfide isomerase.

Rotation about the S–S bond is rather hindered by a high torsional potential that only allows torsional angles of about +90 degree and –90 degree ([Creighton, 1993](#)).

S–S-bonding is reversible, since the energetic equilibrium of this reaction (thiol-disulfide exchange) is close to zero (there were two covalent S–H bonds and one S–S bond, and now there are as many; this resembles the energy balance of hydrogen bonding in proteins, does it not?). Moreover, the available (rather high) concentration of GSH in the cell shifts the equilibrium towards breaking the bonds that might be produced by an “occasional” cysteine approach.

Therefore, the only S–S bonds that can be formed and persist are between cysteines brought close to one another by other interactions (Creighton, 1993; Sevier and Kaiser, 2002).

S–S bonds are of particular importance for proteins that have to reside and function out of the cell. On the one hand, the absence of disulfide isomerase and glutathione is favorable for bonds that have been already formed (either in the cell or when leaving it) as they become “frozen” and run no risk of breaking or rearranging. On the other hand, the external conditions may be different, and the extended margin of safety provided by the stable, “frozen” S–S bonds would not be out of place for the protein. That is why S–S bonds are typical of secreted proteins rather than cellular ones (Creighton, 1993; Sevier and Kaiser, 2002). Usually, in secreted proteins, all available cysteines (less one, if their number is odd) participate in S–S bonds.

Coordinate bonds are formed by N, O, and S atoms of the protein (as well as by O atoms of water) to di- and trivalent ions of Fe, Zn, Co, Ca, Mg, and other metals.

The ions of these metals have vacant orbitals lying low (as to energy), only slightly above their filled electron orbitals. Each of the vacant orbitals is capable of bonding an electron pair. And O, N, and S atoms (electron donors) have electron pairs that can occupy the vacant orbitals of the ions. The resultant bonds are identical to ordinary chemical bonds, except that ordinary bonds comprise electrons from both parent atoms, while coordinate bonds are formed by electrons coming from one bonded atom only (Pauling, 1970).

During coordinate bonding, the metal ion binds to several donors of electrons. Then a small (radius $\sim 0.7 \text{ \AA}$) di- or trivalent ion is surrounded by large-atom donors (radius $\sim 1.5 \text{ \AA}$). Mostly, there are six of these coordinating donor atoms located at the apices of a regular octahedron (Pauling, 1970) (Fig. 6.6).

Since the ion can be bonded to both electron donors of the protein and to oxygens of water, it passes (despite the high energy of each bond) from water

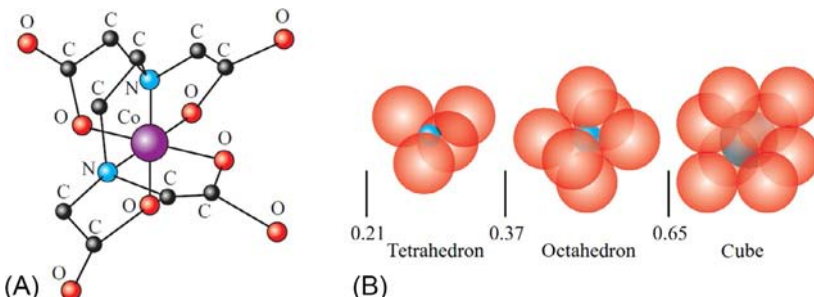


FIG. 6.6 (A) The structure of the octahedral complex between Co^{3+} -atom and EDTA. (B) Typical coordination of the central ion at various ratios between its radius and the radii of the surrounding electron donors. (Adapted from Pauling, L., 1970. *General Chemistry*. W.H. Freeman & Co., New York (Chapter 19).)

to the protein and back without dramatic gains or losses in energy. What is of greater importance is, if the positions of the donor atoms in the protein are “proper” for coordinate bonding, the ion can release the water molecules of its previous water environment and bind to the protein; then a strong bond occurs owing to the gained entropy of motion of the released water molecules (very much like the energy and entropy balance of hydrogen bonding, is it not?). On average, each coordinate bond costs several kilocalories per mole, that is, it is a little more expensive than a hydrogen bond in a water environment.

Such coordinate bonds formed by several atoms of one molecule are called *chelate* (claw-shaped). The role of these bonds in proteins, specifically at their active sites, will be considered later on. Also, we will see later, that chelate complexes coating ions completely can be members of the hydrophobic protein core. At the moment I would like to draw your attention again to Fig. 6.6 presenting the widely used reagent EDTA (ethylenediaminetetraacetic acid) that participates in a chelate bond to the metal. For EDTA, this bond is particularly strong because the negatively charged COO^- groups of EDTA are bound to the positively charged metal ion.

REFERENCES

- Birshtein, T.M., Ptitsyn, O.B., Sokolova, E.A., 1964. Theory of polyelectrolytes. V. Interactions of near groups in stereoregular polyelectrolytes. *Vysokomol. Soedin.* (in Russian) 6, 158–164.
- Creighton, T.E., 1993. Proteins: Structures and Molecular Properties, second ed. W. H. Freeman & Co., New York (Chapters 1, 2, 7).
- Donchev, A.G., Galkin, N.G., Illarionov, A.A., Khoruzhii, O.V., Olevanov, M.A., Ozrin, V.D., Pereyaslavets, L.B., Tarasov, V.I., 2008. Assessment of performance of the general purpose polarizable force field QMPFF3 in condensed phase. *J. Comput. Chem.* 29, 1242–1249.
- Fersht, A., 1999. Structure and Mechanism in Protein Science: A Guide to Enzyme Catalysis and Protein Folding. W. H. Freeman & Co., New York (Chapter 5).
- Finkel'shtein, A.V., 1977. Electrostatic interactions of charged groups in aqueous medium and their influence on the formation of polypeptide secondary structures. *Mol. Biol. (Moscow)* 11, 811–819.
- Halgren, T.A., 1995. Merck molecular force field. I. Basis, form, parameterization and performance of MMFF94. *J. Comput. Chem.* 17, 490–519.
- Jorgensen, W.L., Maxwell, D.S., Tirado-Rives, J., 1996. Development and testing of the OPLS all-atom force field on conformational energetics and properties of organic liquids. *J. Am. Chem. Soc.* 118, 11225–11236.
- Landau, L.D., Lifshitz, E.M., Pitaevskii, L.P., 1984. Electrodynamics of Continuous Media, second ed. A Course of Theoretical Physics, Volume 8. Elsevier Butterworth-Heinemann, Amsterdam–Boston–Heidelberg–London–New York–Oxford–Paris–San Diego–San Francisco–Singapore–Sydney–Tokyo. §§ 6–8, 11.
- Levitt, M., Hirshberg, M., Sharon, R., Daggett, V., 1995. Potential energy function and parameters for simulations of the molecular dynamics of proteins and nucleic acids in solution. *Comput. Phys. Commun.* 91, 215–231.
- MacKerell Jr., A.D., Bashford, D., Bellott, M., Dunbrack Jr., R.L., Evanseck, J.D., Field, M.J., Fischer, S., Gao, J., Guo, H., Ha, S., Joseph-McCarthy, D., Kuchnir, L., Kuczera, K.,

- Lau, F.T.K., Mattos, C., Michnick, S., Ngo, T., Nguyen, D.T., Prodhom, B., Reiher III, W.E., Roux, B., Schlenkrich, M., Smith, J.C., Stote, R., Straub, J., Watanabe, M., Wiorkiewicz-Kuczera, J., Yin, D., Karplus, M., 1998. All-atom empirical potential for molecular modeling and dynamics studies of proteins. *J. Phys. Chem. B.* 102, 3586–3616.
- Nelson, D.L., Cox, M.M., 2012. *Lehninger Principles of Biochemistry*, sixth ed. W.H. Freeman & Co., New York (Chapter 2, 6).
- Pauling, L., 1970. *General Chemistry*. W.H. Freeman & Co., New York (Chapter 19).
- Pereyaslavets, L.B., Finkelstein, A.V., 2012. Development and testing of PFFSol1.1, a new polarizable atomic force field for calculation of molecular interactions in implicit water environment. *J. Phys. Chem. B.* 116, 4646–4654.
- Russel, A.J., Fersht, A.R., 1987. Rational modification of enzyme catalysis by engineering surface charge. *Nature* 328, 496–500.
- Schulz, G.E., Schirmer, R.H., 1979, 2013. *Principles of Protein Structure*. Springer, New York (Chapters 3, 4).
- Sevier, C.S., Kaiser, C.A., 2002. Formation and transfer of disulphide bonds in living cells. *Nat. Rev. Mol. Cell Biol.* 3, 836–847.
- Wang, J., Wolf, R.M., Caldwell, J.W., et al., 2004. Development and testing of a general amber force field. *J. Comput. Chem.* 25, 1157–1174.

Lecture 7

Having dealt with *elementary* interactions, in this lecture we consider the secondary structure of proteins and polypeptides. It is well studied (see Schulz and Schirmer, 1979, 2013; Cantor and Schimmel, 1980; Branden and Tooze, 1999; Creighton, 1993).

First of all, we will discuss regular secondary structures, that is, α -helices and β -structures (Pauling and Corey, 1951a,b; Pauling et al., 1951). These secondary structures are distinguished by regular arrangements of the main chain with side chains of a variety of conformations. The tertiary structure of a protein is determined by the arrangement of these structures in the globule (Fig. 7.1).

We shall consider helices first. They can be right-handed or left-handed (Fig. 7.2) and have different periods and pitches. Right-handed (R) helices come closer to the viewer as they move counterclockwise (which corresponds to positive angle counting in trigonometry), while left-handed (L) helices approach the viewer as they move clockwise.

In the polypeptide chain, major helices are stabilized by hydrogen bonds.

The bonds are formed between C=O and H–N groups of the polypeptide backbone, the latter being closer to the C-terminus of the chain.

In principle, the following H-bonded helices can exist (Fig. 7.3): 2₇, 3₁₀, 4₁₃ (usually called α), 5₁₆ (called π), etc. The 2₇-helix derives its name from the second residue participating in the H-bond (see Fig. 7.3) and seven atoms in the ring (O → H–N–C'–C^α–N–C') closed by this bond. Other helices (3₁₀, 4₁₃, etc.) are named accordingly.

Which of these helical structures are most abundant in proteins? α -Helices are. Why? This question is answered by the Ramachandran map for a typical amino acid residue, alanine (Fig. 7.4), where I marked the conformations that, being repeated periodically, cause formation of the H-bonds shown in Fig. 7.3 (Ramachandran and Sasisekharan, 1968; Schulz and Schirmer, 1979, 2013).

As seen, only the α_R -helix (right-handed α -helix) is deep inside the region allowed for alanine (and for all other “normal,” ie, L amino acid residues). Other helices are either at the very edge of this allowed region (eg, the left-handed α_L -helix or the right-handed 3₁₀-helix), which gives rise to conformational strains, or in the region allowed for glycine only.

Therefore, it may be expected that the right-handed α -helix is the most stable and hence (*what's good for General Motors is good for America*) most abundant in proteins—and this is really so. In the right-handed α -helix (Fig. 7.5), the arrangement of all atoms is optimal, ie, tight but not strained. Therefore, it is no wonder that in proteins α -helices are numerous, and in fibrous proteins, they are extremely extended and incorporate hundreds of residues.

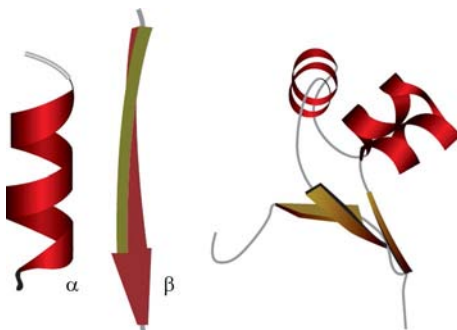


FIG. 7.1 The secondary structures of a polypeptide chain (α -helix and a strand of β -sheet) and the tertiary structure of a protein globule (on the right). Usually, taken together, α - and β -structures make up about a half of the chain in a globular protein.

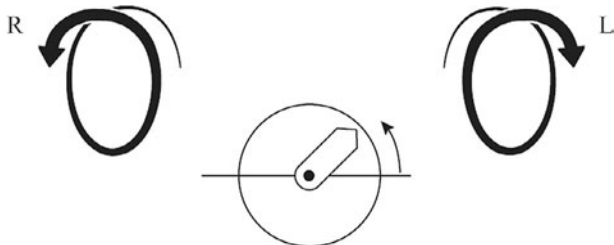


FIG. 7.2 Right-handed (R) and left-handed (L) helices. The spiral naturally must be viewed along its axis, and, with equal success, from either of its ends. The bottom part of the figure shows positive angle counting in trigonometry: the arrow that is “close” to the viewer moves *countrerclockwise*.

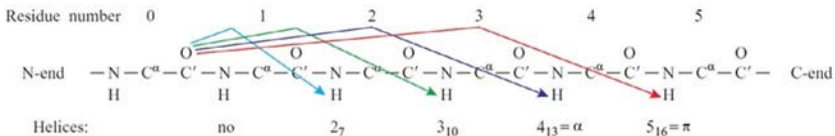


FIG. 7.3 Hydrogen bonds (shown with arrows) typical of different helices. The chain residues are numbered from the N- to the C-end of the chain.

Left-handed α -helices are not (or hardly ever) observed in proteins. This is also true for 2_7 -helices that not only lie at the very edge of the allowed region but also have a large angle between their N–H and O=C groups, that is energetically disadvantageous for hydrogen bonding. π -Helices are absent from proteins too. They also occur at the very edge of the allowed region and their turns are far too wide, which results in an energetically unfavorable axial “hole.” In contrast, 3_{10} -helices (mainly right-handed; left-handed ones are good for glycines only) are present in proteins, although only as short (three to four residues) and distorted fragments: the 3_{10} -helix is too tight and gives rise to steric strains; its conformation lies close to the edge of the allowed region.

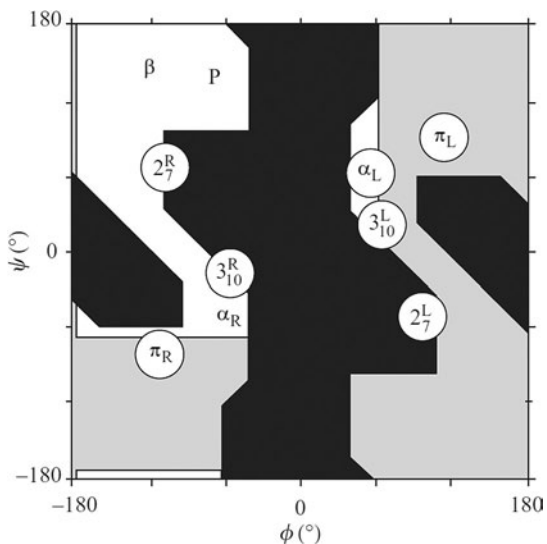


FIG. 7.4 The conformations of various regular secondary structures against the map of allowed and disallowed conformations of amino acid residues. 2_7^R , 2_7^L : the right-handed and left-handed 2_7 -helix; 3_{10}^R , 3_{10}^L : the right-handed and left-handed 3_{10} -helix; α_R , α_L : the right-handed and left-handed α -helix; π_R , π_L : the right-handed and left-handed π -helix. β , the β -structure (for details, see Fig. 7.8B). P, the poly(Pro)II-helix. □, conformations allowed for alanine (Ala); ▨, regions allowed for glycine only, but not for alanine and other residues; ■, regions disallowed for all residues; ϕ and ψ , dihedral angles of rotation in the main chain.

Pay attention to the feature clearly seen in Fig. 7.5A: the helical N-terminus is occupied by “free” H atoms of N–H groups uninvolved in intra-helical H-bonds, while the C-terminus is occupied by H-bond-free O atoms of C=O groups. Since the electron cloud of the H atom is partially pulled off by the electronegative N atom of NH group, and the electronegative O atom attracts the electron of the C' atom of C' O group, the N-terminus assumes a positive and the C-terminus a negative partial charge (Ptitsyn and Finkel'shtain, 1970). That is, the helix is a long dipole where the N-terminal partial “+” charge (coming from three “H-bond-free” H-atoms) amounts to about half of the proton charge, while the C-terminal “-” charge amounts to about half of the electron charge.

Now let us consider the regular main-chain structures lacking hydrogen bonds inside each of them but periodically H-bonded with one another.

The extended (all angles in the main chain are nearly *trans*), slightly twisted chains (“ β -strands”) form the sheet of the β -structure. A β -sheet can be (Fig. 7.6) parallel, ($\beta \uparrow \uparrow$) antiparallel ($\beta \downarrow \uparrow$), and mixed (comprising $\beta \uparrow \uparrow$ and $\beta \downarrow \uparrow$). The β -structure is stabilized by H-bonds (shown in light-blue lines in Fig. 7.6). Since the surface of -structure sheets is pleated (Fig. 7.7), this structure is also called the “pleated β -structure.”

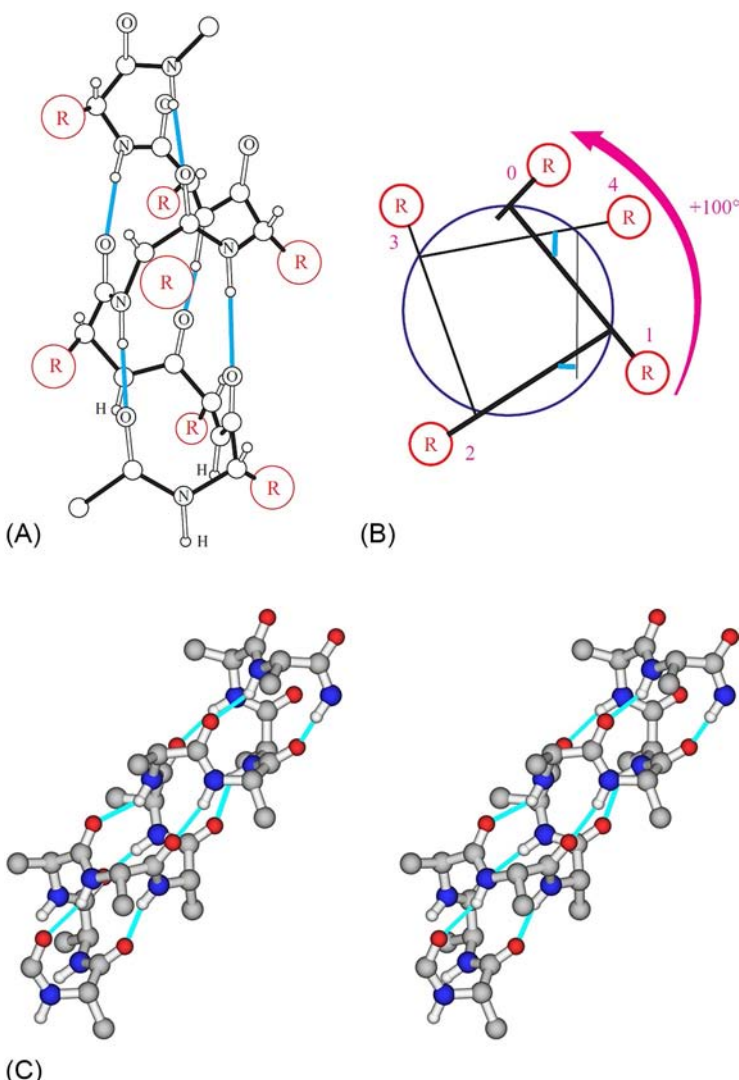


FIG. 7.5 The right-handed α -helix. Hydrogen bonds in the main chain are shown as light-blue lines. (A) Atomic structure; R = side-chains. (B) Axial view of one turn of this α -helix. The arrow shows the turn of the helix (per residue) when it approaches the viewer (the closer to the viewer, the smaller the chain residue number). The circle depicts the cylindrical surface enveloping the C^α atoms of the helix. (Adapted from Schulz, G.E., Schirmer, R.H., 1979, 2013. *Principles of Protein Structure*. Springer, New York (Chapter 5). (C) Stereo drawing (see Appendix E) of an α -helix. In side chains, only C^β atoms are shown.)

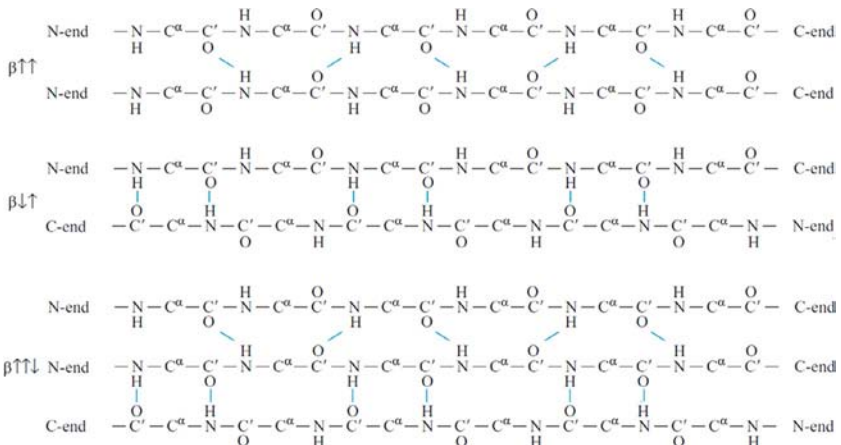


FIG. 7.6 Chain pathway and location of hydrogen bonds in the parallel ($\beta \uparrow \uparrow$), antiparallel ($\beta \downarrow \uparrow$), and mixed ($\beta \uparrow \downarrow \downarrow$) β -structures. As shown, in each β -strand, the H-bonds (light-blue) of one residue are directed oppositely to those of its neighbor in the chain. Periodicity of any β -structure equals two.

As a whole, the β -sheet is usually somewhat twisted (Figs. 7.7A,B, and 7.8A) because each separate β -strand is twisted by itself (Fig. 7.8B), thereby slightly altering the direction of H-bonds along the strand and thus favoring a certain angle between the H-bonded strands. In its turn, as explained by Chothia (1973), this twist of a strand results from shifting the energetically advantageous conformation of all side-chain-possessing residues towards the center of the sterically allowed region (Fig. 7.8C). The twist of an individual β -strand is left-handed (for “normal,” ie, L amino acids; for D, it would be opposite); as seen from Fig. 7.8B, the strand’s side chains turn clockwise (by about -165° per residue) as the strand comes closer to the viewer.

Because the strands twist, H-bonds turn as well (by about -165° per residue, ie, by $-330^\circ + 30^\circ$ per residue pair, a regular periodic element of the β -structure). As a result, the angle between the neighboring β -strands (viewed from the edge of the sheet, Fig. 7.8A) usually amounts to about -25° (as always, “-” means a clockwise turn of the nearby β -strand about the remote one). Thus, the β -sheet has a left-handed twist if viewed from its edge (and right-handed if viewed along the β -strands, as is usually done).

There are also helices without any hydrogen bonds. Their tight (and hence, energetically advantageous) arrangement is stabilized by van der Waals interactions only. This is exemplified by a polyproline helix consisting of three chains; each chain forms a rather extended left-handed helix. Winding these three chains together forms a *triple right-handed superhelix*. Of two possible types of polyproline helix, that of interest to us is poly(Pro)II (Traub and Piez, 1971), since a helix of this kind is realized in collagen. In this helix, the Pro-peptide groups are in the usual (*trans*)conformation. Let us postpone a detailed consideration of the collagen helix until another time and at the

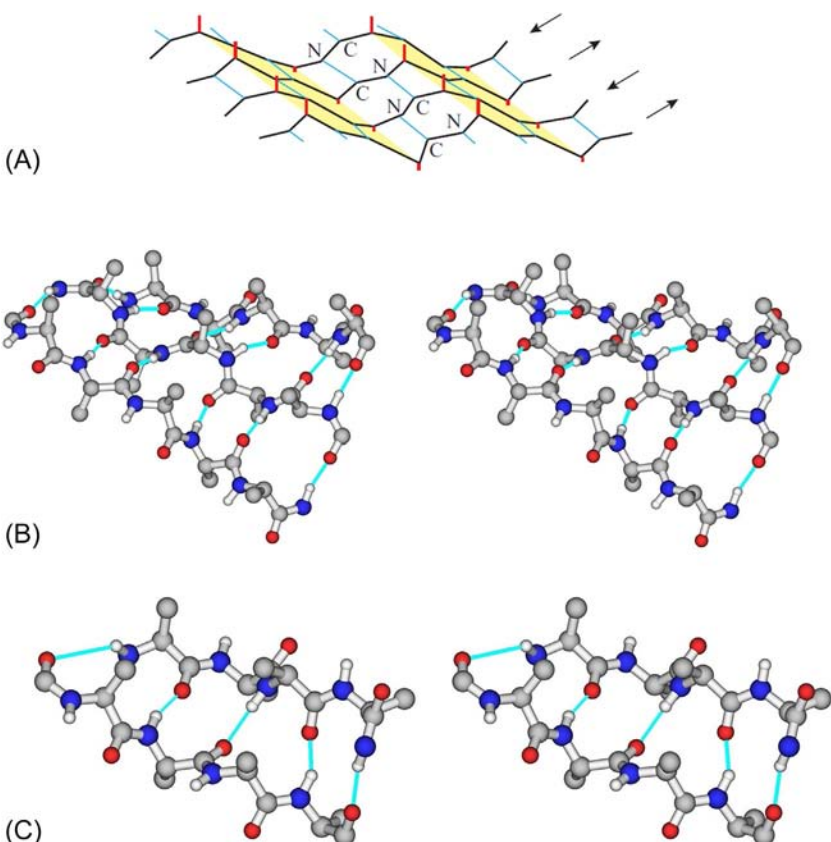


FIG. 7.7 (A) An idealized (nontwisted) antiparallel β -sheet. The β -sheet surface is pleated. The side chains (shown as short red rods here) are at the pleats and directed accordingly; ie, the upward and downward side chains alternate along the β -strand. The H-bonds are shown in light-blue. Adapted from Schulz, G.E., Schirmer, R.H., 1979, 2013. Principles of Protein Structure. Springer, New York (Chapter 5). Below: stereo drawings of β -sheets taken from real protein structures. These β -sheets are twisted a little: (B) an antiparallel β -sheet of three β -strands; (C) a parallel β -sheet of two β -strands.

moment, restrict ourselves to its overall view (Fig. 7.9) and mark in Fig. 7.4 the region P corresponding to its conformation: one can see that it is close to the β -structural conformation.

The features of major regular secondary structures of protein chains are summed up in Table 7.1.

Apart from the regular standard secondary structures, in polypeptide chains there are irregular ones, ie, standard structures that do not form long periodic systems.

The most important are the so-called β -turns (Venkatachalam, 1968) (or β -bends; “ β ” in the name shows that they often bridge the neighboring β -strands

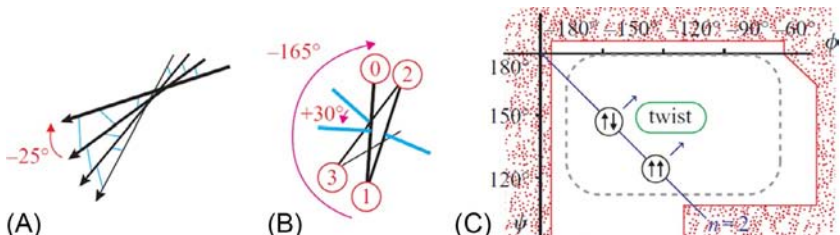


FIG. 7.8 (A) The twist of the β -sheet. β -strands are shown as arrows and hydrogen bonds between them as light-blue lines. (B) Axial view of one turn of the β -strand. Side chains are shown as circles; their numbers increase with increasing distance from the viewer. Blue lines indicate the direction of $C=O$ groups involved in H-bonding in the sheet. The large arrow shows the turn of the β -strand as it comes closer to the viewer by one residue, and the small arrow shows the turn of similarly directed H-bonds when the β -strand comes closer to the viewer by two residues. (C) Conformation of the ideal (nontwisted) parallel ($\uparrow\uparrow$) and antiparallel ($\uparrow\downarrow$) β -structure for poly(Gly), and the averaged conformation of a real twisted β -structure (composed of L amino acids). The dashed line encircles the energy minimum for a separate Ala; the allowed region for its conformations is contoured by the red line. The diagonal of the $\phi\psi$ -map corresponds to the flat regular structure with two residues per turn. Left-handed (L) helices are above the diagonal, and right-handed (R) ones are below it (Ramachandran and Sasisekharan, 1968). (Parts (A) and (C) are adapted from Schulz, G.E., Schirmer, R.H., 1979, 2013. *Principles of Protein Structure*. Springer, New York (Chapter 5).)

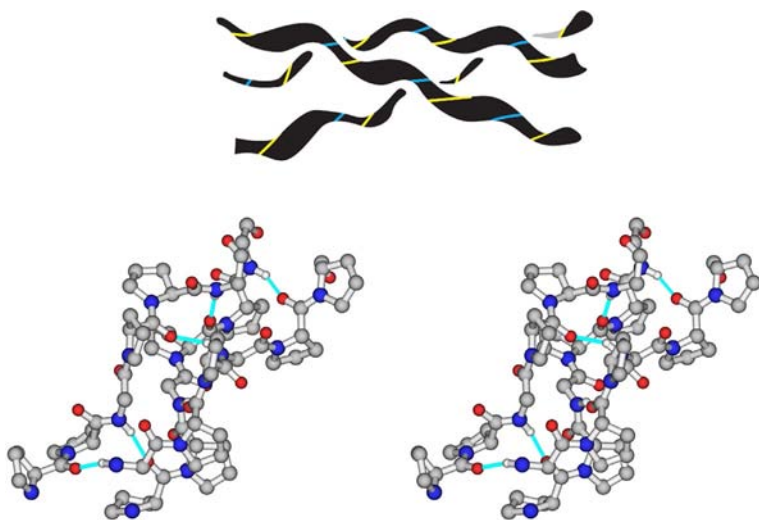


FIG. 7.9 Top: the overall view of poly(Pro)II, the right-handed superhelix composed of three left-handed helices. Below: the collagen triple superhelix (stereo drawing). Each of these three chains consists of Gly-Pro-Pro repeats. H-bonds connect NH-groups of Gly to C' O-groups of the first Pro in the Gly-Pro-Pro triplet: NH group of Gly of chain "1" is bonded to C' O group of Pro of chain "2," and C' O group of Pro of chain "1" is bonded to NH group of Gly of chain "3."

TABLE 7.1 The Main Geometric Parameters of the Most Abundant Secondary Structures in Proteins

Structure	H-Bonding	Residues Per Turn	Shift Per Residue (\AA)	φ (°)	ψ (°)
Helix α_R	$\text{CO}_0-\text{HN}_{+4}$	+3.6	1.5	-60	-45
Helix $(\beta_{10})_R$	$\text{CO}_0-\text{HN}_{+3}$	+3.0	2.0	-50	-25
Sheet $\beta \uparrow \downarrow$	Between chains ^a	-2.3	3.4	-135	+150
Sheet $\beta \uparrow \uparrow$	Between chains ^a	-2.3	3.2	-120	+135
Helix poly(Pro)II	No	-3.0	3.0	-80	+155

Data are from [Schulz and Schirmer \(1979, 2013\)](#) and [Creighton \(1993\)](#). All values are approximate. In the “Residues per turn” column “+” denotes the right-handed helix, and “−” the left-handed.

^aThe distance between strands in the β -sheet is 4.8 Å.

in antiparallel β -hairpins). The appearances of most typical β -bends and conformations of their constituent residues are presented in [Fig. 7.10](#). Compare [Fig. 7.10C](#) with [Fig. 7.4](#) and [Table 7.1](#) and pay attention to the fact that conformations of turn I (and especially of turn III) are close to that of the turn of a β_{10} -helix.

Usually, bends comprise about half of the residues uninvolved in the regular secondary structures of the protein.

Another kind of irregular secondary structure is the β -bulge ([Richardson et al., 1978](#)) ([Fig. 7.11](#)). It is formed by a residue (or sometimes by a few residues) “inserted” in the β -strand and having a non- β -structural conformation. The bulge is typical only for edge strands of a β -sheet (usually of an antiparallel β -sheet); it increases the twist of this sheet and bends it.

A chain without any distinct structure is usually called a “coil.”

When applied to proteins, the term “coil” covers pieces of chains without α and β structures but with a great many various particular conformations. These irregular pieces include β -turns and short portions of polyPro helices ([Adzhubei et al., 1987](#)).

The same term is also applied to unfolded protein chains (ie, those in strong denaturants; [Nozaki and Tanford, 1967](#); [Tanford et al., 1967](#); [Lapanje and Tanford, 1967](#)). Here, it means regions without any regular secondary structure and long-range order in the chain. However, some weak short range order (within a few consecutive residues only) cannot be ruled out in this “coil” (often called a “random coil”).

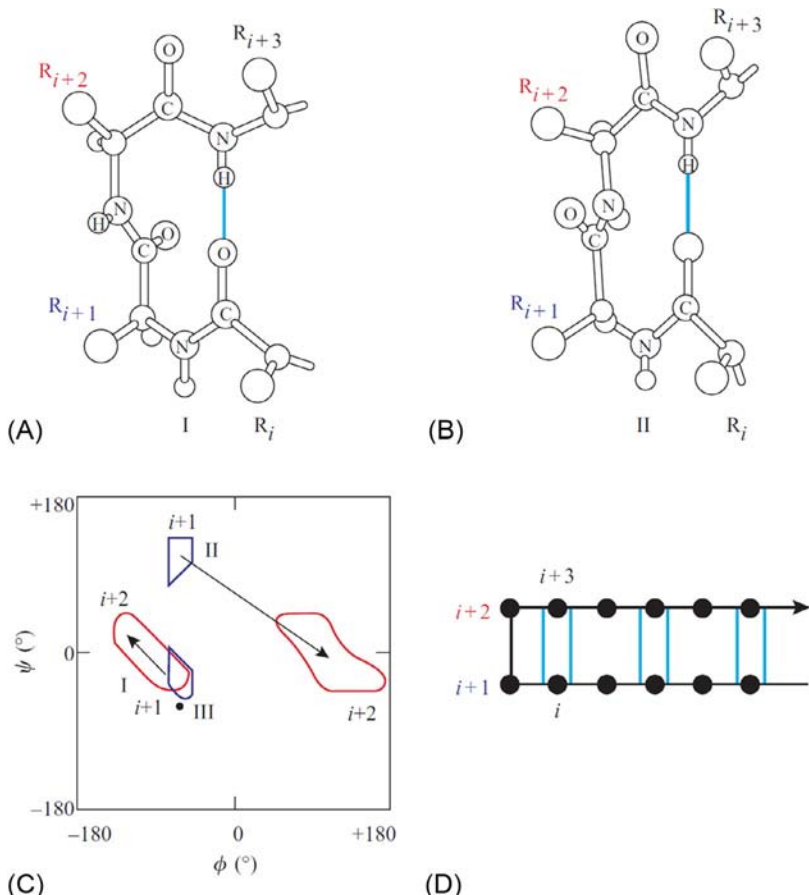


FIG. 7.10 β -turns. (A) The β -turn of type I (type III looks very similar and therefore is not given here). (B) The β -turn of type II. It differs from the β -turn I mainly by the inverted peptide group between the residues $i+1$ and $i+2$. (C) Conformations of the residues $i+1$ and $i+2$ are fixed by the H-bond closing the β -turns. In the β -turn III both these residues have the same conformation (denoted with a bold dot). The conformations of residues i and $i+3$ are not fixed in β -turns; they are fixed by the β -structure, when this structure extends the turn as shown in (D), which sketches a β -hairpin with the β -turn at its top. H-bonds are shown in light-blue. (Parts (A), (B), and (C) are adapted from Schulz, G.E., Schirmer, R.H., 1979, 2013. *Principles of Protein Structure*. Springer, New York (Chapter 5).)

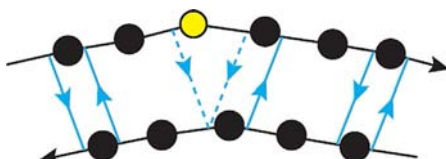


FIG. 7.11 The β -bulge in an antiparallel β -structure. Hydrogen bonds are shown as blue arrows directed from N-H to O=C groups. All residues (shown as circles) have β -structural conformations, except for that shown as a yellow circle, whose conformation is often nearly α -helical. One or even both H-bonds adjacent to this residue (shown by broken arrows) may be broken.

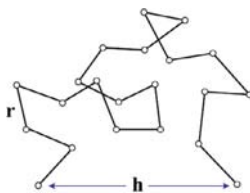


FIG. 7.12 The freely joint (“random-flight”) chain: the simplest model of a random coil.

The most interesting features of the random coil (experimentally observed by using hydrodynamic techniques and light- and X-ray scattering ([Tanford et al., 1967; Lapanje and Tanford, 1967](#)) are its extremely low density and large volume, and a most peculiar dependence of its radius and volume on the chain length.

To shed light upon this peculiarity, let us consider the simplest model of a random coil, the so-called “loose joint chain” ([Birshtein and Ptitsyn, 1966; Flory, 1969; Volkenstein, 1977](#)), see Fig. 7.12. Its “links” are represented as sticks (each link can include a few chain monomers); the main distinctive feature of this model is that each stick can freely turn on the joint about the neighboring sticks. Let us assume that there are M sticks in the chain, and the length of each stick is r .

Such a chain can be described as a sequence of vectors $\mathbf{r}_1, \mathbf{r}_2, \dots, \mathbf{r}_M$ (may I remind you that in math a vector is a directed straight segment). These vectors have identical lengths r , and each of them is directed from the previous joint to the next one.

The sum of these vectors, $\mathbf{h} = \sum_{i=1}^M \mathbf{r}_i$, is just a vector running from the beginning of the chain to its end.

The average over all possible thermal fluctuations vector $\langle \mathbf{h} \rangle = 0$, because each vector \mathbf{r}_i can have any direction.

Now let us find $\langle \mathbf{h}^2 \rangle$, the average value of \mathbf{h}^2 ; ie, let us have \mathbf{h}^2 averaged over all possible thermal fluctuations of the chain conformation (this averaging is denoted by $\langle \rangle$). The squared length of \mathbf{h} is

$$\mathbf{h}^2 = \left(\sum_{i=1}^M \mathbf{r}_i \right)^2 = \sum_{i=1}^M \mathbf{r}_i^2 + \sum_{i=1}^M \sum_{j=1, j \neq i}^M \mathbf{r}_i \mathbf{r}_j \quad (7.1)$$

When averaging \mathbf{h}^2 , we have to keep in mind that $\langle \mathbf{r}_i^2 \rangle$, t average squared vector \mathbf{r}_i , is just r^2 , and the average scalar product of any vectors $\langle \mathbf{r}_i \mathbf{r}_j \rangle$ is zero when $i \neq j$, since free rotation of sticks provides equal probabilities of any direction of these vectors.

Hence, the average squared distance between the ends of a loose joint chain is:

$$\langle \mathbf{h}^2 \rangle = \left\langle \sum_{i=1}^M \mathbf{r}_i^2 \right\rangle + \left\langle \sum_{i=1}^M \sum_{j=1, j \neq i}^M \mathbf{r}_i \mathbf{r}_j \right\rangle = \sum_{i=1}^M \langle \mathbf{r}_i^2 \rangle + \sum_{i=1}^M \sum_{j=1, j \neq i}^M \langle \mathbf{r}_i \mathbf{r}_j \rangle = M r^2 \quad (7.2)$$

ie, the linear dimensions (radius, etc.) of the coil increase with increasing number of chain links M as $M^{1/2}$. Consequently, the coil volume is proportional to $M^{3/2}$ although the volume of all “normal” (ie, fixed density) bodies increases only as the number of particles M , that is, much more slowly than $M^{3/2}$. This abnormally strong dependence of the coil volume on the chain length is the most prominent characteristic feature of the random coil. Specifically, this feature is responsible for the extremely low density of a coil formed by long chains, and consequently, for nearly zero contacts between distant links in the chain.

In addition, since the coil volume is proportional to $M^{3/2}$ and the probability that the chain ends meet is inversely proportional to the volume occupied by the coil, the probability of chain ends meeting is proportional to $M^{-3/2}$. This means that the free energy of loop closing in a coil-like chain increases with its length as $kT \times (3/2) \ln(M)$ (Flory, 1969), where $k \times (3/2) \ln(M)$ is the Flory’s entropy of loop closure.

The free joint model presents a far too ideal coil in which any link may rotate by any angle, which is not actually true. However, Eq. (7.2) can be generalized as:

$$\langle \mathbf{h}^2 \rangle = Lr \quad (7.3)$$

where $L = Mr$ is the full (“contour”) length of the chain proportional to the number of its constituent links, and r is the effective distance between the chain “free joints,” ie, the characteristic length after which the chain “forgets” its direction (*note*: in a polypeptide chain, this characteristic length, also called the “length of the Kuhn segment,” is 30–40 Å (when the polypeptide includes neither too flexible Gly nor too rigid Pro), ie, the Kuhn segment includes about 10 amino acid residues (Flory, 1969)).

The equation for the coil size presented as Eq. (7.3) is general enough to be applied in the description of real polymers.

The more realistic “freely-rotating” model of the random coil (Fig. 7.13) gives the following estimate of the Kuhn segment length r (Birshtein and Ptitsyn, 1966; Flory, 1969):

$$r = l \frac{1 + \langle \cos \alpha \rangle}{1 - \langle \cos \alpha \rangle} \quad (7.4)$$

where l is the distance between the points where the chain turns (ie, the covalent bond length) and $\langle \cos \rangle$ is the average cosine of the turn angle (see Fig. 7.13).

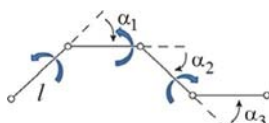


FIG. 7.13 The freely-rotating model of the random coil. Here, the “links” are again represented as sticks of equal lengths l ; each stick can freely rotate about the axis formed by the preceding stick; α_1 , α_2 , ... are angles between adjacent sticks.

In conclusion, a few words on how the secondary structure is determined by experiment. Of course, with X-ray (or accurate multidimensional NMR (nuclear magnetic resonance)) protein structures available (Fig. 7.14), the secondary structure can be derived from atomic coordinates. However, this is hardly possible for disordered proteins or unfolded protein chains. Nevertheless, by detecting closely positioned H-atom nuclei (with $<4\text{--}5\text{ \AA}$ between them), NMR reveals the secondary structure (mainly, α and β) even in these cases (Serdyuk et al., 2007).

NMR spectroscopy is based on applying radiowaves to excite the magnetic moments of nuclei aligned in a strong magnetic field. These nuclei must have an odd number of nucleons (protons and neutrons): then they have a magnetic moment, or spin. In proteins, these are natural “light” hydrogens (^1H), as well as introduced isotopes (^{13}C , ^{15}N , etc.). A key role in structure determination is played by NOESY (nuclear Overhauser effect spectroscopy). The magnetic resonance occurs at a radio frequency typical (in the given magnetic field) of the nucleus in question and slightly modified by its neighbors in chemical bonds and in space (which helps us to understand which atom of which residue is excited) (Serdyuk et al., 2007). The excitation can be propagated from the initial nucleus to a neighboring one (if it has a magnetic moment); the recipient will report on its excitation at its own frequency, thereby demonstrating the closeness of the two nuclei.

The characteristic feature of α -helices is the closeness of the H atom of the C^αH -group to that of the NH-group of the fourth residue down the chain (towards the C-terminus), while the typical feature of the β -structure is closeness between H atoms of NH- and C^αH -groups pertaining to immediate neighbors in the chain and to H-bonded residues in the β -sheet (Figs. 7.14B and 7.15).

However, the most important role in determining the secondary structure (mainly, α and β) is played by circular dichroism (CD) (Greenfield and Fasman, 1969; Creighton, 1993; Serdyuk et al., 2007).

For CD, a knowledge of the overall spatial structure of the protein is not required. On the contrary, structural studies of a protein are usually started with CD. This method is based on differing absorptions of clockwise and

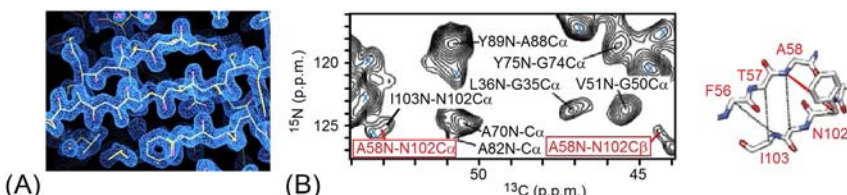


FIG. 7.14 (A) Region of electron density map with the β -structure. (B) A part of the 2D NOESY spectrum; two cross-peaks corresponding to a portion of the β -structure (shown on the right) are marked in red. (The images are taken from <http://learn.crystallography.org.uk/wp-content/uploads/2014/01/electronDensity.jpg> and <http://www.nature.com/nmeth/journal/v9/n12/images/nmeth.2248-F1.jpg>, respectively.)

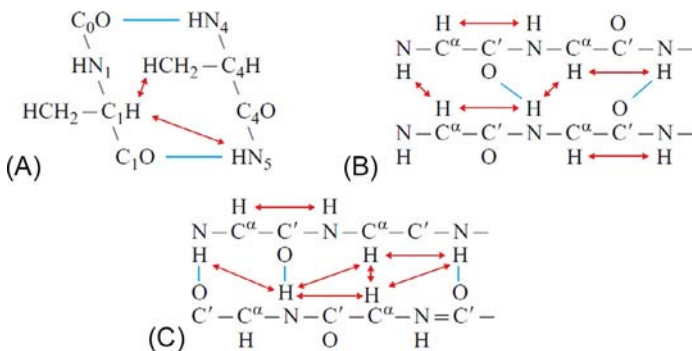


FIG. 7.15 Approach (\leftrightarrow) of the nuclei of H-atoms characteristic of the α -helix (A), and of the parallel (B) and antiparallel (C) β -structure. In (A), indices at atoms of the main chain indicate the relative location of residues in the chain.

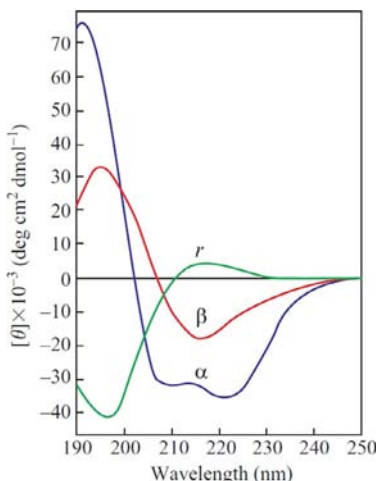


FIG. 7.16 Typical far UV CD spectra for polylysine as the α -helix (α), β -structure (β), and random coil (r). (Adapted from Greenfield, N.J., Fasman, G.D., 1969. Computed circular dichroism spectra for the evaluation of protein conformation. Biochemistry 8, 4108–4116.)

counterclockwise polarized light, which are caused specifically by helices of different handedness. Owing to this difference, plane-polarized light turns into elliptically polarized light.

The typical ellipticity spectra for the “far UV region” (190–240 nm) are given in Fig. 7.16. These spectra depend on the asymmetry of the peptide group environment, and therefore report on the secondary structure.

The optical excitation of peptide groups in the far UV region occurs at a wavelength of about 200 nm. This wavelength is approximately twice as large as that required for excitation of separate atoms. The possibility to excite a

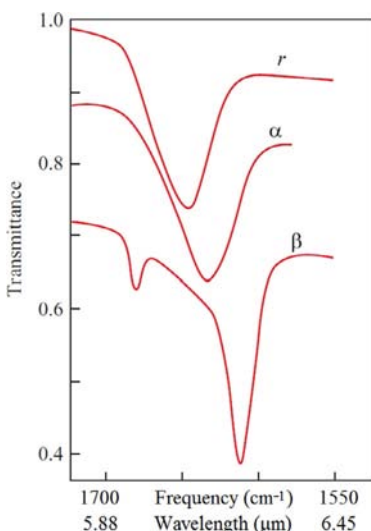


FIG. 7.17 Typical infrared (IR) transmittance spectra measured in heavy water (D_2O) for polylysine as the α -helix (α), β -structure (β), and random coil (r). The measurements were taken in the “amide I” region, reflecting vibrations of the $C=O$ bond. (Adapted from Susi, H., 1972. Infrared spectroscopy—conformation. *Methods Enzymol.* 26, 455–472.)

peptide group with light of lower frequency is explained by delocalization of electrons over the group, which has been discussed previously.

In aromatic side groups, delocalization of electrons is still greater: here, they are “spread over” six atoms (while in peptide groups over three atoms). The CD spectra for aromatic groups fall within the wavelengths of about 250–280 nm (although their “tails” can reach even 220 nm). In this range of 250–280 nm (in the “near-UV region”) the asymmetry of aromatic side-chain environments is studied, ie, the effects characteristic of not the secondary but the tertiary structure of the protein (Creighton, 1993; Serdyuk et al., 2007).

In passing, I could add that when the electron is delocalized still more (ie, in larger molecules with double partial bonds) its excitation moves from UV to visible (400–600 nm) light, and such molecules become dyes.

Apart from UV spectra, IR spectra can be exploited to reveal the secondary structure of polypeptides and proteins. They reflect the difference in vibration of peptide groups involved and uninvolved in various secondary structures (Susi, 1972; Creighton, 1993; Serdyuk et al., 2007) (Fig. 7.17). These measurements are more complicated than study of UV spectra, since the absorption range of ordinary water (H_2O) is nearly the same; therefore, heavy water (D_2O) is used. Also, these measurements, compared with UV ones, require more protein to be used and a higher protein concentration in solution.

REFERENCES

- Adzhubei, A.A., Eisenmenger, F., Tumanyan, V.G., Zinke, M., Brodzinski, S., Esipova, N.G., 1987. Third type of secondary structure: noncooperative mobile conformation. Protein Data Bank analysis. *Biochem. Biophys. Res. Commun.* 146, 934–938.
- Birshtein, T.M., Ptitsyn, O.B., 1966. Conformations of Macromolecules. Interscience Publishers, New York (Chapters 4, 9).
- Branden, C., Tooze, J., 1999. Introduction to Protein Structure, second ed. Garland, New York (Chapter 2).
- Cantor, C.R., Schimmel, P.R., 1980. Biophysical Chemistry. W.H. Freeman, New York (Part 1, Chapters 2, 5).
- Chothia, C., 1973. Conformation of twisted beta-pleated sheets in proteins. *J. Mol. Biol.* 75, 295–302.
- Creighton, T.E., 1993. Proteins: Structures and Molecular Properties, second ed. W.H. Freeman, New York (Chapter 5).
- Flory, P.J., 1969. Statistical Mechanics of Chain Molecules. Interscience Publishers, New York (Chapters 1–3, 7–8; Appendix G).
- Greenfield, N.J., Fasman, G.D., 1969. Computed circular dichroism spectra for the evaluation of protein conformation. *Biochemistry* 8, 4108–4116.
- Lapanje, S., Tanford, C., 1967. Proteins as random coils. IV. Osmotic pressures, second virial coefficients, and unperturbed dimensions in 6 M guanidine hydrochloride. *J. Am. Chem. Soc.* 89, 5030–5033.
- Nozaki, Y., Tanford, C., 1967. Proteins as random coils. II. Hydrogen ion titration curve of ribonuclease in 6 M guanidine hydrochloride. *J. Am. Chem. Soc.* 89, 742–749.
- Pauling, L., Corey, R.B., 1951a. Atomic coordinates and structure factors for two helical configurations of polypeptide chains. *Proc. Natl. Acad. Sci. U. S. A.* 37, 235–240.
- Pauling, L., Corey, R.B., 1951b. The pleated sheet, a new layer configuration of polypeptide chains. *Proc. Natl. Acad. Sci. U. S. A.* 37, 251–256.
- Pauling, L., Corey, R.B., Branson, H.R., 1951. The structure of proteins; two hydrogen-bonded helical configurations of the polypeptide chain. *Proc. Natl. Acad. Sci. U. S. A.* 37, 205–211.
- Ptitsyn, O.B., Finkel'shtein, A.V., 1970. Predicting the spiral portions of globular proteins from their primary structure. *Dokl. Akad. Nauk SSSR* (in Russian) 195, 221–224.
- Ramachandran, G.N., Sasisekharan, V., 1968. Conformation of polypeptides and proteins. *Adv. Protein Chem.* 23, 283–438.
- Richardson, J.S., Getzoff, E.D., Richardson, D.C., 1978. The β -bulge: a common small unit of non-repetitive protein structure. *Proc. Natl. Acad. Sci. U. S. A.* 75, 2574–2578.
- Schulz, G.E., Schirmer, R.H., 1979, 2013. Principles of Protein Structure. Springer, New York (Chapter 5).
- Serdyuk, I.N., Zaccai, N.R., Zaccai, J., 2007. Methods in Molecular Biophysics: Structure, Dynamics, Function. Cambridge University Press, Cambridge (Chapters H1–H3, J1–J2).
- Susi, H., 1972. Infrared spectroscopy—conformation. *Methods Enzymol.* 26, 455–472.
- Tanford, C., Kawahara, K., Lapanje, S., Hooker Jr., T.M., Zarlengo, M.H., Salahuddin, A., Aune, K.C., Takagi, T., 1967. Proteins as random coils. III. Optical rotatory dispersion in 6 M guanidine hydrochloride. *J. Am. Chem. Soc.* 89, 5023–5029.
- Traub, W., Piez, K.A., 1971. The chemistry and structure of collagen. *Adv. Protein Chem.* 25, 243–352.
- Venkatachalam, C.M., 1968. Stereochemical criteria for polypeptides and proteins. V. Conformation of a system of three linked peptide units. *Biopolymers* 6, 1425–1436.
- Volkenstein, M.V., 1977. Molecular Biophysics. Academic Press, New York (Chapters 4, 6).

Lecture 8

At this point, we could pass on to the formation and decay of the secondary structure. However, prior to that I would like to talk about the fundamentals of statistical physics, thermodynamics, and kinetics “in general,” inasmuch as otherwise it is difficult to discuss the stability of the secondary structure, the stability of proteins, cooperative transitions in polypeptides and proteins and the kinetics of these transitions.

Thermodynamics provides an idea of the types of possible cooperative transitions in systems incorporating a great many particles. Statistical physics advises on when and what transitions may occur in the system of particles in question and gives details of these transitions based on the properties of the studied particles and their interactions.

First of all, we will consider the main concepts of statistical physics and thermodynamics, namely, entropy, temperature, free energy and partition function. In doing this, I will follow the generally recognized books *The Feynman Lectures on Physics* (Feynman et al., 1963) and *Statistical Physics* by Landau and Lifshitz (1980).

Systems with numerous degrees of freedom (ie, comprising a lot of molecules or even just one large and flexible molecule) are described by means of statistical physics. It is “statistical” because such a large system has zillions of configurations. Here is an illustrative example. If each of N links of a chain may have only two configurations (eg, “helical” and “extended” ones), then the whole N -link chain has 2^N possible configurations. In other words, a “normal” 100-link protein chain may have at least 2^{100} configurations, that is, about 1 000 000 000 000 000 000 000 000 000 000 000 000 of them! This is an enormous number. Consideration of all of them at a rate of 1 nanosecond (10^{-9} s) per configuration would take 3×10^{13} years, that is more than 1000 lifetimes of the Universe... And in the experimental tube, there are billions of such chains, not to mention the solvent. If we had been going to consider all their configurations, we would have been lost forever. Certainly, we are interested in much more simple and reasonable things, such as the average (ie, *statistically averaged*) helicity of chains and its change upon heating. A peculiar feature of statistical averaging (ie, neglecting all minor details) is a crucial simplification of events.

In statistical averaging, the major role is played by *entropy*. It shows how many configurations (in other words, *microstates*) of the system correspond to its observed *macrostate* (averaged by the observation time and the number of molecules studied). We considered a similar example earlier, though it was only a special case with the number of *microstates* in space for a molecule limited by a volume, and the entropy of the molecule proportional to the

logarithm of this volume (and the molecule's being in the given volume, eg, "in this room," was the "macrostate" of the molecule).

Here, it would be timely to answer the question that is only natural: Why do physicists prefer to consider the *logarithm* of microstate number but not the number itself? The answer is that in considering many separate systems (eg, separate molecules) we have to sum up their energies and degrees of freedom, while the numbers of accessible states are to be multiplied (if one molecule has ten microstates and another as many, these two molecules have 100 different combinations of microstates). This makes the calculations inconvenient and too bulky. But *logarithms* of the numbers of accessible states are to be summed up (you remember that $\ln(AB)=\ln(A)+\ln(B)$), like energies or volumes. Therefore, the logarithms are convenient for calculations. Moreover, the additivity of logarithms allows us to use the potent differential calculus.

Now let us talk about *temperature*, or rather, *absolute temperature*.

First: Why, from the times of Clapeyron and Kelvin, is it counted off -273°C ?

Because (unlike 0°C , the melting point of one of a great many crystals) this point is *universal*: it is obtained by extrapolation to zero of $PV=\text{pressure} \times \text{volume}$ of *all* quantities of *all* gases (Fig. 8.1).

Inner voice: But these extrapolations ignore all visible deviations of experimental points from the straight lines that extrapolate only the linear middles of the PV -on-temperature dependencies!

Lecturer: Exactly! Such deviations are connected with either the gas to liquid transition (at low temperatures) or with dissociation of gas molecules (at too high temperatures). And without *ignoring* these "side-effects," a universal law would be never derived! Note that blind adherence to experiment can prevent from discovering a universal gas law, which can be screened by various "side-effects" such as gas condensation, etc., of various substances...

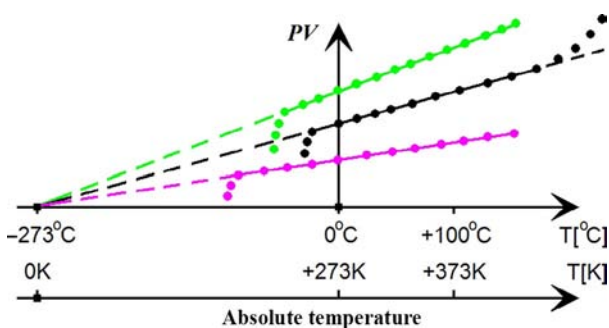
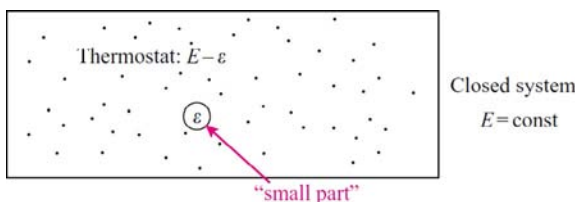


FIG. 8.1 A scheme of determination of the zero point of absolute temperature from extrapolation to zero of $PV=\text{pressure} \times \text{volume}$ of various quantities of various gases at various (but not too high) pressures. Dots represent "experimental" points, dashed lines show extrapolations of linear parts of the PV -on-temperature dependencies.

Second: It is to be shown that *temperature* (which is now only a phenomenological concept) is closely connected with entropy: *where there's no numerous states (no entropy), there's no temperature either.*

To clarify this connection, let us follow J.W. Gibbs and consider a closed system (with no energy exchange with the environment). Let its total energy be E , and let this system be in equilibrium, that is, all its microstates with the energy E are equally probable (and those of different energy $E' \neq E$ have zero probability).

Let us pick out an “observed small part” of the system (eg, a molecule in gas or a macromolecule with its liquid environment). Then the rest of the system may be regarded as a thermostat in which the “small part” is immersed.



Let us divide all the system’s microstates having the total energy E into such classes that each of them corresponds to one microstate of the chosen “small part.” The more microstates incorporated in a given class, the higher probability of observation of this class, that is, the higher the probability of observation of a certain state of our “small part.”

Let a microstate of our “small part” be given (eg, let a molecule in gas have a certain position in space and a certain speed). Let its energy be ε . Since the system (“small part”+“thermostat”) is closed, *its total energy E is conserved* (as stated by the energy conservation law), and thus the thermostat energy is $E - \varepsilon$. Let as many as $M_{\text{therm}}(E - \varepsilon)$ of thermostat microstates correspond to this energy. Then the probability of observation of this state of our “small part” is simply proportional to $M_{\text{therm}}(E - \varepsilon)$.

Note: Here, an implicit assumption has been made that a certain microstate of the system produces no effect on thermostat microstates. Strictly speaking, this is not quite true (or rather, this is true only for an ideal gas as the thermostat), but taking into consideration all events at the border of “our system” and the thermostat would obscure the entire narration. So, to combine strictness and clearness, let us assume for the time being that our “observed part” is encapsulated and thereby separated from thermostat molecules; if required (not in these lectures), the interaction between the “observed part” and the thermostat can be considered separately.

With the number of the thermostat states equal to $M_{\text{therm}}(E - \varepsilon)$, its logarithm *by definition* is proportional to the thermostat entropy:

$$S_{\text{therm}}(E - \varepsilon) = \kappa \ln [M_{\text{therm}}(E - \varepsilon)] \quad (8.1)$$

The coefficient κ is used here only to have the entropy measured in cal K⁻¹, as usual; as you will see later, it appears to be simply the Boltzmann constant.

The energy of the “small part” ε must be relatively small as well. Therefore, we can use an ordinary differential expansion of $S_{\text{therm}}(E - \varepsilon)$ over the small parameter ε (you may remember that $f(x_0 + dx) = f(x_0) + dx \frac{df}{dx}|_0 + \frac{1}{2} (dx)^2 \frac{d^2f}{dx^2}|_0 + \dots = f(x_0) + dx \frac{df}{dx}|_0$ at a small dx with $(df/dx)|_0$ meaning that the derivative df/dx is taken at the point x_0). So,

$$S_{\text{therm}}(E - \varepsilon) = S_{\text{therm}}(E) - \varepsilon \times (\frac{dS_{\text{therm}}}{dE})|_E \quad (8.2)$$

Note: Since both S and E are proportional to the number of particles, dS_{therm}/dE is independent of the number of particles in the thermostat, while d^2S_{therm}/dE^2 is *inversely* proportional to this number, that is, $d^2S_{\text{therm}}/dE^2 \rightarrow 0$ in a very large thermostat; this allows us to neglect members of the order of ε^2 (as well as ε^3 , etc.) in Eq. (8.2).

Thus, the number of accessible thermostat microstates depends on the energy ε of our “small part” as

$$\begin{aligned} M(E - \varepsilon) &= \exp \left[\frac{S_{\text{therm}}(E - \varepsilon)}{\kappa} \right] \\ &= \exp \left[\frac{S_{\text{therm}}(E)}{\kappa} \right] \times \exp \left\{ -\varepsilon \left[\frac{(\frac{dS_{\text{therm}}}{dE})|_E}{\kappa} \right] \right\} \end{aligned} \quad (8.3)$$

Here, neither the common multiplier $\exp[S_{\text{therm}}(E)/\kappa] = M(E)$ nor the number $(dS_{\text{therm}}/dE)|_E$ depends on ε or on a concrete microstate of our “small part” in general.

Since the number of microstates must increase with increasing energy (the higher the energy, the greater the number of ways it can be divided), Eq. (8.3) expresses the following simple idea: the more energy taken from the thermostat by our “small part,” the less energy kept by the thermostat, and hence, the smaller the number of ways it can be divided. Moreover, this equation shows that the decrease of the number of accessible thermostat microstates (the number of ways to divide its energy) depends *exponentially* on the energy of our “small part.”

Conclusion: The probability of observation of a certain microstate of our “small part” (molecule, etc.) is proportional to $\exp[-\varepsilon \{(\frac{dS_{\text{therm}}}{dE})|_E/\kappa\}]$, where ε is the energy of this “small part,” and the magnitude $\{(\frac{dS_{\text{therm}}}{dE})|_E/\kappa\}$ depends *not* on the “small part” but only on averaged features of its environment.

But according to Boltzmann (=Boltzmann–Gibbs) distribution, the probability of a molecule keeping a certain state with energy ε is proportional to $\exp(-\varepsilon/k_B T)$ (where T is temperature, and k_B is the Boltzmann constant). A comparison of the identical expressions $\exp[-\varepsilon \{(\frac{dS_{\text{therm}}}{dE})|_E/\kappa\}]$ and $\exp(-\varepsilon/k_B T)$ yields

$$(dS_{\text{therm}}/dE)|_E = \frac{1}{T} \quad (8.4)$$

and κ in Eqs. (8.1) and (8.3) turns out to be the Boltzmann constant (k_B), provided the energy is measured (as usual) in Joules (J) (or in calories, cal), temperature in K, and entropy in $J K^{-1}$ (or in cal K^{-1}).

Eqs. (8.1) and (8.4) are the main equations of statistical physics and thermodynamics: they define the temperature as the reciprocal of the rate of entropy (or of the logarithm of the number of microstates) change with the system energy E .

In particular, they show that $\ln[M(E+k_B T)] = S(E+k_B T)/k_B = [S(E)+(k_B T)(1/T)]/k_B = \ln[M(E)] + 1$, that is, an energy increase by $k_B T$ results in an “e” ($=2.72$)-fold (approximately three-fold) increase of the number of microstates, *independently* of the system size, its inner forces, etc.

They also allow us to find the corresponding temperature value for each energy of any large system (thermostat), provided we know the number of its microstates at different energies (also called the “energy spectrum density”), or rather, the dependence of the logarithm of the energy spectrum density on this energy. The schematic diagram is given in Fig. 8.2.

It is essential that the microstates are highly numerous because the derivative dS/dE can be taken only when a small (as compared with $k_B T$) energy interval houses many microstates. That is why temperature appears only in sciences dealing with enormous numbers of accessible states.

Let us continue considering a small system in the thermostat whose temperature is equal to T . Eqs. (8.1) and (8.3) show that for our system the probability of being in a given state i with the energy e_i at temperature T is

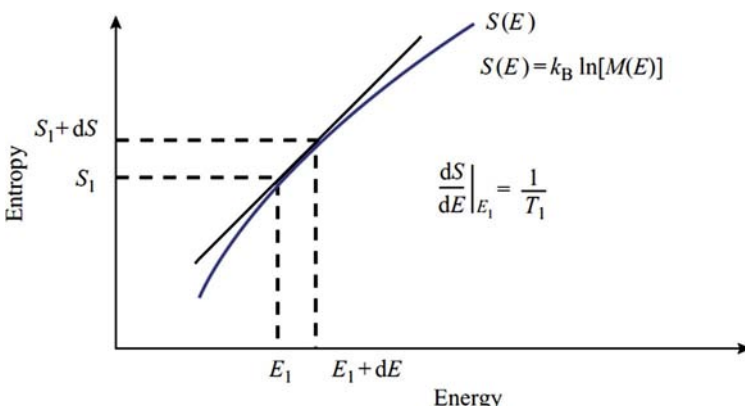


FIG. 8.2 Determination of the temperature of a large system. The bold curve shows the dependence of entropy S on the system energy E . The curve slope, dS/dE , determines the temperature T corresponding to this energy E . $M(E)$ is the number of microstates with the energy E , that is, the density of the energy spectrum of the system.

$$w_i(T) = \frac{\exp(-\varepsilon_i/k_B T)}{Z(T)} \quad (8.5)$$

where

$$Z(T) = \sum_j \exp(-\varepsilon_j/k_B T) \quad (8.6)$$

is the normalization factor which takes into account that the sum of probabilities of all states, $\sum_j w_j$ is necessarily equal to 1 (here and above the sum \sum_j is taken over all microstates j of the studied “small system”).

The value Z is called *partition function* for the studied system. Provided Z is known, Eq. (8.5) allows us to calculate the probability w of each microstate of this system at a given temperature. Then the average energy of the system at this temperature

$$E(T) = \sum_j w_j \varepsilon_j \quad (8.7)$$

and its average entropy

$$S(T) = k_B \sum_j w_j \ln(1/w_j) \quad (8.8)$$

Note that Eq. (8.8) averages $\ln(1/w_j)$ over all microstates j of the system, allowing for their probabilities w_j . This equation provides a direct generalization of the determination of entropy $S = k_B \ln[M(E)]$ already familiar to us (see Eq. 8.1). This is a generalization of averaging for the case when w_j have more than only two values that follow from the energy conservation law: $w_j = 1/M(E)$ for all $M(E)$ states where $E_j = E$ and $w_j = 0$ when $E_j \neq E$.

Inner voice: I feel that the meaning of Eq. (8.8) must be explained better, and that the term $S(T)/k_B$ should be proved to be the logarithm of the average number of system states.

Lecturer: Then, please be tolerant and we will go into some maths...

Following J.W. Gibbs, let us consider a large number N of equal systems each of which may be in the state “1” with the probability w_1 , in the state “2” with the probability w_2 , ..., in the state “ J ” with the probability w_J . Then on average, among N systems considered, those in the state “1” amount to $n_1 = w_1 N$, those in the state “2” amount to $n_2 = w_2 N$, and so on (while $\sum_j w_j N \equiv \sum_j n_j = N$).

$\frac{N!}{n_1! \times n_2! \times \dots \times n_J!}$ is the well-known number of different ways to divide N systems yielding n_1 of them having state “1”, n_2 having state “2”, ..., n_J having state “ J ” (here, $N! \equiv N \times (N-1) \times \dots \times 2 \times 1$ is the number of different enumerations of the N systems, $n_1!$ is the number of enumerations of n_1 systems having the identical state “1”, etc.). Now we use Stirling’s approximation $n! \approx (n/e)^n$ and obtain $\frac{N!}{n_1! \times n_2! \times \dots \times n_J!} \approx \prod_j \left(\frac{N}{n_j}\right)^{n_j} = \left[\prod_j \left(\frac{1}{w_j}\right)^{w_j}\right]^N$.

And since this number (the total number of states for N independent

systems) is simply the number of states of one system to the N th power, the average number of states of *one* system is equal to $\prod_j \left(\frac{1}{w_j}\right)^{w_j}$, and its logarithm is (as it has been expected to be) the term $S(T)/k_B$ of Eq. (8.8). That's all.

The partition function (which may seem to be simply the normalization coefficient in Eq. (5)) plays a most important role in statistical physics because the quantity $Z(T)$ allows direct calculation of the free energy of a system enclosed in a fixed volume,

$$F(T) = E(T) - TS(T) = \sum_j w_j \{ \epsilon_j - T[-k_B \ln(w_j)] \} = -k_B T \ln[Z(T)] \quad (8.9)$$

(here we used Eqs. (8.7) and (8.8) and then Eq. (8.5)).

Derivatives of F determine all other thermodynamic functions:

$$S(T) = -dF/dT$$

We have already seen this equation; please check it up by yourselves using Eqs. (8.9), (8.6), (8.5), (8.8); and

$$E(T) \equiv F(T) + TS(T) = F(T) - T(dF/dT) \equiv d(F/T)/d(1/T).$$

Important secondary notes:

1. If the “small system” has many degrees of freedom, it has its own entropy and therefore its own (internal) temperature. The internal temperature of the “small system,” T_{in} , is equal to the thermostat temperature T because, as follows from the above definitions and equations, $T_{in} \equiv dE_{in}(T)/dS_{in}(T) = d[F_{in}(T) - T(dF_{in}/dT)]/d(-dF_{in}/dT) = [dF_{in}/dT - T(d^2F_{in}/dT^2) - dF_{in}/dT] dT / (-d^2F_{in}/dT^2) dT = T$.
2. The total energy incorporates kinetic and potential energies. The former depends on particle speeds only, while the latter on their positions in space, and not on the speeds. The “microstate” of each particle is determined by its coordinate in space and by its speed. In classical (not quantum) mechanics, any combinations of speeds and coordinates are allowed (as we know, Heisenberg’s Quantum Uncertainty Principle, $\Delta v \Delta x \approx \hbar/m$, imposes restrictions on the speed–coordinate combinations, but at room temperature this is important for very light particles, ie, virtually electrons only). This means that probabilities for coordinates and speeds can be “uncoupled,” that is, $w(\epsilon_{kinet} + \epsilon_{coord}) \sim \exp(-\epsilon_{kinet}/kBT) \times \exp(-\epsilon_{coord}/kBT)$. Further simple calculations (you can make them yourselves) will show that free energies, energies and entropies can also fall into kinetic and coordinate parts, that is, $F = F^{kinet} + F^{coord}$, etc. It is important that kinetic parts are *independent* of the system configuration and can be neglected when considering

conformational changes. Therefore, further on we will discuss *only* configurational (or “conformational”) energy spectra, energies, entropies, etc.

3. Above, we summed over microstates, whereas in the frame of classical mechanics we can equally well integrate over coordinates and speeds that determine the microstate of each particle.
4. Equilibrium temperature must be *positive*. Otherwise, probability integration over speeds, that is, $\int \exp(-mv^2/2k_B T) dv$, turns into infinity at great speeds, and the system “explodes.” Therefore, the stable state cannot be observed in those conformational energy spectrum regions where the spectrum density (and, hence, the entropy of the system) decreases with increasing energy: for these regions, $T < 0$ (see Eqs. (8.4) and (8.1), and Fig. 8.3A).
5. The quantity $k_B T$ is measured in units such as “energy per particle” or “energy per mole ($=6.02 \times 10^{23}$) of particles.” Had temperature been expressed in energy units from the very outset, Boltzmann’s constant k_B would never have been used at all. However, historically it happened that the “degree” was first introduced as a temperature unit, and then it became evident that it could be easily converted into something like “energy per particle” through multiplying by a certain (Boltzmann) constant. Accordingly, k_B is measured in the units “energy per particle per degree.” Its numerical value depends on the energy unit used: “joule per particle,” “calorie per mole of particles,” etc. In accordance with the measured in joules energy cost of a “degree” (K), $k_B = 1.38 \times 10^{-23}$ joule particle $^{-1}$ K $^{-1}$. However, apart from “per particle,” k_B can be calculated per mole ($=6.02 \times 10^{23}$) of particles. To do this we multiply and divide k_B by 6.02×10^{23} , and have: $k_B = 1.38 \times 10^{-23}$ (joule/particle/degree) $= 1.38 \times 10^{-23}$ (joule $\times [6.02 \times 10^{23}]/[6.02 \times 10^{23}$ particles]) degree $^{-1}$ $= [1.38 \times 10^{-23} \times 6.02 \times 10^{23}]$ (joule/mol of particles) degree $^{-1}$ $= 8.31$ (J/mol) degree $^{-1}$ $= 1.99$ (cal/mol) degree $^{-1}$ (since 1 cal $= 4.18$ J).

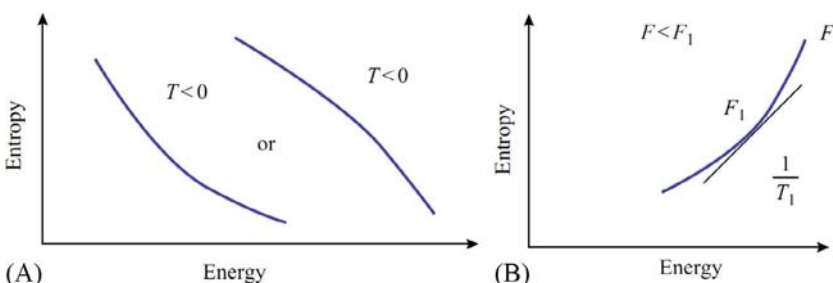


FIG. 8.3 Regions of the $S(E)$ plot that do not correspond with any stable state of the system. (A) Regions where entropy $S(E)$ decreases with increasing energy (E): here $T=1/(dS/dE)<0$. (B) A “concave” region of the $S(E)$ plot: here at the point of contact (where $dS/dE=1/T_1$) the free energy $F=E-TS$ is not lower but higher than that of neighboring sections of the plot $S(E)$; cf. Fig. 8.4.

The last value, $1.99 \text{ cal mol}^{-1} \text{ K}^{-1}$, is traditionally referred to as the “gas constant” R .

6. Specific entropy is often measured in entropy units, “eu”: $\text{eu} = \text{cal mol}^{-1} \text{ K}^{-1} = k_B/1.99 \approx k_B/2$. Hence, 1 eu corresponds to $\approx e^{1/2} \approx 1.65$ states per particle of the system.

Now at last we can start considering *conformational changes*. It was in order to give them a competent consideration that we reviewed the basics of statistical physics and thermodynamics.

Conformational changes can be gradual or sharp (the latter are called “phase transitions”). Let us try and distinguish one kind from the other using energy spectrum density plots such as those presented in [Fig. 8.2](#).

First of all, we have to consider *thermodynamics* and learn how to locate the stable state(s) of our system at a given temperature of the medium.

Let the number of states of our system (macromolecule) be $M(E)$ when its energy is E , and let the medium (thermostat) temperature be T_1 . Given that we have the plot of entropy $S(E) = k_B \ln[M(E)]$ and know T_1 , how can we find the plot’s point corresponding to the stable state of our system? The temperature T_1 determines the plot’s slope dS/dE at the sought point: here $dS/dE = 1/T_1$ since the temperature of our macromolecule is equal to the medium’s temperature. Thus, the corresponding tangent to the curve $S(E)$ gives us the possibility of finding the point we are looking for.

However, there may be several such points with the given plot slope of $1/T_1$ (see [Fig. 8.6](#)). Which of them corresponds to the stable state? Let us consider the tangent at the point E_1 where $dS/dE|_{E_1} = 1/T_1$. The equation describing such tangent is $S - S(E_1) = (E - E_1)/T_1$, or, what is the same, $E - T_1 S = E_1 - T_1 S(E_1)$. The value $F_1 = E_1 - T_1 S(E_1)$ is simply the system’s free energy at temperature T_1 . As seen, along the tangent the value $E - T_1 S$ is constant. Everywhere to the left of the tangent the value of $E - T_1 S$ is lower and everywhere to its right higher than on the tangent itself ([Fig. 8.4](#)).

Specifically, the latter means that concave regions of $S(E)$ ([Fig. 8.3B](#)) cannot correspond to a stable state, since at the contact point, F is not lower but higher than that in the neighboring sections of the curve $S(E)$. The latter means that the system can decrease its free energy (ie, shift towards a more stable state) by moving from the contact point along the concave curve.

If the curve $S(E)$ is convex along its entire length, then its slope decreases with increasing energy E . Hence, each value of slope $1/T$ corresponds to only one point of the curve ([Figs. 8.2](#) and [8.5](#)), that is, this point corresponds to the sought point for the stable state at the given temperature T . As the temperature changes, this point gradually moves and the system gradually changes its entropy and energy ([Fig. 8.5A and B](#)) and its thermodynamic state ([Fig. 8.5C](#)).

If the $S(E)$ slope alternatively decreases and increases with increasing energy E ([Fig. 8.6](#)), then there may be several tangents with the same slope, and the contact point of the extreme left of these tangents (with the lowest F) reflects

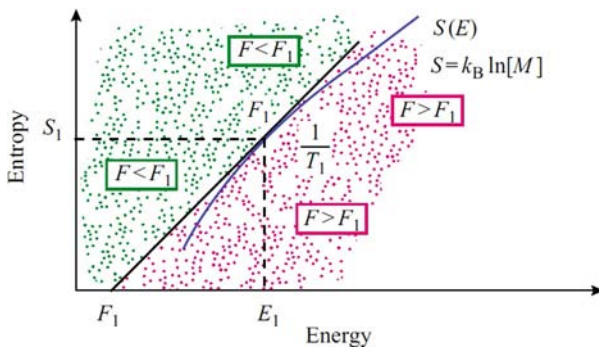


FIG. 8.4 Graphical definition of temperature and free energy. The bold curve $S(E)$ shows the dependence of entropy $S=k_B \ln(M)$ on the energy E . $M(E)$ is the energy spectrum density of the system's states. The slope of $S(E)$ determines the temperature T : $dS/dE=1/T$. Physically possible temperatures $T>0$ correspond to a rise in $S(E)$. F_1 is the free energy (corresponding to the given energy spectrum) at temperature T_1 (that determines the tangent to the $S(E)$ curve). The magnitude $F=E-T_1 S$ is constant along the tangent and equal to $F_1=E_1-T_1 S_1$. At the left and above the tangent, $F=E-T_1 S < F_1$, while at its right and below, $F=E-T_1 S > F_1$. Since here the curve $S(E)$ is convex, that is, it is below the tangent, the contact point corresponds to the minimum free energy at temperature T_1 . For other explanations, see text.

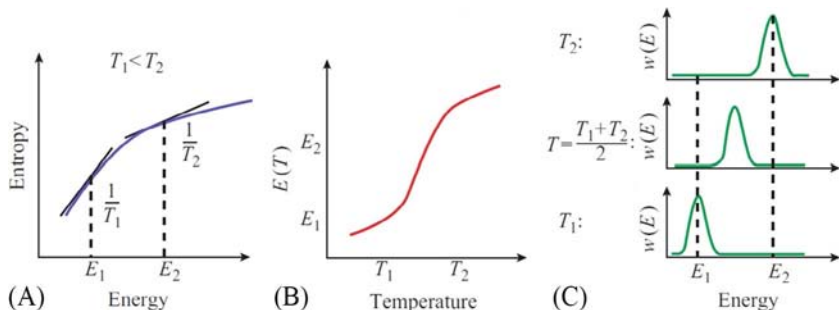


FIG. 8.5 A gradual change of the system state with changing temperature (from T_1 to T_2). The requirement is convexity of the curve $S(E)$. With $S(E)$ known (A), $T(E)$ and then $E(T)$ can be found (B). $w(E)$ (C) is the probability of having energy E at the given temperature T ; $w(E)$ is proportional to $\exp[-(E-TS(E))/k_B T]$.

the most stable state. Up to a certain temperature T^* , the “best” tangent (with the lowest F) will be one in the region of small energies, whereas beyond T^* the “best” tangent will be found in the region of greater energies (and greater entropies).

At temperature T^* , structures with low and high energies will have equal free energies and equal probabilities of existence. This means, that among many identical systems at transition temperature T , half of them are in the low-energy state, while the other half is in the high-energy state (see Fig. 8.6C). In other

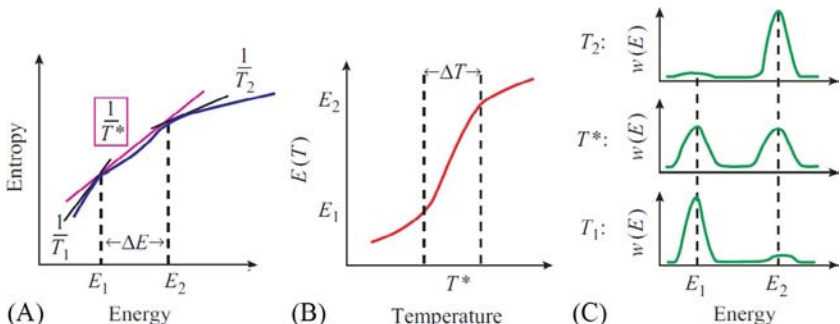


FIG. 8.6 Phase transition of the “all-or-none” type (in macroscopic bodies, it is called a “first-order phase transition”) is characterized by a sharp change of the system’s state with changing temperature. The requirement is a concave region on the curve $S(E)$ in (A): at the transition temperature T^* , the free energy at the center of this region is higher than at its flanks (this region corresponds to unstable states of the system, see Fig. 8.3b). The transition occurs within a narrow temperature range ($\Delta T = T_2 - T_1$) corresponding to the co-existence (ie, approximately equal probabilities) of low- and high-energy states. The tangents correspond to the mid-transition temperature T^* , as well as to $T_1 < T^*$ and $T_2 > T^*$. Note that temperature T^* of the “all-or-none” transition (ie, of the first-order phase transition) exactly coincides with the middle of the sharp energy change (B) and with maximum splitting of the distribution of probability $w(E)$ over the states (C).

words, half of the time each system is in the high-energy state, and for the other half it is in the low-energy state. The “co-existence” of two states of a system, equally probable but utterly different in energy, will occur within a certain very narrow (specifically, for large “macroscopic” systems) temperature range around T^* ; we will estimate it soon.

It is of major importance, that the states with “medium” energies will not be displayed as probable states of the system, since, owing to the $S(E)$ plot concavity, the points for “intermediate” states lie on the right of the tangent corresponding to the transition temperature T^* . In other words, at temperature T^* , the free energy of these “intermediate” states is higher than that of structures corresponding to both contact points, and the probability of manifestation of the intermediates is nearly zero. Then the two stable states are said to be separated by a “free energy barrier.”

These are conditions for the “all-or-none” transition.

In microscopic systems (in proteins, in particular), this transition can occur as a “jump” over the free energy barrier at the transition temperature T^* . We will discuss this later on.

In macroscopic systems (eg, in a tube with freezing water) the barrier (at temperature T^*) is so high that it would take almost infinity to overcome it. Therefore, macroscopic systems possess *hysteresis*, that is, they preserve their state up to slight overcooling (when freezing) or overheating (when melting) as compared with temperature T^* ; after that the transition runs through a temporary (ie, unstable) phase separation in the system (eg, into liquid and

solid). Such a transition in macroscopic systems is called a *first-order phase transition*.

Now I would like to estimate the temperature interval corresponding to coexistence of low- and high-energy states of the system. In the middle of the transition, at temperature T^* , the free energy of the low-energy phase, $F_1(T^*)=E_1-T^*S_1$, is equal to the free energy of the high-energy phase, $F_2(T^*)=E_2-T^*S_2$. That is, in the middle of transition

$$E_2 - E_1 = T^*(S_2 - S_1) \quad (8.10)$$

At a small (δT) temperature deviation from T^* , the free energies of the phases change slightly. The difference between them amounts to:

$$\begin{aligned} \delta F &= F_1(T^* + \delta T) - F_2(T^* + \delta T) = [F_1(T^*) + (dF_1/dT)\delta T] \\ &\quad - [F_2(T^*) + (dF_2/dT)\delta T] = -S_1\delta T + S_2\delta T \\ &= \delta T(S_2 - S_1) \end{aligned} \quad (8.11)$$

The phases co-exist (ie, their probabilities are nearly equal: say, the probability ratio varies from 10:1 to 1:10) as long as $\exp(-\delta F/k_B T^*)$ is between about 10 and 1/10, that is, as long as $\delta F/k_B T^*$ is somewhere between $\ln(10) \approx +2$ and $\ln(1/10) \approx -2$. In this region δT is somewhere between $+2k_B T^*/(S_2 - S_1)$ and $-2k_B T^*/(S_2 - S_1)$. So, the temperature interval of phase co-existence is:

$$\Delta T \approx \frac{2k_B T^*}{S_2 - S_1} - \left(\frac{-2k_B T^*}{S_2 - S_1} \right) = \frac{4k_B T^*}{S_2 - S_1} = \frac{4k_B (T^*)^2}{E_2 - E_1} \quad (8.12)$$

Let us consider an instructive numerical example. When $T^* \sim 300$ K (ie, $k_B T^* \sim 0.6$ kcal mol⁻¹) and $E_2 - E_1$ amounts to about 50 kcal mol⁻¹ $\approx 100 k_B T^*$, which is typical of protein melting (ie, $E_2 - E_1 \approx 50/(0.6 \times 10^{23}) \sim 10^{-22}$ kcal per protein particle), then ΔT is about 10°. This means that molten and intact protein molecules co-exist in the range of a few degrees around the melting mid-point. However, when $E_2 - E_1$ is about 50 kcal per system (equivalent to melting a piece of ice as big as a bottle), then the co-existence range, ΔT , is about 10^{-23} degrees only.

In other words, “all-or-none” phase transitions of small systems are characterized by an energy jump within some temperature range. This is true to a much greater extent for first-order phase transitions in macroscopic systems. In these systems the range of the jump is almost infinitely narrow, while for macromolecules it covers several degrees (and thus still remains narrow as compared with the usual “observation range” from 0 to 100 °C). And in small oligopeptides no jump is observed: here the range of energy change can cover the entire “experimental window” of the temperatures studied.

A few words should be added concerning *second-order* phase transitions. Whereas first-order phase transitions are characterized by a *jump in the energy* of the system (along with its entropy, volume and density), the typical feature of

a second-order phase transitions is *an abrupt change* in the slope of the function $E(T)$, that is *a jump in the heat capacity*.

It should be stressed that a second-order transition occurs as the kink (for macro-systems) or the abrupt change (for macro-systems) in the $E(T)$ curve (Fig. 8.7) which occurs *not* in the middle of the subsequent more-or-less S-shaped dependence of energy (or other observed parameter) on the temperature.

Such a transition is typical, for example, when the system changes up to a certain temperature, and then this change stops (eg, in ferromagnetism, at a temperature below the Curie point, the heat is used to destroy the spontaneously magnetized state; and at a temperature above the Curie point, with the spontaneous magnetization already removed, the added heat is spent to increase the fluctuations only).

Microscopic analogs of the second-order phase transition have been found in proteins only recently, while the gradual and “all-or-none” transitions in poly-peptides and proteins are known already for a long time. We will discuss them in detail later.

Figs. 8.5–8.7 show (deliberately) the cases when the system first changes slowly with increasing temperature, then rapidly, and then slowly again. These are selected to show that such “S-shaped” behavior of $E(T)$ is compatible with both a first-order phase transition and a gradual change of the system in the absence of any phase transition at all, as well as with a gradual change triggered by a second-order phase transition.

I ask you to pay attention to these examples because for unknown reasons, some non-physicists are prejudiced that a “transition” always corresponds exactly in the middle of any S-shaped profile, and that any “transition” that is not first-order is second-order. This is not true.

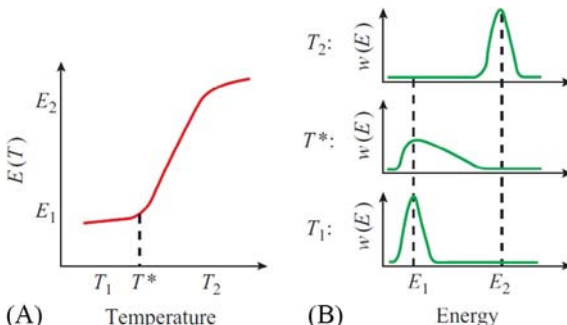


FIG. 8.7 Typical appearance of (A) the energy, $E(T)$, and (B) the energy distribution function, $w(E)$, for a second-order phase transition. T^* is the temperature of this phase transition. At this temperature, the distribution of energies, $w(E)$, becomes dramatically expanded, and the energy *begins* (or *stops*, depending on the direction of temperature change) its rapid change. Note that the second-order phase transition temperature T^* coincides with the *beginning* of this rapid energy change (and not with the middle, which is typical for “all-or-none” transitions shown in Fig. 8.6).

Note that although the curves $E(T)$ in Figs. 8.5–8.7 are alike, the behavior of the distribution curves, $w(E)$, for first-order (all-or-none) transitions is *utterly different* from the others. It is *only* “all-or-none” transitions that are characterized by two peaks on $w(E)$ curves reflecting the *co-existence* of two phases. Therefore, to see whether the transition between two extreme states is jump-like or gradual, it is *insufficient* to register a rapid change of energy or any other parameter in a narrow temperature range.

Some additional measurements are required, which will be the subject of discussion in a future lecture.

Now let us talk about the *kinetics of conformational changes*, or rather, about why their rate is sometimes extremely slow. What is “slow” here? Suppose you know the rate of one elementary step of the process. For example, it takes a residue ~ 1 ns to join the secondary structure. Also, you know that the chain contains 1000 residues. But the entire process takes not 1000 ns but 1000 s. That’s what is “slow”: orders of magnitude slower than expected either from the rate of the steps and their necessary number, or from the rate of diffusion. We have to understand the origin of this difference.

As mentioned, in some processes, the slow rate is caused by slow diffusion (which will be discussed soon) at high viscosity of the media, or by a necessity to make many steps in the course of reaction. However, the slow rate often—not always but often—results from the necessity of overcoming a high *free-energy barrier*. This is a very characteristic feature of “all-or- none” transitions, where the free-energy barrier separates two phases (Fig. 8.6); its value is always considerable here.

This barrier is very similar to the activation energy barrier of chemical reactions, although here it has both energy and entropy constituents (if the latter constituent is the main one, such a barrier is often called a “gate” (Frauenfelder, 2010)); later, we will see that the free energy barrier between the folded and unfolded states of a protein looks like a gate from the side of the unfolded state and as an energy barrier from the side of the folded state.

Let me remind you how to estimate the rate of such “barrier-overcoming” reactions using the classical theory of transition states (Emanuel and Knorre, 1984; Evans and Polanyi, 1935; Eyring, 1935; Pauling, 1970; Pelzer and Wigner, 1932).

First, let us consider the simplest process of a system transition from state 0 to state 1. On the pathway $0 \rightarrow 1$ let there be one barrier # (Fig. 8.8) and no “traps” (Fig. 8.9; the presence of “traps” complicates the process, but its nature remains unchanged).

Note: Kinetics of transition observed for each individual system (in, eg, “single-molecule experiments”) looks *very* different from the “averaged” kinetics observed for a large ensemble of systems (molecules).

A single molecule does not “move” along the reaction coordinate (as it may seem from kinetics observed for a large ensemble, see the bottom panel in Fig. 8.8B): the ensemble demonstrates a smooth kinetics, while each single

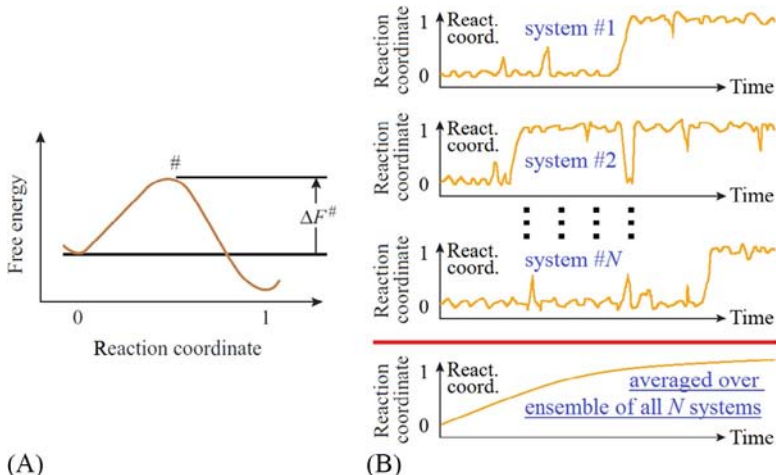


FIG. 8.8 (A) The free-energy barrier (activation barrier) # in the transition from the state “0” to state “1”. $\Delta F^\#$ is the free energy of the barrier (ie, of the “transition state”) counted off the preceding stable state 0. (B) Individual trajectories of overcoming the free energy barrier by single molecules (yellow, red, blue) and the overall kinetics of this process for a multitude of molecules.

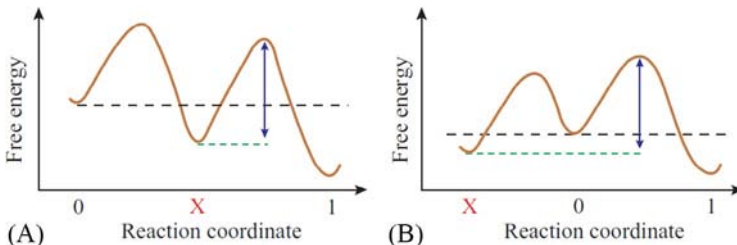


FIG. 8.9 A “trap”: this may be either the on-pathway intermediate “X” (A) or an out-of-pathway (for the reaction $0 \rightarrow 1$) state “X” (B). The kinetic trap occurs provided it is more stable than the initial state “0” but less stable than the final state “1”, and there is a higher free energy barrier (shown with an arrow) between “X” and “1” than between “0” and “X”.

molecule tries to jump—falls back—tries to jump again—fails again—.....—(see upper panels in Fig. 8.9B) and only finally succeeds.

If $\Delta F^\#$ is the free energy of the barrier relative to the free energy of the initial state, with $\Delta F^\# \gg k_B T$, if there are no “traps” (Fig. 8.9), and if n “particles” (molecules, systems, etc.) are in the initial state, then due to fluctuations, $n^\# \approx n \exp(-\Delta F^\#/k_B T)$ particles are on the barrier. Let it take each of these the time τ to jump from the barrier (τ being the time of “an elementary reaction step”). Then, during a time interval of about τ , all $n^\#$ “on-barrier” particles will cross the barrier. For all of the n particles present in state “0”, the time of

performing $n/n^\#$ elementary steps is required to come to state “1”, and this *time* of $0 \rightarrow 1$ transition amounts to:

$$t_{0 \rightarrow 1} \approx \tau(n/n^\#) = \tau \exp(+\Delta F^\#/k_B T) \quad (8.13)$$

The reciprocal

$$k_{0 \rightarrow 1} \equiv 1/t_{0 \rightarrow 1} \approx k_0 \exp(-\Delta F^\#/k_B T) \quad (8.14)$$

is the *rate* of transition from 0 to 1; $k_0 \equiv 1/\tau$ is the rate of an elementary reaction step.

The rate of the reverse $1 \rightarrow 0$ transition amounts to:

$$k_{1 \rightarrow 0} \approx k_0 \exp(-F^\#/k_B T) \times \exp[-(F_0 - F_1)/k_B T] \quad (8.15)$$

where F_0, F_1 are the free energies of states “0” and “1”, respectively. To obtain this equation, we used the well-known ratio

$$k_{1 \rightarrow 0}/k_{0 \rightarrow 1} = \exp[-(F_0 - F_1)/k_B T] \quad (8.16)$$

which follows from the fact that the equilibrium population of these two (“1” and “0”) states, n_1^0 and n_0^0 , must satisfy both the kinetic equation $n_1^0 k_{1 \rightarrow 0} = n_0^0 k_{0 \rightarrow 1}$ (accounting for zero flow of particles from one state to the other in equilibrium) and the thermodynamic ratio $n_1^0/n_0^0 = \exp[-F_1/k_B T]/\exp[-F_0/k_B T]$ (connecting the equilibrium probability of the particle being in either state with its free energy).

With the “trap” X present (Fig. 8.9), the $0 \rightarrow X$ and $X \rightarrow 1$ transition time is estimated in the same way. Then the total time of transition from 0 to 1 is the sum of the times of $0 \rightarrow X$ and $X \rightarrow 1$ transitions.

Note two further points:

First, if there are several transition pathways used *in parallel* (Fig. 8.10A), their *transition rates* must be *summed*:

$$k_{1+2+\dots} = k'_{0 \rightarrow 1^\# \rightarrow 1} + k''_{0 \rightarrow 2^\# \rightarrow 1} + \dots \quad (8.17)$$

Here $k'_{0 \rightarrow 1^\# \rightarrow 1} \equiv 1/t'_{0 \rightarrow 1^\# \rightarrow 1} = (1/\tau) \exp(-\Delta F^{\#1}/k_B T)$ is the transition rate for the first pathway, $k''_{0 \rightarrow 2^\# \rightarrow 1}$ is that for the second pathway, etc. So, if the parallel

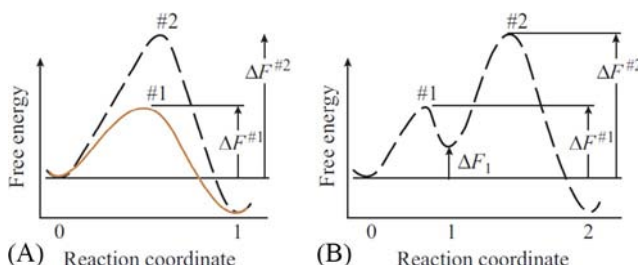


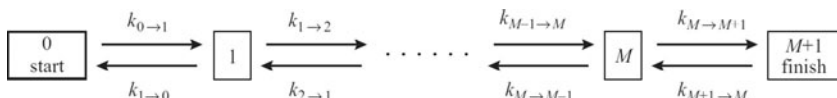
FIG. 8.10 The free energy barriers in parallel (A) and consecutive (B) processes.

pathways are not too numerous, the process time is determined by the most rapid of them, that is, by the one overcoming the *lowest barrier*.

Second, if there are several *consecutive* barriers on the transition path, then the individual barrier-overcoming times must be *summed*.

This statement is evident for the process shown in Fig. 8.9A, where the stable intermediate X is first accumulated before giving rise to the final state 1. However, it is far less evident for the process shown in Fig. 8.10B where the intermediate “1” is *unstable*. Moreover, in this case it should be specified that here “the individual barrier-overcoming time” implies the time required for a particle to reach the on-barrier position from the *deepest* prior minimum of the free energy, and *not* from the *immediately preceding* one (eg, in Fig. 8.10B, the height of barrier #2 must be taken relative to state 0 not to state 1).

To prove this (I will provide the idea only without boring you with calculations), let us consider the process



(where $k_{i \rightarrow i+1}$ is the rate of transition from i to $i+1$, and $k_{i+1 \rightarrow i}$ is the rate of inverse transition from $i+1$ to i).

A general solution of this differential kinetic equation pertaining to this problem has been given by a Moscow scientist, Rakowski (1907), but now we are interested only in a simple estimate (see Becker and Döring, 1935) of the rate of this process for a case where the free energies of all intermediate states ($1, 2, \dots, M$) are higher by many times $k_B T$ than the free energies of both initial (0) and final ($M+1$) states.

Because of their high free energies, all intermediate states accumulate only a few molecules (as compared with the total number of the molecules in the initial and final states). Therefore, the rate at which the numbers of molecules change is also very low for the intermediate states as compared with that for the initial and final states. In other words, it can be assumed that the flow rate is approximately constant over the entire reaction pathway. Thus:

$$\begin{aligned} -dn_0/dt &= k_{0 \rightarrow 1}n_0 - k_{1 \rightarrow 0}n_1 = k_{1 \rightarrow 2}n_1 - k_{2 \rightarrow 1}n_2 = \dots \\ &= k_{M \rightarrow M+1}n_M - k_{M+1 \rightarrow M}n_{M+1} \equiv dn_{M+1}/dt \end{aligned} \quad (8.18)$$

(This assumption is called the “*quasi-stationary*,” or “*steady-state*” approximation, and is widely used in chemical kinetics; Emanuel and Knorre, 1984; Pauling, 1970). Solution to the above equations gives the result:

$$t_{0 \rightarrow \dots \rightarrow M+1} = (1/k_{0 \rightarrow 1}) + (1/k_{1 \rightarrow 2}) \exp(+F_1/k_B T) + \dots + (1/k_{M \rightarrow M+1}) \exp(+F_M/k_B T) \quad (8.19)$$

where $1/k_{i \rightarrow i+1}$ is the barrier i overcoming time, provided the starting point was the immediately preceding state i , and ΔF_i is the free energy of the intermediate state i relative to the free energy of the initial state. To obtain this equation we used Eq. (8.16).

One last point: since in accordance with Eq. (8.13) $1/k_{i-1 \rightarrow i} = \tau_i \exp[(\Delta F^{\#i} - \Delta F_{i-1})/k_B T]$, then $(1/k_{i-1 \rightarrow i}) \exp(\Delta F_{i-1}/k_B T) = \tau_i \exp(\Delta F^{\#i}/k_B T)$. This is just the time required to overcome the individual barrier $\#i$, if it were the only one on the pathway of the process $0 \rightarrow M + 1$; let us refer to this time as $t_{0 \rightarrow \#i \rightarrow \dots}$. Then

$$t_{0 \rightarrow \dots \rightarrow M+1} = t_{0 \rightarrow \#1 \rightarrow \dots} + t_{0 \rightarrow \#2 \rightarrow \dots} + \dots + t_{0 \rightarrow \#M+1} \quad (8.20)$$

which proves the statement that the time of a *consecutive* reaction is the *sum of the times* required to overcome individual barriers the heights of which are taken relative to *the deepest* of the prior free energy minima (Eq. (8.20) gives an approximate solution; a more accurate solution based on generalization of the steady-state approach one can find in [Finkelstein, 2015](#)).

Incidentally, Eq. (8.20) shows that if the sequential barriers are not too numerous, the time of the process is determined simply by the *highest* one among them.

Up to now, we paid attention to the barriers and left aside $k_0 \equiv 1/\tau$, the rate of an elementary step. The value k_0 is often ([Pauling, 1970](#)) taken as $k_{0,\text{el}} = k_B T/h$ (where h is the Planck's constant); $k_B T/h$ is about 10^{13} s^{-1} at $T \approx 300 \text{ K}$: this is the frequency of attacks on the barrier under the action of thermal vibrations.

Considering a multistep process, it is often convenient to express its rate through the rates of one-step transitions between intermediate free energy minima and the heights of these minima (Fig. 8.11). To this end, we can:

1. Take the rate of transition between two adjacent minima as the rate of an elementary step:

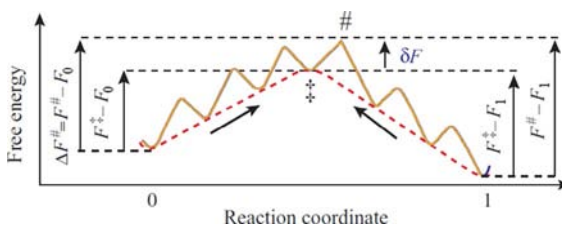


FIG. 8.11 Overcoming of the free energy barrier on the pathway from the stable state “0” to the stable state “1” (the left arrow), and from “1” to “0” (the right arrow). F_0, F_1 are the free energies of the stable states “0”, “1”; F^\ddagger is that of the most unstable intermediate metastable state \ddagger , and $F^\#$ is that of the transition state (ie, the most unstable state on the reaction pathway). δF is the height of the free energy barrier for one step.

$$k_{0,\text{step}} = k_{0,\text{el}} \exp(-\delta F/k_B T) \quad (8.21)$$

(where δF is the free energy barrier that is to be overcome during one step, see Fig. 8.11)

2. Take the maximum free energy of an intermediate metastable state, F^\ddagger , as the effective barrier free energy for the whole process; then:

$$\begin{aligned} k_{0 \rightarrow 1} &= k_{0,\text{el}} \exp[-(F^\# - F_0)/k_B T] = k_{0,\text{el}} \exp[-(F^\ddagger + \delta F - F_0)/k_B T] \\ &= k_{0,\text{step}} \exp[-(F^\ddagger - F_0)/k_B T] \end{aligned} \quad (8.22)$$

This equation looks like Eq. (8.14) with $k_{0,\text{step}}$ in place of k_0 and $F^\# - F_0$ in place of $\Delta F^\# \equiv F^\# - F_0$.

The same substitutions and explanations are, of course, equally true for $k_{1 \rightarrow 0}$ and $t_{1 \rightarrow 0}$.

Finally, let us consider the diffusion rates. As I have already said, the existence of a free energy barrier is suggested by a reaction rate that is much lower than the rate of diffusion. And what is the typical diffusion time? To have some idea, let us talk a little about diffusion.

Before we do this, it is useful to estimate how long a molecule needs to forget the direction of its movement and to start diffusing. That is, we have to know how long it takes for the molecule's kinetic energy to dissipate because of friction against a viscous fluid. One can show that this occurs in picoseconds (ps).

Indeed, the particle's movement in a viscous fluid is described by the Newton equation $m(dv/dt) = F_{\text{frict}}$ where m is the particle's mass, dv/dt is acceleration and F_{frict} is the force of friction. The mass can be estimated as $m = \rho V$, where ρ is the particle's density and V its volume. The friction force, for a spherical particle, is $F_{\text{frict}} = -3\pi D\eta v$ according to Stokes' law, where D and v are the spherical particle's diameter and speed and η is the viscosity of the fluid. The equation:

$$m(dv/dt) = -3\pi D\eta v \quad (8.23)$$

determines the time

$$t_{\text{kinet}} \approx m/(3\pi D\eta) \quad (8.24)$$

typical of the friction-caused movement damping. In fact, $t_{\text{kinet}} \approx 0.1\rho D^2/\eta$, since $m \approx \rho D^3$, and $3\pi \approx 10$. Since $\rho \approx 1 \text{ g cm}^{-3}$ for all the molecules we deal with, and $\eta \approx 0.01 \text{ g cm}^{-1} \text{ s}^{-1}$ for water (see any databook), we have:

$$t_{\text{kinet}} \approx 10^{-13} \text{ s} (D/\text{nm})^2 \quad (8.25)$$

where (D/nm) is the particle's diameter expressed in nanometres. If the molecule is not a ball but an ellipsoid with axes d_1, d_2, d_3 , then the effective $D^2 = (d_1 d_2 + d_2 d_3 + d_3 d_1)/3$ (Landau and Lifshitz, 1987).

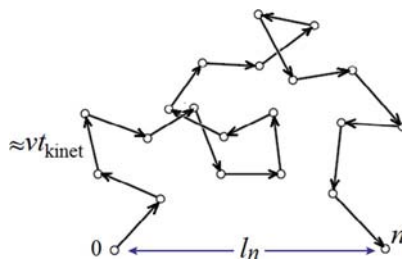
This means that the kinetic energy of a small ($D \approx 0.3$ nm) molecule (eg, water) dissipates within $\sim 10^{-14}$ s, of a small protein ($D \approx 3$ nm) within $\sim 10^{-12}$ s, and of a large protein ($D \approx 10$ nm) within $\sim 10^{-11}$ s. Thus, for aqueous solutions, the typical time is a picosecond.

Note: For a more viscous environment, a membrane for example, the kinetic energy dissipation is proportionally faster.

Of course, collisions with other molecules compensate for this energy loss. But the direction of the initial movement is forgotten within a picosecond.

Now we can turn to the diffusion movement of a molecule.

The heat-maintained kinetic energy of each particle, $mv^2/2$, amounts, on average, to about $k_B T$. The particle “memorizes” the direction of its movement for a time t_{kinet} . During this time, the time of one step, it covers a distance $\Delta l \approx v t_{\text{kinet}}$ (this distance is called the mean free path of the molecule; in water, it can be estimated as ≈ 0.13 nm $(D/\text{nm})^{1/2}$; see Problem 8.8). Then the direction of its movement changes, and it covers approximately the same distance Δl in some new direction. That is, at each step its displacement is about $\pm \Delta l$. The mean square displacement of the molecule from the initial point grows proportionally with time. Indeed, if, after n steps, the particle is moved by a distance l_n in some direction, then its displacement after $n+1$ steps is $l_{n+1} = l_n \pm \Delta l$, and $(l_{n+1})^2 = (l_n \pm \Delta l)^2 = l_n^2 \pm 2l_n \Delta l + \Delta l^2$. That is, since the mean value of the term $\pm 2l_n \Delta l$ is zero, $(l_{n+1})^2 = l_n^2 + \Delta l^2$ on average (recollect coil where the squared end-to-end distance is proportional to the chain length and see the following scheme as an illustration):



The particle makes t/t_{kinet} steps within time t ; thus, its mean square displacement after time t is

$$l_t^2 = (t/t_{\text{kinet}}) \Delta l^2 \quad (8.26)$$

Since $\Delta l \sim v t_{\text{kinet}}$,

$$l_t^2 \sim (t/t_{\text{kinet}})(v t_{\text{kinet}})^2 = t(v^2 t_{\text{kinet}}) \quad (8.27)$$

and since $t_{\text{kinet}} \approx m/(3\pi D\eta)$, and $mv^2/2 \approx k_B T$,

$$l_t^2 \sim t[k_B T / (1.5\pi D\eta)] \quad (8.28)$$

This answer is only approximate, since we have used the symbols “ \approx ” (approximately equal) and “ \sim ” (equal in the order of magnitude) many times. However, as usually happens in such cases, the approximate answer is close to the precise answer (which requires much more refined calculations). The precise answer is:

$$l_t^2 = t[2k_B T / (\pi D\eta)] \equiv t[6D_{\text{diff}}] \quad (8.29)$$

Here $D_{\text{diff}} = k_B T / (3\pi D\eta)$ is the Einstein (more accurately: Stokes–Einstein, 1905—Sutherland, 1905—Smoluchowski, 1906) value of the diffusion coefficient for a ball of diameter D in the medium with viscosity η at temperature T (Landau and Lifshitz, 1987).

The characteristic diffusion time is the time spent by a molecule in diffusing for a distance of its diameter D . It is easy to estimate this time from Eq. (8.29):

$$t_{\text{diff}} = (\pi D^3 \eta) / (2k_B T). \quad (8.30)$$

Since water viscosity $\eta \approx 0.01 \text{ g cm}^{-1} \text{ s}^{-1}$, and $k_B T \approx 600 \text{ cal mol}^{-1} \approx 2500 \text{ J mol}^{-1}$ at room temperature,

$$t_{\text{diff}} \approx 0.4 \times 10^{-9} \text{ s} (D/\text{nm})^3, \quad (8.31)$$

where (D/nm) is again the particle’s diameter expressed in nanometres.

It is possible to show that a particle’s inversion takes approximately the same time (the inversion can be regarded as displacement of the particle’s pole by a distance of $\sim D$).

It is useful also to bear in mind that diffusion at the 1 nm distance takes $\approx 0.4 \times 10^{-9} \text{ s}$ (D/nm).

Thus, we can conclude that in water, the typical diffusion time of a molecule falls within a nanosecond range: within this time a molecule driven by collisions with its fellow molecules covers a distance equal to its size and/or is overturned.

Note: The above estimates are for the aqueous environment. For a more viscous environment (eg, in a cell where viscosity is higher by an order of magnitude, according to some estimates), the times are proportionally longer.

Any process that takes much more time than diffusion allows us to suggest the existence of a free energy barrier on its pathway. For inter-molecular reactions (or reactions between remote chain regions), this barrier is created, in part, by the entropy loss required to bring together the reacting pieces.

REFERENCES

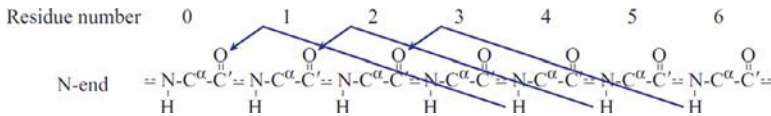
- Becker, R., Döring, W., 1935. Kinetische Behandlung der Keimbildung in Übersättigten Dämpfen. Annalen der Physik (in German) 24, 719–749.

- Einstein, A., 1905. Über die von der molekularkinetischen Theorie der Wärme geforderte Bewegung von in ruhenden Flüssigkeiten suspendierten Teilchen. *Annalen der Physik* (in German) 322, 549–560.
- Emanuel, N.M., Knorre, D.G., 1984. *The Course in Chemical Kinetics*, fourth Russian ed. Vysshaja Shkola, Moscow. Chapters III (§ 2), V (§§ 2, 5).
- Evans, M.G., Polanyi, M., 1935. Some applications of the transition state method to the calculation of reaction velocities, especially in solution. *Trans. Faraday Soc.* 31, 875–894.
- Eyring, H., 1935. The activated complex in chemical reactions. *J. Chem. Phys.* 3, 107–115.
- Feynman, R., Leighton, R., Sands, M., 1963. *The Feynman Lectures on Physics*, vol. 1. Addison-Wesley Publishing Company, Inc., Reading, MA (Chapter 46).
- Finkelstein, A.V., 2015. Time to overcome the high, long and bumpy free-energy barrier in a multi-stage process: the generalized steady-state approach. *J. Phys. Chem. B* 119, 158–163.
- Frauenfelder, H., 2010. *The Physics of Proteins. An Introduction to Biological Physics and Molecular Biophysics*. Springer, NY (Chapter 13).
- Landau, L.D., Lifshitz, E.M., 1987. *Fluid Mechanics (Volume 6 of A Course of Theoretical Physics)*, second ed. Butterworth-Heinemann, Oxford. §§ 58–60.
- Landau, L.D., Lifshitz, E.M., 1980. *Statistical Physics (Volume 5 of A Course of Theoretical Physics)*, third ed. Elsevier, Amsterdam. §§ 7–9, 14–15, 28, 31, 137–138, 150.
- Pauling, L., 1970. *General Chemistry*. W.H. Freeman & Co., NY (Chapter 16).
- Pelzer, H., Wigner, E., 1932. Über die Geschwindigkeitskonstante von Austauschreaktionen. *Z. Phys. Chem.* (in German) B15, 445–471.
- Rakowski, A., 1907. Kinetik der Folgereaktionen erster Ordnung. *Z. Phys. Chem.* (in German) 57, 321–340.
- Sutherland, W., 1905. Dynamical theory of diffusion for non-electrolytes and the molecular mass of albumin. *Phil. Mag.* 9, 781–785.
- von Smoluchowski, M., 1906. Zur kinetischen Theorie der Brownschen Molekularbewegung und der Suspensionen. *Annalen der Physik* (in German) 326, 756–780.

Lecture 9

With basic physics learned, let us move on to discuss the stability of the secondary structure and the kinetics of its formation. We will now consider only *homopolypeptides*, ie, chains formed by identical amino acid residues.

We start by considering an α -helix. The conformations of its first three residues (1, 2, 3) in this helix are fixed with its first hydrogen bond $(CO)_0 \leftarrow (HN)_4$; the next hydrogen bond, $(CO)_1 \leftarrow (HN)_5$, additionally stabilizes the conformation of only one residue (residue 4); the hydrogen bond $(CO)_2 \leftarrow (HN)_6$ provides additional binding for residue 5, and so on.



Thus, n residues are fixed by $n - 2$ hydrogen bonds. Let us consider the free energy of formation of such a helix from a coil in aqueous solution (a coil is a polymer without any fixed structure and without interactions between non-neighboring residues). This free energy is given by:

$$\Delta F_\alpha = F_\alpha - F_{\text{coil}} = (n - 2)f_H - nTS_\alpha = -2f_H + n(f_H - TS_\alpha) \quad (9.1)$$

Here f_H is the free energy of formation of a hydrogen bond in the α -helix. Apart from the free energy of the H-bond per se (which, as you remember, is not just the energy as would be the case in a vacuum, but includes both the energy and entropy of the subsequent H-bond rearrangement in the aqueous environment), it also includes the free energy of other interactions accompanying formation of the H-bond in the helix. S_α is the entropy loss caused by fixation of one residue in the helix.

As you see, ΔF_α has two terms. One of them ($-2f_H$) is independent of the helix length; the quantity

$$f_{\text{INIT}} = -2f_H \quad (9.2)$$

is known as the free energy of helix initiation (actually, f_{INIT} reflects both helix initiation and termination). The other term, $n(f_H - TS_\alpha)$, is directly proportional to the helix length; the quantity

$$f_{\text{EL}} = (f_H - TS_\alpha) \quad (9.3)$$

is known as the free energy of helix elongation per residue. Generally, we have:

$$\Delta F_\alpha = f_{\text{INIT}} + n f_{\text{EL}} \quad (9.4)$$

The relationship between the probabilities of the purely helical state of an n -residue-long sequence and its purely coil (free of any helical admixtures) state is expressed as:

$$\exp(-F_\alpha/kT) = \exp(-f_{\text{INIT}}/kT) \times [\exp(-f_{\text{EL}}/kT)]^n = \sigma s^n \quad (9.5)$$

Here, I have used the conventional notation (Schulz and Schirmer, 1979/2013): $s = \exp(-f_{\text{EL}}/kT)$, the helix elongation parameter; $\sigma = \exp(-f_{\text{INIT}}/kT)$, the helix initiation parameter.

It is obvious that $\sigma \ll 1$, since $\sigma = \exp(-f_{\text{INIT}}/kT) = \exp(+2f_H/kT)$; and the free energy of a hydrogen bond is a large negative value of about several kT .

The quantity $\exp(-\Delta F_\alpha/kT) = \sigma s^n$ is simply the *equilibrium constant* for the two states (“ α ” and “coil”) of an n -residue-long sequence.

Prior to discussing the ways of experimentally determining the σ and s values, let us see whether under varying conditions (temperature, solvent, etc.) the helix forms gradually or through an “all-or-none” transition.

On the face of it, such a distinct structure as the α -helix should be “frozen out” of the coil by a phase (ie, “all-or-none”) transition, like ice out of water.

However, *Landau’s theorem* states that first-order phase transitions never occur in a system consisting of two *one-dimensional* (1D) phases (Landau and Lifshitz, 1980). Let me try to explain this.

First of all, what does one-dimensionality mean? It means that the size (and hence, the free energy) of the phase interface is independent of the phase sizes. In these terms, both helical and coil conformations of a polypeptide are 1D. Fig. 9.1 shows that the interface between the helix and the coil regions is independent of their lengths, unlike the interface of the 3D phases (eg, of a piece of ice with surrounding water). Consequently, the free energy on the helix boundaries does not depend on the helix size, while the free energy of a 3D phase (ice) increases as $n^{2/3}$ with increasing number n of the particles involved in this phase.

Now what does “forming through a first-order phase transition” mean? This means that at a transition temperature either phase can be stable, but their mixture (eg, the mixture of ice and water) is unstable owing to increasing free energy. You must not be misled by the picture of a floating in water piece of

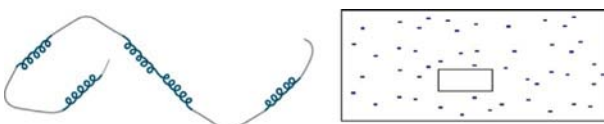


FIG. 9.1 Comparison of 1D (coil with helices) and 3D (a piece of ice in water) systems. The size of the interface between the helix and the coil is independent of their lengths, while the interface of the 3D piece of ice with water varies with its size.

ice: this state is unstable at any temperature (owing to the additional free energy at the interface between ice and water), and with time, at a fixed temperature, ice will either melt or take up the entire water, provided there is no flow of underground heat, streams on other interfering non-equilibrium factors.

Is phase co-existence in a 3D system favorable? *No, it is not. Why?*

Let us return to Fig. 9.1 and consider the temperature at which infinite water and infinite ice have equal values of the free energy (that is a condition of the “mid-transition”). If the floating piece of ice consists of n molecules, the interface free energy is proportional to $\xi n^{2/3}$, where $\sim 6n^{2/3}$ is the characteristic number of interface molecules (suggesting that ice has a more or less cubic form), and $\xi/6 > 0$ is the interface free energy of each of them. (Note that if $\xi < 0$, the thermodynamically favorable (in this case) “mixing up” occurs on the molecular scale, and the two phases do not emerge at all.) Consequently, the ice surface increases the free energy by $\xi n^{2/3}$. True, the piece of ice also possesses positional entropy, since its position in the vessel can vary. But this entropy never exceeds the value of the order of $k \ln(N)$, if there are N molecules (ie, N ice initiation points) in this vessel. In total, the free energy of this piece of ice amounts to about $[\xi n^{2/3} - kT \ln(N)]$. However, at large N values, the logarithm grows only slightly. If the piece of ice occupies a considerable part of the vessel (eg, $n \sim N/10$) and N is very large (eg, 10,000,000,000), then $\ln(N)$ (here, 23) is very small compared with $(N/10)^{2/3}$ (here, 1,000,000); in other words, the interface term $\xi n^{2/3}$ predominates, and this term is unfavorable for the formation of a piece of ice. Therefore, in a 3D system, macroscopic phases fall apart thereby making possible a first-order transition. (Unstable ice pieces of only a few molecules can be neglected as they are no more than microscopic, local fluctuations in water.)

And is phase co-existence in a 1D system favorable? *The answer appears to be yes.*

Let us return to the “mid-transition temperature” at which the helix and the coil have the same free energy, ie, $f_{EL} = 0$. The free energy of the helix boundaries, f_{INIT} , is independent of both helix and coil lengths. The positional entropy of an n -residue-long helix in an N -residue-long chain is $k \ln(N-n)$. In total, the free energy of the helix floating in the sequence is $f_{INIT} - k \ln(N-n)$. At large values of N and not too large n (eg, $n \sim N/10$ or $\sim N/2$), the term containing $\ln(N-n)$ always predominates over the constant (f_{INIT}); this logarithmic term reduces the free energy and promotes insertion of the helix into the coil (as well as insertion of the coil into the helix). That is why, in a 1D system, phase division *does not* happen; the phases tend to mix up, and therefore, a first-order transition (ie, the “all-or-none” type transition) becomes impossible, provided the sequence is sufficiently long. Thus, the Landau theorem is proved.

Note: Strictly speaking, unlike α -helix melting, that of the DNA double helix does not come within the Landau theorem, since the double-stranded DNA is *not* a 1D system: the DNA molten region is a spatial loop closed by double helices at its ends. The loop closing provides an additional contribution to the free

energy of the loop boundaries, which, according to Flory's formula for loops (Flory, 1969), grows logarithmically with increasing loop length.

Now we come to the question, "At which characteristic chain lengths do the coil and helical phases begin to mix up?" Or rather, "What characteristic length n_0 of the helical segment corresponds to the midpoint of the helix-coil transition?"

Let us consider an N -residue sequence at mid-transition temperature when the values of the free energies of the helix and coil are equal, ie, $f_{EL}=0$. Then the free energy of helix elongation (and coil elongation as well) is zero, that of helix initiation is f_{INIT} , the number of possible positions of the ends of a helix in the n -residue chain region is about $n^2/2$ (the helix can be started and ended anywhere; the condition that the helix must contain ≥ 3 residues is not significant when $n \gg 3$). The free energy of the helix is unaffected either by the helix position or by its length. To obtain a qualitative estimate, minor things (numerals in equations) can be neglected, and only major ones (letters in equations) must be taken into account. Then the entropy of the ends is $\approx k \times 2 \ln(n)$; and the total free energy of insertion of a portion of the new phase (a helix with fluctuating ends into the n -residue coil or a coil into the n -residue helix) is $\approx f_{INIT} - 2kT \ln(n)$. If this free energy is greater than zero, the insertion of the new phase will not happen; if it is less than zero, the insertion will happen and may be repetitive until the average phase length n exceeds n_0 that can be found from the equation $f_{INIT} - 2kT \ln(n_0) = 0$. Thus, at the midpoint of the helix-coil transition the characteristic lengths of their fragments is (see Zimm and Bragg, 1959; Schulz and Schirmer, 1979/2013).

$$n_0 \approx \exp(+f_{INIT}/2kT) \equiv \sigma^{-1/2} \quad (9.6)$$

Experimentally, the mid-point of this transition is the point (temperature) corresponding to 50% helicity of a very long polypeptide (as mentioned earlier, the helicity of a polypeptide is usually measured using CD spectra; at 50% helicity, the polypeptide CD spectrum represents a half-sum of the spectra of the polypeptide coil conformation and its totally helical conformation). At this point $f_{EL}=0$, ie, $s=\exp(-f_{EL}/kT)=1$.

The n_0 value can be found as the sequence length that provides 12% helicity at $s=1$. (I will not prove this numerical estimation, as it is beyond the scope of these lectures. You can try and do it yourself using Appendix B.)

I would just like to explain why the helicity of an n_0 -residue chain is several times lower than that of a very long sequence (ie, <50%). This is because this chain can be either completely in the coil state (in this case, its free energy is zero), or include a one helix/coil mixture (with an additional free energy of about $f_{INIT} - kT \ln[(n_0)^2/2] = +kT \ln 2 > 0$, ie, having a <50% probability), where the helix covers only some part of the chain.

Finally, with n_0 known, we can calculate f_{INIT} and σ . For most amino acids, $n_0 \approx 30$, $f_{INIT} \approx 4 \text{ kcal mol}^{-1}$ and $\sigma \approx 0.001$ (see Ptitsyn and Finkelstein, 1979a,b; Muñoz and Serrano, 1994, and references therein).

Now we can find the free energy of H-bonding (together with all the interactions accompanying formation of a hydrogen bond in an α -helix): according to Eq. (9.2), $f_H = -f_{INIT}/2 \approx -2 \text{ kcal mol}^{-1}$. Also, it is possible to determine the loss of conformational entropy caused by fixation of a residue in the α -helix: according to Eq. (9.3), at $f_{EL} = 0$, $TS_\alpha = f_H \approx -2 \text{ kcal mol}^{-1}$.

Both parameters of helix stability, f_{EL} and f_{INIT} , depend on conditions (eg, temperature), but what greatly influences the stability is the deviation of f_{EL} from 0. The reason is that this deviation is multiplied by the large value n_0 (for an n_0 -residue helix), and only in this way does it appear in the free energy of the helix. When the quantity $f_{EL}n_0/kT$ is close to +1 (or more precisely: $f_{EL}n_0/kT = +2$), the helicity almost disappears, and with $f_{EL}n_0/kT \leq -2$ the coil almost ceases to exist. Consequently, in very long ($N \gg n_0$) polypeptide chains the helix-coil transition occurs in a region of $-2/n_0 < f_{EL}/kT < +2/n_0$, ie, in a region of $-0.07 < -f_{EL}/kT < 0.07$ at $n_0 \approx 30$ (Fig. 9.2). This is an example of an abrupt, cooperative, but *not* phase transition (since its width does not tend to zero with increasing length of the chain).

The stability of the α -helix usually decreases with increasing temperature and added polar denaturants; and it increases with added weakly (less than water) polar solvents (which increase the price of H-bonds).

To measure the effect of amino acid residues on helix stability, short ($\sim n_0$ or less) polypeptides are currently most often used. They can house only one helix, and therefore, the effect of each amino acid replacement on the helicity can be estimated most easily. Now it is known that the contribution of an amino acid residue to the helix stability ranges from alanine, the most “helix-forming” residue, with $s \approx 2$, ie, $f_{EL} \approx -0.4 \text{ kcal mol}^{-1}$, to glycine, the most (but for Pro) “helix-breaking” residue, with $f_{EL} \approx +1 \text{ kcal mol}^{-1}$, ie, $s \approx 0.2$, while the majority of other residues have f_{EL} close to zero (Finkelstein et al., 1976; Muñoz and Serrano, 1994). Proline (an *imino* acid with no NH group to participate in the helix-forming H-bond) has a considerably lower value of s (0.01–0.001; it has not been accurately measured yet).

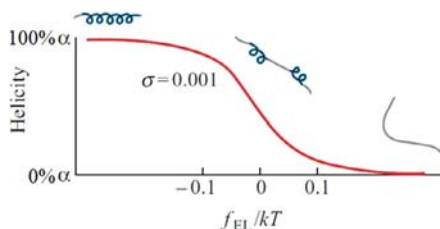


FIG. 9.2 A finite width is typical of any helix-coil transitions, even those in infinitely long chains. This is an example of a cooperative transition, which is *not* a phase transition: at a low value of the helix initiation parameter ($\sigma \ll 1$) it is caused by a certain small change (much less than kT) in the value of f_{EL} , which shows that a “transition unit” involves many chain residues but far from all of them.

Earlier, the estimates of this kind were made (in particular, by one of us, O.B.P.) using statistical co-polymers (eg, chains with a random mixture of 80% Glu and 20% Ala); it is in this way that the first—and hence the most important—estimates were obtained (see [von Dreele et al., 1971](#); [Platzer et al., 1972](#); [Snell and Fasman, 1973](#); [Ptitsyn and Finkelstein, 1979a,b](#), and references therein). But with the advent of pre-set sequence synthesis, the use of such random co-polymers became a thing of the past.

Also, potentiometric titration was used to measure the helical (as well as β -structural) state stability (the quantity f_{EL}) in polypeptides containing acidic or basic side chains (eg, in poly(Glu) or poly(Lys)) ([Bychkova et al., 1971](#); [Barskaya and Ptitsyn, 1971](#); [Pederson et al., 1971](#); [Mandel and Fasman, 1975](#); [Walter and Fasman, 1977](#)). The idea of this approach is that by charging a helix, we destroy it (because in the helix the side chain charges are closer to one another than in the coil, and, hence, their repulsion is stronger). So, the helix stability can be calculated from the dependence of the total charge and helicity of the chain on the medium's pH.

Unfortunately, consideration of this interesting method in more detail is beyond the scope of this course.

Using short peptides with pre-set sequences, an estimate can even be made as to how the helicity is affected by each single amino acid replacement ([Padmanabhan et al., 1990](#); [Fersht, 1999](#)) at a given position in the peptide, ie, in fact, as dependent on the residue position about the N- and C-termini of the helix (and on the residues surrounding the residue in question). The side chains, and in particular charged ones, interact with these termini in opposite ways, because, as mentioned, the N-terminus of the helix houses the main-chain NH groups free of hydrogen bonds (and the resulting partial charge of the α -helix N-terminus is equal to $+e/2$), while its other terminus holds free CO groups (with the total partial charge $-e/2$, half the electron charge ([Ptitsyn and Finkel'shtein, 1970](#); [Finkelstein and Ptitsyn, 1976](#)).

Similar approaches are used to measure the stability of the β -structure in polypeptides. However, they are less developed, since the β -structure aggregates strongly. Currently, β -structure stability is measured right in the proteins by estimating the effect on protein stability of replacements of each of its surface β -structural residues. It is shown that contribution of amino acid residues into β -structure stability ranges from ≈ -1 to $\approx +1 \text{ kcal mol}^{-1}$ ([Finkelstein, 1995](#)). The ability of various residues to stabilize α - and β -structures will be considered in Lecture 10.

Now let us consider *the rate of formation* of the secondary structure in peptides.

Experiment shows that α -helices are formed very rapidly: within $\sim 0.1 \mu\text{s}$ a peptide of 20–30 residues adopts the helical conformation ([Williams et al., 1996](#); [Thompson et al., 1997](#)); such rapid measurements require a pico- or nano-second laser-induced temperature jump of the solution. Consequently, the rate of helix extension is at least a residue per several nanoseconds.

I said “at least” because the rate of helix formation depends not only on its extension rate but also on how rapidly the first “nuclei” of the helical structure appear. Initiation of the helix requires overcoming the activation barrier; therefore, the formation of the first turn is the slowest step, and subsequent growth of the helix is rapid.

Hence, it is possible that nearly the entire observation time might be taken by helix initiation, with its elongation being far more rapid. Let us consider this in more detail (see [Galzitskaya et al., 2002](#), and references therein).

The typical dependence of the free energy of a helix on its length is illustrated in [Fig. 9.3](#). Even if $f_{EL} < 0$, ie, when the rather long helix is stable, formation of its first turn requires overcoming an activation barrier as high as f_{INIT} .

Does the experimentally measured time of α -helix formation agree with our current understanding of this process?

According to the transition state theory, this first step of helix formation (formation of the first helix turn in the given place of the chain) takes the time

$$t_{INIT,\alpha} = \tau \exp(+f_{INIT}/kT) \quad (9.7)$$

where τ is the time of an elementary step (here, helix elongation by one residue), and the exponent allows for low occupancy of the barrier state possessing (by definition of a barrier) the highest free energy. By definition, $\sigma = \exp(-f_{INIT}/kT)$; thus

$$t_{INIT,\alpha} = \tau/\sigma \quad (9.8)$$

However, initiation can occur anywhere in the future helix, and its length (even in very long chains) is limited by $\sim n_0 = \sigma^{-1/2}$. Consequently, the typical time of initiation of the first turn *anywhere* in the future helix is n_0 times less, and $t_{INIT,\alpha}/n_0 = \tau/(\sigma n_0) = \tau/\sigma^{1/2}$.

Propagation of the helix to all its $\sim n_0$ residues takes as much time as the initiation, $\sim \tau n_0 = \tau/\sigma^{1/2}$. Thus, half of the whole transition time, roughly, is spent on helix initiation anywhere in the sequence, and the rest on elongation.

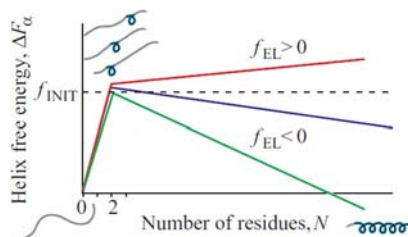


FIG. 9.3 Typical dependence of the α -helix free energy (ΔF_α) on the number (N) of amino acid residues involved in the helix, with various free energies of helix elongation (f_{EL}). When $f_{EL} < 0$, a long helix is stable but its initiation requires overcoming an activation barrier as high as f_{INIT} . When $f_{EL} > 0$, a helix of any length is unstable, and therefore it cannot form. Note that the α -helix-initiating turn can be formed in any place of the future α -helix.

This gives the total helix-coil transition time as approximately $2\tau/\sigma^{1/2}$, and the half-time (ie, the characteristic time) of the whole transition is:

$$t_\alpha \sim \tau/\sigma^{1/2} = \tau \exp(+f_{\text{INIT}}/2kT) \quad (9.9)$$

The time of helix elongation (τ) has been estimated as about a residue per a few nanoseconds (Zana, 1975; Cummings and Eyring, 1975; Thompson et al., 1997), and f_{INIT} as about 4 kcal mol⁻¹ (Barskaya and Ptitsyn, 1971; Ptitsyn and Finkelstein, 1979a,b). Thus, theoretically estimated t_α is about hundreds of nanoseconds, in accordance with experiment.

The kinetics of α -helix formation is relatively simple: all these are formed rapidly. The kinetics of β -structure formation is far more complex and interesting.

Experiment shows that the β -structure often forms extremely slowly in water-soluble polypeptides. It may take hours and even weeks, although sometimes the β -structure folds within milliseconds (Wooley and Holzwarth, 1970; Snell and Fasman, 1973; Fukada et al., 1989), and β -hairpins even faster (Muñoz et al., 1997, 1998). What is the reason for that? Surprisingly, the folding rate of proteins containing β -structures is not much lower than that of α -helical proteins (Fersht, 1999); we will discuss this later on. How do they manage? And what controls the anomalous rate of β -structure formation in large water-soluble polypeptides: slow initiation or slow elongation?

Let us start with formation of β -hairpins. Experiment shows that they are formed rather rapidly, though not as rapidly as α -helices: within $\sim 5 \mu\text{s}$ a peptide of ~ 20 residues adopts the β -hairpin conformation (Muñoz et al., 1997, 1998). Does this agree with our current understanding of formation of β -hairpins?

Formation of a beta turn in the given place of the chain must take the time $\sim \tau_\beta \exp(+f_{\text{INIT},\beta}/kT)$, where the free energy $f_{\text{INIT},\beta}$ of beta turn formation must be similar to that of α -turn (f_{INIT}), and the time of β -structure elongation $\tau_\beta \approx \tau$. However, unlike in the α -helix, the first beta turn initiating a given stable β -hairpin cannot be positioned in any place of the chain, but *only* in its middle (Fig. 9.4). Consequently, initiation of the β -hairpin has to take $\sim n_0 \approx 30$ times

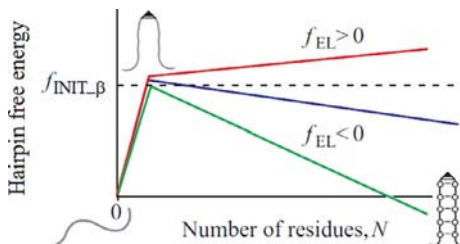


FIG. 9.4 Typical dependence of the β -hairpin free energy (ΔF_β) on the number (N) of amino acid residues forming a hairpin. A hairpin is stable only when the free energy of its elongation (f_{EL}) is negative. Note that the β -hairpin-initiating turn can be only in (approximately) the middle of the chain.

more time than initiation of the α -helix (while the β -hairpin elongation, which resembles the α -helix elongation, must take much less time) (Muñoz et al., 1998; Galzitskaya et al., 2002). This estimate shows a good fit to experiment.

Now, let's pass to the formation of β -sheets.

Theory shows that the “anomalous” (as compared with the coil-helix or coil-hairpin transition) slow kinetics of formation of the β -structure should be connected with its two-dimensionality (in contrast to a 1D helix or coil or hairpin) (Fig. 9.5), which results in a first-order phase transition.

Let us consider this process in more detail (see Finkel'shtein, 1978; Finkelstein, 1991; Galzitskaya et al., 2002).

Edge residues have fewer contacts than internal residues of the sheet. In other words, the edge of a β -sheet (like the boundary of any other phase: a drop of water, a piece of ice or an α -helix) has a higher free energy. However, like a drop of water and in contrast to the α -helix, the β -sheet is not 1D, ie, its boundary (and hence, the boundary free energy) grows with increasing number of residues involved in the sheet. Therefore, the transition from a random coil to the β -structure becomes a first-order phase transition like the formation of a water drop or a piece of ice.

Let us show that this provokes the occurrence of a high free-energy barrier (especially in the formation of an only marginally stable β -structure) capable of slowing down the folding initiation a zillion-fold.

The edge of a β -sheet consists of (a) edge β -strands, and (b) bends or loops connecting the β -strands (Fig. 9.5A). Let the coil free energy be zero (ie, the reference point); f_β , the free energy of a residue in the center of the β -sheet; $f_\beta + \Delta f_\beta$, the free energy of an edge β -strand residue (ie, Δf_β is the edge effect);

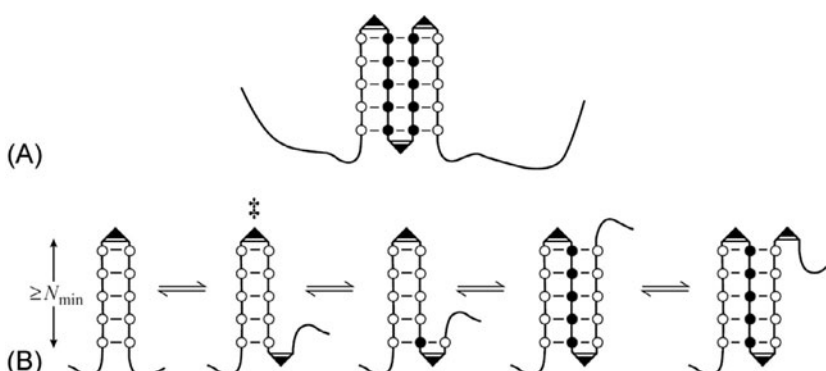


FIG. 9.5 (A) Schematic of a β -sheet. The amino acid residues of internal β -strands are indicated by *closed circles*, and of edge β -strands by *open circles*; the bends (or loops) connecting the β -strands are indicated by angles. (B) Illustration of the β -sheet growth scenario given in the text for the case when separate β -hairpins are unstable. The most unstable structure on the pathway is marked with \ddagger . H-bonds are shown schematically.

and U , the free energy of a bend. Since the β -sheet forms, it is stable (ie, $f_\beta < 0$), and the edge effects prevent it from falling into pieces (ie, $\Delta f_\beta > 0$ and $U > 0$).

In the kinetics of β -sheet formation we must distinguish between the following two cases:

1. $f_\beta + \Delta f_\beta < 0$, ie, in itself a long β -hairpin is more stable than a coil. Then only the turn at its top needs to overcome the activation barrier (which is almost identical to the barrier to be overcome in forming an α -helix), and subsequent growth of the β -structure is rapid, like the elongation of an α -helix or a separate β -hairpin (see the lines with $f_{EL} < 0$ in Figs. 9.3 and 9.4). This case was considered previously.
2. $f_\beta + \Delta f_\beta > 0$, ie, in itself the β -hairpin is unstable, and it is only the association of the initiating hairpin with other β -strands into a β -sheet that stabilizes the β -structure. Then the activation barrier is represented by the formation of a “nucleus,” that is, such a β -sheet or β -hairpin that provides further growth of the sheet accompanied by an overall decrease of the free energy.

We will now consider just this case.

The formation and subsequent growth of the nucleus of a new phase are the most typical feature of first-order phase transitions (Landau and Lifshitz, 1980), β -structure formation among them. However, as we will see, overcoming the nucleus-provoked activation barrier may be an extremely slow process.

Let us consider the following simplest scenario of formation of a stable β -sheet when separate β -hairpins are unstable (Fig. 9.5B): (i) formation of the initiating β -hairpin by a turn and two β -strands N residues long each; (ii) formation of the next turn at its end; (iii) association of another N -residue β -strand; (iv) formation of the next turn; (v) association of another β -strand, and so on.

The formation (in a coil) of a β -hairpin consisting of a turn and two N -residue β -strands contributes as much as $U + 2N(f_\beta + \Delta f_\beta) > 0$ (because $U > 0$ and $f_\beta + \Delta f_\beta > 0$) to the free energy of the chain; formation of the next turn makes it still higher by a value of U . Association of the N -residue edge of this hairpin with a new N -residue β -strand decreases the free energy by Nf_β (since the number of edge residues remains the same, while the number of internal residues increases by N , see Fig. 9.5); formation of the next β -turn increases the free energy again by U ; association of another N -residue β -strand decreases it by Nf_β , and so on.

The cycle of “association of another β -strand and formation of the next β -turn” changes the net free energy by $N\Delta f_\beta + U$. And since this cycle must result in a decrease of the free energy (as a prerequisite of rapid growth), each associating strand should contain not less than

$$N_{\min} = \frac{U}{(-f_\beta)} \quad (9.10)$$

residues. It is noteworthy that this value grows to infinity when $f_\beta \rightarrow 0$, ie, when β -sheet approaches the margin of stability.

The “transition” state, ie, the most unstable state in formation of the β -structure is, according to our scenario, the β -hairpin with a subsequent turn. Since we consider the case where the hairpin stability decreases with increasing length of the hairpin, and since the β -strand of the initiating hairpin must contain at least N_{\min} residues, the minimum free energy of the initiating hairpin and the next turn is

$$F^\ddagger = U + 2N_{\min}(f_\beta + \Delta f_\beta) + U = \frac{2U\Delta f_\beta}{(-f_\beta)} \quad (9.11)$$

This is the free energy of the transition state in β -sheet folding *according to our scenario* (Finkel'shtein, 1978; Finkelstein, 1991). It can be very high when f_β is close to zero.

Now we have to show that, irrespective of the scenario, there cannot exist transition states of a considerably higher stability.

To do so, let us estimate the changes in the minimum free energy of a growing β -sheet. The general course of the free energy changes is presented in Fig. 9.6. When the sheet is small, edge effects predominate, and the free energy of a growing β -sheet increases. In a large sheet, internal residues predominate, and the free energy of a growing β -sheet decreases.

Now we pass to calculations. First, let us estimate the minimum free energy of an M -residue β -sheet. The free energy of a sheet comprising m β -strands (which are of the same length in order to minimize the edge free energy) and $m-1$ turns is

$$F(M, m) = Mf_\beta + 2(M/m)\Delta f_\beta + (m-1)U \quad (9.12)$$

(Here I allowed myself to neglect a relatively small number of residues forming turns.) Varying the number of β -strands m (at a given M) gives the minimum of this free energy from the condition

$$\frac{dF}{dm} = -2(M/m^2)\Delta f_\beta + U \quad (9.13)$$

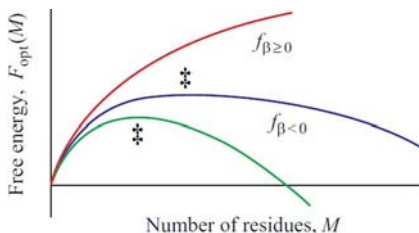


FIG. 9.6 β -Sheet minimum free energy F_{opt} as a function of M , the number of residues in the sheet. The curves refer to various free energies (f_β) of internal residues. The maximum of F_{opt} is marked with \ddagger . In a growing β -sheet (unlike an α -helix or a β -hairpin, see Figs. 9.3 and 9.4) this maximum does not correspond to the very beginning of the process.

This yields the optimal number of β -strands in this sheet, $m_{\text{opt}} = M^{1/2} (2\Delta f_\beta/U)^{1/2}$, and its free energy, $F_{\text{opt}}(M) \equiv F(M, m_{\text{opt}}) = Mf_\beta - U + 2M^{1/2} (2\Delta f_\beta/U)^{1/2}$. Varying the magnitude $F_{\text{opt}}(M)$ over M gives its maximum (see Fig. 9.6) from the condition

$$\frac{dF_{\text{opt}}}{dM} = f_\beta + M^{-1/2} (2\Delta f_\beta/U)^{1/2} = 0 \quad (9.14)$$

Then the sheet size corresponding to this maximum can be determined as $M^* = 2(\Delta f_\beta U)/(-f_\beta)^2$, and its free energy as

$$F^* = F_{\text{opt}}(M^*) = \frac{2U\Delta f_\beta}{(-f_\beta)} - U \quad (9.15)$$

The quantities F^* and F^\ddagger (see Eq. (9.11)) coincide as to their principal term, $\frac{2U\Delta f_\beta}{(-f_\beta)}$ (Finkelstein, 1991). It is because of this term that the free energy of the transition state is *always* high when there is a low free energy of stabilization ($-f_\beta$) of the β -structure, ie, when the β -structure is only marginally stable. (The main thing is that F^* and F^\ddagger equally tend to infinity when the β -structure approaches thermodynamic equilibrium with the coil, ie, when $(-f_\beta) \rightarrow 0$).

Initiation of the β -sheet in the *given* place of the chain must take the time $t_{\text{INIT_}\beta} \sim \tau_\beta \exp(+F^\ddagger/kT)$.

The time of β -folding initiation *somewhere* in a chain of M residues is $\sim t_{\text{INIT_}\beta}/M$ (Finkel'shtein, 1978; Finkelstein, 1991). The expansion of the β -structure all over the chain from *one* initiation center takes $\sim M\tau_\beta$. When the chains are not extremely long, the initiation is the rate-limiting step.

For extremely long chains (and/or for intermolecular β -structures), the time of β -structure formation is about $\tau_\beta \exp(+F^\ddagger/2kT)$. (This problem can be considered in the same way as helix formation in long chains that we discussed earlier. The main idea is that in this case the number of residues (M_{eff}) included in each independently folding sheet is such that its initiation and expansion times are equal, ie, $\tau_\beta \exp(+F^\ddagger/kT)/M_{\text{eff}} = M_{\text{eff}} \tau_\beta$.)

Thus, in both cases, the time of β -sheet formation depends on the β -structure stability per residue, $-f_\beta$, as

$$t_\beta \sim \exp \left[\frac{A}{-f_\beta} \right] \quad (9.16)$$

when the β -structure stability is low, that is, $(-f_\beta) < \Delta f_\beta$. No matter what the numerical value of the constant A may be, it clearly follows from Eq. (9.16) that the time of β -structure formation is enormous at low $-f_\beta$ (in the limit, ie, when β -sheet approaches the margin of stability and $f_\beta \rightarrow 0$, it is *infinity*; see Fig. 9.7A).

Experiments (Snell and Fasman, 1973; Cosani et al., 1974; Walter and Fasman, 1977; Fukada et al., 1989) show a drastic dependence of the β -structure formation rate on its stability, similar to that shown in Fig. 9.7B.

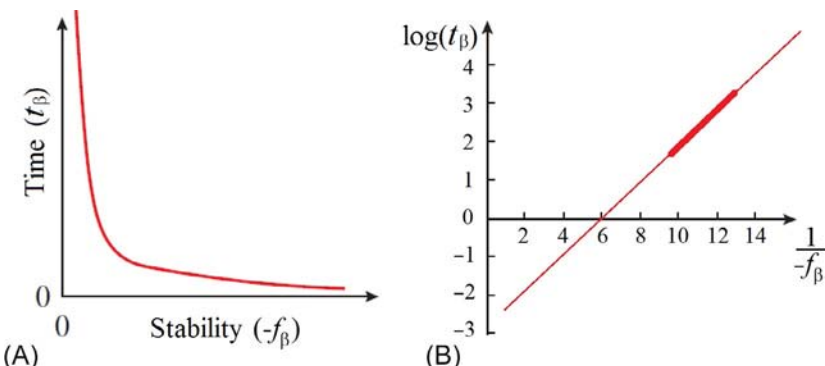


FIG. 9.7 (A) The dependence of the time needed to form a β -sheet on the stability of the β -structure (general view). (B) Time for β -structure formation (s) versus the reciprocal stability (kcal mol^{-1}). The thick line corresponds to experimental data; the thin line is its extrapolation. A high $\frac{1}{-f_\beta}$ value can be due not only to a low stability of the β -structure as related to the competing coil, but also to its low stability in relation to the competing α -helical state. (Adapted from Finkelstein, A.V., 1991. Rate of beta-structure formation in polypeptides. *Proteins* 9, 23–27.)

This explains both for the experimentally observed extremely low rate of β -structure formation in non-aggregating polypeptides (where the stability of the β -structure is always low) and for a drastic increase of this rate with increasing stability of the β -structure (Fig. 9.7B).

Thus, a β -structure of low stability must form very slowly not because of slow elongation but because of slow initiation, although β -sheets and β -hairpins of high stability (which are observed in proteins) must form almost as rapidly as the α -helix.

Inner voice: Now you told us about the coil \rightarrow β -structure transitions. Before, you told us about the coil \rightarrow α -helix transitions. What about the α -helix \rightarrow β -structure transition?

Lecturer: This is a good question which needs an extended answer. I meant to say that, in all the above considerations, kinetics of the β -sheet formation was dependent on stability of the β -structure *counted off* the stability of the preceding state of the polypeptide. This “preceding state” may be the coil state in some experiments and the α -helical state in others.

When α -helices are more stable than the coil, a peculiar kinetics is observed for β -structure formation from the initial coil. It is a very fast formation of α -helices followed by a much slower $\alpha \rightarrow \beta$ transition (Cosani et al., 1974). It may seem that the α -helical intermediates facilitate the β -structure formation in this case. However, this naive idea is wrong, because experiments show that a decrease in the stability of α -helices relative to the coil accelerates the β -structure formation, and a complete destabilization of α -helices and disappearance of the α -helical intermediate makes the β -structure formation even faster. This shows

that the α -helices (which, as mentioned, always fold rapidly) are *not* the on-pathway but rather *off*-pathway intermediates, and that they *do not facilitate* but rather *hinder* the β -structure formation (Finkel'shtein, 1978; Finkelstein, 1991). In other words, as the ancient Romans used to say, *post hoc non est proper hoc* (ie, “after this does not mean because of this”).

A very slow initiation is a common feature of first-order phase transitions when the emerging phase is only marginally stable. Recall the overcooled liquid or the overcooled vapor ... All these effects are connected with a large area and, hence, the high free energy of interface between the phases. And the β -structure is formed through a first-order phase transition with all its consequences ...

In contrast, the α -helix *avoids* the first-order phase transition (remember, the helix boundary, unlike that of the β -structure (or of a piece of ice) *does not increase with its increasing size*), and therefore the barrier to be overcome in helix folding is always of a finite (and small) value; hence, the initiation here can take a fraction of a millisecond.

REFERENCES

- Barskaya, T.V., Ptitsyn, O.B., 1971. Thermodynamic parameters of helix-coil transition in polypeptide chains. II. Poly-L-lysine. *Biopolymers* 10, 2181–2197.
- Bychkova, V.E., Ptitsyn, O.B., Barskaya, T.V., 1971. Thermodynamic parameters of helix-coil transition in polypeptide chains. I. Poly-(L-glutamic acid). *Biopolymers* 10, 2161–2179.
- Cosani, A., Terbojevich, M., Romanin-Jacur, L., Peggion, E., 1974. Potentiometric and circular dichroism studies of the coil- β transitions of poly-L-lysine. In: Proc. Symp. “Peptides, Polypeptides and Proteins”, Israel, pp. 166–176.
- Cummings, A.L., Eyring, E.M., 1975. Helix-coil transition kinetics in aqueous poly(α , L-glutamic acid). *Biopolymers* 14, 2107–2114.
- Fersht, A., 1999. Structure and Mechanism in Protein Science: A Guide to Enzyme Catalysis and Protein Folding. W. H. Freeman & Co., New York (Chapters 17 and 18).
- Finkel'shtein, A.V., 1978. Kinetics of antiparallel β -structure formation. *Bioorganicheskaya Khimiya* (in Russian) 4, 340–344.
- Finkelstein, A.V., 1991. Rate of beta-structure formation in polypeptides. *Proteins* 9, 23–27.
- Finkelstein, A.V., 1995. Predicted beta-structure stability parameters under experimental test. *Protein Eng.* 8, 207–209.
- Finkelstein, A.V., Ptitsyn, O.B., 1976. Theory of protein molecule self-organization. IV. Helical and irregular local structures of unfolded protein chains. *J. Mol. Biol.* 103, 15–24.
- Finkelstein, A.V., Ptitsyn, O.B., Kozitsyn, S.A., 1976. Theory of protein molecule self-organization. II. A comparison of calculated thermodynamic parameters of local secondary structures with experiments. *Biopolymers* 16, 497–524.
- Flory, P.J., 1969. Statistical Mechanics of Chain Molecules. Interscience Publishers, New York (Chapters 1–3).
- Fukada, K., Maeda, H., Ikeda, S., 1989. Kinetics of pH-induced random coil- β -structure conversion of poly[S-(carboxymethyl)-cysteine]. *Macromolecules* 22, 640–645.
- Galzitskaya, O.V., Higo, J., Finkelstein, A.V., 2002. α -Helix and β -hairpin folding from experiment, analytical theory and molecular dynamics simulations. *Curr. Protein Pept. Sci.* 3, 191–200.

- Landau, L.D., Lifshitz, E.M., 1980. Statistical Physics (Volume 5 of A Course of Theoretical Physics), third ed. Elsevier, Amsterdam. §§ 150, 152.
- Mandel, R., Fasman, G.D., 1975. The random coil- β transitions of L-lysine and L-valine: potentiometric titration and circular dichroism studies. *Biopolymers* 14, 1633–1650.
- Muñoz, V., Serrano, L., 1994. Elucidating the folding problem of helical peptides using empirical parameters. *Nat. Struct. Biol.* 1, 399–409.
- Muñoz, V., Thompson, P.A., Hofrichter, J., Eaton, W.A., 1997. Folding dynamics and mechanism of beta-hairpin formation. *Nature* 390, 196–199.
- Muñoz, V., Henry, E.R., Hofrichter, J., Eaton, W.A., 1998. A statistical mechanical model for beta-hairpin kinetics. *Proc. Natl. Acad. Sci. USA* 95, 5872–5879.
- Padmanabhan, S., Marqusee, S., Rigeway, T., Lane, T.M., Baldwin, R.L., 1990. Relative helix-forming tendencies of nonpolar amino acids. *Nature* 344, 268–270.
- Pederson, D., Gabriel, D., Hermans Jr., J., 1971. Potentiometric titration of poly-L-lysine. The coil-to β transition. *Biopolymers* 10, 2133–2145.
- Platzer, K.E.D., Ananthanarayanan, V.S., Andreatta, R.H., Scheraga, H.A., 1972. Helix-coil stability constants for the naturally occurring amino acids in water. IV. Alanine parameters from random poly[(hydroxypropyl)glutamine-co-L-alanine]. *Macromolecules* 5, 177–187.
- Ptitsyn, O.B., Finkel'shtein, A.V., 1970. Relation of the secondary structure of globular proteins to their primary structure. *Biofizika* (in Russian) 15, 757–768.
- Ptitsyn, O.B., Finkelstein, A.V., 1979a. Mechanism of protein folding. *Int. J. Quant. Chem.* 16, 407–416.
- Ptitsyn, O.B., Finkelstein, A.V., 1979b. A problem of protein structure prediction. In: Volkenstein, M.V. (Ed.), ‘Itogi Nauki I Techniki’, Ser. ‘Mol. Biologiya’ (‘Results of Science and Technology’, Ser. ‘Mol. Biology’; in Russian), vol. 15. VINITI, Moscow, pp. 6–41.
- Schulz, G.E., Schirmer, R.H., 1979/2013. Principles of Protein Structure. Springer, New York (Chapters 1 and 2, Appendix).
- Snell, C.R., Fasman, G.D., 1973. Kinetics and thermodynamics of the helix leads to transconformation of poly(L-lysine) and L-leucine copolymers. A compensation phenomenon. *Biochemistry* 12, 1017–1025.
- Thompson, P.A., Eaton, W.A., Hofrichter, J., 1997. Laser temperature jump study of the helix-coil kinetics of an alanine peptide interpreted with a “kinetic zipper” model. *Biochemistry* 36, 9200–9210.
- von Dreele, P.H., Lotan, N., Ananthanarayanan, V.S., et al., 1971. Helix-coil stability constants for the naturally occurring amino acids in water. II. Characterization of the host polymers and application of the host-guest technique to the random poly(hydroxipropylglutamine)-co-(hydroxybutylglutamine). *Macromolecules* 4, 408–417.
- Walter, B., Fasman, G.D., 1977. The random coil- β transitions of copolymers of L-lysine and L-isoleucine: potentiometric titration and circular dichroism studies. *Biopolymers* 16, 17–32.
- Williams, S., Causgrove, T.P., Gilmanshin, R., Fang, K.S., Callender, R.H., Woodruff, W.H., Dyer, R.B., 1996. Fast events in protein folding: helix melting and formation in a small peptide. *Biochemistry* 35, 691–697.
- Wooley, S.Y., Holzwarth, G., 1970. Intramolecular β -pleated-sheet formation by poly-L-lysine in solution. *Biochemistry* 9, 3604–3608.
- Zana, R., 1975. On the rate determining step for helix propagation in the helix-coil transition of poly-peptides in solution. *Biopolymers* 14, 2425–2428.
- Zimm, B.H., Bragg, J.K., 1959. Theory of phase transition between helix and random coil in poly-peptide chains. *J. Chem. Phys.* 31, 526–535.

Lecture 10

Now, let us discuss the properties of the side chains of amino acid residues. In particular, I would like to consider the question of what structures stabilize individual residues.

The list of 20 “standard” DNA-encoded amino acid residues (Cantor and Schimmel, 1980; Lehninger et al., 1993) is given in [Table 10.1](#), and structures of their side chains are presented in [Fig. 10.1](#), together with structures of two “nonstandard,” though equally DNA-encoded, amino acid side chains.

Apart from 20 standard amino acid residues shown in the right part of [Fig. 10.1](#), there are some rare nonstandard ones. Most of them are produced by modifications of standard amino acids, but two, as has become known more or less recently, namely, “selenocysteine” and “pyrrolysine” (see the right part of [Fig. 10.1](#)) are coded by some RNA codons in some organisms. These are stop-codons UGA for selenocysteine and UAG for pyrrolysine positioned in special RNA contexts (Creighton, 1993; Longtin, 2004; Srinivasan et al., 2002).

Also, *N*-formylmethionine (fMet) amino acid (which is a derivative of Met with a formyl group –COH added to its amino group) is a gene-encoded residue that is used for initiation of protein synthesis in some cases. But fMet has the same side chain as Met.

Let us consider the structural tendencies of amino acid residues: these have become known after long-term statistical investigations of protein structures. Such investigations answer the question as to what is most likely to happen and what is not.

[Table 10.2](#) may be helpful in putting these answers in order. Along with the abundance in different parts of proteins, I have tabulated such residue properties as the presence of an NH group in the main chain (it is absent only from the imino acid proline), the presence of the C^β-atom in the side group (it is absent only from glycine), the number of nonhydrogen γ-atoms in the side chain, and the presence and type of polar groups in the side chain (dipoles or charges with a sign; the charged state corresponding to a “normal” pH of 7.0 is shown in bold).

Let us try and understand the major features of [Table 10.2](#), based on what we have already learned. In doing so, we will follow a logical criterion “what’s good for General Motors is good for America”: since the protein as a whole is stable, the majority of its components must be stable, that is, stable components must be most often observed in its structure, while nonstable ones must be rare.

Why does proline dislike the secondary structures? Because it lacks the main-chain NH group, that is, its ability of H-bonding is halved, and H-bonds are of primary importance for the secondary structure. Why does it nevertheless like the N-terminus of the helix? Because here, at the N-terminus, NH groups

TABLE 10.1 The Principal Properties of 20 Standard Natural Amino Acid Residues

Amino Acid Residue	Code		Occurrence in <i>E. coli</i> Proteins (%)	MW at pH 7 (Da)	$G_{\text{water} \rightarrow \text{alcohol}}$ of side chain at 25°C (kcal mol ⁻¹)
	3-Letter	1-Letter			
Glycine	Gly	G	8	57	0
Alanine	Ala	A	13	71	-0.4
Proline	Pro	P	5	97	-1.0
Glutamic acid	Glu	E	≈6	128	+0.9
Glutamine	Gln	Q	≈5	128	+0.3
Aspartic acid	Asp	D	≈5	114	+1.1
Asparagine	Asn	N	≈5	114	+0.8
Serine	Ser	S	6	87	+0.1
Histidine	His	H	1	137	-0.2
Lysine	Lys	K	7	129	+1.5
Arginine	Arg	R	5	157	+1.5
Threonine	Thr	T	5	101	-0.3
Valine	Val	V	6	99	-2.4
Isoleucine	Ile	I	4	113	-1.6
Leucine	Leu	L	8	113	-2.3
Methionine	Met	M	4	131	-1.6
Phenylalanine	Phe	F	3	147	-2.4
Tyrosine	Tyr	Y	2	163	-1.3
Cysteine	Cys	C	2	103	-2.1
Tryptophan	Trp	W	1	186	-3.0

All data are from Schulz and Schirmer (1979/2013), except for those on side chain hydrophobicity ($G_{\text{water} \rightarrow \text{alcohol}}$), which are from Fauchére and Pliska (1983). The volume (in Å³) occupied by a residue (in protein or in water) is close to its molecular weight (in Da) multiplied by 1.3. To be more precise, it is ≈5% higher than MW × 1.3 if the residue contains many aliphatic (–CH₂–, –CH₃) groups and ≈5% lower than MW × 1.3 if the residue contains many polar (O, N) atoms.

protrude from the helix, that is, they do not participate in hydrogen bonds, and proline loses nothing here (the same refers to definite positions at the β-sheet edges). In addition, angle φ is close to -60 degree in the helix, while in proline, its ring fixes the angle φ at about -60 degree, that is, proline is about ready to adopt the helical conformation (Fig. 10.2A).

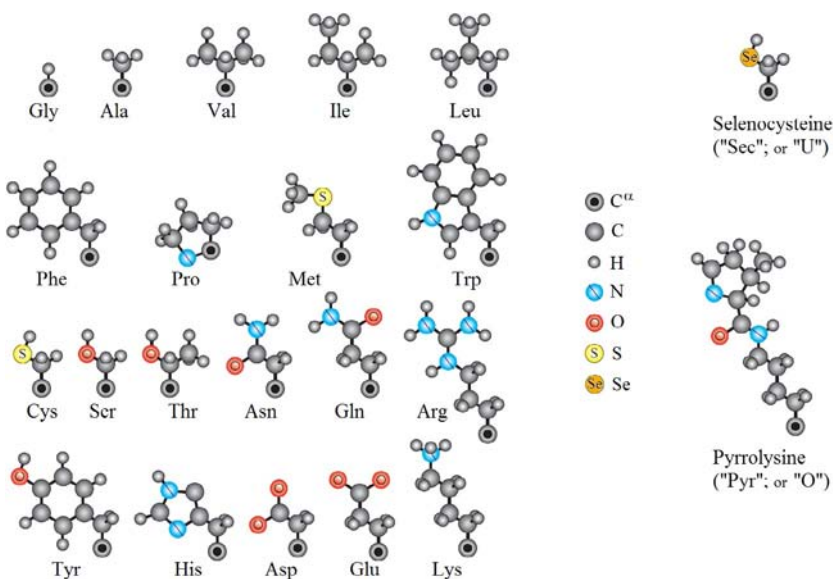


FIG. 10.1 The side chains of 20 standard (on the left) and two rare “nonstandard” (on the right) amino acid residues. Atoms involved in the amino acids are shown in the center.

Why does glycine dislike the secondary structure and prefer irregular segments (coil)? Because its allowed $\varphi\psi$ region in the Ramachandran map is extremely broad (Fig. 10.2B), and it can easily adopt a variety of conformations other than secondary structure.

In contrast, alanine with its more narrow (but including both α and β conformations) region of allowed conformations (Fig. 10.2B) prefers the α -helix (and partially the β -structure) rather than irregular conformations.

Other hydrophobic residues (ie, residues without charges and dipoles in their side chains) prefer, as a rule, the β -structure. Why? Because there is more room for their large γ -atoms (Fig. 10.2C). This is of particular importance for “branched” side chains with two large γ -atoms (Leach et al., 1966), and indeed, these are strongly attached to the β -structure.

As to amino acids with polar groups in their side chains, they prefer irregular (coil) surface regions where these polar groups can easily participate in H-bonds with both the irregular polypeptide chain and water. This tendency is most clearly displayed by most polar residues, which are charged at a “normal” pH of 7.0, as well as by the shortest polar side chains whose polar groups are closest to the main chain. By the way, this possibility of additional H-bonding explains the tendency of short polar side chains to be located at both ends of the helix.

Tryptophan and tyrosine are a kind of exception from amino acids having dipoles in their side chains: they have a small dipole and a large hydrophobic part; another exception is cysteine whose SH groups make extremely weak H-bonds. Their behavior is rather similar to that of hydrophobic residues.

TABLE 10.2 The Principal Structural Properties of Amino Acid Residues

Residue	Main Chain ^a NH	Side Chain ^a		Dipole/Charge ^b	pK _a ^b	Structural Occurrence Tendency ^c									
		Number of C ^β	Number of γ			Before		In helix		After		In			
						α _N	α _N	α	α _C	α _C	β	Loops	Core		
Gly	+	0	0			—					—	+			
Ala	+	1	0			+						—			
Pro	No	1	1			+	—	—	—	—	—	+			
Glu	+	1	1	COOH → CO ₂ [−]	4.3	+	+		—	—	—		—		
Asp	+	1	1	COOH → CO ₂ [−]	3.9	+	+	—	—	—	—	+	—		
Gln	+	1	1	OCNH ₂									—		
Asn	+	1	1	OCNH ₂		+		—		+	—	+	—		
Ser	+	1	1	OH		+						+	—		
His	+	1	1	NH; &N → NH ⁺	6.5		—		+	+					
Lys	+	1	1	NH ₂ → NH ₃ ⁺	10.5	—	—		+	+	—		—		
Arg	+	1	1	HNC(NH ₂) ₂ ⁺	12.5	—	—		+	+	—	+	—		
Thr	+	1	2	OH		+					+				
Ile	+	1	2								+	—	+		
Val	+	1	2								+	—	+		
Leu	+	1	1				+				+	—	+		

Met	+	1	1					+			+	-	+
Phe	+	1	1								+	-	+
Tyr	+	1	1	$\text{OH} \rightarrow \text{O}^-$	10.1			-			+		+
Cys	+	1	1	$\text{SH} \rightarrow \text{S}^-$	9.2			-			+		+
Trp	+	1	1	NH							+		+

^aSee text for a definition of these factors.

^bBold type in the “dipole/charge” column shows the state of the ionizable group at the “neutral” pH 7; pK is that pH value where the group can be in the charged and uncharged states with equal probability (see Fig. 10.5).

^cThese columns refer, respectively, to the tendency to be: immediately before the helix N-terminus; in the α -helix (the N-terminal turn, the body and the C-terminal turn); immediately after the C-terminus; in the β -structure; in irregular structures (loops), including β -turns of the chain; and in the hydrophobic core of the globule, rather than on its surface. The “tendency” is measured as a concentration of a residue in a given structure relatively to the average concentration of this residue in studied proteins. The difference in occurrence between “+” and “-” is approximately a factor of two. A particularly strong tendency is shown by a larger, bold symbol.

Data from Ptitsyn, O.B., Finkel'shtein, A.V., 1970. Relation of the secondary structure of globular proteins to their primary structure. Biofizika 15, 757–768 (in Russian); Ptitsyn, O.B., Finkelstein, A.V., 1979. A problem of protein structure prediction. In: Volkenstein, M.V. (Ed.), Itogi Nauki i Tekhniki (Results of Science and Technology). Mol. Biologiya (Mol. Biology), vol. 15, VINITI, Moscow, pp. 6–41 (in Russian); Schulz, G.E., Schirmer, R.H., 1979/2013. Principles of Protein Structure. Springer, New York, NY/Heidelberg/Berlin; Miller, S., Janin, J., Lesk, A.M., Chothia, C., 1987. Interior and surface of monomeric proteins. J. Mol. Biol. 196, 641–656; Creighton, T.E., 1993. Proteins: Structures and Molecular Properties, second ed. W.H. Freeman & Co., New York (Chapter 5); Stepanov, V.M., 1996. Molecular Biology: Protein Structure and Function. Vysshaya Shkola, Moscow (Chapter 5, in Russian).

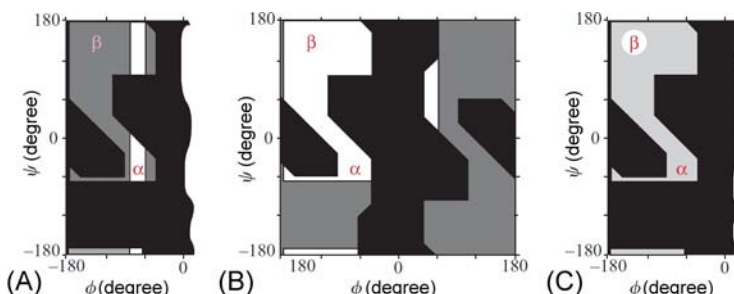


FIG. 10.2 Disallowed and allowed conformations of various amino acid residues as a background for α and β -conformations. (A) Allowed proline conformations (white) against allowed alanine conformations (black); black, conformations disallowed for both of them. (B) Allowed alanine conformations (white) against conformations allowed for glycine only (grey); black, conformations disallowed for all residues. (C) The map of disallowed (black) and allowed (white) conformations of larger residues. White, the region where all side-chain χ^1 angles are allowed; grey, the region where some χ^1 angles are disallowed. (See Lectures 3 and 7 for discussion of these Ramachandran-like plots.)

As it has been observed (Ptitsyn and Finkel'shtein, 1970; Ptitsyn and Finkelstein, 1979) that the negatively charged side chains have a preference for the N-terminus of the helix (or rather, to the N-terminal turn plus one or two preceding residues). At the same time, they avoid the C-terminal turn (plus one or two subsequent residues). The preference of the positively charged groups is just the opposite. What is the reason for that? It is NH groups protruding from the N-terminus and creating a considerable positive charge that attracts “minuses” and repels “pluses” of the side chains (Fig. 10.3). In contrast, the C-terminus is charged negatively, and therefore it is attractive for “pluses” of the side chains, while their “minuses” avoid it.

As to the residue location in the globule, the general tendency is that polar (hydrophilic) side chains are on the protein surface, in contact with polar water molecules (like dissolves in like). Separation from water molecules negatively affects polar groups since then they lose their H-bonds. This negative effect is especially profound when it concerns the charged groups because their transition from the high permittivity medium (water) to that of low permittivity (protein core) is accompanied by a drastic increase in the free energy. Indeed, ionized groups are almost completely absent from the protein interior (nearly all exceptions are connected with either coordinate bonding of metal ions or with active sites which are, in fact, the protein's focus...).

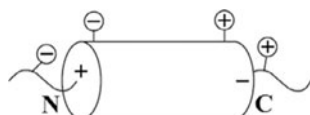


FIG. 10.3 Favorable positions of charged side chains near the N- and C-ends of the helix (Ptitsyn and Finkel'shtein, 1970; Ptitsyn and Finkelstein, 1979).

In contrast, the majority of hydrophobic side chains are in the protein interior to form the hydrophobic core (again, “like dissolves in like”). As we have learned, the hydrophobicity of a group grows with its nonpolar surface that is to be screened from water. For purely nonpolar groups, the hydrophobic effect is directly proportional to their total surface, while in the case of polar admixtures it is proportional to their surface less the surface of these admixtures.

Adhesion of hydrophobic groups is the main, although not the only, driving force of protein globule formation: it is also assisted by H-bonding in the secondary structure (as discussed earlier) and by tight quasicrystal packing within the interior of the protein molecule (to be discussed later).

To form the protein hydrophobic core, the chain must enter it with hydrogen bonds already formed (or formed in the process) because the rupture of H-bonds between polar peptide groups and water molecules occurring in any other way is expensive. That is why the chain involved in hydrophobic core formation has already formed its secondary structure (or forms it in the process), and thereby saturates the hydrogen bonds of the main-chain peptide groups.

The core must mostly comprise hydrophobic side chains from secondary structures, while polar side chains of the same secondary structures must remain outside; therefore, both α -helices and β -strands located at the surface have hydrophobic and hydrophilic surfaces created by alternating appropriate groups of the protein chain in a certain order (Fig. 10.4).

All the regularities just discussed are used to build artificial (*de novo*) proteins and to predict the secondary structure of proteins from their amino acid sequences, and also to predict internal and surface portions of protein sequence segments either deeply immersed in the protein or positioned on its surface. We will discuss this later.

In conclusion, a few more words about ionized side groups. Increasing pH (ie, decreasing H^+ concentration) always shifts the charged state of a group “in the negative direction,” that is, a neutral group acquires a negative charge, and a positive group becomes discharged (see Fig. 10.5).

Different groups change from the uncharged to the charged state or vice versa at different pH, but the transition width always remains the same—about 2 units of pH (within this range the charged/uncharged state ratio changes from 10:1 to 1:10).

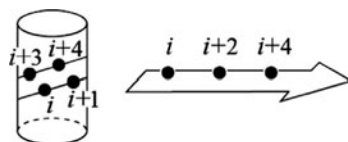


FIG. 10.4 The positions at which nonpolar side groups can form continuous hydrophobic surfaces on α -helices and β -strands. The numbers show residue positions in the chain. Similar combinations of polar groups result in the formation of hydrophilic areas on opposite surfaces of α -helices and β -strands (Lim, 1974a,b).

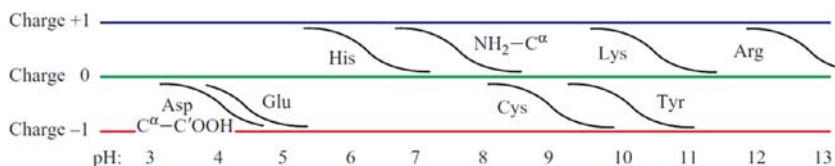


FIG. 10.5 The polarization of ionized side groups, as well as the N- and C-termini of the polypeptide chain ($\text{NH}_2\text{-C}^\alpha$ and $\text{C}^\alpha\text{-C}'\text{OOH}$, respectively) in water at various pH values. The pH value corresponding to the “half-charged” state of a group is the pK value of its ionization (cf. Table 10.2). A quickly installed equilibrium of two (with an H and without it) forms of acids and bases shows that transition of an H atom from water to acid or base is relatively easy, despite the chemical nature of the covalent bonds O–H and N–H. The ratio of probabilities of charged and uncharged states is $10^{(pK-pH)}$: 1 for a positively charged group, and $10^{-(pK-pH)}$: 1 for a negatively charged group. (Data from Stepanov, V.M., 1996. *Molecular Biology: Protein Structure and Function*. Vysshaya Shkola, Moscow (Chapter 5, in Russian).)

Special attention should be paid to groups that change their uncharged state to a charged one at a pH of about 7.0 typical of proteins in a living eukaryotic cell; these easily rechargeable groups (histidine in particular) are often used in protein active sites.

As it has been already mentioned, an ionizable group easier penetrates into a nonpolar medium (eg, protein or membrane interior) in its uncharged form. Indeed, the estimated cost of an ion penetration into such a medium is as high as several dozen kcal mol^{-1} . And what does the discharging cost? This can be easily estimated from Fig. 10.5. The probability of uncharged state is $W_0 = 1/[1 + 10^{(pK-pH)}]$ for a positively charged group, and $W_0 = 1/[1 + 10^{-(pK-pH)}]$ for a negatively charged group in water. Thus, the free energy of uncharging is $F_0 = -kT \ln W_0$. That is, for a positively charged group $F_0 \approx 0$ at $\text{pH} > pK$, and $F_0 \approx 2.3kT(pK - \text{pH})$ at $\text{pH} < pK$; for a negatively charged group $F_0 \approx 0$ at $\text{pH} < pK$, and $F_0 \approx -2.3kT(pK - \text{pH})$ at $\text{pH} > pK$. Thus, the free energy of discharging does not exceed several kcal mol^{-1} (at a “normal” $\text{pH} \approx 7$) for all the ionizable groups shown in Fig. 10.5.

REFERENCES

- Cantor, C.R., Schimmel, P.R., 1980. *Biophysical Chemistry*. W.H. Freeman & Co., New York, NY (Part 1, Chapter 2).
- Creighton, T.E., 1993. *Proteins: Structures and Molecular Properties*, second ed. W.H. Freeman & Co., New York, NY (Chapter 5).
- Fauchére, J.L., Pliska, V., 1983. Hydrophobic parameters of amino acid side chains from the partitioning of N-acetyl-amino acid amides. *Eur. J. Med. Chem. Chim. Ther.* 18, 369–375.
- Leach, S.J., Némethy, G., Scheraga, H.A., 1966. Computation of the sterically allowed conformations of peptides. *Biopolymers* 4, 369–407.
- Lehninger, A.L., Nelson, D.L., Cox, M.M., 1993. *Principles of Biochemistry*, second ed. Worth Publishers, New York (Chapter 5).

- Lim, V.I., 1974a. Structural principles of the globular organization of protein chains. A stereochemical theory of globular protein secondary structure. *J. Mol. Biol.* 88, 857–872.
- Lim, V.I., 1974b. Algorithm for prediction of α -helices and β -structural regions in globular proteins. *J. Mol. Biol.* 88, 873–894.
- Longtin, R., 2004. A forgotten debate: Is selenocysteine the 21st amino acid? *J. Natl. Cancer Inst.* 96, 504–505.
- Ptitsyn, O.B., Finkel'shtein, A.V., 1970. Relation of the secondary structure of globular proteins to their primary structure. *Biofizika* 15, 757–768 (in Russian).
- Ptitsyn, O.B., Finkelstein, A.V., 1979. A problem of protein structure prediction. In: Volkenstein, M.V. (Ed.), *Itogi Nauki I Techniki. Results of Science and Technology. Mol. Biologiya (Mol. Biology)*, vol. 15. VINITI, Moscow, pp. 6–41 (in Russian).
- Schulz, G.E., Schirmer, R.H., 1979/2013. *Principles of Protein Structure*. Springer, New York, NY/Heidelberg/Berlin (Chapter 5).
- Srinivasan, G., James, C.M., Krzycki, J.A., 2002. Pyrrolysine encoded by UAG in Archaea: Charging of a UAG-decoding specialized tRNA. *Science* 296, 1459–1462.

Lecture 11

Now that we know the features of polypeptide secondary structures and the properties of amino acid residues, we can, at last, pass to proteins.

The “living conditions,” structure-stabilizing interactions and overall architecture of proteins provide the basis for classifying them as (1) fibrous proteins; (2) membrane proteins; (3) water-soluble globular proteins; and (4) natively disordered (or “intrinsically disordered”) proteins.

In this lecture, we will consider fibrous proteins. Their structure is simpler than that of other well-ordered proteins (Volkenstein, 1977; Schulz and Schirmer, 1979/2013; Cantor and Schimmel, 1980; Creighton, 1993; Lehninger et al., 1993; Stryer, 1995; Stepanov, 1996; Branden and Tooze, 1999).

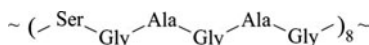
The function of fibrous proteins is mostly structural. They form microfilaments fibrils, hair, silk, and other shielding textures; they reinforce membranes and maintain the structure of cells and tissues. Fibrous proteins are often very large. Among them, there is the largest known protein, titin, of about 30,000 amino acid residues.

Fibrous proteins often form enormous aggregates; their spatial structure is mostly highly regular, usually composed of huge secondary-structure blocks, and reinforced by interactions between adjacent polypeptide chains. The primary structure of fibrous proteins is usually characterized by high regularity and periodicity, which ensures the formation of vast regular secondary structures.

We shall consider some typical representatives of fibrous proteins.

(a) *β-Structural proteins like silk fibroin.* As we know, periodicity of a β-sheet is manifested by residues pointing alternately above and below the sheet (Fig. 11.1).

In silk fibroin, the major motif of the primary structure is an octad repeat of six residue blocks, each consisting of alternating smaller (Gly) and larger residues, for example,



and this octad repeat occurs about 50 times, separated by less regular sequences (Stepanov, 1996).

Antiparallel (such as those in Fig. 11.1) β-sheets of silk fibroin are placed onto one another in the “face-to-face, back-to-back” manner (Dickerson, 1964): a double sheet of glycines (the distance between the planes is

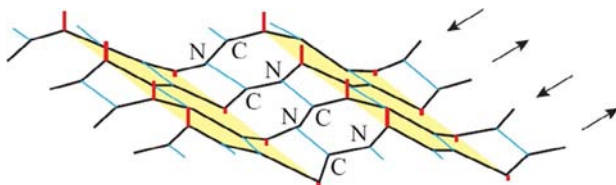
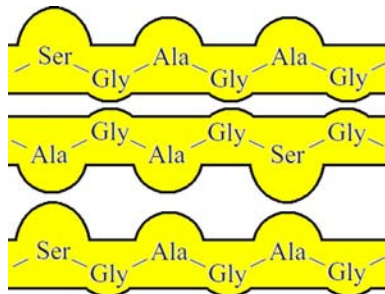


FIG. 11.1 A β -sheet with its pleated structure and periodicity emphasized. Hydrogen bonds between the linked β -strands are shown in light blue; the distance between the β -strands is 4.8 Å. (Adapted from Schulz, G.E., Schirmer, R.H., 1979/2013. *Principles of Protein Structure*. Springer, New York/Heidelberg, Berlin (Chapter 5), with permission.)

3.5 Å)—a double sheet of alanines/serines (as clearly seen by X-rays, the distance between the planes is 5.7 Å)—a double sheet of glycines—and so on:



In a silk fiber, these quasicrystals consisting of many β -sheets are immersed in a less-ordered matrix formed by irregular parts of fibroin, as well as by sericin, a special disordered matrix protein, that is S–S-bonded into a huge aggregate.

(b) α -Structural fibrous proteins formed by long coiled-coil helices (Fig. 11.2). In α -keratin, in all proteins of intermediate filaments (that have very different primary structures), in tropomyosin such helices cover the entire protein chain, and the major part of the myosin chain also forms a fibril of this type. These structures are also observed in some silks (not in the silkworm product considered above but in silk produced by bees and ants).

Associated helical chains form a superhelix known as a “coiled coil” (Figs. 11.2 and 11.3) (Crick, 1953; Dickerson, 1964).



FIG. 11.2 Right-handed coiled-coil α -helices. In the complex they are parallel and slightly wound around each other to form a left-handed supercoil with a repeat of 140 Å. The interhelical contacts are formed by amino acid residues at repeating chain positions **a** and **d** (see Figs. 11.3 and 11.4).

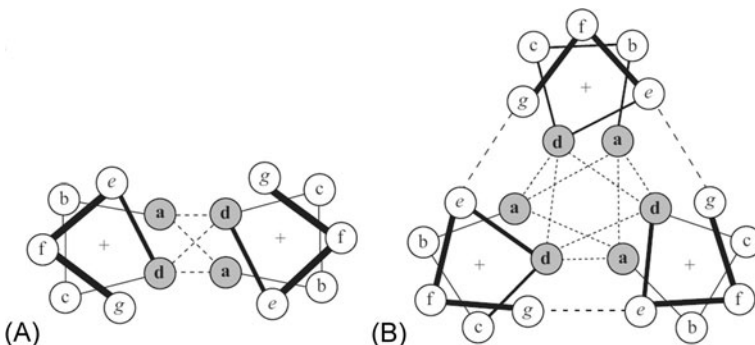


FIG. 11.3 Interactions of α -helices in double (A) and triple (B) superhelices (as viewed along the helix axis). In the double helix, only residues **a** and **d** are in immediate contact with another helix, while in the triple helix **e** and **g** residues are also involved in contacts (although to a lesser extent). (Adapted from Creighton, T.E., 1993. *Proteins: Structures and Molecular Properties*, second ed. W.H. Freeman & Co., New York (Chapter 5).)

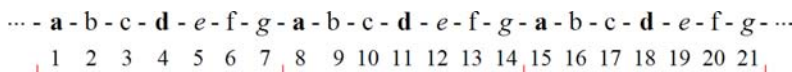


FIG. 11.4 Typical 7-residue repeats in primary structures of α -supercoil-forming chains.

The coiled coil is usually formed by parallel α -helices. In different proteins there may be two, three, or more α -helices forming the coiled coils.

As we know, a regular α -helix has 3.6 residues per turn, while the residue repeat of coiled-coil helices is 7.0, that is, 3.5 residues per turn (Figs. 11.3 and 11.4). The typical primary structure of a supercoil-forming chain has the same 7.0 residue repeat (Fig. 11.4; here, lettering in bold corresponds to hydrophobic amino acids forming the main interhelical contacts, while other letters refer to hydrophilic amino acids).

Interestingly, a slight increase in the hydrophobicity of “intermediate” residues *e* and *g* turns the double supercoiled helix (Fig. 11.3A) into a triple one (Fig. 11.3B), a greater increase turns it into a quadruple helix, and so on.

The next higher structural level is the association of supercoiled helices (shown in Fig. 11.2) into fibrils; this happens often, though not always, for example, it happens in myosin but not in tropomyosin.

It is also of interest that mechanical tension of a wet fiber formed by α -helices may result in its transformation into the β -structure, and when the tension is released and moisture decreased, the α -helical structure restores (Kreplak et al., 2004).

Let us consider in more detail how the helices associate (Crick, 1953; Chothia et al., 1977). Crick observed that there are regular knobs (side chains) on the surface of an α -helix with regular holes between them and suggested that “knob-to-hole” complementarity provides some privileged angles of contact between helices stuck together. This was a crude but correct picture of

helix-with-helix interaction. Subsequent refinement (Chothia et al., 1977) pointed out that the α -helix has several “ridges” formed by side groups coming close together (Fig. 11.5A), partly due to existence of privileged side-chain rotamers. The periodicity of some of these ridges is of the 1–4–7–… type (ridges “ $i, i+3$,” or simply “+3”). The other ridges have periodicity of the 0–4–8–12–… type (ridges “ $i, i+4$,” or simply “+4”). The helix-to-helix contact-zone-involved parts of ridges of the former type consist of residue pairs $\mathbf{a}_1\text{--}\mathbf{d}_4$, $\mathbf{a}_8\text{--}\mathbf{d}_{11}$,… (Fig. 11.5B), while those of ridges of the latter type consist of the residue pairs $\mathbf{d}_4\text{--}\mathbf{a}_8$, $\mathbf{d}_{11}\text{--}\mathbf{a}_{15}$,… (Fig. 11.5C).

The angle between the helix axis and the “ $i, i+4$ ” ridges is about –25 degree, that between the axis and the “ $i, i+3$ ” ridges is about +45 degree (Fig. 11.5).

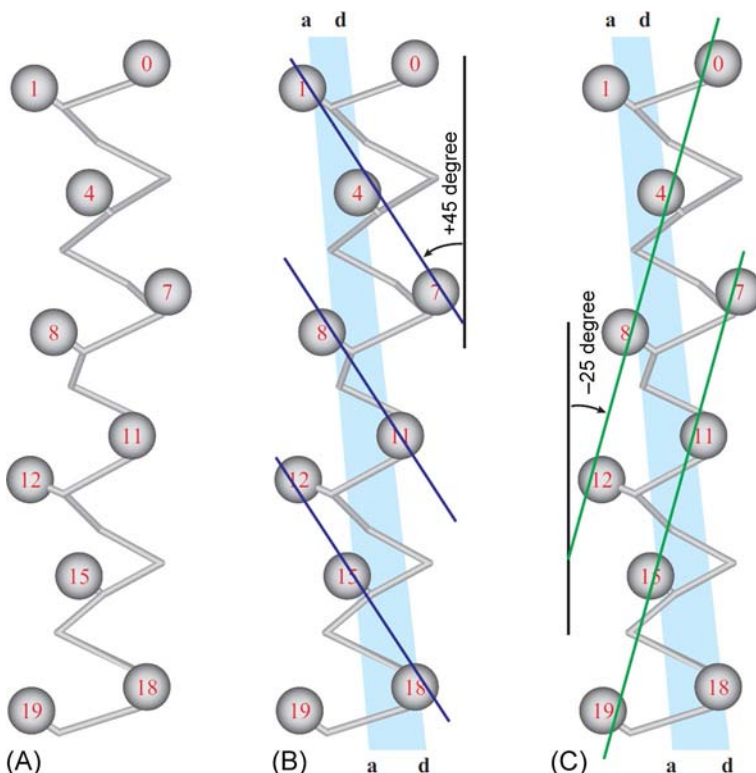


FIG. 11.5 (A) The α -helix (main chain and C^β -atoms). (B and C) Two types of ridges (thin lines) formed by side groups on its surface that are close in space. (B) Ridges of “ $i, i+3$ ” type; (C) ridges of “ $i, i+4$ ” type. The bands show the “contact surface” acting in the coiled coil; its edges are formed by the lines of residues **a** and **d**. Typical angles between the helix axis and ridges $i, i+3$ and $i, i+4$ are given (the angles in the figure look smaller than the typical angles given, since the typical ridges run, not through centers of C^β -atoms, but through massive side groups). (Adapted from Branden, C., Tooze, J., 1999. *Introduction to Protein Structure*, second ed. Garland Publishing Inc., New York/London (Chapter 3).)

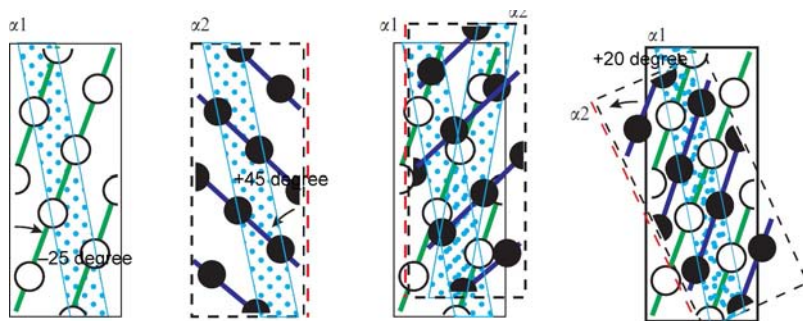


FIG. 11.6 To ensure close packing of helix side-chain ridges, a +20 degree turn of one helix about the other is required. The contact area is viewed through the α_2 helix turned around its axis. Residues of the “lower” (α_1) helix are light circles, of the “upper” (α_2) helix, dark circles. The lines of contact for the residues **a** and **d** are shown in light blue. (Adapted from Chothia, C., Levitt, M., Richardson, D., 1977. Structure of proteins: packing of α -helices and pleated sheets. Proc. Natl. Acad. Sci. U. S. A. 74, 4130–4134.)

If one helical surface is turned about the vertical axis and superimposed on the other surface (Fig. 11.6) with a subsequent turn by +20 degree around the axis perpendicular to the plane of the picture, the 1–4–7 ridges of one helix will fit between the 0–4–8 ridges of the other helix (and vice versa) and ensure a close contact between the helices (Fig. 11.6, right). Then **a**-groups of one helix fit between **d**-groups of the other, and a slightly twisted contact line arises on the surface of each helix. And when these helices become intertwined (Fig. 11.2) and coiled around the common axis, the interaction area becomes straight and appears in the middle of a slightly twisted helical bundle.

This is not the only way to ensure a close contact of helices; others will be considered when discussing globular proteins. But this is the only good way for the very long helices typical of fibrous proteins. It was predicted by Crick (1953), the same year that he and Watson predicted the DNA double helix.

(c) *Collagen* (“glue forming,” in Greek). This is the major structural protein amounting to a quarter of the total mass of proteins of vertebrates. It forms strong nonsoluble fibrils. A collagen molecule is formed by a special superhelix consisting of three polypeptides (Fig. 11.7) that are free of intra-chain H-bonding (Traub and Piez, 1971) and supported by some interchain hydrogen bonds only.

The conformation of all residues of each collagen chain is close to that of a proline (or rather, a poly(Pro)II helix), but collagen chains form additional interchain H-bonds. This helix is a left-handed helix with a 3.0 residue repeat. Accordingly, in collagen, the main motif of the primary structure is the repeated triad of residues (Gly-Pro-Pro)_n or rather (Gly-something-Pro)_n. Gly is essential for hydrogen bonding in collagen since it (unlike Pro) has an NH group and no side chain; and any side chain would be unwanted in the middle of a tight collagen superhelix where the H-bonding glycine is positioned.

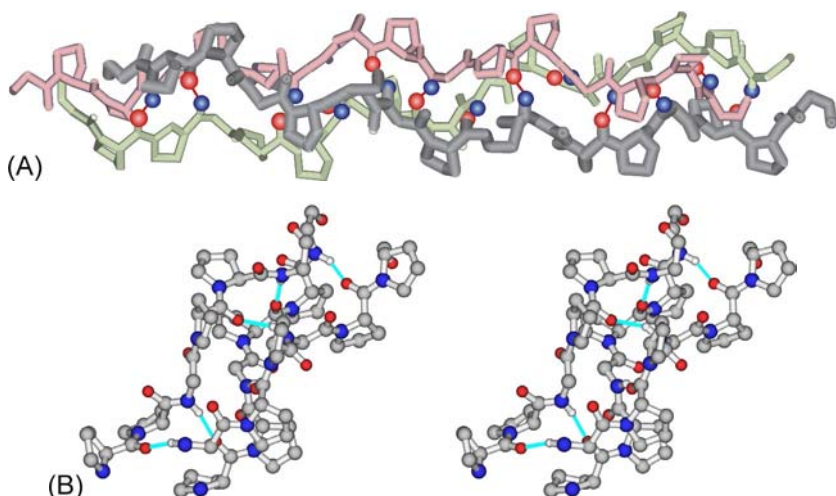


FIG. 11.7 (A) A model of the triple collagen helix with the $(\text{Gly-Pro-Pro})_n$ repeat. Each chain is colored differently. H-atoms of NH-groups of glycines (blue) and O-atoms of the first proline in the Gly-Pro-Pro repeat (red) are shown to participate in hydrogen bonds. Gly of chain “1” binds to chain “2,” while its Pro binds to chain “3,” and so on. Each chain is wound around two others forming a right-handed superhelix. It is called a *superhelix* because at a lower structural level, the level of conformation of separate residues, each individual collagen chain is already helical (it forms a left-handed “microhelix” of the poly(Pro)II type, with three residues per turn, which is easily seen from the alignment of the proline rings). A collagen molecule is about 15 Å wide and about 3000 Å long. (B) A stereo drawing of the triple collagen superhelix.

Interestingly, the collagen chain-coding exons almost always start with glycines, and the number of their codons is a multiple of three. As you may remember, eukaryotic genes contain protein-coding exons separated by introns that are cleaved from mRNA (and therefore do not encode proteins) (Creighton, 1993; Stepanov, 1996).

At the next higher structural level collagen superhelices associate into collagen fibrils.

The biosynthesis of collagen, its subsequent modification and the formation of the mature structure of a collagen fibril have been well studied (Fig. 11.8) (Schulz and Schirmer, 1979/2013; Creighton, 1993; Stepanov, 1996).

As with folding of many fibrous (and membrane) proteins, collagen folding is an externally assisted process. This distinguishes it from the most interesting spontaneous folding typical of water-soluble globular proteins, which is to be discussed close to the end of this course. Besides, collagen folding always involves several chains, which is typical of fibrous proteins, unlike membrane and water-soluble globular proteins.

Correct collagen folding needs to be initiated by procollagen that contains, apart from collagen chains, globular heads and tails. Without these heads and tails, the collagen chains fold into “incorrect” triple helices that lack the

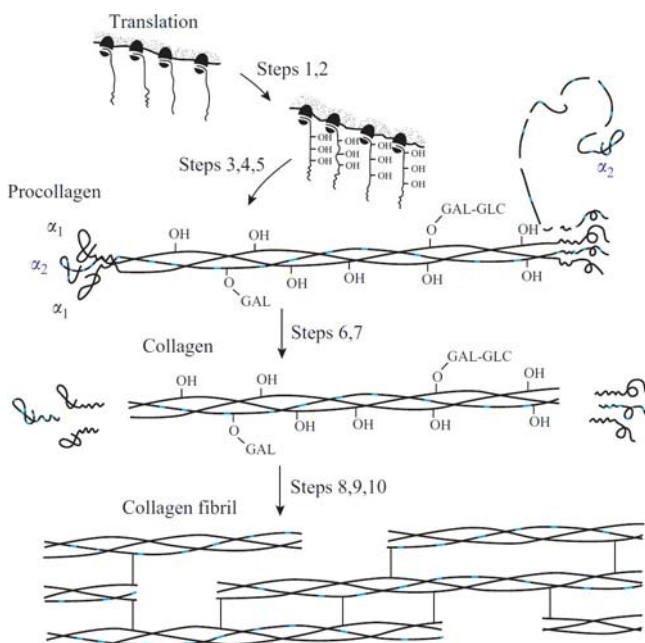


FIG. 11.8 In vivo formation of collagen. Step 1. Biosynthesis of pro- α_1 -chains and pro- α_2 -chains (≈ 1300 residues long each) in the ratio of 2:2. Step 2. Enzymatic cotranslational hydroxylation of some Pro and Lys residues positioned prior to Gly. Step 3. Association of sugars (GLC-GAL) with some hydroxylated residues. Step 4. Formation of the tetramer from C-terminal globules of two pro- α_1 and two pro- α_2 chains; subsequent degradation of one pro- α_2 chain and formation of the pro-collagen (pro- α_1 - α_2 - α_1 trimer) with S-S-bonds between globular ends. Step 5. Formation of a triple helix in the middle of pro-collagen. Step 6. Procollagen secretion into extracellular space. Step 7. Cleavage of globular parts. Steps 8–10. Spontaneous formation of fibrils from the triple superhelices, final modification of amino acid residues and crosslinking (caused by a special enzyme) between modified residues of collagen chains. (Adapted from Schulz, G.E., Schirmer, R.H., 1979/2013. *Principles of Protein Structure*. Springer, New York/Heidelberg, Berlin (Chapter 4), with permission.)

heterogeneity typical of native collagen (which contains one α_2 and two α_1 chains), its inherent register (ie, the correct shift of chains about one another), etc. Thus, a separately taken collagen triple helix is incapable of spontaneously self-organizing its correct spatial structure in vitro. In this respect, it is similar to silk fibroin and distinct from some of the previously described α -helical coiled coils and especially from globular proteins that we will discuss later.

As temperature is increased, the collagen helix melts (this is how gelatin is formed). The collagen melting temperature is strongly dependent on the proportion of proline and oxyproline (the higher the concentration of these rigid residues, the higher the melting temperature, naturally). This melting temperature is usually only a few degrees higher than the body temperature of the host

animal ([Alexandrov, 1965](#)). Please note this fact, as we will return to it in a future lecture.

Collagen folding is particularly interesting because a number of hereditary diseases are known to be associated with mutations in collagens ([Stepanov, 1996](#)), the best characterized of which is *osteogenesis imperfecta* or “brittle bone” disease. The most common cause of this syndrome is a single base substitution that results in the replacement of glycine by another amino acid. This breaks the $(\text{Gly-X-Y})_n$ repeating sequence that gives rise to the characteristic triple-helical structure of collagen. It appears that at least one effect of this is to slow folding and allow abnormal posttranslational modifications to occur. In order to overcome the difficulty of studying collagen itself, the effect of mutations relevant to disease is explored through the study of highly simplified repeating peptides.

This allows detailed biophysical investigations to be carried out, including “real-time” NMR experiments, in order to probe the nature of the folding steps at the level of individual residues ([Baum and Brodsky, 1997](#)). Interestingly, this example illustrates both the increasingly well-established link between protein misfolding and human disease ([Bychkova and Pitsyn, 1995](#)), and the power of properly applied structural methods in probing its molecular origins.

I would like to emphasize that most of fibrous proteins (such as silk fibroin, collagen, etc.) are structurally simple owing to the periodicity of their primary structure and, hence, to their large secondary structures.

However, one more addition would not be out of place here.

Proteins forming huge aggregates without any distinct inner structure are also often classified as fibrous proteins. They form a chemically linked elastic matrix in which other more structural proteins are immersed.

Elastin is a typical matrix protein ([Stepanov, 1996](#)). It plays an important role in building artery and lung walls, etc. Its long chain is rather hydrophobic and consists of short residue repeats of several types. The resultant product resembles rubber: each elastin chain forms a disordered coil, and together these chains form a net linked by enzyme-modified lysines, four per knot. I cannot but mention that the disturbed function of lysine-modifying enzymes causes the loss of elasticity of vessel walls, and sometimes even a rupture of the aorta.

Note: Sometimes fibrils formed by globules (eg, actin) are regarded as fibrous proteins. We will not consider them here—globular proteins are to be discussed later on.

Instead, I would like to make an additional note on proteins which are usually considered as fibrous ones. It has been relatively recently observed that many “normal” water-soluble proteins (as to membrane proteins, no such data are available yet) are capable of reorganizing so that to form the so-called amyloid fibrils, which are known to be related to human diseases (see [Chiti et al., 2003](#), and references therein). Lysozyme, myoglobin, etc., and some of their mutants, but primarily the notorious prions belong to this group of proteins (see [Prusiner, 2012](#), and references therein).

Amyloid fibrils are insoluble protein aggregates sharing specific structural traits. Though long known, these fibrils were hardly associated with proteins, until it was noticed that prions, these “infectious proteins,” form amyloid-like fibrils in the infected cells. Later, it became clear that similar amyloids could also be formed by proteins of a most common nature that seemingly differ from prions only by lack of the ability to transmit the disease from one organism to another (see Afanasieva et al., 2011); however, there are recent reports on infectious nature of the peptide A β causing Alzheimer’s disease (Nussbaum et al., 2012).

Amyloid fibrils are polymorphic. So far, studied ones had the individual protein chains folded as a double- or multilayer sandwich with, as a rule, the parallel β -structure (Lührs et al., 2005; Nelson et al., 2005), though some polypeptide chains were observed to form no compact globules at all, Fig. 11.9D (Lu et al., 2013) or to display an antiparallel β -structure (Qiang

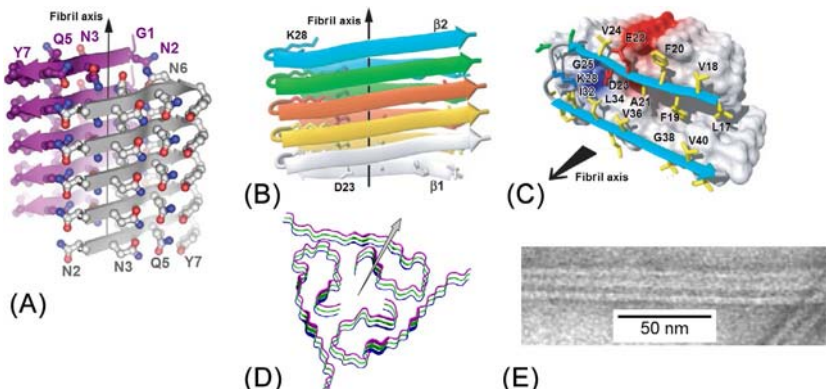


FIG. 11.9 (A) A portion of the X-ray crystallography-solved structure of an amyloid fibril formed by a short (seven residues) fragment of the yeast protein Sup35 (causing a yeast disease similar to a disease of mammals caused by prions; adapted from Nelson et al. (2005), with some simplifications). Note that the “hydrophobic core” of this fibril is composed by *polar* (more so than water) amino acids Asn (N) and Gln (Q), the side groups of which are H-bonded. (B and C) Views from different sides on the structure (solved by a less direct NMR technique) of an amyloid fibril formed by the 42-residue peptide A β (1–42), a part of Alzheimer’s disease-causing protein; adapted from Lührs et al. (2005), with some simplifications. In the A β (1–42) peptide, the fragment 1–17 is disordered (that is why in the figure, only as much as Leu17 is seen), while the rest of it belongs to the protofilament spine whose hydrophobic core comprises mostly “normal” nonpolar amino acids, although the ion pair Asp23-Lys28 is present there as well. (D) The 3D structure of three layers of an amyloid fibril formed by the A β (1–40) peptide (model no. 1 from the PDB; Bernstein et al., 1977) structure 2M4J solved by NMR (Lu et al., 2013). (E) Electron microscopy image of a fragment of the amyloid fibril formed by human insulin after 24 h of incubation; the fibril diameter is \approx 3–4 nm. (Adapted from Selivanova, O.M., Suvorina, M.Y., Dovidchenko, N.V., Eliseeva, I.A., Surin, A.K., Finkelstein, A.V., Schmatchenko, V.V., Galzitskaya, O.V., 2014. How to determine the size of folding nuclei of protofibrils from the concentration dependence of the rate and lag-time of aggregation. II. Experimental application for insulin and Lys-Pro insulin: aggregation morphology, kinetics and sizes of nuclei. *J. Phys. Chem. B* 118, 1198–1206, with some simplifications.)

et al., 2012). β -Strands are perpendicular to the fibril axis, while interstrand H-bonds are parallel to it (Fig. 11.9A–C). The β -sandwiches are tightly packed as protofilaments, tubular or tape-shaped depending on the protein nature and conditions; the protofilaments in turn form long amyloid fibrils (Fig. 11.9E).

The β -structure usually comprises not the entire protein chain but only a part of it, while the remainder may either keep a globular form or be unfolded and remains off the protofilament spine. Presumably, in amyloid fibrils, a unique spatial structure is typical of solely the sequences involved in β -structural protofilament spine.

Typically, the amyloidogenic sites are rich in amino acids characteristic for the β -structure (see Fig. 11.9C), but sometimes (see Fig. 11.9A) they are composed of Gln- and Asn-rich oligopeptide repeats (Parham et al., 2001).

Amyloid formation includes rearrangement of the protein chain structure, which is not just protein folding (or rather, misfolding) but an aggregation process implying both chain refolding and sticking together many protein molecules. It is known to frequently happen very slowly.

This slowness may underlie the extremely long incubation periods of prion infections like scrapie or mad cow disease. We have already met a simple, “peaceful,” and well-studied example of this kind—I mean the structure formation, which is very slow due to a rearrangement. The water-soluble polypeptide poly(Lys), at pH > 10 and 20–50°C, undergoes a very fast coil to α -helix transition followed by a very slow conversion of α -helices into the β -structure. The latter can be accompanied by association and can take hours or weeks; we have already discussed it when considering the kinetics of β -structure formation.

Amyloid formation is sometimes a rather complicated process. Some amyloid fibrils assemble through a series of conformational transitions, including even transitions between antiparallel and parallel β -structure (Liang et al., 2014). Amyloid aggregation commonly includes formation of the β -structure and usually has a lag-period, that is, a delay before the beginning of observable fibril growth (Fig. 11.10); this lag-period often is very pronounced.

This lag-period is a result of a very slow spontaneous initiation of fibrils and their subsequent exponential growth and multiplication (due to fragmentation, branching, or “growth from the surface”) (Xue et al., 2008; Dovidchenko et al., 2014). In the case of an extremely slow spontaneous initiation, fibril formation can be observed only after introduction of “seeds” (pieces of disrupted mature fibrils) into solution of a potentially amyloidogenic protein (Harper and Lansbury, 1997); when the amyloid formation is initiated by seeding, the lag-period is usually absent.

There are, however, good reasons to believe that the organism is not so much harmed by large mature amyloid fibrils themselves as by short active oligomers

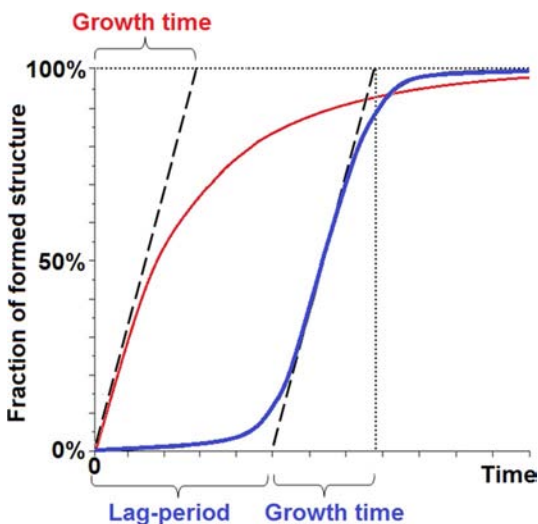


FIG. 11.10 A scheme showing kinetics of unseeded amyloid formation (blue line) where the lag-period is sometimes much shorter and sometimes much longer than the growth time, and kinetics of seeded amyloid formation (red line) where the lag-period is often absent. This kinetics looks rather similar to that of protein folding, which, as we will see soon, is commonly free of any lag-period.

emerging at the beginning of their formation (Ferreira et al., 2007). Anyway, the process and/or the result of amyloid fibril formation underlie serious diseases which may have an extremely long incubation period (eg, kuru, mad cow disease, Alzheimer’s disease, etc.). These and other “conformation-related” diseases had been long predicted by Bychkova and Ptitsyn (1995); they now are the “hot spots” in molecular biology research.

REFERENCES

- Afanasieva, E.G., Kushnirov, V.V., Ter-Avanesyan, M.D., 2011. Interspecies transmission of prions. *Biochemistry (Mosc)* 76, 1375–1384.
- Alexandrov, V.Ya., 1965. On the biological significance of the correlation between the level of thermostability of proteins and the environmental temperature of the species. *Usp. Sovr. Biol.* 60, 28–44 (in Russian).
- Baum, J., Brodsky, B., 1997. Real-time NMR investigations of triple-helix folding and collagen folding diseases. *Fold. Des.* 2, R53–R60.
- Bernstein, F.C., Koetzle, T.F., Williams, G.J.B., Meyer, E.F., Brice, M.D., Rogers, J.R., Kennard, O., Shimanouchi, T., Tasumi, M., 1977. The protein bank. A computer-based archival file for macromolecular structures. *Eur. J. Biochem.* 80, 319–324. modern version: <http://www.rcsb.org/>.

- Branden, C., Tooze, J., 1999. Introduction to Protein Structure, second ed. Garland Publishing Inc., New York, London (Chapter 3).
- Bychkova, V.E., Pitsyn, O.B., 1995. Folding intermediates are involved in genetic diseases? FEBS Lett. 359, 6–8.
- Cantor, C.R., Schimmel, P.R., 1980. Biophysical Chemistry: Part 1. W.H. Freeman & Co., New York (Chapter 2).
- Chiti, F., Stefani, M., Taddei, N., Ramponi, G., Dobson, C.M., 2003. Rationalisation of mutational effects on protein aggregation rates. *Nature* 424, 805–808.
- Chothia, C., Levitt, M., Richardson, D., 1977. Structure of proteins: packing of α -helices and pleated sheets. *Proc. Natl. Acad. Sci. U. S. A.* 74, 4130–4134.
- Creighton, T.E., 1993. Proteins: Structures and Molecular Properties, second ed. W.H. Freeman & Co., New York, NY (Chapter 5).
- Crick, F.H.C., 1953. The packing of α -helices: simple coiled coils. *Acta Crystallogr.* 6, 689–697.
- Dickerson, R.E., 1964. X-ray analysis of protein structure. In: Neurath, H. (Ed.), second ed. In: The Proteins, vol. 2. Academic Press, New York, NY, pp. 603–778.
- Dovidchenko, N.V., Finkelstein, A.V., Galzitskaya, O.V., 2014. How to determine the size of folding nuclei of protofibrils from the concentration dependence of the rate and lag-time of aggregation. I. Modeling the amyloid photofibril formation. *J. Phys. Chem. B* 118, 1189–1197.
- Ferreira, S.T., Vieira, M.N., De Felice, F.G., 2007. Soluble protein oligomers as emerging toxins in Alzheimer's and other amyloid diseases. *IUBMB Life* 59, 332–345.
- Harper, J.D., Lansbury Jr., P.T., 1997. Models of amyloid seeding in Alzheimer's disease and scrapie: mechanistic truths and physiological consequences of the time dependent solubility of amyloid proteins. *Annu. Rev. Biochem.* 66, 385–407.
- Kreplak, L., Doucet, J., Dumas, P., Briki, F., 2004. New aspects of the α -helix to β -sheet transition in stretched hard α -keratin fibers. *Biophys. J.* 87, 640–647.
- Lehninger, A.L., Nelson, D.L., Cox, M.M., 1993. Principles of Biochemistry, second ed. Worth Publishers, New York (Chapter 7).
- Liang, C., Ni, R., Smith, J.E., Childres, W.S., Mehta, A.K., Lynn, D.G., 2014. Kinetic intermediates in amyloid assembly. *J. Am. Chem. Soc.* 136, 15146–15149.
- Lu, J.X., Qiang, W., Yau, W.M., Schwieters, C.D., Meredith, S.C., Tycko, R., 2013. Molecular structure of beta-amyloid fibrils in Alzheimer's disease brain tissue. *Cell* 154, 1257–1268.
- Lührs, T., Ritter, C., Adrian, M., Riek-Lohr, D., Bohrmann, B., Döbeli, H., Schubert, D., Riek, R., 2005. 3D structure of Alzheimer's amyloid-beta (1–42) fibrils. *Proc. Natl. Acad. Sci. U. S. A.* 102, 17342–17347.
- Nelson, R., Sawaya, M.R., Balbirnie, M., Madsen, A.Ø., Riekel, C., Grothe, R., Eisenberg, D., 2005. Structure of the cross-beta spine of amyloid-like fibrils. *Nature* 435, 773–778.
- Nussbaum, J.M., Schilling, S., Cynis, H., Silva, A., Swanson, E., Wangsanut, T., Tayler, K., Wiltgen, B., Hatami, A., Röncke, R., Reymann, K., Hutter-Paier, B., Alexandru, A., Jagla, W., Graubner, S., Glabe, C.G., Demuth, H.U., Bloom, G.S., 2012. Prion-like behaviour and tau-dependent cytotoxicity of pyroglutamylated amyloid- β . *Nature* 485, 651–655.
- Parham, S.N., Resende, C.G., Tuite, M.F., 2001. Oligopeptide repeats in the yeast protein Sup 35 p stabilize intermolecular prion interactions. *EMBO J.* 20, 2111–2119.
- Prusiner, S.B., 2012. Cell biology. A unifying role for prions in neurodegenerative diseases. *Science* 336, 1511–1513.
- Qiang, W., Yau, W.-M., Luo, Y., Mattson, M.P., Tycko, R., 2012. Antiparallel β -sheet architecture in Iowa-mutant β -amyloid fibrils. *Proc. Natl. Acad. Sci. U. S. A.* 109, 4443–4448.
- Schulz, G.E., Schirmer, R.H., 1979/2013. Principles of Protein Structure. Springer, New York/Heidelberg/Berlin (Chapters 4 and 5).

- Stepanov, V.M., 1996. Molecular Biology: Protein Structure and Function. Vysshaya Shkola, Moscow (Chapter 5, in Russian).
- Stryer, L., 1995. Biochemistry, fourth ed. W.H. Freeman & Co., New York (Chapter 9).
- Traub, W., Piez, K.A., 1971. The chemistry and structure of collagen. *Adv. Protein Chem.* 25, 243–352.
- Volkenstein, M.V., 1977. Molecular Biophysics. Academic Press, New York/London (Chapter 4).
- Xue, W.F., Homans, S.W., Radford, S.E., 2008. Systematic analysis of nucleation-dependent polymerization reveals new insights into the mechanism of amyloid self-assembly. *Proc. Natl. Acad. Sci. U. S. A.* 105, 8926–8931.

Lecture 12

Let us now focus on membrane proteins. As concerns their specific transmembrane parts “living” in hydrophobic environment, these proteins are almost as simple as fibrous proteins (Creighton, 1993; Stryer, 1995; Branden and Tooze, 1991; Nelson and Cox, 2012).

Membranes are films of lipids (fat) and protein molecules (Fig. 12.1). They envelop cells and closed volumes within them (the so-called “compartments”). The peculiar role of membrane proteins (they amount to half of the membrane weight) is to act as a power plant dam wall in the cell (this we will consider later) and to provide transmembrane transport of various molecules and signals—this we will consider now.

In transmitting a signal, the lipids of a membrane work as a kind of “insulator” while its proteins (or rather, as we will see later, protein channels) act as “conductors.” These conductors are specific, each ensuring transmembrane transport of molecules of a particular kind or signals from particular molecules (by a slight change in the protein’s conformation).

True membrane proteins reside within the membrane where there is virtually no water. The intramembrane parts have a regular secondary structure, and their size is determined by the membrane thickness (Fig. 12.1).

Let us consider the structure of membrane proteins using several examples.

As a matter of fact, structures of membrane proteins so far constitute <1% of protein structures collected in the Protein Data Bank (Berman et al., 2012), although membrane proteins constitute about one-third of all proteins (Neumann et al., 2012). This is due to their poor solubility in water (detergents have to be used, etc.) and difficulties of crystallization caused by their tendency to disordered association (Huber, 1989).

Fig. 12.2 gives the structure of bacteriorhodopsin which pumps protons across the membrane. This structure was originally determined from many high-resolution electron microphotographs (Amos et al., 1982; Henderson et al., 1990), because it was too difficult to obtain good 3D crystals of bacteriorhodopsin. Therefore, its X-ray structure (which appeared to be very much the same) was reported much later (Pebay-Peyroula et al., 1997).

As we can see, the transmembrane portion of bacteriorhodopsin comprises seven regular α -helices that form a membrane-spanning bundle slightly tilted with respect to the plane of the membrane, while the single β -hairpin and all irregular segments (connecting loops) protrude from the membrane.

The highly regular arrangement of the transmembrane chain backbone is only natural. Each H-bond is expensive in the fatty, waterless environment. Therefore, the protein chain has to adopt a structure with fully accomplished hydrogen bonding, that is, either the α -helix or the β -cylinder (see later).

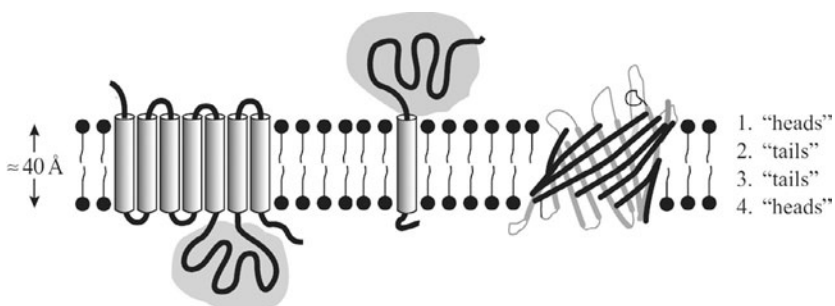


FIG. 12.1 Membrane-embedded proteins. Extramembrane domains are shown, very schematically, in gray. Protein sequences within the membrane are virtually free of irregular segments. In eukaryotes, chain portions projecting from the membrane out of the cell are strongly glycosylated and therefore more hydrophilic. 1. Polar “heads” of lipids of one membrane layer. 2. Nonpolar “tails” of lipids of the same membrane layer. 3. Non-polar “tails” of lipids of second membrane layer. 4. Polar “heads” of lipids of second membrane layer. (*Adapted from Branden, C., Tooze, J., 1991. Introduction to Protein Structure. Garland Publishing Inc., New York (Chapter 12).*)

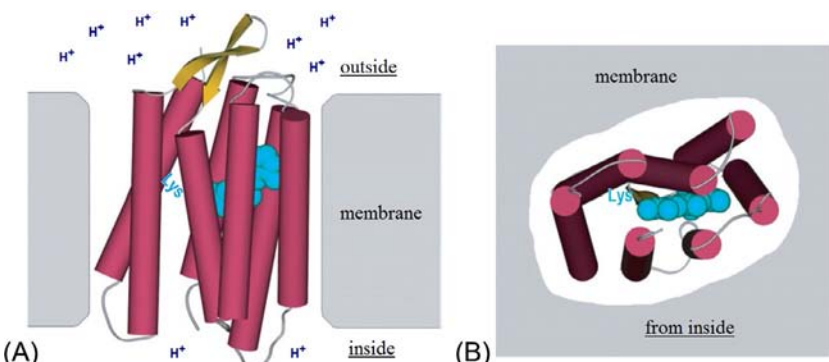


FIG. 12.2 Membrane-embedded bacteriorhodopsin: (A) as viewed along the membrane; (B) as viewed from the bottom (from the cytoplasm). Its seven helices are shown as cylinders. The connecting loops are also shown together with the bound retinal molecule (light-blue). The lipid layer is schematic. H^+ concentration presented in (A) is greatly exaggerated: the distance between the ions shown in (A) is ~ 1 nm, while at pH7 this distance is ~ 250 nm. (*Adapted from Branden, C., Tooze, J., 1991. Introduction to Protein Structure. Garland Publishing Inc., New York (Chapter 12).*)

The hydrophobic groups positioned on the bacteriorhodopsin α -helices are turned rather “outwards,” towards lipids that are also hydrophobic, while the few polar groups face the interior and form a very narrow proton-conducting channel. The proton flow is mediated by a cofactor, which is the retinal molecule chemically bound to Lys of helix G inside the bundle of helices. Retinal blocks the central channel of bacteriorhodopsin.

Bacteriorhodopsin is a light-driven proton pump. Having accepted a photon, retinal changes its form, from *trans* to *cis* (Fig. 12.3), that is, bends by rotation about the bond C₁₃=C₁₄ (with a simultaneous slight change of the protein body conformation) and moves a proton (H⁺) from one (inside) end of the seven-helix bundle to the other, extracellular end. Then retinal regains its previous *trans*-shape, but this time without a proton (Branden and Tooze, 1991), and then receives H⁺ from the cytoplasm. In this way the H⁺ pump works and transports H⁺ from the cytoplasm (where there are few H⁺) to the outside (where there are a lot of them). That is, the photon-induced H⁺ transport goes *against* the H⁺ concentration gradient.

The point is that retinal-bound N-atom of Lys (Fig. 12.3) binds H⁺ very strongly when retinal is in the *trans* form; and the bacteriorhodopsin construction is such that the retinal having its ground-state *trans* form turns its H⁺-binding site towards the inner side of the membrane, and this strong binding site only can bind H⁺ from this (cytoplasm) side, although H⁺ concentration here is low. But when retinal has absorbed a photon, obtaining its activated *cis* form and bent, it binds H⁺ very loosely, and simultaneously, the H⁺-binding site faces the outer side of the membrane. Thus, the loose binding site releases H⁺, which only can go to the outer side of the membrane, although H⁺ concentration there is high.

It is interesting that the same retinal works differently in rhodopsin (a protein quite similar to bacteriorhodopsin), though it is bound to Lys in both of these proteins. In rhodopsin, the retinal ground state is *cis* (rather than *trans*, as in bacteriorhodopsin); its photoactivated state is *trans* (rather than *cis*); and the *cis-trans* transition in rhodopsin-localized retinal results from a turn around the C₁₁=C₁₂ bond (rather than around the C₁₃=C₁₄ one, as in bacteriorhodopsin). This demonstrates how the protein environment can change the behaviour of a co-factor.

Bacteriorhodopsin's central channel is narrow. Similar (but usually wider) pores arranged like a hollow bundle of helices can be formed in other cases from separate α -helical transmembrane peptides (Branden and Tooze, 1991).

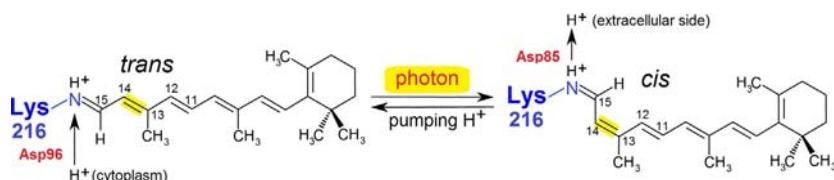


FIG. 12.3 Photoisomerization of retinal in bacteriorhodopsin. Retinal is bound to the N atom of the bacteriorhodopsin's Lys; this N atom (shown in blue) accepts and releases H⁺. Two other groups of bacteriorhodopsin that facilitate binding (Asp96) and release (Asp85) of H⁺ are also shown. (Adapted from <https://en.wikipedia.org/wiki/Bacteriorhodopsin>; <https://en.wikipedia.org/wiki/Retinal>.)

By the way, helical bundles are also abundant in quite different membrane proteins. These do not transport molecules across the membrane but conduct signals.

I am now speaking about receptors, and specifically about hormone receptors (Fig. 12.4). There are two principal signal transduction pathways involving the so-called G protein-coupled receptors: the phosphatidylinositol signal pathway and the cyclic adenosine monophosphate (cAMP) signal pathway. Let us briefly consider one of many G protein-coupled receptors connected with the cAMP signal pathway. I will use β_2 -adrenergic G protein-coupled receptor as an example; like many receptors of this kind, it contains seven helices and looks very much like bacteriorhodopsin (Cherezov et al., 2007).

Having bound a hormone, this receptor somehow changes the conformation of its transmembrane helical bundle thereby “announcing” the hormone’s arrival (for details, see Cherezov et al., 2007; Trzaskowski et al., 2012), but many of them are not completely clear. This signal causes the α -subunit of the receptor-associated *G-protein* (*Guanine-binding protein*) to release its own guanosine diphosphate (GDP) molecule and take up a guanosine triphosphate (GTP) molecule from the surrounding cytosol. Then this α -subunit leaves both its fellow subunits and the receptor, thus providing an opportunity for another GDP-loaded G-protein α -subunit to contact the receptor and then, in its turn, to leave it having exchanged its GDP for GTP (Fig. 12.4).

The α -subunit of G-protein can cleave GTP (guanidine triphosphate) and convert it to GDP (guanidine diphosphate) and phosphate (P) but, importantly, the process is slow. That is, it has been tailored by the Nature as a “very bad” enzyme; the reason for the slow enzyme action will be considered in the last part of this course. Meanwhile, together with GTP, the α -subunit (with its “tail” buried inside the membrane) drifts along the membrane, reaches adenylate

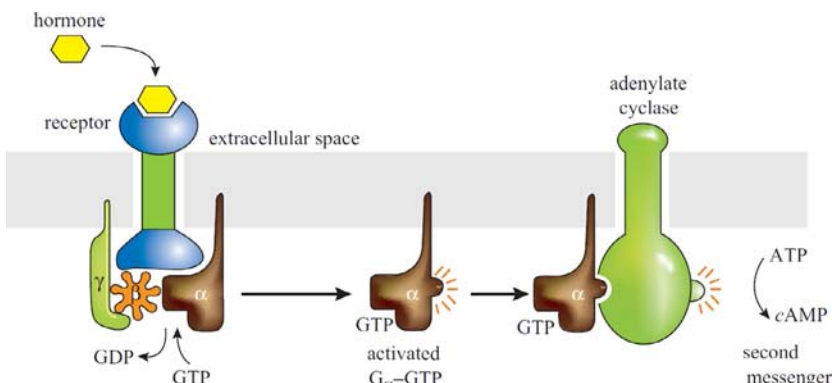


FIG. 12.4 Activation of adenylate cyclase by G-protein, which, in turn, is activated by the hormone-binding transmembrane receptor. (Reproduced from Branden, C., Tooze, J., 1991. *Introduction to Protein Structure*. Garland Publishing Inc., New York (Chapter 12). Reproduced by permission of Garland Science/Taylor & Francis Group LLC.)

cyclase and binds to it; as a result, adenylate cyclase starts functioning and converts many molecules of adenosine triphosphate into cAMP. This initiates a physiological reaction of the cell in response to hormone binding. But the α -subunit's impact upon adenylate cyclase eventually ends when α -subunit-bound GTP turns into GDP. Then, with this GDP, the α -subunit drifts along the membrane and eventually comes back to the host receptor. If the latter is still bound to hormone, the cycle repeats; if not, it is over (Sprang, 1997; Branden and Tooze, 1991).

Hence, the signal of a molecule of hormone is enhanced many-fold, but its duration is finite. This outlines a peculiarity of all G-proteins (not only those activating adenylate cyclase): they function until GTP is cleaved, and a slow GTP cleavage serves as a peculiar timer.

G protein-coupled receptors are found only in eukaryotes (King et al., 2003), where they play an extremely important role in various types of signal transduction. They are involved in many diseases and are also the target of approximately 40% of all modern medicinal drugs (Filmore, 2004; Overington et al., 2006). So, no wonder that many Nobel Prizes have been awarded for various aspects of G protein-mediated signaling.

Now we will consider porin (Fig. 12.5), another transmembrane protein. Its structure is highly regular too and looks like a wide cylinder built up from β -structures. Note that here the β -sheet forms a *closed* β -cylinder, thus avoiding the “free” H-bond donors and acceptors typical of edges of a planar β -sheet. The cylinder comprises 16 very long β -segments, and the diameter of a pore in its center is about 10 Å. The side-groups of polar residues pertaining to the β -strands face the pore, while nonpolar residues alternating with them in the strand face the membrane.

Porin is responsible for the transport of polar molecules, but it is not very selective (Branden and Tooze, 1991).

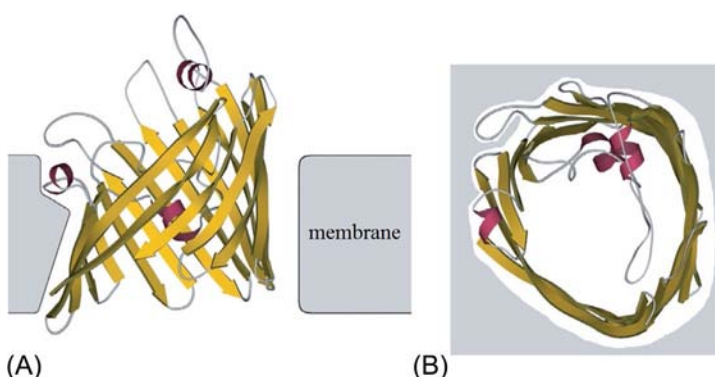


FIG. 12.5 Porin, as viewed (A) along and (B) across the membrane plane. (Adapted from Branden, C., Tooze, J., 1991. *Introduction to Protein Structure*. Garland Publishing Inc., New York (Chapter 12).)

The transport selectivity, that is, specificity of function, of membrane proteins is, of course, dependent on the pore diameter and size of the molecule that tries to pass through it: too large molecules cannot penetrate into it (but the penetration is also difficult for molecules that are a little too small, because (Finkelstein et al., 2006) they are separated from the channel walls by a vacuum gap that is too (narrow to accommodate a water molecule).

The selectivity also is strongly determined by the fact that separate polar groups, not to mention charged ones, can hardly penetrate inside the membrane by themselves.

As you may remember, the free energy of a charge q in the medium with permittivity ϵ is equal to $+q^2/2\epsilon r$, where r is the van der Waals radius of the charge. It can be easily estimated that, with q equal to the electron charge and $r=1.5 \text{ \AA}$ (the typical radius of a singly charged ion), the value of $+q^2/2\epsilon r$ is close to $1.5 \text{ kcal mol}^{-1}$ at $\epsilon=80$ (ie, in water), while at $\epsilon_{\text{membr}}=3$ (ie inside a “purely lipid” membrane), this value will amount to nearly 37 kcal mol^{-1} . In total, an increase in the free energy ΔF of $+35 \text{ kcal mol}^{-1}$ results. According to Boltzmann, the probability of accumulation of such free energy is $\exp(-\Delta F/kT)=\exp(-35/0.6)=10^{-25}$. This means that only one in 10^{25} ion attacks on the membrane will be successful. Given the attack time is no less than 10^{-13} s (as you know, this is the thermal fluctuation time), for an ion passing through a purely lipid membrane would take at least $\sim 10^{12} \text{ s}$, that is about 10,000 years. Thus, a purely lipid membrane appears to be virtually impermeable for ions.

It is quite another matter if the membrane includes protein with a more or less broad water-filled channel where ions at least partly enjoy the high permittivity of water, although to some extent restricted by the surrounding membrane. Roughly (Finkelstein et al., 2006), the membrane-caused increase in the ion’s free energy amounts to about $+q^2/[(\epsilon_{\text{membr}} \epsilon_{\text{water}})^{1/2} R]$, where R is the channel radius, $\epsilon_{\text{membr}}=3$ and $\epsilon_{\text{water}}=80$. It is easy to calculate that with $R \approx 1.5 \text{ \AA}$, it takes an ion a fraction of a second to pass through the channel, and with $R \approx 3 \text{ \AA}$ the time is a tiny fraction of a millisecond.

The channel sites that can attract (or repulse) the ion and thereby reduce (or increase) the barrier to be overcome regulate the selectivity of ion transfer across the membrane. For example, the presence of a positive charge near the channel accelerates transport of negatively charged ions and strongly hampers transport of positively charged ions (Fig. 12.6). In the case of a negatively charged channel, the transport of positive ions is accelerated while that of negative ions is hampered. This effect (and, of course, the pore diameter) underlies the selectivity of membrane proteins responsible for the transport of molecules.

Fig. 12.6 is merely a scheme, but Fig. 12.7 (taken from Long et al., 2007) shows the key part of a transmembrane pore, the “filter,” in the potassium channel. Such channels are found in most cell types; they control a wide variety of cell functions and are targets for many drugs (Jessell et al., 2000; Hille, 2001;

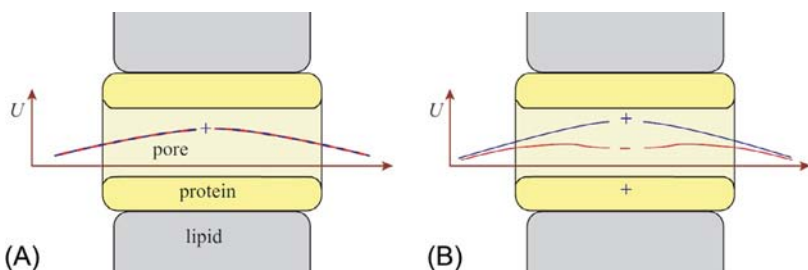


FIG. 12.6 Very schematic diagram of a transmembrane pore (here the membrane is vertical and the pore is horizontal) and the electrostatic free energy U for positively (---+---) and negatively (—+—) charged ions: (A) with no charge on the inner pore surface; (B) with a positive charge close to the pore.

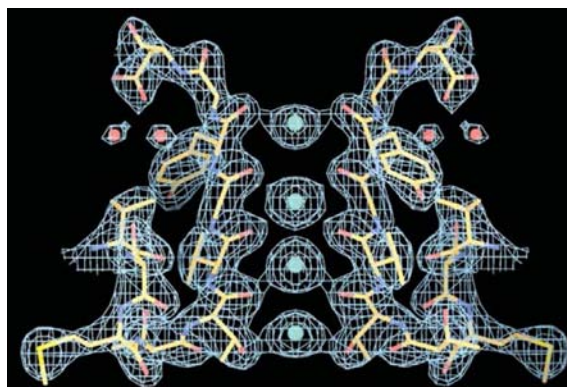


FIG. 12.7 The bottleneck of the potassium channel: the K^+ selectivity filter. For clarity, the parts of only two out of four subunits surrounding the channel are shown (yellow/red sticks surrounded by electron density contours). K^+ (blue spheres) surrounded by electron density contours and water molecules (small red spheres surrounded by electron density contours) are also shown. (Adapted from Long, S.B., Tao, X., Campbell, E.B., MacKinnon, R., 2007. Atomic structure of a voltage-dependent K^+ channel in a lipid membrane-like environment. *Nature* 450, 376–382, with permission.)

Rang, 2000). The membrane voltage-dependent channel is shown here in its “open,” K^+ -transmitting state. One can see that the pore diameter exactly fits the potassium (K^+) ion size, and that walls of the pore are paved with carbonyl oxygens (red short sticks in Fig. 12.7), which are strongly electro-negative and attractive for cations (ie, “plus” charges). The shown intramembrane filter selects and transmits K^+ (and does not transmit smaller Na^+ (Armstrong, 1998); the explanation is given above, while the voltage-sensitive gating (controlling opening and closing of the channel) is performed by a significant displacement of the extramembrane domains of the same protein.

Now let us focus on the photosynthetic reaction center (Fig. 12.8) (Deisenhofer et al., 1985; Huber, 1989; Branden and Tooze, 1991). Its function is to ensure the transport of light-released electrons from one side of the membrane to the other, thereby creating the transmembrane potential that underlies photosynthesis.

The photosynthetic reaction center comprises cytochrome with four hemes (actually, this protein is not a membrane protein: it is outside the membrane in the periplasmic space) and three membrane subunits, L, M, and H (though the transmembrane part of the last is represented by one α -helix only). Subunits L and M are very much alike.

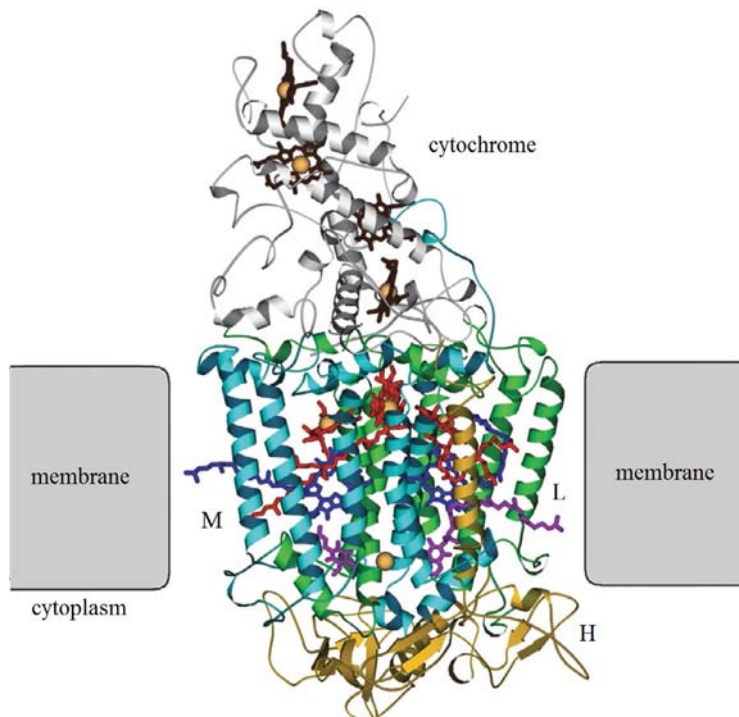


FIG. 12.8 A photosynthetic reaction center. The membrane is shown schematically. The transmembrane subunit M appears in light-blue, L in green and H (with its single transmembrane helix) in yellow, while cytochrome is gray. Notice how distinctly more regular the transmembrane chain portions are compared with those outside the membrane. The subunits L and M bind photosynthetic pigments, chlorophylls (shown in red with a yellow spot for the magnesium ion) and pheophytins (shown in dark-blue). Each has a long hydrophobic tail projecting from the protein into the membrane. The subunits L and M also bind the two quinones, shown in violet. Cytochrome positioned outside the membrane binds four hemes (grayish-black with yellow spots for iron ions). All cofactors are shown as wire models; see also Fig. 12.9. (Adapted from Branden, C., Tooze, J., 1991. *Introduction to Protein Structure*. Garland Publishing Inc., New York (Chapter 12).)

All transmembrane parts are α -helical. As usual, they are long (equal to the membrane thickness) and regular. There are no irregular loops inside the membrane. The outer chain portions are considerably less regular and contain many loops; in fact, their fold is the same as that of “ordinary” water-soluble proteins, which we will discuss later.

Notice the many rather small cyclic molecules, pigments, embedded in this protein: these form the “conductors,” that is, the pathways for the electron flow (the flow of electrons can be followed by the changing electron spectra of pigments during electron transport). The polypeptide only serves as a “shaping insulator.”

First, a light quantum (either originating directly from sunlight or transferred as excitation energy via a light-harvesting antenna system, see later) displaces an electron from the “special pair” of chlorophylls (see the schematic diagram, Fig. 12.9), where it has low energy, to the chain of pigments where it has an elevated energy. Having passed (within a few picoseconds) through the “accessory” chlorophyll B_A , this electron then instantly, within a picosecond, joins to pheophytin P_A (note: P_A and not P_B), and about 200 ps later, it arrives at quinone Q_A . Then it spends about a fraction of millisecond to reach Q_B (Branden and Tooze, 1991; Leonova et al., 2011). We still do not know why the electron prefers this roundabout way to Q_B .

An electron coming from the cytochrome heme replaces the electron released from the special pair of chlorophylls. This completes the first half-cycle of the reaction.

The other similar half-cycle brings another electron to Q_B making it doubly charged and therefore capable of leaving the membrane more easily to participate in further photosynthetic events.

Thus, the photosynthetic reaction center performs electron transport from the upper (in Figs. 12.8 and 12.9) to the lower compartment, that is, against the apparent difference in electric potential between the compartments. The efficiency is about 50% (in other words, 50% of the captured light is converted into the energy of separated charges, which is not bad at all).

The following three important physical aspects must be emphasized:

1. If a special pair of bacteriochlorophylls were to absorb light alone, it would use only a small portion of the light flux. However, the photosynthetic reaction center is surrounded by a light-harvesting antenna. The antenna is not directly involved in photochemical reactions, but is designed to absorb light and transfer excitations toward the photosynthetic reaction center (Liu et al., 2004; Barros and Kuhlbrandt, 2009) consisting (in bacteria) of one “large” complex LH1 (probably embracing the photosynthetic reaction center) and 8–10 “small” complexes LH2 located around (see Branden and Tooze, 1991; Cogdell et al., 2003, and references therein). The LH1 complex is composed of 32 transmembrane α -helices collected in a hollow cylinder, and 32 bacteriochlorophylls seating between these helices and providing

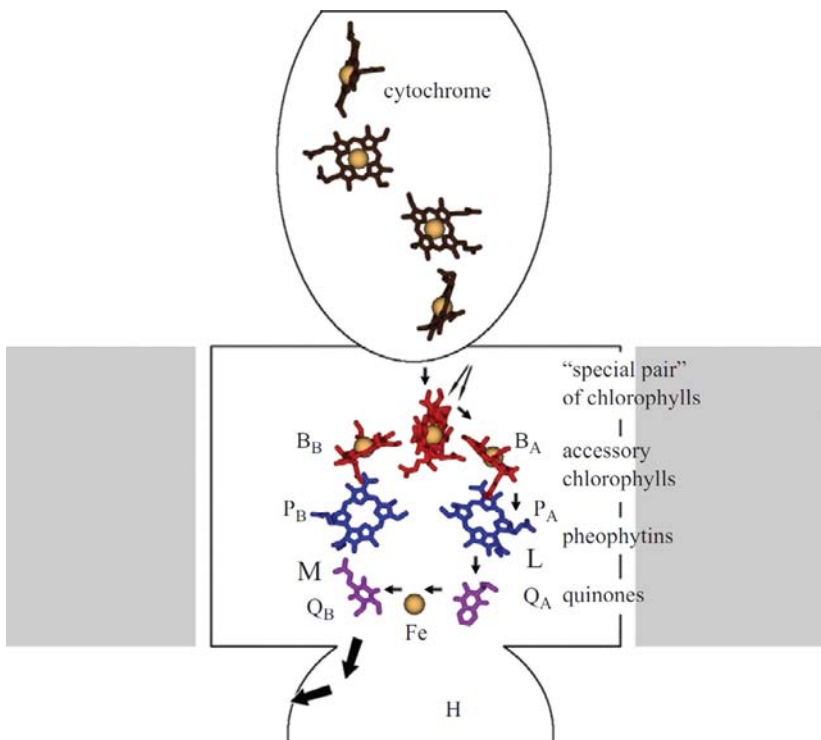


FIG. 12.9 Schematic arrangement of the photosynthetic pigments in the reaction center. The reaction center orientation is the same as in Fig. 12.8. The pseudo-twofold symmetry axis of the L and M subunits passes through the “special pair” of chlorophylls and the Fe ion. The pigments’ long “tails” are omitted as unnecessary details. Electron transfer proceeds preferentially along the branch associated with the L subunit (on the right of the figure). The electron pathway is shown as small arrows. The large arrow indicates release of the quinone with two consecutively accepted electrons. The left chain is not used. Presumably, it was used in the past, but in present-day reaction centers it is an appendix-like relic. (Adapted from Branden, C., Tooze, J., 1991. *Introduction to Protein Structure*. Garland Publishing Inc., New York (Chapter 12).)

their contacts. Each “small” LH₂ complex consists of 18 transmembrane α -helices forming a hollow cylinder, and 27 bacteriochlorophylls seating between these helices and providing their contacts

Thus, a special pair of bacteriochlorophylls of the photosynthetic reaction center is surrounded by about 300 other bacteriochlorophylls. Upon reaching any bacteriochlorophyll of this huge system, a photon excites the collective resonance energy transfer embracing entire bacteriochlorophyll system, and this excitation persists in the system until it knocks out an electron from the special pair of bacteriochlorophylls.

2. All chlorophylls (Fig. 12.10), pheophytins, quinones, and other pigments contain partial double (p-electron) bonds of the $\cdots-C=C-C=\cdots$ type. In other words, owing to Pauling resonance ($\cdots-C=C-\cdots \Leftrightarrow \cdots-C-C= \cdots$), each

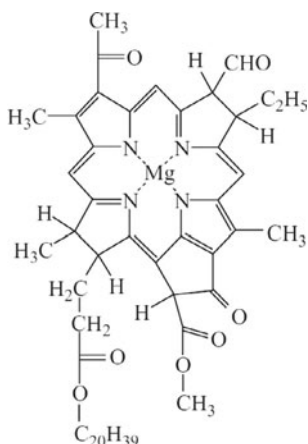


FIG. 12.10 A molecule of bacteriochlorophyll. (Adapted from Branden, C., Tooze, J., 1991. *Introduction to Protein Structure*. Garland Publishing Inc., New York (Chapter 12).)



FIG. 12.11 Schematic representation of tunneling. The profile of the electron potential energy U is shown as a solid line. The dashed line shows the level of total (potential + kinetic) energy of the electron. The bell-shaped line (with hatching below) represents the density of the electron cloud ρ . Initially, the electron stays in the left well (as shown in the figure) with the edge of its cloud (although at an extremely low density) reaching the right well, where the electron can move with time if the energy proves to be lower there. Given a well depth of a few electron Volts or about 100 kcal mol⁻¹ (the typical energy required for molecular ionization), the typical distance at which the density of the electron cloud is reduced by an order of magnitude is about 1 Å.

of these molecules is covered by a common electron cloud, and on such a molecule electrons move as on a piece of metal. This provides a potential well where electrons are “delocalized,” that is, where they can shift by distances greater than the atom diameter. (Note that it is electron delocalization that underlies the typical pigment colors: an electron localized in a separate covalent bond is excited by short-wave UV light, whereas a delocalized electron is excited by “ordinary” visible light of a longer wavelength.)

3. Electron transfer from one “piece of metal” (pigment) to another requires no direct contact of these pigments. It is performed by *quantum tunneling* (see Fig. 12.11).

The main point about quantum tunneling (also called the “sub-barrier” transition because it is as if the electron passes *under* the energy barrier), is that in accordance with quantum mechanics, an electron (like any other particle,

and especially a light particle) “projects” slightly beyond the potential well in which it resides ([Landau and Lifshitz, 1977](#)). The host molecule of the electron (chlorophyll, pheophytin, etc.) serves as the “potential well,” that is, the area of low potential energy U .

When outside the “well” ([Fig. 12.11](#)), the electron’s potential energy is higher than its total (potential + kinetic) energy when in the well. But for the quantum effect, this deficient energy would not let the electron density project a straw beyond the well. However, owing to the quantum effect the electron wave function (or, simply, the density of the electron cloud) extends beyond the potential well, although the value of this density decreases exponentially with growing distance from the well.

The latter point is another manifestation of the same quantum effect that prevents an electron from falling onto the nucleus: although this would decrease the potential energy of the electron, its kinetic energy would increase still more. The thing is that if the distance between the electron and the nucleus (Δx) tends to zero, the potential energy of the electrostatic interaction of the electron with the nucleus tends to minus infinity as $1/(\Delta x)$, while according to the Heisenberg Uncertainty Principle, the electron’s kinetic energy tends (at $\Delta x \rightarrow 0$) to plus infinity far more rapidly, as $1/(\Delta x)^2$.

Indeed, according to the Heisenberg principle, uncertainty in speed (Δv) and uncertainty in coordinate (Δx) of a particle are related as $m\Delta v\Delta x \sim \hbar$, where \hbar is Planck’s constant divided by 2π , and m is the mass of the particle. In other words, the absolute value of the particle’s speed (v) in the well of a Δx width is about $\hbar/(m\Delta x)$ (with complete uncertainty of the direction in which the particle moves at the given moment). Hence, the kinetic energy of the particle, $E = mv^2/2$, is a value of about $m[\hbar/(m\Delta x)]^2 = (\hbar^2/m)\Delta x^2$.

The same is true for an electron staying in the potential well: provided it does not project a straw beyond the well, its total energy would be higher.

That is why the electron slightly “comes out” of the potential well and its density decreases exponentially, like the electron cloud of an atom. The typical distance at which the cloud density becomes an order of magnitude (10-fold) lower is about 1 Å (which, as we know, is the typical radius of an atom).

Clarification. Quantum-mechanical calculation (see [Landau and Lifshitz, 1977](#)) shows that the characteristic distance λ , where electron cloud density decreases by 10 times, is, approximately, $\ln 10 \cdot \hbar / \sqrt{8m \cdot \Delta E}$ (where m is the electron mass and $\Delta E > 0$ is the difference between the barrier energy and the level of electron’s energy in the well); a typical value of $\Delta E \sim 5$ electron-volts (≈ 120 kcal mol⁻¹) leads to $\lambda \approx 1$ Å.

Hence, the electron cloud density becomes 1000 times lower at a distance of 3 Å from the “home well.” This means that the probability of electron’s moving as far as 3 Å off its “home well” during one vibration is about 10^{-3} (for 5 Å it is about 10^{-5} , for 10 Å about 10^{-10} , and so on). When in the “well” (in a pigment molecule), an electron performs $\sim 10^{15}$ vibrations per second (it vibrates at visible light frequencies: this is seen from light absorption spectra of such

molecules). Hence, the typical time of its transition into another “well” (another pigment molecule) 3 \AA away is about $10^{-15} \text{ s}/10^{-3} = 10^{-12} \text{ s}$; for 5 \AA it is about 10^{-10} s , for 10 \AA about 10^{-5} s and for 15 \AA about 1 s . This simple relationship between transition rates and distances is in a qualitative agreement with what we observe in the photosynthetic reaction center.

The following points deserve your special attention:

First. The total distance of the electron transition in the photosynthetic center is about 40 \AA . This distance cannot be covered by one tunnel jump (it would take $\sim 10^{-15} \text{ s}/10^{-40} \sim 10^{25} \text{ s}$ or $\sim 10^{17} \text{ years}$, which is beyond the lifetime of the Universe). However, because of the protein arrangement, this great jump is divided into four small jumps from one electron-attracting pigment to another; as a result, an electron covers the entire 40 \AA distance during a fraction of a millisecond.

Second. To prevent an electron’s prompt return to the first pigment from the second one, and to promote its further movement to the third pigment, and so on, its total (potential + kinetic) energy must decrease along the pathway; in other words, every step of the electron path must be a descent from a high-energy orbital to a low-energy one. The arrangement of the photosynthetic reaction center is believed to provide such a decrease in electron energy from pigment to pigment.

Third. An electron spends no energy on tunneling (since there is no “friction” here). The energy is decreased by the electron-conformational interaction ([Volkenstein, 1979](#)). Specifically, when arriving at the next pigment, an electron faces the pigment’s conformation corresponding to the energy minimum *without* the newcomer. In its presence, the energy minimum corresponds to another, slightly deformed, conformation of the pigment (ie, another location of the nuclei of its atoms). When adopting this new conformation, the pigment atoms rub against the surroundings, and the excess energy dissipates. As a result, at each step, the electron changes a high-energy orbital for a low-energy orbital, its energy decreases and appears to be spent on making the tunnel transition “efficient,” that is, irreversible.

Fourth. A tunneling (sub-barrier) transition can be distinguished from an ordinary activation mechanism that requires the overcoming of an energy barrier ([Frauenfelder, 2010](#)). The rate of tunneling is virtually temperature-independent (and therefore tunneling does not disappear at low temperatures), whereas the rate of an activation transition (proportional to $\exp(-\Delta E^\# / kT)$, where $\Delta E^\#$ is the energy of the activation barrier, and T is temperature) decreases dramatically with decreasing temperature.

In conclusion, let me say a few words on folding of membrane proteins. Some membrane proteins fold spontaneously ([Roman and González Flecha, 2014](#)) like water-soluble proteins; this phenomenon we will consider in one of the subsequent lectures. But usually membrane protein folding is not spontaneous; rather, it is assisted by some special cellular mechanisms ([Skach, 2009](#)).

- *Inner voice:* Do you mean chaperones?
- *Lecturer:* From my point of view, real chaperones are used just to fold membrane proteins. But for some historical reasons which I do not know, the term “chaperones” is only applied to proteins that somehow, and in any case much less manifestly, assist folding the water-soluble proteins. We will come to chaperones in one of the subsequent lectures.

As far as membrane proteins are concerned, the mentioned “special cellular mechanisms” solve two problems:

1. To establish protein topology by selective peptide transport to the opposite sides of a cellular membrane;
2. To insert, integrate, and fold transmembrane segments within the lipid bilayer.

In eukaryotes, the membrane protein folding usually takes place in the endoplasmic reticulum, coincident with protein synthesis, and is facilitated by the “translating ribosome and the translocon” complex (Fig. 12.12). At its core, this complex is assumed to form a dynamic pathway through which the elongating nascent polypeptide moves as it is delivered. The complex is assumed to function as a protein-folding machine that restricts conformational space by establishing transmembrane topology (maybe with the aid of some factors that bind to specific signals contained in the nascent protein sequence) and yet provides a permissive environment that enables nascent transmembrane domains to efficiently fold.

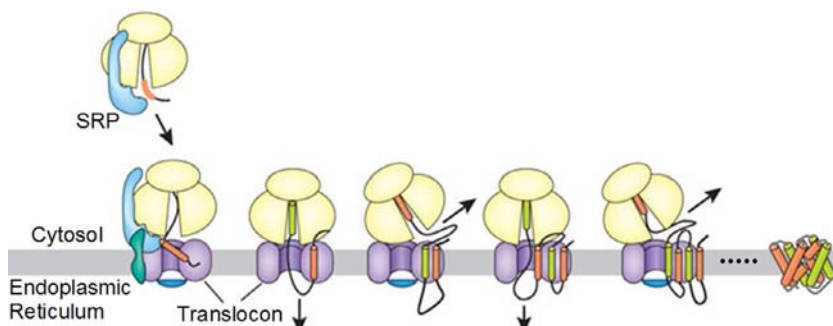


FIG. 12.12 Tentative mechanism of transmembrane integration. For explanations, see the text. SRP is the signal protein recognition particle that binds to the signal sequence of a nascent peptide as it emerges from the ribosome and targets them both to the membrane. Arrows show directions of protrusion of the loops. The translocon (the structure of which remains unknown) is a protein complex that is involved in translocation of the nascent protein chain across the membrane and its folding. (Adapted from Skach, W.R., 2009. Cellular mechanisms of membrane protein folding. *Nat. Struct. Mol. Biol.* 16, 606–612.)

REFERENCES

- Amos, L.A., Henderson, R., Unwin, P.N., 1982. Three-dimensional structure determination by electron microscopy of two-dimensional crystals. *Prog. Biophys. Mol. Biol.* 39, 183–231.
- Armstrong, C., 1998. The vision of the pore. *Science* 280, 56–57.
- Barros, T., Kuhlbrandt, W., 2009. Crystallisation, structure and function of plant light-harvesting complex II. *Biochim. Biophys. Acta Biogeosci.* 1787, 753–772.
- Berman, H.M., Kleywegt, G.J., Nakamura, H., Markley, J.L., 2012. The Protein Data Bank at 40: reflecting on the past to prepare for the future. *Structure* 20, 391–396. <http://www.wwpdb.org/>.
- Branden, C., Tooze, J., 1991. Introduction to Protein Structure. Garland Publishing Inc., New York (Chapter 12).
- Cherezov, V., Rosenbaum, D.M., Hanson, M.A., Rasmussen, S.G., Thian, F.S., Kobilka, T.S., Choi, H.J., Kuhn, P., Weis, W.I., Kobilka, B.K., Stevens, R.C., 2007. High-resolution crystal structure of an engineered human β_2 -adrenergic G protein-coupled receptor. *Science* 318, 1258–1265.
- Cogdell, R.J., Isaacs, N.W., Freer, A.A., Howard, T.D., Gardiner, A.T., Prince, S.M., Papiz, M.Z., 2003. The structural basis of light-harvesting in purple bacteria. *FEBS Lett.* 555, 35–39.
- Creighton, T.E., 1993. Proteins: Structures and Molecular Properties. second ed. W. H. Freeman & Co., New York (Chapter 7).
- Deisenhofer, J., Epp, O., Miki, K., Huber, R., Michel, H., et al., 1985. Structure of the protein subunits in the photosynthetic reaction centre of *Rhodopseudomonas viridis* at 3 Å resolution. *Nature* 318, 618–624.
- Filmore, D., 2004. It's a GPCR world. *Modern Drug Discov.* 7, 24–28.
- Finkelstein, A.V., Ivankov, D.N., Dykhne, A.M., 2006. <http://arxiv.org/abs/physics/0612139> (physics.bio-ph).
- Frauenfelder, H., 2010. The Physics of Proteins. An Introduction to Biological Physics and Molecular Biophysics. Springer, New York (Chapter 13).
- Henderson, R., Baldwin, J.M., Ceska, T.A., Zemlin, F., Beckmann, E., Downing, K.H., 1990. Model for the structure of bacteriorhodopsin based on high resolution electron cryo-microscopy. *J. Mol. Biol.* 213, 899–929.
- Hille, B., 2001. Ion channels of excitable membranes. Potassium Channels and Chloride Channels. Sinauer, Sunderland, MA (Chapter 5), pp. 131–168.
- Huber, R., 1989. Nobel Lecture. A structural basis of light energy and electron transfer in biology. *EMBO J.* 8, 2125–2147.
- Jessell, T.M., Kandel, E.R., Schwartz, J.H., 2000. Principles of Neural Science, Ion Channels, fourth ed. McGraw-Hill, New York (Chapter 6), pp. 105–124.
- King, N., Hittinger, C.T., Carroll, S.B., 2003. Evolution of key cell signaling and adhesion protein families predates animal origins. *Science* 301, 361–363.
- Landau, L.D., Lifshitz, E.M., 1977. Quantum Mechanics. A Course of Theoretical Physics, vol. 3. Pergamon Press, New York (Chapter 3, Section 25).
- Leonova, M.M., Fufina, T.Y., Vasilieva, L.G., Shuvalov, V.A., 2011. Structure-function investigations of bacterial photosynthetic reaction centers. *Biochemistry (Mosc.)* 76, 1465–1483.
- Liu, Z., Yan, H., Wang, K., Kuang, T., Zhang, J., Gui, L., An, X., Chang, W., et al., 2004. Crystal structure of spinach major light-harvesting complex at 2.72 Å resolution. *Nature* 428, 287–292.
- Long, S.B., Tao, X., Campbell, E.B., MacKinnon, R., 2007. Atomic structure of a voltage-dependent K⁺ channel in a lipid membrane-like environment. *Nature* 450, 376–382.
- Nelson, D.L., Cox, M.M., 2012. Lehninger Principles of Biochemistry, sixth ed. W.H. Freeman & Co., New York (Chapters 11, 12).

- Neumann, S., Hartmann, H., Martin-Galiano, A.J., Fuchs, A., Frishman, D., 2012. CAMPS 2.0: exploring the sequence and structure space of prokaryotic, eukaryotic, and viral membrane proteins. *Proteins* 80, 839–857.
- Overington, J.P., Al-Lazikani, B., Hopkins, A.L., 2006. How many drug targets are there. *Nat. Rev. Drug Discov.* 5, 993–996.
- Pebay-Peyroula, E., Rummel, G., Rosenbusch, J.P., Landau, E.M., 1997. X-ray structure of bacteriorhodopsin at 2.5 Angstroms from microcrystals grown in lipidic cubic phases. *Science* 277, 1677–1681.
- Rang, H.P., 2003. *Pharmacology*. Churchill Livingstone, Edinburgh, p. 60.
- Roman, E.A., González Flecha, F.L., 2014. Kinetics and thermodynamics of membrane protein folding. *Biomolecules* 4, 354–373.
- Skach, W.R., 2009. Cellular mechanisms of membrane protein folding. *Nat. Struct. Mol. Biol.* 16, 606–612.
- Sprang, S.R., 1997. G protein mechanisms: insight from structural analysis. *Annu. Rev. Biochem.* 66, 639–678.
- Stryer, L., 1995. *Biochemistry*, fourth ed. W.H. Freeman & Co., New York (Chapters 10-13, 15, 35-36).
- Trzaskowski, B., Latek, D., Yuan, S., Ghoshdastider, U., Debinski, A., Filipek, S., 2012. Action of molecular switches in GPCRs—theoretical and experimental studies. *Curr. Med. Chem.* 19, 1090–1109.
- Volkenstein, M.V., 1979. Electronic-conformational interactions in biopolymers. *Pure Appl. Chem.* 51, 801–829.

Lecture 13

Now we will focus on globular proteins or, rather, on water-soluble globular proteins.

They are the best-studied group: for many hundreds of them the spontaneous self-organization is known; for many thousands, their atomic 3D structure (with mutants and various functional states taken into account, these numbers are increased many-fold). Therefore, it is this type of proteins that is usually meant when “the typical protein structure,” “the regularities observed in protein structure and folding,” etc., are discussed (Volkenstein, 1977; Cantor and Schimmel, 1980; Creighton, 1993; Stryer, 1995; Branden and Tooze, 1991; Nelson and Cox, 2012).

After this remark, let us consider the structures of globular proteins (Figs. 13.1 and 13.2).

They have been yielded first by X-ray (Kendrew and Perutz, 1957; Perutz, 1992), and later by two- and many-dimensional NMR studies (Wüthrich, 1986) by hundreds of laboratories, and storied in the Protein Data bank (PDB) (Berman et al., 2012). PDB forms a basis for protein structure presentation, analysis, and classification (Murzin et al., 1995) used ubiquitously and, in particular, in this book. Many structures have been yielded by various firms for their own purposes.

Inner voice: Does the structure seen by X-rays in the crystal coincide with the protein structure in solution?

Lecturer: It virtually does, as a rule. This is supported by three groups of data. First, it can often be shown that a protein preserves its activity in the crystal form (see, eg, Vas et al., 1979; Fersht, 1999). Second, sometimes one protein can form different crystals, with its structure virtually unchanged. Finally, the NMR-resolved structure of a protein in solution and its X-ray-resolved structure in a crystal are virtually the same (Fig. 13.3). However, a reservation should be made that some flexible portions of proteins (some side chains, loops, as well as interdomain hinges in large proteins) may have a changed structure after or due to crystallization. But this only concerns either details of protein structures or connections between domains and subglobules in large proteins, rather than small single-domain protein globules, which usually are virtually solid.

I should add that X-rays see not only the “static,” averaged structure of a protein (which is the subject of this lecture and the next) but also thermal vibrations of protein atoms, which will be discussed briefly later.

So, what is the bird’s-eye view of water-soluble globular proteins?

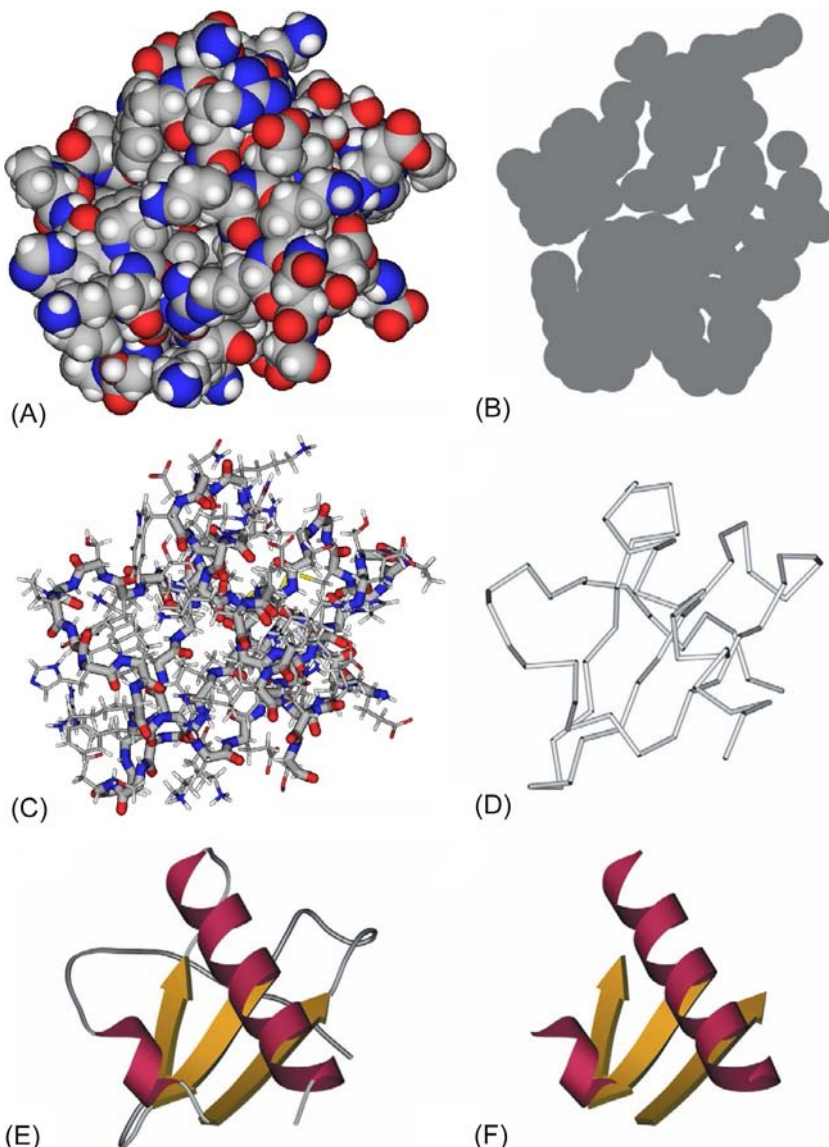


FIG. 13.1 The structure of a small protein, interleukin 8, shown in different ways. (A) The atomic model (nitrogens in blue, oxygens in red, carbons in gray, hydrogens in white); because of the close packing of the chain, we see only the protein surface. (B) The cross-section of the atomic model emphasizes the close packing. (C) Wire model of the main chain (dark line) and side chains (the lighter projections). (D) The pathway of the main chain. (E) Diagram of the protein fold showing the secondary structures involved (two α -helices and one β -sheet consisting of three β -strands). (F) Structural framework (stack) of the protein globule built up from secondary structures. The projection and scale are the same for all drawings.

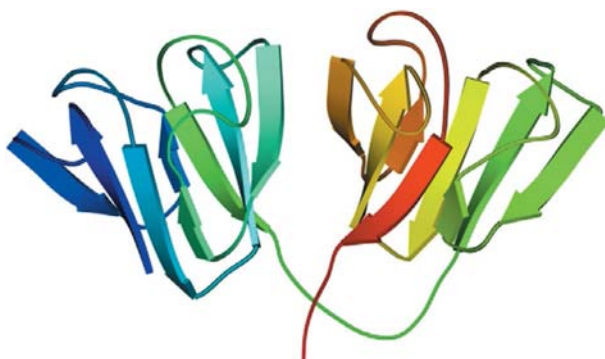


FIG. 13.2 Globular domains in γ -crystallin. The pathway of the chain is traced in the “rainbow” colors (from blue at the N-terminus via green in the middle to yellow and red at the C-terminus).

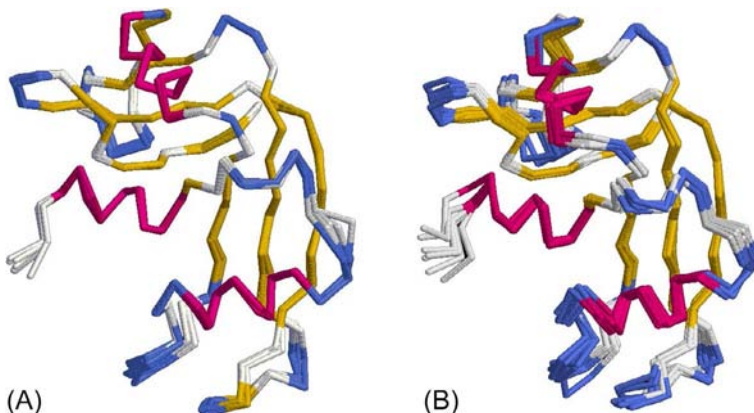


FIG. 13.3 Protein structure in crystal and in solution is nearly the same. (A) The best superposition of seven X-ray structures of the bovine ribonuclease A main chain in different crystals. All differences in these structures are small; the smallest ones are observed in α -helices (red) and β -structures (yellow); the largest in β -turns (blue) and irregular parts of the chains (white). (B) The same protein in solution: seven variants of the structure corresponding to one NMR experiment. The differences in these variants are somewhat larger than those in panel (A), which shows that the NMR solution structure is less accurate than the X-ray crystal structure.

We see that short chains (of 50–150 or, less frequently, 200–250 residues) pack into a compact 25–40 Å globule (Fig. 13.1), and that larger proteins consist of a few such subglobules, or domains (Fig. 13.2) (Schulz and Schirmer, 1979, 2013; Cantor and Schimmel, 1980; Creighton, 1993; Stryer, 1995; Branden and Tooze, 1991; Fersht, 1999; Nelson and Cox, 2012).

The protein chain is packed into a globule as tightly as organic molecules into a crystal. This is clear when you look at both the protein surface (Fig. 13.1A) and the cross-section of a protein globule shown in Fig. 13.1B. However, when examining a protein, we will not focus on the closely packed

electron clouds (or van der Waals surfaces) of atoms: then we cannot see the protein anatomy, that is, nothing can be seen inside the protein; instead, we will inspect the atom-“flesh”-free (Fig. 13.1C) and even side-chain-free (Fig. 13.1D) skeletons (wire models) of protein molecules. But do not submit to the impression (often created by drawings) that a protein molecule has a loose structure!

The frameworks of spatial structures of nearly all globules (domains) are composed of the regular secondary structures already familiar to us: α -helices and β -sheets (Fig. 13.1E) stabilized by regular H-bonds in the regular main chain. In globular proteins the total proportion of α - and β -structures amounts to 50–70% of the number of residues. By the way, Pauling, Corey, and Branson theoretically predicted these and β secondary structures prior to the resolution of atomic structures of protein molecules.

The arrangement of α -helices and β -sheets is not only the most fixed in each molecule (Fig. 13.3), and it is most nonvariable (more so than the position of irregular loops and tails chain) throughout the evolution (Fig. 13.4). Therefore, it is this arrangement determining the main features of protein architecture that forms a basis for structural classification of proteins.

The hydrophobic core (or cores) of the protein is surrounded by α - and β -structures, while irregular loops are moved towards the edge of the globule. The loops almost never enter the interior of the protein. This can be easily explained by the necessity for their peptide groups, uninvolved in secondary structures, to preserve their H-bonds to water, otherwise the globule’s stability would be compromised. (Note that X-rays often find H-bonds between loops, α -helix ends and β -sheet edges and water molecules.)

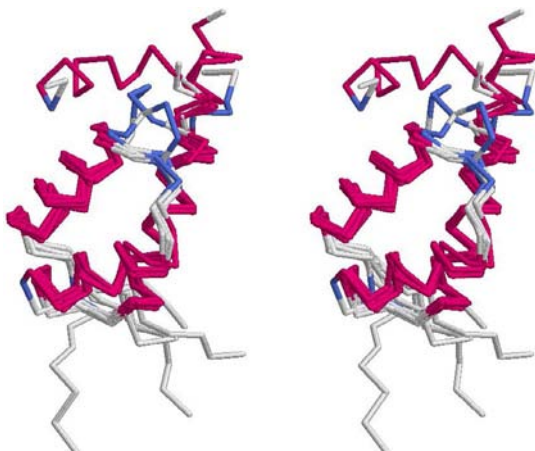


FIG. 13.4 Stereo drawing of the superposed structures of seven distantly related proteins (homodomains of different eukaryotes, from yeast to mammals). The greatest similarity is observed in the general structural core mainly composed of α -helices (here, the difference is about 1 Å); in most of irregular regions the similarity is smaller, and at the ends of chains the differences are maximal.

The structural features of the main chain are the basis for subdivision of globular proteins into “pure” β -proteins, “pure” α -proteins, and “mixed” α/β and $\alpha+\beta$ -proteins. Strictly speaking, this classification refers to small proteins, as well as to separate domains (ie, to compact subglobules forming large proteins); large proteins can contain, say, both β - and α -domains.

Of particular interest to us are: (1) the architecture of packing of α - and β -structural segments into a compact globule (Fig. 13.1F) and (2) the pathway taken by the chain through the globule (Fig. 13.1E) or, as it is often called, “the topology of the protein globule” (taken together, the architecture and topology form a “folding pattern” of the protein molecule).

We will frequently use simplified models of protein structures (Fig. 13.5). The simplification implies not only focusing on secondary structures (with details of loop structures neglected) but also paying no attention to the difference in size of these structures or to details of their relative orientation (in this way, we pass from “folds” (Fig. 13.5A) to “folding patterns” (Fig. 13.5B) of protein chains).

The simplification is justified by the change in the details of loop structures and precise sizes and orientations of structural segments (and even of some small structural segments themselves) that occurs when the protein is compared with another one of similar sequence (ie, with its close relative of the same origin, Fig. 13.4)—eg, when hemoglobin α is compared with hemoglobin β (Fig. 13.6).

The next, higher level of simplification necessary for classification of protein structures is restricted to the packing of structural segments in a globule, that is, the stacks are composed of secondary structures, with no attention paid to loops connecting these secondary structures in a molecule (Fig. 13.5C).

I will purposely use such simplified models of chain folds and packing along with computer-produced “true” protein structures. It might seem

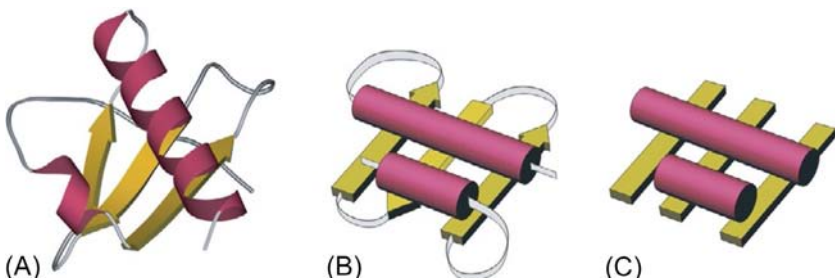


FIG. 13.5 Simplified models of protein structures. (A) A detailed *fold* describing the positions of secondary structures in the protein chain and in space (see also Fig. 13.1E). (B) The *folding pattern* of the protein chain with omitted details of loop pathways, the size and exact orientation of α -helices (shown as cylinders) and β -strands (shown as arrows). (C) *Packing*: a stack of structural segments with no loop shown and omitted details of the size, orientation and direction of α -helices and β -strands (which are therefore presented as ribbons rather than as arrows).

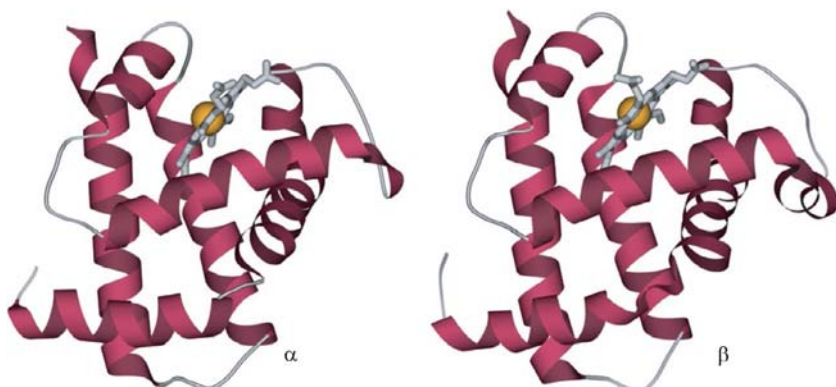


FIG. 13.6 Two close relatives: horse hemoglobin α and horse hemoglobin β (both possessing a heme shown as a wire model with iron in the center). Some differences are in details of loop conformations, in details of the orientation of some helices, and in one additional helical turn available in the β globin, on the right.

pointless to use the simplified models when a computer can describe the structure “as it is.” However, this “as it is” picture has a lot of unnecessary details, while models embody the main features that are the same in similar proteins. Therefore, the models are useful both in classifying protein structures and in outlining their major typical features. When scrutinizing a picture of a protein, we cannot but outline its typical features in our minds—exactly what is done by models, which simply help viewers to systematize their intuitive perception. Besides, models allow us to compose the “verbal portrait” of a protein. Because these models and “verbal portraits” embody the main features and omit details, they will be of practical use as soon as you would like to find out how a protein under consideration resembles others. Of course the omitted details can be basic in protein functioning (as we will see later), but this only emphasizes that the function of a protein is relatively independent of the folding pattern of its chain.

Chain “packings” and “folding patterns” do not bring into focus all possible (loose, open-work, etc.) complexes of structural segments but only those closely packed. Thus, they outline the configuration areas corresponding to close (although free of steric overlapping) packing of the protein chain into a globule, that is, the vicinity of sufficiently deep energy minima of non-bonded interactions. These areas allow us not only to classify known protein structures but also to predict new ones yet to be detected (Levitt and Chothia, 1976; Richardson, 1977, 1981; Finkelstein and Ptitsyn, 1987; Chothia and Finkelstein, 1990).

It is not out of place to mention that, when speaking about classification of protein structures about similarities displayed, and so on, I will not mean the commonplace that all globins are alike irrespective of whether their host is a man or a lamprey—this is certainly true, and proteins can be divided into

phylogenetic classes within which their functions and, importantly, their amino acid sequences do not vary much. However, similar structural features are often intrinsic to proteins that, as revealed by numerous tests, evolutionarily have nothing in common. I will concentrate on this purely structural (not genetic) similarity.

We begin with the architecture of β -proteins. Structurally, β -structural domains turn out to be simpler than others: two (or sometimes several) β -sheets composed of extended chain segments are stacked one onto another. In other words, the “stacks” of secondary structures look quite simple in β -proteins. The *antiparallel* β -structure predominates in β -proteins.

Since proteins are composed of asymmetric (L) amino acids, the extended β -strands are slightly twisted individually: as you may remember, the energy minimum of an extended conformation is positioned above the diagonal in the Ramachandran plot (Chothia, 1973). The twisted β -strands are H-bonded into β -sheets that are arranged in a twisted propeller-like assembly (Fig. 13.7). The angle between adjacent extended strands of the β -sheet is about -25 degree. This propeller-like assembly looks *left-handed* when viewed across the β -strands (Fig. 13.7A) and *right-handed* when viewed along the β -strands (Fig. 13.7B). The latter is a common viewpoint (*along* the β -strands), and hence the β -sheet is said to have a *right-handed* twist.

There are two basic packing types for two β -sheets (Efimov, 1977; Chothia and Janin, 1981), namely, *orthogonal* packing and *aligned* packing (Fig. 13.8A and B). In both cases the sheets pack “face-to-face” around a hydrophobic core of the domain, though their relative arrangement is different: in the second case the angle between the sheets is about -30 degree only ($\pm 10\text{--}15$ degree), while in the first case it amounts to 90 degree ($\pm 10\text{--}15$ degree); angles beyond these two ranges (specifically, angles of about $+30$ degree) are rare.

In *orthogonal* packing (Fig. 13.8A), the β -strands are twisted and usually slightly bent, so that the overall architecture of the “stack” resembles a cylinder

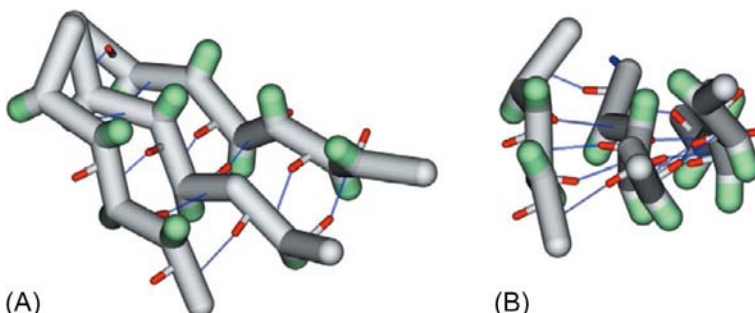


FIG. 13.7 The β -sheet as viewed (A) across and (B) along its β -strands. The sheet is pleated (which is emphasized by projecting the C^β -atoms shown in green) and usually, like here and in the majority of most β -proteins shown below, has a right-handed (viewed along the strands) propeller-like twist. H-bonds between β -strands are shown by thin lines.

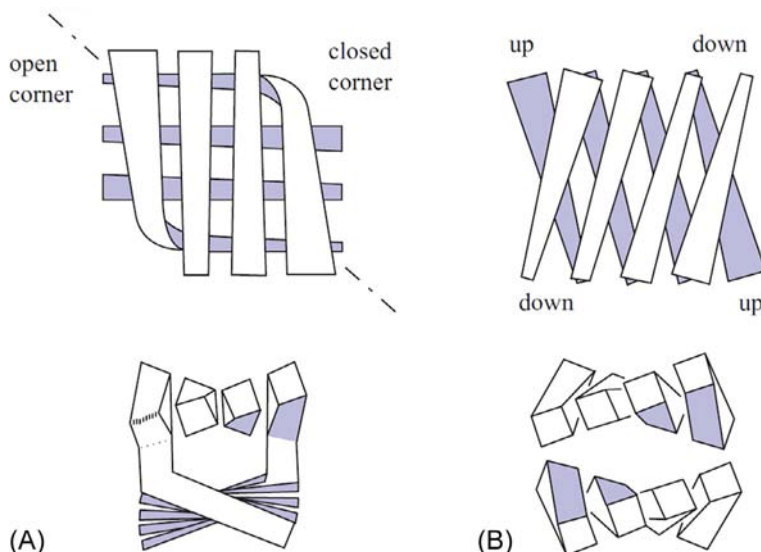


FIG. 13.8 The orthogonal (A) and aligned (B) packing of β -sheets viewed face on (top) and from their lower end (bottom). In the face view, the β -strands are wider as they approach the viewer. The dashed line shows the axis of the orthogonal β -barrel to which both “open” corners belong. Here the two β -sheets are most splayed. At the two “closed” corners the sheets are extremely close together; here the chain bends and passes from one layer to the next. In the orthogonal packing the hydrophobic core is almost cylindrical. In contrast, in the aligned packing, the core is flat, the distance between the twisted sheets remains virtually unchanged, and the relative arrangement of the twisted sheets allows the hydrophobic faces of twisted β -strands to make contact over a great length. (Adapted from Chothia, C., Finkelstein, A.V., 1990. The classification and origins of protein folding patterns. *Ann. Rev. Biochem.* 59, 1007–1039.)

with a significant angle between its axis and the β -strands. This type of β -sheet packing is often called the β -cylinder or the β -barrel, although in β -cylinders composed of *antiparallel* β -structures (unlike in those of parallel β -structures to be discussed later) the two β -sheets are usually clearly distinguished, because on opposite sides of the barrel the H-bond net is often fully or partially broken. In the “closed” corner of this packing, β -segments of both sheets come close together, which enables the chain to pass from one sheet to the other at the expense of a 90 degree bend; it can be said that a single sheet is bent with one part imposed on the other. At the opposite (open) corners, the β -sheets splay apart, the open corner being filled with either an α -helix or irregular loops (Chothia and Janin, 1981), or even with an active site, as in the case of retinol-binding protein (Fig. 13.9).

The *aligned* packing (Fig. 13.8B) is typical of nonbent sheets with a propeller-like twist. This packing type is usually called a β -sandwich. Its ends are covered with irregular loops protruding from the ends of the β -strands (as seen in Fig. 13.10). In some β -sandwiches the edge strands of the β -sheets

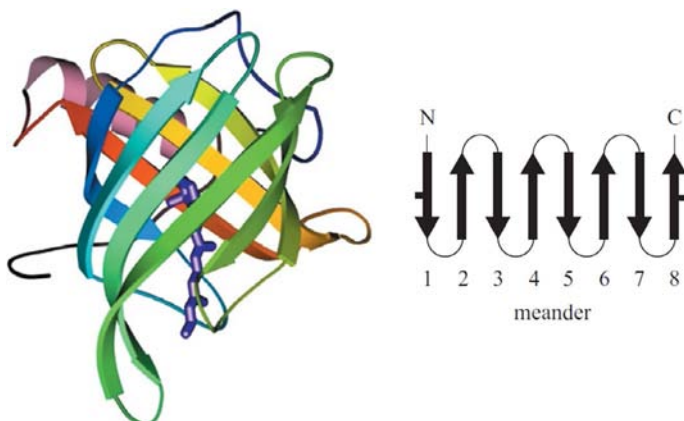


FIG. 13.9 Retinol-binding protein exemplifies β -sheet orthogonal packing. The chain pathway resembles the “meander” pattern (Richardson, 1977) (see the topological diagram, ie, the planar presentation of the β -sheet, on the right). In this diagram β -strands are shown as arrows. The “meander” results from the fact that β -strands adjacent in the chain are also adjacent at the surface of the cylinder; there are H-bonds between them (the H-bonding between the edge (in the planar diagram) β -strands is shown by small thick lines). The retinol-binding site is at the cylinder axis. Retinol is shown in violet. The numbers in the topological diagram reflect the order of structural segments in the chain.

are so close (and sometimes even H-bonded) that the packing acquires the shape of a cylinder with a small angle between its axis and the β -strands.

It should be stressed that the folding patterns are much less numerous than the known protein globules, and the types of stacks are in turn much fewer than the folding patterns of the protein chain. One and the same stack, that is, one and the same packing of structural segments, can conform to various patterns of chain folding in a globule; in other words, these segments can be arranged in the polypeptide chain in different ways.

Fig. 13.10 shows how one and the same β -sandwich (with a variety of topologies, that is, with different pathways taken by the chain through this sandwich) serves as the structural basis of three distinct protein domains: (a) a domain of γ -crystallin, (b) the β -domain of catabolite activating protein, and (c) the virus coat protein. The folding patterns of the last two proteins are the same, that is, in these proteins the chain takes the same pathway through identical β -structural stacks (this is emphasized by the brace in Fig. 13.10).

In continuation of this line, Fig. 13.11 shows how one and the same β -cylinder (with two different chain topologies, ie, with two different pathways taken by the chain through the orthogonal packing of the β -sheets) serves as the basis for both a serine protease like chymotrypsin (a) and an acid protease like pepsin (b).

Examples of such structural similarity in the absence of any other apparent relationship between the proteins are plentiful.

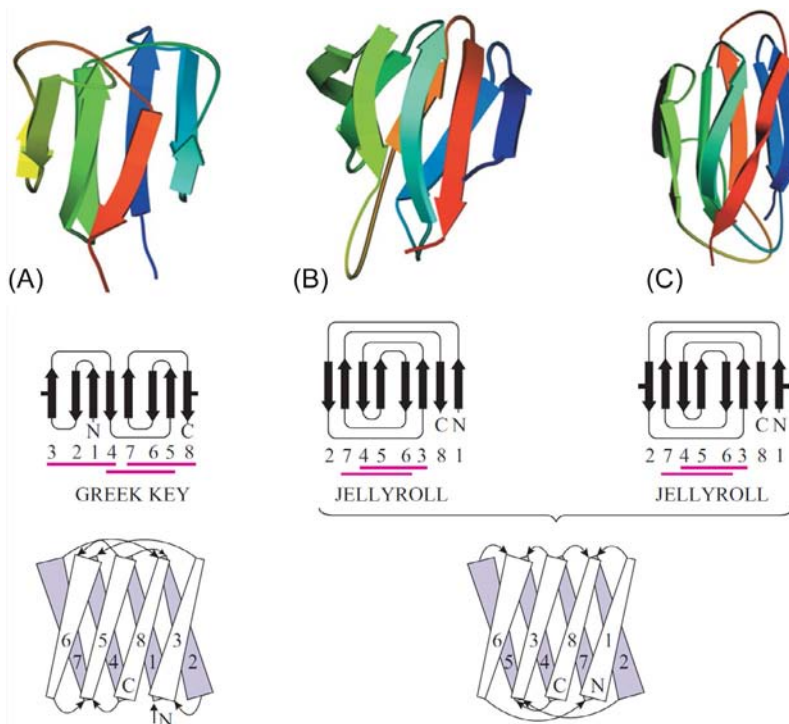


FIG. 13.10 Examples of β -sheet aligned packings. The chain folding patterns for (A) γ -crystallin (see also Fig. 13.2), (B) the β -domain of catabolite activating protein and (C) the coat protein of satellite tobacco necrosis virus. The topological diagrams for these proteins are shown below. For all these proteins, the topology contains a “Greek key” (Richardson, 1977) (a “long hairpin bent in two”) where four β -strands are adjacent in the chain and antiparallel, and there are H-bonds between the first and the fourth strand. In the topological diagrams, structures of the two-layer β -sandwich are drawn in one plane (as for a cylinder cut along its side and unrolled flat). The place of cutting is chosen to stress the symmetry of the chain fold. For example, in γ -crystallin, the slit between β -strands 3 and 8 stresses the similarity of the first (strands 1–4) and the last (strands 5–8) halves of the domain. A shorter distance between the edge β -strands are shown as small thick projecting lines. A gap between the β -strands separates two β -sheets of the sandwich (if there are no H-bonds between them). The domain of γ -crystallin contains a repeated Greek key: one formed by strands 1–4, and the other by strands 5–8; still another Greek key is composed of the β -strands 4–7. The proteins shown in drawings (B) and (C) have Greek keys formed by strands 3–6 and 4–7. Moreover, their topology can be described as a repeatedly bent hairpin (usually called a “jellyroll”) where β -strand 1 is H-bonded to 8, and 2–7, in addition to the H-bonds between strands 3 and 6, 4 and 5, typical of Greek keys. Note that for the purpose of enveloping the globule core by the chain a Greek key proves to be better than “meander” topology (Fig. 13.9) because apart from the β -structure on the sides, it provides enveloping by loops from below and above. Usually, β -sheet aligned packings are β -sandwiches (A,B), but some of them (eg, the coat protein of satellite tobacco necrosis virus and coat proteins of some other viruses) can also be seen as β -cylinders with colinear β -strands (C).

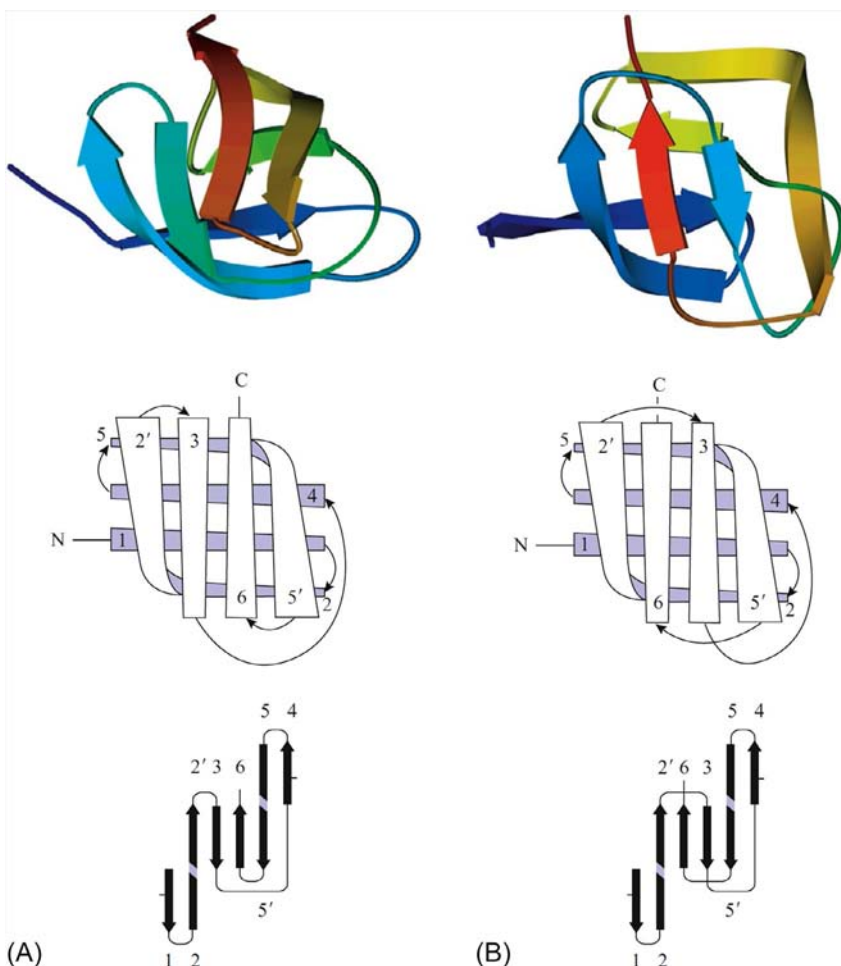


FIG. 13.11 The chain folding patterns in a serine protease such as chymotrypsin (A) and in an acid protease such as pepsin (B). For the latter, the loops are shortened and rather schematic. The orthogonal packings of β -sheets in these proteins are shown along with the β -sheet topology diagrams. In both folding patterns the β -sheets has a bend, such that their edges move away from the reader and stick together by H-bonding (marked as short lines); the places where the β -sheet bends are colored lighter in the topology diagrams (see β -strands 2 and 5).

Here I cannot resist the temptation of showing you another β -sandwich-based protein. It is immunoglobulin; each domain of this large protein is arranged in (or close to) the way shown in Fig. 13.12.

Folding patterns of this type are intrinsic to the chains of about 50 other superfamilies, bearing no sequence similarity to immunoglobulin (although some also are responsible for specific binding to certain agents, eg, in the course of cell recognition).

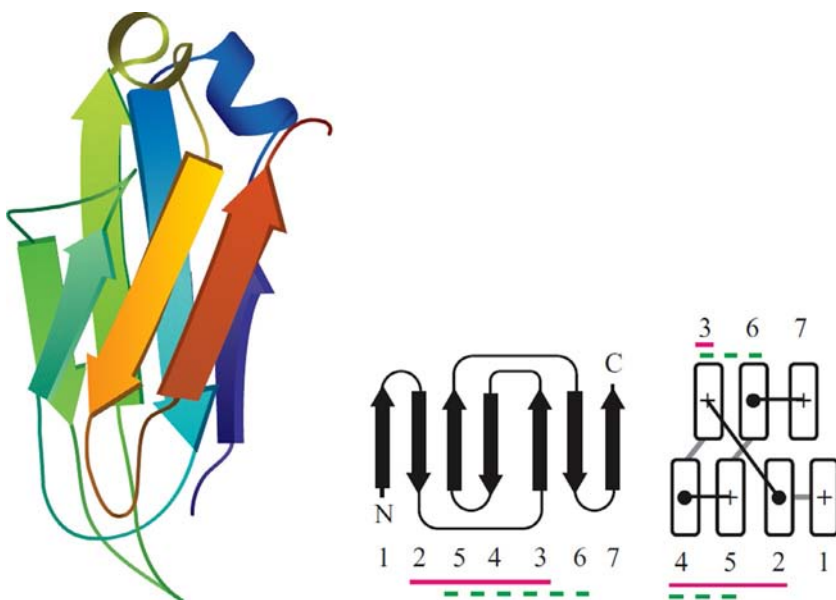


FIG. 13.12 The aligned packing of β -sheets in the constant domain of the light chain of immunoglobulin κ . On the left, a detailed diagram of the protein is shown; the chain pathway is traced in color (rainbow from blue to red) from the N- to the C-terminus. The topological diagram (in the center) accentuates the “Greek keys.” On the right, the protein is shown as viewed from below (ie, from the butt-ends of structural segments; the butt-ends shown as rectangles). The cross corresponds to the strand’s N-end (ie, “the chain runs from the viewer”), and the dot to the C-end (ie, “the chain runs towards the viewer”). The segment-connecting loops close to the viewer are shown by black lines, and those distant (on the opposite side of the fold) by light lines. Note that such a diagram allows the presentation of the colinear packing of these segments (β -strands) in the simplest possible way. It also visualizes the spatial arrangements of “Greek keys” and makes evident that two of them (formed by strands 2–5 and 3–6, respectively) differ in their spatial arrangements. The structure formed by two Greek keys that overlap as shown in this figure is sometimes called a “complete Greek key.”

Some members of these superfamilies are somewhat different from the “standard” structure presented in Fig. 13.12. So, in some proteins β -strand 1 forms a parallel β -structure with strand 7 (and then it can even lose contact with strand 2); in others β -strand 4 moves to strand 3 from strand 5; sometimes an additional β -hairpin forms in the connection between β -strands 3 and 4. But the core of the fold, which involves β -strands 2, 3, 5, 6, 7, remains unchanged.

Apart from the pleasure of showing you this very popular folding pattern, I also aim to show that the easiest way to illustrate the folding pattern of a protein with more or less colinear packing of its structural segments is to use the diagram giving a view from the butt-ends of β -strands.

So far, we have considered the most significant “basic” arrangements of β -proteins. However, there are other “basic arrangements,” for example, the “multiple-blade propeller.”

In the neuraminidase “propeller” (Fig. 13.13), six inclined β -sheets form a rosette (in other proteins of this kind there may be as many as eight sheets).

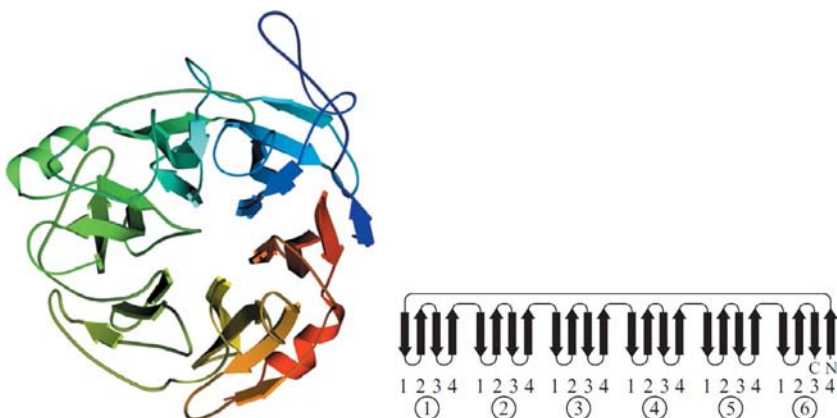


FIG. 13.13 The β -structure in the form of a “six-blade propeller” in neuraminidase, and a topological diagram of this protein, which is composed of six antiparallel β -sheets. In some other proteins, “blades” are formed by separate chains. (Adapted from Branden, C., Tooze, J., 1991. *Introduction to Protein Structure*. Garland Publishing Inc., New York, London (Chapter 5), with minor modifications.)

If considered in pairs, the sheets form β -sandwiches; therefore the “propeller” can be described as a supercylinder built up from β -sandwiches.

As you can see, the axis is not covered with loops and the “indent” at the supercylinder axis contains the active site. We have already seen one similar position of the active site: in the retinol-binding protein (Fig. 13.9), it is also located in an indent in the middle of the cylinder; and we will see it again later.

The structural arrangement of the “ β -prism” (also called the “ β -helix”) type (Fig. 13.14) is of interest mostly due to its regularity. The three facets of this prism are formed by three β -sheets (note: parallel β -sheets) such that the chain

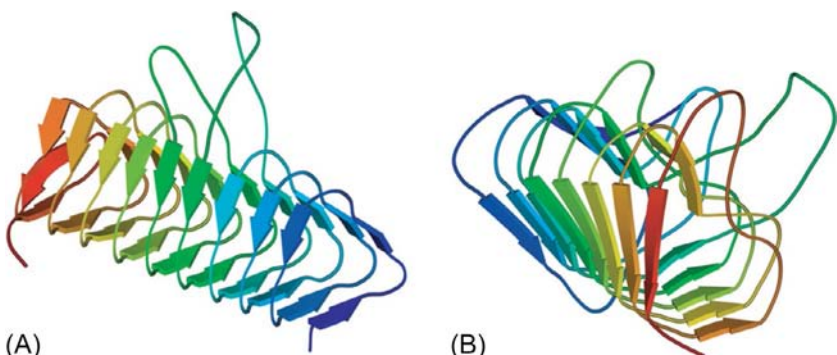


FIG. 13.14 The β -prism in acyl transferase (A) and in pectate lyase (B). Notice the handedness of the chain’s coiling around the axis of the prism: it is unusual, *left*, in (A) and common, *right*, in (B). Also note that when the chain’s coiling is uncommon, that is, left-handed as in (A), the common twist of the β -sheet is absent. This common twist, that is, the right-handed (viewed along the β -strands) propeller twist, is seen also in Figs. 13.7–13.13.

takes its pathway through them continuously passing from one sheet to the next. The chain appears to coil around the axis of this prism and forms either a right-handed helix, which is typical for joining parallel β -strands, or (in the other prism) a left-handed helix, which is extremely rare for the case of joining β -strands in other proteins. It is worth noting that in some primitive fishes (eg, lampreys) the immune role is performed by proteins built not on a classical immunoglobulin fold (Fig. 13.12) but on β -prisms (Fig. 13.14).

It would not be out of place here to discuss the *topology* of β -proteins. We have observed that β -proteins are built up from mostly antiparallel β -structures. The structure of the majority of β -proteins that have been discussed so far is purely antiparallel. Although sometimes a minor admixture of the parallel structure was observed (see Fig. 13.11B), proteins built up from a purely parallel β -structure are extremely rare, although they do exist (see Fig. 13.14).

The fact that an admixture of parallel and antiparallel structures rarely occurs is not surprising since parallel and antiparallel β -structures have somewhat different conformations, and therefore their connection is likely to be energetically unfavorable. The extent of correlation between the unfavorability and the uncommon occurrence of various structures will be discussed in a later lecture, but in principle, it is clear that a stable system (such as protein) must be composed of mostly stable elements and avoid those internally unstable.

The mostly *antiparallel* character of β -sheets in β -proteins is closely connected with the fact that their architecture is usually based on β -hairpins (Fig. 13.15). These hairpins are often bent and sometimes may even have two or three such bends (see Fig. 13.15 and also Fig. 13.10B and C).

The pathways of loops connecting β -segments usually start and finish on the same edge of the fold (ie, the loops do not cross the “stack” but cover its butt-end). This is well seen from almost all drawings. The loops, even long ones, tend to connect ends of β -segments that are close in space. That is why, as a rule, β -segments adjacent in the chain are not parallel and tend to form antiparallel β -hairpins.

Also note that “overlapping” loops (or “crossed loops”) occur rarely (an exception of this kind is shown in Fig. 13.11B), probably because one of the crossed loops must have an energetically unfavorable additional bend (to avoid a collision or dehydration). The avoidance of loop overlapping is a general structural rule for proteins (Lim et al., 1978; Ptitsyn and Finkelstein, 1979).

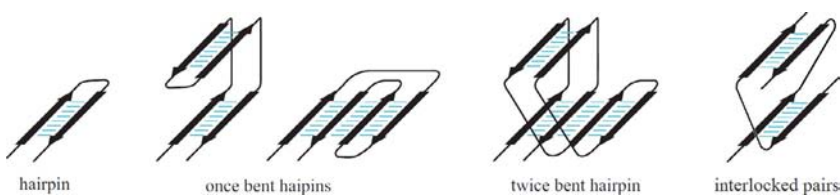


FIG. 13.15 Antiparallel β -hairpins (bent β -hairpins are typical of edges of β -sandwiches) and interlocked pairs of β -strands typical of middles of β -sandwiches (Kister et al., 2002).

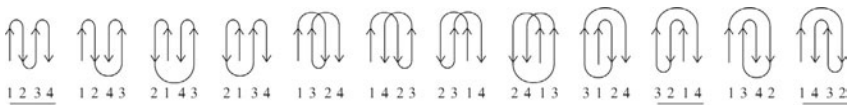


FIG. 13.16 Possible topologies of sheets composed of four β -strands. The scheme includes only the sheets where two β -strands adjacent in the chain are oppositely directed. Among these, the common topologies are “meander” (underlined once) and two “Greek keys” (underlined twice), the latter two being different only in the direction of the chain turn from the hairpin consisting of strands 1 and 4 to the hairpin consisting of strands 3 and 2. The “meander”-containing protein is exemplified by retinol-binding protein (see Fig. 13.9); the examples of “Greek key”-containing proteins are γ -crystallin and other proteins shown in Fig. 13.10, or trypsin (Fig. 13.11).

Among a variety of configurations of a β -sheet formed by a continuous chain (Fig. 13.16), those really abundant are only three: two “Greek keys” and the “meander” (underlined in Fig. 13.16)—by the way, “Meander” is the name of a very winding river in Ancient Greece (now Turkey)—in the meander pattern, β -strands adjacent in the chain are also adjacent in space (Figs. 13.10 and 13.16) and usually linked with H-bonds. The “popular” folding patterns have none of the disadvantages mentioned above: a mixture of antiparallel and parallel β -structures and the crossed loops.

It is characteristic of the “Greek key” pattern (which can be seen on ancient vases and garden railings), that four β -strands adjacent in the chain are antiparallel, and that there are H-bonds between the first and the fourth strands. Actually, the second and/or the third β -strand of the “Greek key” usually belong to another β -sheet rather than to the same one (as it may appear from Fig. 13.16). This gives rise to various spatial structures (the so-called Efimov’s “abcd” structures) with the same Greek key topology but with different shapes in space (Efimov, 1995) (Fig. 13.17). Look for them in Figs. 13.10–13.12.

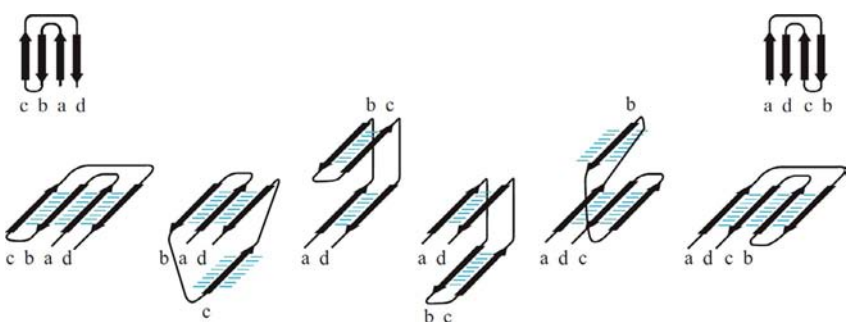


FIG. 13.17 Several kinds of the supersecondary structure: various spatial Efimov’s “abcd” structures with the Greek key topology. Notice the *right-handedness of the superhelix* that consists of two parallel β -strands from one β -sheet and one β -strand (between them) from another β -sheet. It is seen, for example, in the superhelices b-c-d (the second drawing from the left in the lower line) and a-b-c (the second drawing from the right in the lower line). The “right-handed” connection of parallel strands of the same β -sheet is typical for proteins (Nagano, 1973; Richardson, 1976); the reverse (left-handed) is extremely rare.

These typical protein structures (hairpins, meanders, Greek keys, *abcd* structures, etc.), which are built up from elements of the β - (and/or α -) structure that are adjacent in the chain, are often called “supersecondary” structures.

REFERENCES

- Berman, H.M., Kleywegt, G.J., Nakamura, H., Markley, J.L., 2012. The Protein Data Bank at 40: reflecting on the past to prepare for the future. *Structure* 20, 391–396. <http://www.wwpdb.org/>.
- Branden, C., Tooze, J., 1991. *Introduction to Protein Structure*. Garland Publishing Inc., New York, London (Chapter 5).
- Cantor, C.R., Schimmel, P.R., 1980. *Biophysical Chemistry*. W.H. Freeman & Co., New York (Part 1, chapters 2, 9; part 2, chapter 13).
- Chothia, C., 1973. Conformation of twisted beta-pleated sheets in proteins. *J Mol Biol* 75, 295–302.
- Chothia, C., Finkelstein, A.V., 1990. The classification and origins of protein folding patterns. *Annu. Rev. Plant Physiol. Plant. Mol. Biol.* 59, 1007–1039.
- Chothia, C., Janin, J., 1981. Relative orientation of close-packed beta-pleated sheets in proteins. *Proc Natl Acad Sci U S A* 78, 4146–4150.
- Creighton, T.E., 1993. *Proteins: Structures and Molecular Properties*, second ed. W. H. Freeman & Co., New York (Chapter 6).
- Efimov, A.V., 1977. Stereochemistry of the packing of alpha-spirals and beta-structure into a compact globule. *Dokl. Akad. Nauk. SSSR* (in Russian) 235, 699–702.
- Efimov, A.V., 1995. Structural similarity between two-layer α/β and β -proteins. *J. Mol. Biol.* 245, 402–415.
- Fersht, A., 1999. *Structure and mechanism in protein science: a guide to enzyme catalysis and protein folding*. W. H. Freeman & Co., New York (Chapter 1).
- Finkelstein, A.V., Ptitsyn, O.B., 1987. Why do globular proteins fit the limited set of folding patterns? *Prog. Biophys. Mol. Biol.* 50, 171–190.
- Kendrew, J.C., Perutz, M.F., 1957. X-ray studies of compounds of biological interest. *Annu. Rev. Biochem.* 26, 327–372.
- Kister, A.E., Finkelstein, A.V., Gelfand, I.M., 2002. Common features in structures of sandwich-like proteins. *Proc. Natl. Acad. Sci. U. S. A.* 99, 14137–14141.
- Levitt, M., Chothia, C., 1976. Structural patterns in globular proteins. *Nature* 261, 552–558.
- Lim, V.I., Mazanov, A.L., Efimov, A.V., 1978. Stereochemical theory of the 3-dimensional structure of globular proteins. I. Highly helical intermediate structures. *Mol. Biol.* (in Russian) 12, 206–213.
- Murzin, A.G., Brenner, S.E., Hubbard, T., Chothia, C., 1995. SCOP: a structural classification of proteins database for the investigation of sequences and structures. *J. Mol. Biol.* 247, 536–540.
- Nagano, K., 1973. Logical analysis of mechanism of protein folding. I. Prediction of helices, loops and β -structures from primary structure. *J. Mol. Biol.* 75, 401–420.
- Nelson, D.L., Cox, M.M., 2012. *Lehninger Principles of Biochemistry*, sixth ed. W.H. Freeman & Co., New York (Chapters 3–6, 27).
- Perutz, M.F., 1992. *Protein Structure. New Approaches to Disease and Therapy*. W.H. Freeman & Co., New York.
- Ptitsyn, O.B., Finkelstein, A.V., 1979. Prediction of Protein Three-Dimensional Structure by Its Amino-Acid Sequence. In: 12th FEBS Meeting (Dresden, 1978). 52. Pergamon Press, New York, pp. 105–111.
- Richardson, J.S., 1976. Handedness of crossover connections in β sheets. *Proc. Natl. Acad. Sci. U. S. A.* 73, 2619–2623.

- Richardson, J.S., 1977. β -Sheet topology and the relatedness of proteins. *Nature* 268, 495–500.
- Richardson, J.S., 1981. The anatomy and taxonomy of protein structure. *Adv. Protein Chem.* 34, 167–339.
- Schulz, G.E., Schirmer, R.H., 1979, 2013. *Principles of Protein Structure*. Springer, New York (Chapter 5).
- Stryer, L., 1995. *Biochemistry*, fourth ed. W.H. Freeman & Co., New York (Chapter 2).
- Vas, M., Berni, R., Mozzarelli, A., Tegoni, M., Rossi, G.L., 1979. Kinetic studies of crystalline enzymes by single crystal microspectrophotometry. Analysis of a single catalytic turnover in a D-glyceraldehyde-3-phosphate dehydrogenase crystal. *J. Biol. Chem.* 254, 8480–8486.
- Volkenstein, M.V., 1977. *Molecular Biophysics*. Academic Press, London (Chapter 4).
- Wüthrich, K., 1986. *NMR of Proteins and Nucleic Acids*. Wiley-Interscience, New York.

Lecture 14

Now we pass to α -proteins, which are proteins built up from α -helices. They are more difficult to classify than β -proteins (Levitt and Chothia, 1976). The reason is that the arrangement of β -strands in the sheets is stabilized by hydrogen bonds of the main chain (which is the same everywhere), while the arrangement of α -helices in a globule is maintained by close packing of their side chains, which vary greatly in size. This is why, unlike β -strands, α -helices do not pack into more or less standard sheets.

The α -proteins composed of long α -helices have the simplest structure. This structure is a bundle formed by almost parallel or antiparallel (in a word, co-linear) long α -helices. We have already met such bundles when considering fibrous and membrane proteins.

Fig. 14.1 presents three 4-helix proteins. These proteins, structurally very close, have different functions: cytochrome binds an electron, hemerythrin binds oxygen, and tobacco mosaic virus coat protein binds molecules that are much greater in size—other coat proteins and RNAs (Branden and Tooze, 1991). The first two proteins may have something in common in their function because they both act as carriers in the respiratory chain. This resemblance is far from close, though: in cytochrome, the polypeptide binds the heme that binds an iron that binds an electron, while in hemerythrin the polypeptide binds iron ions without any mediating heme, and two iron ions bind an oxygen. Thus, functionally, hemerythrin and cytochrome bear some resemblance, although only a minor one, and they have no common function with the RNA-binding virus coat protein—in spite of the fact that all three of them are very similar structurally. The similarity is not restricted to the overall architecture (a 4-helix bundle) but also involves the pathway taken by the chain through this bundle, that is, the folding pattern of the chain. The latter is well illustrated by a common topological diagram (Fig. 14.1, inset) that shows a view along the bundle axis.

Thus, proteins with the same folding pattern may have utterly different functions; the same we have seen for β -proteins. In contrast, hemerythrin and the classical oxygen-binding protein myoglobin (Fig. 14.2) have identical functions (the former in worms and the latter in vertebrates, including ourselves), while their architectures are utterly different except that they are both α -proteins. However, in hemerythrin all the α -helices are parallel, while in myoglobin they are assembled into two perpendicular layers. This is another example showing that proteins with different architectures can carry out similar functions, while similarly arranged proteins may have different duties.

Again, I am drawing your attention to nontrivial cases of the lack of relationship between protein structure and function, because undoubtedly you know

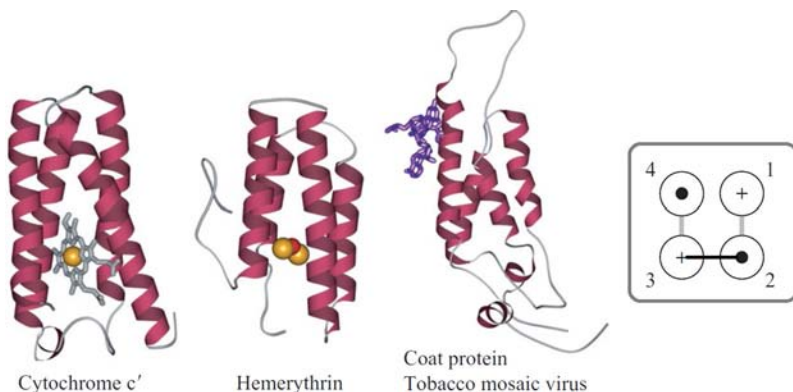


FIG. 14.1 Three α -proteins that are similar in architecture (4-helix bundle) but different in function: cytochrome c' , hemerythrin, and tobacco mosaic virus coat protein. Both the protein chain and co-factors are shown: wire models represent the heme (in cytochrome) and an RNA fragment (in virus coat protein), orange balls are for iron ions (in the cytochrome heme and in hemerythrin), and the red ball is for iron-bound oxygen (in hemerythrin). The overall architecture of such “bundles” resembles the co-linear packing of β -sheets. The topological diagram (inset) shows all these proteins as viewed (in the same orientation) from their lower butt-ends. The circles represent the ends of α -helices. The cross corresponds to the N-end of the segment (ie, the segment goes away from the viewer); the dot corresponds to its C-end (ie, the segment comes towards the viewer). The loops connecting the structural segments are shown by the black line (if it is close to the viewer) and by the light line (if it is on the opposite side of the fold). The numerals indicate the order of structural elements in the chain (from the N- to the C-terminus).

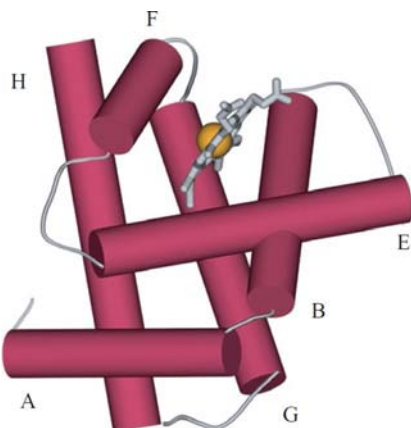


FIG. 14.2 The structure of globin: crossed layers of three α -helices each. The helices A, E, and F (lettered in accordance with their sequence positions) belong to the upper layer, while H, G, and B to the lower layer. The short helices (of 1–2 turns each) C and D are not shown since they are not conserved in globins. A crevice in the upper layer houses the heme. Such “crossed layers” resemble the orthogonal packing of β -sheets (the orthogonal contact of helices B and E is especially close, since both helices have glycine-formed dents at the contact point).

that the kindred proteins (eg, myoglobin and other globins) are similar in both architecture and function.

Besides, by comparing myoglobin with hemerythrin, I want to draw your attention to the fact that in both cases the active site (for the former, it is the heme with an iron ion inside; for the latter, two iron ions) is localized in the “architectural defect” of the protein structure, namely, in a crevice between the helices.

The “bundles” described above are typical of quite long α -helices. They are observed in water-soluble globular proteins, as well as in fibrous and membrane proteins. The protein core enveloped by the helices has an elongated, quasi-cylindrical shape. It is hydrophobic in water-soluble globular and fibrous proteins and hydrophilic in membrane ones.

The “crossed layers” ([Fig. 14.2](#)) are also formed by rather long helices; they have a flat hydrophobic core.

However, relatively short helices are more typical of globular proteins. For these helices (with a length of about 20 Å), a quasi-spherical packing around a ball-like core is more typical ([Murzin and Finkelstein, 1983, 1988](#)).

[Fig. 14.3](#) illustrates a typical packing of helices in a globular protein. This packing cannot be described in terms of a parallel or perpendicular helical arrangement because the angles between helices are usually 40–60 degrees.

But even such intricate packings can be described and classified accurately enough using the “quasi-spherical polyhedron model” ([Murzin and Finkelstein, 1983, 1988](#)). For example, let us see ([Fig. 14.4](#)) how this model describes the α -helical globule of [Fig. 14.3](#). Incidentally, these two figures are from a review of this work by A.G.M. and A.V.F., published in *Nature* by [Chothia \(1989\)](#).

I will not deny myself the pleasure of showing you another pair of figures from the same review ([Fig. 14.5A](#)).

By the way, the quasi-spherical polyhedron model is also sufficiently good for describing rather long helical bundles (such as those we saw in [Fig. 14.1](#)). This is illustrated by [Fig. 14.5B](#).

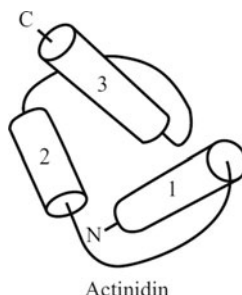


FIG. 14.3 Typical packing of helices in a globular protein exemplified by the N-terminal domain of actinidin (the loops are traced very schematically). Note that the architecture of this domain cannot be described in terms of colinear and orthogonal packings of α -helices. (Adapted from Chothia, C., 1989. Polyhedra for helical proteins. *Nature* 337, 204–205.)

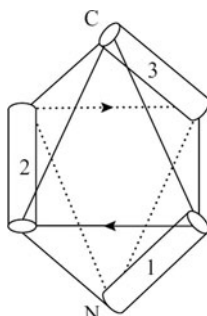


FIG. 14.4 The α -helix positions on the ribs of a quasi-spherical polyhedron that models the N-terminal domain of actinidin shown in Fig. 14.3. The shortcuts for helix-connecting loops are shown by arrows. (Adapted from Chothia, C., 1989. Polyhedra for helical proteins. *Nature* 337, 204–205.)

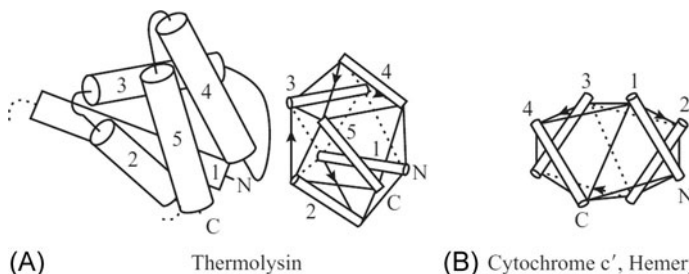


FIG. 14.5 More examples showing how the geometry of helix packings in globular proteins can be described by the quasi-spherical polyhedron model. (A) The C-terminal domain of thermolysin and its model showing the helix positions on the polyhedron ribs. (B) The model for the four-helix globule presented in Fig. 14.1. ((A) Adapted from Chothia, C., 1989. Polyhedra for helical proteins. *Nature* 337, 204–205.)

Essentially, the quasi-spherical polyhedron model focuses on the positioning of α -helices packed around the ball-like core of the globule (Fig. 14.6).

The model only takes into account that α -helices, solid extended particles, surround the core closely, and that the polar helix ends are located on the globule surface. The geometry of any helix packing can be described by a polyhedron (Fig. 14.6) where each vertex corresponds to half of the helix. The most compact “quasi-spherical” polyhedra (Fig. 14.7) describe compact globules. The helix packings actually observed in globular α -proteins are close to these ideal packings. For a given number of helices, there is only one most compact polyhedron; it allows for a number (from 2 to 10) variants of helix positioning on the ribs of this polyhedron. The previously considered “helix bundles” “crossed layers” are among these arrangements.

Interestingly, in the observed architectures of α -proteins, it is not only helices that fit on the ribs of quasi-spherical polyhedra but also, as a rule, the helix-connecting irregular loops (see Figs. 14.4 and 14.5). In other words, a typical

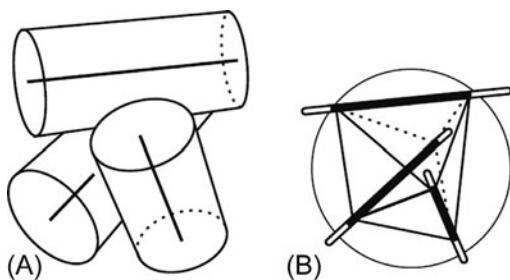


FIG. 14.6 This figure illustrates how the geometry of helix packings can be described by a polyhedron. (A) Three packed helices are shown as cylinders of diameter 10 Å (their axes are also shown). (B) To construct the polyhedron, a sphere of radius 10 Å is drawn from the center of the packing; the polyhedron vertices occur at its intersection with the helix axes. The sections of the ribs enclosed by the sphere are shown as dark lines. Each vertex corresponds to one-half of one helix. The helix axes form one set of the ribs of the polyhedron; it is completed by another set of ribs formed by connections linking the helix ends. (*Adapted from Murzin, A.G., Finkelstein, A.V., 1988. General architecture of α -helical globule. J. Mol. Biol.* 204, 749–770.)

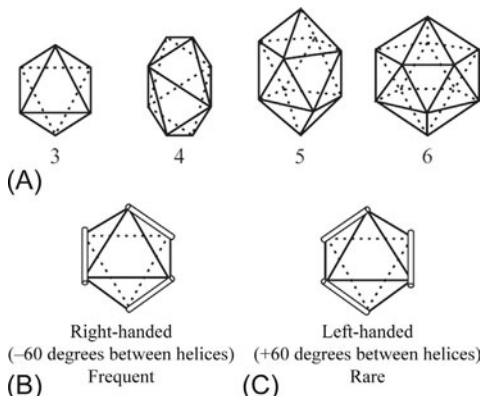


FIG. 14.7 (A) Quasi-spherical polyhedra describe the compact packing of three, four, five and six helices. Larger assemblies of helices cannot be placed around a single spherical core without screening the polar ends from water. Each polyhedron simultaneously describes several packing arrangements, ie, several types of “stacks” of helices; the stacks differ in helix positioning on the polyhedron ribs. For example, three helices form two different arrangements: (B) a right-handed bundle (as that in Figs. 14.3 and 14.4); (C) a left-handed bundle. Four helices form 10 arrangements, five helices form 10 arrangements, and six helices form eight arrangements [“stacks” for four-, five- and six-helix globules are not shown, but one can easily construct them by placing the helices on the polyhedral ribs in all possible ways such that each vertex corresponds to one end of a helix (Murzin and Finkelstein, 1988)]. The packings with inter-helical angles favorable for close helix contacts (see Fig. 14.9) are observed in proteins more often than others. ((A) Adapted from Murzin, A.G., Finkelstein, A.V., 1988. General architecture of α -helical globule. *J. Mol. Biol.* 204, 749–770.)

protein chain envelops its hydrophobic core, as if taking a continuous path along the ribs of a quasi-spherical polyhedron.

Now let us see how close packing forms in a protein globule. The existence of such packing follows from observations that protein is as compact and solid as an organic crystal although it may resemble a glass by the criterion of the free volume distribution (Liang and Dill, 2001). However, it is still to be explained how it comes about that such packing emerges regardless of the vast variety of most intricate shapes of side-groups of a protein chain.

Actually, the outline of close-packing formation is more or less clear only for α -helices (Crick, 1953; Efimov, 1977, 1979; Chothia et al., 1977, 1981) [for β -sheets, it is more intricate due to lesser stiffness of β -strands, see Finkelstein and Nakamura (1993)], and that is why it would not be out of place to consider it here.

The first model of the close packing of α -helices, that of the “knob (side chain) into hole (between side chains)” type, was proposed by Crick (1953) earlier than the solution of the first 3D protein structure. Later, this model was further developed by Efimov (1977, 1979), and independently, by the Chothia-Levitt-Richardson team (1977, 1981), and by now it has acquired the “ridge (of side chains) into groove (between them)” description.

According to this model, side chains in the surface of an α -helix tend to turn about the knobs formed by C^β atoms and form ridges separated by grooves. The “ridges and grooves” prove to be a bit better in describing the reality than “knobs and holes” because a turn of one “extended knob” (one side chain) towards another (another side chain) can make this or that “ridge composed of knobs” more definite. There are two types of ridges (and their parallel grooves): those of the “+4” type formed by side chains of residues at sequence positions “ i ,” “ $i+4$,” “ $i+8$,” etc. (in other words, separated in sequence by four chain residues), and ridges of the “+3” type formed by side chains of residues at sequence positions “ i ,” “ $i+3$,” “ $i+6$,” etc. (ie, separated by three residues). Fig. 14.8 shows that ridges of these two types form angles of opposite signs with the helix axis.

The close packing brings the ridges from one helix into the grooves from another.

This gives two types of possible packing (Fig. 14.9).

In the first type, “+4” ridges of one helix fit into grooves between similar “+4” ridges of the other (Fig. 14.9A; as seen, the close packing results from superimposing the overturned helix $\alpha 2$ onto helix $\alpha 1$ and turning it further until the “+4” ridges of both helices become parallel). In such packing the angle between the helix axes is close to -50 degrees. This is the most typical angle formed by helices in α -helical globules (Chothia et al., 1977; Murzin and Finkelstein, 1988). Also, it is typical for α/β and $\alpha+\beta$ proteins to be discussed later. Such an angle provides for a twist of the α -helix layer (in which the twist angle is close to -50 degrees/ 10 \AA , where -50 degrees is the angle between axes of adjacent helices, and 10 \AA is the width of an α -helix), which is in good agreement with the typical twist of a β -sheet (characterized by the same -25

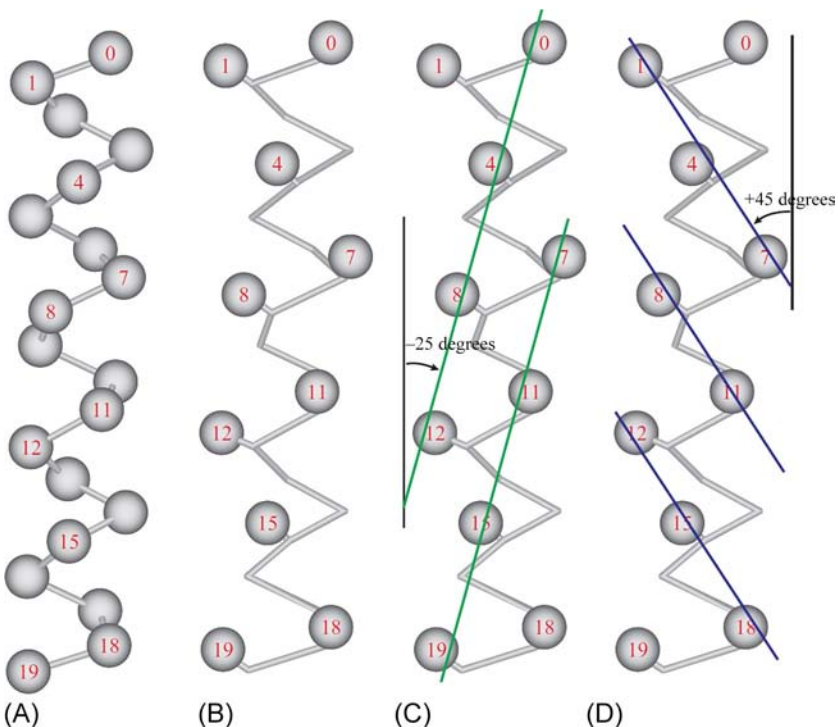


FIG. 14.8 Ridges at the surface of the α -helix. The C^α -atoms (A) and C^β -atoms (B–D) are shown. Numbered residues face the viewer. Two kinds of ridges (thin lines in the helix face) from close side-groups are shown (C, D). The ridges “+4” from side-groups “ i ” – “ $i+4$ ” – “ $i+8$...” are inclined at -25 degrees to the helix axis (C), the ridges “+3” from groups “ i ” – “ $i+3$ ” – “ $i+6$...” are inclined at $+45$ degrees (D); in the drawing these angles look smaller because typical ridges pass through massive side-groups, while in (C) and (D) they run through the centers of the C^β -atoms. (Adapted from Branden, C., Tooze, J., 1991. *Introduction to Protein Structure*, second ed. Garland Publishers, New York (Chapter 3).)

degrees/5 Å value, where -25 degrees is the angle between axes of adjacent β -strands and 5 Å is the width of a β -strand).

In the second type, “+3” ridges of one helix fit into grooves between “+4” ridges of the other (Fig. 14.9B). In such packing, the angle between the helix axes is close to $+20$ degrees. This is the most typical angle for helix contacts in long bundles that occur in α -helical globules, as well as in fibrous and membrane proteins (Chothia et al., 1977, 1981; Murzin and Finkelstein, 1988).

In addition, “+3” ridges of one helix can fit into grooves between similar “+3” ridges of the other, thereby forming an extremely short contact of almost perpendicular helices (Efimov, 1979). The contact is so short that I did not show it in Fig. 14.9 although it is quite typical of α -helical globules.

Concluding the consideration of close packing, I would like you to note that the actual interhelical angles in proteins may differ from the above given “ideal” values because side chains vary considerably in size. For the same reason, the picture of

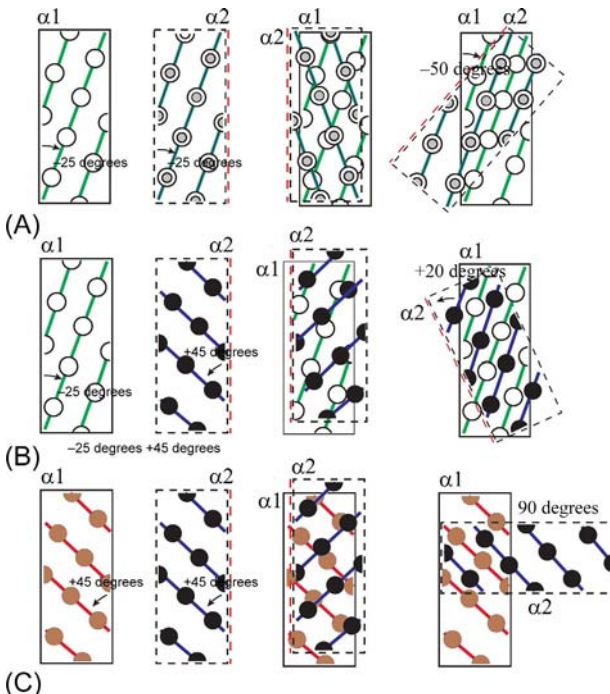


FIG. 14.9 Three variants of close packing of side chains of two helices: large contacts with helix axes inclined at -50 degrees (A) and $+20$ degrees (B) and small contact at 90 degrees (C). We look at the contact area through one helix (through α_2 turned over through 180 degrees around its axis). The residues of the “lower” (α_1) helix are shown as lighter circles and those of the upper helix (α_2) by darker circles. (Adapted from Branden, C., Tooze, J., 1991. *Introduction to Protein Structure*, second ed. Garland Publishers, New York (Chapter 3).)

the ridge-into-groove fitting is slurred over in β -structures (where the side chains project much less: unlike the cylindrical α -helix, the β -sheet has a rather flat surface) and is clearly observed only in rare cases (Finkelstein and Nakamura, 1993).

Finally in this section, let us see how the close packing of helices conforms to the positioning of helices on the ribs of quasi-spherical polyhedra. As a matter of fact, it does so quite curiously. The “polyhedral” packings with angles between helices close to -50 degrees and/or $+20$ degrees (which are favorable for close packing of helices) are observed frequently; others are rare (Murzin and Finkelstein, 1988) although occasionally these can be observed too. For example, the first of the two three-helix packings shown in Fig. 14.7, a bundle with a right-handed twist, causes inter-helical angles of -60 degrees (close to the -50 degrees angle optimal for close packing, see Fig. 14.9A). This three-helix bundle is observed frequently. The other packing, with the left-handed twist, causes interhelical angles of $+60$ degrees (which differs greatly from

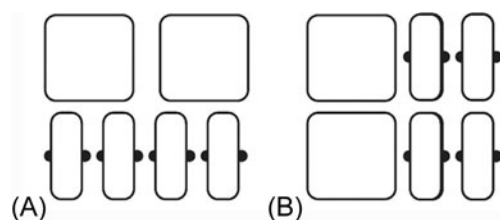


FIG. 14.10 (A) The layer structure of mixed (α/β and $\alpha+\beta$) proteins viewed along the α -helices and β -strands to stress their close packing (helix ends are shown as squares and strand ends as rectangles). (B) α -Helices and β -strands cannot belong to the same layer because this would cause dehydration of H-bonds at the β -sheet edge (H-bond donors and acceptors in the β -sheet are shown as dots).

all angles optimal for close contacts, ie, -50 degrees, $+20$ degrees, and 90 degrees), and this bundle can be observed an order of magnitude less frequently.

Now let us consider “mixed” proteins built up from β -sheets and α -helices. Typically, they consist of separate α - and β -layers, and never have “mixed” ones, which would cause energetically unfavorable dehydration of H-bonds at the β -sheet edges (Fig. 14.10) (Finkelstein and Ptitsyn, 1987).

There are α/β (α slash β) and $\alpha+\beta$ (α plus β) proteins (or rather, domains), and sometimes they are combined into the common class of $\alpha\&\beta$ (ie, “ α and β ”) or $\alpha\cdot\beta$ proteins.

In α/β domains the β -structure is parallel, the α -helices are also parallel to one another (and antiparallel to the β -strands), and along the chain they alternate (Levitt and Chothia, 1976):



Two folding patterns are most typical for α/β proteins (Fig. 14.11): the α/β -cylinder where the β -cylinder lies inside a cylinder formed by α -helices (Richardson, 1977, 1981) and the “Rossmann fold” (Rao and Rossmann, 1973) where a more or less flat (except for the ordinary propeller twist) β -layer is sandwiched between two α -helix layers whose twist is complementary to that of the β -layer.

Unlike previously considered domains, α/β domains usually have two hydrophobic cores: in the Rossmann fold, they are between the β -sheet and each α -layer; in the α/β -cylinder the smaller core is inside the β -cylinder, while the larger one is between the β - and α -cylinders.

β -Cylinders are formed by more or less straight β -strands. Each pair of neighboring (H-bonded) strands has the usual propeller twist. Therefore, the

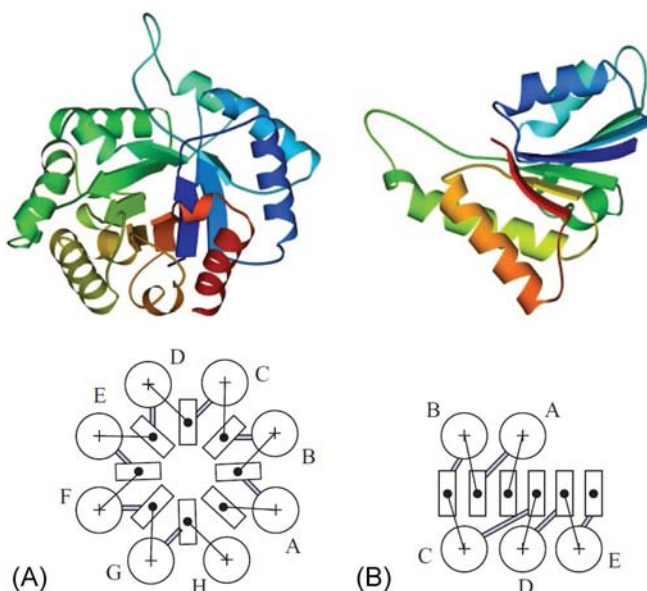


FIG. 14.11 Typical folding patterns of α/β proteins and their simplified models as viewed from the β -layer butt-end: (A) the “ α/β -cylinder” in triose phosphate isomerase; (B) the “Rossmann fold” in the NAD-binding domain of malate dehydrogenase. The detailed drawing of the former shows a viewer-facing funnel formed by rosette-like loops and directed towards the center of the β -cylinder. The latter has a crevice at its upper side; the crevice is formed by loops going upwards and downwards from the β -sheet.

strands form an angle with the cylinder’s axis, and the β -cylinder has a hyperbolic shape (Fig. 14.12). The β -cylinder is rigid, being stitched up with a closed hydrogen bond network. The H-bonds are perpendicular to the strands. Going from one residue to another along the line of H-bonds (along the shaded band in Fig. 14.12), one returns to the initial strand but not to the initial residue (because the strands are tilted with respect to the cylinder’s axes). The resulting shear between the two ends of the hydrogen bond line is expressed as a number of residues. This number is even, since the H-bond directions alternate along the strand. Two digits, the number of β -strands and the “shear number,” allow a precise discrete classification (Murzin et al., 1994) of the closed β -cylinders given by Lesk and Chothia (Lesk, 2001).

By the way, there also exist α/β “almost” cylinders that do not complete the circle and, hence, have no closed hydrophobic core inside the β -cylinder. They are known as “ α/β -horseshoes” and contain up to a dozen and a half α/β repeats.

Usually, an α/β -cylinder contains eight α - and eight β -segments, and the topologies of all α/β -cylinders (and of “ α/β -horseshoes”, too) are alike: β - and α -segments form a right-handed superhelix, where β - and α -segments adjacent in the chain are antiparallel, while two β -strands forming a β - α - β unit are parallel and form an H-bonded contact with each other (see Figs. 14.14–14.16).

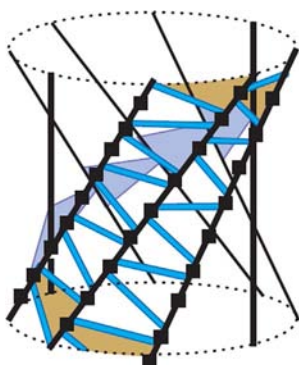


FIG. 14.12 The closed β -cylinder. H-bonds (the blue lines) are shown for one strand only. One line of H-bonding is shown as a shaded band. The number of β -stands is 8, and the “shear number” (follow the shaded band!) also is equal to 8 in the given case. (Adapted from Lesk, A.M., 2001. *Introduction to Protein Architecture*. Oxford University Press, Oxford (Chapter 4).)

Presumably this overall structure provides particular stability to the protein globule, since numerous protein globules with such architecture (10% of all proteins) display close similarity in their shape, although most of them have nothing in common as concerns their origin (ie, nothing in common as concerns their amino acid sequences) or functions.

No common functions, no similarity in the sequences or the structure of their active sites; but when it comes to *location* of the active site, α/β -cylinders have much in common: each architecture has a special place (a dent on the surface at the axis of the β -cylinder), as if specially designed for the active site, no matter what function it performs.

I would like to draw your attention to the “funnel” on the axis of the β -cylinder (Fig. 14.13A). As you can see, it is a dent in the overall protein architecture; this dent is determined by the folding pattern and is not covered with loops. This is where the active site is located. Or rather, one of two such “funnels” (to be found at both ends of the β -cylinder) is used to house the active site—it is the one where C-termini of β -strands and N-termini of α -helices are directed (Branden and Tooze, 1991; Lesk, 2001). These termini (connected with relatively short loops and having numerous open NH groups at N-ends of the helices) are believed to be most useful in binding various substrates. This is, however, still to be studied.

In the Rossmann fold the active site is located similarly: it is in a dent, in the crevice, and again in the crevice to which the C-termini of β -strands and N-termini of α -helices are directed (Rao and Rossmann, 1973). The only difference is that this crevice is formed not by loops drawn outwards from the cylinder center but by loops some of which are drawn to the upper and some to the lower α -layer (Fig. 14.13B).

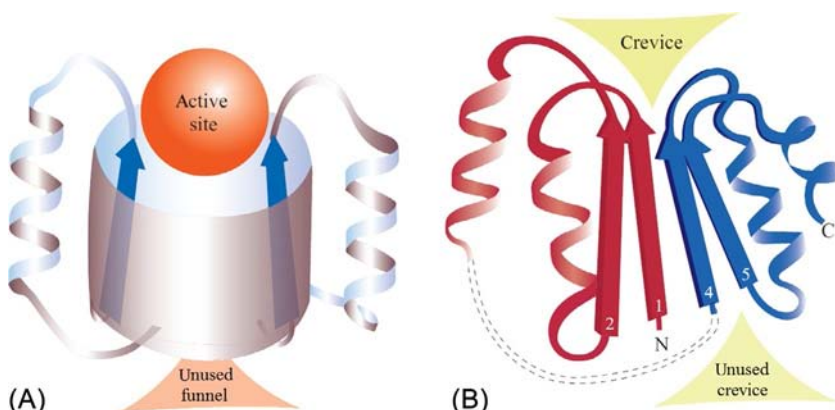


FIG. 14.13 Typical locations of the active site in α/β proteins: (A) in the “funnel” on the α/β -cylinder axis; (B) in the crevice formed by separated loops in the “Rossmann fold”. (Adapted from Branden, C., Tooze, J., 1991. *Introduction to Protein Structure*, second ed. Garland Publishers, New York (Chapter 4).)

Inner voice: Should I believe that the active site always occupies an obvious dent? Maybe it happens often, but far from always?

Lecturer: Right. As a rule (in about 80% of instances), the active site occupies the largest dent on the globule; in turn, this dent is usually determined by the globule architecture built up by the secondary structures. Nevertheless, in many cases a search for the active site took much time—even with the spatial structure of the protein known—and was not always successful...

Now let us consider $\alpha+\beta$ proteins. They are based on the antiparallel β -structure (in contrast to α/β proteins based on the parallel β -structure) (Levitt and Chothia, 1976; Branden and Tooze, 1991; Lesk, 2001, 2010).

The $\alpha+\beta$ proteins can be divided into two subclasses. Those of the first subclass (also known as “ $\alpha\beta$ -plaits”) resemble α/β proteins in that the α -layer is packed against the β -sheet. Like α/β proteins, they are characterized by a regular alternation (though distinct from that of α/β proteins) of α - and β -regions both in the chain and in space. Proteins of the other subclass (“usual” $\alpha+\beta$ proteins) have no such alternation; their α -structures are more or less separated from β -structures in the chain.

The typical alternation of α - and β -regions in the $\alpha\beta$ -plait is either ... $\alpha-\beta-\beta-\alpha-\beta \dots$ or ... $\alpha-\beta-\beta-\beta-\alpha-\beta-\beta \dots$ (Fig. 14.14). Here separate α -helices are placed between β -hairpins or β -sheets composed of an even number of β -strands. The β -strands adjacent in the sequence form antiparallel β -sheets; and because of the even number of β -strands between α -helices (in contrast to the odd number of these observed in α/β proteins), as well as the general co-linearity of the strands and helices, α -helices form antiparallel hairpins too. The “pleated” protein structure is observed as one of the most abundant protein architectures; it is observed, in particular, among ferredoxins and ... RNA-binding proteins.

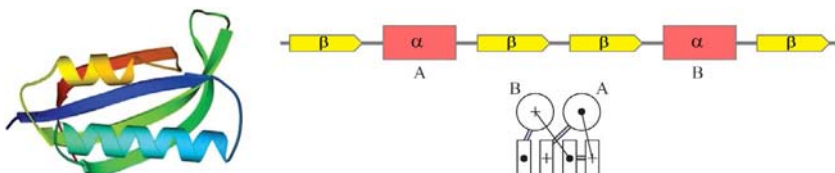


FIG. 14.14 A typical structural motif for $\alpha+\beta$ proteins: the $\alpha\beta$ -plait in the ribosomal protein S6. The $\alpha\beta$ -plait is distinct from other $\alpha+\beta$ proteins because it has a more regular alternation of secondary structures in the chain (in this case, the alternation is $\beta\alpha\beta\alpha\beta$). S6 represents an example of the so-called “ferredoxin fold”. The rainbow coloring (blue-green-yellow-orange-red) traces the pathway of the chain from the N- to the C-terminus. On the right, a schematic diagram of the secondary structure of this protein and its folding pattern as viewed along its almost co-linear structural elements. The helices are lettered. An α - or β -region going away from the viewer (ie, viewed from its N-terminus) is marked with “+”, and that approaching the viewer with a dot.

In “normal” $\alpha+\beta$ domains (Fig. 14.15) α - and β -regions alternate irregularly and tend to form something like blocks (Levitt and Chothia, 1976). They commonly look like a β -sheet (which is often bent on itself thus forming a sub-domain) covered by separate α -helices or by an α -helical subdomain. The β -structure is mostly antiparallel in $\alpha+\beta$ proteins (as in “pure” β proteins).

Now, let me draw your attention to protein topology.

A very typical feature of topology of α/β and $\alpha+\beta$ proteins (as well as of many β -proteins) is the *right-handed* (ie, counterclockwise, when approaching the viewer) topology of connections between parallel β -strands of the β -sheet (see Figs. 14.11 and 14.13–14.15) (Nagano, 1973; Richardson, 1976; Efimov, 1995). In α/β and $\alpha+\beta$ proteins such a connection usually contains

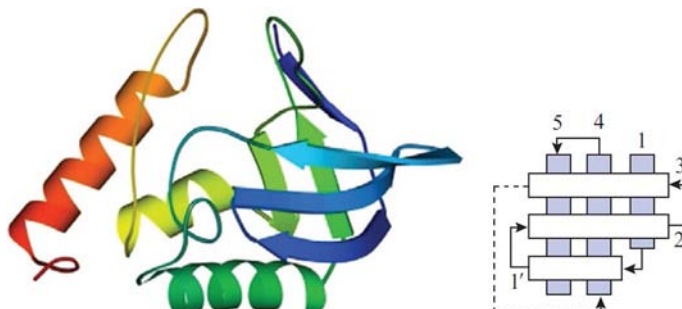


FIG. 14.15 Staphylococcus nuclease, a “normal” $\alpha+\beta$ protein characterized by a less regular (as compared with α/β proteins or $\alpha\beta$ -plaits) alternation of secondary structures in the chain (in this case, $\beta\beta\alpha\beta\beta\alpha\alpha$); here, the α and β structures are more separated in space. The folding pattern observed in the β -sub-domain of the nuclease is called the “OB-fold” (ie, “oligonucleotide-binding fold”) (Murzin, 1993). On the right: a schematic diagram of the OB-fold (the orthogonal packing of β strands is viewed from above). The OB-fold is abundant in various multi- and mono-domain proteins. The β -strands are marked with numerals. The first strand is bent (actually, it is broken); its two halves are marked as 1 and 1'. Notice the “Russian doll effect” (Shindyalov and Bourne, 2000): one characteristic fold (the OB-fold) is a part of another characteristic fold (the nuclease fold).

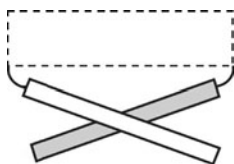


FIG. 14.16 Typical right-handed topology of connections between parallel β -strands of the same sheet. The connection usually contains an extra secondary structure.

an α -helix (Fig. 14.16). In β -proteins (and sometimes in $\alpha+\beta$ too) such a connection contains, as you may remember from the previous lecture (on “abcd” structures and so on), a β -strand from another sheet, and sometimes even a separate β -sheet with odd number of strands. It also happens, though rarely, that the connection between parallel β -strands contains neither α - nor β -structures; but in this, as well as in all other cases, it usually appears to be a *right*, not left-handed connection.

It will become clear from the next two lectures that such handedness of the connection usually contributes to protein stabilization, thus allowing a greater variety of the structure-stabilizing sequences; that’s why the *right*-handed connection is quite frequently observed in different proteins, while the left-handed connection is rare.

In conclusion of this brief outline of globular protein structures, I would like to stress again that the same or very close architectures are often observed in proteins quite different both functionally and phylogenetically. This finding underlies the physical (also known in literature as “rational”) classification of proteins. This will also be discussed in [Lecture 15](#).

REFERENCES

- Branden, C., Tooze, J., 1991. Introduction to Protein Structure. Garland Science, New York (Chapters 2–5, 18).
- Chothia, C., 1989. Polyhedra for helical proteins. *Nature* 337, 204–205.
- Chothia, C., Levitt, M., Richardson, D., 1977. Structure of proteins: packing of α -helices and pleated sheets. *Proc. Natl. Acad. Sci. U. S. A.* 74, 4130–4134.
- Chothia, C., Levitt, M., Richardson, D., 1981. Helix to helix packing in proteins. *J. Mol. Biol.* 145, 215–250.
- Crick, F.H.C., 1953. The packing of α -helices: simple coiled coils. *Acta Crystallogr.* 6, 689–697.
- Efimov, A.V., 1977. Stereochemistry of the packing of alpha-spirals and beta-structure into a compact globule. *Dokl. Akad. Nauk SSSR* (in Russian) 235, 699–702.
- Efimov, A.V., 1979. Packing of alpha-helices in globular proteins. Layer structure of globin hydrophobic cores. *J. Mol. Biol.* 134, 23–40.
- Efimov, A.V., 1995. Structural similarity between two-layer α/β and β -proteins. *J. Mol. Biol.* 245, 402–415.
- Finkelstein, A.V., Nakamura, H., 1993. Weak points of antiparallel β -sheets. How are they filled up in globular proteins? *Protein Eng.* 6, 367–372.

- Finkelstein, A.V., Ptitsyn, O.B., 1987. Why do globular proteins fit the limited set of folding patterns? *Prog. Biophys. Mol. Biol.* 50, 171–190.
- Lesk, A.M., 2001. *Introduction to Protein Architecture*. Oxford University Press, Oxford.
- Lesk, A., 2010. *Introduction to Protein Science: Architecture, Function, and Genomics*, second ed. Oxford University Press, Oxford (Chapters 2–4).
- Levitt, M., Chothia, C., 1976. Structural patterns in globular proteins. *Nature* 261, 552–558.
- Liang, J., Dill, K.A., 2001. Are proteins well-packed? *Biophys. J.* 81, 751–766.
- Murzin, A.G., 1993. OB (oligonucleotide/oligosaccharide binding)-fold: common structural and functional solution for non-homologous sequences. *EMBO J.* 12, 861–867.
- Murzin, A.G., Finkelstein, A.V., 1983. Polyhedrons describing packing of helices in a protein globule. *Biofizika* (in Russian) 28, 905–911.
- Murzin, A.G., Finkelstein, A.V., 1988. General architecture of α -helical globule. *J. Mol. Biol.* 204, 749–770.
- Murzin, A.G., Lesk, A.M., Chothia, C., 1994. Principles determining the structure of β -sheet barrels in proteins. I. A theoretical analysis. II. The observed structures. *J. Mol. Biol.* 236, 1369–1400.
- Nagano, K., 1973. Logical analysis of mechanism of protein folding. I. Prediction of helices, loops and β -structures from primary structure. *J. Mol. Biol.* 75, 401–420.
- Rao, S.T., Rossmann, M.G., 1973. Comparison of super-secondary structures in proteins. *J. Mol. Biol.* 76, 241–256.
- Richardson, J.S., 1976. Handedness of crossover connections in β -sheets. *Proc. Natl. Acad. Sci. U. S. A.* 73, 2619–2623.
- Richardson, J.S., 1977. β -Sheet topology and the relatedness of proteins. *Nature* 268, 495–500.
- Richardson, J.S., 1981. The anatomy and taxonomy of protein structure. *Adv. Protein Chem.* 34, 167–339.
- Shindyalov, I.N., Bourne, P.E., 2000. An alternative view of protein fold space. *Proteins* 38, 247–260.

Lecture 15

This lecture is an attempt to explain why the majority of proteins fit a small set of common folding patterns, which should already be your impression from the previous lectures.

Actually here, we come across the “80%:20%” law. In its initial form, this law suggests that 80% of the total amount of beer is consumed by only 20% of the population.

As for the proteins, 80% of protein families are covered by only 20% of observed folds. In the previous lectures, I took the liberty of focusing mainly on these typical structures.

So, why do most proteins fit a limited set of common folds? And why not all of them (like DNA chains)? And what is behind this limited number of common folds: common ancestry? Common functions? Or the necessity to meet some general principles of folding of stable protein structures? Also, at what structural level is the similarity of proteins of distinct ancestry and function displayed?

For now we will consider these questions only qualitatively, passing to more strict answers in the next lecture, and when we know more about protein folding, I will add a couple of words on the matter.

When only a few protein structures were known (approximately up to the middle of the 1970s) each tertiary structure was believed to be absolutely unique, that is, proteins of evolutionarily different families were thought to share no similarity at all. However, with increasing information on the spatial structure of protein molecules it became more and more clear that there are “standard designs” for protein architectures (Levitt and Chothia, 1976). The architectures of newly solved proteins (or at least of their domains) more and more often appeared to resemble those of known proteins (Chothia, 1992), although their functions and amino acid sequences were utterly different. This generated the idea discussed more than once in our previous lectures, namely, that similarity of protein tertiary structures is caused *not only* by evolutionary divergence and *not* (or not only) by functional convergence of proteins, but simply by restrictions imposed on protein folds by some physical regularities (Richardson, 1977).

By the end of the 1970s it became absolutely clear that there is an intermediate structural level sandwiched between two “traditional” ones, that is, between the secondary structure of a protein and its detailed 3D atomic structure. This intermediate level is already known to us as the “folding pattern” determined by the positions of α - and/or β -regions in the globule, and it is at this level that we observe similarities in proteins having no common ancestry or function. Unlike the detailed 3D atomic protein structure, folding patterns are surprisingly simple and elegant (Fig. 15.1).

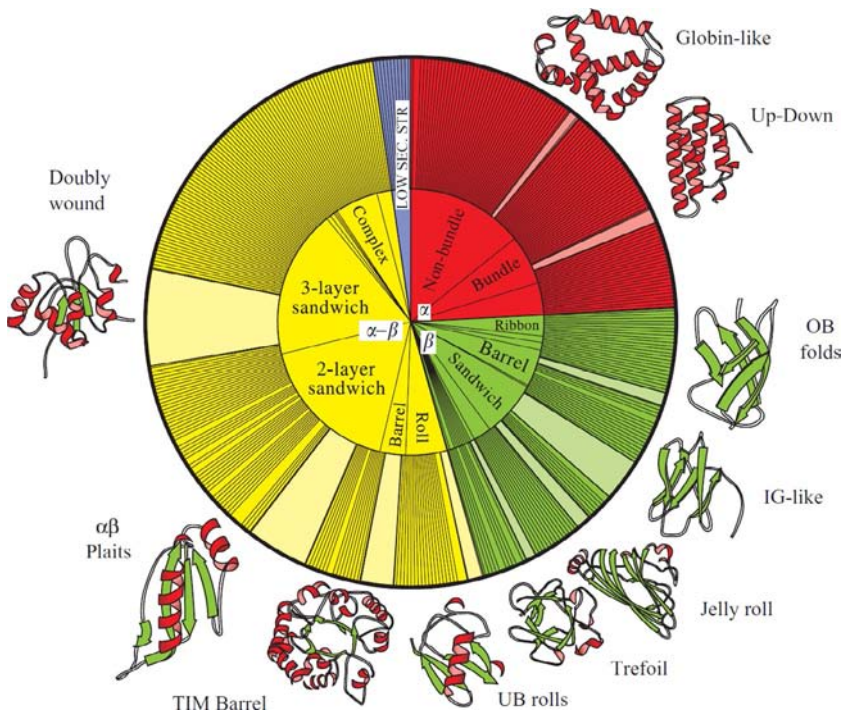


FIG. 15.1 Structural classes of proteins (“ α ,” “ β ,” “ $\alpha\text{-}\beta$,” and “low secondary structure”), typical architectures (“nonbundle,” “bundle,” etc.), and typical folding patterns (topologies) according to physical classifications of proteins (CATH). Class “ $\alpha\text{-}\beta$ ” comprises classes that we have already considered. The sector width shows the abundance of structures of the given type in nonhomologous proteins. Note that α - and β -structures are layered, and that each layer comprises exclusively α -helices or β -strands and never houses both structures (From [Orengo et al., 1997](#).)

The finding that the same or very similar architectures are often observed in proteins utterly different functionally or phylogenetically (Richardson, 1977, 1981; Ptitsyn and Finkelstein, 1980) sets the basis of physical (or “rational”) classification of proteins.

The most complete computer classifications of protein folds are “Dali/FSSP,” developed by Holm and Sander (1997); “CATH” (class-architecture-topology-homology) by Thornton’s team ([Orengo et al., 1997](#)); and, perhaps the most popular among them, “SCOP” (structural classification of proteins) developed by Murzin et al. (1995) after he left Pushchino for Cambridge.

Actually, the classified folds refer to protein domains that are compact globules existing either separately or as a part of a multidomain protein. Classification begins (Fig. 15.1) with structural *classes* (α , β , etc.). The classes are subdivided into *architectures* of protein frameworks built up from α - and/or β -regions. In turn, the architectures are subdivided into *topologies*, that is, pathways taken by the chain through the frameworks; in other words, they are subdivided into folding patterns.

Further on, the folding patterns are subdivided into superfamilies displaying at least some sequence homology (a trace of common ancestry); those, in turn, into families with clearly displayed homology, and so on, down to the separate proteins of concrete organisms.

The physical classification of protein structures (class-architecture-topology) allows not only the systematizing of studied structures but also the prediction of protein structures yet to be found. For example, for a long time, only β -proteins composed of antiparallel β -structures were known, while a lacuna gaped where β -proteins composed of parallel β -structures should be. However, later it was filled (remember β -prisms?).

[Fig. 15.2](#) exemplifies such a classification of the structures of protein globules, which explicitly leaves “vacancies” for possible but not (yet?) found chain folds.

Interestingly, this classification (Efimov’s tree) is based on the initial small “nuclei” of various types that gradually “grow” and become more and more complicated (Ptitsyn et al., 1979; Ptitsyn and Finkel’shtein, 1979; Ptitsyn and Finkelstein 1980; Efimov, 1997). This scheme can be interpreted as an imitation of protein folding; here it should be stressed that the modern idea of this process (supported by experimental and some theoretical (Garbuzynskiy and Kondratova M.S., 2008) data to be discussed in a later lecture) is based on the concept of folding started by the formation of a small folded part of the native globule. However, these “trees” may also be interpreted as an imitation

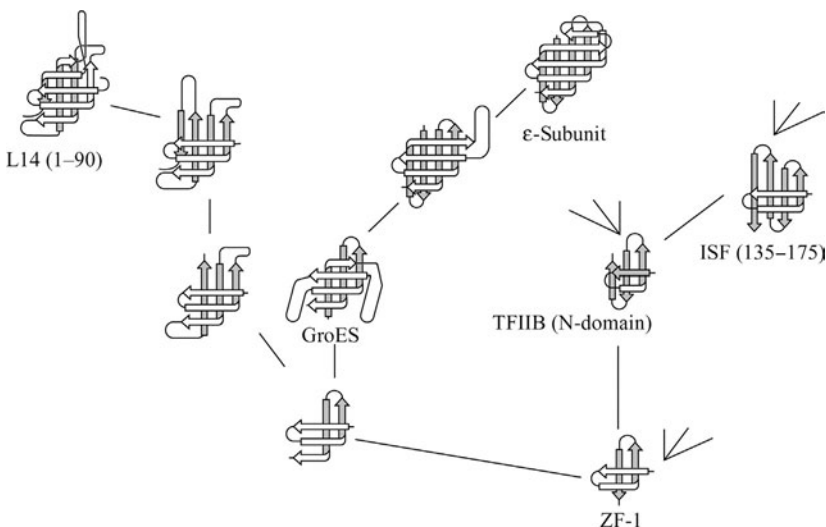


FIG. 15.2 A fragment of the “tree of structures” (Efimov, 1997) based on the initial small “nuclei” of various types gradually growing and becoming more and more complicated. Notice the “Russian doll effect,” that is, that a simpler structure is contained within a more complex one. The branch fragment shown relates to β -proteins “growing” from the “ β -corners” (bent β -hairpins). In this fragment, the known native structures are named, while the remaining unnamed structures were not identified in native proteins until 1997.

of the evolutionary history of proteins. The connection between these two phenomena, folding process and evolutionary history, is yet to be understood.

Now we will discuss the question that always excites a biologist: do we see the evolution of protein structures?

Actually, this question contains two questions: (1) whether we see a microscopic evolution of proteins, that is, whether we see (apart from a simple “drift,” ie, change from organism to organism) some connection between a change in the protein structure and a change of the entire organism; (2) whether there is a macroscopic evolution of proteins, that is, whether their structure becomes more complex with increasing complexity of the organism.

The first question definitely has a positive answer. Although far from all the changes occurring in a protein play a clear functional role (which is stressed by Kimura’s “neutral evolution theory” ([Kimura, 1979](#))), in some cases the functional role of changes in a protein is understood and well-studied. For example, hemoglobin from a llama (a mountain animal) binds oxygen more strongly than hemoglobin from its animal relatives living on the plain. Such adaptation to living conditions is still more clearly illustrated by comparison of hemoglobins from adult animals with fetal hemoglobins: the latter has to derive oxygen from the mother organism, so oxygen binding to fetal hemoglobin must be stronger. And Max Perutz showed which microscopic changes in the hemoglobin structure are responsible for this strengthening ([Perutz, 1970](#)).

It is believed ([Volkenstein, 1977](#); [Schulz and Schirmer, 1979/2013](#); [Cantor and Schimmel, 1980](#); [Branden and Tooze, 1999](#); [Lesk, 2010](#)) that evolution often occurs through amplification of a gene with subsequent mutations of its copies, so that one copy of this gene keeps maintaining the “previous” function (and the organism’s life as well), while another copy, or other copies, become free to mutate in a (random) search for a change that could adapt the protein’s function to a biological need. For example, α -lactalbumin of milk undoubtedly originated from lysozyme at the advent of the vertebrates ([Prager and Wilson, 1988](#)). It is known that there is usually only one gene copy of each major protein (or rather, two identical copies, with diploidy taken into account); however, the living conditions are capable of changing the situation. An “almost fatal” dose of poison can provoke multiplication of copies of the gene responsible for its elimination ([Wannarat et al., 2014](#)). And then random mutations of these copies go into operation, then the selection...

Evolution of proteins is supported by their domain structure. It is known that the domain-encoding genes can migrate, as a whole, from one protein to another, sometimes in various combinations and sometimes individually ([Lesk, 2010](#)). Closely related domains are often observed both as parts of different proteins and as separate proteins (eg, the calcium-binding domain of calmodulin, parvalbumin, etc.; various kringle domains, and so on). Presumably, such exchange is facilitated by the intron-exon structure of genes (specifically, this is well seen in immunoglobulins) ([Maki et al., 1980](#)); however, the hypothesis that the role of

a “module” in the exchange is generally played by an exon rather than by the whole domain (Go, 1985) seems to lack confirmation.

The other question (whether there is macroscopic evolution of proteins, ie, whether their structures become more complex with increasing complexity of the organism) must most probably be answered negatively. A review of protein structures shows that the same folding patterns (specifically, those shown in Fig. 15.1) are observed both in eukaryotes, unicellular and multicellular, and in prokaryotes, although eukaryotic proteins and their domains seem to be larger than prokaryotic proteins sharing the same folding pattern, and the distribution of the most “popular” folds in eukaryotes is somewhat different from that in prokaryotes (Gerstein and Levitt, 1997; Orengo et al., 1999). Besides, eukaryotic proteins often include intrinsically disordered regions, which is not typical of prokaryotic proteins (Bogatyreva et al., 2006; Lobanov and Galzitskaya, 2012; Xue et al., 2012). However, we do not see that protein domains become more complicated with increasing organism complexity, as happens, for example, at the cellular level, as well as at the level of chromatin and organelles, down to ribosomes. (On the contrary: we see that fibrous proteins having the simplest structures, as well as “simple” disordered regions, are more typical for higher organisms rather than for prokaryotes, and especially for archaeabacteria. The simplest proteins are less typical for the simplest organisms. This is strange, is it not?)

However, there exists one more important “macroscopic” structural difference, though it is not connected with the chain folds. It is as follows: the proteins of eukaryotes, of multicellular ones in particular, are much more liable to co- and posttranslational chemical modifications (such as glycosylation, iodination, etc.) (Sambucetti et al., 1986). Modification sites are marked by the primary structure, while the modification is carried out by special enzymes, and often only partially, which causes a variety of forms of the same proteins, although their biochemical activity usually remains unchanged. An alternative splicing, the privilege of eukaryotes, also contributes to the diversity of their proteins (Matlin et al., 2005).

Inner voice: Nevertheless, there is evidence that eukaryotic proteins are not only larger in size but also contain a greater number of domains than prokaryotic proteins (a typical eukaryotic protein contains four or five domains, while a prokaryotic protein only two) (see Branden and Tooze, 1999).

Lecturer: True. However, probably the general idea that eukaryotic proteins are larger in size is connected with the fact that higher organisms have many large multidomain “outer” proteins like immunoglobulins rather than with changes of the “housekeeping” cellular proteins.

It should be mentioned that the investigation of the “macroevolution” of protein chain folds is strongly hampered by the possibility of horizontal gene transfer (see Dunning Hotopp et al., 2007), which may result in penetration of “new” proteins into “old” organisms.

Inner voice: I should like to come back to the “drift” of protein structures (that you had left aside) and to a problem of the origins of protein folds. There is a hypothesis that the “jumping elements” of protein evolution are not domains, as you say, and even not a few times smaller “modules” considered by [Go \(1985\)](#), but short sequences of about 10 residues rather than whole domains. After all, a difference between the folds of distantly similar sequences is often caused by addition or deletion or displacement of such a short chain region (see [Branden and Tooze, 1999](#); [Fersht, 1999](#)). And since it often contains α - or β -structure, kindred protein domains are sometimes attributed to different folding patterns. Thus, a “drift” of protein structures includes transitions from one folding pattern to another due to additions or deletions or displacements of structural modules. If so, is it possible that protein folds originated from the association of small structural modules?

Lecturer: These questions are intensively discussed from time to time, but no definite general answer has been achieved so far. The structural modules considered are so small, and their sequences are so diverse, that it is impossible to prove their relationship or reject this hypothesis. Only short fragments with similar functions (eg, some heme binding fragments) have sufficiently similar sequences. However, the same similarity is sometimes observed for “discontinuous” active sites (eg, for sites of hydrolysis) formed by remote chain residues in proteins having completely different folds. In this case, one can hardly say that these sites are “transferred” from one protein to another. Therefore, coming back to fragments that possibly serve as functional and structural modules: maybe, they are transferred from one protein gene to another; maybe, they arise anew in each protein family. This is not yet known.

However, it is more correct to say that this question is still open for globular proteins. Fibrous proteins, as I have already mentioned, definitely look like multiple repeats of short fragments. Thus, their origin from “modules” looks highly probable, the more so as the repeated structural modules of fibrous proteins are often coded by separate exons. There is every reason to believe that current genomic, and especially structural genomic, and proteomics will answer all these exciting questions.

With a huge number of filed and systematized protein structures available, there arise philosophical questions such as ([Finkelstein and Ptitsyn, 1987](#)): (1) What is the physical reason for the simplicity and regularity of typical folding patterns? (2) Why are the same folding patterns shared by utterly different proteins, and what are the distinctive features of these patterns?

In scientific terms, we would like to elucidate what folding patterns are most probable in the light of the protein physics laws we have studied, how numerous these are and to what extent they coincide with folding patterns observed in native proteins. To answer these questions, we will first of all study the stability of various structures. This approach—to study stability prior to folding—is justified by the fact that the same spatial structures of proteins can be yielded by

kinetically quite different processes: *in vivo* (in the course of protein biosynthesis on ribosomes or during secretion of more or less unfolded proteins through membranes) and *in vitro* when the entire protein refolds from a completely unfolded state. This means that a detailed sequence of actions does not play a crucial role in protein folding.

Let us start with a simple question: why do globular proteins have the layered structure that we discussed in the previous lecture? In other words, let us try and see why the stability of a dense globule requires that the protein framework should look like a close packing of α - and β -layers, why it requires that α - and β -regions should extend from one edge of the globule to the other, and why it requires that the irregular regions should be outside the globule.

In principle, we have already discussed that. Hydrogen bonds are energetically expensive and therefore must be saturated in any stable protein structure. Hydrogen-bond donors and acceptors are present in the peptide group of any amino acid residue. They can be saturated when participating either in H-bonds to water molecules or in the formation of secondary structures. That is why only the secondary structures of a stable (if it wants to be so) globule but not the irregular loops have the right to be out of contact with water and belong to the molecule's interior, and why the elements containing free (from intramolecular H-bonds) NH- and CO-groups, that is, irregular loops, bends, edges of β -sheets, and ends of α -helices, should emerge at the surface.

For the sake of globule stability, extended α - and β -structures must closely surround the hydrophobic core created by their side chains, thereby screening it from water. At the same time, α -helices and β -sheets cannot share the same layer because in this case edge H-bonds of the β -sheet edges would be lost. This means that globule stability demands the formation of purely α -layers and, separately, purely β -layers (Fig. 15.1). In other words, separate α - and β -layers are stable elements of the globular protein structure, while α - and β -structures mixed in the same sheet would be a *structural defect*, or, more accurately, an *energy defect* of the protein globule. It is also evident that a *stable* globule must contain a majority of stable elements (as you know, “*what’s good for General Motors is good for America*”) and avoid structural defects. Since we can observe only stable globules (unstable ones fall apart and therefore cannot be observed), the observed protein structural elements must be mostly stable, and defects must be only occasionally observed.

In particular, this is true for α - and β -layers. They are stable if not mixed. And as we have seen, such layers (usually they are not flat but twisted, cylindrical, and even quasi-spherical, as in α -helical globules) are indeed typical of protein globules. The layered structure simplifies protein construction, and the large majority of domains can be represented by two-, three- or four- (rarely) layer packings.

Some proteins (especially those containing metalorganic complexes or numerous S—S-bonds) are sometimes observed to deviate from the “layered packing” scheme (Fig. 15.3), but such deviating proteins are very rare and they have “unusual” amino acid sequences as a rule.

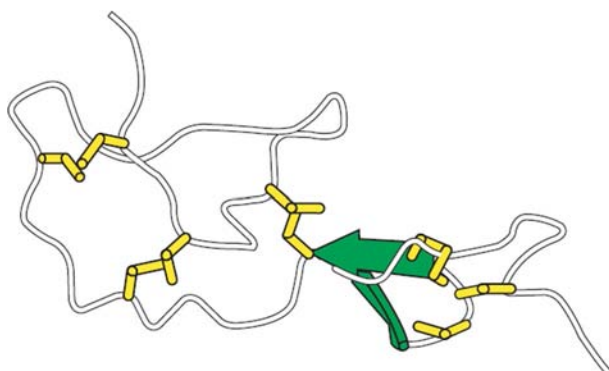


FIG. 15.3 An unusual globule with no α - and almost no β -structure (the protein huristatin, a representative of the “low secondary structure” class). This protein has a very special sequence with many Cys residues that form S—S bonds (their side chains are shown as yellow rods).

Domains with more than four layers are extremely rare, and in principle, it is clear why. They would contain too many residue positions screened from water, which means (for the 1:1 ratio of polar and nonpolar side chains typical of globular water-soluble proteins) that many polar residues would be brought into the interior of the globule. (By the way, the 1:1 ratio of polar to nonpolar residues is just what can be expected from the genetic code (Volkenstein, 1981).) This is energetically most unfavorable, and such a protein would be unstable. That is why very large (and hence, many-layered) compact globules of a “normal” amino acid composition must be unstable, and therefore, large proteins have to be divided into the subglobules that we now know as domains (Bresler and Talmud, 1944a,b; Fisher, 1964).

Actually, a chain consisting mostly of hydrophobic amino acids could pack into a very large stable globule, but such sequences are many times less numerous than those of the mixed “hydrophobic/hydrophilic” type, and, moreover, such a chain would be brought into the membrane instead of acting as a “water-soluble globular protein.”

In principle, a sequence can be suggested in which some specially positioned polar side chains would provide the “cure” for all “defects,” for example, for all broken hydrogen bonds between the main chain and water molecules that result from immersion of a loop or the β -sheet edge in the interior of the globule. Or a sequence can possibly be proposed that would compensate for the broken bonds with some powerful interactions, for example, with covalent (Cys-Cys) or coordinate (through the metal ion) bonds. *In principle*, this seems to be possible. But these sequences would be *very special*, and hence, *very rare...*

Perhaps this is the heart of the matter: maybe, “common” globular proteins are formed by “normal” (not too strictly selected) sequences rather than by those “strictly selected,” which, therefore, are simply very rare.

Let us consider the primary structures of proteins (Fig. 15.4). Statistical analysis shows that the sequences of water-soluble globular proteins appear to be quite “random” (Finkel’shtein, 1972; Poroikov et al., 1976).

That is, in these sequences various residues are as mixed as would be expected for the result of random copolymerization. Certainly, each sequence does not result from random biosynthesis but is gene-encoded. Still, the sequences of water-soluble globular proteins look like "random" ones: they lack the blocks typical of membrane proteins (where clearly hydrophobic regions that must stay within the membrane alternate with more hydrophilic ones that have to form loops and even domains projecting from the membrane), and also they lack the periodicity characteristic of fibrous proteins (with their huge regular secondary structures).

Inner voice: I cannot but note that a coded message may also look like a random sequence of letters, although this is not at all the case...

Lecturer: Of course, the amino acid sequences of globular proteins are not truly random (that would imply that any sequence can fold into a globular protein; anyway, this will be discussed in later in [Lecture 16](#)). Protein sequences are certainly selected to create stable protein globules. But the shape of these globules may vary greatly. Therefore, the set of observed primary structures includes the entire spectrum of regularities inherent to all these shapes, that is, a vast set of various “codes.” And when calling the primary structure “random” (or rather, “quasi-random”), we mean only that in the totality of primary structures of globular proteins, the traces of selection of protein-forming sequences are not seen as clearly (and therefore are not as restrictive) as traces of selection for periodicity in fibrous proteins or traces of selection for blocking in membrane proteins. This is what is meant when I say that amino acid sequences of water-soluble globular proteins look like random sequences.

And what is it like “to look like a *random sequence*”? This means to look like the *majority* of all possible sequences. Then in considering water-soluble globular proteins it would certainly not be pointless to try to find out which spatial

FIG. 15.4 Typical patterns of alternation of hydrophobic (●) and polar (○) amino acid residues in the primary structures of water-soluble globular proteins, membrane proteins and fibrous proteins.

structures are usually stabilized by the most common, random sequences (see [Bresler and Talmud, 1944a,b; Ptitsyn, 1984; Ptitsyn and Volkenstein, 1986](#)) or by those similar to them (by “quasi-random” sequences).

Still more. If a protein globule has a “structural defect” (eg, immersion of an irregular loop or the edge of a β -sheet in the hydrophobic core), then its stability can be ensured only by an extremely thorough selection of the amino acid sequence (to collect as many structure-supporting interactions as possible). The greater the “defect,” the more rigorous the selection. And if there is no defect, then less rigorous selection is required. In other words, a “defect-free” structure can be stabilized by many sequences, a structure with a minor defect by a few, and a structure with a great defect can be stabilized only by a vanishingly small number of sequences.

And (if only physics is taken into account), the structures coded by many sequences must be observed quite often, while those coded by a small number of sequences only rarely. This is how the “physical selection” of protein structures can occur.

Since typical packings, “stacks,” of secondary structures of globular proteins ([Fig. 15.1](#)) look like stable packings of random or almost random sequences should look, it is evident that, at least at the packing level, the observed result of natural (biological) selection of packings does not conflict with physical selection.

Let us proceed by considering the *folding patterns* of protein chains from the same viewpoint, from the viewpoint of structural defects and the physical selection of structures that are “defect-free” (and hence, “eligible” for many sequences).

As we have seen, protein folding patterns are often most elegant. The pathway of protein chains often resembles the patterns on pottery ornaments ([Fig. 15.5](#)). And according to the neat idea of Jane Richardson who discovered this resemblance, this is not a coincidence: both the ornament line and the protein chain aim to solve *the same* problem, that is, how to envelop a volume (in protein, its hydrophobic core) by a line avoiding self-intersection.

In proteins, this effect is achieved by surrounding the core (or two cores, as typical for α/β proteins) with secondary structures and with loops sliding over the core surface. It is also important that the loops connect *antiparallel* (and *not parallel*) secondary structures ([Fig. 15.6A](#)), and that they *do not intercross* ([Fig. 15.6B](#)). Note that the latter decreases the probability of knot formation in the protein chain.

Why are parallel connections worse than antiparallel for the secondary structure elements adjacent in the chain? Is it perhaps because then a too long irregular loop (unsupported by H-bonds) is required? Or is it because the rather rigid polypeptide chain has then to be bent, which is energetically expensive (or rather, causes a free-energy loss; see [Landau and Lifshitz \(1980\)](#))?

And what is wrong with loop crossing? After all, we do not mean that one loop runs into another, we only mean that one loop passes over another. Perhaps

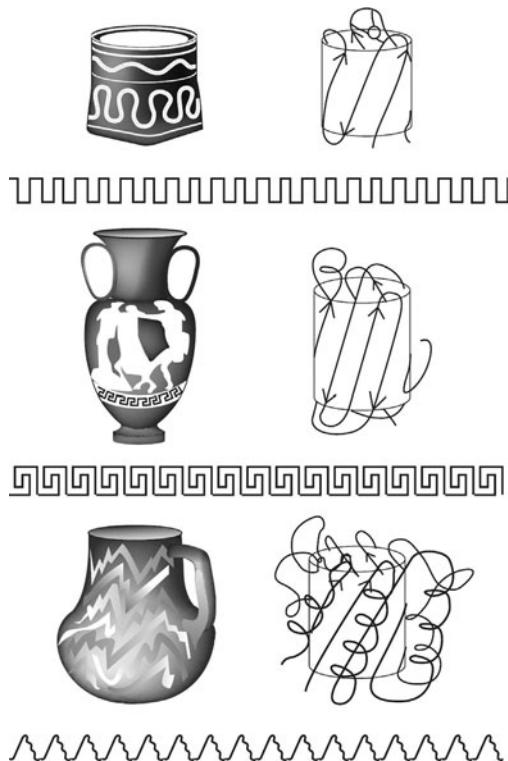


FIG. 15.5 Folding patterns of protein chains and ornaments on American-Indian and Greek pottery: two solutions to the problem of enveloping a volume with a non-self-intersecting line. On top, the meander motif; in the center, the Greek key motif; at the bottom, the zigzag “lightning” motif. (Reprinted with permission from Richardson, J.S., 1977. β -Sheet topology and the relatedness of proteins. *Nature* 268, 495–500, © 1977, Macmillan Magazines Limited.)

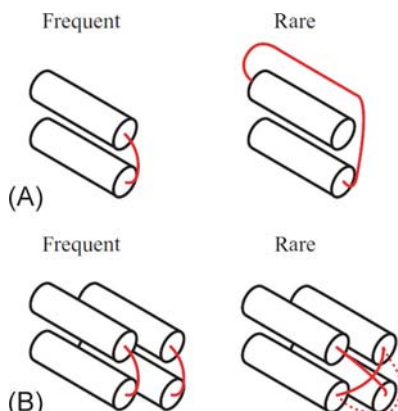


FIG. 15.6 As a rule, loops connect *antiparallel* (and *not parallel*) adjacent regions of a secondary structure (A), and any loop crossing is rarely observed in proteins, no matter if one loop covers another or by-passes it (B).

the problem is that the “lower” loop is pressed to the core and loses some of its hydrogen bonds to water molecules. And to compensate for this loss (the “energy defect”), again a “rare” sequence is needed...

It should be noted that structures with relatively small defects such as loop crossing are still observed in proteins (unlike structures with the large packing defects like mixed layers of α and β structures discussed earlier). But “faulty” protein structures are rare, which is especially significant because a “structure with a defect” can be formed in many more ways than a “defect-free” one.

Thus, we see that “structural defects” have a great effect on the occurrence of various protein structures in nature (Finkelstein and Ptitsyn, 1987).

Here, however, we might be confused by the fact that only one or two H-bonds are lost by loop crossing, that is, the loss is energetically inexpensive and amounts to only $3\text{--}5 \text{ kcal mol}^{-1}$. This is very much less than the total energy of interactions within the globule, which amounts to hundreds of kilocalories (as follows from protein melting data that we will consider in later lectures). Moreover, it is considerably less than the usual “margin of stability” of the native globule, that is, the free-energy difference between the folded and unfolded protein, which amounts to about 10 kcal mol^{-1} under native conditions (according to the same data). Then, why does an “energy defect” of only 5 kcal mol^{-1} virtually rule out loop crossing in native protein globules?

And one more question: why cannot the upper loop make an additional bend (dashed line in Fig. 15.6) to avoid the crossing (ie, to have it replaced by bypassing)? Perhaps the matter is, again, that the polypeptide chain is rigid and an additional bend would cost, as estimated (Finkelstein and Ptitsyn, 1987), a few (again a few!) kilocalories?

Let us postpone answering these questions until the next lecture, and consider now another characteristic feature of protein architectures, namely, that connections between parallel β -strands are almost always *right-handed* and not *left-handed* (Fig. 15.7).

In this case, the stability criterion allows us to point out the “better” of these two asymmetrical connections. Their difference is based on asymmetry of native amino acids. It causes, as you remember, a predominantly *right-handed* twist (shown in Fig. 15.7) of β -layers composed of L-amino acids.

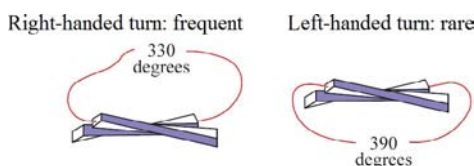


FIG. 15.7 The right-handed turn (counter clockwise rotation when the chain is approaching) of connections between parallel β -strands is frequently observed in proteins, while the left-handed turn is very rare. (The connections shown here as simple lines usually incorporate α - or β -regions.)

The angle between adjacent β -strands is close to 30 degree, such that the total rotation angle is close to 330 degree for a right-handed connection, while it is close to 390 degree for a left-handed one. As a result of polypeptide chain rigidity, the right-handed connection is more favorable: its elastic free energy is lower, although—again—by a couple of kilocalories only ([Finkelstein and Ptitsyn, 1987](#)).

Inner voice: I cannot but note that polymer elasticity is *not* an energy but rather an entropy effect (see [Birshtein and Ptitsyn, 1966](#); [Flory, 1969](#); [Landau and Lifshitz, 1980](#)). That is, a significantly bent chain is not as free in its fluctuation as an extended or slightly bent chain. In other words, a smaller number of conformations are possible for a bent chain than for a straight chain. Thus, you must be speaking about a fluctuating loop, whereas in the protein globule loops are *not* fluctuating, they are fixed, and no matter what pathway they take, they have a single conformation. Then, what do the entropy losses have to do with the native protein structure where the entropy of fixed chains is equal to zero anyway!?

Lecturer: I see you know polymer physics! Let me now answer your question concerning “entropic,” to all appearances, defects of too sharp turns of the chain qualitatively.

The thing is that a chain with a limited choice of conformations cannot adjust well to its constituent amino acid residues. A certain conformation has low energy only for a certain sequence (or a small number of sequences) and high energy for others, that is, for most sequences. But if the chain can choose among a large set of conformations, then many more sequences can be adequately fitted. Thus, we see that the “entropy defect” can be translated into “energy defect” (or into “decreased number of sequences”) language. The entropy effects will be considered more rigorously later on.

We will also consider the postponed question as to why a “defect” of only a few kilocalories per mole plays a significant role in the occurrence of protein structures. We will remember these two problems and consider them in detail in our [Lecture 16](#) (meanwhile, you can take a look at [Finkelstein and Ptitsyn \(1987\)](#) and [Finkelstein et al. \(1995a,b\)](#)).

And right now, not to find the final answer to the latter question but just to drop a hint, let us consider relationships between the energy and other statistical rules known for protein structures. For example, let us consider the immersion of hydrophobic and hydrophilic side-groups in the protein globule, different angles of rotation in the chain ([Pohl, 1971](#)) and others. Similar to the previously discussed folding patterns, here “defects” are rare and “good elements” are usual. However, here more detailed statistics allow not only qualitative but also quantitative estimates to be made.

And the estimates obtained show the following. Both the rare occurrence of “defects” (no matter whether it is a “bad” rotation angle or the deep immersion of a polar group in the globule) and the frequent occurrence of “good elements”

(eg, salt bridges formed by oppositely charged groups) are described by the common phenomenological formula (Pohl, 1971; Finkelstein et al., 1995a,b):

$$\text{Occurrence} \sim \exp(-\text{free energy of element}/kT_C), \quad (15.1)$$

where T_C is a temperature (called “conformational” or “selective” temperature), which is close to either room (comfortable for proteins) temperature or the characteristic protein melting temperature (protein statistics do not allow us to distinguish between 300 and 370 K).

Expression (15.1) describing the occurrence of protein structural elements is surprisingly similar to Boltzmann statistics *in its exponential shape*, while its physical sense is *absolutely different*. It should be remembered that Boltzmann statistics originate from the particles’ wandering from one position to another and staying for a longer time in places where their energy is lower. In contrast, structural elements of the observed (native) protein globules are fixed, they do *not* appear and disappear, and they do *not* wander from one place to another.

That is, the usual Boltzmann statistics cannot be applied to the occurrence of elements of the native protein structure. And if so, why does the statistics of occurrence of these elements have such a familiar “quasi-Boltzmann” shape?

Let us again postpone a detailed answer to this question until the next lecture. Meanwhile, let us accept, as a phenomenological fact, the estimate that the defect of about kT_C , that is, of about 1 kcal mol⁻¹, decreases the occurrence of the defect-containing structures by a few times. And, as is clear to us now, this defect must decrease by a few times the number of amino acid sequences maintaining the stability of the defect-bearing protein.

Thus, our conclusions are as follows:

1. “Popular” folding patterns look so “standard,” so simple and regular, because the framework of a protein structure is a compact layered packing of extended standard solid bodies (α -helices and β -strands), and their irregular connections slide over the surface of the globule, avoiding intercrossing and crossing the ends of structural segments. Physically, this arrangement is most favorable for the globule’s stability because it ensures the screening of nonpolar groups from water and H-bonding of all main-chain peptide groups immersed in the compact globule.
2. The number of such “standard” stable folding patterns is not large (numbered in the hundreds, while proteins are numbered in tens of thousands); therefore, it is not surprising that some of these “common” structures are shared by proteins different in all other respects.
3. At the same time, other (defective) folding patterns are not prohibited either. They are simply rare, since only a small number of sequences can ensure their stability. The greater the defect, the lower the occurrence of such folds.
4. A “*multitude principle*” can be proposed to describe structures of domains of water-soluble globular proteins with their typical “quasi-random” amino

acid sequences. It would read as follows: *the more sequences fit the given architecture without disturbing its stability, the higher the occurrence of this architecture in native proteins.* Proposed by us in 1993 ([Finkelstein et al., 1993](#)), this principle is now better known as the principle of “designability of protein structures” ([Helling et al., 2001](#)).

REFERENCES

- Birshtein, T.M., Ptitsyn, O.B., 1966. Conformations of Macromolecules. Interscience Publishers, New York (Chapters 3, 8).
- Bogatyreva, N.S., Finkelstein, A.V., Galzitskaya, O.V., 2006. Trend of amino acid composition of proteins of different taxa. *J. Bioinf. Comput. Biol.* 4, 597–608.
- Branden, C., Tooze, J., 1999. Introduction to Protein Structure, second ed. Garland Publishing, Inc., New York, London (Chapters 2, 4, 7, 17).
- Bresler, S.E., Talmud, D.L., 1944a. On the nature of globular proteins. *Dokl. Akad. Nauk SSSR* (in Russian) 43, 326–330.
- Bresler, S.E., Talmud, D.L., 1944b. Some consequences of a new hypothesis. *Dokl. Akad. Nauk SSSR* (in Russian) 43, 367–369.
- Cantor, C.R., Schimmel, P.R., 1980. Biophysical Chemistry. W.H. Freeman & Co., New York. (Part 1, Chapter 2).
- Chothia, C., 1992. Proteins. One thousand families for the molecular biologist. *Nature* 357, 543–544.
- Dunning Hotopp, J.C., Clark, M.E., Oliveira, D.C., Foster, J.M., Fischer, P., Muñoz Torres, M.C., Giebel, J.D., Kumar, N., Ishmael, N., Wang, S., Ingram, J., Nene, R.V., Shepard, J., Tomkins, J., Richards, S., Spiro, D.J., Ghedin, E., Slatko, B.E., Tettelin, H., Werren, J.H., 2007. Widespread lateral gene transfer from intracellular bacteria to multicellular eukaryotes. *Science* 317, 1753–1756.
- Efimov, A.V., 1997. A structural tree for proteins containing 3 β -corners. *FEBS Lett.* 407, 37–46.
- Fersht, A., 1999. Mechanism in Protein Science: A Guide to Enzyme Catalysis and Protein Folding. W. H. Freeman & Co., New York.
- Finkel'shtein, A.V., 1972. Feedback between primary and secondary the structure of globular proteins. *Dokl. Akad. Nauk SSSR* (in Russian) 207, 1486–1489.
- Finkelstein, A.V., Ptitsyn, O.B., 1987. Why do globular proteins fit the limited set of folding patterns? *Prog. Biophys. Mol. Biol.* 50, 171–190.
- Finkelstein, A.V., Gutin, A.M., Badretdinov, A.Ya., 1993. Why are the same protein folds used to perform different functions? *FEBS Lett.* 325, 23–28.
- Finkelstein, A.V., Gutin, A.M., Badretdinov, A.Ya., 1995a. Boltzmann-like statistics of protein architectures. Origins and consequences. In: Biswas, B.B., Roy, S. (Eds.), Subcellular Biochemistry. Proteins: Structure, Function and Protein Engineering, vol. 24. Plenum Press, New York, pp. 1–26.
- Finkelstein, A.V., Badretdinov, A. Ya, Gutin, A.M., 1995b. Why do protein architectures have Boltzmann-like statistics? *Proteins* 23, 142–150.
- Fisher, H.F., 1964. A limiting law relating the size and shape of protein molecules to their composition. *Proc. Natl. Acad. Sci. U. S. A.* 51, 1285–1291.
- Flory, P.J., 1969. Statistical Mechanics of Chain Molecules. Interscience Publishers, New York (Chapters 1–3).

- Garbuzynskiy, S.O., Kondratova M.S., 2008. Structural features of protein folding nuclei. *FEBS Lett.* 582, 768–772.
- Gerstein, M., Levitt, M., 1997. A structural census of the current population of protein sequences. *Proc. Natl. Acad. Sci. U. S. A.* 94, 11911–11916.
- Go, M., 1985. Protein structures and split genes. *Adv. Biophys.* 19, 91–131.
- Helling, R., Li, H., Mélin, R., Miller, J., Wingreen, N., Zeng, C., Tang, C., 2001. The designability of protein structures. *J. Mol. Graph. Model.* 19, 157–167.
- Holm, L., Sander, C., 1997. DALI/FSSP classification of three-dimensional protein folds. *Nucleic Acids Res.* 25, 231–234.
- Kimura, M., 1979. The neutral theory of molecular evolution. *Sci. Am.* 241, 98–100. 102, 108 *passim*.
- Landau, L.D., Lifshitz, E.M., 1980. Statistical Physics, third ed. A Course of Theoretical Physics, Vol. 5. Elsevier, Amsterdam–Boston–Heidelberg–London–New York–Oxford–Paris–San Diego–San Francisco–Singapore–Sydney–Tokyo (Section 151).
- Lesk, A., 2010. Introduction to Protein Science: Architecture, Function, and Genomics, second ed. Oxford University Press, Oxford, New York (Chapters 2–4, 7).
- Levitt, M., Chothia, C., 1976. Structural patterns in globular proteins. *Nature* 261, 552–558.
- Lobanov, M.Y., Galzitskaya, O.V., 2012. Occurrence of disordered patterns and homorepeats in eukaryotic and bacterial proteomes. *Mol. Biosyst.* 8, 327–337.
- Maki, R., Traunecker, A., Sakano, H., Roeder, W., Tonegawa, S., 1980. Exon shuffling generates an immunoglobulin heavy chain gene. *Proc. Natl. Acad. Sci. U. S. A.* 77, 2138–2142.
- Matlin, A.J., Clark, F., Smith, C.W.J., 2005. Understanding alternative splicing: towards a cellular code. *Nat. Rev.* 6, 386–398.
- Murzin, A.G., Brenner, S.E., Hubbard, T., Chothia, C., 1995. SCOP: a structural classification of proteins database for the investigation of sequences and structures. *J. Mol. Biol.* 247, 536–540.
- Orengo, C.A., Michie, A.D., Jones, S., Jones, D.T., Swindells, M.B., Thornton, J.M., 1997. CATH—a hierachic classification of protein domain structures. *Structure* 5, 1093–1108.
- Orengo, C.A., Pearl, F.M., Bray, J.E., Todd, A.E., Martin, A.C., Lo Conte, L., Thornton, J.M., 1999. The CATH database provides insights into protein structure/function relationships. *Nucleic Acids Res.* 27, 275–279.
- Perutz, M.F., 1970. Stereochemistry of cooperative effects in haemoglobin. *Nature* 228, 726–734.
- Pohl, F.M., 1971. Empirical protein energy maps. *Nat. New Biol.* 234, 277–279.
- Poroikov, V.V., Esipova, N.G., Tumanian, V.G., 1976. Distribution of identical amino acid residues in the primary structure of proteins. *Biofizika* (in Russian) 21, 397–400.
- Prager, E.M., Wilson, A.C., 1988. Ancient origin of lactalbumin from lysozyme: analysis of DNA and amino acid sequences. *J. Mol. Evol.* 27, 326–335.
- Ptitsyn, O.B., 1984. Protein as an edited statistical copolymer. *Mol. Biol.* (in Russian) 18, 574–590.
- Ptitsyn, O.B., Finkel'shtein, A.V., 1979. Folding and topology parallel β -structure. *Biofizika* (in Russian) 24, 27–31.
- Ptitsyn, O.B., Finkelstein, A.V., 1980. Similarities of protein topologies: evolutionary divergence, functional convergence or principles of folding? *Quart. Rev. Biophys.* 13, 339–386.
- Ptitsyn, O.B., Volkenstein, M.V., 1986. Protein structures and neutral theory of evolution. *J. Biomol. Struct. Dyn.* 4, 137–156.
- Ptitsyn, O.B., Finkelstein, A.V., Falk, P., 1979. Principal folding pathway and topology of all-beta proteins. *FEBS Lett.* 101, 1–5.
- Richardson, J.S., 1977. β -Sheet topology and the relatedness of proteins. *Nature* 268, 495–500.
- Richardson, J.S., 1981. The anatomy and taxonomy of protein structure. *Adv. Protein Chem.* 34, 167–339.

- Sambucetti, L.C., Schaber, M., Kramer, R., Crowl, R., Curran, T., 1986. The fos gene product undergoes extensive post-translational modification in eukaryotic but not in prokaryotic cells. *Gene* 43, 69–77.
- Schulz, G.E., Schirmer, R.H., 1979/2013. Principles of Protein Structure. Springer, New York (Chapter 9).
- Volkenstein, M.V., 1977. Molecular Biophysics. Academic Press, London, NY (Chapters 1, 4).
- Volkenstein, M.V., 1981. Biophysics. Nauka, Moscow (Chapters 4, 6, in Russian).
- Wannarat, W., Motoyama, S., Masuda, K., Kawamura, F., Inaoka, T., 2014. Tetracycline tolerance mediated by gene amplification in *Bacillus subtilis*. *Microbiology* 160, 2474–2480.
- Xue, B., Dunker, A.K., Uversky, V.N., 2012. Orderly order in protein intrinsic disorder distribution: disorder in 3500 proteomes from viruses and the three domains of life. *J. Biomol. Struct. Dyn.* 30, 137–149.

Lecture 16

We will now discuss in detail how general structural regularities are connected with protein stability and with the number of protein structure-coding amino acid sequences.

We learned that the framework of a typical protein globule is a compact packing of layers built up from extended solid bodies (α -helices and β -structures), and that irregular connections slide over the surface of the globule virtually never intercrossing or crossing the ends of structural segments (Fig. 16.1).

We concluded that the physical reason for such an arrangement is its contribution to the stability of the globule, since it provides screening of nonpolar side chains from water simultaneously with H-bonding of the main-chain peptide groups when they are immersed in the compact globule. In turn, this increased stability allows a greater number of amino acid sequences to fit the given architecture without its destruction (which can cause a more frequent occurrence of this architecture in native proteins—we called this “the multitude principle”).

As we have mentioned, the peculiarity of typical water-soluble globular proteins consists in the absence of any striking features common for their primary structures (and that is why these sequences are most diverse and numerous, so the “multitude principle” can be applied to them). Indeed, their primary structures are free of any obvious correlation, such as the periodicity characteristic of fibrous proteins or block alternation typical of membrane proteins; their polar groups are rather evenly mixed with nonpolar ones. Moreover, in water-soluble globular proteins, the amounts of polar and nonpolar residues are almost equal. As a result, their primary structures look very much like “random copolymers” synthesized from hydrophobic and hydrophilic amino acids.

Are these “random” sequences compatible with the compact chain fold in the globule? (I have to note that the first to pose this question were Bresler and Talmud (1944a,b).) In particular, are they compatible with the observed secondary structures (whose share in the protein chain is somewhat above a half)? To answer these questions, let us consider hypothetical “protein chains” that result from occasional copolymerization of equal amounts of polar and nonpolar groups (Ptitsyn and Volkenstein, 1986; Finkelstein and Ptitsyn, 1987).

To be able to fit a compact globule, an α - or β -structural segment should have a continuous hydrophobic surface that includes several hydrophobic groups. An α -helical surface is formed, as we know, by nonpolar residues positioned as $i - (i+4) - \dots$ (sometimes, as $i - (i+3)$) in the chain, while the alternation $i - (i+2) - \dots$ is suitable for the hydrophobic surfaces of β -strands (Fig. 16.2). It can be easily shown that even a random copolymer contains

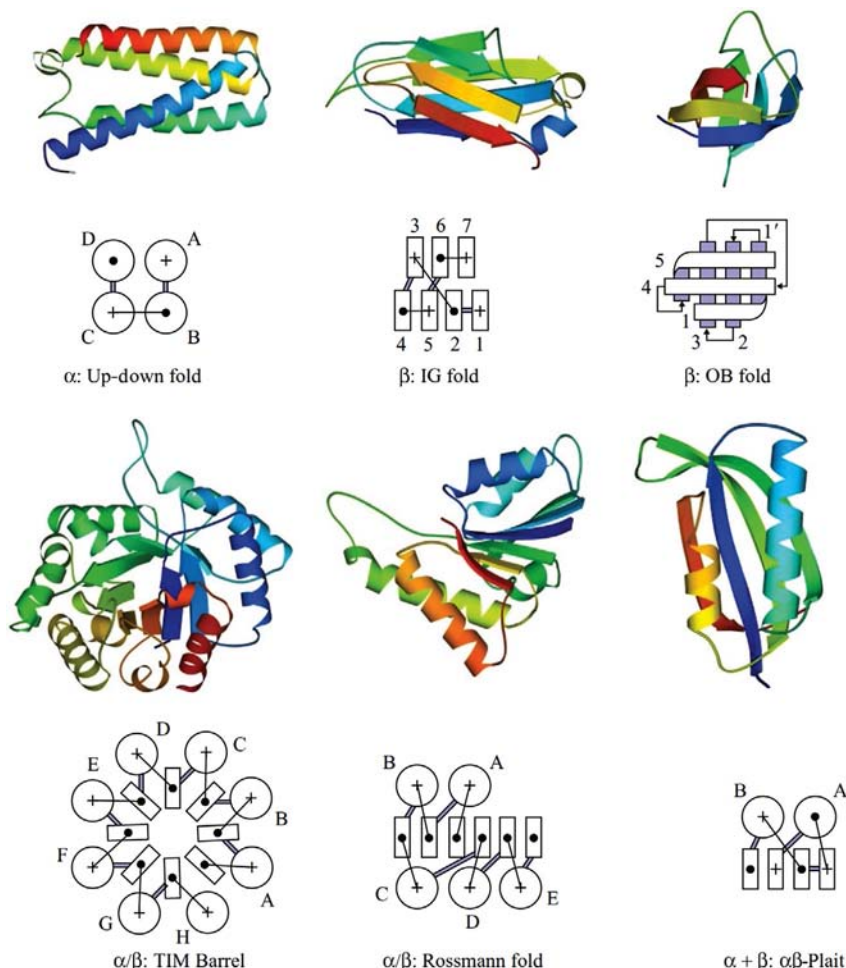


FIG. 16.1 Typical folding patterns of the protein chain in α , β , α/β , $\alpha+\beta$, and proteins. Simplified diagrams are shown below each. The packings of α - and β -structures are layered, and each layer is composed of either α -helices or β -strands but never contains both structures.

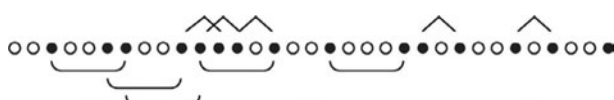


FIG. 16.2 The typical pattern of alternation of hydrophobic (●) and polar (○) amino acids in “quasi-random” primary structures of water-soluble globular proteins. Arcs (below) and angles (above) indicate the positions of potential hydrophobic surfaces suitable for α -helical and β -structural segments, that is, pairs of hydrophobic residues in positions $i, i+4$ and $i, i+2$, respectively.

enough nonpolar periodic aggregates for hydrophobic surfaces of α - and β -segments of a medium-sized protein domain.

Let “ p ” be the portion of nonpolar groups in a copolymer, and “ $1 - p$ ” be the portion of polar ones. Then a periodic sequence of exactly r nonpolar groups restricted at its ends by two polar residues can start at a given point with the probability:

$$W(r) = (1-p)p^r(1-p) \quad (16.1)$$

The “hydrophobic surface” of the α - and β -segment forms if $r > 1$, and the average number of groups involved is

$$\langle r \rangle = \sum_{r>1} [W(r) \cdot r] / \sum_{r>1} W(r) = \sum_{r>1} [p^r \cdot r] / \sum_{r>1} p^r = 2 + p/(1-p) \quad (16.2)$$

(I have taken the liberty of omitting the summation of series because this can be found in any maths handbook.) At $p = 1/2$, both an “average” α -helix and an “average” β -segment include $\langle r \rangle = 3$ of regularly positioned hydrophobic groups, that is, 3 ± 0.5 of the full periods of the α - or β -structure (± 0.5 —because the hydrophobic group may be at the beginning, or in the middle, or at the end of the period). The expected average numbers of residues in α - and β -segments (their periods are 3.6 and 2) are $\langle n_\alpha \rangle = 11 \pm 2$ and $\langle n_\beta \rangle = 6 \pm 1$, respectively, which practically coincide with the average lengths of α - and β -segments in globular proteins (Finkelstein and Ptitsyn, 1987). Interestingly, in random sequences, as well as in primary structures of real proteins, the residue clusters good for α -surfaces often overlap those good for β -surfaces (Fig. 16.2).

Similar estimates show that the average length of loops between secondary structures in a random copolymer amounts to about $3 + 0.5p^{-2}$, that is, at $p \approx 1/2$, the loops should be somewhat shorter, on the average, than the secondary structure segments—which is indeed observed.

Thus, a random copolymer provides continuous hydrophobic surfaces that can stick α - and β -segments to the hydrophobic core at least with their one side, while the loops are relatively short. Therefore, “mediocre” random sequences are quite capable of folding into at least a two-layer arrangement of secondary structures.

Inner voice: However, one should not forget that in some, though not many, proteins (eg, in hemagglutinin or leucine zipper) there are extremely long helices that do not fit the above principles. And in some other proteins (eg, in superoxide dismutase) there are extremely long disordered loops...

Lecturer: True. These exceptions look either like blocks borrowed from fibrous helical proteins or (as concerns long loops) like anomalous hydrophilic blocks. But *on the average, in general*, α -, β -, and irregular segments are not too long, and their length is close to that expected for a “random” sequence containing equal proportions of hydrophobic and polar groups.

The harmony between random sequences and compact, potentially stable shapes of globules exists as long as the chain comprises fewer than ~ 150 residues. However, as the globule increases, as the number of its secondary structure layers grows, its “eligibility” for a random amino acid sequence decreases. This is explained by the fact that the segments belonging to the protein interior must be almost exclusively composed of hydrophobic residues, because otherwise the globule would not survive the presence of numerous water-screened hydrophilic groups and would explode, and the length of such a sequence must be proportional to the diameter of the globule. A small number of such long and almost exclusively hydrophobic segments may also be built up in a “random” copolymer from $\sim 50\%$ of hydrophobic and $\sim 50\%$ of hydrophilic residues, but only a small number indeed. Therefore, for a random sequence, we can expect not more than two or three, or sometimes four, layers of secondary structures, and this is what we really observe in single-domain water-soluble globular proteins and in the domains of such proteins (Fig. 16.1). And, for the reasons given above, large proteins must be composed of subglobules, which we know as domains, and this is indeed observed.

Now we have to return to the two questions left unanswered since the previous lecture, namely:

1. Why an “energetic defect” of a few kilocalories per mole, so very minor as compared with the total energy of protein, can virtually prohibit many protein architectures?
2. What do “entropic effects” have to do with the native protein structure where the chain is known to be fixed?

We start with the first question concerning the manifestation of the “defect” energy in protein architecture statistics. First, we will aggravate the matter: as you may remember, the stated (at the qualitative level) low occurrence of “structural defects” was supported by the observed “quasi-Boltzmann” statistics of “small elements” of protein structures, which we have to understand as well. And the statistics of “small elements” are exactly what we start with.

For example, let us consider the statistics of the distribution of amino acid residues between the interior and the surface of a protein globule and consider the interrelation between these statistics and the hydrophobicity of amino acid residues.

The hydrophobicity of amino acid residues is usually measured as the free energy of their transfer from octanol (simulating the hydrophobic core of a protein) to water. In Fig. 16.3 this free energy of transfer (divided by RT , at $T \approx 300$ K) is the vertical coordinate, while the horizontal coordinate is the logarithm of the ratio between the frequencies of the outer and inner residues in proteins. As seen, the points are arranged more or less linearly with a slope around 1–1.5.

Thus, the observed statistics of residue distribution between the interior and the surface are more or less adequately described by the expression:

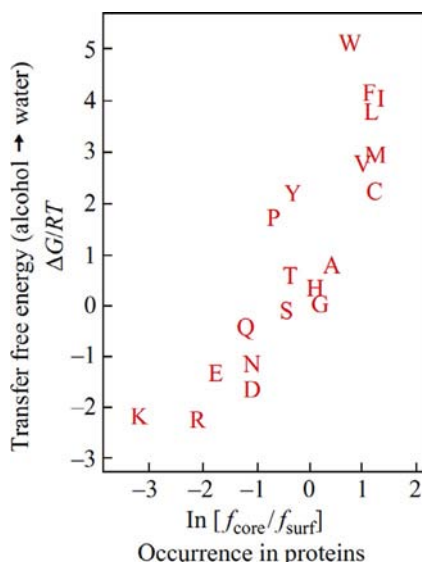


FIG. 16.3 Experimentally found free energy of transfer of residue side-groups from a nonpolar solvent to water (ΔG , expressed in RT units), and “apparent free energy of transfer of a residue from the protein core to its surface,” derived from observed frequencies of residue occurrence in the interior (f_{core}) and on the surface (f_{surf}) of the protein using the formula $\Delta G_{\text{app}}/RT = -\ln [f_{\text{surf}}/f_{\text{core}}]$. (Adapted from Miller, S., Janin, J., Lesk, A.M., Chothia, C., 1987. Interior and surface of monomeric proteins. *J. Mol. Biol.* 196, 641–656.)

$$\text{Occurrence} \sim \exp(-\text{free energy in given medium}/kT_C) \quad (16.3)$$

where the “conformational temperature” T_C is about 300–400 K.

Inner voice: I would be more cautious as concerns the data presented in Fig. 16.3 because in experiment, hydrophobicity was derived from residue transfer from water to high-molecular-weight alcohol. But why is the protein hydrophobic core believed to be like an alcohol? As well as the fact that alcohol is liquid while the core is solid, purely hydrophobic cyclohexane could be proposed as probably a better model of the hydrophobic core. And since the solubility of polar groups in cyclohexane is extremely low, the transfer free energy coordinate in Fig. 16.3 would inevitably be much more *extended*... True, the correlation between hydrophobicity and occurrence will also be preserved in this case, but the slope of the “cyclohexane line” drawn through the experimental points will appear to be much greater, around 3–4, or so. Incidentally, this is close to the slope, shown in the upper part of Fig. 16.3, that refers to hydrophobic amino acids which, by the way, would be least affected by replacing the core-simulating agent...

Lecturer: What is to be used to model the hydrophobic core really deserves consideration. I would say, an alcohol is still better than cyclohexane because of the presence of polar (NH and especially CO) groups in the protein core

(although these usually participate in H-bonds within the core-surrounding secondary structure, the CO group is still capable of forming a “fork-like” H-bond, one branch of which remains unsaturated in the secondary structure). So the hydrophobicity coordinate is hardly to be adjusted to purely nonpolar cyclohexane. On the other hand, speaking of quantitative estimates, we have to bear in mind that Fig. 16.3 reflects a rough division of all side-groups into two classes (those immersed in the protein and those located at its surface), and therefore their exposures differ by only about a half of the group surface. Accordingly, the experimentally derived hydrophobicities are to be *decreased* approximately twofold, which (in contrast to alcohol replacement by cyclohexane) would decrease the tilt of the interpolation line... In principle, I do agree that the presented *numerical* data are to be treated cautiously, but the qualitative relationship between the energies of various elements and their occurrence in proteins should receive full attention.

Thus, the statistics of the occurrence of amino acid residues in the interior of a protein and at its surface exhibit a surprising *outward* similarity to Boltzmann statistics. This was first noted by Pohl (1971) for rotamers. Later, the same was shown for the statistics of many other structural elements: for occurrence of ion pairs, for occurrence of residues in secondary structures, for occurrence of cavities in proteins, and so on, and so forth. To date, this analogy has become so common that protein structure statistics are often used to estimate the free energy of a variety of interactions between amino acid residues (Miyazawa and Jernigan, 1996).

However, it should be stressed that the protein statistics resemble Boltzmann statistics only in the *exponential form* but *not* in the physical sense. As you may remember, the basis of Boltzmann statistics is that particles move from one position to another and spend more time at the position where their energy is lower, whereas in native proteins, *no* residue wanders from place to place. For example, Leu72 of sperm whale myoglobin is *always* inside the native globule and *never* on its surface. And although, according to the statistics, 80–85% of the total amount of Leu residues belong to the protein interior and 15–20% to its surface, this does not mean that each Leu spends 80–85% of the time inside the native globule and 20–15% on its surface. Rather, it means that natural selection has fixed most Leu residues at positions that belong to the interior of the globule.

That is, the usual Boltzmann statistics, the statistics of fluctuations in the usual 3D space, have nothing to do with the distribution of residues between the core and the surface of a protein. A globule has no fluctuations that could take each Leu (in accordance with its hydrophobicity) to the surface for 15–20% of the time and then take it back to the interior of the globule and keep it there for 80–85% of the time. That is, for *each separate* Leu, there is *no* Boltzmann distribution determined by its particular hydrophobicity. Then how can we explain that the occurrence of the *total amount* of leucines inside and outside proteins

agrees with the Boltzmann distribution determined from leucine's particular hydrophobicity?

Let us change the viewpoint.

Why is the predominant internal location of leucines favorable? Because it contributes to globule stability (you remember the saying “*what's good for General Motors is good for America*”). Then why were not all leucines fixed inside the protein by natural selection? Presumably, because 80–85% of internal leucines are already *enough* to ensure protein stability, and dealing with the rest would be too expensive for selection.

Let us give up the psychology of natural selection as a pointless and non-scientific topic and pursue the matter on how the internal free energy of a protein structural element affects the *number of amino acid sequences* capable of stabilizing the protein that contains the structural element in question.

For example, let us see how the Leu → Ser mutation in the protein interior can change the number of fold-stabilizing sequences.

The native (observed) structure is stable if its free energy is lower than that of the unfolded chain and of all kinds of misfolded structures. Let us now assume, for simplicity that (1) the observed fold competes only with the unfolded state rather than with other compact folds; (2) the residue's contribution to the native state stability is determined only by the residue's hydrophobicity; (3) the internal residues are completely screened from water, and the external residues are completely exposed; and (4) the residues in the unfolded protein are completely exposed to water. These statements are only approximately correct. Therefore, the following theory is rather rough—but it has the important advantage of simplicity.

The transfer free energy of a Ser side-group from the hydrophobic surroundings into water is about 0, while that of leucine is about +2 kcal mol⁻¹. Let us put aside the difference in the Leu and Ser volumes and shapes and consider only their hydrophobicity. Leu is more hydrophobic than Ser. When Leu is inside, the protein fold is more stable against unfolding than the same fold with Ser inside. This means that the sequences which can stabilize a fold with Ser inside can *also* stabilize the fold with Leu inside—but the fold with Leu inside will, *in addition*, be stabilized by some sequences which cannot stabilize the fold with Ser inside.

How does the number of fold-stabilizing sequences change when a more stable structural element (Leu inside) is replaced by a less stable one (Ser inside)? Consideration of this problem will help us to understand why occurrence of various elements depends exponentially on their free energy and what the sense of the temperature T_C in Eq. (16.3) is.

I apologize in advance for giving here calculations in a most simplified form (see Finkelstein et al. (1993, 1995a,b) and Appendix D for rigorous calculations), because a simplified form of calculations implies their incomplete accuracy. I am aiming to describe the essence of the matter without losing you in the

maths labyrinth through which one of us (A.V.F.), advised by E.I. Shakhnovich, used to ramble a lot together with A.M. Gutin and A.Ya. Badretdinov.

Let $\Delta\epsilon + \Delta F$ be the free energy difference between the given chain fold and the unfolded state of the chain. Here $\Delta\epsilon$ is the free energy difference for the concerned element in the fold (including all the element's interactions with the surroundings, eg, the Leu's hydrophobic free energy in the core), and ΔF is the free energy difference for the remaining chain. The fold is stable against unfolding when $\Delta F + \Delta\epsilon < 0$, that is, when

$$\Delta F < -\epsilon \quad (16.4)$$

The values ΔF and $\Delta\epsilon$ depend on the amino acid sequence. Let us consider all those sequences which preserve the $\Delta\epsilon$ value (eg, all sequences with Leu (or Ser) at the given point of the chain; for the core positions, $\Delta\epsilon \approx 2$ kcal mol⁻¹ for Leu (and ≈ 0 for Ser), while for the surface positions, $\Delta\epsilon \approx 0$ for all residues). The value ΔF will change with the sequence. The probability P^* that $\Delta F < -\Delta\epsilon$ is

$$P^*(\Delta F < -\epsilon) = \int_{-\infty}^{-\epsilon} P(\Delta F) d(\Delta F) \quad (16.5)$$

where $P(\Delta F)$ is the probability of the given ΔF value for a randomly taken sequence.

The ΔF value is composed of energies and entropies of many residues that independently mutate in random sequences. Therefore (according to the Central Limit Theorem of mathematical statistics), $P(\Delta F)$ has a simple, so-called Gaussian (see Fig. 16.4) form:

$$P(\Delta F) = (2\pi\sigma^2)^{-1/2} \exp \left[-(\Delta F - \langle \Delta F \rangle)^2 / 2\sigma^2 \right] \quad (16.6)$$

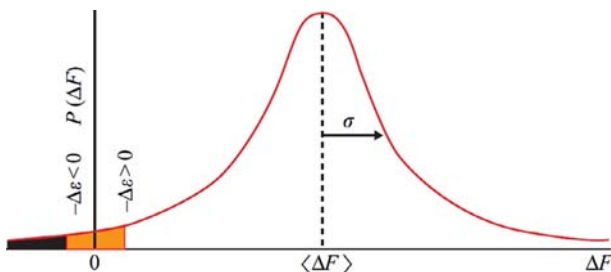


FIG. 16.4 The typical Gaussian curve for ΔF distribution among random sequences. ΔF contains the entire free energy difference between the given fold and the unfolded state of the chain, except for the fixed $\Delta\epsilon$ value of the structural element in question. The values of $\Delta F < -\Delta\epsilon$ (ie, those satisfying the condition that $\Delta F + \Delta\epsilon < 0$) meet the requirements of a stable fold. The area shown in black corresponds to $\Delta F < -\Delta\epsilon$ values at $\Delta\epsilon > 0$, while the “red+black” area is for $\Delta\epsilon < 0$. The latter is larger, which means that a greater number of random sequences stabilize the fold when the free energy of the element in question is below zero ($\Delta\epsilon < 0$) as compared with its being above zero ($\Delta\epsilon > 0$).

Here $\langle \Delta F \rangle$ is the mean (averaged over all the sequences) value of ΔF , and σ is the root-mean-square deviation of ΔF from the mean $\langle \Delta F \rangle$.

I would like to remind you that the Central Limit Theorem describes the expected distribution of the sum of *many* random terms and answers the question as to the probability of this or that value of the sum. Here, “the sum of many random terms” is ΔF (composed of many interactions in a randomly taken, ie, “random,” sequence). As mathematics state, for the majority ($\approx 70\%$) of sequences, the ΔF value must lie between $\langle \Delta F \rangle - \sigma$ and $\langle \Delta F \rangle + \sigma$, and the probability $P(\Delta F)$ decreases dramatically (exponentially) with increasing difference between ΔF and $\langle \Delta F \rangle$ (see Fig. 16.4).

Since the great majority of random sequences are obviously incapable of stabilizing the fold, the values of P and P^* must be far less than 1 near the “stability margin” ($\Delta F \approx 0$). Thus, the $\langle \Delta F \rangle$ value is not only positive but also *large*, much larger than σ .

The value of $(\Delta F - \langle \Delta F \rangle)^2$ is equal to $\langle \Delta F \rangle^2 - 2\langle \Delta F \rangle \Delta F + \Delta F^2$, that is, at small (as compared with large $\langle \Delta F \rangle$) values of ΔF , the value $(\Delta F - \langle \Delta F \rangle)^2 \approx \langle \Delta F \rangle^2 - 2\langle \Delta F \rangle \Delta F$, and consequently,

$$P(\Delta F) \approx \left\{ (2\pi\sigma^2)^{-1/2} \exp\left[-\langle \Delta F \rangle^2/2\sigma^2\right] \right\} \times \exp\left[-\Delta F \times (\langle \Delta F \rangle/\sigma^2)\right] \quad (16.7)$$

I would like you to believe (or better—to take the integral and check) that in this case the probability of $\Delta F < -\varepsilon$ is

$$P^*(\Delta F < -\varepsilon) = \int_{-\infty}^{-\varepsilon} P(\Delta F) d(\Delta F) \approx \text{const} \times \exp\left[-\frac{\Delta \varepsilon}{\sigma^2/\langle \Delta F \rangle}\right] \quad (16.8)$$

where the constant, equal to $[(2\pi\sigma^2)^{-1/2} \times \exp(-\langle \Delta F \rangle^2/2\sigma^2)] \times (\sigma^2/\langle \Delta F \rangle)$, is of no interest to us, while the really important term $\exp[-(\Delta \varepsilon/(\sigma^2/\langle \Delta F \rangle))]$ demonstrates that an element’s free energy ($\Delta \varepsilon$) has an *exponential* impact upon the probability that a random sequence is capable of stabilizing the fold with the given element. Thus, increasing $\Delta \varepsilon$ decreases the number of fold-stabilizing sequences *exponentially*.

Note: Our previous belief was that “eligible” sequences are all those providing $\Delta F + \Delta \varepsilon < 0$, that is, at least a minimal stability of the protein structure. After a few more lectures, you will know that the “solid” protein structure should possess a certain “stability reserve.” Otherwise, it would melt in our hands and be incapable of rapid and unique folding. Therefore, to be more accurate, we have to consider as “eligible” the sequences that provide $\Delta F + \Delta \varepsilon < -F_{\min}$ (where $-F_{\min} < 0$), that is, $-\Delta F < -\Delta \varepsilon - F_{\min}$. To ensure stability of the native globule, it is enough to have F_{\min} of only a few kilocalories per mole, that is, it can be believed that $F_{\min} \ll \langle \Delta F \rangle$. Then Eq. (16.8) has the form:

$$P^*(\Delta F < -\varepsilon) \approx \text{const} \times \exp\left[-\frac{\Delta \varepsilon + F_{\min}}{\sigma^2/\langle \Delta F \rangle}\right] = \text{const}^* \times \exp\left[-\frac{\Delta \varepsilon}{\sigma^2/\langle \Delta F \rangle}\right] \quad (16.9)$$

In other words (since a change of the preexponential constant is of no interest to us), we come again to the same idea that an element's energy has an exponential impact on the probability that the element will be fixed in the protein structure as a result of the “selection for stability.”

Note that a requirement of enhanced stability of the native fold (ie, an increase in the F_{\min} value) decreases the number of appropriate sequences also exponentially, in proportion to $\exp[-(\Delta F_{\min}/(\sigma^2/\langle \Delta F \rangle))]$.

The dependence (16.8) is as exponential as the Boltzmann formula but it has the term Δe divided not by the temperature of the environment (kT) but by the as yet unknown value of $\sigma^2/\langle \Delta F \rangle$.

What is this value? First of all, note that $\sigma^2/\langle \Delta F \rangle$ is independent of the protein size. Indeed, according to the mathematical statistics laws, the mean value (here, $\langle \Delta F \rangle$) is proportional to the number of terms summarized in ΔF (which is, in our case, approximately proportional to the protein size), while the mean square deviation from σ is proportional to the square root of the number of these terms, ie, σ^2 is also approximately proportional to the protein size.

The fact that $\sigma^2/\langle \Delta F \rangle$ does not increase with increasing protein size is most important: this means that the “defect’s” free energy Δe must be compared (using Eq. 16.8) not with the total protein energy but rather with some characteristic energy unit $\sigma^2/\langle \Delta F \rangle$, which is something like the average energy of non-covalent interactions per residue in the chain (which is also independent of the protein size, provided the small impact of the surface is neglected).

Taken together with the exponential form of Eq. (16.8), this provides an immediate answer to the question as to why Δe of only a few kilocalories per mole can produce a considerable effect upon the occurrence of protein structure elements (eg, why inside a protein globule Leu residues are an order of magnitude more numerous than Ser ones). This happens because the number of fold-stabilizing sequences decreases e-fold (approximately threefold) when Δe increases by a value of $\sigma^2/\langle \Delta F \rangle$.

Thus, $\sigma^2/\langle \Delta F \rangle$ is something like chain energy per residue. One can present $\sigma^2/\langle \Delta F \rangle$ as kT_C , where T_C is a certain temperature (as you may remember, the “heat quantum” kT also has the sense of characteristic heat energy per particle). Exactly what temperature is T_C ? For a “random” globule, there is only one characteristic temperature—that of “freezing out” its most stable fold. A protein chain has one characteristic temperature as well, that is, its denaturation temperature ≈ 350 K (which is close to that of protein’s life, ≈ 300 K). Eventually, it can be shown that as long as only the minimum protein structure stability is required (ie, if selection of primary structure is determined only by this minimal restriction), the protein melting temperature is close to the freezing temperature of a random chain. Therefore, it can be suggested that the value of “conformational temperature” T_C is determined by the temperature T_M of protein melting. In other words, $\sigma^2/\langle \Delta F \rangle$ can be considered as amounting to about $0.5\text{--}1$ kcal mol⁻¹.

This can be not only believed but can be shown as well. The words “can be shown” imply a quite complex theoretical physical proof, the Shakhnovich-Gutin theorem (Shakhnovich and Gutin, 1989, 1990), which I shall spare you. (Nevertheless, I would like to outline the main ideas involved. (1) Random replacement of one sequence by another changes its free energy essentially in the same way as a random replacement of one fold by another. (2) $kT_C = \sigma^2 / \langle \Delta F \rangle$ is determined by the growth in the number of random sequences close to the edge separating the fold-stabilizing sequences from the others. (3) T_M is essentially determined by the growth in the number of folds close to the low-energy edge of energy spectrum of a random sequence. These two edge temperatures are close since (4) the native and denatured states of a chain are close in stability, and (5) the energy gap between the most stable (native) chain fold and its close nonnative competitors is not wide (this will be discussed in Lectures 17, 18, and in Appendix D); therefore, T_C and T_M are also close.)

Thus, we have cleared up why a defect of only a few kilocalories per mole (against the background of the much higher total energy of the protein) can virtually prohibit many motifs of protein architecture. This happens because the defect’s free energy is to be compared with $kT_C \approx 0.5\text{--}1 \text{ kcal mol}^{-1}$ rather than with the total energy of the protein; and then we see that any defect of $\approx 1 \text{ kcal mol}^{-1}$ decreases roughly fivefold the number of sequences “eligible” for this protein, a defect of $\approx 2 \text{ kcal mol}^{-1}$ decreases them roughly 20-fold, and so on.

Specifically, that is why the crossing of irregular connections (this defect, caused by screening from water and loss of 1–2 H-bonds, usually costs 2–3 but never more than 5 kcal mol^{-1}) is rarely observed (Fig. 16.5) (Finkelstein and Ptitsyn, 1987).

Inner voice: I accept the argument about the loss of bonds when loops overlap, but I do not understand why the “upper” loop cannot make an additional bend and avoid overlapping the “lower” loop! Or perhaps the loops are always so short that just cannot do this?

Lecturer: No, loops are not always that short. The thing is that an additional bend of the polymer chain causes an entropy loss just like an additional bend in left-handed connection between parallel β -strands (Fig. 16.6), which was briefly discussed in the previous lecture and will be discussed in more detail right now.

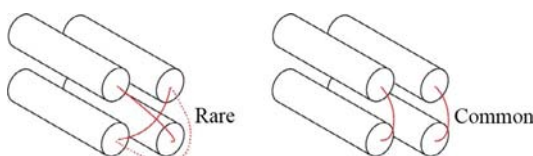


FIG. 16.5 Loop crossing (even with overlap replaced by bypassing) is rarely observed in proteins.

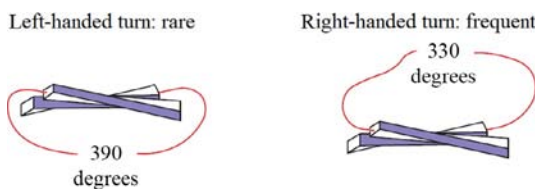


FIG. 16.6 In proteins with the right-handed (as in the figure) twist of β -sheets, the left-handed (*more bent*) connections between parallel β -strands are very rare, while right-handed ones are common.

Inner voice: OK, I will wait, but at the moment I cannot but cut in with a more general question. The entire logic of your narration is based on the assumption that sequences unable to fold into a stable structure are rejected. This is quite probable. But then, are those yielding *too stable* structures rejected too?

Actually, the observed stability of native structures is *never* very high. Moreover, a correlation between the denaturation temperature of a protein and the life temperature of the host organism has been mentioned by [Alexandrov \(1965\)](#). Then we have to conclude that *too stable* protein structures (and, according to your logic, *too stable* structural elements as well) are to be rejected. Seemingly, you do not take this into account at all.

Lecturer: It is difficult to make a stable protein. This has been demonstrated by the entire experience of designing *de novo* proteins. That is, sequences capable of folding into something stable are rare. It is still more difficult to create a “superstable” protein because its eligible sequences occur still more rarely. [Fig. 16.4](#) also serves as an illustration of how small the fraction of sequences eligible for creating “superstable” protein structures (ie, those with the extremely low free energy ΔF) is; see also the exponential effect of F_{\min} on P^* in Eq. (16.9). The sequences good for “superstable” proteins constitute only a minor fraction of the sequences that are good for stable proteins... If the selection does not insist on “superstability” and has nothing against it, the fraction of such proteins *automatically* appears to be negligible. This explains quite satisfactorily all the experimental facts and correlations you have pointed out.

Now we, at last, pass to the question as to the role played by entropy effects in the stability of the native protein structure, although the chain there is fixed.

Let us again compare right-handed and left-handed connections between parallel β -strands (see [Fig. 16.6](#)). As we know, due to the intrinsic *right*-handed twist of a β -sheet formed by L amino acid residues, a *right-handed* connection has to turn by about 360 degrees $- 30$ degrees $= 330$ degrees, while a *left-handed* connection would have to turn by about 360 degrees $+ 30$ degrees $= 390$ degrees. As stated by polymer physics, the more bent the chain, the less numerous its possible conformations. This means that the right-handed (less bent)

connection is compatible with a greater number of chain conformations than the left-handed one. This is clear. But what is the impact of the number of possible conformations on the number of sequences stabilizing this or that connection pathway?

A randomly taken sequence can provide the highest stability (among all other chain structures) of either one of the numerous conformations corresponding to the less-bent connection or one of a few conformations corresponding to the more bent connection; alternatively, it may be unable to ensure stability of any of them. The latter is certainly the most probable, since randomly composed amino acid sequences possess no stable 3D structure. However, if we have to choose only between the left- and right-handed connections, which of them has a better chance to become the more stable?

Each separate conformation containing a less bent connection is neither better nor worse than each separate conformation with a more bent connection, provided that these conformations are equal in compactness, in secondary structure content, etc. Still, the less bent conformations are much more numerous...

Actually, here, we have a kind of lottery with a small chance of winning the main prize (that is creating a stable 3D structure); in this lottery, the right-handed (less bent) connection has many tickets (possible conformations), while the left-handed connection has only a few. Which of them, if either, will win the prize? Almost certainly the right-handed connection that has many more tickets and hence a better chance of success, since the probability of winning is directly proportional to the available tickets (conformations).

In other words, the broader the set of *possible* conformations, the more frequently (in direct proportion to the set range) this set contains the most stable structure of a random sequence. This is exactly what we observe in globular proteins: here the right-handed (less restricted) pathway of a connection is the rule, while the more restricted left-handed pathway (or bypassing loop with an additional bend) is the exception.

Allow me to remind you of one of these very rare exceptions. I mean the left-handed β -prism discussed a couple of lectures back. Its spatial structure is indeed unique as it consists almost entirely of left-handed connections between β -segments. And what about the twist of its β -sheet? The twist is absent... And what about its primary structure? It appears to be unique as well: first, it does not look like “random” (that would be typical of globular proteins) but contains 10 repeats of an 18-residue peptide forming each turn of the left-handed superhelix (with three β -strands per turn); second, its β -strands contain abnormally numerous glycines (which are neither L nor D amino acids and therefore do not twist β -sheet, as you know). So, a unique spatial structure is combined with a unique primary structure...

Let us consider one more problem connected with entropic defects. It concerns not folding patterns but the layered structure of the globule. Which should occur more often, proteins with α - or β -structure in the center?

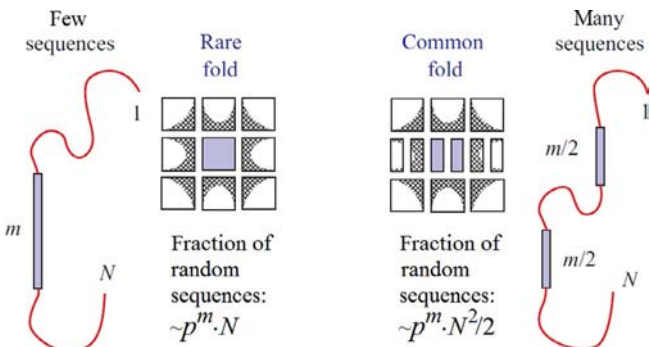


FIG. 16.7 In a large globule, a multiple-layer packing with an α -helix in its center should be less probable (and, indeed, is observed more rarely) than a multiple-layer packing with two β -segments in its center. The reason is that the segment occupying the globule's center should contain exclusively hydrophobic residues, and its large length is dictated by the large globule diameter (which is proportional to $N^{1/3}$). Since an α -helix contains twice as many residues as an extended β -strand of equal length, a central α -helix (with a large block of hydrophobic groups) will require a much less common sequence than is required for the creation of two central β -segments (with two hydrophobic blocks of half the length positioned somewhere in the chain). The probability of occurrence of one entirely hydrophobic block of m residues in a given position of the random chain is about p^m (where p is the fraction of hydrophobic residues in the chain); there is an equal probability of two hydrophobic blocks of half the length occurring in two given positions of a random chain: $(p^{m/2}) \times (p^{m/2}) = p^m$. However, one block can be placed in the N -residue chain in only $\approx N$ different ways, while there are many more ways ($\approx N \times N/2$) to position two blocks, that is, there are many more sequences with two short hydrophobic blocks than with one long block.

Fig. 16.7 explains why globules with β -strands in the center can be stabilized by many more primary structures than those with α -helices in the center.

And indeed, the internal α -helix occurs in proteins most rarely (the green fluorescent protein shown in Fig. 16.8 is a striking example of such the most unusual fold), while the internal β -strands are typical (eg, for “Rossmann folds,” see Fig. 16.1).

The same standpoint (How often is this structural element stabilized by random sequences?) may be used to explain many other structural features observed in globular proteins. Among them, the average domain size for a chain with a given ratio between hydrophobic and hydrophilic groups (this problem was studied by Bresler and Talmud in Leningrad as far back as in 1944, and then by Fisher (1964) in the USA), and also the previously discussed average lengths of α -helices, β -segments, and irregular loops.

Thus, our analysis shows that the probability of observing the given structural element in stable folds formed by those random sequences that are able to stabilize at least some 3D structure should be greater, the lower the element’s energy and the greater the number of conformations appropriate for this element.

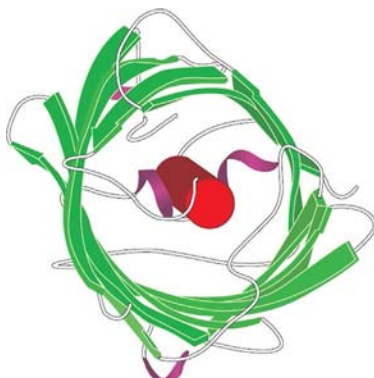


FIG. 16.8 Green fluorescent protein has an unusual fold in which the α -helix is surrounded by the β -sheet. The central α -helix is not continuous: actually, it is broken by the chromophore into two approximately equal halves (not shown).

And since the energy and the number of conformations unite in the free energy, the statistics of occurrence of various structural elements in *randomly created stable globules* should have the form:

$$\text{Occurrence} \sim \exp(-\text{free energy}/kT_C), \quad (16.10)$$

where T_C is close to (but not equal to, as a thorough analysis shows) the freezing temperature of the globule formed by a random amino acid sequence; in turn, this temperature is close to the protein melting temperature T_M .

And, in fact, general protein statistics have the form outlined above, which is typical for statistics of structures built up by random sequences that have been selected only for creation of stable globular structures.

Let me remind you once again of the physical basis of the above relationship. The free energy of a given structural element *exponentially* changes the number of sequences capable of stabilizing the protein whose native structure contains this element. If the element itself is stable, its host protein can stand many even unfavorable mutations, that is, the protein containing this element can be stabilized by a quite large number of sequences. If the element is unstable, its host protein demands a most thorough selection of its primary structure (stability of its 3D structure can be easily ruined by even a few mutations), and these “thoroughly selected” sequences are rare.

Here, it should be stressed that the so-called prohibited (not observed or rarely observed) protein structures are *not* impossible in principle but simply improbable because they can only be created by a small number of sequences.

Thus, structures of globular proteins resemble those which can be expected for folds of random copolymers (Ptitsyn, 1984)—or maybe for little “edited” ones (Finkelstein and Ptitsyn, 1987; Shakhnovich and Gutin, 1990; Finkelstein et al., 1993).

It appears that globular proteins could quite easily originate from random amino acid sequences (to be more accurate, from pieces of DNA coding random amino acid sequences). It would only require slight stabilizing (through a few mutations) of the most stable 3D structure of the initial random polypeptide and “grafting” an active site on its surface (to provide “biologically useful” interactions with surrounding molecules). Also, it would be necessary to clean the protein’s surface of the residues that could involve it in “biologically harmful” associations (like those provoking sickle cell anemia by sticking hemoglobins together).

Inner voice: Are we to understand that you are suggesting that proteins with “new architectures” originated from random sequences rather than through strong mutations of proteins with some “old” architectures? And that the folding patterns whose stability is compatible with many random sequences originated from them many times (as many as there are homologous families in them), while other patterns covering only one homologous family each arose only once?

Lecturer: All we can say with confidence is that more than a negligibly small fraction of random sequences can give rise to proteins, and that the stability of some folds (specifically, of those often observed in proteins) is compatible with a larger number of random sequences than the stability of other, “rare” folds. As to your questions about the historical happenings, I think they cannot be answered at present. In particular, it is impossible to say whether representatives of “popular” folding patterns arose many times or not. Perhaps they originated many times from different random sequences. Perhaps only once (and not from a random sequence but from pieces of some other proteins). It is also possible that later, in the course of evolution, sequences of the same root fell so wide apart within the frames of the preserved folding pattern (since “popular” patterns are compatible with so very different sequences), that all signs of homology and genetic relationships have been wiped out, and we cannot trace them. I only want to stress that the “popular” folding patterns compatible with so many sequences give much more space for any kind of origin and subsequent evolution than the “rare” patterns.

In this connection, I cannot but note that contemporary attempts at *de novo* protein design widely use both multiple random mutations of sequences, necessarily accompanied by selection of “appropriate” (say, capable of binding to something) variants, and random shuffling of oligopeptides (accompanied by similar selection). The modern methods of selecting “appropriate” random sequences (I would like to mention perhaps the most powerful of them: it is called phage display; do read about it in molecular biology textbooks) allow

examining about 10^{12} of random sequences. The fact that “protein-like” products were now and then found among these samples shows that the fraction of such “protein-like” chains amounts to $\sim 10^{-11}$ of all random polypeptides composed of a few dozens of amino acid residues (Keefe and Szostak, 2001).

I stress that origination from random sequences is especially appropriate for globular proteins because it is their sequences that outwardly resemble “random” (ie, most abundant) copolymers (Fig. 16.2). At the same time, *nonrandomness* is obvious for primary (and also spatial) structures of fibrous and membrane proteins (but incidentally, the principles of their construction are simple too: repeats of short blocks for fibrous proteins and alternation of hydrophobic and hydrophilic blocks for membrane proteins).

The above analysis emphasizes the fact that evolution-yielded protein structures look very “reasonable” from the physical point of view, just like the DNA double helix and the membrane bilayer. Presumably, at the level of protein domain architectures as well, evolution does not “invent” physically unlikely structures but “selects” them from physically sound ones (ie, those that are stable and therefore capable of rapid self-organizing, as we will see soon). This is what the sense of “physical selection” consists in.

REFERENCES

- Alexandrov, V.Ya., 1965. On the biological significance of the correlation between the level of thermoresistance of proteins and the environmental temperature of the species. Usp. Sovr. Biol. (in Russian) 60, 28–44.
- Bresler, S.E., Talmud, D.L., 1944a. On the nature of globular proteins. Dokl. Akad. Nauk SSSR (in Russian) 43, 326–330.
- Bresler, S.E., Talmud, D.L., 1944b. On the nature of globular proteins. II. Some consequences of a new hypothesis. Dokl. Akad. Nauk SSSR (in Russian) 43, 367–369.
- Finkelstein, A.V., Ptitsyn, O.B., 1987. Why do globular proteins fit the limited set of folding patterns? Progr. Biophys. Mol. Biol. 50, 171–190.
- Finkelstein, A.V., Gutin, A.M., Badretdinov, A.Ya., 1993. Why are the same protein folds used to perform different functions? FEBS Lett. 325, 23–28.
- Finkelstein, A.V., Gutin, A.M., Badretdinov, A.Ya., 1995a. Boltzmann-like statistics of protein architectures. Origins and consequences. In: Biswas, B.B., Roy, S. (Eds.), Subcellular Biochemistry. Proteins: Structure, Function and Protein Engineering, vol. 24. Plenum Press, New York, pp. 1–26.
- Finkelstein, A.V., Badretdinov, A.Ya., Gutin, A.M., 1995b. Why do protein architectures have Boltzmann-like statistics? Proteins 23, 142–150.
- Fisher, H.F., 1964. A limiting law relating the size and shape of protein molecules to their composition. Proc. Natl. Acad. Sci. U. S. A. 51, 1285–1291.
- Keefe, A.D., Szostak, J.W., 2001. Functional proteins from a random-sequence library. Nature 410, 715–718.
- Miyazawa, S., Jernigan, R.L., 1996. Residue-residue potentials with a favorable contact pair term and an unfavorable high packing density term, for simulation and threading. J. Mol. Biol. 256, 623–644.
- Pohl, F.M., 1971. Empirical protein energy maps. Nat. New Biol. 234, 277–279.

- Ptitsyn, O.B., 1984. Protein as an edited statistical copolymer. *Mol. Biol.* (in Russian) 18, 574–590.
- Ptitsyn, O.B., Volkenstein, M.V., 1986. Protein structures and neutral theory of evolution. *J. Biomol. Struct. Dyn.* 4, 137–156.
- Shakhnovich, E.I., Gutin, A.M., 1989. Formation of unique structure in polypeptide chains. Theoretical investigation with the aid of a replica approach. *Biophys. Chem.* 34, 187–199.
- Shakhnovich, E.I., Gutin, A.M., 1990. Implications of thermodynamics of protein folding for evolution of primary sequences. *Nature* 346, 773–775.

Lecture 17

In a previous lecture, we considered the stability of fixed, “well-folded,” “solid” protein structures. However, depending on ambient conditions, the most stable state of a protein molecule may be not solid but molten or even unfolded. Then the protein denatures and loses its native, “working” 3D structure.

Usually, protein denaturation is observed *in vitro* as a result of an abnormal temperature or denaturant (ie, urea, H⁺ or OH⁻ ions (ie, abnormal pH), etc.). However, decay of the “solid” protein structure and its subsequent refolding can also occur in a living cell; specifically, this is important for transmembrane transport of proteins, for protein degradation, etc.

Moreover, even under physiological conditions, not all proteins “by themselves” have a fixed 3D structure.

Those having no fixed structure under normal cellular conditions were called “intrinsically disordered” or “natively unfolded” proteins; currently, they attract a great interest (Wright and Dyson, 1999; Uversky et al., 2000; Uversky, 2013; Dunker et al., 2001, 2008; Tompa, 2010). In some cases, the entire protein is “natively disordered,” while in others, only some portions of the chain (having no X-ray-revealed structure) may be called so. Some “natively disordered” proteins are in the coil state, others are in the “molten globule” (MG) state (which will be described soon). It is now becoming clear that many protein functions require the disordered state. Native disorder is often an integral feature of proteins involved in recognition, signaling, and regulation (especially in eukaryotes), but never of enzymes (Uversky, 2013) whose work requires rigidity (we will see it in one of the next lectures).

Some of natively unfolded proteins (or natively unfolded chain segments) have a strange, simple amino acid composition, and may never have a definite spatial structure, even when contacting their targets, although many “natively unfolded” proteins acquire their unique spatial structure when binding to a ligand (Bychkova et al., 1988), or another protein, or DNA, or RNA.

It is assumed that binding of protein with natively disordered structure has that advantage that it is not too strong, and therefore, reversible even when the binding area is large (and hence, providing a significant selectivity of binding; see Schulz, 1977; Schultz and Schirmer, 1979). It is also assumed that disorder speeds up scanning of possible targets (Drobnak et al., 2013).

From my point of view, two features of intrinsically disordered proteins are of a great interest: (1) their functions (we will consider them in one of the next lectures) and (2) their ability to survive in aggressive biological environment for a rather long time. As to physics of disordered protein chains, it is not as exciting as physics of “well-folded” proteins where each atom knows its place.

Physics of disordered chains is the same as that of artificially denatured (disordered) protein chains in vitro. Not more—but not less. Therefore, in vitro studies of denatured proteins are not only interesting by themselves and in their relationship to protein folding, but also directly concern the states of some proteins in the cell.

Denaturation of globular proteins in vitro is the subject of intensive studies.

This continues to be of interest because of its relationship to the problem of protein folding, that is, to the question as to how a protein chain finds its unique 3D structure among zillions of alternatives. Today, in fact, I will not touch upon the kinetic aspects of protein denaturation and folding; rather, I will concentrate on the thermodynamic and structural aspects of these events.

Water-soluble globular proteins are the best studied in this respect, and I will speak about them.

What does experiment show?

It is well established that denaturation of small proteins is a cooperative transition with a simultaneous abrupt (“S-shaped”) change of many (though sometimes not all) characteristics of the molecule (Fig. 17.1). The S-shaped form of experimental curves shows that the plotted characteristics of the molecule change from the values corresponding to the native molecule to those corresponding to its denatured state, and the narrow transition region suggests that the transition embraces many amino acid residues.

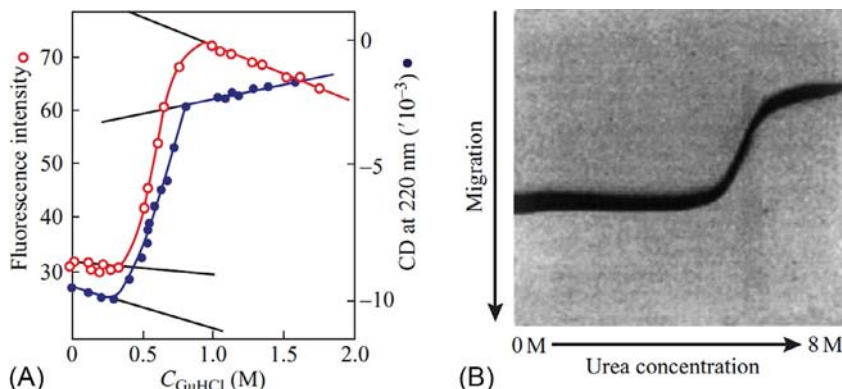


FIG. 17.1 Protein denaturation is accompanied by an abrupt “S-shaped” change of many characteristics of the molecule. In the given case, protein unfolding is induced by increasing denaturant concentration; the latter is measured in mol L⁻¹ (often denoted as M). (A) Simultaneous change of circular dichroism (CD) (at 220 nm) and fluorescence in the process of denaturation of phosphoglycerate kinase in solution with increasing concentration of guanidine dihydrochloride. (B) Electrophoresis of cytochrome c at various urea concentrations. ((A) Adapted from Nojima, H., Ikai, A., Oshima, T., Noda, H., 1977. Reversible thermal unfolding of thermostable phosphoglycerate kinase. Thermostability associated with mean zero enthalpy change. *J. Mol. Biol.* 116, 429–442. (B) Reproduced with permission from Creighton, T.E., 1979. Electrophoretic analysis of the unfolding of proteins by urea. *J. Mol. Biol.* 129, 235–264.)

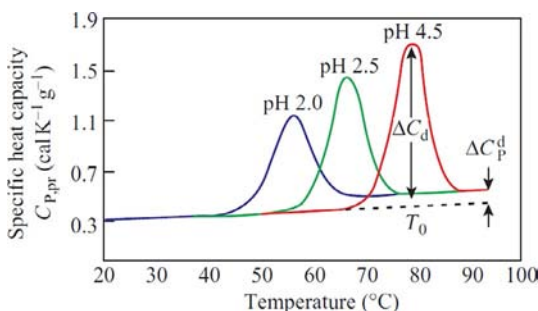


FIG. 17.2 Calorimetric study of lysozyme heat denaturation at various pH values. The position of the heat capacity ($C_{P,\text{pr}}$) peak determines the transition temperature T_0 ; the peak width gives the transition width ΔT ; and the area under the peak determines ΔH , the heat absorbed by 1 g of the protein. The values ΔT , $\Delta H \times (\text{protein's M.W.})$ and T_0 satisfy Eqs. (17.5), (17.6), indicating that the denaturation occurs as an “all-or-none” transition. The increased heat capacity of the denatured protein (ΔC_d^P) originates from the enlarged interface between its hydrophobic groups and water after denaturation. (Adapted from Privalov, P.L., Khechinashvili, N.N., 1974. A thermodynamic approach to the problem of stabilization of globular protein structure: a calorimetric study. *J. Mol. Biol.* 86, 665–684.)

Moreover, protein denaturation occurs as an “all-or-none” transition (Fig. 17.2).

You may remember that the latter means that only the initial (native) and the final (denatured) states amount to visible quantities (Fig. 17.3), while “semidenatured” states are virtually absent. (Though, of course, they do exist to a very small extent, since a native molecule cannot come to its denatured state without passing the intermediate forms, and their presence has a crucial effect on kinetics of the transition, which we will discuss later.)

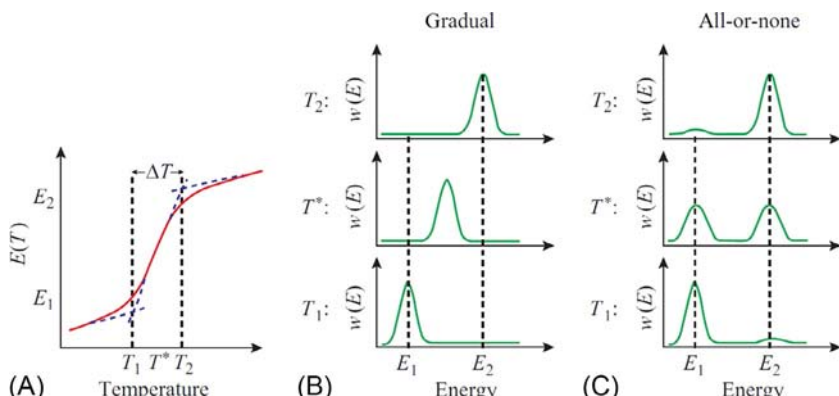


FIG. 17.3 With the same temperature dependence (A) of energy E (or any other observable parameter), the cooperative (S-shaped) transition can be either (B) gradual (eg, helix-coil transition in polypeptides), or (C) of the “all-or-none” type (eg, protein denaturation). The difference is displayed in the shape of the function $w(E)$ showing (B, C) the distribution of molecules over energy (or over any other observable parameter) rather than in the shape of the curve $E(T)$. Dashed lines in (A) show a graphical determination of ΔT , the width of the temperature transition.

In other words, the “all-or-none” transition is a microscopic analog of the first-order phase transitions in macroscopic systems (eg, crystal melting). However, unlike true phase transitions, the “all-or-none” transitions in proteins have a nonzero width, since this transition embraces a microscopic system. A little later, I will show you how protein denaturation was proved to be of the “all-or-none” type (Privalov and Khechinashvili, 1974; Privalov, 1979).

Inner voice: As I understand, you say that a protein molecule can be either solid or denatured... Are there proteins which contain both solid and denatured (or somehow unfolded) parts?

Lecturer: First, I have to specify that “all-or-none” denaturation actually refers to small proteins and to separate domains of large proteins, while denaturation of a large protein as a whole is the sum of the denaturation of its domains (Privalov, 1982). In the latter case, the protein, in the course of denaturation, simultaneously contains a yet part and an already denatured part.

But I think, you are asking, actually, if there are proteins containing both well-folded and poorly folded or unfolded parts in their native state, having in mind the intrinsically disordered proteins. The answer is yes, and clear examples of proteins with well-folded and poorly folded parts are known for a long time. I mean, first of all, histones with their solid cores and long charged and disordered tails (Klug, 1984). But what at that time was considered a kind of exotic, now is considered as a large kingdom of protein structures (Fig. 17.4) (Tompa, 2010).

As for me, a physicist, this coexistence of two native phases, well-folded and poorly folded, is the most interesting physical phenomenon concerning intrinsically disordered proteins. In all other respects, physics of disordered proteins is neither less nor more interesting than that of artificially denatured protein chains.

Another interesting question connected with natively disordered proteins is why their disordered parts are not cleaved by cellular proteases: it used to be commonly believed that the folding only protects polypeptide chains against them. I do not know a good answer to this question.

One can denature a protein, not only by heating (see Fig. 17.2), but sometimes also by cooling (this will be considered later). Besides, proteins denature under the action of too low or too high pH (which annihilates the charges of one sign and thus causes repulsion between remaining charges of the opposite sign). Also, protein denaturation results from addition of denaturants like urea ($\text{NH}_2-\text{CO}-\text{NH}_2$) or guanidine dihydrochloride ($(\text{NH}_2)_3\text{C}^+\text{Cl}^-$): these molecules, with excess hydrogen-bond donors, seem to withdraw the hydrogen bonds of O-atoms of water molecules, disturb the balance of H-bonds in water, and thus force water molecules to break H-bonds in the protein more actively (Finkelstein and Ptitsyn, 2012).

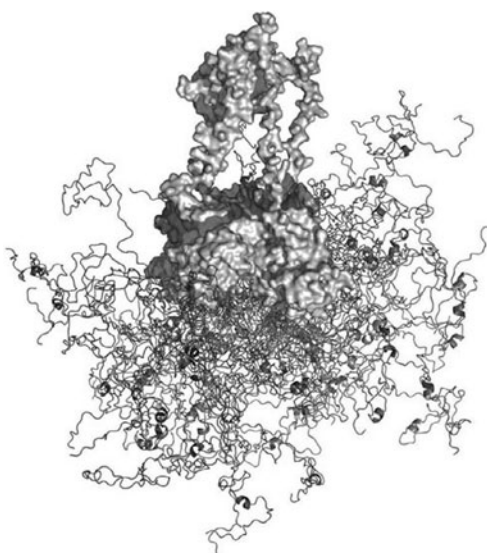


FIG. 17.4 Partly ordered and partly disordered protein p53. The structure of the ordered part was created from the X-ray structure and shown in space filling model; the image of the disordered part (shown as thin traces of the polypeptide chain) represents 20 copies of the NMR-based models. (Reproduced with permission from Wells, M., Tidow, H., Rutherford, T.J., Markwick, P., Jensen, M.R., Mylonas, E., Svergun, D.I., Blackledge, M., Fersht, A.R., 2008. Structure of tumor suppressor p53 and its intrinsically disordered N-terminal transactivation domain. *Proc. Natl. Acad. Sci. U. S. A.* 105, 5762–5767, © by the National Academy of Science of the USA.)

It is not out of place to mention here that some substances like Na_2SO_4 , having excess O atoms, on the contrary, work as “renaturants” of protein structures, that is, they increase the native structure stability (look at Problem 17.4).

Proteins can also be denatured by sodium dodecyl sulfate (SDS) molecules (their hydrophobic tails penetrate into the hydrophobic core of the protein and break it down), by various alcohols, salts, etc., as well as by very high pressure (Cantor and Schimmel, 1980; Serdyuk et al., 2007).

It is worthy of note that proteins of organisms living under extreme (for us!) conditions, such as hot-acidic-salty wells are “extremophilic”: they have their solid native form just under such extreme conditions, and denature under “physiological” (for most organisms) conditions. It should be mentioned that the architectures of these “extremophilic” proteins have no striking features that distinguish them from normal (mesophilic) proteins; rather, adaptation to the extreme conditions is provided through more careful fitting of their amino acid sequences aiming to reinforce structure-supporting (in the given environment) interactions (Glyakina et al., 2007). But this story can take us too far...

Is a denatured protein able to renature and to restore its native structure? That is, is denaturation reversible?

Yes, it is (this has been known since Anfinsen's experiments in the 1960s ([Anfinsen et al., 1961](#); [Anfinsen, 1973](#)) that brought him a Nobel Prize): the protein can renature if it is not too large and has not been subjected to substantial chemical modifications after *in vivo* folding. In this case, a “mild” (without chemical decay) destruction of its native structure (by temperature, denaturant, etc.) is reversible, and the native structure spontaneously restores after environmental conditions have become normal. However, effective renaturation *in vitro* needs thorough optimization; otherwise, the renaturation can be hindered by precipitation or aggregation (for large multidomain proteins it can also be an intramolecular aggregation of remote chain regions; it is known that the ability to renature usually decreases, and the experimental difficulties increase with protein size) ([Chiti et al., 2003](#)).

The reversibility of protein denaturation is very important: it shows that the entire information necessary to build up the protein structure is contained in its amino acid sequence, and that the protein structure itself (to be more exact, the structure of a not-too-modified and not-too-large protein) is thermodynamically stable. And this allows the use of thermodynamics to study and describe de- and renaturation transitions.

The fundamental fact that protein denaturation occurs as an “all-or-none” transition, that is, that “semidenatured” states are virtually absent, has been established by P.L. Privalov, who worked at our Institute of Protein Research, Russian Academy of Sciences. He studied heat denaturation of proteins, which is usually accompanied by a large heat effect, in the order of 1 kcal mol^{-1} of amino acid residues ([Privalov and Khechinashvili, 1974](#); [Privalov, 1979, 1982](#)).

How has it been proven that protein melting is an “all-or-none” transition?

To this end, it is not enough to demonstrate the existence of a heat capacity peak connected with protein melting (or, which is the same, the S-shaped temperature dependence of protein's energy). This only shows an abrupt cooperativity of melting, that is, that melting embraces many amino acid residues. However, this does not prove that melting embraces the entire protein chain, that is, this does not tell us if the protein melts as a whole or in parts. To prove that melting is an “all-or-none” transition, one has to compare (1) the “effective heat” of transition calculated from its width (ie, the amount of heat consumed by one independent “melting unit”) with (2) the “calorimetric heat” of this transition, that is, the amount of heat consumed by one melting protein molecule. A coincidence of these two independently measured values proves that the molecule melts as a single unit.

If the “effective latent heat” of a melting unit is less than the calorimetric heat consumed by one protein molecule, then the “melting unit” is smaller than the whole protein, that is, the protein melts in parts. If the effective heat of transition is greater than the calorimetric heat, then the “melting unit” is greater than the protein, that is, it is not one protein molecule but some aggregate of them that melts.

This is the van't Hoff criterion for existence (or nonexistence) of the “all-or-none” transition. Since it is important, we shall consider it in some detail ([Privalov and Khechinashvili, 1974](#)).

How is the effective heat of transition related to its width?

Let us consider a “melting unit,” which can be in two states: “solid,” with energy E and entropy S , and “molten,” with energy E' and entropy S' . For simplicity, let us assume that E, E', S, S' do not depend on temperature T (consideration of a more general case I leave to the reader... or read the paper by [Privalov and Khechinashvili \(1974\)](#)).

Since there are only two states of this unit, the probability of its molten state, according to the Boltzmann formula, is:

$$\begin{aligned} P_{\text{MOLTEN}} &= \frac{\exp [-(E' - TS')/kT]}{\exp [-(E - TS)/kT] + \exp [-(E' - TS')/kT]} \\ &= \frac{1}{\exp [(\Delta E - T\Delta S)/kT] + 1} \end{aligned} \quad (17.1)$$

where $\Delta E = E' - E$, $\Delta S = S' - S$. The probability of its solid state (for the “all-or-none” transition) is $P_{\text{SOLID}} = 1 - P_{\text{MOLTEN}}$. The derivative dP_{MOLTEN}/dT shows how steeply P_{MOLTEN} changes with temperature. A simple calculation (using the equation $d(F/T)/dT = d[(E - TS)/T]/dT = -E/T^2$ derived earlier) shows that

$$dP_{\text{MOLTEN}}/dT = P_{\text{MOLTEN}}(1 - P_{\text{MOLTEN}})(\Delta E/kT^2). \quad (17.2)$$

I think I should give you the details of this calculation: you have to understand rather than just believe. Thus, let us denote $\Delta F/T \equiv (\Delta E - T\Delta S)/kT$ as X . Then $dX/dT = -\Delta E/kT^2$, while $P_{\text{MOLTEN}} = 1/(e^X + 1)$, $P_{\text{SOLID}} = 1 - P_{\text{MOLTEN}} = e^X/(e^X + 1)$, and

$$\begin{aligned} dP_{\text{MOLTEN}}/dT &= d[1/(e^X + 1)]/dT = -[1/(e^X + 1)^2] \times (de^X/dT) \\ &= -[1/(e^X + 1)^2] \times e^X \times (dX/dT) = -[1/(e^X + 1)] \\ &\quad \times [e^X/(e^X + 1)] \times (dX/dT) = P_{\text{MOLTEN}}(1 - P_{\text{MOLTEN}}) \times (-dX/dT) \\ &= P_{\text{MOLTEN}}(1 - P_{\text{MOLTEN}})(\Delta E/kT^2) \end{aligned}$$

The mid-transition temperature corresponds to $T_0 = \Delta E/\Delta S$. Here $P_{\text{MOLTEN}} = P_{\text{SOLID}} = 1/2$, and here the value $P_{\text{MOLTEN}}(1 - P_{\text{MOLTEN}})$ has its maximum equal to 1/4. The point of the steepest change of P_{MOLTEN} , that is, the maximum of the derivative dP_{MOLTEN}/dT is very close to T_0 when $\Delta E/kT \gg 1$, that is, when P_{MOLTEN} changes in a narrow temperature range. Here the slope of the curve $P_{\text{MOLTEN}}(T)$ has its maximum and equals to

$$(dP_{\text{MOLTEN}}/dT)|_{T=T_0} = \frac{1}{4} \Delta E/kT_0^2 \quad (17.3)$$

A graphical determination of the transition width ΔT is shown in Fig. 17.3A. It is done by a linear extrapolation of the maximum slope of the curve $P_{\text{MOLTEN}}(T)$ up to its intersection with the base lines corresponding to the native ($P_{\text{MOLTEN}}=0$) and the denatured ($P_{\text{MOLTEN}}=1$) states. In the transition zone, the extrapolated value of $P_{\text{MOLTEN}}|_{T=T_0}^{\text{extrap}}$ changes from 0 to 1 (ie, the change $\Delta P_{\text{MOLTEN}}|_{T=T_0}^{\text{extrap}}=1$), and the temperature changes by ΔT . Thus,

$$(dP_{\text{MOLTEN}}/dT)|_{T=T_0} = \frac{\Delta P_{\text{MOLTEN}}|_{T=T_0}^{\text{extrap}}}{\Delta T} = \frac{1}{\Delta T}. \quad (17.4)$$

That is, ΔT is determined (see Fig. 17.3) by the width of the zone of the steep rise in P_{MOLTEN} (or, more generally: by the width of the steep rise zone of any experimental parameter determining the fraction of the denatured state, for example, protein helicity).

Finally, the heat consumed by the “melting unit” (ΔE) is connected with the transition width (T) and temperature (T_0) by the relationship

$$\frac{1}{\Delta T} = \frac{1}{4} \Delta E / kT_0^2$$

or

$$\Delta E = \frac{4kT_0^2}{\Delta T}. \quad (17.5)$$

The heat ΔE consumed by the “melting unit” (and calculated *only* from the shape of the transition curve) is to be compared with the heat consumed by the whole protein molecule. The latter is calculated as $\Delta H/N$, where ΔH is the heat consumed by all N protein molecules contained in the calorimeter ($N=m/M$, where m is the total mass of the protein taken, and M is its molecular mass). If

$$\Delta E = \Delta H/N \quad (17.6)$$

then melting of the *whole* protein is an “all-or-none” transition. This is the van’t Hoff criterion.

If $\Delta E < \Delta H/N$, that is, if the transition width ΔT is greater than $4kT_0^2/(\Delta H/N)$, then the “melting unit” is smaller than the whole protein; this means that the protein melts in parts.

If $\Delta E > \Delta H/N$, then the “melting unit” is greater than the protein, that is, the “melting unit” is some aggregate of protein molecules rather than one protein molecule.

Inner voice: As I understand it, thermodynamic measurements, like microcalorimetric studies of protein melting, should be performed in equilibrium, that is, very slowly; but I know that microcalorimeter heating cannot be very slow. Can this affect the results you are talking about?

Lecturer: Good question. Indeed, microcalorimeter heating cannot be slower than a fraction of degree per minute; thus, the complete protein melting takes

many minutes, but not hours, while protein denaturation, which is especially slow at the point of equilibrium denaturation, may take hours, as we will see when discussing protein folding and unfolding kinetics. This increases the melting temperature observed in microcalorimetric studies as compared with the temperature of the equilibrium melting: the heated protein melts not at the equilibrium melting point, but at a somewhat higher temperature. However, this has only a minor effect on the heat consumed by the melting protein molecule (Potekhin and Kovrigin, 1998; Dragan et al., 2004; Potekhin, 2012). On the other hand, when protein melting is observed at various rates of heating (and cooling), this gives us some additional information on its melting kinetics (Potekhin and Kovrigin, 1998; Dragan et al., 2004).

Protein melting, that is, the decay of its structure due to elevated temperature, looks natural; however, a “cold” denaturation of proteins also exists at abnormally low temperatures (Fig. 17.5). It is not observed for all proteins, however, since the water in the tube usually freezes first...

Experimentally, the existence of the cold denaturation of proteins has been shown by Privalov and Griko’s group (1988); they have also shown that it is an “all-or-none” transition, like protein melting.

Cold denaturation occurs because of an abnormal temperature dependence of the strength of hydrophobic forces (here I present the arguments of Brandts and Hunt (1967), who predicted cold denaturation long before the experiments by Griko and Privalov).

These forces decrease drastically with decreasing temperature. The strong temperature dependence of the hydrophobic effect is manifested by the increased heat capacity of the denatured, less-compact state of the protein

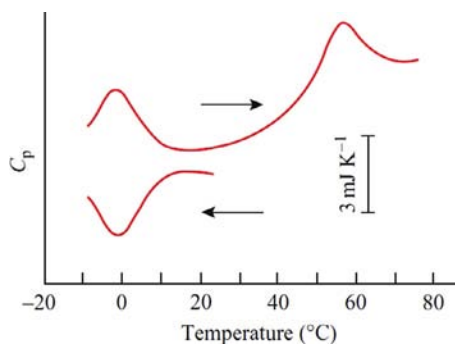


FIG. 17.5 Reversible “cold” denaturation of protein (apomyoglobin) at an abnormally low temperature (the lower curve; the arrow shows that temperature decreases during the experiment). The upper curve shows renaturation of the cold-denatured protein (the left heat capacity peak) with increasing temperature and its subsequent melting (the right peak) at high temperature. The curves show the excess of the protein solution heat capacity C_p over that of the solvent; they are not normalized by the amount of protein in solution. (Adapted from Griko, Yu.V., Privalov, P.L., Venyaminov, S.Yu., Kutyshenko, V.P., 1988. Thermodynamic study of the apomyoglobin structure. *J. Mol. Biol.* 202, 127–138.)

(see ΔC_P^d in Fig. 17.2). As a result, the latent heat of protein denaturation increases significantly with increasing temperature—and *decreases* significantly with decreasing temperature (Figs. 17.2 and 17.6A).

Indeed, it may fall to negative values (Fig. 17.6A)! That is, the energy of the more ordered (native) structure (plus the energy of the surrounding water) is *lower* than that of the less ordered, denatured state (plus surrounding water) at normal temperatures; but it can *exceed* the energy of the denatured state (plus surrounding water) at low temperatures ($\approx +10^\circ\text{C}$ and below). As a result, the native structure's stability (ie, the free energy difference between the native and the denatured state) has its maximum at about room temperature, and starts to

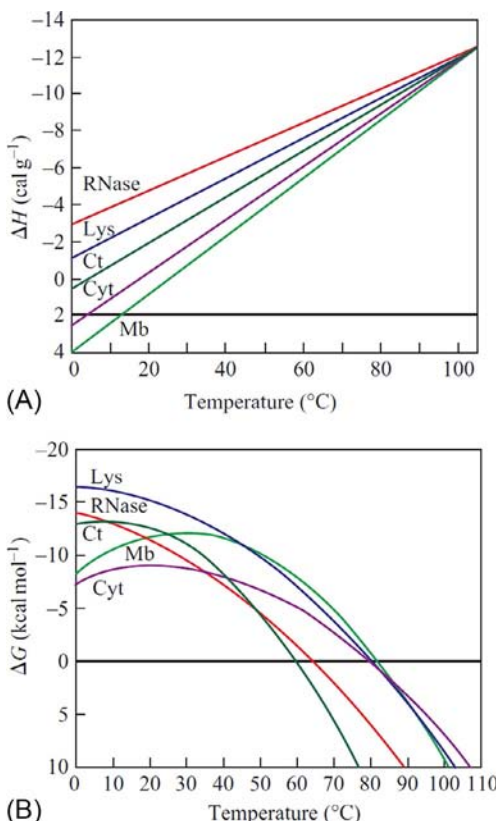


FIG. 17.6 Temperature dependence of (A) the specific (per gram of protein) difference between the energies of the native and denatured states, and (B) the free energy difference (per mole of proteins) between these states. Notice that the protein melting temperature is $60-80^\circ\text{C}$ ($330-350\text{ K}$); that the melting heat (at this temperature) is $\approx 8\text{ cal g}^{-1}$ (or $\approx 1\text{ kcal mol}^{-1}$) per residue, since an average residue is about 110 Da ; and that the “stability reserve” of the native protein molecule is $10-15\text{ kcal mol}^{-1}$ at room temperature. (Adapted from Privalov, P.L., Khechinashvili, N.N., 1974. A thermodynamic approach to the problem of stabilization of globular protein structure: a calorimetric study. *J. Mol. Biol.* 86, 665–684.)

decrease at low temperatures (Fig. 17.6B). For some proteins, the stability decreases so much that the native structure decays at an abnormally low (from the physiological point of view: $\approx 0^\circ\text{C}$) temperature. However, this event is usually unobserved since water usually freezes at such a low temperature, and all denaturation processes freeze as well (which allows us to store proteins in the cold).

Paradoxically, there is some similarity between the denaturation of proteins and water boiling. As you know, there are two ways to boil water: either to increase temperature or to decrease pressure. The hydrophobic pressure condensing the protein globule decreases significantly at low temperatures, and the protein begins to “boil.”

By the way, it really “boils” (meaning a great decrease in its density): the protein chain always unfolds completely, and its volume grows many-fold after cold denaturation, while heat denaturation usually only “melts” the protein, and its volume increases only slightly.

This naturally brings us to the question as to what a denatured protein looks like.

A heated debate on this subject started in the 1950s, continued over the next three decades and only then yielded a kind of consensus.

The problem was that different experimental techniques led to different conclusions.

Specifically, numerous *thermodynamic* experiments have shown that there are no cooperative transitions within the denatured state of a protein molecule. Therefore, it was initially assumed that the denatured protein is always a very loose random coil (which is actually true for denatured proteins in “very good” solvents like concentrated solutions of urea (Tanford et al., 1967; Lapanje and Tanford, 1967)).

However, numerous *structural* studies of denatured proteins reported some large-scale rearrangements within the denatured state (Tanford, 1968), that is, on some “intermediates” between the completely unfolded coil and the native state of proteins (Figs. 17.7 and 17.8).

Actually, experimental data on the state of proteins after denaturation were rather contradictory. In some cases, proteins seemed to be completely unfolded and “unstructured” (Privalov and Khechinashvili, 1974); in others, they seemed to be rather structured (Kuwajima and Sugai, 1978) and/or compact (Dolgikh et al., 1981), and they completely unfolded only under the action of highly concentrated denaturants.

This contradictory picture of protein denaturation was clarified only by using a variety of methods. Measurements of protein solution viscosity gave information about the hydrodynamic volume of protein molecules; far-UV CD spectra (circular dichroism (CD) in the far-UV region) revealed their secondary structure; near-UV CD spectra investigated asymmetry, that is, the ordering of the environment of aromatic side chains in the protein; while infrared (IR) spectroscopy, nuclear magnetic resonance (NMR), measurements of

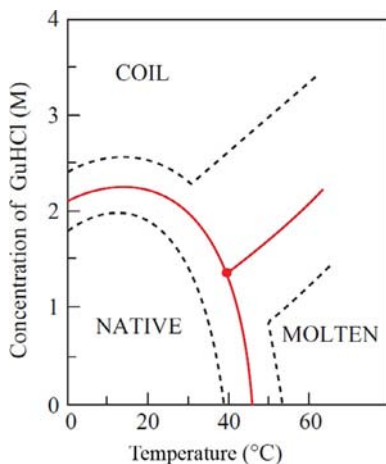


FIG. 17.7 Phase diagram of the conformational states of lysozyme at pH 1.7 in guanidine dihydrochloride solution at various temperatures. It shows the regions of existence of the NATIVE state, of the COIL, and of a more compact temperature-denatured state (MOLTEN). The red line corresponds to the mid-transition, the dashed lines outline the transition zone (approximately from the proportion 9:1 in favor of one state to 1:9 in favor of the other). One can see that the COIL-MOLTEN transition is much wider (less cooperative) than the NATIVE-COIL or the NATIVE-MOLTEN transitions. (Adapted from Tanford, C., 1968. *Protein denaturation. Adv. Protein Chem.* 23, 121–282.)

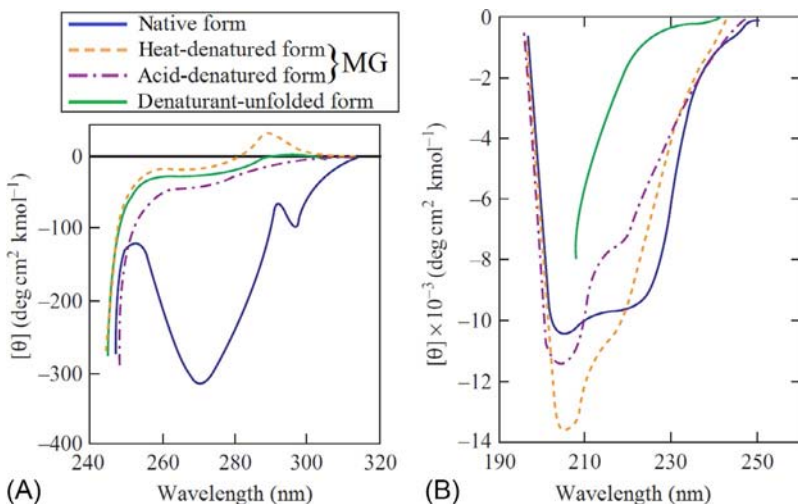


FIG. 17.8 CD spectra in (A) the near- and (B) the far-ultraviolet regions for α -lactalbumin in the native, heat-denatured, acid-denatured and denaturant-unfolded forms. Near-UV CD spectra are always changed by denaturation. Far-UV CD spectra are significantly changed only by unfolding. Heat- and acid-denatured forms have the molten globule (MG) state. (Adapted from Dolgikh, D.A., Abaturov, L.V., Bolotina, I.A., Brazhnikov, E.V., Bychkova, V.E., Bushuev, V.N., Gilmanishin, R.I., Lebedev, Yu.O., Semisotnov, G.V., Tiktupulo, E.I., Ptitsyn, O.B., 1985. Compact state of a protein molecule with pronounced small-scale mobility: bovine alpha-lactalbumin. *Eur. Biophys. J.* 13, 109–121.)

protein activity, etc., gave additional information. This whole arsenal of methods has been applied to the study of protein denaturation by the team of O.B.P. (Dolgikh et al., 1981; Gil'manshin et al., 1982; Ptitsyn, 1995), and A.V.F. belonged to this group as a theoretician.

It has become clear that, apart from activity, only two protein properties always abruptly change during denaturation. These are: (1) the ordering of the environment of aromatic side chains observed by near-UV CD (Fig. 17.8A) and by NMR, and (2) the rigidity of the globular structure followed (using NMR) by exchange of hydrogens (H) of the protein's polar groups for deuteriums (D) of water, and by acceleration of the protein chain proteolysis (Ptitsyn, 1995).

On the other hand, the ordering of the protein main chain (ie, its secondary structure), the volume of the protein molecule and the density of its hydrophobic core can be virtually preserved in some cases and strongly changed in others, depending on the denaturation conditions (Fig. 17.8B).

These studies have revealed the compact state of a protein molecule without the unique 3D structure and with a pronounced small-scale mobility (Dolgikh et al., 1981; Gil'manshin et al., 1982) (Figs. 17.9 and 17.10), which turned to be a universal, or nearly universal, intermediate of protein unfolding and folding (Uversky and Ptitsyn, 1996). This intermediate is now known as the (MG); a term coined by Ohgushi and Wada (1983).

The most important properties of this intermediate (see Ptitsyn, 1995, and references therein) are summarized in Table 17.1.

On the face of it, the properties of the MG are contradictory. Its secondary structure is usually nearly as developed as that of the native protein. On the other hand, the MG (like the completely unfolded protein) has very little of the ordering of its side chains, which is so typical of the native “solid” protein. However, some portion of the native side-chain contacts evidently remains intact in the

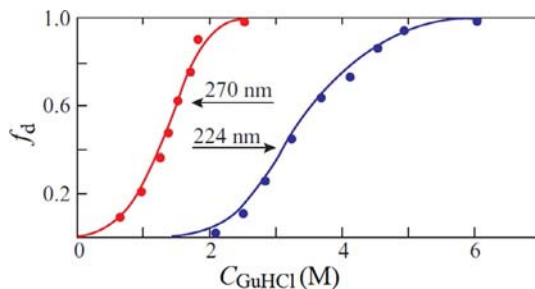


FIG. 17.9 Relative changes of α -lactalbumin CD in the near-(270 nm) and far-(224 nm) UV regions at increasing denaturant (guanidine dihydrochloride) concentrations. $f_d=0$ refers to the signal from the native structure, $f_d=1$ refers to the signal from the completely denatured molecule. The “intermediate state” exists between the first and the second transitions. At $C_{\text{GuHCl}}=2 \text{ M}$, all α -lactalbumin molecules are in the “molten globule” state (as shown by subsequent studies). (Adapted from Pfeil, W., Bychkova, V.E., Ptitsyn, O.B., 1986. Physical nature of the phase transition in globular proteins: calorimetric study of human alpha-lactalbumin. FEBS Lett. 198, 287–291.)

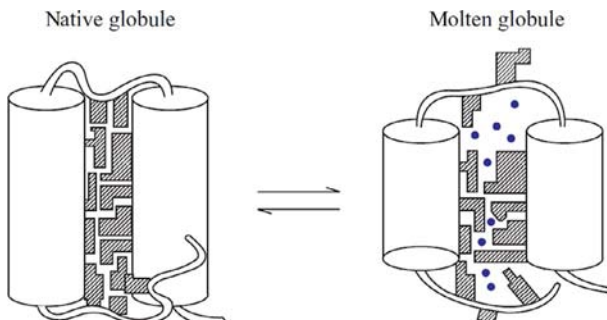


FIG. 17.10 Schematic model of the native and the molten globule protein states. For simplicity, the protein is shown to consist of only two helices connected by a loop. The backbone is covered with numerous side chains (shaded). Reinforced by H-bonds, the secondary structures are stable until the globule is “dissolved” by a solvent. Usually, water molecules are unable to do this job without a strong denaturant. In the molten globule, side chains lose their close packing, but acquire freedom of movement, that is, they lose energy but gain entropy. The water molecules (●) enter into pores of the molten globule (which appear when the close packing is lost), but may cause no further decay of the molten globule.

MG; NMR shows that this applies to aromatic side chains (which are large and rigid) and not to aliphatic side chains (which are smaller and more flexible). The MG is a little less compact than the native protein (as hydrodynamic volume measurements indicate), and its core is virtually as compact as that of the native protein (as shown by “middle-angle” X-ray scattering); on the other hand, a rather high rate of hydrogen exchange shows that at least separate solvent molecules easily penetrate into the globule.

Inner voice: I accept that the volume of MG and its secondary structure content is nearly the same as those of the native protein. But is the secondary structure of a compact globule similar to that of the native protein or not?

Lecturer: Good question. Experiment shows that they are of the same type, as the rule. This is not surprising because what’s good for the MG is good for a well-folded protein. However, there are interesting exceptions. The best known one concerns the MG of β -lactoglobulin (see review in [Ikeguchi, 2014](#)). The native protein is a β -structural molecule, but the MG (which is an intermediate of its folding) contains non-native α -helices, according to the CD spectra.

To some extent, these contradictions may be reconciled by the assumption that the MG is heterogeneous: that it has a relatively dense, native-like core and more loose loops ([Ptitsyn, 1995](#)). However, the assumption that the MG has a completely native core and completely unfolded loops is in clear contradiction to experiment, and specifically with the absence of the ordered environment of even aromatic side chains in the MG. The latter is observed by near-UV CD and by NMR spectroscopy.

TABLE 17.1 Methods of Investigating the “Molten Globule” State, and Conclusions Drawn From Them

“Globule” (Like Native Protein)		“Molten” (Unlike Native Protein)	
<i>Investigation</i>	<i>Conclusion</i>	<i>Investigation</i>	<i>Conclusion</i>
Hydrodynamic volume, small and medium-angle X-ray scattering	Compactness	Near-UV CD, H ¹ NMR spectra	No unique packing of side chains
Large-angle X-ray scattering	Presence of core	H↔D exchange +NMR; proteolysis	Vibrations
NMR (spin echo)	Some aromatic side chains are fixed	NMR (spin echo)	Mobility of aliphatic side chains
Far-UV CD, IR spectra, NMR +H↔D exchange	Secondary structure	Scanning and isothermal microcalorimetry	No further melting (as a rule)
Fluorescence	Some Trp residues are not accessible to water	Fluorescence	Some Trp residues are accessible to water
2D NMR	Preservation of some long-range contacts	2D NMR	Decay of most long-range contacts
Chromatography (HPLC)	Possibility of “correct” S–S bond formation		

Notes: The molten globule state differs from both the native and the unfolded states in showing enhanced binding of nonpolar molecules (demonstrated by enhanced fluorescence of the protein-bound hydrophobic dye ANS ([Semisotnov et al., 1991](#))).

Inner voice: You told that the MG can be somewhat heterogeneous... What about the native protein globule—is it heterogeneous or not?

Lecturer: Actually, heterogeneity of protein globules is only natural, because amino acids chains are of different kinds... But I think, you ask about heterogeneity that embraces large regions of the globules. Many of already discussed intrinsically disordered proteins are clearly heterogeneous in this sense ([Fig. 17.4](#)). As to well-folded proteins, they are heterogeneous only to a certain extent. Thermal fluctuations at their surfaces are, roughly, twice as large as those inside ([Parthasarathy and Murthy, 1997](#)), but one cannot take their surface for liquid. Actually, some structural differences

between a few layers of surface molecules and the crystal interior are generally typical of solids ([Ubbelohde, 1965](#)). The “pre-melting” observed for some globular proteins ([Privalov, 1979](#)) also seems to be connected with their heterogeneity.

For very many (though not for all) proteins, the “MG” arises from a moderately denaturing impact upon the native protein, and decays (turning into a random coil) only under the impact of a concentrated denaturant. The molten-globule-like state often occurs after temperature denaturation (melting), and this melting has been observed always to be an “all-or-none” transition. The MG does not usually undergo further cooperative melting with a greater rise in temperature (see [Fig. 17.7](#)), but its unfolding caused by a strong denaturant looks like a cooperative though rather broad S-shaped transition (see [Ptitsyn, 1995](#), and references therein).

However, some proteins (especially small ones) unfold directly into a coil without the intermediate MG state; and many other proteins are converted into the MG by some denaturing agents (eg, by temperature or by acid), while other agents (eg, urea) directly convert them into a coil ([Tanford, 1968](#); [Ptitsyn, 1995](#)).

A theoretical explanation was required for the contradiction between the results of structural studies and those of thermodynamic studies of protein denaturation, as well as for the physical nature of the new state of proteins, the “MG.”

To understand the physics of the MG, it is important to take into account that this state arises from the native state by cooperative melting, which is a first-order (all-or-none) phase transition. This means that the MG has a much higher energy and entropy than the native state, that is, that the intrachain interactions are much weaker and the chain motility is much higher in the MG. Since the majority of the protein chain degrees of freedom are connected with small-scale fluctuations of the structure, and predominantly with side chain movements, it is the liberation of these fluctuations that can make the MG thermodynamically advantageous. The liberation of small-scale fluctuations does not require the complete unfolding of the globule; slight swelling would be enough. This swelling, however, leads to a significant decrease of the van der Waals attraction: this attraction strongly depends on the distance, and even a small increase of the globule’s volume is enough to reduce it greatly ([Fig. 17.10](#)).

Generally, all this is similar to the melting of a crystal, where a small increase in volume reduces van der Waals interactions and liberates the motions of the molecules.

It was unclear, however, why a system so heterogeneous as a protein melts by a phase transition (like a crystal built up from the same or a few kinds of molecules): protein has no regular crystal lattice the decay of which leads to a first-order phase transition at crystal melting.

Studies of the “MG” furnished the clue to an understanding of the cooperativity of protein denaturation. This process turned out to be very different from what happens in synthetic polymers, DNA or RNA. The last two have no “all-or-none” denaturation, and the same applies to the helix-coil transition.

But what about the previously studied β -structure formation? As we have seen, the “all-or-none” transition exists there... Yes, it does indeed. However, the “non- β -structural” chain is in the coil state: its volume is huge, and it has no secondary structure. And the denatured protein often (in the MG state) virtually preserves its volume and the secondary structure content; but, nevertheless, the MG arises from the native protein by an “all-or-none” way...

Can synthetic polymers serve as an analog?

They do have globule-coil transitions. May be, these resemble protein denaturation?

However, the events observed in protein denaturation are very different from those observed in experimental studies (Fig. 17.11) of globule-coil transitions in synthetic homopolymers (which are extremely difficult because of the threat of aggregation) and which are explained by physical theories of homopolymers (Lifshitz et al., 1978; Grosberg and Khokhlov, 1994) and of heteropolymers (Shakhnovich and Gutin, 1989) (not of “selected” ones, as are proteins, but of random heteropolymers).

All of the latter suggests that the unfolding of a dense polymer globule must start with a gradual increase in its volume, and up to (or nearly up to) its very end, that is, to conversion into a coil, it must go without any abrupt change in the

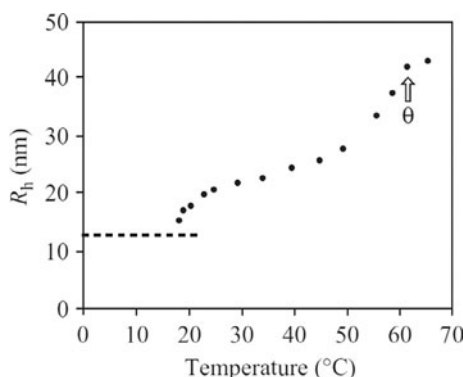


FIG. 17.11 Hydrodynamic radius R_h vs temperature for poly(methyl-methacrylate) chains (M.W. = 6.5×10^6 Da). A very diluted isoamyl acetate solution of the polymer is studied. The point of the globule-coil transition (the “θ-point”) corresponds to 61°C (shown by the arrow). The globule exists below 61°C, the coil above 61°C. Dashed line, is the computed radius of solid poly(methyl-methacrylate) with M.W. of 6.5×10^6 Da. One can see that the radius of the coil is four times larger than that of the solid polymer globule (ie, the coil is nearly 100 times larger in volume and nearly 100 times less dense), and that after the coil → globule transition (with decreasing temperature) the chain undergoes a gradual compaction down to the swollen globule whose radius is two times larger (ie, whose volume is 10 times larger and density 10 times less) than those of the solid polymer globule (see the 50–30°C region). This first compaction is followed (as the temperature decreases) by the second one (see the 25–20°C region), and only this second compaction leads to a dense globule. (Adapted from Kayaman, N., Guerel, E.E., Baysal, B.M., ve Karasz, F., 1999. Kinetics of coil-globule collapse in poly(methyl methacrylate) in dilute solutions below theta temperatures. *Macromolecules* 32, 8399–8403.)

molecule's density. They also suggest that the globule-to-coil transition starts when the globule is already rather swollen, and that the main difference between the globular and coil phases is the difference not in density, but rather in the scale of fluctuations (small in globule, large in coil). This means that the globule-to-coil transition is quite different from the first-order phase transition exemplified by melting, boiling or sublimation, while protein denaturation is essentially similar to melting or sublimation of a solid.

Although the conventional theory of globule-coil transitions in *homopolymers* is *not* applicable to protein denaturation, it would not be out of place to present it to you here—of course, in a simplified form (for more details, see Appendix A). This will allow me later, to emphasize the difference in behavior between the “selected” protein chains and normal polymers. On the other hand, this conventional theory is applicable to the behavior of already denatured protein chains. And, last but not least, I think that acquaintance with the basic physical models is a necessary part of general culture.

The conventional globule-coil transition theory ([Grosberg and Khokhlov, 1994](#)) starts with consideration of similarity and difference between the globule-coil transition in a homopolymer chain and evaporation of a liquid. Let us consider the situation at a low temperature T when the effect of liquid-vapor phase separation is the strongest.

The theory emphasizes that the chain-bound monomer cannot go far away from its neighbor in the chain, while a free molecule (monomer) in liquid or a vapor cloud can do so (until it hits a wall of the vessel). Therefore, free monomers can be in either of the *two* stable states: in a dense phase (whose free energy is dominated by the energy E of attraction) and in an extremely sparse cloud (whose entropy is huge, and whose free energy is therefore dominated by the entropy term TS even at a very low temperature T). On the contrary, the states of intermediate density are unstable: here, the attraction is *already* weak, while the entropy is *still* low. This is the origin of the liquid-gas phase separation and an abrupt evaporation of the dense phase with rising temperature.

And what about the polymer? Here the situation is quite *different*, because a monomer cannot go far away from its chain neighbor even in the most diffuse coil. This means that the coil entropy cannot exceed a certain limit, and thus the entropy is not able (at low temperatures) to compete with the energy gained by compaction of the polymer. Thus, the polymer has no alternative: at low temperature its monomers cannot scatter, and it has to be a dense globule only, which means that (unlike liquid) it cannot jump from the dense to the sparse phase. Therefore, rising temperature can cause only a gradual swelling of the polymer globule rather than its abrupt “evaporation.”

Clarification. Strictly speaking, the general theory ([de Gennes, 1979; Grosberg and Khokhlov, 1994](#)) states that an abrupt transition of the more-or-less dense globule into the coil, though possible in principle, occurs only under hardly obtainable conditions, for example, when monomers in the chain are repelled in pairs but attracted to one another when there are many simultaneously interacting particles. This effect can be observed in homopolymers with

very rigid chains (recollect β -sheets with their straight rigid strands). But in contrast to proteins, in these rigid polymers, the jump in energy (per monomer) during coil-globule transitions is very small (as for liquid crystal formation of rigid elongated molecules), if the monomer lacks internal degrees of freedom. A large energy jump requires a very special construction of the chain monomers. Normal polymers do not have such a construction of their links, unlike protein chains. As we will see, protein residues become strongly attracted together when many of them are simultaneously involved in interactions. Why this is so, we will see in [Lecture 18](#).

Thus, the conventional theory of coil-globule transitions in normal homopolymers cannot explain protein denaturation. (The same is true for the theory of coil-globule transitions in random heteropolymers ([Gutin and Shakhnovich, 1993](#); [Sfatos et al., 1993](#)), but consideration of this complicated theory is beyond the scope of these lectures.)

Conventional theories state that the globule expands gradually, and that the coil arises from a globule of very low density, and *not* by a first-order phase transition; but denaturation of proteins, these Schrödinger's "aperiodic crystals," occurs at a high density of the globule, often does not lead to random coil formation, and resembles the destruction of a crystal, that is, a first-order phase transition.

The explanation of these peculiarities of protein denaturation, and of its "all-or-none" phase nature in particular, will be given in [Lecture 18](#).

REFERENCES

- Anfinsen, C.B., 1973. Principles that govern the folding of protein chains. *Science* 181, 223–230.
- Anfinsen, C.B., Haber, E., Sela, M., White, F.H., 1961. Kinetics of formation of native ribonuclease during oxidation of the reduced polypeptide chain. *Proc. Natl. Acad. Sci. U. S. A.* 47, 1309–1314.
- Brandts, J.F., Hunt, L., 1967. The thermodynamics of protein denaturation. 3. The denaturation of ribonuclease in water and in aqueous urea and aqueous ethanol mixtures. *J. Am. Chem. Soc.* 89, 4826–4838.
- Bychkova, V.E., Pain, R.H., Ptitsyn, O.B., 1988. The molten globule state is involved in the translocation of proteins across membranes? *FEBS Lett.* 238, 231–234.
- Cantor, C.R., Schimmel, P.R., 1980. *Biophysical Chemistry*. W.H. Freeman & Co., New York (Part 2, Chapters 8, 12; Part 3, Chapter 21).
- Chiti, F., Stefani, M., Taddei, N., Ramponi, G., Dobson, C.M., 2003. Rationalisation of mutational effects on protein aggregation rates. *Nature* 424, 805–808.
- de Gennes, P.-G., 1979. *Scaling Concepts in Polymer Physics*. Part A. Cornell University Press, Ithaka, London.
- Dolgikh, D.A., Gil'manshin, R.I., Brazhnikov, E.V., Bychkova, V.E., Semisotnov, G.V., Venyaminov, S.Yu., Ptitsyn, O.B., 1981. Alpha-lactalbumin: compact state with fluctuating tertiary structure? *FEBS Lett.* 136, 311–315.
- Dragan, A.I., Potekhin, S.A., Sivolob, A., Lu, M., Privalov, P.L., 2004. Kinetics and thermodynamics of the unfolding and refolding of the three-stranded alpha-helical coiled coil, Lpp-56. *Biochemistry* 43, 14891–14900.

- Drobnak, I., De Jonge, N., Haesaerts, S., Vesnaver, G., Loris, R., Lah, J., 2013. Energetic basis of uncoupling folding from binding for an intrinsically disordered protein. *J. Am. Chem. Soc.* 135, 1288–1294.
- Dunker, A.K., Lawson, J.D., Brown, C.J., Williams, R.M., Romero, P., Oh, J.S., Oldfield, C.J., Campen, A.M., Rattliff, C.M., Hippis, K.W., Ausio, J., Nissen, M.S., Reeves, R., Kang, C., Kissinger, C.R., Bailey, R.W., Griswold, M.D., Chiu, W., Garner, E.C., Obradovic, Z., 2001. Intrinsically disordered protein. *J. Mol. Graphics Model.* 19, 26–59.
- Dunker, A.K., Oldfield, C.J., Meng, J., Romero, P., Yang, J.Y., Chen, J.W., Vacic, V., Obradovic, Z., Uversky, V.N., 2008. The unfoldomics decade: an update on intrinsically disordered proteins. *BMC Genomics* 9 (suppl. 2), S1.
- Finkelstein, A.V., Ptitsyn, O.B., 2012. Protein physics. A course of lectures with color and stereoscopic illustrations and problems with solutions, 4th extended ed. Publishing House ‘Universitet’, Moscow (in Russian). Problems 17.6, 17.7.
- Gil'manshin, R.I., Dolgikh, D.A., Ptitsyn, O.B., Finkel'shtein, A.V., Shakhnovich, E.I., 1982. Protein globule without the unique three-dimensional structure: experimental data for alpha-lactalbumins and general model. *Biofizika* 27, 1005–1016 (in Russian).
- Glyakina, A.V., Garbuzynskiy, S.O., Lobanov, M.Y., Galzitskaya, O.V., 2007. Different packing of external residues can explain differences in the thermostability of proteins from thermophilic and mesophilic organisms. *Bioinformatics* 23, 2231–2238.
- Griko, Yu.V., Privalov, P.L., Venyaminov, S.Yu., Kutyshenko, V.P., 1988. Thermodynamic study of the apomyoglobin structure. *J. Mol. Biol.* 202, 127–138.
- Grosberg, A.Yu., Khokhlov, A.R., 1994. Statistical Physics of Macromolecules. American Institute of Physics, New York (Chapters 1, 2, 3, 7).
- Gutin, A.M., Shakhnovich, E.I., 1993. Ground state of random copolymers and the discrete random energy model. *J. Chem. Phys.* 98, 8174–8177.
- Ikeguchi, M., 2014. Transient non-native helix formation during the folding of β -lactoglobulin. *Biomolecules* 4, 202–216.
- Klug, R., 1984. Structure of the nucleosome core particle at 7 Å resolution. *Nature* 311, 532–537.
- Kuwajima, K., Sugai, S., 1978. Equilibrium and kinetics of the thermal unfolding of alpha-lactalbumin. The relation to its folding mechanism. *Biophys. Chem.* 8, 247–254.
- Lapanje, S., Tanford, C., 1967. Proteins as random coils. IV. Osmotic pressures, second virial coefficients, and unperturbed dimensions in 6 M guanidine hydrochloride. *J. Am. Chem. Soc.* 89, 5030–5033.
- Lifshitz, I.M., Grosberg, A.Yu., Khokhlov, A.R., 1978. Some problems of the statistical physics of polymer chains with volume interactions. *Rev. Mod. Phys.* 50, 683–713.
- Ohgushi, M., Wada, A., 1983. ‘Molten-globule state’: a compact form of globular proteins with mobile side-chains. *FEBS Lett.* 164, 21–24.
- Parthasarathy, S., Murthy, M.R.N., 1997. Analysis of temperature factor distribution in high-resolution protein structures. *Protein Sci.* 6, 2561–2567.
- Potekhin, S.A., 2012. The potential of scanning microcalorimetry for studying thermotropic conformational transitions in biomacromolecules. *Polym. Sci. Ser. C* 54, 108–115.
- Potekhin, S.A., Kovrigin, E.L., 1998. Influence of kinetic factors on heat denaturation and renaturation of biopolymers. *Biofizika* 43, 223–232 (in Russian).
- Privalov, P.L., 1979. Stability of proteins: small globular proteins. *Adv. Protein Chem.* 33, 167–241.
- Privalov, P.L., 1982. Stability of proteins. Proteins which do not present a single cooperative system. *Adv. Protein Chem.* 35, 1–104.
- Privalov, P.L., Khechinashvili, N.N., 1974. A thermodynamic approach to the problem of stabilization of globular protein structure: a calorimetric study. *J. Mol. Biol.* 86, 665–684.

- Ptitsyn, O.B., 1995. Molten globule and protein folding. *Adv. Protein Chem.* 47, 83–229.
- Schulz, G.E., 1977. Nucleotide binding proteins. In: Balaban, V. (Ed.), *Molecular Mechanism of Biological Recognition*. Elsevier/North-Holland Biomedical Press, New York, pp. 79–94.
- Schulz, G.E., Schirmer, R.H., 1979, 2013. *Principles of Protein Structure*. Springer, New York (Chapter 8).
- Semisotnov, G.V., Rodionova, N.A., Razgulyaev, O.I., Uversky, V.N., Gripas', A.F., Gilmanshin, R.I., 1991. Study of the ‘molten globule’ intermediate state in protein folding by a hydrophobic fluorescent probe. *Biopolymers* 31, 119–128.
- Serdyuk, I.N., Zaccai, N.R., Zaccai, J., 2007. *Methods in Molecular Biophysics: Structure, Dynamics, Function*. Cambridge University Press, Cambridge, NY (Chapters C2, C3).
- Sfatos, C.D., Gutin, A.M., Shakhnovich, E.I., 1993. Phase-diagram of random copolymers. *Phys. Rev. E* 48, 465–475.
- Shakhnovich, E.I., Gutin, A.M., 1989. Formation of unique structure in polypeptide-chains theoretical investigation with the aid of a replica approach. *Biophys. Chem.* 34, 187–199.
- Tanford, C., 1968. Protein denaturation. *Adv. Protein Chem.* 23, 121–282.
- Tanford, C., Kawahara, K., Lapanje, S., Hooker Jr., T.M., Zarlengo, M.H., Salahuddin, A., Aune, K.C., Takagi, T., 1967. Proteins as random coils. 3. Optical rotatory dispersion in 6 M guanidine hydrochloride. *J. Am. Chem. Soc.* 89, 5023–5029.
- Tompa, P., 2010. *Structure and Function of Intrinsically Disordered Proteins*. Chapman & Hall/CRC Press, Taylor & Francis Group, Boca Raton, FL (Chapters 2, 10–12).
- Ubbelohde, A.R., 1965. *Melting and Crystal Structure*. Clarendon Press, Oxford (Chapters 2, 11, 12, 14).
- Uversky, V.N., 2013. A decade and a half of protein intrinsic disorder: biology still waits for physics. *Protein Sci.* 22, 693–724.
- Uversky, V.N., Ptitsyn, O.B., 1996. All-or-none solvent-induced transitions between native, molten globule and unfolded states in globular proteins. *Fold. Des.* 1, 117–122.
- Uversky, V.N., Gillespie, J.R., Fink, A.L., 2000. Why are ‘natively unfolded’ proteins unstructured under physiologic conditions? *Proteins* 41, 415–427.
- Wright, P.E., Dyson, H.J., 1999. Intrinsically unstructured proteins: re-assessing the protein structure-function paradigm. *J. Mol. Biol.* 293, 321–331.

Lecture 18

As we have learned from the previous lecture, the conventional theories of coil-globule transitions either in homo- or in heteropolymers cannot explain protein denaturation. They state that the globule expands gradually, that a coil arises only when the globule's density is very low, and that this does *not* happen by a pronounced first-order (all-or-none) phase transition. On the contrary, denaturation of proteins, these Schrödinger's “aperiodic crystals,” occurs at a high density of the globule without its preceding swelling, often does not lead to random coil formation and resembles the destruction of a crystal, that is, it resembles a first-order phase transition.

A “normal” crystal melting ([Ubbelohde, 1965](#)) also cannot explain protein denaturation: proteins have no periodic crystal lattice, which distinguishes a crystal from liquid or glass (which is nothing but a very viscous liquid). And the origin of crystal melting is just a decay of this lattice.

It is really astonishing that protein denaturation occurs as a normal sharp all-or-none transition (which is an analogue of the first-order phase transition in macroscopic systems): any protein is a small (or rather, “mesoscopic”) highly heterogeneous system (where, nevertheless, each atom sits at its own place), and heterogeneity in “common” macroscopic systems is known to slur over the phase transitions in normal molecular systems.

Inner voice: Does protein denaturation always occur just as an “all-or-none” transition from one state to another, between which there is no interim?

Lecturer: First, I am, as usual, talking about single-domain proteins; large multidomain ones undergo several successive transitions of the “all-or-none” type ([Privalov, 1979, 1982](#)), that is, such proteins can be “semidenatured” (similar to some “intrinsically disordered” proteins that we discussed in the previous lecture). Second, both in the “all-or-none” and first-order phase transitions certain transient intermediates can be observed, though mostly indirectly, by their influence on kinetics of transition over the free-energy barrier separating two directly observable states. This is discussed in [Lecture 19](#). Third, it has been found that in some small proteins this free-energy barrier is so small that the transition bears a close similarity to the second-order phase transition ([Muñoz et al., 2008](#)). But this is true only for some small proteins and looks like an exception from the general rule (established for large and medium-size proteins and for the vast majority of small proteins).

It is not out of place here to draw your attention to an aspect that distinguishes conventional physics from the physics of proteins and of complex systems in general. What I am speaking about are not physical laws: they are certainly the same for both cases; I am speaking about the effects that attract the attention

of researchers. The normal subjects of conventional physics are more or less uniform or “averaged”: gases, crystals, fields, spin glasses, etc. Therefore, special attention is paid to each heterogeneity arising in these uniform objects; for example, to quasi-particles. Protein physics, on the contrary, deal with a highly heterogeneous object from the very beginning. Protein is full of heterogeneous tensions; it can be said to be full of various frozen fluctuations; but this is just a figure of speech to describe protein heterogeneity. In contrast, the uniform phenomena that deal with the entire heterogeneous system (like denaturation that involves the entire protein) are indeed of special interest for protein physics.

To understand protein denaturation, one has to explain why there exist two equally stable states, that is, equally stable phases of the protein chain (which, as we already know, is impossible for normal polymers), and why they are separated by a free energy barrier (which, as we also know, is necessary for an “all-or-none” transition). That is, one has to explain why the protein globule cannot decay by gradual swelling, as usual polymer globules do.

In doing so ([Shakhnovich and Finkel'shtein, 1982](#); [Shakhnovich and Finkelstein, 1989](#); [Finkelstein and Shakhnovich, 1989](#)), one has to take into account the main peculiarities of proteins (those which differ them from normal polymers): that each protein has one chain fold distinguished by its peculiar stability; that flexible side groups are attached to a more rigid protein-chain backbone; and that the native protein is packed as tightly as a molecular crystal (although without a crystal lattice): in the protein, as in a molecular crystal, the van der Waals volumes of atoms occupy 70–80% of space, while in liquids (melts) they occupy only 60–65% ([Schulz and Schirmer, 1979, 2013](#); [Branden and Tooze, 1999](#)).

Side groups of the protein chain are capable of rotational isomerization, that is, jumps from one allowed conformation to another. Each jump requires some vacant volume around the jumping side chain; but the native protein fold is distinguished by tight chain packing (which contributes to the peculiar stability of this fold). Besides, the side chains sit at the rigid backbone, which is especially rigid inside the globule, because here the chain forms the α - and β -structures that are necessary to involve the backbone with its polar groups in the dense hydrophobic globule ([Fig. 18.1](#)). These structures are stable at least until the solvent penetrates into the globule (which requires approximately the same free volume as well). Thus, each of these rigid structures has to move as a whole (at least at the beginning of the globule’s expansion), with the entire forest of side chains attached. Therefore, expansion of the closely packed globule through the movement of α - and β -structures creates approximately equal free spaces near each side chain, and these spaces are either insufficient for isomerization of each of the side chains (when the globule’s expansion is too small), or sufficient for isomerization of many of them at once. This means that liberation of the side chains (as well as solvent penetration) occurs only when the globule’s expansion crosses some threshold, the “barrier” ([Fig. 18.2](#)). These two events can make a less dense state of the protein chain as stable as its native state, but only after the density barrier has been passed.

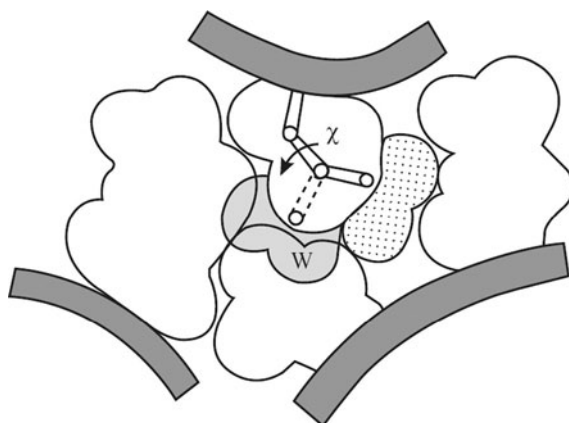


FIG. 18.1 A sketch of the side chain packing. Only a small piece of the globule is shown. The dashed region W corresponds to an alternative rotamer of the side chain (χ being its rotational angle); this rotamer is forbidden by close packing. Its appearance requires additional vacant volume W of at least 30 \AA^3 (ie, the volume of a methyl group), or $\approx 1/5$ of the average amino acid volume. Nearly the same volume is required for H_2O penetration in the core. (Adapted from Shakhnovich, E.I., Finkelstein, A.V., 1989. Theory of cooperative transitions in protein molecules. I. Why denaturation of globular protein is a first-order phase transition. *Biopolymers* 28, 1667–1680.)

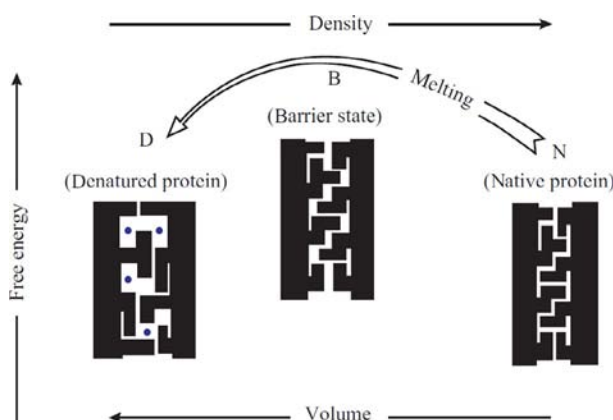


FIG. 18.2 Origin of the free-energy barrier between the native and any denatured state of the protein. The “barrier” state B arises at a small expansion of the native, closely packed state N. The pores formed in the state B already cause a great increase in the van der Waals energy, but yet allow neither side chain liberation nor penetration of the solvent (●) inside the protein. This requires a further expansion of the globule to the state D. (Adapted from Shakhnovich, E.I., Finkelstein, A.V., 1989. Theory of cooperative transitions in protein molecules. I. Why denaturation of globular protein is a first-order phase transition. *Biopolymers* 28, 1667–1680.)

Thus, a small (prebarrier) expansion of the native globule is *always* unfavorable: it *already* increases the energy of the globule (since its parts move apart and lose their close packing) but does not increase its entropy because it does not yet liberate the rotational isomerization of the side chains. That is, the free energy of the globule increases with a slight expansion. On the contrary, a large (postbarrier) expansion of the globule liberates the rotational isomerization and leads (at a sufficiently high temperature) to decreasing free energy. As a result, protein denaturation does not occur gradually but as a jump over the free energy barrier, in accordance with the “all-or-none” principle.

Therefore, the protein tolerates, without a change, modification of ambient conditions up to a certain limit, and then melts altogether, like a macroscopic solid body. This resistance and hardness of protein, in turn, provides the reliability of its biological functioning.

In other words, the “all-or-none” transition between the native and denatured state is explained by a sudden jump in entropy (mainly side chain entropy) which occurs only when the globule’s expansion crosses a certain threshold ([Figs. 18.2](#) and [18.3](#)). And the latter exists because the side chains sit at the rigid backbone that coordinates their positions and cannot be liberated one-by-one.

Prior to the discovery of the molten globule state, protein denaturation was usually considered to be a complete decay of the protein structure, that is, as a transition to the coil. After this discovery ([Dolgikh et al., 1981](#)), it became clear that the denatured protein can be rather dense as well as loose depending on the solvent’s strength and the hydrophobicity of the protein chain. The pores in the molten globule (ie, the vacant space necessary for the side-chain movements, see [Figs. 18.1](#) and [18.2](#)) are “wet,” that is, they are occupied by the solvent because a water molecule inside the protein is still better than a vacuum. Experimentally, the “wetness” of the molten globule is proved by the absence of a visible increase in the protein partial volume ([Kharakoz and Bychkova, 1997](#)) after denaturation of any kind.

When the solvent is poorly attracted by the protein core (consisting mainly of hydrophobic groups, although including some polar backbone atoms too), it only occupies the pores that already exist in the molten core to ensure side-chain movements, but it does not create new pores and does not expand the globule (just as water does not expand a sponge, although it occupies its pores). Then, the denatured protein remains in the wet molten globule state.

Inner voice: Where there’s a “wet” molten globule there’s a “dry” one, is not there?

Lecturer: Yes. Like the “wet” one, a “dry” molten globule (without water in its pores) was predicted from theoretical considerations ([Finkelstein and Shakhnovich, 1989](#)); a further analysis of theoretical and experimental data showed that the dry molten globule was less stable than the wet one, and therefore, hardly fits to play the role of an intermediate in protein melting.

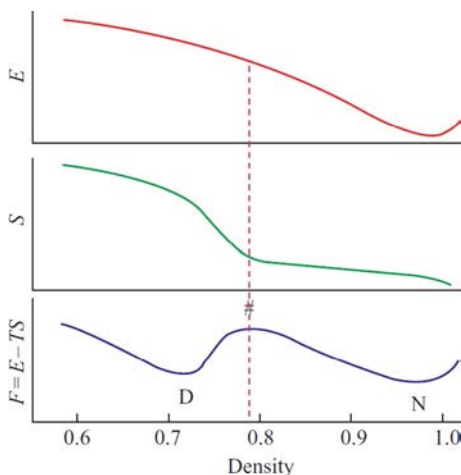


FIG. 18.3 Origin of the “all-or-none” transition in protein denaturation. The energy E is at its minimum at close packing (here the globule’s density $\rho = 1$). The entropy S increases with decreasing density. Initially, this increase is slow (at $\rho = 1.0\text{--}0.8$, until the side chains can only vibrate, but their rotational isomerization is impossible), rapid (when rotational isomerization becomes possible), and then slow again (when free isomerization has been reached). The nonuniform growth of the entropy is due to the following. The isomerization needs some vacant volume near each side group, and this volume must be at least as large as a CH_3 -group. And, since the side chain is attached to the rigid backbone, this vacant volume cannot appear near one side chain only but has to appear near many side chains at once. Therefore, there exists a threshold (barrier) value of the globule’s density after which the entropy starts to grow rapidly with increasing volume of the globule. This density is rather high, about 80% of the density of the native globule, since the volume of the CH_3 -group (a typical unit of rotation, see Fig. 18.1) amounts to $\approx 20\%$ of the volume of an amino acid residue. Therefore, the dependence of the resulting free energy $F = E - TS$ on the globule’s density ρ has a maximum (“barrier” $\#$) separating the native, tightly packed globule (N) from the denatured state (D) of lower density. Because of this free energy barrier (its width depends on the heterogeneity of the side chain rotation units) protein denaturation occurs as an “all-or-none” transition, independent of the final state of the denatured protein.

Nevertheless, as found recently ([Jha and Udgaonkar, 2009](#)), the dry molten globule emerges during fluctuations preceding protein melting.

The molten globule compactness is maintained by residual hydrophobic interactions. They are not very strong. Even in the apomyoglobin molten globule that has developed a secondary structure and almost native topology of packing of the most of its chain ([Jennings and Wright, 1993](#)), the residual interaction between hydrophobic side-groups appears to be at least three times weaker than that in the native protein ([Samatova et al., 2009](#)), and some of these groups lack these residual interaction at all (which emphasizes heterogeneity of molten globules; see [Ptitsyn, 1995](#)).

If the residual hydrophobic interactions are weak, that is, if either the solvent is strongly attracted by the protein chain or the chain hydrophobicity is low, the solvent starts to expand the pores, and the globule starts to swell. The greater the attraction between the solvent and the protein chain, and the smaller the attraction within the chain, the greater the swelling: up to transition to the random coil.

The coil arises directly from the native state if the temperature is low, that is, when the role of the entropy of side chain liberation is not crucial, and a significant part of the denaturation effect is produced by the solvent (recall cold denaturation); and at a higher temperature the coil can arise after the swelling of the molten globule (recall the experimental protein phase diagram by Tanford).

It seems that the swelling of the molten globule can be described by the conventional theory of globule-coil transitions we have considered. Fig. 18.4 shows what is predicted to happen: if the intrachain interactions remain strong, that is, $-\varepsilon/kT$ is large (ie, if the protein chain is hydrophobic enough or/and the solvent is not strong enough), the denatured protein will have the dense molten globule state; otherwise (with decreasing $-\varepsilon/kT$), the globule will swell or even unfold completely—but without any jump in density.

This is a result of the most simplified physical theory of the molten globule state. Actually, the theory states that the molten globule is separated by an “all-or-none” transition from the native state, but not from the coil. This result does not account for a possible heterogeneity of the molten globule, though. Perhaps a more advanced theory is needed...

And what do experiments show? Is unfolding of the molten globule of the “all-or-none” type?

This is not quite clear yet. Some experiments demonstrate that denaturant-induced unfolding of the molten globule to coil is a cooperative, “S-shaped” transition (Fig. 18.5). However, such a form of the experimental curve is compatible both with an “all-or-none” transition and with a gradual (Fig. 18.4) globule-to-coil transition via states of intermediate density.

True, GuHCl- or urea-induced molten globule unfolding is a narrow transition, not much wider than the denaturation ($N \rightarrow MG$) transition itself (Fig. 18.5), and its width (like the width of denaturation) is shown to be inversely proportional to the protein domain molecular weight, which is in

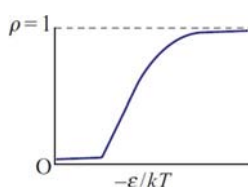


FIG. 18.4 Qualitative dependence of the polymer’s density ρ on the energy of the monomer interaction ε expressed in kT units (see Appendix A). There is no density jump here, that is, this transition is not of the “all-or-none” type.

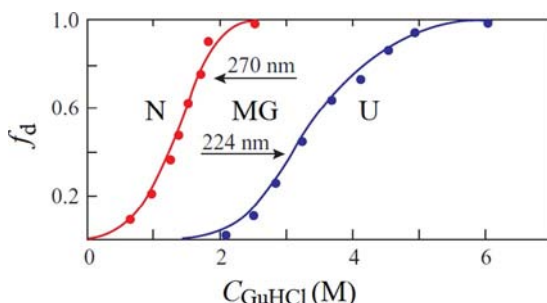


FIG. 18.5 Relative changes of the α -lactalbumin CD in the near-UV region (270 nm; this transition reports on decay of the tertiary structure) and in the far-UV region (224 nm; this transition reports on decay of the secondary structure) at increasing denaturant (guanidine dihydrochloride) concentrations. $f_d=0$ refers to the signal from the native structure, $f_d=1$ refers to the signal from the completely denatured molecule. The “intermediate state” exists between the first and the second transitions, that is, between the native state (N) denaturation and transition to the completely unfolded state (U); at $C_{\text{GuHCl}}=2 \text{ M}$, the α -lactalbumin molecules have the “molten globule” (MG) state. (Adapted from Pfeil, W., Bychkova, V.E., Ptitsyn, O.B., 1986. Physical nature of the phase transition in globular proteins: calorimetric study of human α -lactalbumin. FEBS Lett. 198, 287–291.)

qualitative agreement with the van't Hoff criterion. This led [Uversky and Ptitsyn \(1996a\)](#) to conclude that the transition in question can be of the “all-or-none” type.

Calorimetric investigations can, in principle, give the final answer; but molten proteins have been never observed to undergo further melting ([Tanford, 1968](#); [Ptitsyn, 1995](#)) (though, “all-or-none” melting seems to appear in calorimetric studies of some de novo designed proteins, which usually have a molten globule rather than a solid form).

It has also been shown ([Uversky et al., 1992](#)) that the molten globule (more compact) denatured state can be separated by chromatography from some “less compact” state by an all-or-none transition (at least in carbonic anhydrase). The coexistence of two denatured states is demonstrated by the split peak in the chromatography elution profile of the denatured protein. This split peak shows that the protein molecule exists *either* in one form *or* in another, but the states of intermediate compactness are absent; that is, the split peak is clear evidence of an “all-or-none” transition. However, carbonic anhydrase is a β -structural protein, and the observed transition may refer not to decay of the molten globule, but rather to decay of the β -structure (which is of an “all-or-none” type in synthetic polypeptides, as you may remember). There is one more intriguing thing connected with this transition: it is so slow (takes at least minutes) as to be detected by chromatography, while the unfolded chain-to-molten globule transition (to be considered in the next lecture) usually takes much less time...

At the moment of transition, the “less compact” state is only a little less compact than the molten globule and has half of its secondary structure, but it is far

more compact and far more structured than the coil ([Uversky and Ptitsyn, 1996b](#)) (therefore, this “less compact” state is called the “premolten” globule). It should be noted that structural features of the “premolten” and “molten” globules are not that different, and this is the cause of frequently occurring ambiguity in the use of the term “molten globule.” But let me repeat again that the nature of the molten globule-to-coil transition is yet to be understood, that is, further experiments and a physical theory of this phenomenon are needed.

A short digression. It is quite possible that denaturant-induced unfolding of the molten globule is an all-or-none transition for some proteins and a gradual transition for others. We must not be surprised by that. This may reflect not a qualitative difference between proteins, but rather the fact that we observe each protein through a relatively small “experimental window” ([Finkelstein and Shakhnovich, 1989](#)), with temperature ranging from water freezing to boiling and the action of denaturant is limited by its zero concentration. Therefore, for example, the proteins with less hydrophobic amino acids, that is, the proteins whose native globule is more susceptible to denaturants, demonstrate (in the “window”) only the native state-to-coil transition (since the molten globule is maintained only by residual hydrophobic interactions that are weak in this case). Proteins of this kind (especially if they are “weakened,” eg, apomyoglobin, which is myoglobin weakened by deprivation of the heme) tend to demonstrate the cold denaturation that leads to the coil. The more hydrophobic, more stable proteins demonstrate (in the “window”) the native state-to-molten globule transition, but do not demonstrate cold denaturation: apparently, it can occur only at subzero temperatures, when water freezes and thus stops our experiments.

Further consideration of the thermodynamics of protein molecules will be now done from the following point of view: which physical property distinguishes the protein chain from a random heteropolymer and allows the protein native structure to be capable of “all-or-none” rather than gradual destruction? That is, what makes the protein tolerate, without softening, a change of ambient conditions and then break suddenly? It is clear that this behavior ensures the reliability of the protein function: as long as it works, it works properly...

Having plotted the dependence of both the protein entropy S and its energy E on its density ρ ([Fig. 18.3](#)), we can now plot the S -on- E dependence and then grasp the typical appearance of the spectrum of protein energy ([Fig. 18.6A](#)). We want to see how the structures are distributed over the energy; it is of no interest to us now *what* structure has this or that energy, the question is *how many* structures have this or that energy. We can answer it if $S(E)$ is known. Let me remind you that $S(E)$ is proportional to the logarithm of the number of structures with energy E . Let me also remind you that $dS(E)/dE = 1/T(E)$, where $T(E)$ is the temperature corresponding to the energy E .

The distinctive feature of a protein energy spectrum ([Fig. 18.6A](#)) is the large gap between the energy of the most stable, that is, the native protein structure, and the region where the energies of many other, “misfolded” structures appear.

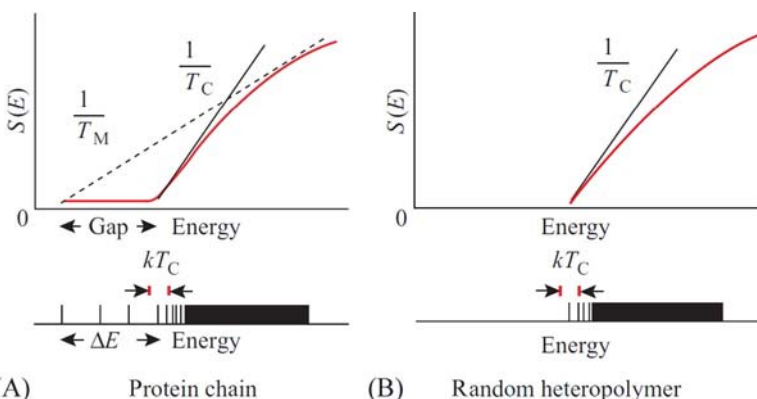


FIG. 18.6 Tentative dependence of the entropy S on the energy E for (A) the protein chain and (B) for a random heteropolymer. Typical energy spectra are shown below. Each spectrum line (only a few of them can be shown) corresponds to one chain conformation (more precisely, to one local energy minimum of the conformational space). The right, high-energy part of each spectrum has plenty of such lines, and they merge into a virtually continuous spectrum. The main peculiarity of the spectrum of protein (the “selected” heteropolymer) is a large energy gap ($\Delta E \gg kT_C$) between the lowest-energy fold and other “misfolded” structures. The energies of only a few structures get into this “gap”; some of them are somewhat disordered or nearly folded variants of the lowest-energy fold. The tangent touching the lower part of the $S(E)$ curve to the right of the gap determines the temperature T_C of chain vitrifying [the same temperature, by the way, appears in the statistics of protein structures (Finkelstein et al., 1995)]. The tangent is touching also the lowest-energy fold; the slope of this tangent determines the temperature T_M of protein melting (the temperature of coexistence of the lowest-energy structure and a multitude of high-energy ones). Since the slope of the latter is somewhat less than that of the former, $1/T_M < 1/T_C$, that is, $T_M > T_C$. This means that cooling of the protein (ie, a chain with a large “energy gap” ΔE) leads to “all-or-none” freezing of its lowest-energy structure prior to vitrifying of the chain, that is, prior to freezing of misfolded structures corresponding to the high-energy side of the gap. A typical random heteropolymer (a chain having no “gap”), on the contrary, has only a vitrifying transition.

(Their energy spectrum is very dense, virtually continuous: the spectrum width is proportional to the number of residues N , while the number of structures is at least $\sim 2^N$ in order of magnitude, since each residue can have more than one conformation.)

It is just the “energy gap” between the native structure and its numerous high-energy competitors (see Appendix D) that creates a *free energy barrier* between them. This barrier corresponds to the concave $S(E)$ region. As we have learned, the free energy in such a region is higher than at the ends. It is the “gap” that makes $S(E)$ concave, thereby ensuring the protein’s tolerance to heating up to a certain temperature with subsequent melting through an “all-or-none” transition. A few “nearly correctly folded” structures, whose energies get into the gap play no role in the thermodynamics of this transition but are very important for its kinetics (as we will see later) as well as for thermal fluctuations of the lowest-energy structure.

Two peculiar temperatures are determined by the energy spectrum. These are the melting temperature T_M and the critical vitrifying temperature T_C . The melting temperature T_M is determined by the coexistence of the “abnormally stable” lowest-energy structure and a multitude of high-energy ones (see Fig. 18.6A). The vitrifying temperature T_C is determined by the rise of the $S(E)$ curve just after the “gap” (Fig. 18.6A), that is, by the abrupt increase in the entropy of “misfolded” structures (or simply, in their number) at the low-energy end of the dense energy spectrum (see Appendix D).

If it were not for the jump over the “gap” to the native fold, a temperature decrease would lead to vitrifying of the chain in the ensemble of the low-energy misfolded structures at T_C . This is typical of glasses with very complicated and eroded energy landscapes in the region of low energies (Frauenfelder, 2010). This is also typical of random heteropolymers (Gutin and Shakhnovich, 1993; Sfatos et al., 1993) that do not have “abnormally stable” fold and the “gap” (or rather, as the physical theory states (see Appendix D), only have a very narrow gap, about kT_C , see Fig. 18.6); their low-energy folds can be rather various. Vitrification is not what happens to the protein: its lowest-energy fold—or rather, a set of very similar folds (Frauenfelder, 2010)—one must not take Fig. 18.6 too literally... is separated from misfolded structures by the energy gap. As the temperature is decreased, the protein chain jumps to its lowest-energy fold (or rather, a set of very similar folds) before vitrifying—at the freezing (=melting) temperature T_M which is above T_C (see Fig. 18.6A). The same figure (and Appendix D) shows that T_M is close to T_C if the “gap” is not too wide, and that $T_M = T_C$ when the gap is absent or close to kT_C in width.

This means that the “all-or-none” protein melting needs a sufficiently broad energy gap (with a width of $\Delta E \gg kT_C$) between the lowest-energy fold and the bulk of “misfolded” structures, and that this energy gap is a privilege of selected, “protein-suitable” chains only. Only such chains allow a unique stable fold, and this fold is both formed and protected against gradual softening by the “all-or-none” transition.

It seems that natural selection picks up such sequences because of their unique ability to form solid protein globules with fixed 3D structures: only among them can it find those capable of reliable functioning (as substrate-specific enzymes, etc.) in the organism.

The fraction of random heteropolymers with an energy gap of the given width ΔE is obtained from the extrapolation of the low-energy side of the $S(E)$ curve for random heteropolymers to the still lower energies. The result is:

$$\text{FRACTION}(\Delta E) \sim \exp(-\Delta E/kT_C). \quad (18.1)$$

This fraction is quite small when the gap is pronounced ($\Delta E \gg kT_C$), which is reasonable: protein creation is not at all easy. However, this fraction is not negligible: if $\Delta E \approx 20kT_C$, that is, $\approx 10\text{--}15 \text{ kcal mol}^{-1}$ (which is plenty to create a reliable barrier between the native fold and its competitors), this fraction amounts to $\sim 10^{-9}$.

Modern experimental methods in molecular biology (eg, the phage display method; Pande et al., 2010) are, in principle, able to select such a small fraction of polypeptides provided they can acquire some structure and become capable of strong binding to something. Therefore, it is no great surprise that some recent experiments with random polypeptides proved to be able to produce “protein-like” molecules (see, eg, Keefe and Szostak, 2001; Pande et al., 2010). By the way, these experiments can do what, by now unfortunately, has not been done by physical experiment: they can help to establish the width of the energy gap ΔE using Eq. (18.1).

Experiments (Keefe and Szostak, 2001) show that “protein-like” molecules amount to 10^{-11} of random polypeptides; thus, $\Delta E \approx 20kT_C$ or (because $T_C \approx T_M$, see below, and the protein melting temperature $T_M \approx 350$ K) $\Delta E \approx 10\text{--}15$ kcal mol⁻¹.

It is noteworthy that the theory yielding Eq. (18.1) also predicts that it is much harder to produce a chain that can stabilize two (or more) different folds. The gap ΔE (that separates the lowest-energy fold from its competitors) occurs in $\sim \exp(-\Delta E/kT_C)$ fraction of “random” chains, but the gap of the same width that separates two folds from their competitors occurs in $\sim \exp(-2\Delta E/kT_C)$ of “random” chains only. In other words, to make a chain with one native fold is a wonder, to make a chain with two native folds is a squared wonder, with three a cubed wonder, and so on... Therefore, it is no surprise that there are almost no proteins having alternative native structures (here I am speaking of course about really different structures, not about small thermal or functional deformations; and I say “almost,” because there are some “chameleon” proteins that have different native folds in associated and not associated states or in different environments, and at least one protein—serpin—that slowly passes from its active to its inactive fold (Stein and Chothia, 1991; Tsutsui et al., 2012) without any association with other molecules or change of the environment; we will come to this protein when discussing protein folding).

The T_C value does not depend on the gap width, that is, on the existence of the native fold. It depends on the distribution of many nonnative structures over energy. Thus, it has to be the same for random sequences and for protein sequences equal in amino acid content. And it is remarkable that the same T_C appears (but see Eq. 18.1) in protein statistics that we discussed a few lectures ago.

[Fig. 18.6](#) (and Appendix D) shows that T_C has to be only a little lower than the protein melting temperature T_M if the ΔE value is relatively low. However, it seems that very wide energy gaps, that is, very large ΔE values, are not necessary for “protein-like” behavior of the chain. Therefore, natural selection must not seek too large ΔE values, and hence, these have to be highly improbable according to Eq. (18.1). It is now a question of experiment.

The energy gap is fundamental for protein physics. It is this gap that provides the reliability of a protein’s biological functioning: without it, the protein would not be able to tolerate a change of ambient conditions without changing

its fold. After a few lectures you will see that the gap is necessary for rapid and reliable folding of a protein structure (and it is quite possible that this determines the appropriate ΔE value). Therefore, an experimental estimate of this gap (and of temperatures T_C , T_M) would be most interesting. Alas, this has not yet been done in physical experiments—and measuring this gap is a challenge to protein physics.

REFERENCES

- Branden, C., Tooze, J., 1999. Introduction to Protein Structure, second ed. Garland Publishing, Inc., New York (Chapter 6).
- Dolgikh, D.A., Gilmanshin, R.I., Brazhnikov, E.V., Bychkova, V.E., Semisotnov, G.V., Venyaminov, S.Yu., Ptitsyn, O.B., 1981. Alpha-lactalbumin: compact state with fluctuating tertiary structure? FEBS Lett. 136, 311–315.
- Finkelstein, A.V., Shakhnovich, E.I., 1989. Theory of cooperative transitions in protein molecules. II. Phase diagram for a protein molecule in solution. Biopolymers 28, 1681–1694.
- Finkelstein, A.V., Gutin, A.M., Badretdinov, A.Ya., 1995. Boltzmann-like statistics of protein architectures. Origins and consequences. In: Biswas, B.B., Roy, S. (Eds.), Subcellular Biochemistry. Proteins: Structure, Function and Protein Engineering. vol. 24. Plenum Press, New York, pp. 1–26.
- Frauenfelder, H., 2010. The Physics of Proteins. An Introduction to Biological Physics and Molecular Biophysics. Springer, New York (Chapters 11, 12, 14).
- Gutin, A.M., Shakhnovich, E.I., 1993. Ground state of random copolymers and the discrete random energy model. J. Chem. Phys. 98, 8174–8177.
- Jennings, P.A., Wright, P.E., 1993. Formation of a molten globule intermediate early in the kinetic folding pathway of apomyoglobin. Science 262, 892–896.
- Jha, S.K., Udgaonkar, J.B., 2009. Direct evidence for a dry molten globule intermediate during the unfolding of a small protein. Proc. Natl. Acad. Sci. U. S. A. 106, 12289–12294.
- Keefe, A.D., Szostak, J.W., 2001. Functional proteins from a random-sequence library. Nature 410, 715–718.
- Kharakoz, D.P., Bychkova, V.E., 1997. Molten globule of human alphasalbutamol: hydration, density, and compressibility of the interior. Biochemistry 36, 1882–1890.
- Muñoz, V., Sadqi, M., Naganathan, A.N., de Sancho, D., 2008. Exploiting the downhill folding regime via experiment. HFSP J. 2, 342–353.
- Pande, J., Szewczyk, M.M., Grover, A.K., 2010. Phage display: concept, innovations, applications and future. Biotechnol. Adv. 28, 849–858.
- Pfeil, W., Bychkova, V.E., Ptitsyn, O.B., 1986. Physical nature of the phase transition in globular proteins: calorimetric study of human alpha-lactalbumin. FEBS Lett. 198, 287–291.
- Privalov, P.L., 1979. Stability of proteins: small globular proteins. Adv. Protein Chem. 33, 167–241.
- Privalov, P.L., 1982. Stability of proteins. Proteins which do not present a single cooperative system. Adv. Protein Chem. 35, 1–104.
- Ptitsyn, O.B., 1995. Molten globule and protein folding. Adv. Protein Chem. 47, 83–229.
- Samatova, E.N., Katina, N.S., Balobanov, V.A., Melnik, B.S., Dolgikh, D.A., Bychkova, V.E., Finkelstein, A.V., 2009. How strong are side chain interactions in the folding intermediate? Protein Sci. 18, 2152–2159.
- Schulz, G.E., Schirmer, R.H., 1979, 2013. Principles of Protein Structure. Springer, New York (Chapter 8).

- Sfatos, C.D., Gutin, A.M., Shakhnovich, E.I., 1993. Phase-diagram of random copolymers. *Phys. Rev. E.* 48, 465–475.
- Shakhnovich, E.I., Finkel'shtein, A.V., 1982. The theory of cooperative transitions in protein globules. *Dokl. Akad. Nauk SSSR* 267, 1247–1250 (in Russian).
- Shakhnovich, E.I., Finkelstein, A.V., 1989. Theory of cooperative transitions in protein molecules. I. Why denaturation of globular protein is a first-order phase transition. *Biopolymers* 28, 1667–1680.
- Stein, P., Chothia, C., 1991. Serpin tertiary structure transformation. *J. Mol. Biol.* 221, 615–621.
- Tanford, C., 1968. Protein denaturation. *Adv. Protein Chem.* 23, 121–282.
- Tsutsui, Y., Cruz, R.D., Wintrode, P.L., 2012. Folding mechanism of the metastable serpin $\alpha 1$ -anti-trypsin. *Proc. Natl. Acad. Sci. U. S. A.* 109, 4467–4472.
- Ubbelohde, A.R., 1965. Melting and Crystal Structure. Clarendon Press, Oxford (Chapters 2, 5, 6, 10–12, 14, 16).
- Uversky, V.N., Ptitsyn, O.B., 1996a. All-or-none solvent-induced transitions between native, molten globule and unfolded states in globular proteins. *Fold. Des.* 1, 117–122.
- Uversky, V.N., Ptitsyn, O.B., 1996b. Further evidence on the equilibrium “pre-molten globule state”: four-state guanidinium chloride-induced unfolding of carbonic anhydrase B at low temperature. *J. Mol. Biol.* 255, 215–228.
- Uversky, V.N., Semisotnov, G.V., Pain, R.H., Ptitsyn, O.B., 1992. “All-or-none” mechanism of the molten globule unfolding. *FEBS Lett.* 314, 89–92.

Lecture 19

In this lecture, we will see how protein folding proceeds in time, and consider kinetic intermediates of protein folding. I will talk mainly about water-soluble globular proteins which demonstrate a spontaneous folding. Folding of membrane proteins is much less studied; it often is not a spontaneous folding; I have already touched on it. For all these reasons, I will consider membrane proteins only briefly. Folding of fibrous proteins is better studied, though at the biochemical rather than physical level; usually, it is not spontaneous either; we have considered this already when speaking about collagen.

We will start with various aspects of experimental studies of protein folding *in vivo*, or nearly *in vivo*.

In a living cell, protein is synthesized by a ribosome. The whole life cycle of a bacterium can take only 20 min; the biosynthesis takes about 1 min and yielding of a “ready” folded protein lasts as long: experiments do not detect any difference (Creighton, 1993; Stryer, 1995). Therefore, it may be reasonable to assume that protein chain folding starts on the ribosome before protein chain synthesis is completed.

Unfortunately, reliable experimental data on protein folding *in vivo* (in the cell) were quite scarce until recently: it was (and still is) extremely difficult to see a structural transformation of a nascent protein chain against the background of thick cell “soup.” Usually people have to stop the biosynthesis, to extract the nascent protein and to study it separately. All this takes time, many minutes, during which the three-dimensional (3D) structure of the protein chain can change.

A number of experiments of this kind on large proteins showed that their N-terminal domains are able to fold before the biosynthesis of the whole chain is completed.

I have to stress, though, that these data refer to *multi-domain* proteins; this is an important qualification, since the above mentioned *in vivo* and numerous *in vitro* experiments (as discussed later) show that the “folding unit” is a protein domain rather than the whole protein. A “semi-folded” domain is usually not observed, and we cannot say whether its N-terminal half folds before the C-terminal half.

There are two groups of evidence (provided by *in vitro* rather than *in vivo* experiments) that the folding unit is a domain. On the one hand, separate domains are usually capable of folding into the correct structure (Petsko and Ringe, 2004). On the other hand, single-domain proteins usually cannot fold when as few as 10 of their C- (or N-) terminal amino acids are deleted (Flanagan et al., 1992; Neira and Fersht, 1999a,b).

On the other hand, though, it has been shown (Komar et al., 1997) that a globin chain can bind the heme when only slightly more than its half has been synthesized by the ribosome in a cell-free system (Baranov and Spirin, 1993; Kolb et al., 1994). Globin is a single-domain protein from both structural and thermodynamic points of view (the latter means that its denaturation is of the “all-or-none” type in vitro) (Privalov, 1979); its N-terminal half forms a compact sub-domain where the heme binding site is located; we have seen its structure when talking on α -helical proteins.

Some other interesting experimental data on protein folding have also been obtained using biosynthesis in a cell-free system (ie, not entirely in vitro, but not entirely in vivo). This system includes ribosomes, tRNAs, mRNA, and other factors necessary for matrix synthesis of a protein.

It is not out of place to mention again here that the terms “in vivo” and “in vitro” are often understood differently by physicists and biologists. Strictly speaking, between the pure “in vivo” and the pure “in vitro” there are a number of ambiguous steps. For example, protein folding in a cell-free system (with all its ribosomes, initiation factors, chaperones, etc.) is unequivocally an “in vivo” experiment in the physicist’s view (for him, “in vitro” would be a separate protein in solution; as to the cell-free system ... it contains too many complicating life realities). But for a biologist, this is undoubtedly an “in vitro” experiment (since “in vivo” is referred, for him, to a living and preferably intact organism). However, structural studies of a separate protein in an organism are hardly possible. Therefore, reasonable people compromise by making biologically significant “in vivo” events accessible for experimental “in vitro” studies.

Unfortunately, it is difficult to see the structure of a nascent protein chain (against the background of the huge ribosome) even in the cell-free system. But, if lucky, one can watch the activity of the synthesized protein.

Luciferase provides such a lucky opportunity. Having folded into its native structure, this protein catalyzes the light-emitting reaction. Therefore, it is easy to observe its appearance: nothing else but the native luciferase emits light in the cell. In their study on luciferase folding and activity, Kolb, Makeev, and Spirin from our Protein Research Institute, RAS, have shown (Kolb et al., 1994) that the first active protein appears 10 min after switching on its synthesis in a cell-free system, and that it abruptly stops appearing when its synthesis is switched off (Fig. 19.1). This means that there is virtually no *already* synthesized but *yet not* folded luciferase molecules, that is, folding of this large protein (comprising more than 500 residues in two structural domains) occurs either during biosynthesis or immediately after it.

However, most up-to-date experiments on co-translational structure acquisition of nascent polypeptides monitored by nuclear magnetic resonance (NMR) spectroscopy have shown that “polypeptides [at a ribosome] remain unstructured during elongation but fold into a compact, native-like structure when the entire sequence is available” (Eichmann et al., 2010) and that “... folding [occurs] immediately after the emergence of the full domain sequence ...

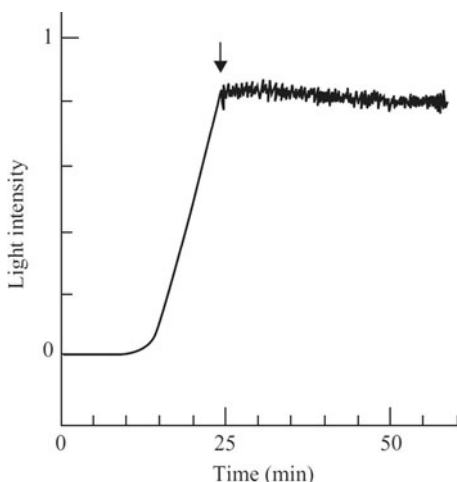


FIG. 19.1 Light emission by luciferase synthesized in a cell-free system. Time “0”: biosynthesis is switched on. Light emission stops increasing as soon as biosynthesis is switched off (denoted by arrow). (Adapted from Kolb, V.A., Makeev, E.V., Spirin, A.S., 1994. Folding of firefly luciferase during translation in a cell-free system. *EMBO J.* 13, 3631–3637, with permission from A.S. Spirin.)

displaying two epitopes simultaneously when the full sequence is available” ([Han et al., 2012](#)). In these experiments, the ribosome synthesis of ^{15}N , ^{13}C -labeled chains of small proteins was stopped at several points, and structures of these not wholly synthesized chains were studied by NMR. Because the nascent chains were ^{15}N , ^{13}C -labeled, NMR could distinguish their structures from those of all other constituents of the biological soup. The experiments by [Han et al. \(2012\)](#) used even intact mammalian cells. The incompletely synthesized chains failed to form a specific (solid) spatial structure both when hanging on the ribosome and when released from it.

Thus, incompletely synthesized protein chains behave at the ribosome in the same way as truncated protein chains lacking only several C-terminal (or N-terminal) amino acid residues *in vitro*. These truncated chains showed that significant stable native-like conformations are present only in polypeptide chains with length close to the size of the full-length protein ([Flanagan et al., 1992](#); [Neira and Fersht, 1999a,b](#)): they show low levels of native-like secondary structure, do not melt cooperatively with temperature, and do not form a specific, solid 3D structure (which does not rule out formation of the molten globule by them).

Co-translational folding, that is, the folding of a nascent chain while it is still attached to the ribosome, is of special interest at present because of the tremendous progress being made in defining the structure of the ribosome at atomic resolution and in elucidating the structure of a small nascent protein against the background of the giant ribosome.

To study not only the result, but also the process of protein folding, one has to carry out “pure” *in vitro* studies (without any ribosomes, chaperones, etc.), that is, to study protein folding in solution.

In about 1960, a remarkable discovery was made ([Anfinsen et al., 1961](#); [Anfinsen, 1973](#)): it was shown that a globular protein is capable of spontaneous folding *in vitro* (renaturation) if its chain has not been heavily chemically modified after the initial (*in vivo*) folding. In such a case, a protein that has been gently unfolded by temperature, denaturant, etc. (without damage to the chain) spontaneously restores its activity and structure after solvent “normalization.” True, the effective renaturation requires a careful selection of experimental conditions; otherwise, aggregation can prevent the protein from folding.

The Anfinsen’s discovery was that it is the amino acid sequence that determines protein conformation.

Inner voice: Is it possible that some features of the native structure are preserved even in the denatured protein, and these residual structures, “remembered” from the *in vivo* folding, direct the *in vitro* protein folding to the right pathway?

Lecturer: No, it is not, if the protein is denatured properly. I mean, if native S–S bonds are disrupted and if the memory of native (*cis*- or *trans*-) states of prolines is erased (which occurs in a few minutes after unfolding), and if the denaturant is strong enough to destroy the secondary structure and to disrupt other non-covalent contacts, ie, to convert the chain into the coil so that its volume increases many-fold. All this can be checked experimentally (see [Tanford et al., 1967](#); [Lapanje and Tanford, 1967](#); [Tanford, 1968](#); [Anfinsen, 1973](#)). And the protein still renatures ...

Inner voice: However, there are reliable data—in particular, by [Lietzow et al. \(2002\)](#) and [Basehore and Ropson \(2011\)](#)—on preservation of some native contacts even in a quite unfolded protein chain!

Lecturer: There are such data; they concern mainly contacts between residues which are more-or-less close in the chain (if proteins with preserved S–S bonds are not taken into account). The question is, however: are these contacts inherited from the native protein fold and “frozen,” or are they occasionally formed spontaneously in the unfolded chain? Unfortunately, NMR (which is the main source of information about these contacts) cannot distinguish “frozen” contacts from those formed spontaneously from time to time. The point is that the NMR signal decreases as R^{-6} with increasing contact distance R . Therefore, the same signal is produced by a contact having $R = 4.5 \text{ \AA}$ and existing for 100% of the time, and a contact having $R = 3 \text{ \AA}$ and existing for 10% of the time. I do not see any physical forces which can freeze contacts between non-neighbor residues in unfolded protein chain (if preserved covalent S–S bonds are not considered, of course). I think that the contacts we are discussing are sometimes formed spontaneously between those unfolded

chain regions that attract each other (and let me remind you that a native protein structure typically contains just those contacts that give sufficient stability by themselves). The same consideration refers, I think, to the “residual” secondary structure sometimes observed by circular dichroism (CD).

As already mentioned, the phenomenon of a spontaneous protein folding was discovered by Anfinsen’s team in 1961. This phenomenon was first established for bovine ribonuclease: its biochemical activity and its correct S–S bonds were restored (after complete unfolding of the protein and disruption of all its S–S bonds) when the protein chain was placed again into the “native” solvent.

Later, numerous research groups dealing with a great many other proteins experimentally confirmed this discovery. Furthermore, it was demonstrated ([Gutte and Merrifield, 1969](#)) that a protein chain synthesized chemically, without any cell or ribosome, and placed in the proper ambient conditions, folds into a biologically active protein.

The phenomenon of spontaneous folding of protein native structures allows us to detach, at least to a first approximation, the study of protein folding from the study of its biosynthesis.

Protein folding *in vitro* is the simplest (and therefore, the most interesting to me as a physicist) case of pure *self-organization*: here there is nothing “biological” (but for the sequence) to help the protein chain to fold. As a matter of fact, self-organization of the unique 3D structures of proteins (and RNAs) is a physical phenomenon having no close analogs in inanimate nature. However, this self-organization resembles the formation of crystals (but very peculiar crystals: with no regular space lattice, very complicated and very small).

From the mathematical point of view, this self-organization belongs to the “order from order” class (according to Prigogine’s classification): the protein structure emerges as a 3D “aperiodic crystal” (in Schrödinger’s wording) from the order of amino acid residues in its chain. Notice that the self-organization of 3D structures of proteins (and RNAs, and crystals) results from the tendency to thermodynamic stability, which distinguishes this self-organization from the more widely discussed self-organization of the “order from disorder” class (existing in oscillating Belousov-Zhabotinsky chemical reactions, in ecological “predator-prey” systems, etc.), which occurs in non-equilibrium systems at the cost of energy flow.

However, before beginning to consider the physics of protein folding *in vitro*, I would like to come back to the cell and to remind you briefly of the machinery that is used by a cell to increase the efficiency of protein folding under the conditions faced by a nascent protein chain in the cell.

A ribosome makes a protein chain residue by residue, from its N- to its C-end, and not quite uniformly: there are pauses, temporary pauses in the synthesis at the “rare” codons (they correspond to tRNAs, which are rare in the cell, and these codons are rare in the cell’s mRNAs, too). It is assumed that the pauses may correspond to the boundaries of structural domains, that can help a quiet

maturation of the domain structures (Komar, 2009). But this speculation is quite questionable in the light of already discussed novel experiments that demonstrate resemblance of protein folding *in vivo* and *in vitro*.

Some enzymes, like prolyl peptide isomerase or disulfide isomerase accelerate *in vivo* folding. The former catalyzes slow, if unaided, *trans* ↔ *cis* conversions of prolines; in some cases, this is the rate-limiting step of the *in vitro* folding. The latter catalyzes the formation and decay of S–S bonds (Kersteen, 2005).

The next point to consider is that in the cell, a protein chain folds under the protection of special proteins, chaperones. Chaperones are the cell's trouble-shooters; their main task is to fight the consequences of aggregation (Ellis and Hartl, 1999; Hardesty et al., 1999) (which would be only natural in a thick and crowded cell "soup").

The phenomenon of macromolecular crowding attracted a significant attention during last decades (Ellis, 2001); crowding can alter the properties of macromolecules at their high concentration (in the cell, they occupy ~30% of the volume). It is often believed that this effect (which can stimulate protein folding, oligomerization or aggregation) results from the conformational entropy, which is affected by decrease of the volume available for molecules in the crowded solution (Zimmerman and Trach, 1991). For a physicist, this opinion sounds strange, because it virtually ignores another, much stronger effect: namely, innumerable, large and various macromolecular surfaces that each macromolecule can meet in a crowded environment—and bind to them. This binding can be entropy-driven (remember hydrophobic and electrostatic forces!); but there is some evidence that the crowding effect is driven by enthalpy, not entropy (Benton et al., 2012).

As to me, I would rather consider "crowding" as an effect similar to aggregation (which is the main obstacle for *in vitro* folding) or amyloid formation (which often occurs when proteins occupy 0.1–1% of the volume or less, and thus are connected with binding and have nothing to do with excluded volume).

Many chaperones are produced in response to heat shock, since a rise in temperature intensifies the hydrophobic forces causing aggregation.

It seems that the molten globule is a key element here: it seems to appear in the process of biosynthesis and then it is protected by the chaperones against aggregation (Dobson, 1994, 2003).

Protein aggregation in a cell often leads to the formation of "inclusion bodies" where the proteins do not have their native structures (specifically, their S–S bonds are formed randomly). However, the "correct" native protein can be obtained after dissolving the inclusion bodies and subsequently allowing protein renaturation *in vitro* (Singh and Panda, 2005).

A more complicated chaperone-like machinery is used in folding of membrane proteins (Kim et al., 2012); it contributes to their proper passing through the membrane; this has been shortly discussed already.

“Small” chaperones, like hsp70 (heat shock protein, of 70 kDa), bind to a nascent protein to protect it against aggregation, and then they dissociate from the protein (at the cost of ATP consumption). “Large” chaperones, also called “chaperonins,” such as GroEL/GroES (in bacteria) or TRiC (in eukaryotes), work mainly with multi-domain proteins, and especially with proteins whose domains are composed of remote chain regions. The “large” chaperonin GroEL (it consists of 14 subunits, 60 kDa each) belongs to the hsp60 family. The sub-units form a kind of nano-test-tube (a few nanometers in diameter), with two co-chaperonins GroES as two lids that sometimes come to GroEL, sometimes go away. It is widely assumed that the nascent protein or rather its domain (initially covered with hsp70 and/or hsp40 chaperones) comes into this tube. However, it seems that encapsulation is not an absolute requirement for successful re/folding (Farr et al., 2003). According to Marchenko et al. (2009), Marchenkov and Semisotnov (2009) the unfolded, or rather, not folded protein chain binds in vitro to the very edge of the cavity. It is assumed that this “tube” (sometimes called the “Anfinsen cage”) protects the nascent protein against aggregation and against the action of the cell “soup” with all its proteases, etc., thereby ensuring undisturbed protein folding. GroEL undergoes some conformational changes increasing and decreasing its hydrophobic surface, ie, the “test-tube” “shakes” from time to time, and the GroES lid closes and opens (all this at the cost of ATP consumption). The chaperone lets the protein go only when it is already folded and has ceased sticking to the “tube.” Thus, chaperones are assumed to work as “incubators” of protein folding.

The old idea that chaperons may direct the folding process and determine the final tertiary structure of a protein is now abandoned—as far as the water-soluble globular proteins are concerned; as for some membrane proteins, their penetration through the membrane seems to be indeed directed by a kind of chaperone machinery (though the word “chaperone” is not used just in this case—I do not know why). However, an intriguing question is whether chaperones catalyze, ie, accelerate protein folding.

Actually, chaperones must be very peculiar catalysts (if they are catalysts at all). For example, GroEL, which works for far from all proteins but mostly for large ones, constitutes 1% of the total protein mass in a normally living cell, and this number grows up to 10% at heat shock (Herendee et al., 1979). Thus, each GroEL molecule can shape, over all its life span, only a few other proteins, while a normal enzyme processes thousands other molecules per second (Hagen, 2006) (though one cannot rule out the possibility that GroEL has to reshape other proteins many times because they denature in the cell once and again).

The idea that chaperones (eg, the above mentioned GroEL) may have an intrinsic foldase/unfoldase activity is supported by many scientists (see, eg, Libich et al., 2015, and literature therein). And indeed, Libich et al. have shown that GroEL does accelerate *one* of the folding steps, namely, interconversion of

partly and completely folded forms of a protein. However, a thorough analysis of kinetic data reported by Libich et al. revealed strict evidence that, contrary to the authors' statement, GroEL *cannot* accelerate the overall folding process (Marchenko et al., 2015) because another step of the GroEL-assisted folding, namely, the GroEL binding to a protein, is slow. As a result, the GroEL-assisted folding is slower (even with highest GroEL concentrations obtained at a heat shock) than the GroEL-*unassisted* folding (and it remains unclear how the observed fast, at GroEL, interconversion of partly and completely folded forms of a protein is used by the cell)!

The experimental results by Libich et al. (2015) and their analysis by Marchenko et al. (2015) challenge a widely spread dogma that chaperonins make proteins fold faster, and corroborate the conclusion that apo GroEL is *not* a catalyst of protein folding and, possibly, it serves as a transient trap that binds excess unfolded protein chains, thus preventing them from irreversible aggregation.

The works by Semisotnov's team suggest (Marchenkov et al., 2004; Marchenko et al., 2009) that GroEL rather acts as a “buffer” that binds redundant non-folded proteins and removes them from solution, which allows the remaining ones to avoid aggregation and fold correctly (though slowly) by themselves. Thus, this chaperone works rather as an “incubator” (but not a catalyst) of folding. And, as it has been shown by studies of Spirin's team (Svetlov et al., 2006), some chaperones can work also as “freezers” that postpone folding up to the time when the protein is to be assembled into a quaternary structure or is transported to a proper place of the cell.

The folding of nascent peptides may possibly occur in the sheltered ribosomal environment, in which (many researchers believe) they are protected from aggregation and degradation. Moreover, there is some (incomplete) evidence that ribosomes and some of their components can function as molecular chaperones to mediate and accelerate the refolding of denatured proteins.

It looks as though, then, that the biosynthetic machinery of the cell (ribosomes + chaperones + ...) not only ensures synthesis of the protein chain but also serves as a kind of incubator that helps folding of 3D protein structures. This “incubator” does not determine the protein structure, though, but rather provides “hothouse” conditions for its maturation—just like a normal incubator, which helps a nestling to develop but does not determine whether a chicken or a duckling will be developed. And, now there is no reason to assume that anything other than the amino acid sequence alone (and, of course, the environment and posttranslational chemical modifications) determines protein conformation in the cellular environment.

Numerous experiments on *in vitro* protein folding show (Anfinsen, 1973; Fersht, 1985, 1999; Matouschek et al., 1990; Stryer, 1995) that the work of the whole cellular machinery can be replaced by careful selection of the experimental conditions (a low protein concentration, a suitable redox potential, etc.). This substitution does not change the result of the chain folding: if the protein folds rather than precipitates *in vitro*, then the resultant native structure is the

same as in vivo folding yields. True, this can take more time (or much less, for some small proteins) than in vivo folding, but the *result* is the same. Moreover, as I have already mentioned, it has been shown that the chain of a small protein can be synthesized in a test-tube by purely chemical methods, and this chain folds into a correct native (and active) 3D structure. All this proves that all the information necessary to build up the 3D protein structure is inscribed in its amino acid sequence.

Inner voice: All that you have just said about the in vitro refolding refers mostly to small water-soluble globular proteins or to the separate domains of large proteins. They usually renature easily, that's true. However, to be frank, you have to say that one faces far greater difficulties when dealing with whole large proteins, especially with those from higher organisms: far from all of them renature spontaneously. As for the spontaneous renaturation of membrane and fibrous proteins, this only happens with some of them; usually their complete renaturation cannot be obtained ...

Lecturer: Concerning the proteins that are “difficult” for renaturation, I would suggest that aggregation is the common major obstacle (eg, some membrane proteins renature in detergents and do not fold in water because of aggregation). Multi-domain proteins can also experience “aggregation” of remote chain regions which is absent in vivo since ribosomal synthesis allows folding of the N-terminal domains prior to synthesis of the C-terminal domains. Also, refolding difficulties caused by post-folding modifications should not be neglected, especially for eukaryotic proteins. Let us agree that for now I am considering relatively small water-soluble proteins and let us understand the folding of these first.

The fundamental physical problem of spontaneous folding of proteins (and RNA, by the way) has come to be known as the Levinthal paradox ([Levinthal, 1968, 1969](#)). It reads as follows: on the one hand, the same native state is achieved by various folding processes: in vivo on the ribosome, in vivo after translocation through the membrane, in vitro after denaturation with various agents ... The existence of spontaneous renaturation and the correct folding of chemically synthesized protein chains suggests that the native state is thermodynamically the most stable state under “biological” conditions. On the other hand, a chain has zillions of possible conformations (at least 2^{100} for a 100-residue chain, since at least two conformations, “right” and “wrong,” are possible for each residue; the estimate 3^{100} for a 100-residue chain looks more reasonable for a physicist, since each residue has at least three well-defined energy minima: α -right, α -left, β). And the protein can “feel” the correct stable structure only if it is achieved exactly this conformation, since even a 1 Å deviation can strongly increase the chain energy in a closely packed globule. Thus, the chain needs *at least* $\sim 2^{100}$ (or rather $\sim 3^{100}$) picoseconds, that is $\sim 10^{10}$ (or rather $\sim 10^{25}$) years to sample all possible conformations in its search for the most stable fold (while $\sim 10^{10}$ years is the age of our Universe!).

So, how can the chain find its most stable structure within a “biological” time (minutes)?

The paradox is that, on the one hand, the achievement of the same (native) state by a variety of processes is (in physics) clear-cut evidence of its stability. On the other hand, Levinthal’s estimate shows that the protein simply does not have enough time to prove that the native structure is the most stable among all possible structures!

Then, how does the protein chain choose its native structure among zillions of others, asked Levinthal, and answered: It seems that there exists a specific folding pathway, and the native fold is simply the end of this pathway rather than the most stable chain fold. Should this pathway be narrow, only a small part of the conformational space would be sampled, and the paradox would be avoided.

In other words, Levinthal suggested that the native protein structure is under kinetic rather than under thermodynamic control, ie, that it corresponds not to the global but rather to the easily accessible free energy minimum.

The question as to whether the protein structure is under kinetic or thermodynamic control is not a purely speculative question. It is raised again and again when one faces practical problems of protein physics and engineering. For example: when trying to predict a protein structure from its sequence, what do we have to look for? The most stable or the most rapidly folding structure? When designing a de novo protein, what do we have to do? To maximize the stability of the desired fold or to create a rapid pathway to this fold?

A discussion on protein folding mechanisms started immediately after solution of the first 3D protein structures and the discovery of spontaneous folding and lasts even today. The Levinthal paradox was not for nothing called “the Fermat’s last theorem of protein science” by Eugene Shakhnovich. It seems that the first proposed hypothesis was that by [Phillips \(1966\)](#), who suggested that the folding nucleus is formed by the N-end of the nascent protein chain, and that the remaining part of the chain wraps around it. In various forms this appealing hypothesis is present in some works up to now. However, this hypothesis has been refuted experimentally (as far as single-domain proteins are concerned). The elegant works of [Goldenberg and Creighton \(1983, 1984\)](#) have shown that the N-terminus has no special role in in vitro folding. It was demonstrated that it is possible to glue the ends of the chain of a small protein (trypsin inhibitor) with a peptide bond, and it folds into the correct 3D structure, nevertheless. Moreover, it is possible to cut this circular chain so as to make a new N-end at the former middle of the chain; and it still folds to the former native structure. Nowadays, protein engineering routinely produces circularly modified proteins ([Fersht, 1999](#)).

In an effort to solve the folding problem, O.B.P. proposed model of sequential protein folding ([Ptitsyn, 1973](#)) ([Fig. 19.2](#)). Later given the name of a “framework model,” this hypothesis stimulated further investigation of folding intermediates. It postulated a sequential involvement of different interactions

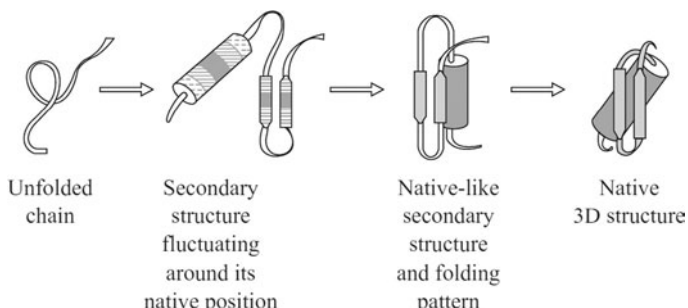


FIG. 19.2 Framework model of sequential protein folding according to Ptitsyn (1973). The secondary structures are shown as *cylinders* (α -helices) and *arrows* (β -strands). Both predicted intermediates have already been observed; the first is now known as the “pre-molten globule” and the other as the “molten globule.”

and structures in protein structure formation, stressing the importance of rapidly folded α -helices and β -hairpins in the initial folding steps, the gluing of these helices and hairpins into a native-like globule, and the final crystallization of the structure within this globule at the last step of folding.

The cornerstone of this concept was the then hypothetical and now a well-known folding intermediate, the “molten globule” (Dolgikh et al., 1984; Dobson, 1994; Ptitsyn, 1995).

The theoretically predicted molten globule was experimentally discovered and studied by Dolgikh, Semisotnov, Gil'manshin, Bychkova, and others at the laboratory of O.B.P. in the 1980s—first as the equilibrium state of a “weakly denatured” protein (Dolgikh et al., 1981; Gil'manshin et al., 1982) (I mentioned this in my previous lectures), and then as a kinetic folding intermediate (Dolgikh et al., 1984).

The molten globule is assembled in the course of the folding of many proteins. In the experiments shown (Fig. 19.3), the initial coil state is obtained by incubation of a protein in solution with a high denaturant concentration. The renaturation is achieved by rapidly diluting this solvent with water. That is, the folding process starts from the coil and ends with the native protein. However, different properties of the native protein have two quite different rates of restoration, which is evidence for the accumulation of some “intermediate” state of the protein molecule at the beginning of the folding process.

Fig. 19.3 shows that the “native” values of intrinsic viscosity (which characterize the globule’s volume) and ellipticity at 222 nm (ie, CD in the far-UV region, which characterizes the secondary structure) are restored, or, rather, nearly restored in the course of renaturation much faster than the ellipticity at 270 nm (ie, CD in the near-UV region, which characterizes the side chain packing) or protein activity (which is a general indication of the native state of the protein). This indicates the presence of a metastable (ie, quasi-stable, since it lives long but then disappears) kinetic intermediate, accumulated in a

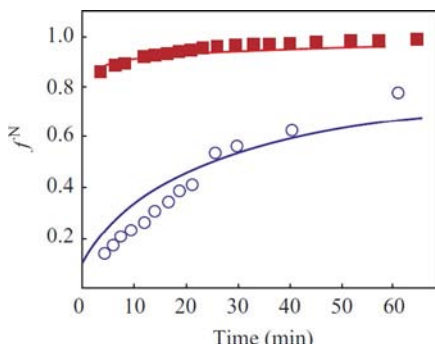


FIG. 19.3 Kinetics of recovery of a “degree of nativity” (f_N) in the process of carbonic anhydrase B renaturation. Transition of the protein from its fully unfolded state (existing at 5.45 M GuHCl concentration) to the native state (at 0.97 M GuHCl) is followed by intrinsic viscosity (■), by ellipticity at 222 nm (red line) and at 270 nm (blue line), and by enzymatic activity (○). (Adapted from Dolgikh, D.A., Kolomietz, A.P., Bolotina, I.A., Ptitsyn, O.B., 1984. “Molten globule” state accumulates in carbonic anhydrase folding. *FEBS Lett.* 164, 88–92.)

large quantity. This intermediate was at first colloquially called by us in Russian *komok* (= “a clot” in English); later Wada (in the paper [Ohgushi and Wada, 1983](#)) coined the name “molten globule,” since its compactness and secondary structure are close to those of the native protein, although it has neither native side chain packing nor the enzymatic activity of the native “solid” protein.

The molten globule is an early folding intermediate in the *in vitro* folding of many proteins ([Ptitsyn, 1995](#)). It is noteworthy that it can be observed under physiological conditions. This intermediate takes a few milliseconds to form ([Gilmanshin and Ptitsyn, 1987](#); [Roder et al., 2006](#); [Samatova et al., 2010](#)), while the complete restoration of the native properties of a 100–300 residue chain can take seconds or less for some proteins and up to hours for others. Thus, the rate-limiting folding step is the formation of the native “solid” protein from the molten globule rather than the formation of the molten globule from the coil (Fig. 19.3).

The molten globule is not the only intermediate observed in protein folding. A state with a partially formed secondary structure and a partially condensed chain (that also fits the “framework model”) has been observed to precede formation of the molten globule. This intermediate was discovered with the use of ultrafast (sub-millisecond) measuring techniques. This state of the folding chain resembles the “pre-molten” globule. In addition, proteins with disulfide bonds allow the trapping of various intermediates indicative of the order of formation of S–S bonds, etc.

As a matter of fact, the “kinetic control” hypothesis initiated very intensive and numerous studies of protein folding intermediates. Actually, it was clear almost from the very beginning that the stable intermediates are not obligatory for folding (since the protein can also fold near the point of equilibrium between the native and denatured states ([Segava and Sugihara, 1984](#)), where the

transition is of the “all-or-none” type, which excludes any stable intermediates). The idea was, though, that the intermediates, if trapped, would help to trace the folding pathway, just as intermediates in a complicated biochemical reaction trace the pathway of this reaction. This was, as it is now called, “chemical logic.” However, this logic worked only in part when it came to protein folding. Intermediates (like molten globules) were found for many proteins, but the main question as to how the protein chain can rapidly find its native structure among zillions of alternatives remained unanswered.

Progress in understanding was achieved when the studies involved small proteins (of 50–100 residues). Many of them fold *in vitro* without any observable intermediates accumulating in the experiment, and have only two observable states: the native fold and the denatured coil (Matouschek et al., 1990; Fersht, 1999). The absence of folding intermediates refers not only to the vicinity of the denaturation point (where the two-state kinetics can be expected *a priori* because of the “all-or-none” thermodynamics of denaturation, which means the absence of a visible quantity of intermediates). For these small proteins, this absence also refers to “physiological” conditions where folding intermediates of larger proteins are usually observed (Fersht, 1999).

The investigation of small proteins having no S–S bonds or *cis*-prolines (features that were widely used previously to trap the folding intermediates) has led to a striking result. It turned out that, in the absence of such “unnecessary complications” as folding intermediates, these proteins fold very rapidly: not only much faster than larger proteins (which would not be a surprise), but also at least as rapidly as small proteins that have folding intermediates that would be expected to accelerate their folding. We will discuss this later.

Some small proteins with *no* observable folding intermediates fold within milliseconds (Fig. 19.4) or even faster under nearly physiological conditions. The absence of folding intermediates was established by the equal rates of restoration of secondary structure, side chain packing, hydrogen exchange, etc.

What can these experiments provide to shed light on the nature of protein folding? What are we supposed to study if there are no intermediates to single out and investigate?

The answer is: just here one has the best opportunity to study the *transition state*, the bottleneck of folding (Fersht, 1999).

I think it is important to emphasize from the very beginning that the transition state, which is of crucial importance for folding kinetics and the folding rate, is, by definition, the *most unstable* state along the protein folding pathway. Thus, it is *not* a kind of previously discussed “folding intermediate” (and, specifically, it is *not* a molten globule). The “intermediates” correspond to free energy minima; that is, they are stable at least for some time and therefore can accumulate during folding and can be directly observed. On the contrary, the transition state corresponds to the free energy maximum; it never accumulates and therefore is never observed directly. It can *only* be followed by its influence on the folding rate (Fersht, 1999).

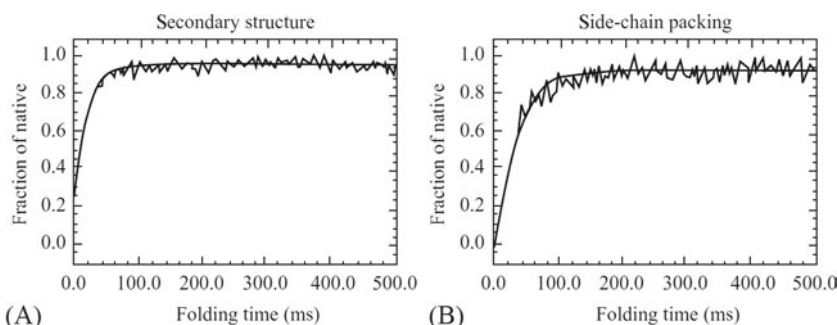


FIG. 19.4 Two-state renaturation of ACBP (acetyl coenzyme A binding protein), registered by the restoration of ellipticity (A) at 225 nm and (B) at 286 nm. The former reflects restoration of the secondary structure, the latter restoration of the tertiary structure (specifically, restoration of the aromatic side-group packing). The experimental signal (*broken line*) and the result of its smoothening and extrapolation (*smooth line*) are shown. Note the absence of changes within the measurement dead-time: this provides evidence that no intermediates accumulate within this time. (*Reprinted with permission from Kragelund, B.B., Robinson, C.V., Knudsen, J., Dobson, C.M., Poulsen, F.M., 1995. Folding of a four-helix bundle: studies of acyl-coenzyme A binding protein. Biochemistry 34, 7217–7224, ©1995, American Chemical Society.*)

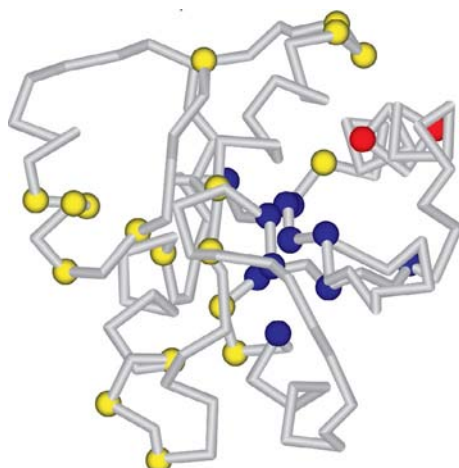


FIG. 19.5 Experimentally outlined folding nucleus for CheY protein according to López-Hernández and Serrano (1996). The residues studied experimentally are shown as *beads* against the background of the native chain fold. The residues forming the folding nucleus are shown in *dark blue*. The *yellow beads* indicate the residues that are not involved in the nucleus. The *red beads* show two residues that are difficult to interpret.

Let us postpone a detailed consideration of the transition states observed in protein folding till the next lecture and just see what results they produce. Transition state studies outlined the “folding nucleus,” ie, a part of the chain that is folded already in the transition state (Fig. 19.5). A relatively small fraction of residues are deeply involved in the nucleus; there, they already have their

native-like (ie, the same as in the native protein) conformations and contacts; some of the others are involved only partly. The remaining residues are not involved in the nucleus and remain in the unfolded state. All this will be discussed in detail in the Lecture 20.

Thus far, we have considered water-soluble globular proteins.

True, most studies of protein folding deal with these proteins. But nearly a third of proteins in the genome of any organism are membrane proteins. However, advances in study of folding of globular membrane proteins lag far behind in comparison to those for water-soluble globular proteins.

Spontaneous folding is not typical of membrane proteins ([Kim et al., 2012](#); [Roman and Flecha, 2014](#)) that usually need assistance for their proper passing through the membrane; this has been shortly discussed already. Here I will focus on those that undergo a spontaneous folding.

Investigation of membrane protein denaturation needs ionic detergents, and even then it is successful only in few cases (in particular, because these detergents can form their own structures, like brushes, when binding to protein molecules).

Membrane proteins can only achieve their functional state in the presence of a lipid environment or detergents. There is some evidence that the folding of helical membrane proteins occurs through intermediate states that share many features ([Surrey and Jähnig, 1995](#)) of the “molten globules” of water-soluble proteins, ie, have a native-like secondary structure, but disordered tertiary interactions. The presence of exposed hydrophobic residues within a condensed globular form makes them attractive in the context of folding in a membrane. A number of experiments suggest that different helices in membrane proteins fold in a relatively autonomous manner ([van der Goot et al., 1991](#)), consistent with the flexibility anticipated for the molten globule. Membrane proteins having a β -barrel shape (such as porins) seem to fold much more cooperatively ([Surrey and Jähnig, 1995](#); [Kim et al., 2007](#)) than helical membrane proteins, that is, without observable stable intermediates and visible folding steps. The analogy between the folding of membrane-bound and water-soluble proteins may extend to the presence of a structural “core” that might serve as a nucleus for folding.

As well as satisfying our natural curiosity about the folding of this group of proteins, progress in protein folding studies will contribute to our ability to produce membrane proteins efficiently and increase our understanding of the regulation of membrane processes.

In conclusion, it seems to be not out of place to suggest some curious analogy between the folding of proteins and assembling of viral particles. For many simple viruses, the coat proteins appear to have all the properties needed for the formation of the intact particles. For more complex viruses, however, there are known to be assembly pathways that involve “scaffolding proteins” or other components, which are essential to the formation of the particles but are not incorporated in the mature virions. These “molecular chaperones” are clearly

very fascinating from both a structural and a mechanistic point of view. Intriguingly, as simple viruses assemble without the accumulation of intermediates (as simple small proteins fold without populating partially folded states), we know more about the assembly pathways of the more complicated species, where partially structured states can be observed under favorable circumstances.

REFERENCES

- Anfinsen, C.B., 1973. Principles that govern the folding of protein chains. *Science* 181, 223–230.
- Anfinsen, C.B., Haber, E., Sela, M., White, F.H., 1961. The kinetics of formation of native ribonuclease during oxidation of the reduced polypeptide chain. *Proc. Natl. Acad. Sci. U. S. A.* 47, 1309–1314.
- Baranov, V.I., Spirin, A.S., 1993. Gene expression in cell-free system on preparative scale. *Methods Enzymol.* 217, 123–142.
- Basehore, H.K., Ropson, I.J., 2011. Residual interactions in unfolded bile acid-binding protein by ¹⁹F NMR. *Protein Sci.* 20, 327–335.
- Benton, L.A., Smith, A.E., Young, G.B., Pielak, G.J., 2012. Unexpected effects of macromolecular crowding on protein stability. *Biochemistry* 51, 9773–9775.
- Creighton, T.E., 1993. Proteins: Structures and Molecular Properties, second ed. W. H. Freeman & Co, New York (Chapters 2, 7).
- Dobson, C.M., 1994. Protein folding. Solid evidence for molten globules. *Curr. Biol.* 4, 636–640.
- Dobson, C.M., 2003. Protein folding and misfolding. *Nature* 426, 884–890.
- Dolgikh, D.A., Gilmanshin, R.I., Brazhnikov, E.V., Bychkova, V.E., Semisotnov, G.V., Venyaminov, S.Yu., Ptitsyn, O.B., 1981. Alpha-lactalbumin: compact state with fluctuating tertiary structure? *FEBS Lett.* 136, 311–315.
- Dolgikh, D.A., Kolomiets, A.P., Bolotina, I.A., Ptitsyn, O.B., 1984. “Molten globule” state accumulates in carbonic anhydrase folding. *FEBS Lett.* 164, 88–92.
- Eichmann, C., Preissler, S., Riek, R., Deuerling, E., 2010. Cotranslational structure acquisition of nascent polypeptides monitored by NMR spectroscopy. *Proc. Natl. Acad. Sci. U. S. A.* 107, 9111–9116.
- Ellis, R.J., 2001. Macromolecular crowding: obvious but underappreciated. *Trends Biochem. Sci.* 26, 597–604.
- Ellis, R.J., Hartl, F.U., 1999. Principles of protein folding in the cellular environment. *Curr. Opin. Struct. Biol.* 9, 102–110.
- Farr, G.W., Fenton, W.A., Chaudhuri, T.K., Clare, D.K., Saibil, H.R., Horwich, A.L., 2003. Folding with and without encapsulation by *cis*- and *trans*-only GroEL-GroES complexes. *EMBO J.* 22, 3220–3230.
- Fersht, A., 1985. Enzyme Structure and Mechanism, second ed. W.H. Freeman & Co, New York, p. 12 (Chapters 1, 8).
- Fersht, A., 1999. Structure and Mechanism in Protein Science: A Guide to Enzyme Catalysis and Protein Folding. W. H. Freeman & Co, New York (Chapters 15, 18, 19).
- Flanagan, J.M., Kataoka, M., Shortle, D., Engelman, D.M., 1992. Truncated staphylococcal nucleic acid is compact but disordered. *Proc. Natl. Acad. Sci. U. S. A.* 89, 748–752.
- Gil'manshin, R.I., Dolgikh, D.A., Ptitsyn, O.B., Finkel'shtein, A.V., Shakhnovich, E.I., 1982. Protein globule without the unique three-dimensional structure: experimental data for alpha-lactalbumins and general model. *Biofizika* (in Russian) 27, 1005–1016.
- Gilmanshin, R.I., Ptitsyn, O.B., 1987. An early intermediate of refolding alpha lactalbumin forms within 20 ms. *FEBS Lett.* 223, 327–329.

- Goldenberg, D.P., Creighton, T.E., 1983. Folding pathway of a circular form of bovine pancreatic trypsin inhibitor. *J. Mol. Biol.* 165, 407–413.
- Goldenberg, D.P., Creighton, T.E., 1984. Circular and circularly permuted forms of bovine pancreatic trypsin inhibitor. *J. Mol. Biol.* 179, 527–545.
- Gutte, B., Merrifield, R.B., 1969. The total synthesis of an enzyme with ribonuclease A activity. *J. Am. Chem. Soc.* 91, 501–502.
- Hagen, J., 2006. Industrial Catalysis: A Practical Approach. Wiley-VCH, Weinheim, Germany.
- Han, Y., David, A., Liu, B., Magadan, J.G., Bennink, J.R., Yewdell, J.W., Qian, S.-B., 2012. Monitoring cotranslational protein folding in mammalian cells at codon resolution. *Proc. Natl. Acad. Sci. U. S. A.* 109, 12467–12472.
- Hardesty, B., Tsalkova, T., Kramer, G., 1999. Co-translational folding. *Curr. Opin. Struct. Biol.* 9, 111–114.
- Herendee, S.L., Vanbogelen, R.A., Neidhart, F.C., 1979. Levels of major proteins of *Escherichia coli* during growth at different temperatures. *J. Bacteriol.* 139, 185–194.
- Kersteen, E.A., 2005. Protein Folding Enzymes. University of Wisconsin, Madison.
- Kim, N.Yu., Novikova, O.D., Khomenko, V.A., Likhatskaya, G.N., Vostrikova, O.P., Emel'yanenko, V.I., Kuznetsova, S.M., Solov'yeva, T., 2007. Effects of pH on structural and functional properties of porin from the outer membrane of *Yersinia pseudotuberculosis*. I. Functionally important conformational transitions of yersinin. *Biochem. (Mosc.) Suppl. Ser. A Membr. Cell Biol.* 1, 145–153.
- Kim, K.H., Aulakh, S., Paetzl, M., 2012. The bacterial outer membrane β -barrel assembly machinery. *Protein Sci.* 21, 751–768.
- Kolb, V.A., Makeev, E.V., Spirin, A.S., 1994. Folding of firefly luciferase during translation in a cell-free system. *EMBO J.* 13, 3631–3637.
- Komar, A.A., 2009. A pause for thought along the co-translational folding pathway. *Trends Biochem. Sci.* 34, 16–24.
- Komar, A.A., Kommer, A., Krasheninnikov, I.A., Spirin, A.S., 1997. Cotranslational folding of globin. *J. Biol. Chem.* 272, 10646–10651.
- Lapanje, S., Tanford, C., 1967. Proteins as random coils. IV. Osmotic pressures, second virial coefficients, and unperturbed dimensions in 6 M guanidine hydrochloride. *J. Am. Chem. Soc.* 89, 5030–5033.
- Levinthal, C., 1968. Are there pathways for protein folding? *J. Chim. Phys. Physico-Chim. Biol.* 65, 44–45.
- Levinthal, C., 1969. How to fold graciously. In: Debrunner, P., Tsibris, J.C.M., Munck, E. (Eds.), Mössbauer Spectroscopy in Biological Systems. Proceedings of a Meeting Held at Allerton House, Monticello, Illinois. University of Illinois Press, Urbana-Champaign, IL, pp. 22–24.
- Libich, D.S., Tugarinov, V., Clore, G.M., 2015. Intrinsic unfoldase/foldase activity of the chaperonin GroEL directly demonstrated using multinuclear relaxation-based NMR. *Proc. Natl. Acad. Sci. U. S. A.* 112, 8817–8823.
- Lietzow, M.A., Jamin, M., Dyson, H.J., Wright, P.E., 2002. Mapping long-range contacts in a highly unfolded protein. *J. Mol. Biol.* 322, 655–662.
- López-Hernández, E., Serrano, L., 1996. Structure of the transition state for folding of the 129 aa protein CheY resembles that of a smaller protein, CI-2. *Fold. Des.* 1, 43–55.
- Marchenko, N.Yu., Garbuzynskiy, S.O., Semisotnov, G.V., 2009. Molecular chaperones under normal and pathological conditions. In: Zabolotny, D.I. (Ed.), Molecular Pathology of Proteins. Nova Science Publishers, New York, pp. 57–89.
- Marchenko, N.Y., Marchenko, V.V., Semisotnov, G.V., Finkelstein, A.V., 2015. Strict experimental evidence that apo-chaperonin GroEL does not accelerate protein folding, although it does accelerate one of its steps. *Proc. Natl. Acad. Sci. U. S. A.* 112, E6831–E6832.

- Marchenkov, V.V., Semisotnov, G.V., 2009. GroEL-assisted protein folding: does it occur within the chaperonin inner cavity? *Int. J. Mol. Sci.* 10, 2066–2083.
- Marchenkov, V.V., Sokolovskii, I.V., Kotova, N.V., Galzitskaya, O.V., Bochkareva, E.S., Girshovich, A.S., Semisotnov, G.V., 2004. The interaction of the GroEL chaperone with early kinetic intermediates of renaturing proteins inhibits the formation of their native structure. *Biofizika* (in Russian) 49, 987–994.
- Matouschek, A., Kellis, J.T., Serrano, L., Fersht, A.R., 1990. Transient folding intermediates characterized by protein engineering. *Nature* 346, 440–445.
- Neira, J.L., Fersht, A.R., 1999a. Exploring the folding funnel of a polypeptide chain by biophysical studies on protein fragments. *J. Mol. Biol.* 285, 1309–1333.
- Neira, J.L., Fersht, A.R., 1999b. Acquisition of native-like interactions in C-terminal fragments of barnase. *J. Mol. Biol.* 287, 421–432.
- Ohgushi, M., Wada, A., 1983. ‘Molten-globule state’: a compact form of globular proteins with mobile side-chains. *FEBS Lett.* 164, 21–24.
- Petsko, G.A., Ringe, D., 2004. *Protein Structure and Function*. New Science Press Ltd, London (Chapter 1).
- Phillips, D.C., 1966. The three-dimensional structure of an enzyme molecule. *Sci. Am.* 215, 78–90.
- Privalov, P.L., 1979. Stability of proteins: small globular proteins. *Adv. Protein Chem.* 33, 167–241.
- Ptitsyn, O.B., 1973. Stages in the mechanism of self-organization of protein molecules. *Dokl. Akad. Nauk SSSR* (in Russian) 210, 1213–1215.
- Ptitsyn, O.B., 1995. Molten globule and protein folding. *Adv. Protein Chem.* 47, 83–229.
- Roder, H., Maki, K., Cheng, H., 2006. Early events in protein folding explored by rapid mixing methods. *Chem. Rev.* 106, 1836–1861.
- Roman, E.A., Flecha, L.G., 2014. Kinetics and thermodynamics of membrane protein folding. *Biomolecules* 4, 354–373.
- Samatova, E.N., Melnik, B.S., Balobanov, V.A., Katina, N.S., Dolgikh, D.A., Semisotnov, G.V., Finkelstein, A.V., Bychkova, V.E., 2010. Folding intermediate and folding nucleus for I–N and U–N transitions in apomyoglobin: different contributions of conserved and non-conserved residues. *Biophys. J.* 98, 1694–1702.
- Segava, S., Sugihara, M., 1984. Characterization of the transition state of lysozyme unfolding. I. Effect of protein-solvent interactions on the transition state. *Biochemistry* 23, 2473–2488.
- Singh, M.S., Panda, A.K., 2005. Solubilization and refolding of bacterial inclusion body proteins. *J. Biosci. Bioeng.* 99, 303–310.
- Stryer, L., 1995. *Biochemistry*, fourth ed. W.H. Freeman & Co, New York (Part 1, Chapters 2, 9; Part 3, Chapter 27).
- Surrey, T., Jähnig, F., 1995. Kinetics of folding and membrane insertion of a β -barrel membrane protein. *J. Biol. Chem.* 270, 28199–28203.
- Svetlov, M.S., Kommer, A., Kolb, V.A., Spirin, A.S., 2006. Effective cotranslational folding of firefly luciferase without chaperones of the Hsp70 family. *Protein Sci.* 15, 242–247.
- Tanford, C., 1968. Protein denaturation. *Adv. Protein Chem.* 23, 121–282.
- Tanford, C., Kawahara, K., Lapanje, S., Hooker Jr., T.M., Zarlengo, M.H., Salahuddin, A., Aune, K.C., Takagi, T., 1967. Proteins as random coils. 3. Optical rotatory dispersion in 6 M guanidine hydrochloride. *J. Am. Chem. Soc.* 89, 5023–5029.
- van der Goot, F.G., Gonzalez-Manas, J.M., Lakey, J.H., Pattus, F., 1991. A molten-globule membrane insertion intermediate of the pore-forming domain of colicin A. *Nature* 354, 408–410.
- Zimmerman, S.B., Trach, S.O., 1991. Estimation of macromolecule concentrations and excluded volume effects for the cytoplasm of *Escherichia coli*. *J. Mol. Biol.* 222, 599–620.

Lecture 20

As I mentioned in the previous lecture, in the understanding of protein folding a key role was played by the simplest folding event, in which no metastable intermediates accumulate during the process.

Only the native and the completely unfolded state are seen in such a ‘two-state’ transition.

Let us spend a few minutes considering some details of a simplest transition of this kind. An irreversible ([Fig. 20.1A](#)) transition between two states, A → B.

For an ensemble of many molecules, its kinetics is described by the simple differential equations

$$dn_A(t)/dt = -k_{A \rightarrow B} n_A(t) \quad (20.1)$$

$$dn_B(t)/dt = k_{A \rightarrow B} n_A(t) \quad (20.2)$$

where $n_A(t)$, $n_B(t)$ are the number of molecules in the states A and B, respectively, at time t .

It is easy to solve them. Actually, we have to solve only one of them, since $dn_B/dt \equiv -dn_A/dt$. According to school maths, the solution is obtained by rewriting Eq. (20.1) as $dn_A(t)/n_A(t) = -k_{A \rightarrow B} dt$, or $d \ln(n_A(t)) = -k_{A \rightarrow B} dt$; from here $\ln(n_A(t)) = -k_{A \rightarrow B} t + C$ (where C is some constant), or $n_A(t) = \exp(C) \times \exp(-k_{A \rightarrow B} t)$. Having $n_A(t=0) = n_0$ (where $n_0 \gg 1$ is the total number of molecules), $n_B(t=0) = 0$ and $dn_A/dt + dn_B/dt \equiv 0$, we obtain

$$n_A(t) = n_0 \exp(-k_{A \rightarrow B} t) \quad (20.1a)$$

$$n_B(t) = n_0(1 - \exp(-k_{A \rightarrow B} t)) \quad (20.2a)$$

[Fig. 20.1B](#) presents this solution as a plot.

It is worth noting, though, that this single-exponential solution describes a flow of molecules from A to B, which is valid for description of an experiment with many molecules. Each of the molecules does not change smoothly—it jumps ([Fig. 20.1C](#)) over the free-energy barrier # from A to B state—and this is just what will be seen in a single-molecule experiment!

Inner voice: So, we have a single-exponential kinetics in the absence of intermediates... Does this mean that transition with one intermediate is described by two exponents, and so on?

Lecturer: That’s true, from the maths point of view. (See, eg, [Nölting, 2010](#), and especially Fig. 10.9 therein.) And we will observe the two-exponential kinetics in experiment most clearly when (1) the intermediate I is more stable than the initial state A, and (2) the first (along the reaction pathway) transition A → I is much faster than the last transition I → B.

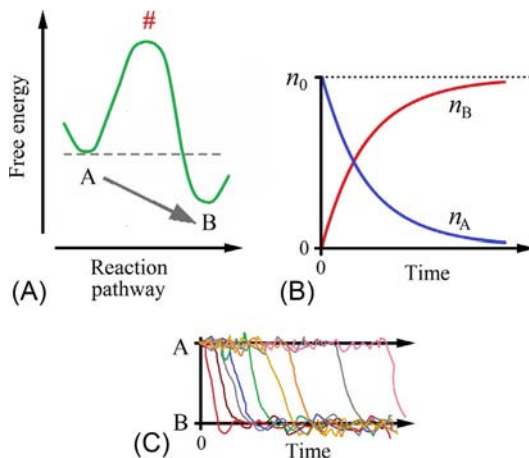


FIG. 20.1 (A) Scheme of the two-well free-energy profile for the two-state transition $A \rightarrow B$; it is irreversible, because the free-energy of state B is much (by many $k_B T$) lower than that of A ; $\#$ denotes the free-energy maximum, ie, the rate-limiting transition state. (B) Kinetics of the $A \rightarrow B$ transition for an ensemble of many molecules ($n_0 \gg 1$). (C) A sketch of transitions of individual molecules from this ensemble.

When the first transition is not much faster than the second one, the intermediate is present in a small amount for kinetic reason: molecules escape from it to the final state as fast as or faster than they come from the initial state (see Problems 20.1, 20.2).

When the intermediate is less stable than the initial state, it is present in a small (compared with the initial state) amount for the thermodynamic reason, that is, according to the Boltzmann distribution (see Problem 20.3).

In both of these cases, the increment of the second exponent is minor (see Fig. 20.2A and Problems 20.1–20.3), and the low-populated intermediate can be virtually invisible experimentally (unless it has some very bright property, like a specific colour or fluorescence, see Fig. 20.2B).

This is typical for global features of the ‘on-pathway’ intermediates, eg, when the degree of helicity grows from the unfolded chain to molten globule to native state.

However, the second transition is seen much more clearly when the measured signal changes in different directions upon the two transitions (compare panels (a) and (b) in Fig. 20.2).

But this difference does not necessary mean that the intermediate is an ‘off-pathway’ one: eg, the Trp fluorescence is more intensive in the molten globule than in both the native and unfolded states of apomyoglobin (Samatova et al., 2010), but this seems to imply only that the surface Trp is exposed to water in the native protein, partly screened from water in the molten globule, and again exposed in the unfolded apomyoglobin.

Now, coming back from the *multi-state* to *two-state* folding.

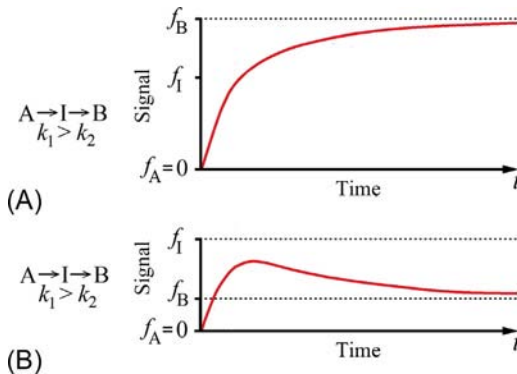


FIG. 20.2 Sketch of changing of the experimental signal in the course of the $A \rightarrow I \rightarrow B$ transition for the case when the first transition is not much (eg, as in this Figure, only four-times) faster than the last one. (A) In strength, signal f_I from the intermediate I is in-between signals f_A and f_B from states A and B ; then existence of the three states can be masked—compare the red curve here and the red curve in Fig. 20.1B. (B) Signal f_I is stronger than signals f_A and f_B ; then existence of the intermediate is clearly seen.

The absence of folding intermediates is usually established by the equal rates of restoration of each of the properties: secondary structure, side chain packing, etc.

Notice that two-state kinetics can be *a priori* expected around the mid-point of the de/renaturation, ie, close to the point of co-existence of the native and denatured states of the protein molecule—since the thermodynamics of denaturation are known to be of the ‘all-or-none’ type. The latter means that no intermediates are present in any visible amount around the mid-point of this transition. Less trivial is the fact that the two-state folding is observed (in many small proteins) also under physiological conditions (which are far from the equilibrium mid-point), where the folding is most rapid, and where the majority of larger proteins display accumulating folding intermediates (like the molten globule).

The two-state folding, which occurs within a wide range of conditions (and has no such complications as accumulating intermediates), provides the best opportunity to study the *transition state*, that is, the bottleneck of folding that determines the folding rate (Fersht, 1999; Nölting, 2010).

As you may remember, the transition state corresponds, by definition, to the free energy *maximum* on the pathway from one stable state (the free energy *minimum*) to another. Let me also remind you that the kinetics of the simplest transition between two stable states are satisfactorily described by the *transition-state theory*.

The rates of the $A \rightarrow B$ and of the $B \rightarrow A$ transitions are given; let me remind you, by the equations:

$$\begin{aligned} k_{A \rightarrow B} &= k_0 \exp [-(F^\# - F_A)/RT] \\ k_{B \rightarrow A} &= k_0 \exp [-(F^\# - F_B)/RT] \end{aligned} \quad (20.3)$$

Here F_A , F_B and $F^\#$ are the free energies of the states A, B and the transition state (free energy maximum) $\#$, and k_0 is the rate of an “elementary step” of the process.

It is noteworthy that the temperature dependence of the $A \rightarrow B$ reaction rate allows us to estimate the transition state energy relative to that of state A. According to Arrhenius, we obtain:

$$d[\ln(k_{A \rightarrow B})]d(1/T) = d[\ln(k_0) - (F^\# - F_A)/RT]/d(1/T) \approx -(E^\# - E_A)/R \quad (20.4)$$

Here, I have used the known relationship $d(F/T)/dT = -E/T^2$ and neglected the weak dependence of the elementary step rate k_0 on temperature T . The latter is usually acceptable in chemical reactions, and thus should be at least as acceptable in proteins where the energies $E^\#$ and E_A , determined by many interactions, are large.

Fig. 20.3 shows the dependence of lysozyme folding and unfolding rates on the reciprocal temperature value (T^{-1}). The plot shows that the rates of both processes are close to $e^{-2.5} \approx 0.1 \text{ s}^{-1}$ (ie, their times are close to 10 s) at the mid-transition (where the folding rate $k_{u \rightarrow N}$ is equal to the unfolding rate $k_{N \rightarrow u}$, so that the curves for $\ln(k_{u \rightarrow N})$ and $\ln(k_{N \rightarrow u})$ intersect).

This plot also shows that the denaturation accelerates as it gets deeper into the ‘denaturation region’, and the renaturation accelerates as it gets deeper into the ‘renaturation region’.

A most interesting conclusion from this plot is as follows:

The unfolding rate $k_{N \rightarrow u}$ decreases with T^{-1} (ie, it grows with temperature T , which is typical of physicochemical reactions), while the folding rate $k_{u \rightarrow N}$,

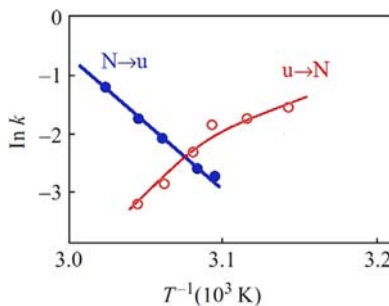


FIG. 20.3 Arrhenius plots for the rates of lysozyme de- and renaturation vs the reciprocal temperature value (T^{-1}); the plot is extracted, with some abridgement, from (Segava and Sugihara, 1984). The rate constants (k) are measured in s^{-1} . Renaturation: rate $k_{u \rightarrow N}$ (experimental points \circ and the thin red interpolation curve); denaturation: rate $k_{N \rightarrow u}$ (experimental points \bullet and the bold dark-blue interpolation line). The mid-transition is the temperature point where $k_{u \rightarrow N} = k_{N \rightarrow u}$, ie, where the curves intersect (at about $1000/3.08 = 325 \text{ K}$). Folding prevails in the ‘renaturation region’ ($u \rightarrow N$) at low temperatures (ie, at high T^{-1} values to the right of the intersection point); unfolding prevails in the ‘denaturation region’ ($N \rightarrow u$) at high temperatures (ie, at low T^{-1} values to the left of the intersection point).

on the contrary, increases with T^{-1} (ie, it drops with temperature T , which is atypical of physicochemical reactions). According to Eq. (20.4), this means that $E^\# - E_N > 0$ and $E^\# - E_u < 0$. In other words, $E_u > E^\# > E_N$, ie, the barrier energy $E^\#$ is above the native state energy E_N , but below the unfolded state energy E_u ; the latter is atypical of chemical reactions where the barrier energy is higher than both the initial and the final state energy. Additional analysis of this plot (taken now in the form $T \ln(k/k_0)$ vs T) shows that the same relationship, $S_u > S^\# > S_N$, is valid for the entropies of the native, transition and denatured states. This means that the barrier between the native and denatured states looks like a normal energy barrier when viewed from the native state, but from the denatured state it looks like an abnormal entropy barrier.

However, just this could be expected from our previous analysis of the free energy barrier between the native and denatured states and of the reasons for the ‘all-or-none’ protein melting.

Let us return to Eqs. (20.3) once again. They show that the ratio between the rates of the direct and reverse reactions, $k_{A \rightarrow B}/k_{B \rightarrow A}$, is simply the constant of equilibrium between the final (B) and initial (A) states:

$$K_{B:A} = \frac{k_{A \rightarrow B}}{k_{B \rightarrow A}} = \exp[-(F_B - F_A)/RT] \quad (20.5)$$

The $K_{B:A}$ value gives the ratio between the equilibrium numbers (n_A^∞ , n_B^∞) of molecules in the states B and A, which is achieved, after a very long time, as a final result of the transition process under given conditions (temperature, etc.), ie, when (in the final equilibrium) the flow $A \rightarrow B$ equilibrates the flow $B \rightarrow A$ (so that $n_A^\infty k_{A \rightarrow B} = n_B^\infty k_{B \rightarrow A}$):

$$K_{B:A} = \frac{k_{A \rightarrow B}}{k_{B \rightarrow A}} = \frac{n_B^\infty}{n_A^\infty} \quad (20.6)$$

What is the rate of approach to this equilibrium? To answer this question, we have to solve the differential equation which is very similar to (20.1), but takes into account the reverse process $B \rightarrow A$ as well:

$$dn_A(t)/dt = -k_{A \rightarrow B} n_A(t) + k_{B \rightarrow A} n_B(t) \quad (20.7)$$

Here, again, $n_A(t)$, $n_B(t)$ are the numbers of molecules in the states A and B, respectively, at time t (and again there is no need to solve equation for dn_B/dt , since $n_A(t) + n_B(t) \equiv n_0$, and this full number of molecules is constant).

Substituting $n_B(t) = n_0 - n_A(t)$ into (20.7), one obtains $dn_A(t)/dt = -(k_{A \rightarrow B} + k_{B \rightarrow A})n_A(t) + k_{B \rightarrow A}n_0$. Now, using $n_A^\infty k_{A \rightarrow B} = n_B^\infty k_{B \rightarrow A}$, see Eq. (20.6) and $n_A^\infty + n_B^\infty = n_0$, so that $n_0 k_{B \rightarrow A} = n_A^\infty (k_{A \rightarrow B} + k_{B \rightarrow A})$, we have:

$$dn_A(t)/dt = -(k_{A \rightarrow B} + k_{B \rightarrow A})[n_A(t) - n_A^\infty] \quad (20.8)$$

The final answer (I recommend you to verify the calculation yourselves) is:

$$n_A(t) = [n_A(t=0) - n_A^\infty] \cdot \exp[-(k_{A \rightarrow B} + k_{B \rightarrow A})t] + n_A^\infty \quad (20.9)$$

This means that the apparent rate of *approach to the equilibrium* is

$$k_{\text{app}} = k_{A \rightarrow B} + k_{B \rightarrow A} \quad (20.10)$$

ie, it is equal to the sum of the rates of the forward and reverse reactions. The value k_{app} depends only on the conditions of the process rather than on the initial numbers of folded and unfolded molecules.

The most rapid reaction dominates in the k_{app} value. When the conditions (solvent, temperature, etc.) stabilize the native state, the folding rate $k_{u \rightarrow N}$ dominates in k_{app} . When the denatured state is more stable, then the unfolding rate $k_{N \rightarrow u}$ dominates in k_{app} .

The above shows that a reversible transition between two stable states (ie, folded and unfolded protein) is described by a *single*-exponential kinetics with *one* characteristic folding rate.

The rate of approach to the equilibrium, k_{app} , can be measured *directly* (unlike $k_{u \rightarrow N}$ and $k_{N \rightarrow u}$ separately) both when the native state is more stable and when it is less stable than the denatured one (Fig. 20.4); this is an important advantage of the k_{app} value.

Values of k_{app} are commonly presented as a function of the denaturant's concentration, in the form of so-called 'chevron plots' ('chevron', because its shape resembles the military long-service stripe) (Fig. 20.4). This plot shows that:

1. The rate of coming to equilibrium (and the rates of folding and unfolding, see Fig. 20.3) is minimal at the mid-transition; however, it is not infinitely big, which is typical of the first order phase transitions in macroscopic systems (Nicolis and Prigogine, 1977; Slezov, 2009) (including the coil to β -sheet transition that we have touched on already). In macroscopic systems this phenomenon leads to hysteresis (which means that the transition is observed *not* in the transition point but later on); but this is not observed for folding and unfolding of globular proteins (in Fig. 20.4, the hysteresis would look like the absence of both folding and unfolding dots in the mid-transition vicinity; this would be exactly so, if the time of kinetic experiments were limited to 100–1000 seconds (s)).
2. The rates of folding ($k_{u \rightarrow N}$) and unfolding ($k_{N \rightarrow u}$) are oppositely dependent on the denaturant's concentration. We have already seen (Fig. 20.3) a similar case when considering the temperature dependence of the folding and unfolding rates. As in that case, the opposite slopes of the two branches indicate that the transition state is intermediate in properties between the native and denatured states.

Indeed, the ability of a denaturant to unfold the protein means that it is attracted to the denatured state more than to the native state. The denaturant-induced decrease in the folding rate of the initially unfolded protein (see the left part of the chevron in Fig. 20.4) means that the denaturant is more strongly attracted to the unfolded state than to the transition state (ie, that the denaturant

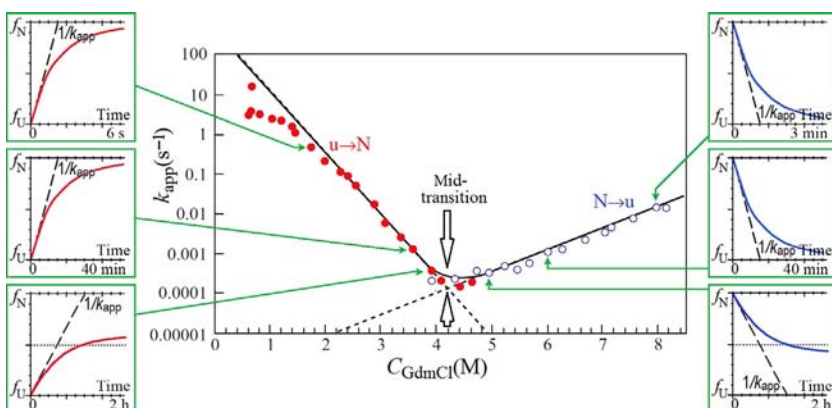


FIG. 20.4 Central panel: ‘chevron plot’ for the apparent rate (k_{app}) of approach to the equilibrium between the native and unfolded forms of hen egg-white lysozyme vs C_{GdmCl} , the concentration of guanidine dihydrochloride. The experiment was carried out in the presence of native S–S bonds. To obtain every point of the plot, separate kinetic experiments were performed (they took from seconds to hours; panels in the margins show results of some of them very schematically; f_N, f_U correspond to signals from the native and unfolded states). The filled circles are obtained when diluting a concentrated GdmCl solution of the denatured protein, ie, they correspond to refolding ($u \rightarrow N$); $k_{app} \approx k_{u \rightarrow N}$ in this region (since here the refolding rate $k_{u \rightarrow N}$ is greater than the unfolding rate $k_{N \rightarrow u}$). The open circles are obtained when adding GdmCl to aqueous solution of the native protein, ie, they correspond to unfolding ($N \rightarrow u$); $k_{app} \approx k_{N \rightarrow u}$ here (since $k_{u \rightarrow N} < k_{N \rightarrow u}$ upon unfolding). At the lowest part of the chevron (in the mid-transition), where $C_{GdmCl} \approx 4.2\text{M}$, $k_{u \rightarrow N} \approx k_{N \rightarrow u} \approx k_{app}/2$. Note the overlapping of the open and filled circles in this region. It shows that here, at the mid-transition, the protein folds at the same rate as it unfolds (which means that the folded and unfolded states have equal free energy, in accordance with definition of the mid-transition). Also note the absence of hysteresis. The dotted lines show extrapolation of the $k_{u \rightarrow N}$ and $k_{N \rightarrow u}$ values to the chevron bend region and beyond. The solid line shows the $k_{u \rightarrow N}$ extrapolation to the low-GdmCl region. The points that deviate from the solid line at low GdmCl concentrations (ie, far from the mid-transition) indicate either some rearrangement of the transition state or the appearance of some additional metastable intermediates (possibly molten globules); these may be on, as well as off the main renaturation pathway. Note that these rearrangements and/or intermediates (or traps) do not increase the renaturation rate compared with what could be expected in their absence: although they correspond to the highest observed renaturation rate, they are *below* the extrapolation line. (Adapted from Kiefhaber, T., 1995. Kinetic traps in lysozyme folding. *Proc. Natl. Acad. Sci. USA* 92, 9029–9033.)

destabilizes the transition state relative to the initial unfolded state). The denaturant-induced increase in the unfolding rate of the initially native protein (see the right part of the chevron in Fig. 20.4) means that the denaturant is more strongly attracted to the transition state than to the native state. This shows that the denaturant’s contact with the transition state is stronger than with the native state, but weaker than with the denatured state. Thus, in terms of protein–solvent contact, the transition state is intermediate between the native and denatured states. The plot shows even a little more: since the $k_{u \rightarrow N}$ slope is a little steeper than the $k_{N \rightarrow u}$ slope, the compactness of the transition state is

somewhat closer (in this case) to that of the native state than to the compactness of the denatured state.

[Fig. 20.4](#) (and also [Fig. 20.3](#)) refers to lysozyme, the protein whose GdmCl-induced denaturation leads directly to the coil state, rather than to the molten globule state. Its folding takes hours at moderate GdmCl concentrations. However, in ‘almost pure’ water the folding time is as short as $\approx 0.1\text{--}0.3$ s.

Inner voice: Does this mean that the protein has no such characteristic as the folding rate?

Lecturer: That’s true. The protein does not have a strictly defined ‘folding rate’. Indeed, [Fig. 20.4](#) shows that lysozyme folding takes about 0.1 s under native conditions and about 10 000 s when close to the denaturant-induced equilibrium between its native and denatured forms. And at high temperature (but without denaturant) its folding takes about 10 s, while at the mid-transition caused by temperature it takes ~ 10 min (see [Fig. 20.3](#)). Therefore, when discussing the protein’s folding rate, one has either to refer to the entire observed range of its folding rates, or specify the ambient conditions (eg, those which refer to the protein folding in the cell, or in water at 20–25°C, as is also often done).

Coming back to lysozyme folding in water (*far* from the denaturant-induced equilibrium between the native and the coil forms), we see a shoulder where the folding rate is at a maximum, and is virtually independent of denaturant concentration (this is called a ‘rollover’ of the chevron). This is typical of the folding of middle-sized and especially larger proteins at low denaturant concentrations (see, eg, [Melnik et al., 2008](#)); therefore, the in-water folding time is often taken as the characteristic folding time of a given protein.

It has been shown that here, in pure or almost pure water, lysozyme folding has a compact intermediate that does not appear at higher GdmCl concentrations ([Kieffhaber, 1995](#)). Thus, lysozyme exhibits “three-state” folding far from the equilibrium of the native and denatured states, and “two-state folding” in the vicinity of this equilibrium. This means that there is no difference—in the sense of the number of states—between “three-” and “two-state” folding proteins, if we consider the vicinity of mid-transition only.

In the example shown in [Fig. 20.5](#), the transition from U to N occurs in two steps only when the folding intermediate I is more stable than the unfolded state U, which frequently occurs under strong renaturing conditions ([Fig. 20.5A](#)). With other things being equal, folding of a protein with *unstable* I is *faster* because there’s no need to escape from the stable (as compared to the initial state U) intermediate I before reaching the rate-limiting transition state #. When I is unstable, folding ([Fig. 20.5B](#)) or unfolding ([Fig. 20.5C](#)) occurs in one step.

Although there seems to be no principal difference between “three-” and “two-state” folding proteins, the study of proteins exhibiting only two-state folding is more straightforward: their in-water folding transition state is the

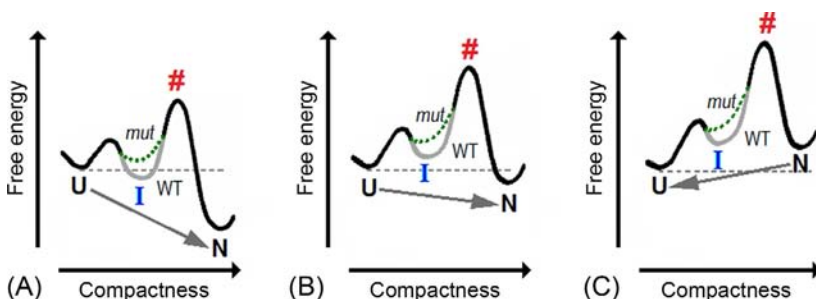


FIG. 20.5 Scheme of the free-energy profile for the wild type (WT) and mutated (*mut*) protein. Following the experimental observations, the rate-limiting transition state # here is positioned between the folding intermediate I and the native state N. The mutation-caused change of the profile is shown with the dotted line for the mutated (*mut*) protein (while the corresponding part of the profile is shown with the gray line for WT). It is assumed that mutation affects only the intermediate I, and that the conditions-caused change of the profile is strictly proportional to protein compactness. The transition from the unfolded (U) to the native (N) state via the intermediate (I) and transition state (#) is shown for strong (A) and mild (B) renaturing conditions, and the transition from N to U occurs under denaturing conditions (C). Under strong renaturing conditions (A), the intermediate I is stable (as compared with U) for the WT protein, but not stable for the mutated (*mut*) protein. Under mild renaturing conditions (B), as well as for denaturing conditions (C), the intermediate is unstable in all cases. Note that the shown N → I → U transition (C) always looks as the two-state one, because the first free energy barrier # for this process (at the N → I step) is higher than the last barrier at the I → U step; see Problems 20.2, 20.3. (Adapted from Finkelstein, A.V., Galzitskaya, O.V., 2004. Physics of protein folding. *Phys. Life Rev.* 1, 23–56.)

same as that at other denaturant concentrations. Another advantage is technical: the extrapolation of the long, straight chevron branches is easier. Therefore, the “two-state folders” played a key role in investigations of transition states (Matouschek et al., 1990; Fersht, 1999). However, in principle, all transition states that appear in the course of a multi-state folding can be investigated in a similar way (Nölting, 2010; Samatova et al., 2010).

The appearance of compact intermediates always makes the folding rate dependence more shallow (or even changes the sign of the slope) because the rate-limiting step of the folding now starts from a more compact intermediate, ie, from the state whose properties (such as interaction with the denaturant) are closer to those of the transition state than to the properties of the former starting state, ie, the unfolded state. It is known also that the rate of folding that starts from the molten globule rather than from the coil state (eg, carbonic anhydrase folding) shows a very shallow dependence on the denaturant concentration (Melnik et al., 2008). This means that the compactness of the transition state in this folding is close to that of the molten globule state.

In other words, the ‘intermediate’ character of the transition state properties makes them similar to the properties of the molten globule. However, this similarity refers only to some averaged properties of these two states (such as energy or compactness), and *does not* mean that the transition state *is* the molten

globule: the transition state is (by definition) most unstable, while the molten globule is stable or at least metastable.

Experiments (to be described later) show that the transition state is far less uniform than the molten globule. As far as the ‘coil → native protein’ transition is concerned, the transition state can be imagined as similar to a piece of the native protein, while the rest of the chain remains in the unfolded state. Transition states in the ‘molten globule → native protein’ and especially ‘coil → molten globule’ transitions have not yet been determined experimentally, but it is plausible that they also include a piece of the more structured state, while the rest of the chain remains in a less structured state.

The nature of the transition state is established using many mutants of the protein (ideally, each separate chain residue is mutated), and analyzing changes in the chevron plots (see Figs. 20.4 and 20.5). This allows one to find out, at the cost of hard work, which residues are involved in the native-like part of the transition state (their mutations change the folding rate substantially), and which are not (their mutations do not change the folding rate, but change the rate of unfolding). This protein-engineering method was developed by A. Fersht and his co-workers in England (Matouschek et al., 1990; Fersht, 1999). It can be applied to all ‘all-or-none’ transitions. However, up to now it is mostly (but not exclusively, see, eg, Samatova et al., 2010) used for proteins whose denatured state is the coil rather than the molten globule.

To estimate the involvement of a residue in the native-like part of the transition state (‘folding nucleus’), one estimates: (a) the mutation-induced shift of the folding rate and (b) the mutation-induced shift of the native protein stability (Fig. 20.6). Usually, in mutants, small amino acid residues (Ala or Gly) are substituted for larger ones, and not *vice versa*, to avoid distortion of the native protein structure.

The folding ($u \rightarrow N$) rate is determined (see Eq. (20.2)) by the free energy difference between the transition state (#) and the initial unfolded (u) state of the protein (ie, by the $F^{\#} - F_u$ value).

The stability of the native (N) relative to the unfolded (u) form of the protein is determined by their free energy difference, $F_N - F_u$, which is in turn determined (see Eq. (20.5)) by the ratio between the folding and unfolding rates. (These values depend on the ambient conditions. Since it is in-water folding that is usually of interest, the rates of protein unfolding (and folding) are usually extrapolated to zero denaturant concentration. It should be noted, though, that a smaller and therefore more accurate extrapolation (Fig. 20.6) is needed to determine the folding nucleus at mid-transition.)

Mutations influence both the folding rate and the stability of the protein. This provides an opportunity to use them in outlining the folding nucleus experimentally. The interpretation is done under the assumption that the rate-limiting step of protein folding is the nucleation of its native structure, and that the residues involved in the *folding nucleus* (the globular part of the transition state) are positioned there in the same way as in the native protein.

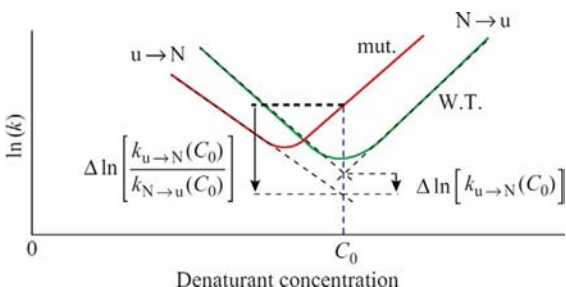


FIG. 20.6 A scheme illustrating a mutation-induced change of the chevron plot: k , apparent rate of transition. Green line, the initial, ‘wild type’ protein (W.T.); red line, the same protein with one residue mutated (mut.). C_0 , the denaturant concentration at the mid-transition for the W.T. protein. The dotted lines show extrapolation of the folding and unfolding rates, $k_{u\rightarrow N}$ and $k_{N\rightarrow u}$, to the W.T. chevron bend region. Two measured mutation-induced shifts are shown with arrows. The first is the change in the height of the free energy barrier on the pathway from the unfolded to the native state: $\Delta(F^\# - F_u) = -RT\Delta\ln[k_{u\rightarrow N}]$. The other is the change in protein stability, ie, in the free energy difference between the native and unfolded states: $\Delta(F_N - F_u) = -\Delta\ln[k_{u\rightarrow N}/k_{N\rightarrow u}]$. The ratio $\Delta(F^\# - F_u)/\Delta(F_N - F_u)$ is called ‘ Φ_f value’ for the mutated residue of the chain. In the shown case $\Phi_f \approx 1/4$, ie, in the transition state, the mutated residue has only a quarter of its native interactions. (A mnemonic rule. If the left branches of the W.T. and mut. chevrons are closer to each other than the right branches, Φ_f is closer to 0 than to 1. If otherwise, Φ_f is closer to 1 than to 0.) The values shown in the plot refer to the C_0 denaturant concentration, where the necessary extrapolations (and therefore, extrapolation errors) are minimal. However, usually one makes the extrapolation to $C=0$ and determines the change in protein stability, $\Delta(F_N - F_u)$, the change in the barrier height, $\Delta(F^\# - F_u)$, and the Φ_f value referring to pure water rather than to the denaturant concentration C_0 .

The nucleation mechanism is typical of the first-order phase transitions ([Ubbelohde, 1965](#); [Landau and Lifshitz, 1980](#); [Slezov, 2009](#)) in conventional physics (such as crystal freezing), and therefore it is highly plausible that it should occur in protein folding: it is an ‘all-or-none’ transition, which, as we know, is a microscopic analog of a first-order phase transition in macroscopic systems.

The experimental check of this assumption will be described shortly. First, I would like to tell you how one can interpret the mutation-induced shifts of the $F_N - F_u$ and $F^\# - F_u$ values to outline, under the above assumption, the residues involved in the nucleus.

If the residue’s mutation changes the transition state stability value $F^\# - F_u$ and the native protein stability value $F_N - F_u$ *equally*, this means that the residue in question is involved in the folding nucleus and has there the same contacts and conformation as in the native protein ([Fersht, 1999](#); [Nölting, 2010](#)).

If, on the contrary, the residue’s mutation changes *only* the native protein stability value $F_N - F_u$, but *does not* change the folding rate (and thus does not change the transition state stability value $F^\# - F_u$), this means that the residue in question is *not* involved in the nucleus and comes to the native structure only after the rate-limiting step.

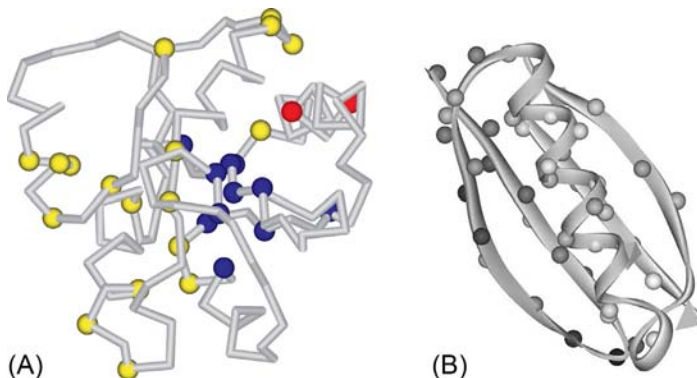


FIG. 20.7 (A) Folding nucleus for CheY protein according to (López-Hernández and Serrano, 1996). The residues studied experimentally are shown as beads against the background of the native chain fold. Dark-blue beads show the residues involved in the nucleus, ie, in the folded part of the transition state (in the given case, if they have $\Phi_f > 0.3$, ie, each of them forms >30% of its native contacts there). Yellow beads show residues having $\Phi_f < 0.3$; they are not involved in the folded part of the transition state. Red beads show two residues that are difficult to interpret experimentally. They have such low ($\ll kT$) values $\Delta(F^\# - F_u)$ and $\Delta(F_N - F_u)$ (the latter is more important, since this value is the denominator in Eq. (20.11)), that the errors in their determination exceed the measured values themselves. (B) Folding nucleus for L protein according to (Wikström et al., 1994). The experimentally studied residues are shown as beads against the background of the native chain fold and coloured according to the Φ_f -values from white ($\Phi_f = 0$) to black ($\Phi_f = 1$). (Adapted from Finkelstein, A.V., Ivankov, D.N., Garbuzynskiy, S.O., Galzitskaya, O.V., 2014. Understanding the folding rates and folding nuclei of globular proteins. In: Dunn, B.M. (Ed.), eBook Series Frontiers in Protein and Peptide Sciences, vol. 1. Bentham Science, Oak Park, IL, pp. 91–138 (Chapter 5).)

And, lastly, if the residue's mutation affects the transition state stability to a lesser degree (but with the same sign) than the native protein stability, this means that the residue in question either belongs to one of a few alternative folding nuclei or forms only a part of its native contacts within the nucleus (ie, that this residue is at the surface of the nucleus).

This is how the folding nucleus is outlined (Fig. 20.7): one estimates the value:

$$\Phi_f = \Delta(F^\# - F_u) / \Delta(F_N - F_u) \equiv \Delta \ln [k_{u \rightarrow N}] / \Delta \ln [k_{u \rightarrow N} / k_{N \rightarrow u}] \quad (20.11)$$

for each mutated residue (this is called 'Φ-analysis'). If its Φ_f is close to 1, the residue is interpreted as participating in the folding nucleus; if its Φ_f is close to 0, as non-participating. If $0 < \Phi_f < 1$, the residue is interpreted as either a surface residue of the nucleus, or as a member of one of a few alternative folding nuclei.

It is significant that only a negligible part of residues cannot be interpreted in such a way (and *this is experimental evidence for the nucleation folding mechanism*). In other words, only a negligible fraction of mutations have their Φ_f values beyond the range 0–1. That is, almost no mutations influence the folding

rate only leaving stability unaffected (these would have $\Phi_f \gg 1$ or $\Phi_f \ll -1$), or stabilize the native fold but decrease the folding rate (these would have $\Phi_f < 0$), and even these exceptions are mostly connected with unreliably measured (too small) differences $\Delta(F^\# - F_u)$ and especially $\Delta(F_N - F_u)$.

The above facts allow us to believe that the nucleation mechanism, first suggested by [Wetlaufer \(1973\)](#), is basically correct, ie, that the residues, if involved in the folding nucleus, are positioned there in (approximately) the same way as in the native protein.

Inner voice: Actually, you are saying that any mutation affecting the protein folding rate affects its stability as well. But there are experiments showing the opposite...

Lecturer: All that I have said refers only to “two-state” transitions, ie, to those without stable folding intermediates. If such an intermediate is present (which is possible only far from the mid-transition, see the upper left part of [Fig. 20.4](#)), the mutation may affect it without affecting either the final native structure or the initial coil (as, eg, mutation of a surface residue (in the native fold) can affect the stability of the intermediate molten (or pre-molten) globule, not to mention possible transient association of these intermediates, but affects neither the native nor the coil form stability). Then the effect you mentioned (which, incidentally, is always observed far from the transition point) becomes possible.

[Fig. 20.7](#) shows that in this way detected residues of the folding nucleus (ie, residues having the highest Φ_f values, those of key importance for the protein folding) form a relatively small compact region, a relatively small (but not grain-sized!) compact folding nucleus positioned at the periphery rather than in the center of the protein globule.

A similar picture is usually observed in other proteins already studied experimentally: usually, the folding nucleus is compact and does *not* coincide with the protein’s hydrophobic core.

As I have told, the nucleation mechanism seems to be basically correct. However, it is an oversimplification that the folding nucleus is a completely folded piece of the native protein structure, while the rest of the chain is completely unfolded. Some non-native interactions occur in a protein folding nucleus ([Li et al., 2000](#); see also [Shakhnovich, 2006](#)): it seems that the transition state includes a native-like nucleus surrounded by something like a loose, amorphous molten globule, and the folding nucleus is bigger than its part outlined by the Φ value analysis.

A number of proteins have a very “diffuse” folding nucleus, which is “weak” (characterized by low Φ_f -values), has no clear boundaries, but occupies a large part of the protein. Apparently, these proteins fold by many parallel paths with different nuclei. This view is supported by the fact that some mutations localize the nucleus, though some of them localize it in one place and others in another ([Tseng and Liang, 2004](#); [Burton et al., 1997](#); [Otzen et al., 1999](#)).

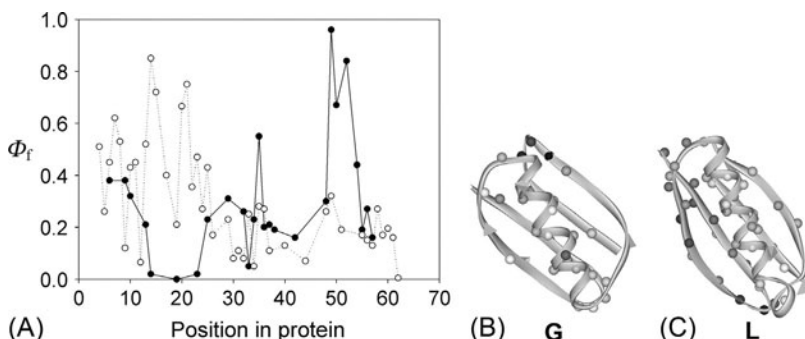


FIG. 20.8 (A) Profiles of experimental Φ_f -values obtained for B1 domains of G protein (filled circles) and L protein (open circles). (B, C) Schemes of 3D structures of these proteins (Gallagher et al., 1994; Wikström et al., 1994) (which have very similar folds but a relatively low, $\approx 15\%$, sequence identity) coloured according to the Φ_f -values of their amino-acid residues, from white ($\Phi_f=0$) to black ($\Phi_f=1$). The experimentally studied residues are shown as beads against the background of the native chain folds. As seen, the location of folding nucleus is quite different in these similar proteins. (Adapted from Finkelstein, A.V., Ivankov, D.N., Garbuzyanskiy, S.O., Galzitskaya, O.V., 2014. Understanding the folding rates and folding nuclei of globular proteins. In: Dunn, B.M. (Ed.), eBook Series Frontiers in Protein and Peptide Sciences, vol. 1. Bentham Science, Oak Park, IL, pp. 91–138 (Chapter 5).)

Proteins with different sequences but similar 3D structures usually have similar folding nuclei. However, there are some exceptions (Steensma and van Mierlo, 1998) (Fig. 20.8). The observed abundance of Φ_f values of about 0.5 in virtually all proteins and the observed sensitivity of nuclei to mutations, together with the results of computer simulations, led to two conclusions: (1) that a ‘nucleus’ is an ensemble of structures rather than a single structure, and (2) that mutations, both artificial and natural, can radically change folding pathways (create and destroy folding intermediates, transforming two- into multi-state folding proteins and *vice versa*, shift the folding nuclei at the opposite side of the molecule, etc.), without any considerable variation of 3D structures of native proteins (Grantcharova et al., 2001; Shakhnovich, 2006).

This means that the folding nucleus is less ‘invariant’ and more sensitive to mutations than the native protein structure (Finkelstein and Galzitskaya, 2004). The native protein structure is a subject of much more severe natural selection than the folding nucleus and folding pathways.

REFERENCES

- Burton, R.E., Huang, G.S., Daugherty, M.A., et al., 1997. The energy landscape of a fast-folding protein mapped by Ala→Gly substitutions. *Nat. Struct. Biol.* 4, 305–310.
- Fersht, A., 1999. Structure and Mechanism in Protein Science: A Guide to Enzyme Catalysis and Protein Folding. H. Freeman & Co., New York. Chapters 15, 18, 19.
- Finkelstein, A.V., Galzitskaya, O.V., 2004. Physics of protein folding. *Physics of Life Reviews* 1, 23–56.

- Gallagher, T., Alexander, P., Bryan, P., Gilliland, G.L., 1994. Two crystal structures of the B1 immunoglobulin-binding domain of streptococcal protein G and comparison with NMR. *Biochemistry* 33, 4721–4729.
- Grantcharova, V., Alm, E.J., Baker, D., Horwich, A.L., 2001. Mechanisms of protein folding. *Curr. Opin. Struct. Biol.* 11, 70–82.
- Kiefhaber, T., 1995. Kinetic traps in lysozyme folding. *Proc. Natl. Acad. Sci. USA* 92, 9029–9033.
- Landau, L.D., Lifshitz, E.M., 1980. Statistical Physics (Volume 5 of A Course of Theoretical Physics), third ed. Elsevier, London. Section 150.
- Li, L., Mirny, L.A., Shakhnovich, E.I., 2000. Kinetics, thermodynamics and evolution of non-native interactions in a protein folding nucleus. *Nat. Struct. Biol.* 7, 336–432.
- López-Hernández, E., Serrano, L., 1996. Structure of the transition state for folding of the 129 aa protein CheY resembles that of a smaller protein, CI-2. *Fold. Des.* 1, 43–55.
- Matouschek, A., Kellis, J.T., Serrano, L., Fersht, A.R., 1990. Transient folding intermediates characterized by protein engineering. *Nature* 346, 440–445.
- Melnik, B.S., Marchenkov, V.V., Evdokimov, S.R., et al., 2008. Multi-state protein: Determination of carbonic anhydrase free-energy landscape. *Biochem Biophys. Res. Commun.* 369, 701–706.
- Nicolis, G., Prigogine, I., 1977. Self-Organization in Nonequilibrium Systems: From Dissipative Structures to Order through Fluctuations. Wiley Interscience, New York.
- Nöltning, B., 2010. Protein Folding Kinetics: Biophysical Methods. Springer, New York. Chapters 4–6, 8, 10, 11.
- Otzen, D.E., Kristensen, O., Proctor, M., Oliveberg, M., 1999. Structural changes in the transition state of protein folding: alternative interpretations of curved chevron plots. *Biochemistry* 38, 6499–6511.
- Samatova, E.N., Melnik, B.S., Balobanov, V.A., et al., 2010. Folding intermediate and folding nucleus for I–N and U–N transitions in apomyoglobin: different contributions of conserved and non-conserved residues. *Biophys. J.* 98, 1694–1702.
- Segava, S., Sugihara, M., 1984. Characterization of the transition state of lysozyme unfolding. I. Effect of protein-solvent interactions on the transition state. *Biochemistry* 23, 2473–2488.
- Shakhnovich, E., 2006. Protein folding thermodynamics and dynamics: where physics, chemistry, and biology meet. *Chem. Rev.* 106, 1559–1588.
- Slezov, V.V., 2009. Kinetics of First-Order Phase Transitions. Wiley-VCH, Weinheim, Germany. Chapter 3.
- Steensma, E., van Mierlo, C.P.M., 1998. Structural characterisation of apoflavodoxin shows that the location of the stable nucleus differs among proteins with a flavodoxin-like topology. *J. Mol. Biol.* 282, 653–666.
- Tseng, Y.Y., Liang, J., 2004. Are residues in protein folding nucleus evolutionarily conserved? *J. Mol. Biol.* 335, 869–980.
- Ubbelohde, A.R., 1965. Melting and Crystal Structure. Clarendon Press, Oxford. Chapters 2, 10, 14.
- Wetlaufer, D.B., 1973. Nucleation, rapid folding, and globular intrachain regions in proteins. *Proc. Natl. Acad. Sci. USA* 70, 697–701.
- Wikström, M., Drakenberg, T., Forsén, S., et al., 1994. Three-dimensional solution structure of an immunoglobulin light chain-binding domain of protein L. Comparison with the IgG-binding domains of protein G. *Biochemistry* 33, 14011–14017.

Lecture 21

In this lecture, we shall continue to discuss protein folding.

All the experimental data we discussed, though very interesting by themselves, cannot answer the main question as to how a protein manages to find ([Anfinsen, 1973; Levinthal, 1968](#)) its native structure among zillions of others within those minutes or seconds that are assigned for its folding.

And the number of alternative structures is vast indeed: it is at least 2^{100} but may be 3^{100} or even 10^{100} for a 100-residue chain, because at least 2 (but more likely 3 or 10) conformations are possible for each residue. Since the chain cannot pass from one conformation to another faster than within a picosecond (the time of a thermal vibration), their exhaustive search would take at least $\sim 2^{100}$ picoseconds (or 3^{100} or even 10^{100}), that is, $\sim 10^{10}$ (or 10^{25} or even 10^{80}) years. And it looks like the sampling has to be really exhaustive, as the protein can ‘feel’ that it has come to the stable structure only when it hits it precisely, because even a 1 Å deviation can strongly increase the chain energy in the closely packed globule.

How does the protein choose its native structure among zillions of possible others?, asked Levinthal (who first noticed this paradox), and answered ([Levinthal, 1968, 1969](#)): It seems that the protein folding follows some specific pathway, and the native fold is simply the end of this pathway, no matter if it is the most stable chain fold or not. In other words, Levinthal suggested that the native protein structure is determined by kinetics rather than stability and corresponds to the easily accessible local rather than the global free energy minimum.

The difficulty of this problem is that it cannot be solved by direct experiment. Indeed, suppose that the protein has some structure that is more stable than the native one. How can we find it if the protein does not do so itself? Shall we wait for $\sim 10^{10}$ (or even $\sim 10^{80}$) years?

On the other hand, the question as to whether the protein structure is controlled by kinetics or stability arises again and again, when one has to solve practical problems of protein physics and engineering. For example, in predicting a protein’s structure from its sequence, what should we look for? The most stable or the most rapidly folding structure? In designing a protein *de novo*, should we maximize the stability of the desired fold, or create a rapid pathway to this fold? However, is there a real contradiction between “the most stable” and the “rapidly folding” structure? Maybe, the stable structure *automatically* forms a focus for the “rapid” folding pathways, and therefore it is *automatically* capable of fast folding?

Before considering these questions, ie, before considering the *kinetic* aspects of protein folding, let us recall some basic facts concerning protein *thermodynamics* (as before, I will talk about single-domain proteins only, ie, chains

of 50–200 residues). These facts will help us to understand what chains and what folding conditions we have to consider. The facts are as follows:

1. Protein unfolding is reversible, and it occurs as an “all-or-none” transition. The latter means that only two states of the protein molecule, native and denatured, are present (close to the denaturation point) in a visible quantity, while all others, semi-native or misfolded, are virtually absent. Such a transition (as we already know) requires an amino acid sequence that provides a large energy gap between the most stable structure and the bulk of misfolded ones.
2. The denatured state, at least that of small proteins unfolded by a strong denaturant, is often the random coil.
3. Even under normal physiological conditions the native state of a protein is only more stable than its unfolded state by a few kilocalories per mole (and these two states have equal stability at mid-transition, naturally).

The native structure is stable because of its low energy, ie, because of strong interactions within this structure, and the coil state is stable because of its high entropy, that is, because of the vast number of unfolded conformations.

Inner voice: You say “entropy” and then mention solely “the vast number of unfolded conformations”, as if solvent entropy does not contribute to the total entropy!

Lecturer: It is essential that you note the following: (1) as is customary in the literature on this subject, the term “entropy” as applied to protein folding means only the conformational entropy, and this “entropy” does not include the solvent entropy; (2) correspondingly, the term “energy” means, actually, the “free energy of interactions” (often called the “mean force potential”) since, eg, the hydrophobic and other solvent-mediated forces, with all their solvent entropy, are included in the “energy”. This terminology is commonly used to concentrate on the main problem of sampling the protein chain conformations.

Throughout this lecture I will use the terms “energy” and “entropy” only in the above mentioned sense, which allows me to avoid speaking on the solvent—or rather, to take it into consideration in an implicit way.

Thus, to solve the Levinthal’s paradox...

Inner voice: Are you sure that the “Levinthal’s paradox” *is* a paradox indeed? [Bryngelson and Wolynes \(1989\)](#) have already mentioned that this ‘paradox’ is based on the absolutely flat (and therefore unrealistic) ‘golf course’ model of the protein potential energy surface ([Fig. 21.1A](#)), and somewhat later, [Leopold et al. \(1992\)](#), following the line of [Go and Abe \(1981\)](#), considered more realistic (tilted and biased to the protein’s native structure) energy surfaces and introduced the ‘folding funnels’ ([Fig. 21.1B](#)), which seems to eliminate the “paradox” completely!

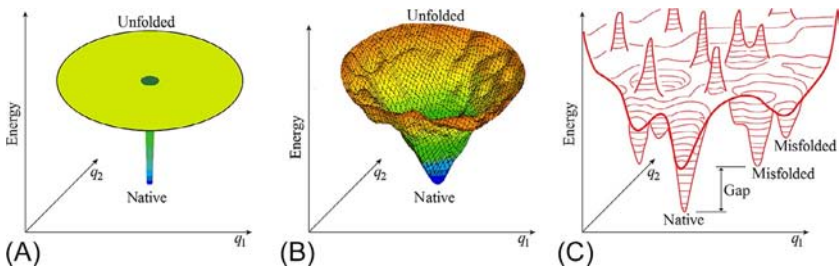


FIG. 21.1 (A) The “golf course” model of the protein potential energy landscape. (B) The “funnel” model of the protein potential energy landscape. The funnel is centered in the lowest-energy (“native”) structure. (C) In more detail: the bumpy potential energy landscape of a protein chain. A wide (of many $k_B T$) energy gap between the global and other energy minima is necessary to provide the “all-or-none” type of decay of the stable protein structure. The gap makes the protein function specific: like a light bulb, either the protein works or it does not. Only two coordinates (q_1 and q_2) can be shown in the drawings, while the protein chain conformation is determined by hundreds of coordinates.

Lecturer: It’s not as simple as that... The problem of huge sampling time exists: it has been mathematically proven that, despite the folding funnels and so on, finding the lowest free-energy conformation of a protein chain is the so-called “NP-hard” problem ([Ngo and Marks, 1992](#); [Unger and Moult, 1993](#)), which, loosely speaking, requires an exponentially large time to be solved (by a folding chain or by a man).

But, indeed, various “folding funnel” models became popular for explaining and illustrating protein folding ([Wolynes et al., 1995](#); [Karplus, 1997](#); [Nölting, 2010](#)). The “energy funnel”, centered in the lowest-energy structure, seems to allow protein chains to avoid the “Levinthal’s” sampling all conformations.

However, it can be shown that the energy funnels *per se* do not solve the Levinthal’s paradox—this, as Eugene Shakhnovich used to say, “Fermat’s Last Theorem of protein science”...

Strict analysis ([Bogatyreva and Finkelstein, 2001](#)) of the straightforwardly presented funnel models ([Zwanzig et al., 1992](#); [Bicout and Szabo, 2000](#)) shows that they cannot simultaneously explain both major features observed in protein folding: (1) its non-astronomical time, and (2) co-existence of the native and unfolded protein molecules during the folding process.

By the way, a stepwise mechanism of protein folding (which we discussed recently) also cannot ([Finkelstein, 2002](#)) simultaneously explain both these major features observed in protein folding.

Thus, neither stepwise nor simple funnel mechanisms solve the Levinthal’s problem, although they give a hint of what accelerates protein folding.

A solution of the paradox is provided by special (so-called “capillarity”; see [Wolynes, 1997](#)) nucleation funnels ([Finkelstein and Badretdinov, 1997a,b](#)), allowing for separation of the unfolded and native phases within the folding chain. It is this solution that I am going to present.

So, I continue. To solve the “Levinthal paradox” and to show that the most stable chain fold can be found within a reasonable time, we could, to a first approximation, consider only the rate of the “all-or-none” transition between the coil and the most stable structure. And we may consider this transition only for the crucial case when the most stable fold is as stable as (or only a little more stable than) the coil, all other forms of the chain being unstable, ie, close to the “all-or-none” transition midpoint.

Here the analysis can be made in the simplest form, without accounting for accumulating intermediates. True, the maximum folding rate is achieved when the native fold is considerably more stable than the coil, and then observable intermediates often arise. But let us first consider the situation when the folding is not the fastest but the simplest.

Since, as you may remember, the “all-or-none” transition requires a large energy gap between the most stable structure and the misfolded ones ([Fig. 21.1C](#)), we will assume that the considered amino acid sequence provides such a gap. I am going to show you that the “gap condition” provides a rapid folding pathway to the global energy minimum, to estimate the rate of folding and to prove that the most stable structure of a normal size domain can fold within seconds or minutes.

To prove that the most stable chain structure is capable of rapid folding, it is sufficient to prove that at least one rapid folding pathway leads to this structure. Additional pathways can only accelerate the folding since the rates of parallel reactions are additive. (One can imagine water leaking from a full to an empty pool through cracks in the wall between them: when the cracks cannot absorb all the water, each additional crack accelerates filling of the empty pool. And, by definition of the “all-or-none” transition, all semi- and misfolded forms together are too unstable to absorb a significant fraction of the folding chains and trap them.)

To be rapid, the pathway must consist of not too many steps, and most importantly, it must not require overcoming of a too high free-energy barrier. An L -residue chain can, in principle, attain its lowest-energy fold in L steps, each adding one fixed residue to the growing structure ([Fig. 21.2](#)). If the free energy went downhill along the entire pathway, a 100-residue chain would fold in $\sim 100\text{--}1000$ ns, since the growth of a structure (eg, an α -helix) by one residue is known to take a few nanoseconds ([Zana, 1975](#)).

Protein folding takes seconds or minutes rather than a microsecond because of the free-energy barrier: most of the folding time is spent on climbing up this barrier and falling back, rather than on moving along the folding pathway.

You should remember that, according to conventional transition state theory, the time of the process is estimated as:

$$\text{TIME} \sim \tau \times \exp (+\Delta F^\# / RT) \quad (21.1)$$

where τ is the time of one step, and $\Delta F^\#$ the height of the free-energy barrier.

For protein folding, τ is about 1–10 ns (according to the experimentally measured time of the growth of an α -helix by one residue; see [Zana, 1975](#)).

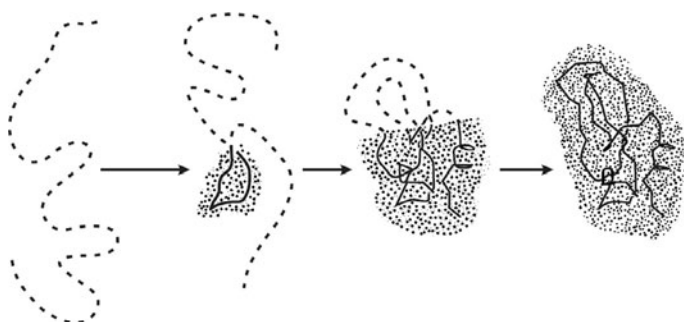


FIG. 21.2 Sequential folding pathway. At each step one residue leaves the coil and takes its final position in the lowest-energy structure. The folded part (shaded) is compact and native-like. The bold line shows the backbone fixed in the already folded part; the fixed side chains are not shown for the sake of simplicity (the volume that they occupy is shaded). The broken line shows the still unfolded chain. A rapid pathway requires compactness of the folded phase, ie, the minimal border between folded and unfolded phases. (Adapted from Finkelstein, A.V., Badretdinov, A.Ya., 1997b. Rate of protein folding near the point of thermodynamic equilibrium between the coil and the most stable chain fold. *Fold. Des.* 2, 115–121.)

As for $\Delta F^\#$, this is our main question: how high is the free-energy barrier $F^\#$ on the pathway leading to the lowest-energy structure? Folding of this structure decreases both the chain entropy (because of an increase in the chain's ordering) and its energy (because of the formation of contacts stabilizing the lowest-energy fold). The former increases and the latter decreases the free energy of the chain.

If the fold-stabilizing contacts start to arise only when the chain comes very close to its final structure (ie, if the chain has to lose almost all its entropy *before* the energy starts to decrease), the initial free energy increase would form a very high free-energy barrier (proportional to the *total* chain entropy lost). The Levinthal paradox claiming that the lowest-energy fold cannot be found within any reasonable time since this involves exhaustive sampling of all chain conformations originates exactly from this picture (loss of the entire entropy *before* the energy gain).

However, this paradox can be avoided if there is a folding pathway where the entropy decrease is immediately or nearly immediately compensated for by the energy decrease.

Let us consider a *sequential* (Fig. 21.2) folding pathway, which was first suggested by Wetlaufer (1973). At each step of this process, one residue leaves the coil and takes its final position in the lowest-energy 3D structure.

Inner voice: This pathway looks a bit artificial... How can the residue know its position in the lowest-energy fold?

Lecturer: As I told, we have to trace *one* pathway leading to the native fold. And the outlined pathway does so. As for the impression of its being artificial: look, it is exactly the pathway that you expect to see watching the movie on unfolding, but in the opposite direction.

Inner voice: And why cannot the protein use one way to unfold and quite another to fold?

Lecturer: It cannot: the direct and reverse reactions follow *the same* pathway(s) under the same ambient conditions (and we have already agreed to consider the fixed ambient conditions corresponding to the mid-point of the folding-unfolding equilibrium). This is the *detailed balance* law of physics. Its proof is very simple: if the direct and reverse reactions followed different pathways under the fixed ambient conditions, a *perpetual circular flow would arise in equilibrium*. And you could use it to rotate a small turbine. That is, your suggestion would lead to a device (called a *perpetuum mobile* of the second-order) that converts surrounding heat into work. And, as you know, or should know, the second law of thermodynamics, the law of maximum possible entropy, states that such a *perpetuum mobile* is impossible ([Landau and Lifshitz, 1980](#)). (Being more specific, the direct and reverse reactions must follow the same pathway under the same conditions, but under different conditions the pathways can be different, of course. That is, folding in water need not follow the same pathway as unfolding in concentrated denaturant; but at the same (fixed) denaturant concentration (eg, at mid-transition) they *must* use the same pathway.)

Inner voice: Still, a movie about explosion of a building, even watched in the opposite direction, is quite different from a movie about building construction ...

Lecturer: Both construction and explosion proceed at the expense of a huge energy (or, to be more precise, free energy): fuel, manpower, explosives. There are no “fixed ambient conditions” for the building. On the contrary, protein folding and unfolding do not consume any “fuel”, and, as the chevron plots show (see [Fig. 21.7](#) in the last part of this lecture), they can occur around and even at the equilibrium point ([Fersht, 1999](#)). This fact (I have stressed it many times) is very significant for an understanding of protein folding. Here, near the equilibrium point, the free energy difference between the folded and unfolded states is very small: zero or about $\pm k_B T$. And, at the very mid-transition (ie, the point where unfolding is in equilibrium with folding and the free energy difference is completely absent), these two processes occur simultaneously under the same ambient conditions, and here the direct and reverse reactions must follow exactly the same pathway and equilibrate one another.

Inner voice: So, you are going to estimate the time of protein *unfolding* (*not* folding!), and then use the detailed balance law to prove that the folding time is exactly the same?

Lecturer: Precisely. I shall estimate the protein *unfolding* time because it is easier (it is easier to outline a good *unfolding* pathway than a good folding pathway!) and, according to the detailed balance law, the folding time, under the same ambient conditions, is exactly the same as the unfolding time.

And then, to complete the solution of Levinthal's problem, we shall come back to considering the *folding* process.

Thus, let us consider the energy change ΔE , the entropy change ΔS and the resultant free energy change $\Delta F = \Delta E - T\Delta S$ along the *sequential* (Fig. 21.2) folding pathway.

When a piece of the final globule grows sequentially, the interactions that stabilize the final fold are restored sequentially as well. If the folded piece remains compact, as in Fig. 21.2, the number of restored interactions grows (and their total energy decreases) approximately in proportion to the number n of residues that have taken their final positions (Fig. 21.3A).

Approximately in proportion—but with one significant deviation:

At the beginning of folding, the energy decrease is a little slower, since the contact of a newly joined residue with the surface of a small globule is, on average, smaller than its contact with the surface of a large globule. This results in a

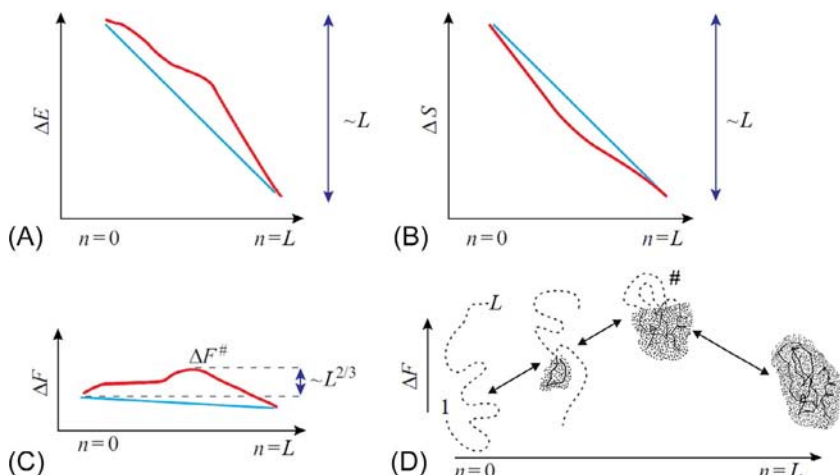


FIG. 21.3 The change of energy (A), entropy and (B) free energy (C) along the sequential folding pathway (D) close to the point of thermodynamic equilibrium between the coil ($n=0$) and the final structure ($n=L$: all the L chain residues are folded). The full energy and entropy changes, $\Delta E(L)$ and $\Delta S(L)$, are approximately proportional to L . The blue lines show the linear (proportional to the number of already folded residues n) parts of $\Delta E(n)$ and $\Delta S(n)$. The non-linear parts of $\Delta E(n)$ and $\Delta S(n)$ result mainly from the boundary between the folded and unfolded halves of the molecule. The maximum deviations of the $\Delta E(n)$ and $\Delta S(n)$ values from linear dependences are proportional to only $L^{2/3}$. As a result, the $\Delta F(n) = \Delta E(n) - T\Delta S(n)$ value also deviates from linear dependence (the blue line) by a value of $\sim L^{2/3}$. Thus, at the equilibrium point (where $\Delta F(0) = \Delta F(L)$), the maximal, along the pathway, free energy excess $\Delta F^\#$ over the blue free energy baseline is also proportional to only $L^{2/3}$. (Adapted from Finkelstein, A.V., Badretdinov, A.Ya., 1997a. Physical reason for fast folding of the stable spatial structure of proteins: A solution of the Levinthal paradox. *Mol. Biol. (Moscow, Eng. Trans.)* 31, 391–398; Finkelstein, A.V., Badretdinov, A.Ya., 1997b. Rate of protein folding near the point of thermodynamic equilibrium between the coil and the most stable chain fold. *Fold. Des.* 2, 115–121.)

non-linear *surface* term (proportional to $\approx n^{2/3}$ for an n -residue folded part) in the energy E of the growing globule. Thus, the maximum deviation from a linear energy decrease is proportional to the surface of the folded part, that is, to $L^{2/3}$, while the total energy decrease is proportional to the total number L of residues.

The entropy decrease is also *approximately* proportional to the number of residues that have taken their final positions (Fig. 21.3B). At the beginning of folding, though, the entropy decrease can be a little faster owing to disordered but closed loops protruding from the growing globule (Figs. 21.2 and 21.4). Their number is proportional to the interface between the folded and unfolded phases, and the free energy of a loop is known (Flory, 1969) to have a very slow, logarithmic dependence on its length. This again results in a non-linear *surface* term in the entropy ΔS of the growing globule. The overall entropy decrease is proportional to L again, and the maximum deviation from the linear entropy decrease again is proportional to $L^{2/3}$ (actually, it is $\approx L^{2/3} \times \ln(L^{1/3})$) at the maximum, but, on the average, the multiplier of the main term, $L^{2/3}$, is not more than 1 (Finkelstein and Badretdinov, 1997a); you may also take a look at the later rigorous mathematical papers (Fu and Wang, 2004; Steinhofel et al., 2006)).

Both linear and surface constituents of ΔS and ΔE enter the free energy $\Delta F = \Delta E - T\Delta S$ of the growing globule. However, when the final globule is in thermodynamic equilibrium with the coil, the large linear terms *annihilate* each other in the difference $\Delta E - T\Delta S$ (since $\Delta F = 0$ both in the coil (ie, at $n=0$) and in the final globule (at $n=L$)), and only the surface terms remain: $\Delta F(n)$ would be zero all along the pathway in the absence of surface terms.

Thus, the free-energy barrier (Figs. 21.3C and 21.5) is connected only with the relatively small surface effects at the coil–globule boundary, and the

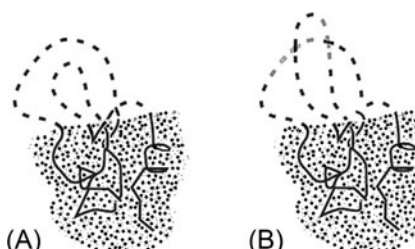


FIG. 21.4 (A) Compact semi-folded intermediate with protruding unfolded loops. Its growth corresponds to a shift of the boundary between the folded (globular) and unfolded parts. Successful folding requires correct knotting of loops: the structure with incorrect knotting (B) cannot change directly to the correct final structure: it first has to unfold and achieve the correct knotting. However, since a chain of ~ 100 residues can only form one or two knots, the search for correct knotting can only slow down the folding two-fold or at most four-fold; thus, the search for correct chain knotting does not limit the folding rate of normal size protein chains. (Adapted from Finkelstein, A.V., Badretdinov, A.Ya., 1998. Influence of chain knotting on the rate of folding. Erratum to Rate of protein folding near the point of thermodynamic equilibrium between the coil and the most stable chain fold. *Fold. Des.* 3, 67–68.)

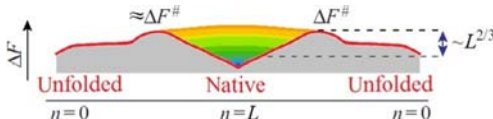


FIG. 21.5 The entropy converts the *energy funnel* (Fig. 21.1B) into a volcano-shaped (as it is called now, see [Rollins and Dill, 2014](#)) free-energy folding landscape with free-energy barriers (Fig. 21.3C) on each pathway leading from an unfolded conformation to the native fold.

height of this barrier on a sequential folding pathway (Figs. 21.2 and 21.3D) is proportional *not to* L (as Levinthal's estimate implies), but to $L^{2/3}$ only (Fig. 21.3C).

As a result, the time of folding of the most stable chain structure grows with the number of the chain residues L *not* “according to Levinthal” (ie, *not* as 2^L , or 10^L , or any exponent of L), but as $\exp(\lambda L^{2/3})$ only. The value $L^{2/3}$ arises from the separation of the “native” and “unfolded” phases, and it is much smaller than L . A thorough estimate of the coefficient λ (which is based on only one experimental parameter, namely, the average heat of protein melting per residue that is known from [Privalov's \(1979\)](#) work to be equal to about $2k_B T_{melt}$) shows that $\lambda = 1 \pm 0.5$, the particular value of λ depending on the distribution of strongly and weakly attracted residues within the lowest-energy structure, and in the main, on the *topology* of the lowest-energy structure (λ is large when this structure is such that its folding requires intermediates with many closed loops protruding from the native-like part, and λ is small if such loops are not required; (see [Finkelstein and Badretdinov, 1997a,b, 1998](#)) and Supporting Information for [Garuzynskiy et al., 2013](#)).

The observed protein folding times (for the coil → native globule transition at the point of equilibrium between these two states) are indeed (Fig. 21.6) in the range $10 \text{ ns} \times \exp(0.5 L^{2/3})$ to $10 \text{ ns} \times \exp(1.5 L^{2/3})$ ns, in accordance with the estimate obtained.

The reason for the “non-Levinthal” estimate, obtained for the mid-transition conditions (where the native fold free energy ΔF counted off that of the denatured state equals zero by definition),

$$\text{TIME} \sim \tau \times \exp \left[(1 \pm 0.5) L^{2/3} \right] \quad (21.2)$$

is that (1) the entropy decrease is almost immediately compensated for by the energy gain along the sequential folding pathway and (2) the free-energy barrier occurs owing to the surface effects only, which are relatively weak; $\tau = 10 \text{ ns}$ ([Zana, 1975](#)).

It is noteworthy that the sequential folding pathway does not require any rearrangement of the globular part (which could take a lot of time): all rearrangements occur in the coil and therefore are rapid.

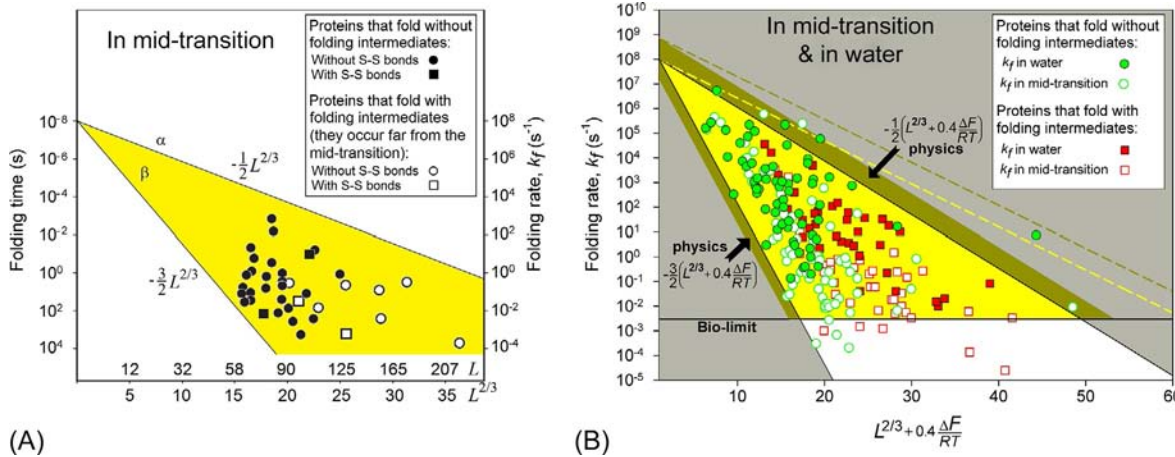


FIG. 21.6 (A) Observed (before 2000) folding time at the point of equilibrium between the unfolded and the native states, vs $L^{2/3}$ (L being the number of residues in the chain). The circles and squares refer to all 36 proteins listed in (Jackson, 1998), whose folding time at the mid-transition can be calculated from the available data. The symbols α , β refer to α -helical (Thompson et al., 1997) and β -hairpin (Muñoz et al., 1997) peptides. For many proteins, the folding intermediates are observed, but this occurs far from the mid-transition. The theoretically allowed (gold) region of $\ln(\text{time})$ is limited by the lines $\ln(10^{-8}\text{ s}) + 0.5L^{2/3}$ and $\ln(10^{-8}\text{ s}) + 1.5L^{2/3}$. As seen, all the experimental points are within this range (except for that of the α -helix, which is a one-dimensional rather than 3D object). (Adapted from Galzitskaya et al., 2001.) (B) Experimentally measured *in vitro* folding rate constants in water and at the mid-transition for 107 single-domain proteins (or separate domains) without disulfide bonds or covalently bound ligands. The rates are shown in the background of the golden (with the bronze belt) triangle, theoretically outlined for “biologically normal” conditions, plus the white extension of the triangle, additionally outlined for mid-transition conditions. Yellow dashed line limits the area allowed only for oblate (1:2) and oblong (2:1) globules at mid-transition; bronze dashed line means the same for “biologically normal” conditions. L is the number of amino acid residues in the experimentally investigated protein chain. ΔG is the free energy difference between the native and unfolded states of the chain. (Adapted from Garbuzynskiy et al., 2013.) The left edges of triangles in plots (A) and (B) (at $\Delta F=0$) approximately coincide with the estimated (Finkelstein and Garbuzynskiy, 2015; Finkelstein, 2015) time necessary for exhaustive sampling of all protein folds at the level of secondary structure formation and assembly.

Another similar scaling law ($\ln(\text{TIME}) \sim L^{1/2}$) was obtained by Thirumalai (1995) for the case of a very high native fold stability ($\Delta F \ll -k_B T$). Then protein folding essentially goes “downhill” in energy all the way, but the “downhill slope” has (due to protein heterogeneity) random bumps, whose energy is proportional to $L^{1/2}$.

The estimate obtained in Eq. (21.2), illustrated by Fig. 21.6 shows that a chain of L 80–90 residues will find its most stable fold within minutes or hours even near the mid-transition, where the folding is the slowest (Fig. 21.7). The native structures of such relatively small proteins are under thermodynamic control: they are the most stable among all structures of such chains. Native structures of larger proteins (of \approx 90–400 residues) are additionally under kinetic control, in a sense that some too entangled folds of their chains cannot be achieved within days or weeks even if they are thermodynamically stable (Garbuzynskiy et al., 2013). This equation also explains why a large protein should consist (according to the “divide and rule” principle) of separately folding domains: otherwise, chains of more than 300 residues would fold too slowly. The above estimates (80–90 and \approx 400 residues) are somewhat increased if the native fold’s free energy F is by many $k_B T$ lower than that of the unfolded chain (see below), but essentially remains the same (Garbuzynskiy et al., 2013).

The following points are noteworthy:

(1) Having found the free energy of the transition state (Fig. 21.3), one can further estimate the size of its globular part. This estimate shows that the nucleus must be as large as about half the protein. This is more or less compatible with

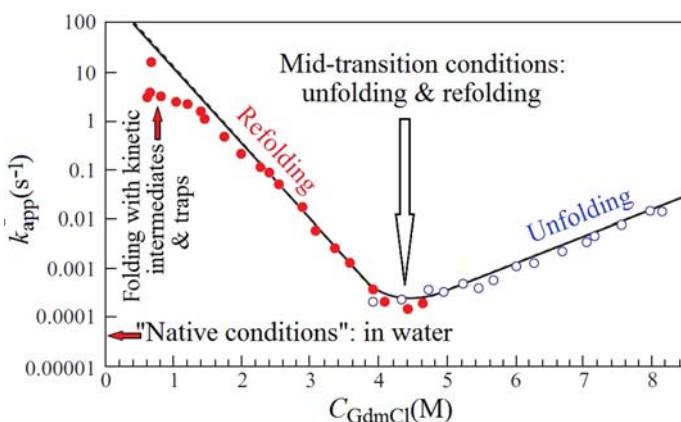


FIG. 21.7 Refolding and unfolding rates of hen egg-white lysozyme vs the concentration of guanidine dihydrochloride. The experimental points show the apparent rate k_{app} of approach to the equilibrium between the native and denatured forms of the protein. The filled circles correspond to refolding obtained upon diluting a concentrated GdmCl solution of the denatured protein. The open circles correspond to unfolding occurring after GdmCl addition to aqueous solution of the native protein. Note that these points overlap at the GdmCl concentration of ≈ 4.2 M, which corresponds to kinetic (and thermodynamic) equilibrium between folded and unfolded protein molecules. (Adapted from Kiefhaber, T., 1995. Kinetic traps in lysozyme folding. Proc. Natl. Acad. Sci. USA 92, 9029–9033.)

experiment ([Fig. 21.7](#)), which shows a crudely equal (but of opposite sign) dependence of the folding and unfolding rates on the denaturant concentration.

This means that the solvent-accessible area of the chain in the transition state is between the solvent-accessible areas of the unfolded and the globular states. It seems that the globular part of the transition state is somewhat larger than the folding nucleus itself at the cost of non-native interactions ([Li et al., 2000](#)). A large (comprising about half the protein) folding nucleus implies that there cannot be many alternative folding nuclei, which means that there cannot be too many parallel, alternative folding pathways, and thus consideration of only one of them can give a reasonable estimate of the folding time.

(2) The “quasi-Levinthal” search over intermediates with different chain knotting ([Fig. 21.4](#)) can, in principle, be a rate-limiting factor, since knotting cannot be changed without a decay of the globular part. However, since the computer experiments show that one knot involves about a hundred residues, the search for knotting can only be important for extremely long chains ([Finkelstein and Badretdinov, 1998](#)), which cannot fold within a reasonable time (according to Eq. [\(21.2\)](#)) in any case.

(3) Our estimate, Eq. [\(21.2\)](#), refers to $\Delta F = 0$, ie, to the point of equilibrium between the unfolded and the native states where the observed folding time is at a maximum and can exceed by orders of magnitude the folding time under native conditions ([Fig. 21.7](#)).

How will the folding rate change when the native state becomes somewhat more stable than the coil (ie, $\Delta F < 0$, but still $\Delta F \sim -k_B T$)? (In the opposite case, ie, if $\Delta F > 0$ no folding will happen, and that’s all.)

The initial growth of native fold stability has to increase the folding rate, since the transition state is stabilized as well, and the competing misfolded structures are still unstable (relative to the coil) owing to the energy gap between them and the most stable fold ([Fig. 21.8A](#)). This acceleration is indeed observed (see the left chevron limb in [Fig. 21.7](#)). However, the acceleration proceeds up to a certain limit only (see the short plateau at the top of the left chevron limb in [Fig. 21.7](#); in larger proteins such a plateau is much more pronounced ([Baryshnikova et al., 2005; Melnik et al., 2008](#))). It seems that the maximum folding rate is achieved when the metastable “misfolded” states (which include molten globules and serve as the on- or off-pathway kinetic intermediates) become as stable as the unfolded state. After that, the further increase in stability of the folded states leads to a rapid misfolding followed by a slower conversion into the native state that may occur via the unfolded state ([Fig. 21.8B](#)).

Leaving temporarily aside the latter case, ie, rare proteins with extremely stable folding intermediates, let us estimate the time of folding under the native conditions. It depends on the mid-transition folding time and on the native (relative to the unfolded) state free energy ΔF under the native conditions, and can be estimated as:

$$\text{TIME} \sim \tau \times \exp \left[(1 \pm 0.5) \times \left(L^{2/3} + 0.4 \times \Delta F / RT \right) \right] \quad (21.3)$$

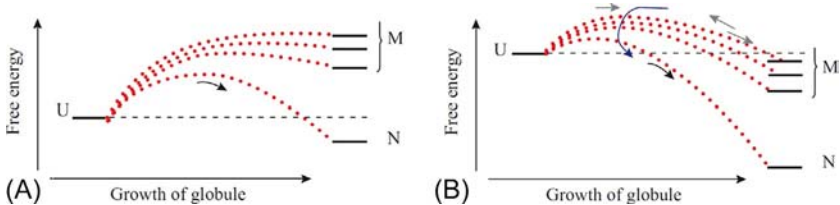


FIG. 21.8 Folding under different conditions. The bold lines show the free energies of the unfolded chain (U), of the most stable ('native') fold (N), and of the mis- or semi-folded structures (M). Dotted lines schematically show the behaviour of the free energy along the folding pathways leading to different structures (ignoring small irregularities); their maxima correspond to the transition states on these pathways. The main folding scenarios are given. (A) Fold N is more stable than the coil U, and the coil is more stable than all misfolded states M taken together. Misfolding and kinetic traps do not hinder rapid folding to the native state. The chain virtually does not explore the pathways leading to misfolded states, since on these pathways the free energy rises too high. (B) Both native and some of the misfolded folds are more stable than the coil (which is the phase where a fast rearrangement occurs). The chain rapidly comes to some misfolded form and then slowly undergoes transition to the stable state N via the partly unfolded state. Arrows show the mainstream of the folding process. (*Adapted from Finkelstein, A.V., Badretdinov, A.Ya., 1997b. Rate of protein folding near the point of thermodynamic equilibrium between the coil and the most stable chain fold. Fold. Des. 2, 115–121.*)

The multiplier 0.4 corresponds to the average (between 0.3 and 0.5) fraction of a chain involved in the folding nucleus (Garbuzyanskiy et al., 2013), so that $0.4 \times \Delta F$ is, proportionally, the average free energy of the folding nucleus. This equation gives a unified, though approximate estimate (Fig. 21.6B) of folding rates occurring under various conditions.

(4) Eqs. (21.2) and (21.3) estimate the *range* of possible folding rates rather than folding rates of an individual protein, which may differ (Fig. 21.6) from one another by many orders of magnitude. The influence of a protein chain fold upon the folding time (the factor $\lambda = 1 \pm 0.5$ in Eqs (21.2) and (21.3)) can be estimated (Ivankov et al., 2003) using a phenomenological “contact order” parameter (CO%) (Plaxco et al., 1998). CO% is equal to the average chain separation of the residues that are in contact in the native protein fold, divided by the chain length. (A somewhat different order parameter, proportional to the average chain separation squared has been suggested by Nölting et al. (2003) and later analyzed in Nölting (2010).) A high CO% value reflects entangling of the chain in the native protein (ie, existence of many long closed loops in the protein fold), while a high value of the factor λ reflects entangling of the chain in a semi-folded globule (Fig. 21.4). Therefore, CO% is more or less proportional to the λ value (Ivankov et al., 2003). CO% is a good predictor of folding rates of proteins equal in size, but it fails to compare folding rates of small proteins with those of large ones, because CO% decreases with decreasing protein size (which reflects a low entangling of chains forming large domains (Ivankov et al., 2003; Garbuzyanskiy et al., 2013)), while the folding rate grows, on the average, with increasing protein size (Fig. 21.6).

As a result of collaboration of A.V.F.'s and Plaxco-Baker's groups, it was shown that logarithms of the folding rates correlate well (Ivankov et al., 2003) with the "absolute contact order" value $\text{AbsCO} = \text{CO}\% \times L$, which grows with L as $L^{2/3}$ on the average. The AbsCO (and $\ln(\text{AbsCO})$) even better (Finkelstein et al., 2013)) allows predicting the folding rate of a protein from its size and structure.

Moreover, protein folding rates can be predicted from the chain length and the secondary structure content (Ivankov and Finkelstein, 2004), and, because the latter can be predicted from the amino acid sequence (Jones, 1999), one can rather successfully predict protein folding rates from their amino acid sequences alone. (Here, I put aside those numerous works on protein folding or unfolding rate prediction that do not contain physical insights and are based simply on correlation of folding or unfolding rates with amino acid content, and so on. I also put aside works on relationship between folding nuclei and conservatism of some sites of amino acid sequences; cf. Shakhnovich et al., 1996.)

The estimate of the folding time that I gave above is based on consideration of protein *unfolding* rather than *folding*. I considered *unfolding* because it is easier to outline a good *unfolding* pathway than a good folding pathway, while the result must be the same.

You may remember that I considered the free-energy barrier between the unfolded and folded states, focusing on its *unfolding* side (connected with energy increase), and did not consider it from its folding side connected with entropy loss. Since the rates of direct and reverse reactions are equal under the mid-transition conditions (as follows from the physical "detailed balancing" principle), here the "*unfolding*" and "*folding*" sides of the barrier are of equal heights, and therefore, examination of only one ("*unfolding*") side is sufficient to estimate the barrier height.

However, a complete analysis of folding urges us to look at the barrier from its folding (connected with entropy loss) side as well; I promised to do this, and will do it now.

To analyze folding, we have to analyze sampling of configurations of the protein chain.

The total volume of the protein conformation space, considered at the level of amino acid residues by Levinthal, is huge indeed. However, interactions occurring inside the chain are mainly connected with secondary structures. Thus, a question arises as to how large the total volume of the protein conformation space is, if considered at the level of formation and assembly of secondary structures, that is, at the level that had been considered by Ptitsyn (1973) in his model of stepwise protein folding.

To estimate this volume, one has to enumerate the number of local energy minima in the space of interacting secondary structures.

It turns out that the total volume of the protein chain conformation space is by many orders of magnitude smaller at the level of secondary structures than that at the level of amino acid residues: the latter, according to Levinthal's estimate, scales up as something like 10^L or 3^L with the number L of residues in the

chain, while the former scales up no faster than $\sim L^N$ with the number N of the secondary structure elements. N is much less than L , and this is the main reason for the drastic decrease of the conformation space.

The estimate L^N has been obtained as follows (see Fig. 21.9):

The number of architectures (ie, types of dense stacks of secondary structures) is small (cf. Levitt and Chothia, 1976; Murzin and Finkelstein, 1988; Chothia and Finkelstein, 1990), since the architectures are packagings of a few secondary structure layers, and their combinatorics is small compared with other factors. The number of packings, ie, combinations of positions of N elements in the given protein architecture cannot exceed $N!$ The number of topologies, ie, combinations of directions of these elements cannot exceed 2^N . Transverse shifts and tilts of an element within each architecture are prohibited (Fig. 21.9D). Shifts and turns of secondary structure elements within an architecture are coupled (this is shown in Fig. 21.9E using β -sheet as the most evident example, but it also refers to α -helices—remember ‘knobs in the holes’ close packing (Crick, 1953); as a result, each α or β element can have about L/N possible shift/turns in the globule formed by N secondary structures of the L -residue chain. All this limits the space to

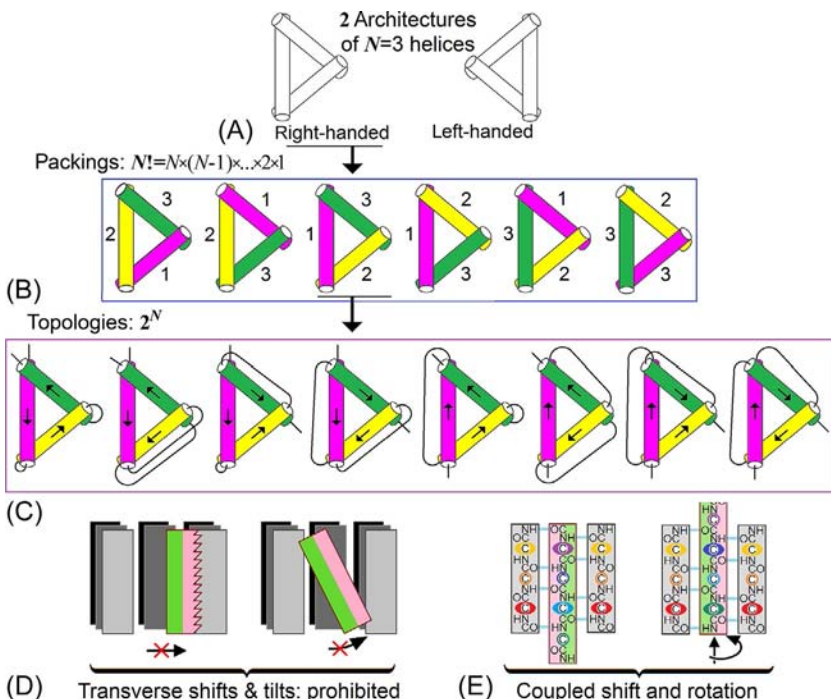


FIG. 21.9 A scheme of estimate of the volume of conformation space at a level of assembly of secondary structures. (Adapted from Supplement to Finkelstein, A.V., Garbuzyanskiy, S.O., 2015. Reduction of the search space for the folding of proteins at the level of formation and assembly of secondary structures: A new view on solution of Levinthal's paradox. *Chem. Phys. Chem.* 16, 3373–3378.)

$\sim(L/N)^N \times 2^N \times N!$ configurations, or $\sim L^N$ in the main term (if $L \gg N \gg 1$). This number can be somewhat reduced by symmetry of the globule; also, no α -helix can take the place of a β -strand, and vice versa, and short or crossing loops between secondary structures can prevent these from taking arbitrary positions and directions in the globule, etc. (Ptitsyn and Finkelstein, 1980). However, this reduction is not important to us, because our aim is to estimate the upper limit of the number of configurations.

Inner voice: How does the chain know where to form a secondary structure and what secondary structure is to be formed there?

Lecturer: Most of the secondary structures are well outlined by local amino acid sequences (Jones, 1999). Besides, its “existence or non-existence” adds only one state to the number L/N of its possible shift/turns, which is already taken into account.

The value of L/N (ie, the number of residues per secondary structure element plus accompanying loops) is 15 ± 5 according to protein statistics (Rollins and Dill, 2014), and it should scale as $\sim 3 L^{1/3}$ in a large globule, because the secondary structures go from one end of the globule to another, so that the resulting L^N scales up, in the main term, approximately as the upper limit of the estimate given by Eq. (21.2) (*cf.* also Fu and Wang, 2004; Steinhofel et al., 2006).

Taking, from folding of the smallest proteins, a few microseconds as a rough estimate of the time necessary to sample one configuration, we see that the time necessary to sample the whole conformation space at the level of secondary structure formation and assembly approximately coincides with the upper limit of the time estimate obtained from consideration of unfolding, as well as from experiment (Fig. 21.6).

Inner voice: Does this mean that a folding protein samples the entire conformation space at the level of secondary structure formation and packing?

Lecturer: Not at all. This means only that the funnels and all that starting their work from the level of secondary structures have to accelerate folding by several orders of magnitude, rather than by many tens of orders, which would have been the case if the funnels were to start working from the level of amino acid residues.

Actually, protein folding resembles crystallization (*cf.* Ubbelohde, 1965; Slezov, 2009); at the freezing temperature a perfect large single crystal (the lowest-energy structure) arises, although extremely slowly. As the temperature is lowered, a little the single crystal grows faster; and a further temperature decrease leads to rapid formation of a multitude of small crystals rather than of a perfect large single crystal.

I would like to mention that the similarity of the thermodynamic aspects of protein folding to those of first-order phase transitions has been experimentally proved by Privalov (1979), and the similarity of the kinetic aspects of these two events has been outlined by the experiments of Fersht and his co-workers

(Matouschek et al., 1989, 1990; Fersht, 1999) and by the analytical studies (Shakhnovich and Gutin, 1989, 1990) and computer experiments (Abkevich et al., 1994; Gutin et al., 1996) by Shakhnovich and Gutin.

Šali et al. (1994) used simple computer models of protein chains to show that even a small (several $k_B T$) difference in stability displayed by the lowest-energy fold and its competitors provides a reliable and fast folding to the global energy minimum. This work had a significant impact on the subsequent development of the theory of protein folding.

Then the same simple computer models of protein chains were used to explore the region of fastest folding. It has been shown (Gutin et al., 1996) that the folding time grows with the chain length L in this region much more slowly than predicted by Eq. (21.2) for the mid-transition. Specifically, in this region, the folding time grows with L not as $\sim \exp(L^{2/3})$ but as L^6 for “random” chains and as L^4 for the chains selected to fold most rapidly (ie, having a large energy gap between the most stable fold and the other ones). This emphasizes once again the dependence of the folding rate on the experimental conditions and on the difference in stability between the lowest-energy fold and its competitors (Wolynes, 1997).

Now, it would be only natural if here you asked me the question as to what happens if *two* structures instead of one are separated from others by a large energy gap.

The answer is: If these two structures are stable relative to the denatured state, the one with the better folding pathway (with a lower barrier) will be the first to fold. However, if this “more rapidly folded structure” is even a little less stable than the other one, a very slow transition to the more stable structure will follow. The transition will be slow since unfolding of the first stable structure will be required (Fig. 21.8B). This transition is similar to a polymorphous transition in crystals (recall the “tin disease”, ie, the transition of white tin into grey tin: in the 16th–18th centuries, this “disease” is known to have destroyed whole stores of tin soldier buttons during unusually severe frosts). It seems, though, that “polymorphous” proteins must be rare: as I told you, theoretical estimates show that the amino acid sequence coding one stable chain fold is a kind of wonder, but the sequence coding two of them is a squared wonder!

There is evidence, though, for polymorphous transitions in some proteins (Tsutsui et al., 2012). I mean serpins (a family of serine protease inhibitors, Fig. 21.10) and a few other “chameleon” proteins (putting aside already considered amyloids, because their alternative folds are achieved in aggregates, ie, in an environment that differs from conditions in which a single chain folds; so, this is not surprising; the surprising thing is that a separate protein molecule undergoes rearrangement under unchanged environmental conditions).

The serpin works as follows: it works as an inhibitor for some time and then stops working—without causing any damage to the chain or aggregation. Being denatured and then renatured *in vitro*, it regains its active state (Fig. 21.10, left), works as an inhibitor for an hour or so, and then stops working—and again

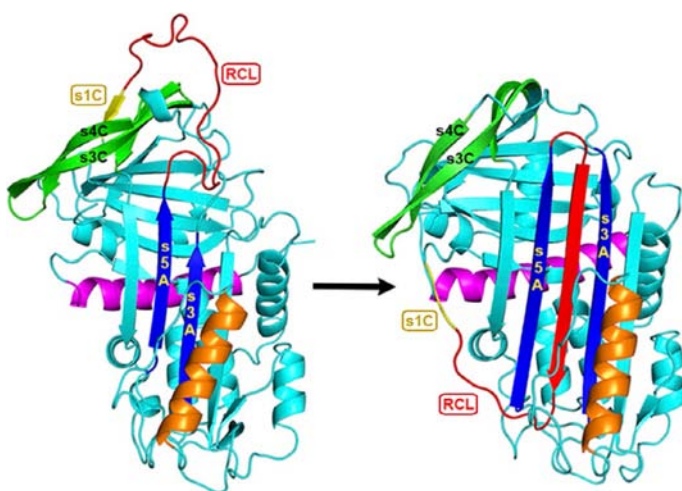


FIG. 21.10 Polymorphous latency transitions in serpin. Left panel: in the active state, the RCL region (red, on the top) is solvent-exposed, and the s1C region (yellow β -strand, on the top) is hydrogen-bonded to β -sheet C. The active state contrasts with the latent state (right panel), where s1C (yellow) is released from sheet C and the RCL (now in the bottom, left) is inserted in the centre of β -sheet A as the fourth (red) strand in a now six-stranded, fully antiparallel β -sheet. (Adapted with permission from Cazzolli, G., Wang, F., Beccara, S., Gershenson, A., et al., 2014. Serpin latency transition at atomic resolution. Proc. Natl. Acad. Sci. USA 111, 15414–15419.)

without damaging the chain or aggregation. And this cycle can be repeated a few times. This means that the “working” state of serpin is *not* the free energy minimum: it is a metastable state, while the stable state, ie, the global free energy minimum corresponds to its “latent” state (Fig. 21.10, right). The transition from the active, metastable state of serpin to its latent, inactive but stable state requires a large change in its conformation.

With this, I have redeemed my promise to return to the “rare proteins with extremely stable folding intermediates”.

In conclusion, let us return to the energy (Fig. 21.1) and free energy (Fig. 21.5) landscapes to visualize the fast folding pathways that automatically lead to the global energy minimum, provided it is much deeper than other energy minima.

Each low-energy structure, each energy minimum is surrounded by a rosette of tracks going to the minimum through the hilly, even rocky landscape (the “rocks” stressed by Frauenfelder (2010) correspond to powerful but short-range repulsions at collisions of chain fragments). They form a “folding funnel” (Leopold et al., 1992; Wolynes et al., 1995; Karplus, 1997; Wolynes, 1997; Dill and Chan, 1997; Nölting, 2010). Some of these tracks, more or less smooth, correspond to the sequential (Fig. 21.2) pathways of folding to the given energy minimum; the most advantageous are those that provide separation of the dense, compact (and thus relatively stable) already folded part of the native globule from the still unfolded chain. No rearrangements of the already folded part

of the globule take place on the sequential pathways, and therefore they have no large pits and bumps (and small ones pose no obstacle when the temperature is not too low). When moving along these pathways to the energy minimum, the molecule gains energy but loses entropy (Fig. 21.3), since its structure becomes more and more fixed. The deeper the energy minimum, the greater the energy gain—and the easier it is to overcome the “entropic resistance”. The strength of this resistance is proportional to temperature. At too high a temperature the resistance is strong, and it does not allow the chain to fold into any fixed structure. At too low a temperature the resistance is too small, and the chain falls in any neighboring energy well; then it spends a lot of time to get out of it just to fall in a local minimum again—and thus it cannot approach the global energy minimum for a very long time (Fig. 21.8B). And at last, when the temperature is good for folding, the entropic resistance is overcome only on the pathways to the deepest energy minimum (which is much deeper than other minima: just recall the “energy gap”), and the chain gets there rapidly (Fig. 21.8A).

The scheme given above of entropy-by-energy compensation along the folding pathway with separation of folded and unfolded phases, and the conclusion that it can solve the Levinthal’s paradox are applicable to formation of the native protein structure not only from the coil but also from the molten globule or from another intermediate. However, for these scenarios, all the estimates would be much more cumbersome, while these processes do not show (experimentally) any drastic advantage in the folding rate. Therefore, I will not go beyond the simplest case of the coil-to-native globule transition.

All the above emphasizes the significance of development of the “new view” on folding, the view based on the nature of the free energy surfaces or “landscapes” that define the folding reaction rather than on discrete accumulation of folding intermediates. This process differs from the more familiar reactions of small molecules by the following: (1) a particular protein structure is the result of many weak interactions; (2) a large change in configurational entropy occurs during folding; (3) the native and denatured phases separate during folding.

One of the most satisfying features of recent conceptual advances is the emergence of a “unified mechanism” of folding and the realization that apparently disparate patterns of experimental behavior result from the interplay of different contributions to the overall free energy under different circumstances. This unification of ideas provides a framework for joint work by experimentalists and theoreticians in order to obtain a more detailed understanding of the intricate folding process.

In particular, special attention is now paid to the link between the fundamental process of folding and the multiplicity of folding protein states that can exist in a crowded cellular system, which leads to the need to consider their intermolecular as well as intramolecular interactions, such as the interaction of the folding nuclei with chaperones or other proteins, RNA and DNA.

The understanding of protein folding is much more than just a challenge to the skills and intellects of protein scientists. Folding (or self-organization)

represents a bridge between the laws of physics and the results of the evolutionary pressure under which the character of biology has developed. For many years we could only discuss this issue in very general terms, emphasizing the biological importance of this complex physical process. Now, we are beginning to understand that folding is a physical process taking place only in systems that have been biologically selected to ensure its efficiency.

Protein physics is grounded on two fundamental experimental facts: (1) protein chains are capable of forming their native structures spontaneously in the appropriate environment, and (2) the native state is separated from the unfolded state of the chain by an “all-or-none” phase transition. The latter ensures the robustness of protein action and minimal populations of partially folded and therefore aggregation-prone species.

It appears that biological evolution selects only those sequences that fold into a well-defined 3D native structure. This is necessary for the protein to work reliably. Such a well-defined structure can be formed only by a sequence with a free energy that is much lower than that of alternative structures. And this is precisely the sequence that is capable of “all-or-none” folding and unfolding. The enhanced stability of the native structure seems to be due to its tight packing (even though it is not yet clear exactly what constraint is placed on protein chains by their capability of tight packing). Interestingly, these selected sequences appear to meet the requirement of correct folding into the stable structure simultaneously with the ability to fold quickly. It is probable that the latter helps incompletely folded polypeptide chains to avoid the competing process of intermolecular aggregation. The ability of stable structures to fold quickly solves the long-standing contradiction between the kinetic and thermodynamic choice of the native fold.

The sequences of globular proteins look rather “random”, and their secondary and tertiary structures bear many features typical of all more or less stable folds of random co-polymers. However, the ability of polypeptides to fold rapidly and reproducibly to definite tertiary structures is not a characteristic feature of random sequences. The main feature of “protein-like” amino acid sequences, the feature that determines all their physical properties, is the enhanced stability of their native fold, ie, the existence of a large gap between the energy of the native fold and the minimum energy of misfolded globular structures. Although the size of this energy gap is not yet established by a physical experiment, some theoretical estimates show that even a rather narrow gap (of a few kilocalories per mole) can cause “protein-like” behavior of a protein domain. And it is already clear that the necessary reinforcement of the lowest-energy fold can be achieved by a gradual evolutionary selection among many random point mutations.

Protein folding is perhaps the simplest example of a biological morphogenesis that can only take place in a system evolutionarily designed to allow it to happen. Nevertheless, protein folding has the typical physical characteristics associated with a complex process obeying the laws of statistical mechanics.

In particular, folding of globular proteins involves a capillarity nucleation mechanism generally typical for “all-or-none” (ie, first-order) phase transitions.

Folding pathways seem to be not unique: various pathways can lead to one target, although their rates may be different and may depend on the folding conditions. (A low-speed folding may be, though, dangerous: as shown by ([Dobson, 2003](#)), non-folded proteins tend to aggregate, which, as have been mentioned, can lead to “conformational diseases”.) Folding is the result of statistical fluctuations within the unfolded protein chain, which (under appropriate temperature and solvent conditions) result in its transition to the native state, which is almost always the structure of the lowest free energy. In this way a single well-defined structure can emerge from the statistical ensemble of unfolded or partially folded species.

All this once again emphasizes a connection between protein structure, stability and ability to fold spontaneously and the role of natural selection in the introduction and maintenance of these qualities.

It is easy to imagine and it is possible to show by computer simulations (but much more difficult to prove experimentally) that selection could start from the slightly increased stability of some structure of a polypeptide coded by a “random” piece of DNA, provided this structure can do something even marginally useful for a cell. And that then the pressure of evolution results, by random mutations and selection of the more and more reliably folding sequences, in the emergence of a sequence with the rare quality of spontaneously folding into a definite fold, which also allows specificity of function to be achieved, by additional selection, in a manner susceptible to feedback control and regulation in a complex and crowded cellular environment.

However, this way of originating new globular proteins, origination from random sequences, seems to play no role at observable (ie, not the earliest) stages of biological evolution (this concerns water-soluble globular proteins, while fibrous and membrane proteins seem to evolve by multiplication of relatively short repeats or merging of relatively short blocks). As I have already mentioned, it is commonly accepted that now “new” proteins originate in two ways. One is gene duplication, which allows the “old” protein to keep working, while the sequence of the “new” one is free to mutate and to drift (with the aid of selection) towards some “new” function. The other is the merging of separate domains and small proteins into a multi-domain protein capable of performing more complicated functions and thus more susceptible to regulation because of the physical interactions of these domains. It is worth mentioning that multi-domain proteins are more typical of higher organisms than of bacteria and unicellular eukaryotes. (Though I have to say that there is no evidence that, historically, proteins went from “small and simple” to “large and complicated”; the already considered observation that natively disordered proteins are more typical of eukaryotes than of prokaryotes provokes some suspicions to this idea.)

However, this does not revoke the privilege of some (“defect-free”) protein architectures, whose stability is compatible with a greater variety of sequences

to ensure more freedom for evolution and selection. Of course, selection is capable of creating even most improbable structures if they give an advantage to a species (the eye and brain being examples). However, protein function has only a little connection with its architecture, as we have seen and will see again. Therefore, it is not really surprising (although it is remarkable) that protein structures often look like those to be expected for stable folds of random sequences; that is, the “multitude principle” still seems to work in biological evolution.

REFERENCES

- Abkevich, V.I., Gutin, A.M., Shakhnovich, E.I., 1994. Specific nucleus as a transition state for protein folding: evidence from the lattice model. *Biochemistry* 33, 10026–10031.
- Anfinsen, C.B., 1973. Principles that govern the folding of protein chains. *Science* 181, 223–230.
- Baryshnikova, E.N., Melnik, B.S., Finkelstein, A.V., et al., 2005. Three-state protein folding: experimental determination of free-energy profile. *Protein Sci.* 14, 2658–2667.
- Bicout, D.J., Szabo, A., 2000. Entropic barriers, transition states, funnels, and exponential protein folding kinetics: A simple model. *Protein Sci.* 9, 452–465.
- Bogatyreva, N.S., Finkelstein, A.V., 2001. Cunning simplicity of protein folding landscapes. *Protein Eng.* 14, 521–523.
- Bryngelson, J.D., Wolynes, P.G., 1989. Intermediates and barrier crossing in a random energy model (with applications to protein folding). *J. Phys. Chem.* 93, 6902–6915.
- Chothia, C., Finkelstein, A.V., 1990. The classification and origins of protein folding patterns. *Ann. Rev. Biochem.* 59, 1007–1039.
- Crick, F.H.C., 1953. The packing of α -helices: Simple coiled coils. *Acta Crystallogr.* 6, 689–697.
- Dill, K.A., Chan, H.S., 1997. From Levinthal to pathways to funnels. *Nat. Struct. Biol.* 4, 10–19.
- Dobson, C.M., 2003. Protein folding and misfolding. *Nature* 426, 884–890.
- Fersht, A., 1999. Structure and Mechanism in Protein Science: A Guide to Enzyme Catalysis and Protein Folding. W.H. Freeman, New York (Chapters 2, 15, 18, 19).
- Finkelstein, A.V., 2002. Cunning simplicity of a hierarchical folding. *J. Biomol. Struct. Dyn.* 20, 311–313.
- Finkelstein, A.V., 2015. Two views on the protein folding puzzle. Available at: <http://atlasofscience.org/two-views-on-the-protein-folding-puzzle/>.
- Finkelstein, A.V., Badretdinov, A.Ya., 1997a. Physical reason for fast folding of the stable spatial structure of proteins: A solution of the Levinthal paradox. *Mol. Biol. (Moscow, Eng. Trans.)* 31, 391–398.
- Finkelstein, A.V., Badretdinov, A.Ya., 1997b. Rate of protein folding near the point of thermodynamic equilibrium between the coil and the most stable chain fold. *Fold. Des.* 2, 115–121.
- Finkelstein, A.V., Badretdinov, A.Ya., 1998. Influence of chain knotting on the rate of folding. Erratum to Rate of protein folding near the point of thermodynamic equilibrium between the coil and the most stable chain fold. *Fold. Des.* 3, 67–68.
- Finkelstein, A.V., Garbuzynskiy, S.O., 2015. Reduction of the search space for the folding of proteins at the level of formation and assembly of secondary structures: A new view on solution of Levinthal’s paradox. *Chem. Phys. Chem.* 16, 3373–3378.
- Finkelstein, A.V., Bogatyreva, N.S., Garbuzynskiy, S.O., 2013. Restrictions to protein folding determined by the protein size. *FEBS Lett.* 587, 1884–1890.
- Flory, P.J., 1969. Statistical Mechanics of Chain Molecules. Interscience Publishers, New York (Chapter 3).

- Frauenfelder, H., 2010. *The Physics of Proteins: An Introduction to Biological Physics and Molecular Biophysics*. Springer, New York (Chapters 11, 12, 15).
- Fu, B., Wang, W., 2004. A $2^{O(n^{1-1/d} \cdot \log(n))}$ time algorithm for d-dimensional protein folding in the HP-model. *Lecture Notes in Computer Science* 3142, 630–644.
- Galzitskaya, O.V., Ivankov, D.N., Finkelstein, A.V., 2001. Folding nuclei in proteins. *FEBS Lett.* 489, 113–118.
- Garbuzyntsiy, S.O., Ivankov, D.N., Bogatyreva, N.S., Finkelstein, A.V., 2013. Golden triangle for folding rates of globular proteins. *Proc. Natl. Acad. Sci. USA* 147–150.
- Go, N., Abe, H., 1981. Noninteracting local-structure model of folding and unfolding transition in globular proteins. I. Formulation. *Biopolymers* 20, 991–1011.
- Gutin, A.M., Abkevich, V.I., Shakhnovich, E.I., 1996. Chain length scaling of protein folding time. *Phys. Rev. Lett.* 77, 5433–5436.
- Ivankov, D.N., Finkelstein, A.V., 2004. Prediction of protein folding rates from the amino-acid sequence-predicted secondary structure. *Proc. Natl. Acad. Sci. USA* 101, 8942–8944.
- Ivankov, D.N., Garbuzyntsiy, S.O., Alm, E., et al., 2003. Contact order revisited: Influence of protein size on the folding rate. *Protein Sci.* 12, 2057–2062.
- Jackson, S.E., 1998. How do small single-domain proteins fold? *Fold. Des.* 3, R81–R91.
- Jones, D.T., 1999. Protein secondary structure prediction based on position-specific scoring matrices. *J. Mol. Biol.* 292, 195–202. Modern version available at: <http://bioinf.cs.ucl.ac.uk/psipred/>.
- Karplus, M., 1997. The Levinthal paradox: yesterday and today. *Fold. Des.* 2 (Suppl. 1), S69–S75.
- Landau, L.D., Lifshitz, E.M., 1980. *Statistical Physics (Volume 5 of A Course of Theoretical Physics)*, third ed. Elsevier, London (Sections 7, 8, 150).
- Leopold, P.E., Montal, M., Onuchic, J.N., 1992. Protein folding funnels: a kinetic approach to the sequence-structure relationship. *Proc. Natl. Acad. Sci. USA* 89, 8721–8725.
- Levinthal, C., 1968. Are there pathways for protein folding? *J. Chim. Phys. Chim. Biol.* 65, 44–45.
- Levinthal, C., 1969. How to fold graciously. In: Debrunner, P., Tsibris, J.C.M., Munck, E. (Eds.), *Mössbauer Spectroscopy in Biological Systems: Proceedings of a Meeting Held at Allerton House, Monticello, Illinois*. University of Illinois Press, Urbana-Champaign, IL, pp. 22–24.
- Levitt, M., Chothia, C., 1976. Structural patterns in globular proteins. *Nature* 261, 552–558.
- Li, L., Mirny, L.A., Shakhnovich, E.I., 2000. Kinetics, thermodynamics and evolution of non-native interactions in a protein folding nucleus. *Nat. Struct. Biol.* 7, 336–432.
- Matouschek, A., Kellis, J.T., Serrano, L., Fersht, A.R., 1989. Mapping the transition state and pathway of protein folding by protein engineering. *Nature* 340, 122–126.
- Matouschek, A., Kellis, J.T., Serrano, L., Fersht, A.R., 1990. Transient folding intermediates characterized by protein engineering. *Nature* 346, 440–445.
- Melnik, B.S., Marchenkov, V.V., Evdokimov, S.R., et al., 2008. Multi-state protein: Determination of carbonic anhydrase free-energy landscape. *Biochem Biophys. Res. Commun.* 369, 701–706.
- Muñoz, V., Thompson, P.A., Hofrichter, J., Eaton, W.A., 1997. Folding dynamics and mechanism of beta-hairpin formation. *Nature* 390, 196–199.
- Murzin, A.G., Finkelstein, A.V., 1988. General architecture of α -helical globule. *J. Mol. Biol.* 204, 749–770.
- Ngo, J.T., Marks, J., 1992. Computational complexity of a problem in molecular structure prediction. *Protein Eng.* 5, 313–321.
- Nölting, B., 2010. *Protein Folding Kinetics: Biophysical Methods*. Springer, New York (Chapters 10, 11, 12).
- Nölting, B., Schälike, W., Hampel, P., et al., 2003. Structural determinants of the rate of protein folding. *J. Theor. Biol.* 223, 299–307.

- Plaxco, K.W., Simons, K.T., Baker, D., 1998. Contact order, transition state placement and the refolding rates of single domain proteins. *J. Mol. Biol.* 277, 985–994.
- Privalov, P.L., 1979. Stability of proteins: small globular proteins. *Adv. Protein Chem.* 33, 167–241.
- Pitsyn, O.B., 1973. Stages in the mechanism of self-organization of protein molecules. *Dokl. Akad. Nauk SSSR* 210, 1213–1215 (in Russian).
- Pitsyn, O.B., Finkelstein, A.V., 1980. Similarities of protein topologies: evolutionary divergence, functional convergence or principles of folding? *Quart. Rev. Biophys.* 13, 339–386.
- Rollins, G.C., Dill, K.A., 2014. General mechanism of two-state protein folding kinetics. *J. Am. Chem. Soc.* 136, 11420–11427.
- Šali, A., Shakhnovich, E., Karplus, M., 1994. Kinetics of protein folding. A lattice model study of the requirements for folding to the native state. *J. Mol. Biol.* 235, 1614–1636.
- Shakhnovich, E.I., Gutin, A.M., 1989. Formation of unique structure in polypeptide-chains theoretical investigation with the aid of a replica approach. *Biophys. Chem.* 34, 187–199.
- Shakhnovich, E.I., Gutin, A.M., 1990. Implications of thermodynamics of protein folding for evolution of primary sequences. *Nature* 346, 773–775.
- Shakhnovich, E., Abkevich, V., Ptitsyn, O., 1996. Conserved residues and the mechanism of protein folding. *Nature* 379, 96–98.
- Slezov, V.V., 2009. Kinetics of First-Order Phase Transitions. Wiley-VCH, Weinheim, Germany.
- Steinhofel, K., Skaliotis, A., Albrecht, A.A., 2006. Landscape analysis for protein folding simulation in the H-P model. *Lecture Notes in Computer Science* 4175, 252–261.
- Thirumalai, D., 1995. From minimal models to real proteins: time scales for protein folding kinetics. *J. Phys. I. (Orsay, Fr.)* 5, 1457–1469.
- Thompson, P.A., Eaton, W.A., Hofrichter, J., 1997. Laser temperature jump study of the helix<=>coil kinetics of an alanine peptide interpreted with a ‘kinetic zipper’ model. *Biochemistry* 36, 9200–9210.
- Tsutsui, Y., Cruz, R.D., Wintrode, P.L., 2012. Folding mechanism of the metastable serpin $\alpha 1$ -antitrypsin. *Proc. Natl. Acad. Sci. USA* 109, 4467–4472.
- Ubbelohde, A.R., 1965. Melting and Crystal Structure. Clarendon Press, Oxford (Chapters 2, 5, 6, 10–12, 14, 16).
- Unger, R., Moult, J., 1993. Finding the lowest free energy conformation of a protein is an NP-hard problem: proof and implications. *Bull. Math. Biol.* 55, 1183–1198.
- Wetlaufer, D.B., 1973. Nucleation, rapid folding, and globular intrachain regions in proteins. *Proc. Natl. Acad. Sci. USA* 70, 697–701.
- Wolynes, P.G., 1997. Folding funnels and energy landscapes of larger proteins within the capillarity approximation. *Proc. Natl. Acad. Sci. USA* 94, 6170–6175.
- Wolynes, P.G., Onuchic, J.N., Thirumalai, D., 1995. Navigating the folding routes. *Science* 267, 1619–1620.
- Zana, R., 1975. On the rate determining step for helix propagation in the helix-coil transition of poly-peptides in solution. *Biopolymers* 14, 2425–2428.
- Zwanzig, R., Szabo, A., Bagchi, B., 1992. Levinthal’s paradox. *Proc. Natl. Acad. Sci. USA* 89, 20–22.

Lecture 22

When it became known that the amino acid sequence of a protein chain determines its 3D structure (Anfinsen et al., 1961), the “protein structure prediction problem” arose.

Prediction of protein structures from their amino acid sequences is interesting for two reasons: intellectual and practical.

Intellectual interest in the protein structure prediction problem is aroused not only because it is a challenge (can we do it or not?) but mostly, I think, because we well remember the very great importance of the DNA structure prediction for molecular biology as a whole.

The practical interest is obvious. Experimentally, it is much more difficult to determine a 3D protein structure than an amino acid sequence. The flow of new sequences is immense, counted in millions. Most of them are only read from DNA or RNA, and the functions of these proteins are not yet established experimentally. The flow of new 3D structures is less by two or three orders of magnitude. And understanding of the protein action, the search for protein’s inhibitors and activators (ie, for potential drugs)—all this requires a knowledge of the protein’s 3D structure. Thus, any tips on the 3D folds from the sequences are valuable.

What can be said about the 3D structures of “new” proteins (not yet studied by NMR or X-ray) when only their amino acid sequences are known?

The first thought is to predict the 3D structure of a “new” sequence on the basis of its generic similarity (homology) to a sequence of some “old” (X-ray- or NMR-solved) proteins.

Establishing sequence homology (Fig. 22.1) is indeed a very powerful method for elucidating structural and functional similarity (for proteins, as well as for DNA fragments and RNAs). The main difficulty in making alignments is that even very similar sequences (Fig. 22.1A) or structures (Fig. 22.2A) cannot be well superimposed (see Appendix C) without allowing deletions (gaps) or insertions in them. Establishing of “optimal” penalty for deletions and insertions is a special problem that, up to now, has no good solution; instead, there are more or less satisfactory “experience-based” recipes of various kinds.

It may be worth mentioning that the term “homology of sequences” is somewhat ambiguous. The following are two illustrative examples:

1. Suppose, one additional base is included in the protein gene just after the initiation codon. Then the new and the old DNA (and RNA) sequences are virtually the same; one will find them highly “homologous” (which is correct, in the strict sense of the word “homology,” since their origin is the same). At the same time, the new and the old protein sequences are completely different due to the frame shift, one will find no “homology” between them (which is,

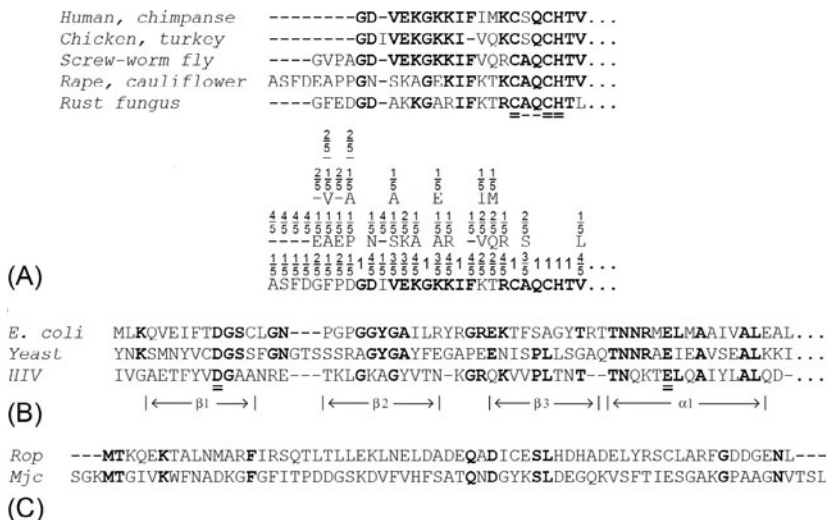


FIG. 22.1 Homology: strong (A), weak (B), and absent (C). Bold letters indicate residues identical in a half or more compared sequences. (A) Multiple alignment of amino acid sequences of the N-terminal fragments of a few cytochromes *c* from mitochondria and chloroplasts. Proteins with such a high similarity of sequences (if it is observed throughout the chain) are known to have nearly identical 3D structures, as a rule. The underlined site Cys-X-X-Cys-His is responsible for heme binding in the majority of cytochromes (adapted from Creighton, T.E., 1993. Proteins: Structures and Molecular Properties, second ed. W. H. Freeman & Co., New York (Chapter 3)). Below: the alignment profile corresponding to this multiple alignment; numbers are “weights” for the matching given residue in the given profile position. (B) Amino acid sequences of the N-terminal halves of ribonucleases *H* from bacteria (*E. coli*), eukaryote (yeast), and virus HIV. The alignment was done so as to rule out sequence gaps (---) within inner regions of α- and β-structures (these are shown at the bottom). The active site residues are marked with = (adapted from Perutz, M.F., 1992. Protein Structure, W. H. Freeman & Co., New York, NY). (C) Alignment of sequences of unlike, nonhomologous proteins (here: α-helical RNA-binding protein, *Rop*, and β-structural cold shock protein, *Mjc*) often shows the same, as in (B), 10–15% coincidence of amino acid residues. The alignment was done using the BLAST program (Altschul et al., 1990). It shows approximately the same sequence identity as *Yeast* and *HIV* ribonucleases *H* shown in (B).

strictly speaking, a wrong conclusion because they have the same genetic origin; but this conclusion is instrumental as far as it simply means that amino acid sequences (and 3D folds) of the proteins have nothing in common).

Later on, I will use the term “homology” in a narrow sense, in the sense of similarity of amino acid sequences only, having in mind that our aim is to use “homology” in finding similarity between 3D structures.

- Sequence alignment is assumed to reflect their common ancestry. Since the true evolutionary alignment is always unknown, accurate alignment of 3D structures (Fig. 21.2) can present its reasonable approximation (Doolittle, 1981) and serve as the alignment “gold standard” (GS). But the protein structure *prediction* can be, of necessity, only based on alignment of

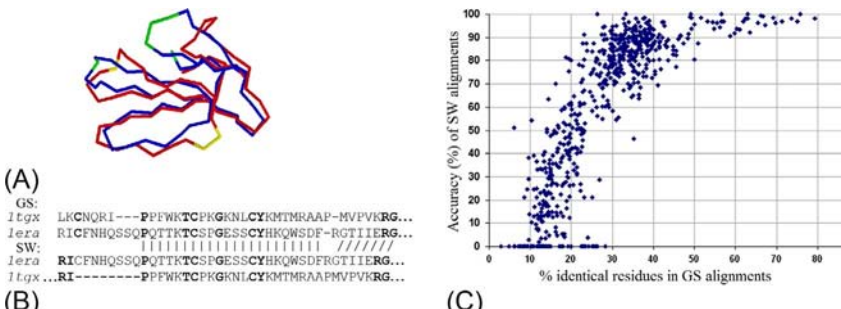


FIG. 22.2 (A) “Gold standard” (GS): structural alignment of 3D folds in 3D space. Cardiotoxin (PDB code: 1tgx) vs. erabutoxin B (PDB code: 1era). Aligned regions are colored in red in 1tgx and in blue in 1era, nonaligned regions are in yellow in 1tgx and in green in 1era. Deviations in C^α positions of aligned residues are usually within 3 Å. (B) Sequence alignments corresponding to the alignment of 3D folds (GS) and to the [Smith and Waterman \(1981\)](#) method (SW) of alignment of sequences. N-terminal fragments of the alignments are only shown; bold letters indicate identical residues. Short lines between the GS and SW alignments connect residues identically superimposed in both alignments. (C) Accuracy of 583 pair-wise SW alignments with respect to the structural GS alignments. “% identical residues” is the number of identical residue matches in the GS alignment, divided by the length of the shorter sequence. Accuracy of the SW alignment is the number of positions identically superimposed in the SW and the GS alignments divided by the total number of positions in the GS alignment. (*Adapted from Sunyaev, S.R., Bogopolsky, G.A., Oleinikova, N.A., Vlasov, P.K., Finkelstein, A.V., Roytberg, M.A., 2004. From analysis of protein structural alignments toward a novel approach to align protein sequences. Proteins 54, 569–582.*)

sequences (Figs. 22.1 and 22.2B). However, one has to bear in mind that an algorithmic alignment of sequences is only an approximation to the GS alignment (Fig. 22.2C), and this approximation can be quite crude if the sequence similarity is below 30%.

Experience tells us that protein structure prediction on the basis of pair-wise sequence alignments is satisfactory when the sequence identity exceeds 30%: even a moderate sequence similarity is sufficient for a high similarity of 3D structures (Fig. 22.3), and this high similarity concerns more than 50% of the chain. It is often said that the 3D structure is much more conservative than the sequence (or that “coding of the 3D structure by sequence is degenerate”). Establishing sequence homology usually leads to a straightforward and sufficiently precise reconstruction of 3D structures when the sequence similarity is high enough (as in Fig. 22.1A).

It is possible to extend homology recognition below the level of 30%, that is, to the “twilight zone,” but this requires comparison of *many* sequences. Involvement of multiple alignments and the corresponding “profiles” (Fig. 24.1A) is the feature that distinguishes the advanced programs like PSI-BLAST (Position-Specific Iterative Basic Local Alignment Search Tool; [Altschul et al., 1997](#)) and HMMer (Hidden Markov Model; [Krogh et al., 1994](#);

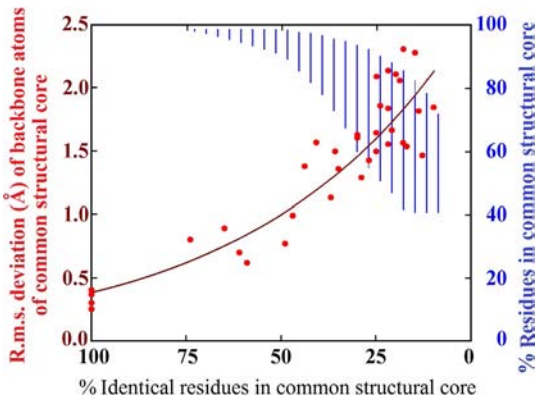


FIG. 22.3 The root mean square deviation between the positions of equivalent backbone atoms in superposed 3D folds of homologous proteins vs. the amino acid identity of residues that occupy the equivalent positions (ie, compose the common structural core). The equivalent positions include 80–95% of protein chain residues when the identity exceeds 50%, but can be as low as about 40% of the residues when the identity is as small as 10–25%. The exponential curve that shows a general tendency is fitted to the experimental points. The initial variation (at 100% identity) in the r.m.s. deviation reflects small variations of the 3D structures obtained under different conditions or/and by different refinement procedures for the same proteins. The plot reflects conservation of homologous 3D protein structures up to a rather low sequence identity. (Adapted from Lesk, A.M., Chothia, C., 1986. The response of protein structures to amino acid sequence changes. *Philos. Trans. R. Soc. Lond. A317*, 345–356.)

Durbin et al., 1998) from, for example, SW algorithm or “simple” BLAST working with separate sequences.

Establishing sequence homology is a very powerful approach to identify similarities of structures and functions of proteins. But it is related to *bioinformatics* (see, eg, Durbin et al., 1998; Lesk, 2008, 2010; Schlick, 2010) rather than to physics.

The “Empire of Bioinformatics” includes many kingdoms. The Protein kingdom, which is so important for proteomics, is grounded on knowledge-based methods that cover the well-established fields of secondary structure prediction (Schulz et al., 1974), fold recognition (Bowie et al., 1991; Finkelstein and Reva, 1991) and homology modeling (Marti-Renom et al., 2000), functional site recognition, etc., as well as a comparatively new field of prediction of natively disordered regions of protein chains (Wright and Dyson, 1999; Uversky, 2002; Garbuzyanskiy et al., 2004; Xue et al., 2010; Tompa, 2010). This kingdom flourishes in the absence of feasible *ab initio* physics-based prediction methods.

Inner voice: Is there any physics behind the knowledge-based rules?

Lecturer: Yes. We have already considered the physical background of protein structure statistics. And, for example, the rules for identification of natively disordered sequences [“more charges, less hydrophobicity → disordered” (Zbilut et al., 2004) or “repeats of pro or hydrophilic residues → disordered”], are definitely based on physics of dissolving in water and H-bonding.

Leaving bioinformatics aside, let us turn to physics-based methods of structure prediction for “new” sequences having no detectable homology with “old” proteins, already solved by X-ray or NMR methods. Here, the problem is to predict structures, and then perhaps their functions as well, from the amino acid sequences and the physics of protein folding: if a protein is capable of spontaneous folding, all the necessary information is to be coded in its sequence (Fig. 22.4).

It has to be said from the very beginning that to date, there are no perfectly precise and sufficiently reliable methods to predict a protein’s structure from its sequence alone.

The reason (leaving aside technical complexity of the huge, even for modern supercomputers, volume of calculations), is twofold: (1) the limited accuracy of the energy or energy-like estimates underlying theoretical computations of protein structures; and (2) a relatively small energy difference (gap) between one “correct” and many possible “wrong” folds of a protein chain: the small gap can be easily erased by a low accuracy of energy estimates. If the gap width is, say, 10 kcal/mol and the latent heat of protein melting is 10 kcal/mol, than the correct prediction of protein’s structure requires 90% correlation between computed and actual (experimental) energies (Finkelstein et al., 1995b), which, as it follows from (Krieger et al., 2004; Piana et al., 2014), seems to exceed the currently available level of accuracy.

I have to emphasize the latter: the small gap radically discriminates between the protein (and RNA) situation and the DNA situation (where the gap is large)—to the deep regret of people dealing with protein structure predictions.

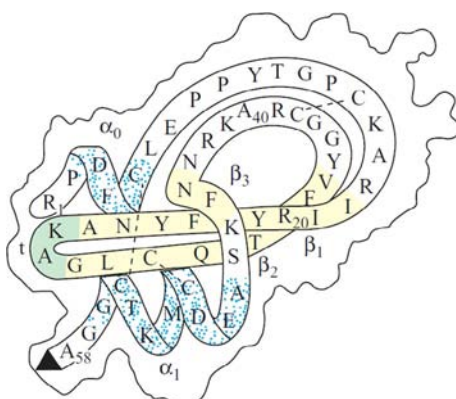


FIG. 22.4 Scheme of the primary and 3D structure of a small protein (bovine pancreatic trypsin inhibitor). The backbone (with the one-letter-coded sequence) is drawn against the background of the molecule’s contour. The α -helices, β -strands, β -turn (t), and S-S bonds (---) are outlined. When a protein is capable of spontaneous folding, all these details can be predicted, *in principle*, from its amino acid sequence alone. The side chains are not shown here, but their conformation, *in principle*, can also be predicted from the sequence.

In DNA, the complementary base pairing exists over the whole double helix, since the sequence of one DNA strand reproduces the sequence of the other. This strict complementarity of the two sequences forming the DNA molecule leads to formation of a continuous double helix and ensures the great energy advantage of the “correct” double helix over all “wrong” structures. The advantage is so great that even a very crude estimate of base pairing was sufficient for the correct prediction of the double helix. The same “base-pairing code” exists in RNA as well, but here the complementarity of sequences is much less strict and covers much shorter regions; therefore, prediction of the RNA structure is much more difficult. And the proteins have neither an unambiguous “code” for interaction of residues nor any strict complementarity of long contacting chain regions and accordingly, they lack the huge energy advantage of the “correct” fold.

However, the existing methods provide fairly rich and quite reliable information on the probable structure (or rather, on plausible structures) of a protein, and specifically on the main structural elements of its 3D structure.

There are two strategies of protein structure prediction: (1) to seek for the structure resulting from the kinetic folding process and (2) to seek for the most stable (or, equally, the most probable) chain structure.

In principle, both these strategies can lead to a correct answer, since the most stable structure of a protein chain has to fold rapidly (recall the previous lecture).

However, it is important that protein structure prediction requires neither consideration nor reproduction of the folding mechanisms, and it is enough to consider only the stability of the folded structure. Moreover, the kinetic approach requires more difficult computations, needs additional (kinetic) parameters, and still does not lead to a substantial success. And all the speculations on the specific (say, hierarchic) rules of protein folding (which looked so attractive and could indeed, if correct, facilitate the search for the native structure enormously) appear to be wrong (at least as far as single-domain proteins are concerned).

The second strategy turned out to be easier and more successful. The evaluation of stability (or, equally, of probability) of various chain folds is based either on physics-derived potentials of interactions, or (what is more common now) on the frequency of occurrence of various structural elements and interactions in proteins. This makes no major difference since, as we already know, the quasiBoltzmann statistics of protein structures are determined by the potentials of interactions. Thus, I shall speak of the “potentials,” even if their evaluation originates from protein statistics rather than from physical experiments. The interactions with water molecules are usually not taken into account explicitly; instead, the water-mediated interactions of the residues (like hydrophobic interactions) are used.

Let us start with secondary structure predictions. α -Helices and β -strands are important elements of the protein; as you remember, they determine many features of its architecture (Fig. 22.4).

Let us forget for a while that the protein chain is packed into a solid globule: it is too difficult to predict the secondary structure simultaneously with the tertiary one. Is it possible to predict, on the basis of stability, the secondary structure of the chain from its amino acid sequence *prior* to the tertiary structure? The answer is: yes, usually it is possible, though the resulting prediction is not absolutely precise.

First of all, what residues stabilize a separate secondary structure, an α -helix, for example, and what residues destroy it?

Experiment gives a direct answer to this question. First of all, the immense work on determining the α - and β -forming propensities of amino acid residues in polypeptides and proteins performed by the groups of Scheraga, Fasman, Baldwin, Fersht, Serrano, DeGrado, Kim and by a number of other groups (and in our laboratory by O.B.P. and Bychkova). Also, a wealth of information (well consistent with and extending physicochemical experiments) is given by the statistics of α - and β -structures in proteins. Fig. 22.5 summarizes the most important results (those worth remembering) obtained by all these methods.

It is necessary to stress that all the rules formulated for protein structures are of a probabilistic nature. Despite many attempts, no strict “code” of protein structures has been found; that is, in proteins there is nothing like the strict A-T and G-C pairings of nucleotides, which is so typical of nucleic acids. However, I have to say that the nucleotide pairing is not all that strict in RNAs either, with their very diverse (in contrast to DNA) repertoire of 3D structures.

The majority of the experimental and statistical data obtained can be easily understood from the physics and stereochemistry of amino acid residues. We have touched on this question already (see also Schulz and Schirmer, 1979/2013; Fersht, 1999). For example: Pro likes to enter neither the α -helix (but for its N-terminal turn), nor the β -structure. Why? Because Pro has no NH-group, and therefore it cannot form the corresponding H-bonds in the

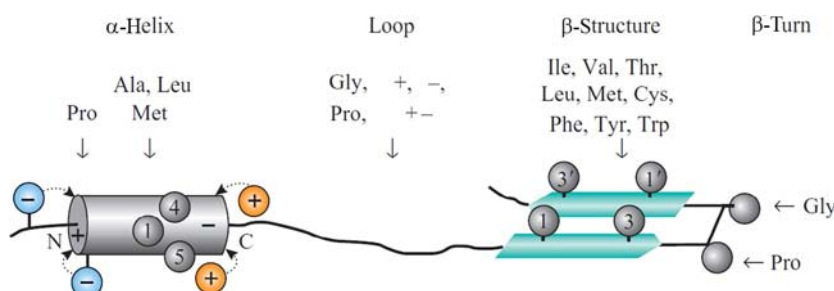


FIG. 22.5 “Templates” for an α -helix, a loop, a β -strand, and a β -turn. The amino acid residues that stabilize these elements or their separate parts are singled out; “+” denotes all positively charged residues; “-” denotes all negatively charged residues; and all residues with a dipole in the side chain are marked with “+-”. The patterns of alternating hydrophobic side chains shown (see the numbered groups) stabilize the α - and β -structure. Such an alternation also leads to the formation of continuous nonpolar and polar surfaces at opposite sides of the α -helices and β -strands.

α -and β -structures. Therefore, Pro destabilizes these structures—and it does not like to enter them. On the other hand, the NH-groups of residues forming the N-terminal turn of the α -helix (and NH-groups in some positions at the β -sheet edges) are not involved in H-bonding; thus, Pro loses nothing here, and it does not avoid these positions. Moreover, Pro often enters the N-ends of helices, since its ϕ angle is already fixed in the α -helical conformation by the proline ring (which stabilizes the α -helix with Pro at its N-end). This is also a reason for the frequent occurrence of prolines at the N-ends of the β -turns.

Another example: Ala stabilizes α -helices in polypeptides (and it is most abundant there in proteins), while Gly destabilizes both α - and β -structures and facilitates the formation of irregular regions. What is the origin of this difference? Gly lacks a side chain, and therefore it has a much larger area than Ala of possible ϕ , ψ angles; that is, while the α - and β -conformations of both residues are essentially the same, the possible irregular conformations of Gly are much more numerous and therefore more probable.

For the same reason, the C $^{\beta}$ -branched residues (Val, Ile, Thr) stabilize the β -structure, where their side chains have all three possible rotamers, and destabilize the α -helix and irregular regions, where only one, on average, side chain rotamer is allowed for any backbone conformation.

Hydrophobic groups generally prefer α - and β -structures, where they can stick together “for free” (the price has been already paid by H-bonds) in a hydrophobic cluster (see Fig. 22.5), and do not like the coil, where they cannot stick together “for free.” On the other hand, polar side chains, and especially short side chains, prefer irregular regions where they can form additional irregular H-bonds to the backbone, and do not like α - and β -structures where all the backbone’s H-bond donors and acceptors are already occupied.

The influence of amino acids on secondary structure formation can be not only measured (Fersht, 1999) or explained (Finkelstein et al., 1977) but also theoretically predicted from physics. For example, in 1970, prior to experimental evidence, we (A.V.F. and O.B.P.) predicted that a negatively charged residue would stabilize the N-end of the α -helix because of attraction to the N-end’s positive charge. We predicted also that a negatively charged residue would destabilize the C-end of the α -helix because of repulsion from the C-end’s negative charge; and that a positively charged residue must act in the opposite direction (Ptitsyn and Finkel’shtein, 1970a,b; Finkelstein and Ptitsyn, 1976; Finkel’shtein, 1977). The potential of such “charged residue-helix terminus” interaction was estimated (from usual electrostatics in water; see Problem 22.2) to be about 0.5–0.25 kcal/mol, or $\approx k_B T/2$ on the average (at $T \approx 300$ K), which is consistent with protein statistics made both previously (when the statistics data were scanty) (Ptitsyn and Finkel’shtein, 1970b) and latterly (when statistics became rich) (Richardson and Richardson, 1988).

When we know what residues stabilize the middle of the α -helix and its N- and C-ends, we obtain a kind of “template” for recognition of helices in amino acid sequences; this again bridges physics and bioinformatics. The α -helical

“template” can be roughly described as follows. A sequence fragment forms the α -helix, when: four or five positions near its N-end are enriched with negatively charged groups and include a Pro in addition; the middle of the fragment is enriched with Ala, Leu, Met rather than with Gly, and does not include any Pro at all; and its C-end is enriched with positively charged groups and avoids negatively charged residues. In addition, the α -helix is stabilized by alternation of hydrophobic groups in the sequence resulting in their sticking together within the helix (Fig. 22.5), and the same order of side chains in the sequence is necessary for incorporation of the helix into the globule. The importance of side-chain ordering for secondary structure formation in globular proteins was demonstrated by Lim (1974a,b). The better the amino acid sequence satisfies this template, the higher the probability that this sequence forms an α -helix.

Other templates have been described for β -strands, for β -turns, for loops, and even for the β - α - β units consisting of two parallel β -strands connected with an α -helix and a loop of variable length (Fig. 22.6). These “supersecondary structures” are typical of nucleotide-binding domains. A special role is played by the so-called “key residue positions” of the templates that can be occupied only by strictly defined amino acids—for example, by Gly which is the only residue that

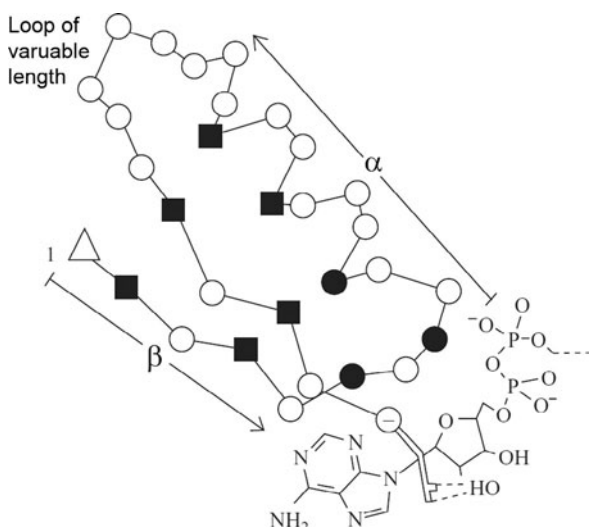


FIG. 22.6 Template of the nucleotide-binding β - α - β unit. Squares indicate positions usually occupied by relatively small hydrophobic residues (Ala, Ile, Leu, Val, Met, Cys): they form a hydrophobic core of the β - α - β superhelix. Filled circles are the key positions (sharp turns) occupied by Gly only. The open triangle indicates the beginning of the β - α - β motif; it is usually occupied by a basic or a dipolar side chain. The last (-) motif's position includes a nucleotide-binding Asp or Glu. (Adapted from Wierenga, R.K., Terpstra, P., Hol, W.G.S., 1986. Prediction of the occurrence of the ADP-binding $\beta\alpha\beta$ -fold in proteins, using an amino acid sequence fingerprint. *J. Mol. Biol.* 187, 101–107.)

can have a conformation with $\phi \approx +60^\circ$: this conformation is forbidden for other amino acids.

It is noteworthy that the “bioinformatic templates” can include not only physical or structural, but also functional information (see the last residue of the nucleotide-binding β - α - β unit in Fig. 22.6). Further, we will see much more complicated templates used for fold recognition by “threading.”

Let us come back to secondary structure predictions. To begin with, let us completely ignore interactions between different secondary structures and consider an “unfolded” polypeptide chain (with separate fluctuating secondary structures).

When the increments of separate interactions to the α -helix and β -hairpin stability are known, one can compute the free energies of these structures in any part of the sequence (see Appendices B and C). Then it is possible to compute the probability of occurrence of α - and β -structures in each chain region and the average content of α - and β -structures in the whole “unfolded,” that is, nonglobular, chain (at a given temperature, pH, and ionic strength of the solution). This can be performed by computer programs like ALB-“unfolded chain” (Finkelstein, 1983; Finkelstein et al., 1991) or AGADIR (Muñoz and Serrano, 1994). The results can be compared with experimental (eg, circular dichroism (CD), spectra-based) data on the secondary structure content in non-globular polypeptides. Fig. 22.7 shows that the theoretical estimates by ALB-“unfolded chain” are in reasonable agreement with experiment.

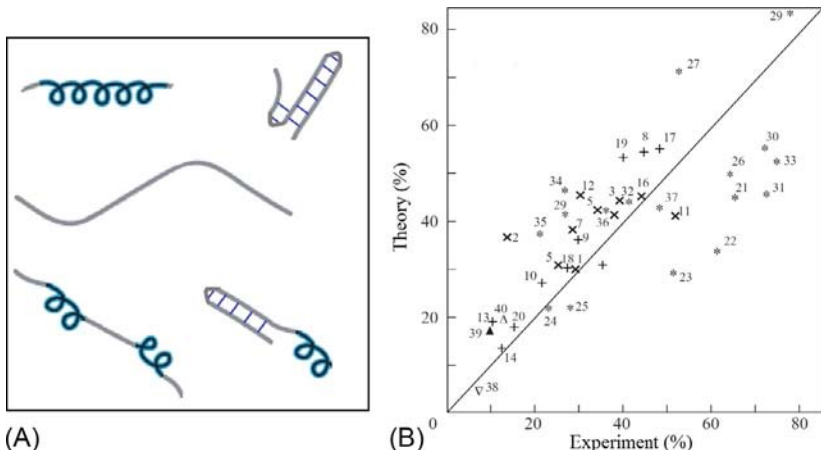


FIG. 22.7 (A) Various secondary structures competing within the program ALB-“unfolded chain.” (B) Theoretical (computed by the program ALB-“unfolded chain”) and experimentally observed helicity (%) of several tens of peptides at 0–5°C and various (marked with different symbols; see the original paper) pH and ionic strengths of the solution. (Adapted from Finkelstein, A.V., Badretdinov, A.Y., Ptitsyn, O.B., 1991. Physical reasons for secondary structure stability. *Proteins* 10, 287–299.)

When predicting the secondary structures of globular proteins, we should take into account the interaction of each secondary structure with the rest of the globule on one its side and with water on the other (Fig. 22.8).

This can be done only approximately, since 3D structure of this globule is not known. One knows, though, that the secondary structures are attached somehow to its hydrophobic core. This interaction can be approximated by interactions of secondary structures with a “hydrophobic lake” (Fig. 22.8).

The strength of hydrophobic interactions is known experimentally. The stereochemistry of α - and β -structures tells us which of their residues face the same direction and can stick to the “hydrophobic lake” simultaneously. Thus, we can estimate the energy of secondary structure adhesion, add it to the internal secondary structure energy, calculate the Boltzmann probability of formation of α - and β -structures in each chain region, and use these probabilistic estimates as a basis for the prediction of secondary structures of globular proteins. This is exactly what the program ALB (Finkelstein, 1983) performs in the operating mode “globular chain.”

Here, the question arises as to what temperature should be used to calculate the above-mentioned Boltzmann probabilities.

If we take an extremely low temperature (0 K), the secondary structures forming only *one*, the lowest-energy (according to our calculations) chain fold is singled out. If we take a higher temperature, the secondary structures common for *many* low-energy folds (again, according to our calculations—with all their errors) are singled out. What temperature is to be preferred?

On the one hand, we are interested in a stable structure of the protein chain, which may suggest that only the secondary structures forming the lowest-energy fold should be singled out, that is, we should compute the probabilities for 0 K.

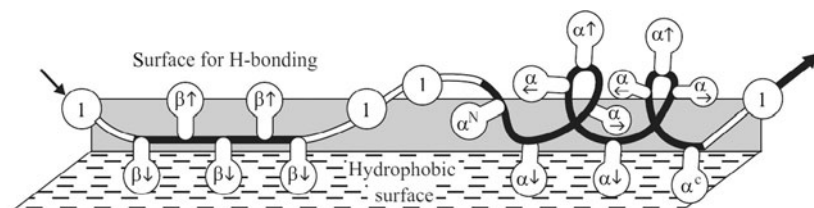


FIG. 22.8 Fluctuating secondary structure of a protein chain (β , β -strand; l , loop; α , α -helix) on the surface mimicking the protein globule (the “floating logs” model). The surface consists of a hydrophobic “lake,” the “shore” of which is capable of H-bonding to β -strands. The model takes into account different alternations of side chains directed to (\downarrow), from (\uparrow), and along (\rightarrow , \leftarrow) the surface in different secondary structures, as well as the N- and C-terminal effects in α -helices (these effects are summed up and attributed to the N- and C-terminal residues of the helix, α^N and α^C). (Adapted from Ptitsyn, O.B., Finkelstein, A.V., 1983. Theory of protein secondary structure and algorithm of its prediction. *Biopolymers* 22, 15-25.)

On the other hand, the protein exists at approximately room temperature ($\approx 300 \text{ K}$), and its structure is maintained by the temperature-dependent hydrophobic interactions; this implies that room temperature should be used.

There is another strong and quite different reason to use a temperature like $\approx 300 \text{ K}$ rather than 0 K (Finkelstein et al., 1995b).

When the protein-stabilizing interactions are known only approximately, which is *always* the case, the characteristic temperature of protein statistics (T_C), which is somewhat lower than the protein melting temperature ($T_M \approx 350 \text{ K}$, as you may remember), is most suitable to single out probable states of the chain's elements.

I will now try to explain rather than to prove this difficult point.

In essence, *any* protein structure prediction is based on only some of the interactions operating in the chain: some interactions are neglected (like close packing in secondary structure predictions), while others are known only approximately (which means that only a part of their energy is properly taken into account). This refers, in particular, to powerful hydrophobic interactions of secondary structures with the rest of the globule (since we do not know its shape).

Then, making *any* prediction is akin to predicting the inner/outer residue position exclusively from the hydrophobicity of this residue. In this case only a minor part of the interactions within the protein are taken into account. Nevertheless, we know that this problem has a solution, though probabilistic rather than precise (Finkelstein et al., 1995a,b). The solution can be found in the statistics of the distribution of residues between the interior and the surface of proteins. We already know what the statistics look like

$$\frac{\text{Probability to be "in"} }{\text{Probability to be "out"} } \sim \exp \left(-\frac{\text{Hydrophobic free energy}}{k_B T_C} \right) \quad (22.1)$$

where T_C is a characteristic temperature of protein statistics, which does not depend on the kind of interaction taken into account.

The above example suggests that the same characteristic temperature T_C should be used for *any probabilistic* protein structure prediction, and that only a probabilistic prediction can be made when we know only a part of the interactions.

If the “known” part is small, our prediction will be rather vague, “highly fluctuating.” On the other hand, if we obtain a prediction without any or with only small uncertainty—the interactions taken into account are sufficient to fix the considered structure (if it is fixed in the protein) at the “temperature of statistics”, T_C , which is somewhat lower than the protein melting temperature T_M .

[Fig. 22.9](#) presents the result of a secondary structure calculation performed by the program ALB-“globular chain” for a small protein. This calculation takes into account the interactions within secondary structures and the interactions of secondary structures with a “hydrophobic lake” that models the protein globule. The solidity of the protein and the close packing of its side chains are not taken into account in these calculations. Thus, one can say that this secondary structure prediction refers rather to the molten globule than to the native, solid

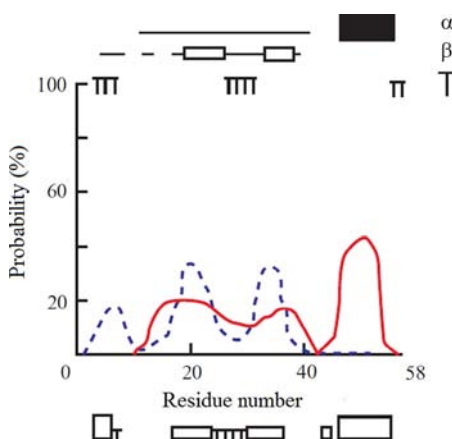


FIG. 22.9 Secondary structure calculation performed by the program ALB-“globular chain” for the sequence of bovine pancreatic trypsin inhibitor. Abscissa, the residue number in the sequence; ordinate, the computed probability of the α -helical (—) and β -structural (---) states for each chain residue. Above the plot: prediction of probable α -helices (α), β -strands (β), and chain turns (T). Filled rectangles, the most probable secondary structures; open rectangles, probable (and also predicted) secondary structures; lines, possible but not predicted secondary structures. Below the plot: α -helices (deep rectangles), β -strands (shallow rectangles), and turns (T) in the native protein structure.

protein; but we already know that the secondary structures of these two are similar. The resulting plot shows that the calculated secondary structure probability, even in the most structured (according to the calculation) chain regions is far from 100%. However, in accordance with the X-ray 3D structure of the protein, the predicted α -helix prevails at the chain’s C-end, and the β -structure (actually, the β -hairpin) in its middle. Thus, the peaks of probability of the α -helical and β -structural states (if they exceed some empirically established level) can be used for protein secondary structure prediction. This is a probabilistic prediction, of course, though many secondary structure elements can be predicted with confidence.

Actually, secondary structure prediction is always probabilistic in nature. This refers not only to the program ALB, which is explicitly a probability-based one. This refers to all other methods, even to those that are aimed, as is usually done, to single out only one, the “best” (read: the most probable from the program’s point of view) position of α - and β -structures in the protein chain.

When the protein’s secondary structure is predicted from its amino acid sequence *alone*, the precision of recognition of α , β , and an “irregular” state is about 65%, which means that the secondary structure is correctly predicted for 65% of protein chain residues.

Inner voice: Is it possible to improve the accuracy of secondary structure prediction?

Lecturer: Yes, it is—with the aid of informatics. The internet-accessible methods PHD (Rost et al., 1994), PSIPRED (Jones, 1999) and some others predict the protein's secondary structure *not* from its sequence alone, but (whenever it is possible) from a *set* of sequences that includes the sequence in question *and* its homologs. This approach leads to the partial annihilation of random errors made in considering each of the sequences (Finkelstein, 1998), and the prediction is made with more confidence (reaching an average level of 75–80% instead of 65%).

Secondary structure prediction has become, in fact, a routine procedure in the analysis of protein sequences, even though its accuracy is still not perfect.

Now we have to consider the problem of predicting the 3D protein fold from its sequence; this problem is much more difficult and much less routine.

Prediction of 3D folds is often based on the predicted secondary structures. Although this way is not, so to speak, self-consistent, since tertiary structure can affect the secondary structure, it is sometimes successful, since a stable 3D fold must consist mostly of intrinsically stable, and therefore “well-predictable,” secondary structures.

Figs. 22.10 and 22.11 illustrate our prediction of 3D fold for interferon (Ptitsyn et al., 1985).

The secondary structure prediction (Fig. 22.10) shows a predominance of α -helices in the interferon chains, especially in its N-terminal part [where the functional domain had been localized by functional studies (Ackerman et al., 1984)]. The α -helices of interferon have been predicted very definitely (which is far from being often), and we dared to sculpture the N-terminal domain from the predicted helices. For the C-terminal domain, where the secondary structure prediction is more ambiguous, we were not able to give an unambiguous prediction of its 3D fold.

Fig. 22.11A shows that the N-terminal domain is predicted to be built up from three large helices and one tiny helix.

The X-ray structure of interferon β was solved (Fig. 22.11B) 5 years after this prediction and showed a rather accurate agreement with the predicted structure. This interferon N-terminal domain fold was one of the first successful *a priori* predictions of a protein structure from its sequence.

I would like to emphasize the factors contributing to this success: the prediction of α -helices was unambiguous, and predictions were very similar for several remote homologs, which allowed us to believe them. (However, such definite and similar predictions for remote homologs are relatively rare. Less definite and less consistent predictions are more common. This is exemplified by the secondary structure prediction made for the interferon C-terminal domain (Fig. 22.10); an unambiguous fold prediction is not possible in this case.) And one more thing was crucial for the successful prediction of the interferon fold. When looking for the folding pattern, we could perform a rational and exhaustive search using the *a priori* classification of α -helical complexes (Murzin and Finkelstein, 1988).

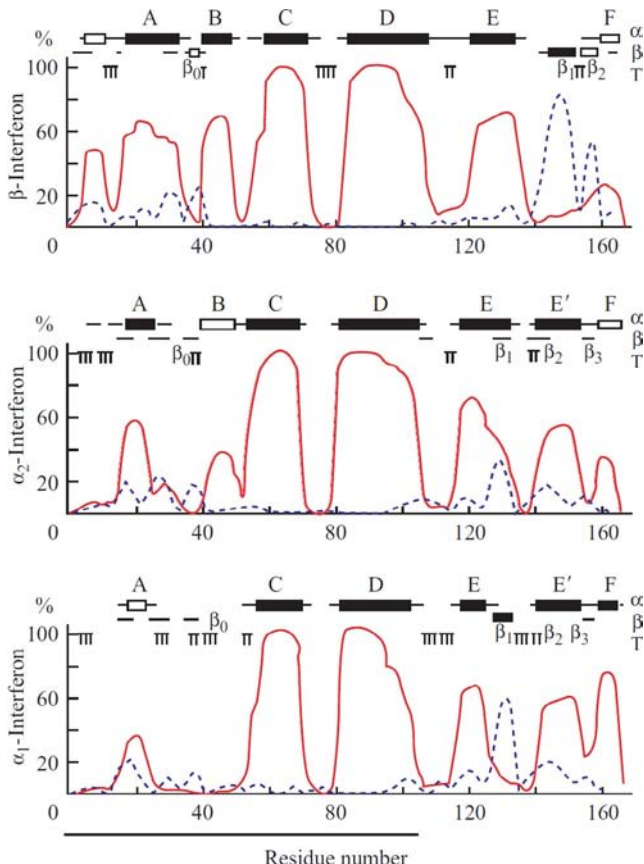


FIG. 22.10 Secondary structure calculation performed by the program ALB-“globular chain” for three interferons. The chain region forming the N-terminal domain is underlined. All other designations are the same as in Fig. 22.9. (Adapted from Ptitsyn, O.B., Finkelstein, A.V., Murzin, A.G., 1985. Structural model for interferons. FEBS Lett. 186, 143–148.)

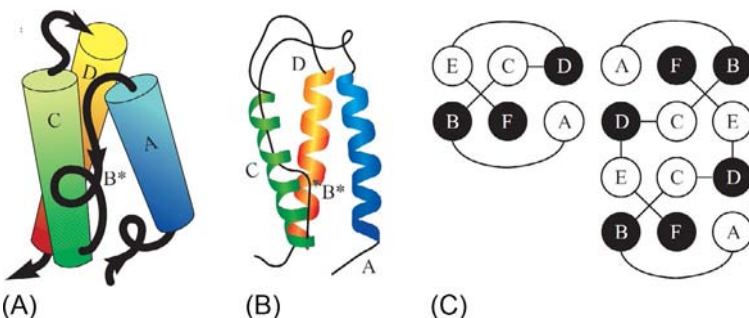


FIG. 22.11 (A) Predicted chain fold for the N-terminal domain of interferon (Ptitsyn et al., 1985). Three large α-helices (A, C, D in Fig. 22.10) are shown as cylinders, the tiny helix B* as a separate helix turn. (B) X-ray structure of the N-terminal domain of interferon β by Senda et al. (1990) (the C-terminal domain is not shown). The structure is given in the same orientation as the predicted model, and the helices are lettered identically. The region B* is helix-like, but it is not an α-helix in interferon β; however, a short α-helix exists in this place in the closely related interferon γ (Ealick et al., 1991). (C) Topologies of β (on the left) and γ (on the right) interferons according to Ealick et al. Interferon γ consists of two subunits. Notice that these subunits “swap” the C-terminal regions (helices E and F).

REFERENCES

- Ackerman, S.K., Nedden, B.Z., Hemtzelman, M., Hunkapiller, M., Zoon, K., 1984. Biologic activity in a fragment of recombinant human interferon alpha. Proc. Natl. Acad. Sci. USA 81, 1045–1047.
- Altschul, S.F., Gish, W., Miller, W., Myers, E.W., Lipman, D.J., 1990. Basic local alignment search tool. J. Mol. Biol. 215, 403–410. Modern version: <http://blast.ncbi.nlm.nih.gov/Blast.cgi>.
- Altschul, S.F., Madden, T.L., Schäffer, A.A., Zhang, J., Zhang, Z., Miller, W., Lipman, D.J., 1997. Gapped BLAST and PSI-BLAST: a new generation of protein database search programs. Nucleic Acids Res. 25, 3389–3402. Modern version available at: <http://blast.ncbi.nlm.nih.gov/Blast.cgi>.
- Anfinsen, C.B., Haber, E., Sela, M., White, F.H., 1961. Kinetics of formation of native ribonuclease during oxidation of the reduced polypeptide chain. Proc. Natl. Acad. Sci. USA 47, 1309–1314.
- Bowie, J.U., Lüthy, R., Eisenberg, D., 1991. A method to identify protein sequences that fold into a known three-dimensional structure. Science 253, 164–170.
- Doolittle, R.F., 1981. Similar amino acid sequences: chance or common ancestry? Science 214, 149–159.
- Durbin, R., Eddy, S., Krogh, A., Mitchison, G., 1998. Biological Sequence Analysis: Probabilistic Models of Proteins and Nucleic Acids. Cambridge University Press, Cambridge. Modern version available at: <http://hmmer.org/>.
- Elalick, S.E., Cook, W.J., Vijay-Kumar, S., Carson, M., Nagabushan, T.L., Trotta, P.P., Bugg, C.E., 1991. Three-dimensional structure of recombinant human interferon-gamma. Science 252, 698–702.
- Fersht, A., 1999. Structure and Mechanism in Protein Science: A guide to Enzyme Catalysis and Protein Folding. W. H. Freeman & Co., New York, NY (Chapters 15 and 17).
- Finkel'shtein, A.V., 1977. Electrostatic interactions of charged groups in aqueous medium and their influence on the formation of polypeptide secondary structures. Mol. Biol. (Mosk) 11, 811–819.
- Finkelstein, A.V., 1983. Program ALB for polypeptide and protein secondary structure calculation and prediction. Submitted to Protein Data Bank, Available version of ALB “globular chain” at: <http://i2o.protres.ru/alb/>.
- Finkelstein, A.V., 1998. 3D protein folds: homologs against errors—a simple estimate based on the random energy model. Phys. Rev. Lett. 80, 4823–4825.
- Finkelstein, A.V., Ptitsyn, O.B., 1976. A theory of protein molecule self-organisation. IV. Helical and irregular local structures of unfolded protein chains. J. Mol. Biol. 103, 15–24.
- Finkelstein, A.V., Reva, B.A., 1991. Search for the most stable folds of protein chains. Nature 351, 497–499.
- Finkelstein, A.V., Ptitsyn, O.B., Kozitsyn, S.A., 1977. Theory of protein molecule self-organisation. II. A comparison of calculated thermodynamic parameters of local secondary structures with experiment. Biopolymers 16, 497–524.
- Finkelstein, A.V., Badretdinov, A.Y., Ptitsyn, O.B., 1991. Physical reasons for secondary structure stability. Proteins 10, 287–299.
- Finkelstein, A.V., Badretdinov, A.Y., Gutin, A.M., 1995a. Why do protein architectures have Boltzmann-like statistics? Proteins 23, 142–150.
- Finkelstein, A.V., Gutin, A.M., Badretdinov, A.Y., 1995b. Perfect temperature for protein structure prediction and folding. Proteins 23, 151–162.
- Garbuzynskiy, S.O., Lobanov, M.Y., Galzitskaya, O.V., 2004. To be folded or to be unfolded? Protein Sci. 13, 2871–2877.

- Jones, D.T., 1999. Protein secondary structure prediction based on position-specific scoring matrices. *J. Mol. Biol.* 292, 195–202. Modern version available at: <http://bioinf.cs.ucl.ac.uk/psipred/>.
- Krieger, E., Darden, T., Nabuurs, S.B., Finkelstein, A., Vriend, G., 2004. Making optimal use of empirical energy functions: force field parameterization in crystal space. *Proteins* 57, 678–683.
- Krogh, A., Brown, M., Mian, I.S., Sjölander, K., Haussler, D., 1994. Hidden Markov models in computational biology. Applications to protein modeling. *J. Mol. Biol.* 235, 1501–1531.
- Lesk, A.M., 2008. Introduction to Bioinformatics, third ed. Oxford University Press, Oxford.
- Lesk, A.M., 2010. Introduction to Protein Science: Architecture, Function, and Genomics, second ed. Oxford University Press, Oxford.
- Lim, V.I., 1974a. Structural principles of the globular organization of protein chains. A stereochemical theory of globular protein secondary structure. *J. Mol. Biol.* 88, 857–872.
- Lim, V.I., 1974b. Algorithm for prediction of α -helices and β -structural regions in globular proteins. *J. Mol. Biol.* 88, 873–894.
- Marti-Renom, M.A., Stuart, A.C., Fiser, A., Sanchez, R., Melo, F., Sali, A., 2000. Comparative protein structure modeling of genes and genomes. *Annu. Rev. Biophys. Biomol. Struct.* 29, 291–325.
- Muñoz, V., Serrano, L., 1994. Elucidating the folding problem of helical peptides using empirical parameters. *Nat. Struct. Biol.* 1, 399–409.
- Murzin, A.G., Finkelstein, A.V., 1988. General architecture of α -helical globule. *J. Mol. Biol.* 204, 749–770.
- Piana, S., Klepeis, J.L., Shaw, D.E., 2014. Assessing the accuracy of physical models used in protein-folding simulations: quantitative evidence from long molecular dynamics simulations. *Curr. Opin. Struct. Biol.* 24, 98–105.
- Ptitsyn, O.B., Finkel'shtein, A.V., 1970a. Predicting the spiral portions of globular proteins from their primary structure. *Dokl. Akad. Nauk SSSR* 195, 221–224 (in Russian).
- Ptitsyn, O.B., Finkel'shtein, A.V., 1970b. Relation of the secondary structure of globular proteins to their primary structure. *Biofizika* 15, 757–768 (in Russian).
- Ptitsyn, O.B., Finkelstein, A.V., Murzin, A.G., 1985. Structural model for interferons. *FEBS Lett.* 186, 143–148.
- Richardson, J.S., Richardson, D.C., 1988. Amino acid preferences for specific locations at the ends of alpha helices. *Science* 240, 1648–1652.
- Rost, B., Sander, C., Schneider, R., 1994. PHD—an automatic mail server for protein secondary structure prediction. *Comput. Appl. Biosci.* 10, 53–60. Modern version available at: <https://www.predictprotein.org/>.
- Schlick, T., 2010. Molecular Modeling and Simulation: An Interdisciplinary Guide, second ed. Springer, New York, NY.
- Schulz, G.E., Schirmer, R.H., 1979/2013. Principles of Protein Structure. Springer, New York (Chapter 6).
- Schulz, G.E., Barry, C.D., Friedman, J., Chou, P.Y., Fasman, G.D., Finkelstein, A.V., Lim, V.I., Ptitsyn, O.B., Kabat, E.A., Wu, T.T., Levitt, M., Robson, B., Nagano, K., 1974. Comparison of predicted and experimentally determined secondary structure of adenilate kinase. *Nature* 250, 140–142.
- Senda, T., Matsuda, S., Kurihara, H., Nakamura, K.T., Kawano, G., Shimizu, H., Mizuno, H., Mitsui, Y., 1990. Three-dimensional structure of recombinant murine interferon-beta. *Proc. Japan Acad. Ser. B* 66, 77–80.
- Smith, T.F., Waterman, M.S., 1981. Identification of common molecular subsequences. *J. Mol. Biol.* 147, 195–197.

- Tompa, P., 2010. *Structure and Function of Intrinsically Disordered Proteins*. Chapman & Hall/CRC Press, Taylor & Francis Group, Boca Raton, FL (Chapters 1, 7, 9 and 10).
- Uversky, V.N., 2002. Cracking the folding code. Why do some proteins adopt partially folded conformations, whereas other do not? *FEBS Lett.* 514, 181–183.
- Wright, P.E., Dyson, H.J., 1999. Intrinsically unstructured proteins: re-assessing the protein structure-function paradigm. *J. Mol. Biol.* 293, 321–331.
- Xue, B., DunBrack, R.L., Williams, R.W., Dunker, A.K., Uversky, V.N., 2010. PONDR-Fit: a meta-predictor of intrinsically disordered amino acids. *Biochim. Biophys. Acta* 1804, 996–1010.
- Zbilut, J.P., Giuliani, A., Colosimo, A., Mitchell, J.C., Colafranceschi, M., Marwan, N., Webber Jr., C.L., Uversky, V.N., 2004. Charge and hydrophobicity patterning along the sequence predicts the folding mechanism and aggregation of proteins: a computational approach. *J. Proteome Res.* 2004 (3), 1243–1253.

Lecture 23

Let us turn now to physics-based or physics-inspired predictions of three-dimensional (3D) folds of protein chains.

The problem of protein structure prediction can be posed as a problem of choice of the 3D structure best fitting the given sequence among many other possible folds.

However, what can be the source of “possible” structures?

One answer is: an a priori classification (see, eg, [Murzin and Finkelstein, 1988](#)); this way was used in predicting the interferon fold ([Ptitsyn et al., 1985](#)). Another, a more practical answer ([Bowie et al., 1991](#)) is: the Protein Data Bank (PDB) where all the solved and publicly available 3D structures are collected ([Berman et al., 2012](#)). In this case, actually, we will deal with “recognition” rather than “prediction”: a fold cannot be recognized if PDB does not contain its already solved analog. This limits the power of recognition. However, it has an important advantage: if the protein fold is recognized among the PDB-stored structures, one can hope to recognize also the most interesting feature of the protein, its function—by analogy with that of an already studied protein.

Certainly, not all protein folding patterns have been collected in PDB yet; however, it hopefully already includes half of all the folding patterns existing in nature. This hope, substantiated by [Chothia \(1992\)](#), is based on the fact that the folds found in newly solved protein structures turn out to be similar to already known folds more and more frequently. Extrapolation shows that perhaps about 1500–2000 folding patterns of protein domains exist in genomes, and we currently know more than half of them (including the majority of the “most popular” folds).

To recognize the fold of a chain having no visible homology with already solved proteins, one can use various superimpositions of the chain in question onto all examined (taken from an a priori classification or from PDB) 3D folds in search of the lowest-energy chain-with-fold alignment (see [Fig. 23.1](#)). This is called the “threading method.” When a chain is aligned with the given fold, it is threaded onto the fold’s backbone until its energy (or rather, free energy) is minimized, including both local interactions and interactions between remote chain regions. The threading alignment allows “gaps” in the chain and in the fold’s backbone (the latter are often allowed for irregular backbone regions only).

The threading approach was suggested by us ([Finkel’shtein and Reva, 1990](#); [Finkelstein and Reva, 1991](#)) and, independently, by David Eisenberg’s group ([Bowie et al., 1991](#); our variant uses a self-consisted molecular force field to calculate the long-range interactions; the Bowie-Lüthy-Eisenberg’s variant, although less “self-consistent,” has the advantage of a simple form and practical convenience). Since then, various threading methods have become popular

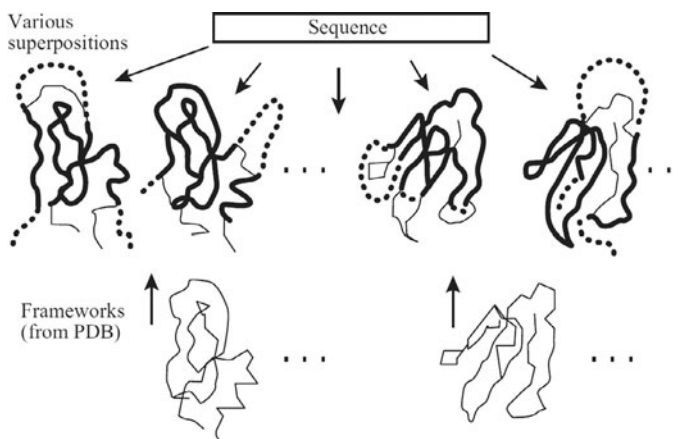


FIG. 23.1 Scheme illustrating the idea of “threading” the studied sequence onto the PDB-stored backbone structures. The bold line shows the regions where the chain is aligned with the backbone of a “known” protein structure; the broken line shows the nonaligned region of the studied chain.

tools for recognizing the folds of “new” proteins by their analogy with “old” ones.

In principle, threading is similar to a homology search; the difference is that only sequences are aligned in a homology search, while threading aligns a “new” sequence with “old” folds.

Being physics-inspired, threading serves now as a powerful tool of bioinformatics. It uses mostly statistics-derived pseudopotentials rather than actual energies (we already know that they are closely related; and it is much easier today, to obtain the former from statistics than the latter from physical experiments).

Before coming to the results, I would like to stress here some of the principal problems of threading methods (actually, no method of protein structure prediction is free of these problems in one form or another).

First, the conformations of the gapped regions remain unknown, together with all interactions in these regions. Second, even the conformations of the aligned regions and their interactions are known only approximately, since the alignment does not include side-chain conformations (which may differ in “new” and “old” structures). Estimates show that threading takes into account, at best, half of the interactions operating in the protein chain, while the other half remain unknown to us. Thus, again, the protein structure is to be judged from only a part of the interactions occurring in this structure. Therefore, this can only be a *probabilistic* judgment.

The next problem is: how do we sort out all possible threading alignments and find which is the best? The number of possible alignments is enormous (remember Levinthal’s paradox?). To be brief, there are powerful mathematical tools. I will only name the main ones here. Dynamic programming (not to be confused with molecular dynamics!—they are absolutely different) and its

variant, statistical mechanics of one-dimensional systems (see Appendix C); are used to sort out the alignment variants. Self-consistent molecular field theory is used to calculate the field acting at each residue in each position of the fold. Stochastic Monte-Carlo energy minimization; various branch-and-bound methods including dead-end elimination, etc., are also in use. And one more: an intuitive estimation of the variants! It seems to be old-fashioned in the computer age, but just this method allowed Alexei Murzin to predict many protein structures and to beat even the best computer programs in this kind of chess game. (There has been a worldwide “critical assessment of protein structure prediction” (CASP) event taking place every 2 years since 1994 when CASP-I happened. There was also the “CASP-0” in 1974 on protein secondary structure prediction only; see [Schulz et al., 1974](#)). The situation with “protein chess: people vs. metaservers” virtually remains unchanged for decades; see computer game FOLDIT and ([Cooper et al., 2010](#)).

Returning to the results: I will intentionally show you rather old results, because current results for sequences whose fold cannot be derived from homology are not much better (“steady progress in the overall accuracy”, according to [Moult et al., 2014](#))—in spite of more than 1000-fold increase in the number of storied protein structures, sequences, and in the computer power. Another thing is that now it is virtually always possible to find “relatives” to a new sequence and then recognize its fold from homology ([Lesk, 2008](#); [Kryshtafovych et al., 2014](#)); but it is bioinformatics (with all its databases, servers and metaservers that collect opinions of many servers, megaservers, etc.), but not physics; so I’ll return to the good old days, when the protein structure prediction, in the absence of rich statistics, was physics-based to a large degree.

As an example, I will show you the structure prediction done for the replication terminating protein (rtp) by threading. Having threaded the rtp sequence onto all PDB-stored folds, Sippl and his Salzburg group using threading with statistics-based pseudopotentials ([Flöckner et al., 1995](#)) showed that the rtp fold must be similar to that of H5 histone ([Fig. 23.2](#)). This a priori recognition turned out to be correct.

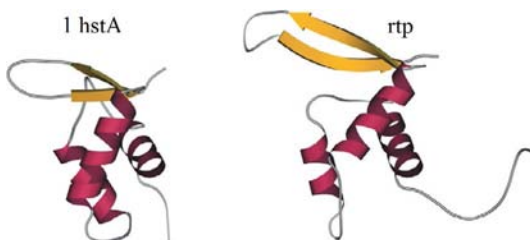


FIG. 23.2 3D structures of chicken histone H5 (1hstA) and replication terminating protein (rtp). In rtp, the last helix is not shown since it has no analog in the histone. The prediction is made by threading ([Flöckner et al., 1995](#)) in the course of a “blind” assessment of protein structure prediction methods (CASP #1, 1994). The root mean square deviation between 65 equivalent C^α atom positions in the presented structures is 2.4 Å.

However, it also turned out that the alignment provided by threading deviates from the true alignment obtained from superposed 3D structures of rtp and H5 histone (Fig. 23.3). On the one hand, this shows that even a rather inaccurate picture of residue-to-residue contacts can lead to an approximately correct structure prediction. On the other hand, this shows once again that all the mentioned flaws (insufficiently precise interaction potentials, uncertainty in conformations of nonaligned regions, of side chains, etc.) allow one to single out only a more-or-less narrow set of plausible folds rather than *one* unique correct fold. The set of the “most plausible” folds can be singled out quite reliably, but it still remains unclear, which of these is the best. The native structure is *a member* of the set of the plausible ones, it is more or less close to the most plausible (predicted) fold, but this is all that one can actually say even in the very best case.

Threading methods became a tool for a tentative recognition of protein folds from their sequences. The advantage of these methods is that they formulate a recipe—do this, this and this, and you will obtain a few plausible folds, one of which has a fairly high chance of being correct.

All the above described approaches to protein structure prediction ignored kinetics of protein folding. An alternative approach assumes that the self-organization begins with the formation of “centers of crystallization” and proceeds with the growth of on such center or by a sequential collapse of two or

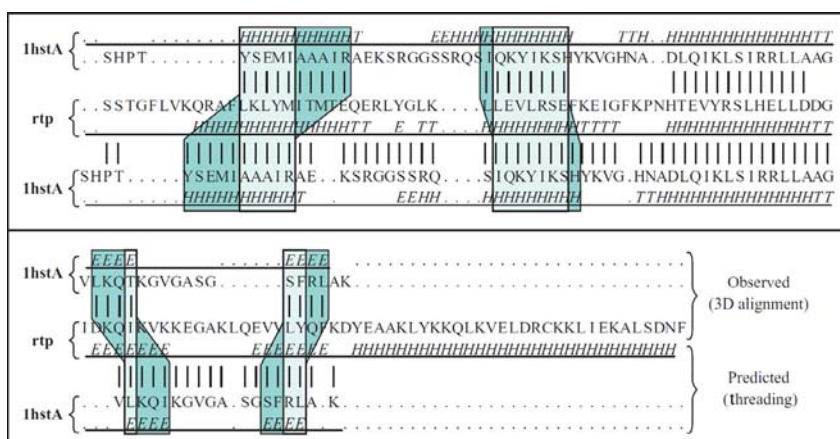


FIG. 23.3 Histone H5 (1hstA) sequence aligned with that of replication terminating protein (rtp) by superposing their 3D structures (the “observed” pair), and the rtp and 1hstA sequences aligned by threading (the “predicted” pair). Ideally, these two alignments should coincide. However, the two 1hstA-with-rtp alignments are shifted (see the gray zones indicating the regular secondary structures; *H*, α -helix; *E*, β -strand; *T*, turn). The gaps in sequences, introduced to optimize the alignments, are shown with dots. The similarity of folds has been recognized by threading in spite of a very low homology of the sequences. (Adapted from Lemer, C.M.-R., Rooman, V.J., Wodak, S.J., 1995. Protein structure prediction by threading methods: evaluation of current techniques. *Proteins*, 23, 337–355, with permission from John Wiley and Sons; there, the CASP-1994 results are summarized.)

more grown centers (Ptitsyn and Rashin, 1975; Lim et al., 1978). It considers different pathways of self-organization, selecting the “best” of alternative structures at every stage of the process.

A real success of protein structure prediction by modeling its folding is connected with prediction of folds for sequences that do not have obvious homologs with already known 3D structures and sometimes show “novel,” so far unexampled fold types. The most famous is David Baker’s Rosetta program (Simons et al., 1999; actually, it is not just a program—it is a method) and its derivatives, including *Rosetta@home* (Das et al., 2007) that you may also use. Rosetta starts by collecting known 3D structure fragments for each short, usually nine-residue long, pieces of the sequence whose fold is to be predicted. This generation of local structures models the initial folding step at which the local interactions work. Then the alternative local structures found are used as blocks to build up many possible 3D structures of the whole chain. At the next step, nonlocal interactions start to work, and the “best” of these chain folds are singled out by energy calculations. In this way, Rosetta succeeded, in the course of CASP III (1998) and in all the following CASPs (IV–XI), to make many “blind” protein structure predictions and not only to “recognize” the folds of many new sequences (ie, to find the PDB-stored analogs to their folds), but also to ab initio predict some folds with no analogs in PDB (Simons et al., 1999; Kryshtafovych et al., 2014). As might be expected, Baker’s method is more successful in predicting folds with many local interactions than in predicting folds supported mainly by interactions between remote chain regions.

Worthy of mention are recent works by Vijay Pande’s team (Voelz et al., 2010), and especially by David Shaw and colleagues (Shaw et al., 2010; Lindorff-Larsen et al., 2011; Piana et al., 2014). These really are movies about folding/unfolding processes lasting for hundreds or thousands of microseconds. During these ultra-long (up to milliseconds) molecular dynamics simulations (performed by Pande’s team using distributed calculations and by Shaw’s team using a specialized supercomputer ANTON) they managed to trace reversible folding and unfolding of several chains, albeit only of very small proteins. A good, 0.5–5 Å precision for the folded structures of these proteins was achieved (Fig. 23.4). The wonder is that such a precision was achieved despite the fact that the errors in assessment of the protein denaturation energy sometimes reached tens of kcal/mol (Piana et al., 2014; and, correspondingly, the correlation between the calculated and actual folding rates was very poor: as we remember, the transition rates exponentially depend on the heights of free-energy barriers). The conclusion by Piana et al. (2014) was that an improvement in the potential-energy function is needed. I agree.

Inner voice: Can one somehow estimate whether it is possible to predict protein structure, provided the level of errors in the energy estimates is given?

Lecturer: It is possible, but needs some assumptions as to the shape of energy spectrum of the protein chain and some calculations which are

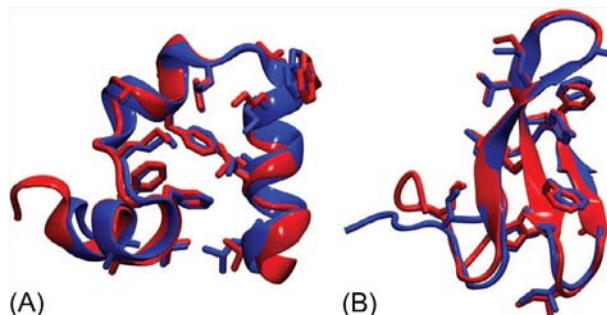


FIG. 23.4 Comparison of X-ray structures (blue) and the one resulted from MD (red): (A) 68 ms simulation of villin at 300 K; (B) 38 ms simulation of Fip35 at 337 K. Simulations were initiated from completely extended structures. (Reproduced from Shaw, D.E., Maragakis, P., Lindorff-Larsen, K., Piana, S., Dror, R.O., Eastwood, M.P., Bank, J.A., Jumper, J.M., Salmon, J.K., Shah, Y., Wriggers, W., 2010. Atom-level characterization of structural dynamics of proteins. *Science* 330, 341–346, with permission from The American Association for the Advancement of Science.)

inappropriate this moment. Take a look at Problem 23.1 and its solution. Now I would like to say only that the result depends on the ratio of the average level of errors to the width of the repeatedly referred to “gap” in the energy spectrum.

Inner voice: Is it possible to compensate somehow for the harmful action of errors in estimates of the interactions in protein chains and thus to improve protein structure recognition and prediction?

Lecturer: Yes, it is possible, if we use a set of homologs and try to predict not the best structure for a single sequence, but the best common structure for the set of them. This approach has already increased the quality of secondary structure predictions of protein (and earlier of RNA) chains. It is also used now in recognizing protein folds. Chains with a homology of ~40% seem to be most useful for the “set of homologs” used in predictions, since they still have a common 3D structure, although coded differently; this allows detection of the “signal” (structure) in spite of the “noise” of errors (Finkelstein, 1998). It should be noted, though, that this approach is not aimed at predicting the 3D structure for an individual protein chain, but rather a common (ie, approximate for each sequence) fold for a protein family.

So far, this lecture has been mainly about globular proteins. What about fibrous and membrane proteins?

Sequences of most of fibrous proteins are so regular that one needs no computer to recognize their large secondary structures. And these can form a basis for only a few higher-order structures; this paves a way to choosing one among a few variants of secondary structure packing into a fibril. Physics here is rather clear. Thus, this problem almost completely belongs to bioinformatics (Gruber et al., 2005); it is easier than, and not as fascinating as, prediction of folds of globular proteins.

Prediction of membrane protein structures is more or less similar to prediction of structures of water-soluble globular proteins, and belongs mostly to bioinformatics (Punta et al., 2007); these predictions suffer from the fact that not as many membrane protein structures have been experimentally solved so far. The methods include: sequence alignment, motif search, functional residue identification, transmembrane segment and protein topology predictions, homology, and ab initio modeling. It is fairly easy to recognize the intramembrane parts of proteins in the sequence: these are nearly continuous hydrophobic blocks; they form intramembrane α - and β -structures, whose length is dictated by the membrane thickness. However, the principles of packing of these blocks are not yet developed enough (although the main principle is clear: membrane proteins need not have a hydrophobic interior, like water-soluble proteins, but rather a hydrophilic one, forming a pore or a channel; it is the external surface that is hydrophobic and is in contact with the membrane's lipids; β -structure must form barrels, not sheets; and contacts between secondary structures must obey to "knobs-to-sockets" rules; all this we have already discussed).

In summary: prediction of the 3D fold of a protein chain, from a physicist's point of view, is a search for the most stable structure for this chain. Such a prediction is possible in principle, and is sometimes successful. The main problem is, however, that we still have insufficient information on the repertoire of possible 3D structures of protein chains and, most importantly, on the potentials of many interactions operating in these chains.

As a result, an unambiguous and reliable prediction of a protein chain structure from its sequence is hardly possible, but one can single out a very narrow set of plausible structures and, importantly, rule out a great many "impossible" folds. And the predictions can be improved by additional information concerning homologous sequences, active sites, etc.

Pragmatically, the protein structure prediction problem is usually set now as a task of recognition: is the 3D structure of a given sequence similar to some already known 3D protein structure? to which exactly? and how can the sequence in question be superimposed on the known 3D fold?

The recognition strategy is restricted. It is restricted to known protein folds (since unknown ones cannot be recognized). However, there is one clear pragmatic advantage of "recognition" over the "a priori" (unrestricted by the set of known folds) prediction. A protein fold once recognized among the PDB-stored structures allows easy analogy-based recognition of the function, active site, etc. of this protein. The a priori prediction by itself provides no hints of the function, which is usually the most interesting feature of the protein.

You should realize that physics-based methods form only one branch of protein structure prediction (or rather, recognition) methods. The mainstream is formed by methods using similarities of the sequence of interest, and often of its genome environment as well, to sequences of already identified proteins.

The latter is completely based on sequence and structure databanks. The amount of data stored in these banks is so tremendous that people try to retrieve

from there all the information necessary for predictions, ie, data on the repertoire of possible structures, energies of various interactions, homologs, functions, active sites, etc.

This is called “bioinformatics.” This branch of science is evolving very rapidly ([Lesk, 2008](#)). A huge amount of money is allocated to its development, as well as to the collection of new data and replenishment of the databases. Genome projects are aimed at collecting the sequences of all the human and not only human chromosomes and genes. The situation with gene identifying and annotating is a little trickier. Identification of a gene in the eukaryotic chromosome is not a trivial task. Recall splicing, and especially alternative splicing: one has to identify all the pieces that compose a gene, and a protein-encoding gene in particular. Hopefully, this problem can be also solved within a few years. The subsequent “Structural genomics,” “Proteomics,” and other “omics” projects aim to proceed from identification of all genes in the genome to experimental identification of the 3D structures, biological functions and roles of their protein products. It has to establish the protein’s biochemical function (does this gene encode an oxireductase? or nuclease? or ...?), to recognize the protein’s role in the cell (is it involved in the nucleotide metabolism? or in regulation? or ...?), as well as to elucidate relationships and interactions between the given protein and products of other genes.

Protein fold recognition can serve as a tool in this project. After all, a biologist wants to know protein functions, while structures and sequences are means to this end.

When the “Structural genomics” project is accomplished (and X-ray or NMR structures of at least one representative of each protein family are collected), it will be possible to recognize the 3D fold of any sequence by homology only, and there will be no practical need for a priori protein structure prediction methods—except to satisfy our natural scientific curiosity and the needs of protein design that I am just going to discuss.

In the last part of this lecture, I want to discuss *protein engineering* that is a directed modification of natural proteins, and about the *design* of new proteins and especially new folds.

Actually, there are two general strategies for protein engineering, “rational” protein design and “directed evolution” (and their combination, of course; [Lutz, 2010](#)). I’ll speak about the former, just because it is physics-based.

Oligonucleotide synthesis and recombinant DNA techniques have provided an opportunity to produce genes for proteins that do not exist in nature. X-ray and NMR have made it possible to see 3D protein structures. Powerful computers (and computer graphics) ensure an interactive dialog with these 3D structures: they enable us to modify these structures and to estimate (and see) the consequences. Taken together, these provide “hands,” “eyes,” and the “brain” of protein engineering, the new field of molecular biology. Its strategic aim is to create proteins with predetermined structures and functions. Its future role in the

creation of new drugs and catalysts, in nanotechnology, etc., can hardly be overestimated.

Directed protein engineering experiments have already answered a number of fundamental questions. Specifically, as concerns protein structure formation, it has been shown that proteins are not “perfect” and that a considerable proportion of mutations (~20%) increase their stability (though the rest ~80% decrease it). It has also been shown that correct folding is not dependent on all the details of side chain packing within the protein structure: the protein can withstand a lot of point mutations. And the loops have little bearing on the 3D fold choice: if a loop is changed and even deleted, the “wound” at the globule’s body is usually healed. (See [Fersht \(1999\)](#), who is widely regarded as one of the main pioneers of protein engineering and by [Branden and Tooze \(1999\)](#) or [Park and Cochran \(2009\)](#), and references therein.)

The role of directed mutations in studies of protein energetics and folding has been already discussed; and the use of directed mutations in elucidating protein action will be discussed in the next lectures.

It is worth mentioning that protein engineering is also used in the chemical and pharmacological industries for creating, by directed mutations, proteins with increased (or decreased, if necessary) stability and with modified catalytic activity.

The essence of a protein engineering approach to protein modification is demonstrated in [Fig. 23.5](#). Suppose we want to graft some site onto the protein structure or simply to stabilize this structure (as a simple example, [Fig. 23.5](#) shows introduction of the site Asp-His, frequently occurring among active sites of proteins). Then, first, we are looking up in the PDB an “old” protein (whose structure has been already established by X-ray or NMR) where some amino

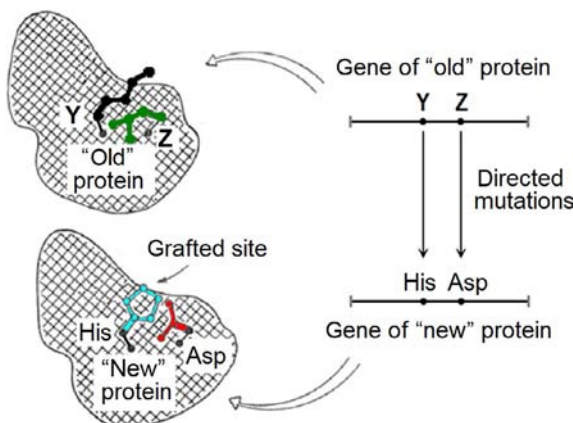


FIG. 23.5 A scheme of protein engineering as applied for grafting a new functional site to the “old” protein. (The figure, with some simplifications, is taken from Finkelstein, A.V., 1989. Is it possible to graft a new active site to the protein molecule? *Biopolym. Cell* 5, 89–93 (in Russian).)

acid residues (Z and Y in the figure) can give the desired site with the desired configuration of Asp and His after substituting Z→Asp and Y→His. Then, in the gene of selected “old” protein we replace the codons encoding the Z and Y by those encoding Asp and His, respectively, and get the gene of the “new” protein containing the desired site (and then we must check whether this “new” protein folds and works, and then establish its X-ray or NMR structure and check whether it has got the desired configuration).

[Fig. 26.5](#) shows no more than a simple scheme of experiment that has not been made for some nonscientific reasons. However, David Baker’s group (independently) realized a very similar scheme and created ([Röthlisberger et al. 2008](#)) an enzyme that never existed in nature and had a new catalytic site for the chemical reaction that did not exist in living organisms (the “Kemp elimination” reaction, ie, the proton transfer from one offshoot of an aromatic molecule to another).

The choice of the type and configuration of functional groups capable of catalyzing this reaction, that is, stabilizing the transition state on its pathway, was based on physics and chemistry of the Kemp process (by the way, for this catalysis, a certain configuration of the above discussed dyad Asp-His, along with several others, proved to be suitable, being localized in a pocket formed by the “old” protein’s aromatic residues).

The choice of this protein was performed by the aforementioned Rosetta program; the grafting was made by genetic engineering; then the protein was expressed. It turned out that the resulting artificial enzyme makes the Kemp elimination a million times faster than the spontaneous process (which is very, very good to start with, although some natural enzymes accelerate reactions by a million of millions times); lastly, the X-ray analysis showed that the grafted active site matched the theoretical design nearly perfectly. So it was done—an artificial enzyme with designed but not existing before in nature activity.

Protein engineering is a method for solving various problems. It was used to find out whether almost the same amino acid sequence can encode two essentially different folds of the protein chain. It turned out to be possible, provided the amino acid sequence was carefully worked upon.

The group of Orban and Brian started with two proteins, called GB1 and PSD1, having equal chain lengths but different structures and functions ([Fig. 23.6](#)), and different sequences where only 9 out of 58 residues coincided. Step-by-step mutations brought these sequences closer to each other, while preserving original functions of the both proteins at each step of mutation and resulted in 88% sequence identity of these proteins retaining unchanged their original functions ([Alexander et al., 2007](#)) and folds ([He et al., 2008](#)). Further work reduced the difference between them to only ONE (!!) residue ([Alexander et al., 2009](#)), while the difference in their structures and functions was preserved!

Another interesting paper by [Gambin et al. \(2009\)](#) shows that a protein having the form of a 4-helix bundle made of two α -helical hairpins acquires, after introduction of several directed mutations, the ability to be in an alternative

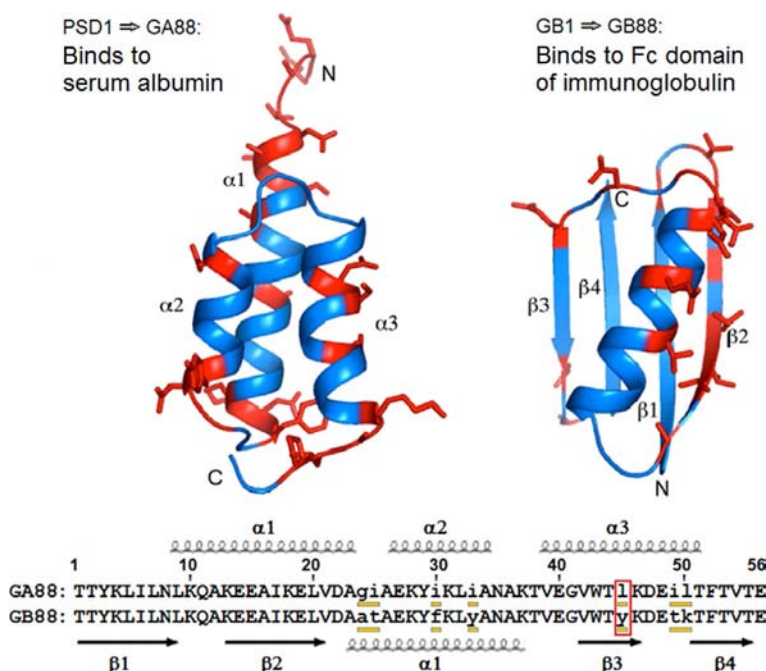


FIG. 23.6 Proteins that preserved their functions and folds but acquired the 88% sequence identity after a set of mutations (GB1 and PSD1: initial proteins; GA88 and PB88: their mutants). The modified residues are shown in red against the background of folds (*upper panel*). Lower panel: identical amino acid residues are shown in capital letters, and different ones in small underlined letters. (The figure is taken from He, Y., Chen, Y., Alexander, P.A., Bryan, P.N., Orban, J., 2008. NMR structures of two designed proteins with high sequence identity but different fold and function. Proc. Natl. Acad. USA, 105, 14412–14417, Copyright (2008) National Academy of Sciences, USA, with some simplifications and additions.) The red frame shows the only residue which, in the later achieved limit (Alexander et al., 2009), distinguishes these proteins that still retain their folds and functions.

conformation, which also is a 4-helix bundle, but with a quite different packing of helices. Some conditions stabilize one structure, some stabilize another, and both structures coexist in intermediate conditions.

Thus, almost the same or even completely the same (but very well selected!) amino acid sequence may, in principle, encode two substantially different packings of the protein chain.

In parallel with mastering the modification of natural proteins, protein engineering turned to the design of new protein molecules (Richardson and Richardson, 1989).

The problem of protein design is the reverse of the protein structure prediction problem. In prediction, we have to find the best 3D structure for a given sequence. In design, we have to find a sequence capable of folding into the given structure.

The design of artificial proteins can be easier than the prediction of the structures of “natural” proteins (just as the stability of an “artificial” TV tower can be

calculated more easily than that of a “natural” tree: the architectural design is based on standard elements and implies simplicity of calculation of their connections). And protein design, based on the theory of protein structures, can use, as building blocks, only those α -helices, β -structures and loops that are internally most stable and capable of effective sticking.

The idea of protein design emerged at the end of the 1970s after a technique for the creation of new genes had been developed. Close to the end of the 1980s the first new protein molecules were designed and synthesized mainly by trial and error. Their architectures mimicked those of natural proteins, but the sequences designed to stabilize these architectures had no homology with the sequences of natural proteins.

The first such protein, a 4-helix bundle, was obtained by DeGrado et al. (1989; Fig. 23.7). The design was made in a permanent dialog with experiment. The protein turned out to be helical and globular, as designed, and its structure seemed to be much more heat-resistant than the structure of any natural protein. Later it turned out, though, that the protein does not melt upon heating because it is a molten globule from the very beginning. Then its 3D structure was

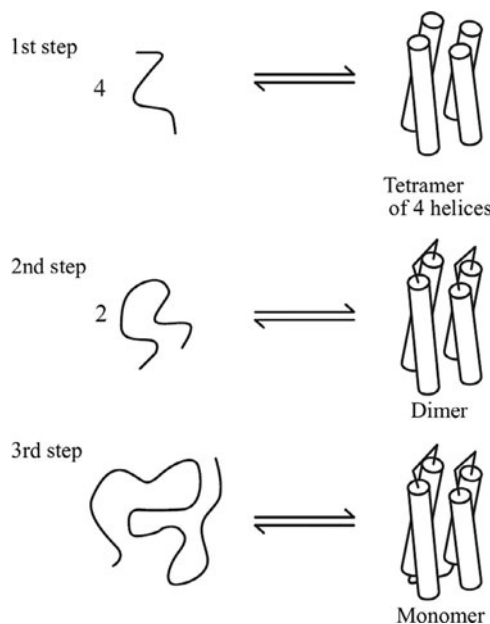


FIG. 23.7 The main steps of design of a 4-helical bundle performed by DeGrado’s group. 1st: design of short helical peptides; selection of those that can form a tetramer. 2nd: design of loops for helical hairpins; selection of those hairpins that can form a dimer. 3rd: design of the last loop; selection of a tetra-helical monomer. (The figure by W. DeGrado is reproduced, with his kind permission, from Creighton, T.E., 1993. Proteins: Structures and Molecular Properties, second ed. W. H. Freeman & Co, New York, NY (Chapter 6).)

reinforced by the introduction of ion-binding histidines (Betz et al., 1996). This ion-binding protein was as solid as natural proteins.

For a long time, all artificial proteins (apart from those reinforced by ion binding) formed a collection of excellent molten globules. They were very compact, they had very good secondary structures—but they were not solid.

Why was a molten globule obtained instead of a solid protein?

It seems that the reason is as follows. Everybody knows how to make stable secondary structures (Leu and Ala in the middle, Asp, Glu, Pro at the N-end, Lys, Arg at the C-end—and you have an α -helix; a lot of Val, Ile, Thr—and you have a β -strand). Everybody also knows how to force these α - and β -structures to stick together (their hydrophobic groups have to form continuous surfaces); and how to rule out aggregation (the opposite surfaces of the α - and β -structures must be composed of polar groups). But nobody has a recipe for forming close side chain packing in the core of the protein (except for the general idea of “knobs-to-sockets” contacts that we have already discussed)—and therefore they fail to obtain such a packing. And a compact globule with secondary structures but without close packing is just a molten globule.

To cope with the insufficient precision of design methods, “rational” design is often supported by the introduction of multiple random mutations and subsequent selection of variants having a “protein-like” activity (eg, those that specifically bind to something). This procedure has been used by Wrighton’s group to make a mini-protein (a dimer of two β -hairpins) that has an erythropoietin hormone activity. It is noteworthy that the natural protein consists of 166 residues, and its artificial analog has 28 residues only (Wrighton et al., 1996; Branden and Tooze, 1999).

However, it seems that the rational design of close packing is a soluble problem—at least for a small protein.

Dahiyat and Mayo (1997) developed an algorithm for sorting out the astronomical number of variants of side group packings and ruling out hopeless variants; in 1997, they designed a small solid protein without any ion binding (Fig. 23.8). The structure of this protein was designed in such a way as to mimic that of a “zinc finger” (a widespread DNA-binding motif), but without the Zn ion forming the structural center of the zinc finger fold. The artificial protein, called FSD-1, was designed so as to have a very low (20%) homology with the natural zinc finger. Nevertheless, it is solid at low temperatures (as shown by NMR). However, it melts within a wide temperature range (Fig. 23.8D), that is, displays a much lower cooperativity than analogous natural proteins.

Some designed architectures, however, do not mimic natural samples. For example, a “nonnatural” structure (Fig. 23.9A) was used to design an artificial protein called *albebetin*. It was designed to consist of two α - β - β repeats (and was named accordingly); although not yet found in nature at that time, this fold satisfied all known principles of protein structure. The sequence was designed in our group, and synthesized and studied by Fedorov, Dolgikh and Kirpichnikov, with his team (Dolgikh et al., 1991; Fedorov et al., 1992).

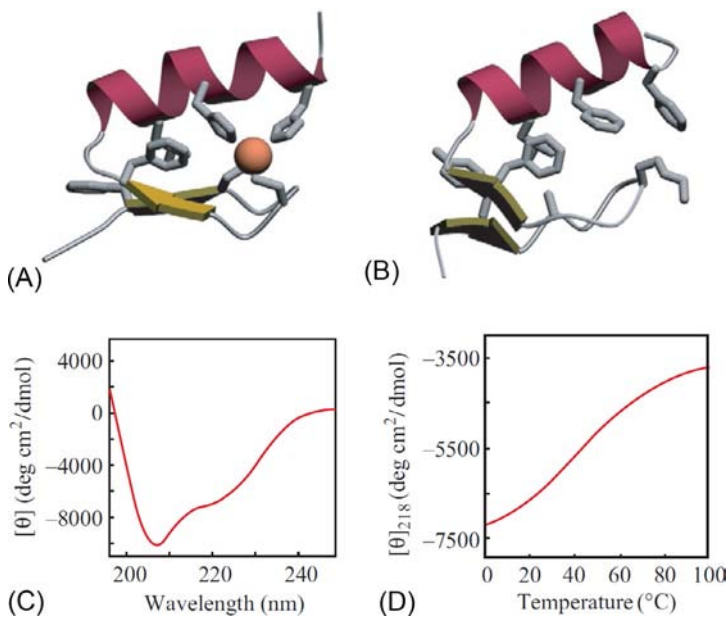


FIG. 23.8 (A) Structure of the natural zinc finger (the second module of Zif 268 protein); the Zn ion is shown as a ball. (B) Structure of the artificial FSD-1 protein designed by Dahiyat and Mayo. (C) CD spectrum for FSD-1 at 1°C shows a rich and correct secondary structure. (D) Temperature change of the FSD-1CD spectrum ellipticity at 218 nm. (*Adapted from Dahiyat, B.I., Mayo, S.L., 1997. De novo protein design: fully automated sequence selection. Science, 278, 82–86.*)

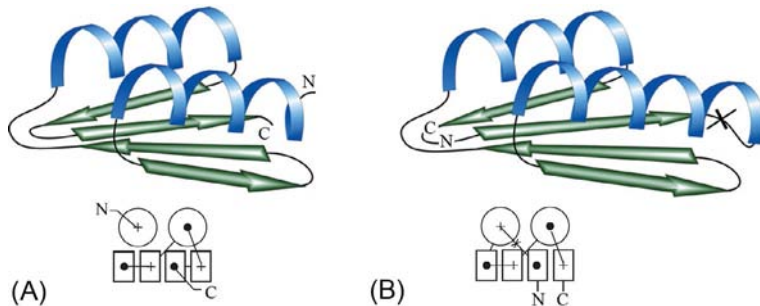


FIG. 23.9 (A) Designed fold of albbebetin and (B) a scheme of the experimentally determined fold of ribosomal protein S6. Topological schemes of these proteins are shown later. An artificial circular permutation of S6, which gives it the albbebetin topology, consists in cutting of one loop (X) and making another loop (N-C) to connect the N- and C-ends of the natural S6 chain.

A structural study of albbebetin showed that it has a rich secondary structure (Fig. 23.10A), that it is very compact, that its structure is rather stable against unfolding by urea and that the protein is proteolysis-resistant. However, it does not melt in a cooperative manner, and is a molten rather than a solid globule.

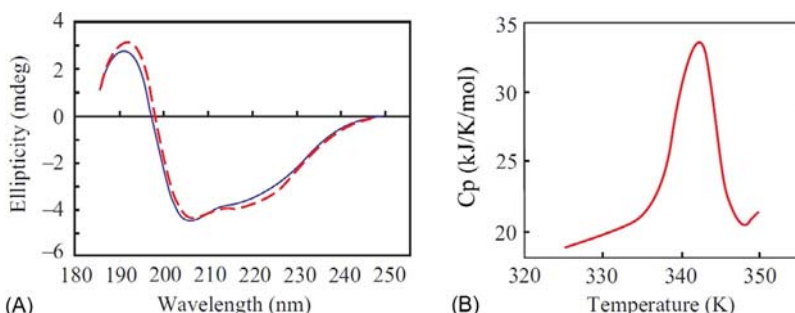


FIG. 23.10 (A) CD spectra of albebetin (---) and albeferon (—); (B) microcalorimetric melting curve of S6 permutant designed to have the albebetin topology. (Part (A) is adapted from Dolgikh, D.A., Gabrielian, A.E., Uversky, V.N., Kirpichnikov, M.P., 1996. Protein engineering of de novo protein with predesigned structure and activity. *Appl. Biochem. Biotech.* 61, 85–96, and part (B) from Abdullaev, Z.K., Latypov, R.F., Badretdinov, A.Y., Dolgikh, D.A., Finkelstein, A.V., Uversky, V.N., Kirpichnikov, M.P., 1997. S6 permutain shows that the unusual target topology is not responsible for the absence of rigid tertiary structure in de novo protein albebetin. *FEBS Lett.* 414, 243–246.)

A solid protein with the albebetin fold was obtained in a different way: by circular permutation of the natural protein S6 (its native fold, as well as several other recently solved protein folds, has the albebetin stack of structural segments, but these are differently connected by the chain; see Fig. 23.9B). The modified protein was shown to have a solid structure that melts in a cooperative manner (Fig. 23.10B).

Albebetin was used as a biological activity carrier. The fragment 131–138 of the human α 2 interferon sequence was attached to it (Dolgikh et al., 1996; the resultant protein was called albeferon). This fragment is responsible for the activation of blast-transformation of thymocytes, and the rest of the interferon body serves as a kind of sheath that protects this fragment against proteolysis and does not allow it to work too actively. Experiments show that the albebetin globule works in the same way.

Experiments on design of functionally active artificial proteins are being carried out by many groups.

By and large, proteins rapidly transform from the object of respectful and amazed observation into the subject of intense engineering and design (but the amazement still remains...).

REFERENCES

- Alexander, P.A., He, Y., Chen, Y., Orban, J., Bryan, P.N., 2007. The design and characterization of two proteins with 88% sequence identity but different structure and function. *Proc. Natl. Acad. Sci. USA* 104, 11963–11968.
- Alexander, P.A., He, Y., Chen, Y., Orban, J., Bryan, P.N., 2009. A minimal sequence code for switching protein structure and function. *Proc. Natl. Acad. Sci. USA* 106, 21149–21154.

- Berman, H.M., Kleywegt, G.J., Nakamura, H., Markley, J.L., 2012. The Protein Data Bank at 40: reflecting on the past to prepare for the future. *Structure* 20, 391–396. Modern version available at: <http://www.wwpdB.org/>.
- Betz, S.F., Bryson, J.W., Passador, M.C., Brown, R.J., O’Neil, K.T., DeGrado, W.F., 1996. Expression of de novo designed alpha-helical bundles. *Acta Chem. Scand.* 50, 688–696.
- Bowie, J.U., Lüthy, R., Eisenberg, D., 1991. A method to identify protein sequences that fold into a known three-dimensional structure. *Science* 253, 164–170.
- Branden, C., Tooze, J., 1999. *Introduction to Protein Structure*, second ed. Garland Publishing, New York, NY; London (Chapter 17).
- Chothia, C., 1992. Proteins. One thousand families for the molecular biologist. *Nature* 357, 543–544.
- Cooper, S., Khatib, F., Treuille, A., Barbero, J., Lee, J., Beenen, M., Leaver-Fay, A., Baker, D., Popović, Z., Players, F., 2010. Predicting protein structures with a multiplayer online game. *Nature* 466, 756–770. Foldit program, available at: <http://fold.it/portal/node/>.
- Dahiyat, B.I., Mayo, S.L., 1997. De novo protein design: fully automated sequence selection. *Science* 278, 82–86.
- Das, R., Qian, B., Raman, S., Vernon, R., Thompson, J., Bradley, P., Khare, S., Tyka, M.D., Bhat, D., Chivian, D., Kim, D.E., Sheffler, W.H., Malmström, L., Wollacott, A.M., Wang, C., Andre, I., Baker, D., 2007. Structure prediction for CASP7 targets using extensive all-atom refinement with Rosetta@home. *Proteins* 69 (Suppl. 8), 118–128.
- DeGrado, W.F., Wasserman, Z.R., Lear, J.D., 1989. Protein design, a minimalist approach. *Science* 243, 622–628.
- Dolgikh, D.A., Fedorov, A.N., Chemeris, V.V., Chernov, B.K., Finkel’shtein, A.V., Shul’ga, A.A., Alakhov, Yu.B., Kirpichnikov, M.P., Ptitsyn, O.B., 1991. Preparation and study of albebetin, an artificial protein with a given spatial structure. *Dokl. Akad. Nauk SSSR* 320, 1266–1269 (in Russian).
- Dolgikh, D.A., Gabrielian, A.E., Uversky, V.N., Kirpichnikov, M.P., 1996. Protein engineering of de novo protein with predesigned structure and activity. *Appl. Biochem. Biotech.* 61, 85–96.
- Fedorov, A.N., Dolgikh, D.A., Chemeris, W., Chernov, B.K., Finkelstein, A.V., Schulga, A.A., Alakhov, Yu.B., Kirpichnikov, M.P., Ptitsyn, O.B., 1992. De novo design, synthesis and study of albebetin, a polypeptide with a predetermined three-dimensional structure. Probing the structure at the nanogram level. *J. Mol. Biol.* 225, 927–931.
- Fersht, A., 1999. *Structure and Mechanism in Protein Science: A Guide to Enzyme Catalysis and Protein Folding*. W. H. Freeman & Co, New York, NY (Chapters 15, 17–19).
- Finkelstein, A.V., 1998. 3D protein folds: homologs against errors—a simple estimate based on the random energy model. *Phys. Rev. Lett.* 80, 4823–4825.
- Finkel’stein, A.V., Reva, B.A., 1990. Determination of globular protein chain fold by the method of self-consistent field. *Biofizika* 35, 402–406.
- Finkelstein, A.V., Reva, B.A., 1991. Search for the most stable folds of protein chains. *Nature* 351, 497–499.
- Flöckner, H., Braxenthaler, M., Lackner, P., Jaritz, M., Ortner, M., Sippl, M.J., 1995. Progress in fold recognition. *Proteins* 23, 376–386.
- Gambin, Y., Schug, A., Lemke, E.A., Lavinder, J.J., Ferreon, A.C., Magliery, T.J., Onuchic, J.N., Deniz, A.A., 2009. Direct single-molecule observation of a protein living in two opposed native structures. *Proc. Natl. Acad. Sci. USA* 106, 10153–10158.
- Gruber, M., Söding, J., Lupas, A.N., 2005. REPPEP—repeats and their periodicities in fibrous proteins. *Nucleic Acids Res.* 33 (Web Server issue), W239–W243.

- He, Y., Chen, Y., Alexander, P.A., Bryan, P.N., Orban, J., 2008. NMR structures of two designed proteins with high sequence identity but different fold and function. *Proc. Natl. Acad. USA* 105, 14412–14417.
- Kryshtafovych, A., Fidelis, K., Moult, J., 2014. CASP10 results compared to those of previous CASP experiments. *Proteins* 82 (Suppl. 2), 164–174.
- Lesk, A.M., 2008. Introduction to Bioinformatics, third ed. Oxford University Press, Oxford.
- Lim, V.I., Mazanov, A.L., Efimov, A.V., 1978. Structure of ribosomal proteins. Prediction of the tertiary structure of proteins from small 30S *Escherichia coli* ribosomal subparticles. *Dokl. Akad. Nauk SSSR* 242, 1219–1222 (in Russian).
- Lindorff-Larsen, K., Piana, S., Dror, R.O., Shaw, D.E., 2011. How fast-folding proteins fold. *Science* 334, 517–520.
- Lutz, S., 2010. Beyond directed evolution—semi-rational protein engineering and design. *Curr. Opin. Biotechnol.* 21, 734–743.
- Moult, J., Fidelis, K., Kryshtafovych, A., Schwede, T., Tramontano, A., 2014. Critical assessment of methods of protein structure prediction (CASP)—round X. *Proteins* 82 (Suppl. 2), 1–6.
- Murzin, A.G., Finkelstein, A.V., 1988. General architecture of α -helical globule. *J. Mol. Biol.* 204, 749–770.
- Park, S.J., Cochran, J.R. (Eds.), 2009. Protein Engineering and Design. CRC Press, Boca Raton, FL.
- Piana, S., Klepeis, J.L., Shaw, D.E., 2014. Assessing the accuracy of physical models used in protein-folding simulations: quantitative evidence from long molecular dynamics simulations. *Curr. Opin. Struct. Biol.* 24, 98–105.
- Pititsyn, O.B., Rashin, A.A., 1975. A model of myoglobin self-organization. *Biophys. Chem.* 3, 1–20.
- Pititsyn, O.B., Finkelstein, A.V., Murzin, A.G., 1985. Structural model for interferons. *FEBS Lett.* 186, 143–148.
- Punta, M., Forrest, L.R., Bigelow, H., Kurnytsky, A., Liu, J., Rost, B., 2007. Membrane protein prediction methods. *Methods* 41, 460–474.
- Richardson, J.S., Richardson, D.C., 1989. The de novo design of protein structures. *Trends Biochem. Sci.* 14, 304–309.
- Röthlisberger, D., Khersonsky, O., Wollacott, A.M., Jiang, L., DeChancie, J., Betker, J., Gallaher, J.L., Althoff, E.A., Zanghellini, A., Dym, O., Albeck, S., Houk, K.N., Tawfik, D.S., Baker, D., 2008. Kemp elimination catalysts by computational enzyme design. *Nature* 453, 190–195.
- Schulz, G.E., Barry, C.D., Friedman, J., Chou, P.Y., Fasman, G.D., Finkelstein, A.V., Lim, V.I., Pititsyn, O.B., Kabat, E.A., Wu, T.T., Levitt, M., Robson, B., Nagano, K., 1974. Comparison of predicted and experimentally determined secondary structure of adenilate kinase. *Nature* 250, 140–142.
- Shaw, D.E., Maragakis, P., Lindorff-Larsen, K., Piana, S., Dror, R.O., Eastwood, M.P., Bank, J.A., Jumper, J.M., Salmon, J.K., Shah, Y., Wriggers, W., 2010. Atom-level characterization of structural dynamics of proteins. *Science* 330, 341–346.
- Simons, K.T., Bonneau, R., Ruczinski, I., Baker, D., 1999. Ab initio protein structure prediction of CASP III targets using ROSETTA. *Proteins* (Suppl. 3), 171–176.
- Voelz, V.A., Bowman, G.R., Beauchamp, K., Pande, V.S., 2010. Molecular simulation of ab initio protein folding for a millisecond folder NTL9(1–39). *J. Am. Chem. Soc.* 132, 1526–1528.
- Wrighton, N.C., Farrell, F.X., Chang, R., Kashyap, A.K., Barbone, F.P., Mulcahy, L.S., Johnson, D.L., Barrett, R.W., Jolliffe, L.K., Dower, W.J., 1996. Small peptides as potent mimetics of the protein hormone erythropoietin. *Science* 273, 458–464.

Lecture 24

This lecture is devoted to protein functions. This is a vast subject to discuss, and my lecture will present only a few illustrations of functioning proteins, which will emphasize the crucial role of their spatial arrangement in their functioning. I showed some illustrations of this kind when talking about membrane proteins. But in this lecture, I shall only be talking about globular, water-soluble proteins.

A very rough scheme of protein functioning looks as follows:

BIND → TRANSFORM → RELEASE

Remember that some proteins may perform only some of these actions; that the words “BIND” and “RELEASE” may imply binding and releasing a few different molecules; and that the word “TRANSFORM” may mean some chemical transformation, a change in conformation (of both the protein and the substrate), and/or movement of the protein or the substrate in space.

We start with proteins whose main function is BINDing.

Among these there are many “natively disordered” proteins. They acquire their unique spatial structure only when bound to a ligand (another protein, or DNA, or RNA or a small molecule). The hard structure provides the binding specificity, but is in demand only when there is a binding; while the protein is unbound, it may be disordered.

The well-known example of disorder is presented by unfolded, in separately taken proteins, histone tails (Peng et al., 2012), which wrap around DNA to form a nucleosome. Many other biologically active proteins contain long disordered regions, such as histones, or are wholly disordered. These intrinsically disordered proteins/regions are common in nature and abundantly found in all organisms, where they carry out important biological functions (Wright and Dyson, 1999; Uversky et al., 2000; Tompa, 2010) that use the initial disorder of the chain.

The most obvious advantage is a possibility illustrated by Fig. 24.1. The intrinsically unfolded chain can bind to a large area, which can lead to a large contact energy, and therefore to a high specificity, but the binding will be not too strong (because a great deal of the contact energy will be spent to fold the unfolded chain). As a result, the binding can be very specific but reversible (Schulz, 1977). The induced folding, that is, binding + folding (as well as unbinding + unfolding) can also be faster than binding of the rigid protein because it can start from any point of the unfolded chain, and this can lead to formation of the “energy funnel,” where the binding energy compensates the entropy loss step-by-step (cf. Fig. 24.1A and B).

The above described effect can lead to acceleration of molecular recognition—if the folding is fast (and you may remember that it can be very fast indeed). Therefore, no wonder that natively disordered proteins are widely

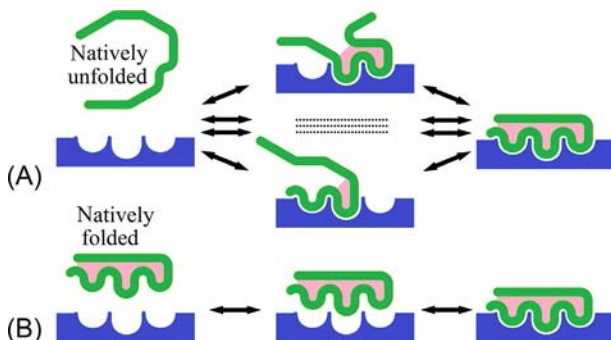


FIG. 24.1 (A) Step-by-step binding + folding of the intrinsically unfolded chain. It does not require a precise preliminary positioning of the chain, because the binding can start from its any point, and then the growing contact energy is spent on compensating the binding and folding entropy. (B) An abrupt binding of a rigid protein requires its precise preliminary positioning (not compensated by the energy), and unbinding of such a protein requires an abrupt energy increase that is not compensated by a simultaneous entropy increase.

involved in recognition, signaling, and regulation (Uversky, 2013), and frequently enough, one protein can be involved in different functions, because its conformation is affected by the interaction partner. The functions of these proteins complement the functional repertoire of “normal” ordered proteins. But they are not used as enzymes: effective catalysis requires hardness, as we will see.

Now we shall speak on DNA-binding proteins—their main function also is BINDing.

To bind to DNA, an ample portion of the protein surface should be approximately complementary to the double helix surface (Fig. 24.2A). Then, protein surface ridges are able to fit deeply into the DNA groove, where protein side-groups perform fine recognition of a concrete DNA sequence (Fig. 24.3) and bind to it. All proteins shown in Fig. 24.2 are dimers, and it is in this form that they are complementary to the DNA duplex. Two identical DNA-recognizing α -helices of such a dimer recognize a *palindrome* in the DNA double helix, that is, such a DNA sequence that preserves the same view after turning by 180 degrees around an axis perpendicular to the duplex, for example:



Here, “—” denotes an arbitrary DNA sequence between two halves of the palindrome, and the rotation axis is indicated as “.”

In such a protein dimer, DNA-binding helices are mutually *antiparallel*, and the distance between them is close to a period of the DNA double helix, so that the dimer fits onto one side of the DNA double helix. However, different

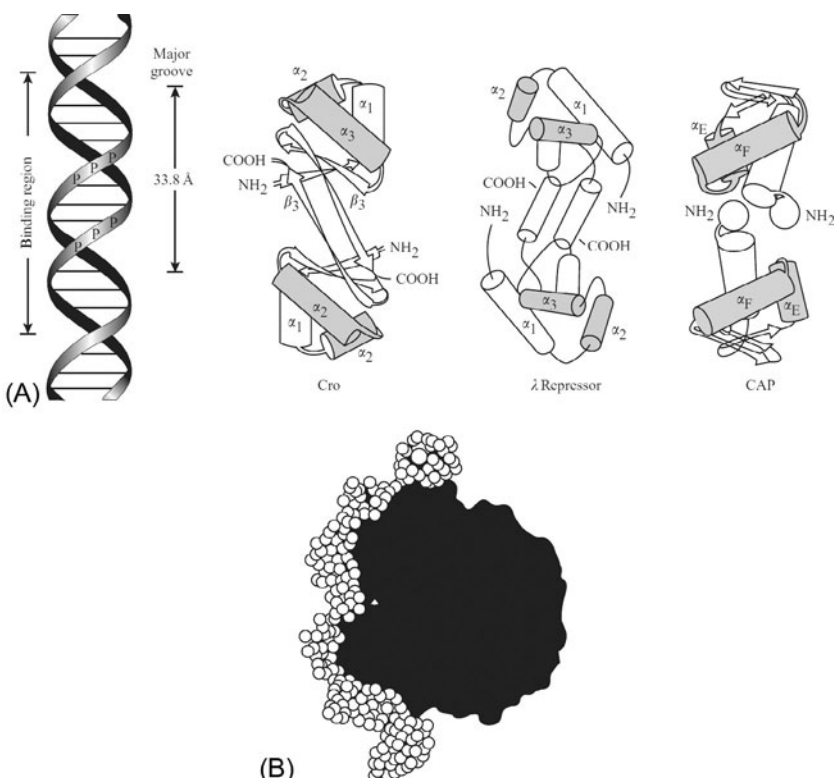


FIG. 24.2 (A) The structure of DNA (left) and a number of proteins with a typical DNA-binding motif “helix-turn-helix” (shown in gray). For catabolite activating protein (CAP), only its C-terminal domain is shown. All these proteins are dimers and all of them recognize the major groove of DNA using their helices α_3 (αF of CAP), the distance between which, in dimers, is close to a period of the DNA double helix (33.8 Å). (B) DNA (a lighter helix on the left) bent by CAP dimer (shown in black on the right). CAP association with DNA requires the presence of cyclic AMP (cAMP). (The drawings by B.W. Matthews are reproduced from Creighton, T.E., 1993. *Proteins: Structures and Molecular Properties*, second ed. W.H. Freeman & Co., New York (Chapter 8), with permission.)

proteins have different tilts of these α -helices with respect to the axis going through their centers, which results in different binding-induced bends in the DNA. Some of these binding-*induced* bends are fairly sharp (Fig. 24.2B).

In some cases, protein-to-DNA binding has to be assisted by *co-factors*, which change, or rather, slightly deform, the structure of the protein, thereby making it change from the inactive to the active state.

This is exemplified by trp-repressor (in *E. coli* it represses the operon in charge of the synthesis of RNA that codes proteins necessary for tryptophan synthesis), in which the role of such *co-factor*, or rather *co-repressor*, is played by tryptophan itself (Fig. 24.4). As long as tryptophan is unbound to the protein,

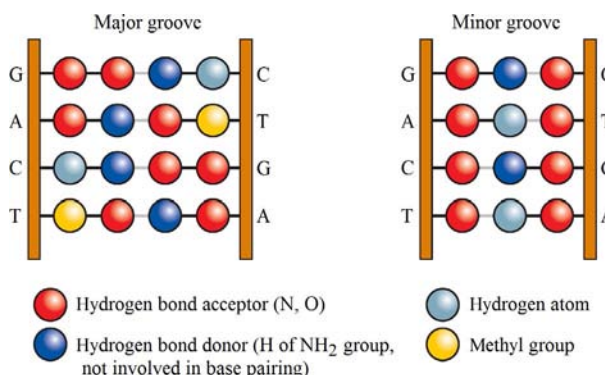


FIG. 24.3 Typical patterns created by various functional groups of A-T and C-G pairs in the major and minor grooves of DNA. (Adapted from Branden, C., Tooze, J., 1999. *Introduction to Protein Structure*, second ed. Garland Publ. Inc., New York and London (Chapter 7), with permission.)

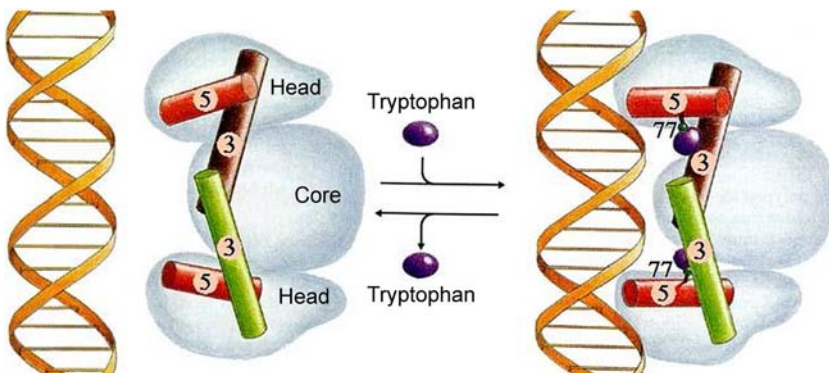


FIG. 24.4 The scheme of action of tryptophan (Trp) repressor. Against the background giving the general outline of the dimer with the common fused core and two identical heads, only those two helices (3 and 5) are shown between which the co-repressor (amino acid Trp) fits. It moves the 77th residue away, and that, in turn, shifts α -helix 5. Only then can both α -helices 5 bind to DNA. (Adapted from Branden, C., Tooze, J., 1999. *Introduction to Protein Structure*, second ed. Garland Publ. Inc., New York and London (Chapter 8), with permission.)

the distance between DNA-binding helices in the dimeric trp-repressor is too small, about 28 Å, instead of the required 34 Å, which prevents DNA binding. The protein-bound tryptophan moves the helices apart, so that they become complementary to the groove in the double helix and bind to it. Thus, when there are many tryptophans in the cell, they bind to the repressor, thus blocking further synthesis of Trp-synthesizing proteins, and hence its (tryptophan's) own further synthesis. This mode of regulation is called *negative feedback*.

In this case, tryptophan acts both as a *stimulator* of trp-repressor's DNA-binding activity and as an *inhibitor* of the synthesis of proteins required for tryptophan synthesis. Here, stimulation of trp-repressor is *allosteric*, since

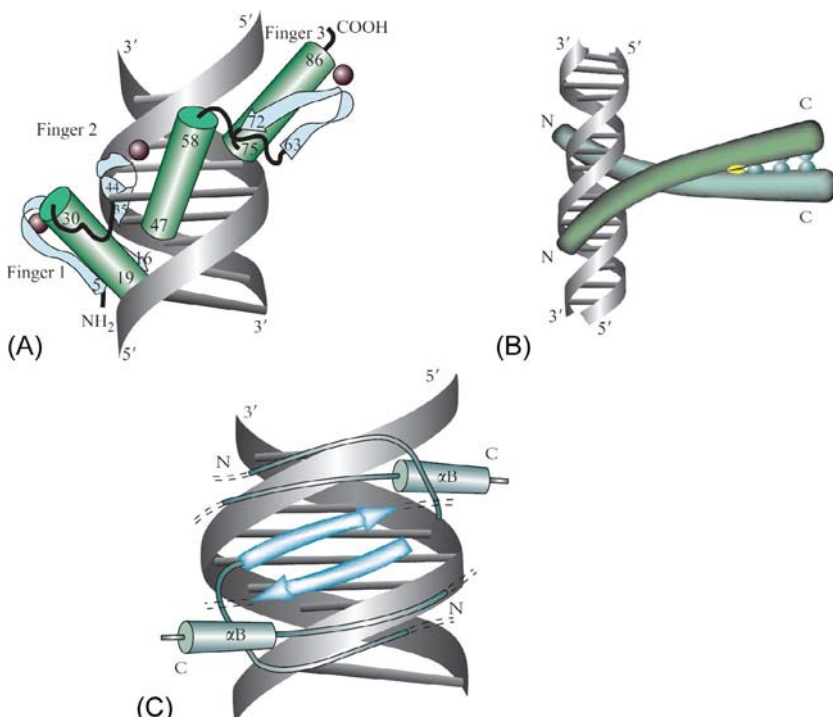


FIG. 24.5 Three more motifs typical of DNA-binding proteins. In two of them the key role is played by α -helices: (A) “zinc fingers” (Zn ions are shown as balls). Adapted from Creighton, T.E., 1993. Proteins: Structures and Molecular Properties, second ed. W.H. Freeman & Co., New York (Chapter 8), with permission. (B) “Leucine zipper”. Adapted from Branden, C., Tooze, J., 1991. Introduction to Protein Structure. Garland Publ. Inc., New York and London (Chapter 10), with permission. In the third, met-repressor motif (C) the key role is played by the β -hairpin, which specifically binds to the major groove of DNA, while the α -helices α B non-specifically bind to the sugar-phosphate backbone of DNA. Adapted from Branden, C., Tooze, J., 1991. Introduction to Protein Structure. Garland Publ. Inc., New York and London (Chapter 10), with permission. The zinc finger (a domain that can be cut-off and isolated from the remaining part of the protein) is one of the smallest among the known globular proteins, while the leucine zipper is structurally the simplest. When the latter is DNA-unbound, it is simply a dimer composed of parallel α -helices whose narrow hydrophobic surfaces are stuck together along their entire length. The surface-forming side-groups are shown as projections. However, each helix has one non-hydrophobic group: it is polar Asn shown as a yellow spot against the helix hydrophobic surface. This Asn ensures formation of a dimer: its replacement by a more hydrophobic residue results in assemblies of not two but ≥ 3 helices. N- and/or C-termini of each chain are denoted.

Trp binding to protein occurs at another site, ie, at a site different from the site that binds to DNA. The motif “helix-turn-helix” shown in Figs. 24.2 and 24.4 is typical, but far from being the only DNA-binding structural motif. To illustrate this statement, I present three other typical motifs in Fig. 24.5. I would like to stress that DNA-binding proteins can pertain to different structural classes

(in the drawings you can see α and $\alpha+\beta$ proteins), and that even DNA binding itself can be performed by the α - as well as by the β -structure.

So far, we have spoken about the coarse features of the protein structure (their characteristic size is about 10–30 Å) that allow it to fit into the DNA groove. Finer features of the protein surface (their characteristic size is that of an atom, ~3 Å) are responsible for recognition of a certain DNA sequence which is to be bound by the protein.

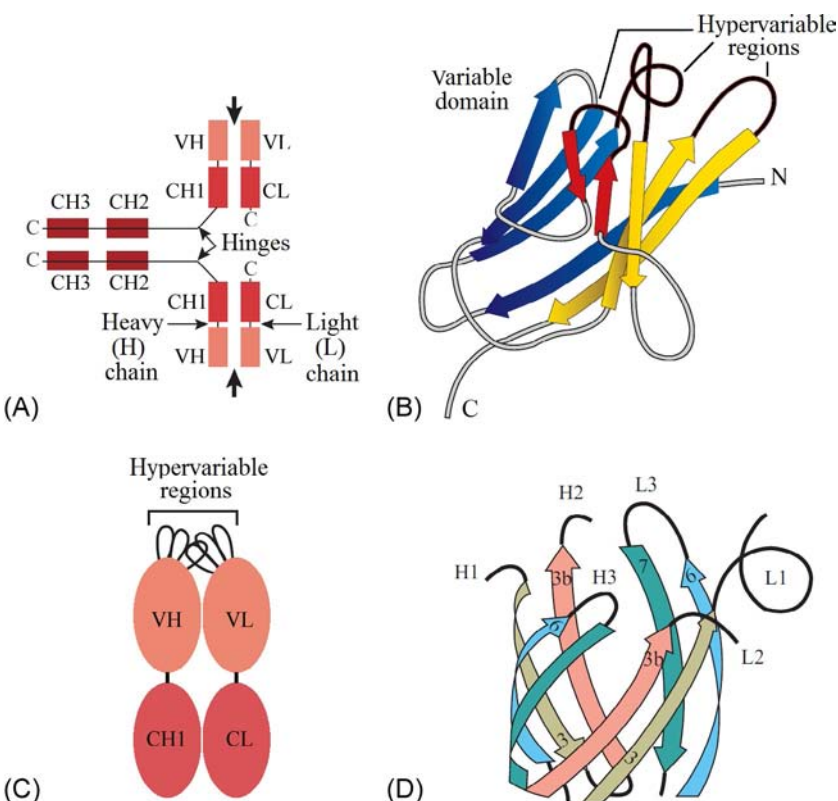
Regrettably, the “general code” used by proteins for selective recognition of DNA fragments is still unknown (if there is a distinct “code” at all). So, the state of the art here is the same as in recognition of one piece of the protein chain by another in the course of folding. However, consideration of the details of each solved DNA-protein contact allows us to understand exactly which H-bonds between protein side-groups and nucleotides, and what other of their close contacts, contribute to the occurrence of the DNA-protein contact at this particular site.

The highly selective recognition of other molecules by proteins is clearly exemplified by *immunoglobulins* or *antibodies*, ie, proteins whose task (in vertebrates) is fine recognition of small-scale *antigenic determinants* (with the characteristic size of an atom or a few atoms) of various molecules. The immunoglobulin-like *receptors of T-cells* similarly recognize small antigenic determinants of specific cells, eg, of virus-infected cells.

Immunoglobulins are built up from many β -structural domains and relatively small flexible hinges between them ([Fig. 24.6A](#)). The diversity of combinations of variable (antigen-binding) domains ensures a great variety of immunoglobulins, and hence, a broad spectrum of their activities, while rigidity of these domains ensures the high selectivity of action of each immunoglobulin. I am not going to recite here the basics of clonal selection theory, which explains the origin of a vast variety of immunoglobulins.

You will remember from other courses that germ cells contain *not* whole genes of light and heavy chains of immunoglobulins but only their fragments. In the genome, these fragments are arranged in cassettes: separately for many types of each of three fragments of the heavy-chain variable domain, separately for the light chains; separately for constant domains of each chain, and separately for hinges. During the formation of somatic immune cells these fragments are shuffled (and also their hyper-variable portions undergo mutations introduced by special DNA polymerases) to build up whole genes of immunoglobulin chains. It is a puzzle why these mutations (which may amount to tens in one domain—too many to be introduced all together with subsequent selection of “survived” proteins) do not explode the protein structure.

What we find important at the moment is that the antigen is recognized jointly by variable domains (VH and VL) of the light and heavy chains, or rather by hyper-variable loops fringing the antigen-binding pocket at the interface between these domains ([Fig. 24.6B–D](#)). The primary structure of these loops varies from immunoglobulin to immunoglobulin (which underlies the vast variety of



immunoglobulin variants). In spite of hyper-variability of their sequences, there is a limited set of canonical structures for these regions (Chothia and Lesk, 1987), and each variant has not only a particular amino acid sequence but also strictly fixed conformations of all loops, and the antigen-binding pocket is positioned on the rigid β -cylinder formed by merged antiparallel β -sheets of the variable domains. Therefore, each immunoglobulin molecule can tightly bind only a particular antigen determinant and does not bind to others.

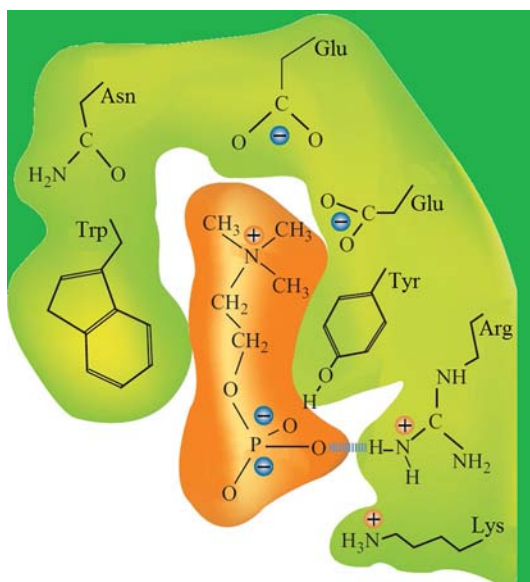


FIG. 24.7 Schematic representation of the specific interaction between an antigen (orange) and the antigen-binding “pocket” of an antibody. Mutually approaching charges and formed H-bonds are shown. The center of the antigen experiences hydrophobic and van der Waals interactions. (Adapted from Branden, C., Tooze, J., 1999. *Introduction to Protein Structure*, second ed. Garland Publ. Inc., New York and London (Chapter 15).)

[Fig. 24.7](#) shows that the selectivity of binding of antigen determinants is dictated *not* by the *overall* protein arrangement (which serves only as a basis) but rather by the complementary shape of the molecule to be bound to the shape of the relatively small (as compared with the whole domain) antigen-binding pocket. Besides, hydrophobic parts of the molecule to be bound are in contact with hydrophobic parts of the pocket, its charges are complementary to those embedded in the pocket, and also the H-bond donors and acceptors of the antigen are complementary to the pocket’s acceptors and donors. All this contributes to the tight binding of only a specific antigen.

A similar location of the active site (in a funnel at the butt-end of a β -cylinder) is observed in many other proteins having nothing in common with immunoglobulins. For example, this is where the active site is usually found in α/β cylinders (which, unlike immunoglobulins, have parallel β -structures).

In general, when studying proteins, it is easy to see that active sites often occupy “standard defects,” ie, standard dents (determined by the chain fold and not by side-groups) in the architectures of protein globules ([Fig. 24.8](#)); such a dent automatically provides contacts with many protein side chains at once.

The interface between domains is another frequent place of location of the active site. [Fig. 24.9](#) shows the active site of trypsin-like serine proteases, which is located at the interface between two β -structural domains.

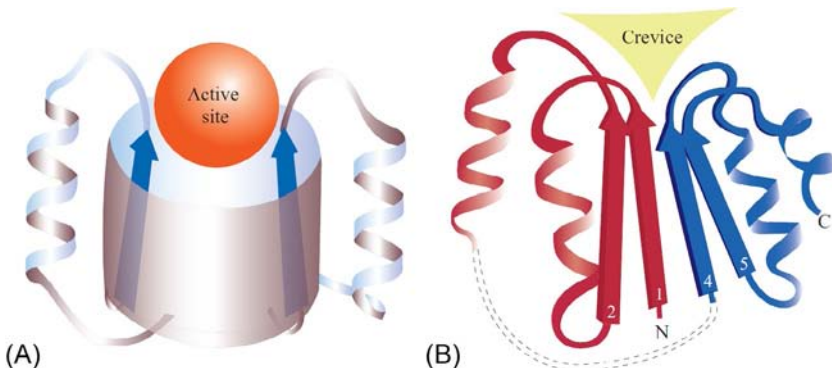


FIG. 24.8 Standard dents in protein globule architectures often dictate the location (but not function) of the active site. (A) The active site lies in the funnel at the top of a β/α -barrel with the parallel β -cylinder; for similar location of the active site in the funnel at the top of the antiparallel β -cylinder, see Fig. 24.6D. (B) The active site in the Rossmann fold crevice is formed by moving apart $\beta\text{-}\alpha\text{-}\beta$ superhelices (in the superhelix $\beta 1\text{-}\alpha\text{-}\beta 2$ the chain goes away from, while in the superhelix $\beta 4\text{-}\alpha\text{-}\beta 5$ it goes towards the viewer). (Reproduced by permission of Garland Science/Taylor & Francis Group LLC, from Branden, C., Tooze, J., 1991. *Introduction to Protein Structure*. Garland Publ. Inc., New York and London (Chapter 4), ©1991 from *Introduction to Protein Structure*, by Branden and Tooze.)

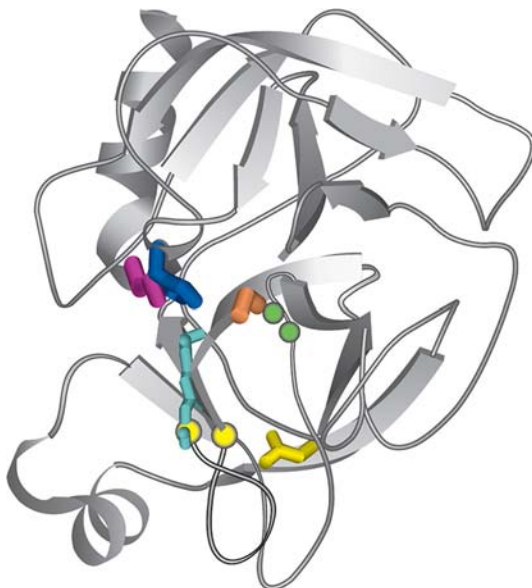


FIG. 24.9 Location of the active site in chymotrypsin (PDB code 1cbw), trypsin-like serine proteases. The figure shows parts of the active site: the *catalytic site* with side-groups of the “charge-transfer relay triad” (Ser195 (orange), His57 (blue), and Asp102 (crimson)), and two NH-groups forming the oxyanion hole are shown in green; the *substrate-binding site* includes this oxyanion hole, the non-specific substrate-binding area (shown in light-blue) and groups lining the specific substrate-binding pocket; they are shown in yellow. The domain interface is between the pair (His57, Asp102) and other active site parts.

Concluding the story of the function “BIND,” it is necessary to say a few words about the symmetrical function “RELEASE.”

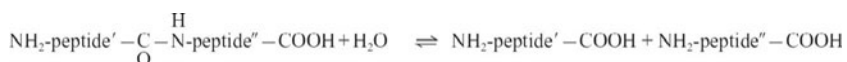
As we remember, many of the natively unfolded proteins acquire their unique spatial structure only when bound to a ligand. Therefore, not surprisingly, these proteins lose their unique spatial structure when RELEASED from a ligand. For example, the retinol-binding protein becomes a molten globule ([Bychkova et al., 1998](#)) when it gets released from retinol.

Now it is time to discuss enzymes, which are proteins whose main function is to chemically TRANSFORM the molecules bound to them. Enzymes do not create new reactions or change their direction; they “only” accelerate spontaneous processes. But sometimes the acceleration is a zillion-fold, many million times stronger than that caused by the most powerful chemical catalysts.

I take the liberty of omitting enzyme classification (it can be found in any biochemical textbook, eg, [Enzyme Nomenclature, 1992](#)), and to focus on how enzymes succeed in providing such a great acceleration of chemical reactions.

Serine proteases are a classic example considered in lectures on simple enzymatic reactions ([Schulz and Schirmer, 1979, 2013](#); [Creighton, 1993](#); [Branden and Tooze, 1991, 1999](#); [Fersht, 1999](#)), and I am not going to depart from that tradition.

Serine proteases cut polypeptide chains, ie, carry out the reaction



The polypeptide chain hydrolysis reaction proceeds spontaneously when there is enough water in the medium, but it proceeds very *slowly* and may take many years; in other words, with free water molecules available, hydrolysis is thermodynamically favorable, although a very high activation barrier has to be overcome. If there are no free water molecules in the medium, the reaction proceeds towards the other side, ie, towards polypeptide synthesis and water release, and again it is very slow.

However, in the presence of an enzyme, the peptide hydrolysis reaction (or, in the absence of free water molecules, the reverse reaction of peptide synthesis from smaller fragments) takes a fraction of a second, that is, the enzyme decreases the activation barrier dramatically. Let us see how this is done.

First, let us consider the main components of the enzyme *active site*. This consists of the *catalytic site* responsible for chemical transformation and of the *substrate-binding site* whose task is to accurately place the substrate under the catalytic cutter (or rather, under the welding/cutting machine, since an enzyme equally accelerates the reaction and its reverse).

In serine proteases, catalysis is carried out by the side chain of one definite serine (whose name “Ser195” has been derived, for historical reasons, from its position in the chymotrypsinogen chain and used for all proteins of the trypsin

family; it is this protein, trypsin, that is shown in Fig. 24.9). Let me remind you the chemical formula for a Ser side-group is $-\text{CH}_2\text{OH}$. However, serine cannot catalyze hydrolysis without the help of certain other groups and certain preparatory steps. It is inactive as long as oxygen is a member of the $-\text{OH}$ group and becomes active after H^+ removal and oxygen conversion into the $-\text{O}^-$ state.

The task of H-atom removal from Ser195 is carried out by the two other members of the “charge transfer triad,” His57 (which accepts the H^+ atom) and “auxiliary” Asp102. Mutations of these two residues, not to mention mutation or chemical modification of catalytic serine, nearly stop the catalytic activity of serine proteases.

The activated oxygen ($-\text{O}^-$) of the Ser195 side-group plays the crucial role in catalysis. It attacks the C' atom of the treated peptide group (Fig. 24.10) and involves it in a temporary covalent bond (that is longer and not so tight as normal C–O bonds), thereby turning the C' atom into the tetrahedral state (when it has covalent bonds not to three but to four atoms: the additional atom is O $^-$ from

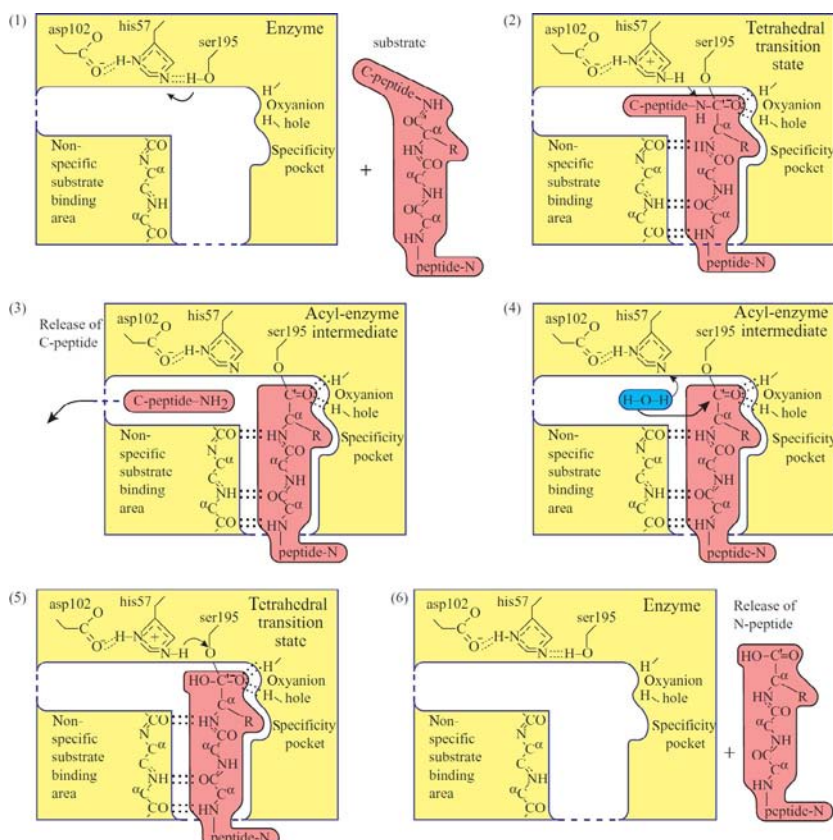


FIG. 24.10 Diagram of enzymatic peptide hydrolysis.

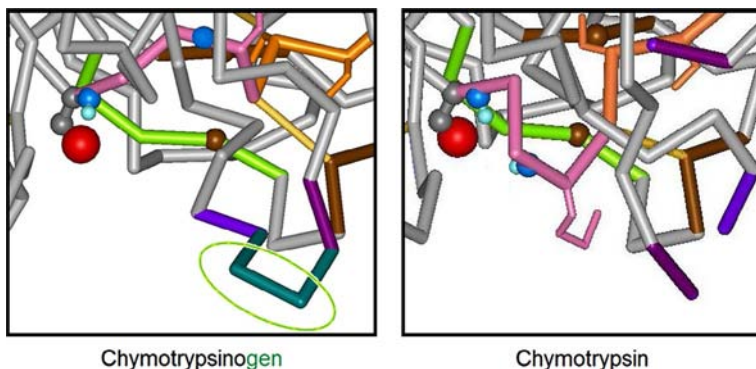


FIG. 24.11 The part of a catalytic site which experiences the greatest change upon conversion of the enzymatically-inactive chymotrypsinogen (PDB code 1ex3) into active chymotrypsin (PDB code 1cbw). The conversion results from proteolysis which cuts out the dipeptide (encircled in the left panel) from chymotrypsinogen. Then the NH group distant from the chemically active O^γ-atom of Ser195, approaches this O^γ atom and another NH group to form the oxyanion hole. The O^γ-atom of Ser195 is presented as a large red ball. Each of the two NH groups participating in formation of the oxyanion hole is presented as a larger blue and a smaller light-blue ball.

the Ser195 side-group). The tetrahedral state of the C' atom is supported by a bond of the peptide's group O atom with the *oxyanion hole* (it is noteworthy that just this hole is created upon conversion of the enzymatically-inactive chymotrypsinogen into active chymotrypsin, see Fig. 24.11). And subsequent disintegration of this complex results in breaking the C'=N bond leading to a breakdown in the treated chain.

The substrate-binding site includes (Figs. 24.9 and 24.10) the mentioned *oxyanion hole* (which binds the oxygen of the treated peptide group), the *non-specific peptide-binding area* (which, together with the oxyanion hole, is responsible for the correct positioning of the treated peptide group relative to the activated O[−] atom of activated Ser195), and the *specific substrate-binding pocket* responsible for recognition of the amino acid preceding the cleavage point.

The general course of the reaction is illustrated in Fig. 24.10. This scheme is a result of long-term studies of many research groups (see Schulz and Schirmer, 1979, 2013; Creighton, 1993; Branden and Tooze, 1991, 1999; Stryer, 1995; Stepanov, 1996; Fersht, 1999). A lot of different data have been used to build it up: data on catalysis of different substrates and on chemical modifications of the enzyme, results of protein engineering studies (which determined the catalysis-participating points of the enzyme) and studies of enzyme complexes with non-cleavable substrate analogs, as well as X-ray structural work, etc.

What does the enzyme do to accelerate a chemical reaction? To answer this question, let us compare the enzymatic reaction (Fig. 24.10) with a similar spontaneous reaction that occurs in water without any help from an enzyme (Fig. 24.12).

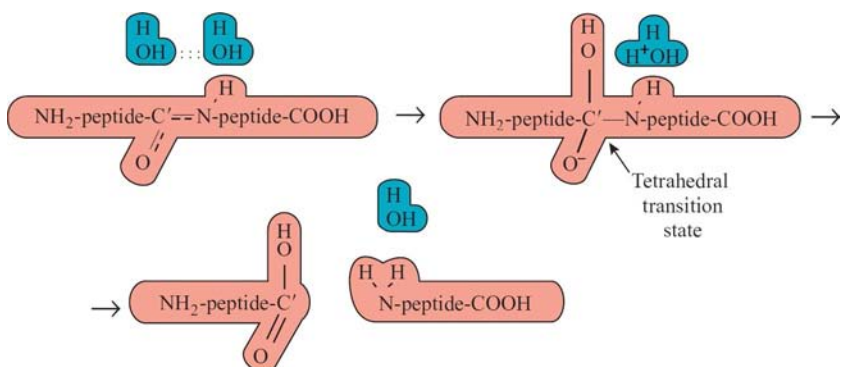


FIG. 24.12 Diagram of spontaneous, non-enzymatic peptide hydrolysis in water. The chemical mechanism is similar to that shown in Fig. 24.10.

We see that the enzymatic reaction occurs in two stages: first, the C-terminal peptide is cleaved off, and the N-terminal peptide forms a complex with the O^γ-atom of serine, and second, this N-peptide changes its bond to the O^γ-atom of serine for a bond to the O atom of water. The enzyme-unassisted reaction has only one stage during which the C-terminal peptide is cleaved off, and the N-terminal peptide forms a complex with the O atom of water. Also, we see that all these three reactions proceed via the tetrahedral activated complex, or rather, via the activated complex where the tetrahedral C-atom (which has formed a covalent bond to the O-atom) is near some proton donor (His⁺ in the enzyme or OH₃⁺ in water).

The fact that the enzymatic reaction proceeds via two activated complexes (and not one as the enzyme-unassisted reaction does) is not an accelerating factor by itself. The acceleration happens because the enzyme-bound activated complex is *less* unstable than the activated complex in water (and it is precisely the instability of the activated complex that limits the reaction rate).

In an enzyme, the activated complex (ie, the transition state) is stabilized as follows:

First, the negative charge of the peptide's C'-O⁻ group (arising with electron shifting from the serine's O⁻ upon tetrahedrization of the C'-atom) is drawn into the enzyme's oxyanion hole having two protons inside. The hydrogen and electrostatic bond between these positively charged protons and the negatively charged O-atom decreases the energy of the latter and hence the energy of the C'-atom's tetrahedral state (unlike in the non-enzymatic reaction where there is no such pre-arranged "hole"). In other words, the energy (enthalpy) of the transition state decreases, and so-called *enthalpic catalysis* occurs.

Second, near the tetrahedral C'-atom there is the proton-holding His⁺, which is approximately as stable as proton-free His⁰. In water, the role of the proton donor is played by OH₃⁺, the concentration of which, owing to its instability, is extremely low and amounts only to about 10⁻⁷ mol L⁻¹. The necessity to "fish

it out” decreases entropy and hence increases the free energy of the non-enzymatic activated complex. Therefore, entropy hampers the association of all the components of the activated complex in water but does not hamper its association on the enzyme, where all the components are already assembled, the entropy of “fishing out” of the substrate being covered by its sticking to the enzyme’s substrate-binding site. This facilitates the association of all the components of the activated complex, decreases its free energy on the enzyme (as compared to that of the non-enzymatic reaction), and results in so-called *entropic catalysis*.

In total, the entropic and enthalpic components of catalysis accelerate the enzymatic reaction by approximately 10^{10} times compared with the non-enzymatic reaction.

The basic feature of both chemical and enzymatic catalysis is a decrease in the free energy of the transition state, ie, a decrease of the maximum free energy to be surmounted in the course of the reaction (Fig. 24.13). The free energy may be decreased at the expense of the entropy that is due to association of all the necessary reaction components on the enzyme. Also, the free energy decrease may be achieved (or strengthened) at the expense of the enthalpy of preferential binding of the molecule’s transition state and not its initial (“substrate”) and/or final (“product”) states.

By the way, too tight binding of the substrate or product (tighter than that of the transition state) will simply cause *inhibition* (the so-called “substrate inhibition” or “product inhibition”) of the enzyme, which will lose its “RELEASE” function and quit the game.

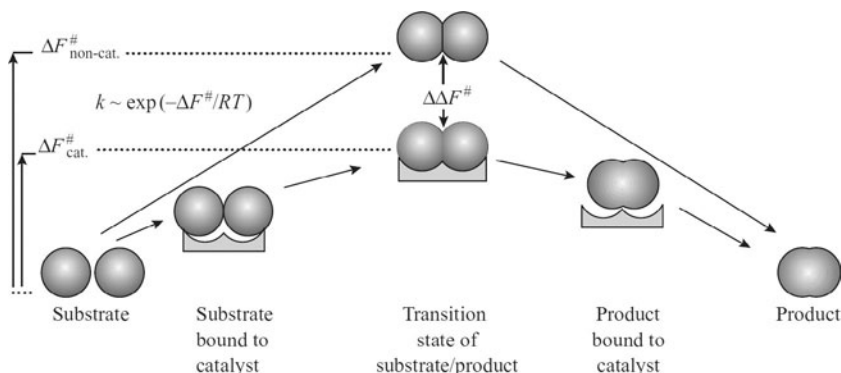


FIG. 24.13 This diagram illustrates the crucial role of catalyst-produced stabilization of the transition (most unstable) state of the substrate/product and stresses the importance of the catalyst’s rigidity in decreasing the free energy barrier ($\Delta F^\#$) and increasing the reaction rate (k). For the sake of clarity, the figure indicates that the contours of the transition state are complementary to those of the enzyme active site, although actually the key role is usually played by temporary covalent bonds between the substrate/product transition state and the enzyme’s catalytic site. The free energies of the initial and final states are not affected by the catalyst. The figure stresses that acceleration of the reaction depends on the $\Delta\Delta F^\#$ value, ie, on how strongly the enzyme binds the transition state.

Typical natural or artificial inhibitors are non-cleavable analogs of the transition state.

The structures of inhibited enzymes are stable and therefore can be readily investigated; this gives us a possibility to peep into the mechanism of enzyme action (see Figs. 24.14–24.16).

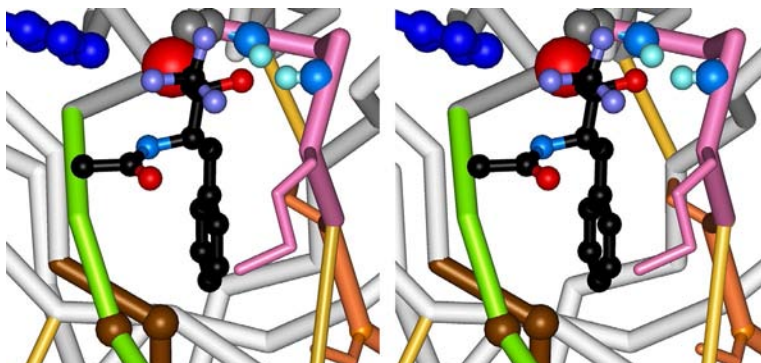


FIG. 24.14 Stereo drawing (see Appendix E) of the chymotrypsin (PDB code 1GG6) catalytic site blocked with the small inhibitor APF (*N*-acetyl-phenylalanine-trifluoromethyl ketone; its three fluorine atoms are gray-blue, C-atoms are black, the N-atom is pale-blue, O-atoms are red). APF is in the right (for hydrolysis) position relative to the active center (the C'-atom of APF even forms a bond with the attacking O^γ-atom of Ser195, which is only a little longer than a “normal” covalent bond; the O-atom of the APF’s C’O group is in the oxyanion hole of chymotrypsin). APF is not cleaved, as its highly electronegative fluorines pull the excess electronic charge away from its C'-atom, thereby stabilizing the tetrahedral shape of the C'-atom covalently attached to the O^γ-atom of Ser195 (shown as a large red ball). The orientation of this and the Fig. 24.15 is somewhat different from that of Fig. 24.11.

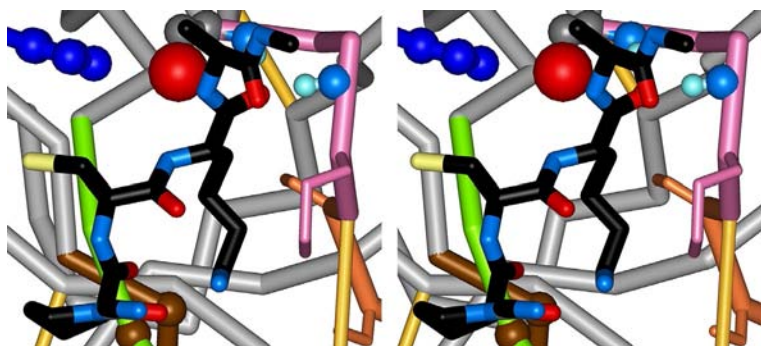


FIG. 24.15 Stereo drawing of the chymotrypsin catalytic site blocked with a fragment of bovine pancreatic trypsin inhibitor protein (PDB code 1cbw); C-atoms of the fragment are painted black. The fragment is in the *almost* right (for hydrolysis) position, but its C' atom is not as close to the O^γ-atom of Ser195 as it would be required for bond formation. Therefore, the inhibitor cannot be cleaved; its conformation corresponds to “unproductive binding,” and the necessary for the completion of the reaction water is not allowed to come to the reaction center by a tight contact of the enzyme and the inhibitor (see the bottom panel in Fig. 24.16).

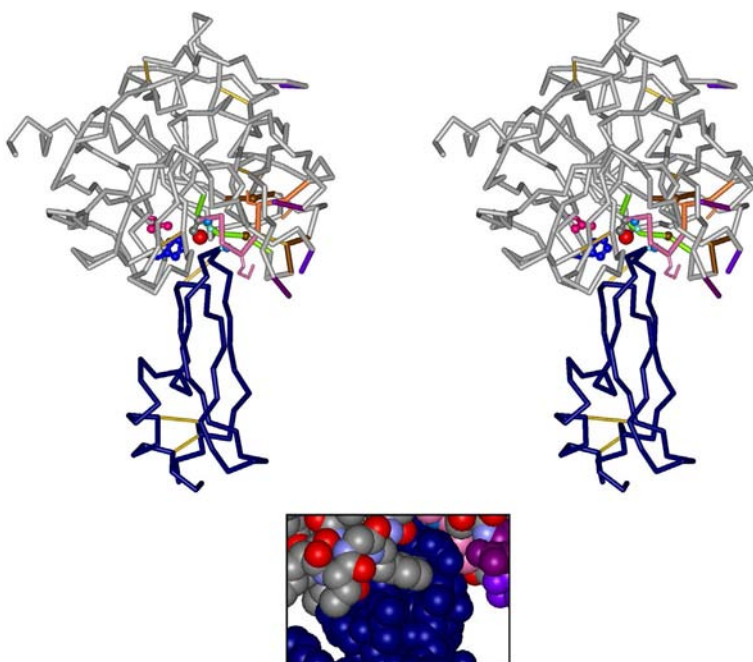


FIG. 24.16 Top panel: stereo drawing of chymotrypsin (PDB code 1cbw), which is painted gray, with colored pieces outlining its active site associated with trypsin inhibitor (dark blue). S–S bonds within each protein are shown by yellow sticks. Bottom panel: enlarged full-atom model of a close contact between the enzyme and the inhibitor.

In the preferential binding of the transition state the key role may be played either by the binding of its deformed electron system to the enzyme (recall the activated Ser and the “oxyanion hole” of serine proteases) or by preferential binding of the deformed (in the transition state) conformation of the whole molecule.

The latter is vividly illustrated by the catalytic function of artificial “abzymes” (antibody enzymes), which are antibodies selected to bind the substrate’s transition state and thus to catalyze its chemical conversion (Kohen et al., 1980; Schultz and Lerner, 1995; Fersht, 1999) (Fig. 24.17).

Some abzymes are able to spend almost the entire energy obtained from substrate binding on decreasing the activation barrier, ie, on deformation of the treated chemical bond. And although the available abzymes are not powerful enzymes (since electron donors and acceptors are not built into them yet, they are only able to accelerate a spontaneous reaction by five orders of magnitude at the most, while this value for natural enzymes can be 10–15 orders), the possibility of their creation confirms the importance of preferential binding of the transition state.

The transition state differs from the initial and final states of a chemical reaction by small details, of an Angström unit in size (Fig. 24.17). To ensure

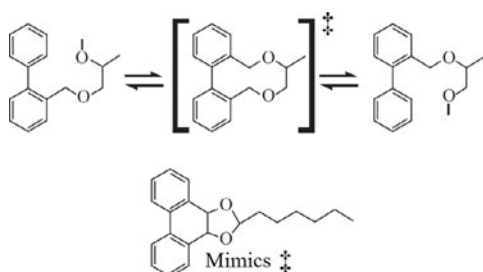


FIG. 24.17 A diagram of chemical conversion catalyzed by abzyme, ie, the antibody selected against the transition state of a slow spontaneous reaction. The transition (\ddagger) state of the given reaction of isomerization has (unlike its initial and final states) a flat three-ring system. To produce antibodies to the transition state of such a shape, the stable molecule (below) with similar rings is injected into the animal's blood. (From Schultz, P.G., Lerner, R.A., 1995. From molecular diversity to catalysis: lessons from the immune system. *Science* 269, 1835–1842.)

preferential binding of the transition state (rather than the initial and the final ones), the protein must be as rigid as possible (see also Problem 24.1). Soft protein, or, rather, a soft active site, is as efficient in catalysis as a rubber razor in shaving (although the opposite opinion can also be found in the literature; see, eg, Chernavskyyii and Chernavskaya, 1999).

Inner voice: Does “rigid” refer to the active site rather than to the entire protein? And when you talk of “rigidity,” do you have mechanical rigidity in mind, or something else?

Lecturer: It is the active site that must be rigid. Rigidity of the entire protein is important for catalysis only so far as it maintains the rigidity (and specificity, see discussed later) of the active site. And I have in mind the energetic rather than the mechanical aspect of rigidity: I mean that a small change in the substrate causes a great change in the energy of its binding to the enzyme. The mechanical picture, see Fig. 24.13, is easier to grasp. However, the same effect can be caused by interactions between the enzyme and the substrate valence electrons: the energy of interaction of the electron clouds changes sharply with a small-scale change of their shapes.

Actually, the deformation of rigid chemical bonds of a substrate (which is the essence of any chemical reaction) is more efficient when transient substrate-to-enzyme binding is performed by rigid covalent bonds rather than by soft van der Waals interactions. This explains why abzymes, which use van der Waals interactions only, are weaker catalysts than natural proteins with their chemically active catalytic sites.

Inner voice: Thus, you mean that flexibility of a protein structure plays no role in catalysis? There are other opinions in the literature (Chernavskyyii and Chernavskaya, 1999; Frauenfelder, 2010) ...

Lecturer: Here, first of all, one has to distinguish the catalytic act itself, which is not facilitated by flexibility, from the stage of substrate penetration

into the active site, where protein flexibility can be required (and when the product leaves this site, too). We will come to this in the Lecture 25. Second, one has to have in mind the following. If the enzyme's active site does not fit the substrate's transition state perfectly (nothing is perfect ...); some flexibility would allow this non-perfect site to be suitable for at least a fraction of the time. But even in this case, the active site must fit the transition state better than both initial and final states of the substrate/product.

Inner voice: All your speculations, up to now, dealt with a static or an almost static enzyme. What if the energy necessary for catalysis is stored as kinetic energy of moving parts of the enzyme, for example, as the energy of its vibration?

Lecturer: This is not possible. In Lecture 8 (see also Problem 24.2), we have seen that kinetic energy dissipates within $\sim 10^{-11}$ s even in a large protein and much faster in a small one, while one act of enzymatic catalysis takes at least $\sim 10^{-6}$ s. This means that the energy released during substrate binding dissipates and converts into heat long before it can be used in catalysis.

This analysis shows that: (1) the potential energy should be put into the substrate (*not* into the protein) to bring it, the substrate, closer to its transition state, and therefore, the protein active site should be rigid; and (2) kinetic energy cannot be used in catalysis.

The theory of catalysis at the expense of preferential binding of transition states was put forward by Holden and [Pauling \(1970\)](#) as far back as the 1930s and 1940s. More recently, the transition states for some enzymatic reactions have been probed by protein engineering techniques ([Fersht, 1985, 1999](#)), ie, by directed replacement of amino acids in the enzyme active sites. It has become clear (and visible, thanks to X-rays) which residues of the enzyme are responsible for the sticking together of components required to build up the activated complex, and which for preferential binding of exactly and exclusively the transition state (previously hypothetical since its arrangement could not be seen in experiment).

For example, Alan Fersht's study of tyrosyl-tRNA synthase has established the residues (Thr40 and His45, see [Fig. 24.18](#)) that bind to ATP γ -phosphate *only* in the transition state ([Fersht et al., 1985; Fersht, 1999](#)). This additional strong binding distinguishes the transition state from bound substrates or products of the reaction.

The transition state is most unstable (by definition!) and therefore cannot be observed directly. So X-rays, which can see only the stable position of the substrate on the enzyme, show us the substrate unbound to Thr40 and His45 (the distance is too large); meanwhile, replacement of Thr40 and His45 by small alanines decreases the mutant protein activity by more than a million times, while binding of the substrate by the mutant protein remains almost unaffected. This shows that Thr40 and His45 bind to ATP γ -phosphate *only* in the transition state, at a strained (five-coordinate) state of α -phosphorus attacking the tyrosine's CO-group.

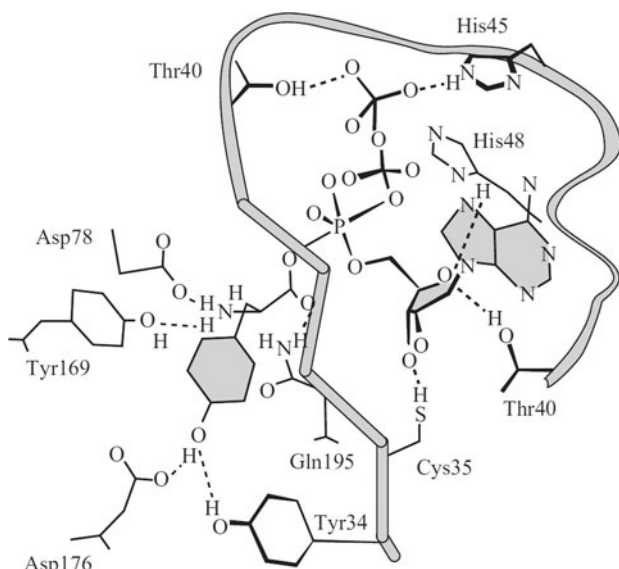


FIG. 24.18 The presumed structural arrangement of the transition state for tyrosyl-AMP formation from tyrosine and ATP on the tyrosyl-tRNA synthetase enzyme. The tyrosine ring is hatched as well as the adenosine rings. The tyrosine-attacking activated five-coordinate α -phosphorus (P) of the ATP molecule is drawn in the center, while ATP γ -phosphate is at the top. This γ -phosphate forms hydrogen bonds to Thr40 and His45 only in the transition state; a stable, X-ray-observed binding of substrates involves no such bonds. (*Adapted from Stryer, L., 1995. Biochemistry, fourth ed. W.H. Freeman & Co, New York (Chapter 34).*)

When discussing the enzymatic reaction we cannot but mention its very high specificity. For example, serine proteases cut a polypeptide only after certain amino acids: chymotrypsin cuts it after aromatic ones, trypsin does so after positively charged residues, elastase only after the smallest. This effect (it is called “key (substrate)-lock (enzyme)” substrate recognition) is ensured by the neat structure of the *specific substrate-binding “pocket”* (Fig. 24.19). This pocket

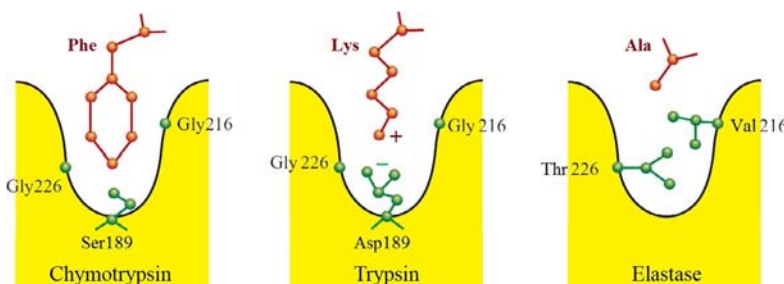


FIG. 24.19 The structural arrangement of the specific substrate-binding pocket in various serine proteases. (*Adapted from Branden, C., Tooze, J., 1999. Introduction to Protein Structure, second ed. Garland Publ., Inc., New York and London (Chapter 11).*)

recognizes the “key” side-group of the treated peptide. In trypsin, the key side-group is last before the cleavage point. In papain, it is last but one; in thermolysin, it is positioned immediately *after* the treated C–N bond.

The key residues mark the possible cleavage point rather accurately; however, the rate of polypeptide digestion also depends on other residues surrounding this point (this is only natural because they also have some interactions with the protease).

A still more important factor affecting cleavage efficiency and even its possibility, is the polypeptide conformation at the cleavage site. The C'=N bond cannot be cut if a fixed substrate conformation does not allow this bond and the key side-group to gain their “correct” (for cleavage) positions simultaneously. This is why proteases are not good at digesting proteins with a rigid structure but easily deal with denatured, flexible proteins. Some definite rigid conformation of the polypeptide chain allows it to stick to a definite protease, to block its active site, and to remain there, intact, forever. Many inhibitors (see Fig. 24.15) use this principle of “unproductive binding.”

The proteases that we have discussed in this lecture are efficient but not absolutely accurate enzymes. Presumably, the organism can still tolerate some mistakes in their selection of the cleavage point. But there are proteins that must be absolutely reliable. Such reliability is ensured by the operation of a few active sites in the same protein.

Having dealt with the elementary functions of proteins, we will consider their more complex functions in the Lecture 25.

REFERENCES

- Branden, C., Tooze, J., 1991. *Introduction to Protein Structure*. Garland Publ. Inc, New York and London (Chapters 4, 10, 15).
- Branden, C., Tooze, J., 1999. *Introduction to Protein Structure*, second ed. Garland Publ. Inc., New York and London (Chapters 7, 8, 11, 15).
- Bychkova, V.E., Dujsekina, A.E., Fantuzzi, A., Ptitsyn, O.B., Rossi, G.L., 1998. Release of retinol and denaturation of its plasma carrier, retinol-binding protein. *Fold. Des.* 3, 285–291.
- Chernavskiyii, D.S., Chernavskaya, N.M., 1999. *Protein as a Machine. Biological Macromolecular Constructions* (in Russian). Moscow University Publishing, Moscow (Chapters 24, 25).
- Chothia, C., Lesk, A.M., 1987. Canonical structures for the hypervariable regions of immunoglobulins. *J. Mol. Biol.* 196, 901–917.
- Creighton, T.E., 1993. *Proteins: Structures and Molecular Properties*, second ed. W.H. Freeman & Co, New York (Chapters 8, 9).
- Enzyme Nomenclature, 1992. Academic Press, San Diego, CA. <http://www.chem.qmul.ac.uk/iubmb/enzyme/rules.html>. <http://www.chem.qmul.ac.uk/iubmb/enzyme/rules.html>.
- Fersht, A., 1985. *Enzyme Structure and Mechanism*, second ed. W.H. Freeman & Co, New York (Chapters 1, 3, 7, 8, 10–12).
- Fersht, A., 1999. *Structure and Mechanism in Protein Science: A Guide to Enzyme Catalysis and Protein Folding*. W. H. Freeman & Co, New York (Chapters 1, 7, 10, 12, 13, 15, 16).

- Fersht, A.R., Shi, J.P., Knill-Jones, J., Lowe, D.M., Wilkinson, A.J., Blow, D.M., Brick, P., Carter, P., Waye, M.M., Winter, G., 1985. Hydrogen bonding and biological specificity analyzed by protein engineering. *Nature* 314, 235–238.
- Frauenfelder, H., 2010. *The Physics of Proteins. An Introduction to Biological Physics and Molecular Biophysics*. Springer, New York (Chapters 11, 15).
- Kohen, F., Kim, J.B., Lindner, H.R., Eshhar, Z., Green, B., 1980. Monoclonal immunoglobulin G augments hydrolysis of an ester of the homologous hapten: an esterase-like activity of the antibody-containing site? *FEBS Lett.* 111, 427–431.
- Pauling, L., 1970. *General Chemistry*. W.H. Freeman & Co, New York (Chapter 12).
- Peng, Z., Mizianty, M.J., Xue, B., Kurgan, L., Uversky, V.N., 2012. More than just tails: intrinsic disorder in histone proteins. *Mol. Biosyst.* 8, 1886–1890.
- Schultz, P.G., Lerner, R.A., 1995. From molecular diversity to catalysis: lessons from the immune system. *Science* 269, 1835–1842.
- Schulz, G.E., 1977. Nucleotide binding proteins. In: Balaban, V. (Ed.), *Molecular Mechanism of Biological Recognition*. Elsevier/North-Holland Biomedical Press, New York, pp. 79–94.
- Schulz, G.E., Schirmer, R.H., 1979, 2013. *Principles of Protein Structure*. Springer, New York (Chapters 10, 11).
- Stepanov, V.M., 1996. *Molecular Biology: Protein Structure and Function* (in Russian). Vysshaya Shkola, Moscow (Chapters 7, 8, 10, 13).
- Stryer, L., 1995. *Biochemistry*, fourth ed. W.H. Freeman & Co, New York (Chapter 34).
- Tompa, P., 2010. *Structure and Function of Intrinsically Disordered Proteins*. Chapman & Hall/CRC Press, Taylor & Francis Group, Boca Raton, FL (Chapters 2, 10–12).
- Uversky, V.N., 2013. A decade and a half of protein intrinsic disorder: biology still waits for physics. *Protein Sci.* 22, 693–724.
- Uversky, V.N., Gillespie, J.R., Fink, A.L., 2000. Why are “natively unfolded” proteins unstructured under physiologic conditions? *Proteins* 41, 415–427.
- Wright, P.E., Dyson, H.J., 1999. Intrinsically unstructured proteins: re-assessing the protein structure-function paradigm. *J. Mol. Biol.* 293, 321–331.

Lecture 25

Having considered elementary protein functions in the previous lecture, we can now proceed to their more complicated functions.

As I have said already, some proteins are supposed to work extremely accurately; this precision in action is achieved by the conjugated work of several active sites of a protein. Specifically, aminoacyl-tRNA synthetases work in this way. They charge tRNAs with the proper amino acids, and precision in their work is crucial for precision of protein biosynthesis. They are allowed to be mistaken only once per many thousands of acts of aminoacyl-tRNA synthesis, while recognition of an amino acid by the substrate-binding cleft is erroneous in about 1% of cases. A “double-sieve” effect used to eliminate these errors (Fig. 25.1) is achieved by the special construction of the enzyme (Fersht, 1999).

Aminoacyl-tRNA hydrolysis is not simply a reversal of the synthesis reaction: both reactions release free phosphates, that is, *both* of them decrease the free energy. Aminoacyl-tRNA synthase has two active sites, one for synthesis and one for hydrolysis, and the substrate-binding cleft of the center of hydrolysis is smaller than the cleft of the aminoacyl-tRNA synthesis site.

The principle of the sieve is to reject particles that are greater than the sieve’s mesh.

The first sieve, the sieve at the aminoacyl-tRNA synthesis site, allows tRNA to be charged with the “proper” amino acid and with a small number of those “wrong” amino acids that are no larger than the “proper” one. All amino acids larger in size are rejected by the rigid cleft. Most of the smaller amino acids are rejected too, since their hydrophobicity/hydrophilicity is different from that of the “proper” amino acid. However, selection on a hydrophobicity/hydrophilicity basis is not as strict as selection caused by the necessity to squeeze into a rigid dent of a given size. Thus, the output of the first step is a lot of aminoacyl-tRNAs charged with a “proper” amino acid and some quantity of aminoacyl-tRNAs charged with “wrong” (smaller) amino acids, all larger ones having been rejected by the first sieve.

The second active site has a smaller “mesh” (substrate-binding cleft); it promotes hydrolysis of aminoacyl-tRNAs, but *only* of those charged with amino acids smaller than the “proper” amino acid. The “proper” amino acid is larger, and therefore the second sieve rejects it, and all the others are hydrolyzed and decay. These two sieves provide production of only the correctly charged aminoacyl-tRNAs.

To complete the story about enzyme specificity, it is worthwhile mentioning some important practical aspects of active site studies. (1) Many people are currently studying various substrate-binding pockets and trying to find—with open eyes, not blindly—the inhibitors that bind to them. Special interest is paid to

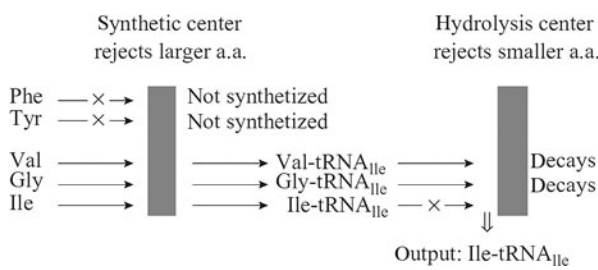


FIG. 25.1 A scheme of the “double-sieve” mechanism used by Ile-aminoacyl-tRNA synthase to produce the Ile-charged isoleucine tRNA (tRNA_{Ile}).

proteins of most harmful viruses. (2) Directed mutations introduced to the substrate-binding site can modify a “natural” substrate specificity (eg, of serine proteases) and even create a new specificity—to meet the needs of medicine and industry. (3) Great interest is attracted by attempts to create, on the solid basis of existing protein globules, new active sites with a new, “grafted” activity.

Studies of enzymatic activity have shown (recall the last lecture) that only a small part of a protein globule is involved in the catalytically active site, while the rest, the largest portion of the protein globule, serves only as a solid base that forms and fixes the active site. Therefore, we must not be surprised that proteins with different primary and even tertiary structures can have similar or even identical biochemical functions.

Serine proteases again serve as a classic example. There are two classes of such proteases: the trypsin type and the subtilisin type. They have no similarity either in sequences or in folds (Fig. 25.2). They belong to different structural classes (trypsin is a two-domain β -protein, subtilisin is a single-domain α/β -protein). They have different substrate-binding clefts. They only

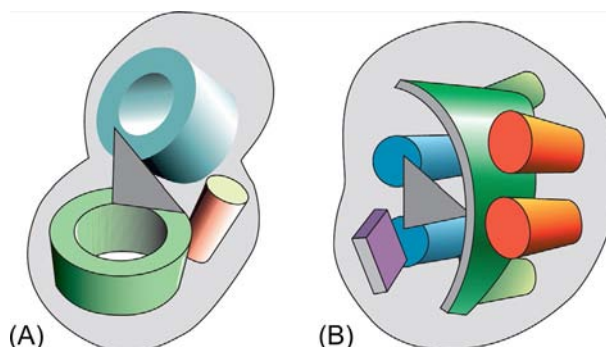


FIG. 25.2 Schemes of serine proteases (A) of the trypsin type and (B) of the subtilisin type. α -helices (cylinders) β -sheets and β -barrels are shown against the background of the molecule’s contour. The active sites are shown as dark-gray triangles. (Adapted from Finkelstein, A.V., 1989. Is it possible to graft a new active site to the protein molecule? Biopolym. Cell (in Russian) 5, 89–93.)

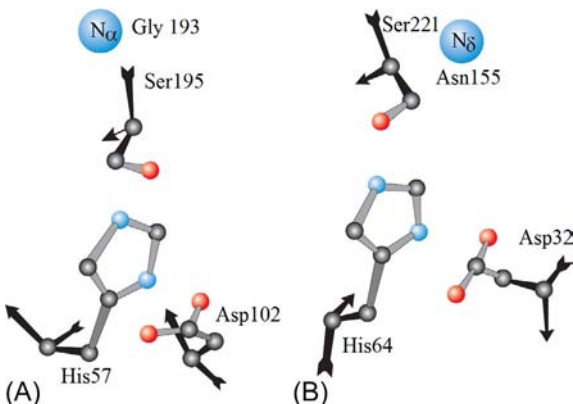


FIG. 25.3 Schemes of the active sites of serine proteases of (A) the trypsin type and (B) the subtilisin type. (Similar active sites exist not only in proteases but also in lipases and in some other enzymes.) The main-chain fragments (up to C_β-atoms) are shown in black; the arrows show the main-chain direction. The circle (with N inside) shows the positions of the oxyanion holes. The main-chain N_αH groups (in trypsin) and the side chain N_δH group (in subtilisin) face these holes. The only invariant feature of the active sites in these two classes of proteins is the position of the tips of the side chains of the catalytic triad (Ser, His, Asp), and with some variation, of the oxyanion hole; all other details are different, including the main chain direction in the catalytic residues His and Asp. (Adapted from Finkelstein, A.V., 1989. Is it possible to graft a new active site to the protein molecule? *Biopolym. Cell* (in Russian) 5, 89–93.)

have similarly positioned key amino acid residues of the catalytic sites (Fig. 25.3), and even this similarity refers mainly to the functional “tips” of the side chains of these residues (Finkelstein, 1989).

Moreover, there are proteases that differ from serine proteases even in the catalytic site zone. I have in mind metalloproteinases such as carboxypeptidase or thermolysin. A key role in their catalytic action is played by a Zn²⁺ ion built into the protein structure by powerful coordinate bonds (Rawlings and Barrett, 1995). Having a small radius because of its lack of outer electrons, a multi-charged metal ion produces a very strong electric field (see Problem 25.1). This allows such an ion, built into the metalloprotease, to activate a water molecule by breaking it into OH[−] and H⁺, and the activated water disrupts a peptide bond. In doing so, the activated water works approximately in the same way as OH[−] in the noncatalyzed reaction described in the previous lecture. A significant difference is that the enzyme activates exactly the water molecule sitting near the peptide bond to be attacked, while in a noncatalyzed reaction the activated water is to be found among a great many nonactivated ones, which takes a lot of time. Simultaneously, the Zn²⁺ charge stabilizes—in metalloproteinases—a negative charge at the tetrahedral transition state of the treated peptide; this mimics the oxyanion hole action in serine proteases.

Metalloproteinases present an example of involvement of nonpolypeptide groups (here, Zn²⁺) in the protein action. We have seen such co-factors in some

of the already studied proteins: retinal in bacteriorhodopsin, chlorophylls, and other pigments in a photosynthetic reaction center, and so on. The co-factors are not substrates but rather instruments of a protein. These instruments greatly extend the variety of protein actions.

Thus, the same chemical reaction can be catalyzed by completely different proteins, and the same key role of a powerful electric cutter can be played by multicharged metal ions, or by environment-activated side chains (as in trypsin), or by organic co-factors that, like hemes or NAD⁺/NADH, accept and release electrons or protons.

On the other hand, as we remember, proteins similarly arranged as α/β -barrels or Rossmann folds can catalyze very different reactions. A classic example of proteins having the same origin and architecture but different functions is the pair lysozyme and α -lactalbumin. These proteins not only have identical, within 1–2 Å, 3D structures, but also display a quite high sequence identity (35%) ([Nitta and Sugai, 1989](#)). Nevertheless, one of them (lysozyme) is an enzyme (it cuts oligosaccharides), and the other (α -lactalbumin, which descended from lysozyme only \sim 100,000,000 years ago, when milk appeared) is not an enzyme at all: it has lost the lysozyme's active site, and now only modifies the enzymatic action of another protein.

The functional features of proteins are fixed by its enzyme classification, “EC” ([Enzyme Nomenclature, 1992](#)); the correlation between EC and protein structure classification (CATH; [Orengo et al., 1997](#)) is not very bright, that is, in outline, a certain biochemical function is not exclusively performed by proteins of a certain structural class. However, “large-scale” protein properties (which depend not on a small catalytic site but on a greater area of the protein surface), such as the capability of binding large ligands, partially correlate with overall protein architecture. Also, partial correlation is observed between the overall architecture of a protein and its involvement in biological processes ([Thornton et al., 1999](#)).

This is most vividly demonstrated by proteins responsible for transmembrane transport of any kind. Being membrane proteins, they have a most regular transmembrane α - or β -structure. We spoke about them in previous lectures.

The architecture-function correlation, although to a lesser extent, can also be traced in water-soluble globular proteins. For example, half of heme- and DNA-binding proteins are α -proteins, while the proportion of α -proteins among carbohydrate- and nucleotide-binding proteins is only 20%. On the other hand, almost all proteins controlling immunity and cell recognition are β -proteins. Nearly half the carbohydrate-binding proteins are also β -proteins, whereas their proportion among heme-, nucleotide-, and DNA-binding proteins only amounts to 10%. Almost all nucleotide-binding proteins belong to the α/β class. They include all 11 proteins of the glycolytic pathway. In general, α/β proteins often (more often than others) appear to be enzymes that are responsible for “cell housekeeping.” But all these preferences are not pronounced ([Thornton et al., 1999](#)).

All this demonstrates that, although the overall structure of a protein is rather independent of its catalytic activity, the architecture of the protein to a certain extent correlates with its “large-scale” substrate-binding activity, with its environment (“living conditions”) and with its involvement in certain biological processes.

So far I have said almost nothing about conformational changes in functioning protein molecules. I have done this on purpose, since, so far we have discussed catalysis of one isolated reaction (where substrate/product was the only mobile element). For catalysis of an isolated reaction, conformational changes in a protein can only worsen its catalytic properties. Indeed, efficient catalysis implies preferential binding of the transition state (which must be stronger than the binding of the initial and final states, although they differ from the transition state by as little as one Angström unit, 1 Å). Catalysis is aimed at either synthesis or disruption of rigid covalent bonds. Any attempt to disrupt the bonds using a “flexible” enzyme would be similar to an attempt to disrupt a wire using a piece of rubber or a pillow.

The following addition would not be out of place here. When the active site does not fit its function ideally (and ideal tuning must be a result of super-thorough natural selection), it may require a minor deformation to adopt the active state. Then this deformation is indeed functionally necessary because from time to time it brings the nonideal protein up to the mark. However, here the necessity (a deformation that compensates for the imperfect geometry of the active site) must be distinguished from virtue (protein perfection)!

Even the best possible protein undergoes deformation in the course of an elementary catalytic action (just because it is not as hard as a diamond), but, functionally, this may be compared with paper deformation under a pen: the less, the better.

Inner voice: So, the catalytic site of the enzyme needs no flexible parts at all?
Lecturer: Why, no. They are needless only if the enzyme must work very quickly (which is often, though wrongly, assumed to be its main purpose). In other cases, the catalytic center may contain such details, eg, in G-proteins ([Sprang, 1997](#); [Fersht, 1999](#)). But—what is the task of a G-protein? Its task is to cleave GTP, but—*very slowly!* The G-protein (we have already talked about it) is a timer. And for its *slow* work, the flexible catalytic center fits perfectly ... While “fast” catalysis needs a solid active center.

It is quite another matter when a protein must change one action for another; then its deformation providing the transition from one role to another is really of great functional importance. For example, in many proteins penetration of the substrate into the active site requires a slight displacement of site-adjacent side-groups (see eg, [Perutz, 1970](#)). But as soon as the substrate has occupied the site, the catalytic activity of this site does not require any further movement of the side-groups. It can be said that mobility is required in preparing the reaction,

while rigidity is necessary in its course. This reminds me of the Napoleon's strategic principle "marching separately, fighting together."

Sometimes the transition from one protein function to another is simply a result of substrate movement from one active site to another (recall aminoacyl-tRNAs synthases: there, the entire mobility is executed by the substrate). However, transition from one elementary function to another often occurs through more or less considerable deformation of the protein structure. The ability to deform in such a way is inherent in the construction of some protein molecules. This is what we are going to consider next.

When discussing protein dynamics and its role in protein functioning ([Frauenfelder, 2010](#)), we have to distinguish between small and large movements.

Actually, small movements are heat-induced fluctuations. Such fluctuations can be seen against the background of the averaged "static" protein structure using high resolution X-ray crystallography. The fluctuations are seen from difused X-ray patterns, whose fuzziness grows with temperature. Surface groups of a protein fluctuate with an average amplitude of about 0.5 Å ([Fersht, 1985, 1999](#)), while the fluctuation amplitude of core groups is a few times less. In loops amino acids fluctuate more strongly than in secondary structures. Side-groups fluctuate much more strongly than the main chain. The strongest fluctuations are typical of those long surface side-groups, whose ends are not fixed to other groups; fluctuations of these ends are so large that X-rays cannot locate these ends which is considered as a local "intrinsic disorder". That is why the protein interior is said to be solid, while its surface resembles a liquid and turns solid only at about –100°C. (I would like to note in parentheses that a semiliquid surface layer of molecules is generally typical of crystals; see, eg, [Ubbelohde, 1965](#); [Sazaki et al., 2012](#).)

The same conclusion on the combination of "solid" and "liquid" components in protein globule dynamics is supported by γ -resonance ("Mössbauer") spectroscopy ([Young et al., 2011](#)).

It follows from absorption of monochromatic γ -quanta by Mössbauer nuclei of some heavy metal isotopes (eg, ^{57}Fe) and allows us to estimate, specifically, the size of a solid part of the protein cemented to these nuclei.

Larger changes in protein structure occur during ligand binding. The relaxation dynamics of such structural deformations are best studied in myoglobin. A laser flash can instantly (within $\sim 10^{-13}$ s) tear the ligand (CO) off the myoglobin heme, and the relaxation towards the initial state can be followed by optical spectra.

The complex kinetics of such relaxation studied for a wide range of temperatures ([Young et al., 2011](#)) indicate that the native conformation can be achieved through a number of energetic barriers, and that the native conformation comprises a number of subconformations differing from one another in minor details.

Such, and even larger, deformations of proteins that accompany their functioning are studied by crystallizing proteins in various functional states. Also, much information can be obtained using various spectral techniques, chemical modifications, etc.

We know from the previous lecture about one functionally important deformation exemplified by regulation of DNA-binding activity of the trp-repressor. Let us consider functionally important deformations in more detail.

First of all, let us see how protein deformation helps to combine the steps of the cycle BIND → TRANSFORM → RELEASE. Fig. 25.4 illustrates *induced fit* (Koshland, 1994) of the phosphorylating protein, hexokinase, to its substrates.

This protein transfers the phosphate group from ATP to glucose. Judging from chemical principles only, this phosphate group might be alternatively transferred to water, but this never actually happens. In an attempt to understand the reasons, Koshland put forward the following postulates: (1) Prior to binding to the substrate, the enzyme is in the “open” form (in which it can take the substrate from water but cannot phosphorylate it). (2) After substrate binding, the enzyme adopts the “closed,” catalytically active form, with all parts of the active site brought together and capable of catalyzing the phosphorylation reaction, but in this form water is removed from the active site and so cannot compete with the substrate for phosphorylation. (3) After the act of catalysis, the enzyme opens again, and the phosphorylated substrate is released.

Later this hypothesis received complete experimental verification (Fig. 25.4) but *only* for proteins that need to screen the treated substrate from competing water molecules (although there were numerous attempts to extend the mechanism of induced fit to cover all enzymatic reactions). For example, trypsin has no such need. No induced fit for the substrate is observed here. Trypsin (as well as chymotrypsin, elastase, subtilisin, etc.) does not undergo deformations and recognizes the substrate using the simplest “key-lock” principle by Emil Fischer (1890).

I would like to draw your attention to the fact that, leaving aside the already discussed induced folding of natively disordered proteins, the induced fit results from *displacement* of either large blocks (discussed in the previous lecture) or whole protein domains (Fig. 25.4) but *not* from complete rearrangement of the

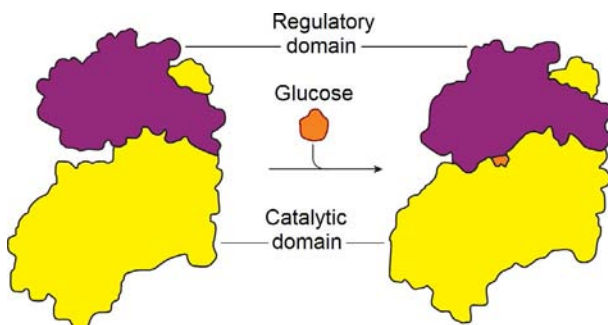


FIG. 25.4 Induced fit in hexokinase. In the open form, two domains are separated by a deep crevice, which the glucose can enter. When the glucose enters the crevice, the domains rotate, closing the crevice and expelling water from it, and all the active site components come together. (Adapted from Branden, C., Tooze, J., 1991. *Introduction to Protein Structure*, first ed. Garland, New York (Chapter 10).)

protein fold. In turn, the displacement is mostly a result of small local deformations. (Analogy: muscles contract (“local deformation”) and make fingers (“domains”) clench into a fist, but the fingers do not turn into teeth or tentacles.)

The same happens in all other cases of “conformational rearrangements in proteins,” except for rare cases when a whole α -helix or β -strand comes out from its place in the globule and adopts an irregular conformation. One of the greatest rearrangements that I know occurs in calmodulin. This protein is dumbbell-shaped, with α -domains as “heads” kept wide apart by a long α -helix playing the role of the “handle.” However, when calmodulin is binding to other proteins, the intact “heads” come together and stick to each other and to the target protein, while the former “handle” (a long α -helix) decays.

Protein domains are mobile not only in space but also in time, in the evolutionary process. As I have already mentioned, domain genes, as a whole, can wander from protein to protein, sometimes combined, sometimes detached. It often happens that in one organism there are several monomeric proteins, while in another they fuse into one multidomain protein.

The relative autonomy of domains is well demonstrated by a large family of proteins called dehydrogenases. These proteins catalyze OH-group oxidation and other similar reactions using co-factors NAD^+/NADH that easily accept and release separated protons. However, they deal with different substances: alcohol dehydrogenase treats alcohol (ethanol), lactate dehydrogenase treats lactate, and so on.

Dehydrogenases consist of two domains (Fig. 25.5) with a hinge between them. One domain is the substrate-binding module; it is structurally individual

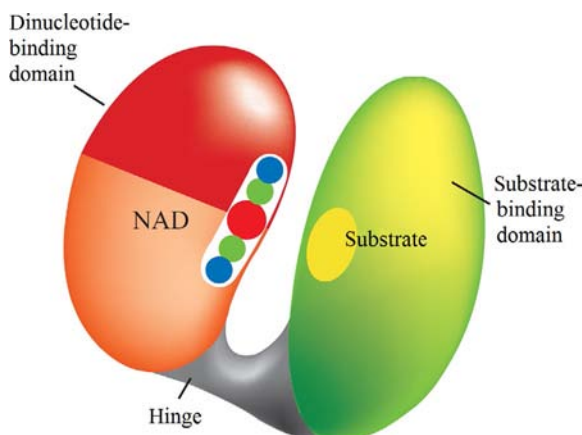


FIG. 25.5 Chains of NAD-dependent dehydrogenases are folded into two independent domains connected by a hinge. One domain is a universal NAD-binding domain; similar domains can be found in many different proteins. The other is a substrate-binding domain; it is individual for each dehydrogenase. (*Reproduced by permission of Branden, C., Tooze, J., 1991. Introduction to Protein Structure, first ed. Garland, New York (Chapter 10).*)

for each dehydrogenase. For example, that of alcohol dehydrogenase contains a β -cylinder, while this domain of glyceraldehyde-3-phosphate dehydrogenase contains a flat β -sheet.

In contrast, the other (NAD (nicotinamide adenine dinucleotide)-binding) domain is nearly the same for all NAD-dependent dehydrogenases, although in some of them it is located in the N-terminal half of the chain, while in others it is closer to the C-terminus, and despite the fact that the primary structures of NAD-binding domains display no notable homology. The chains of NAD-binding domains form the Rossmann fold (of the α/β class), and the structural similarity of these domains from different dehydrogenases is so close that many of them may be superimposed (including the NAD-binding sites) with an accuracy of 2 Å (presumably, this shows that the kinship is better remembered by the spatial structure than by the primary one).

Thus, the catalytic NAD-binding domain is a universal unit, while structurally different substrate-binding domains provide a variety of actions of dehydrogenases.

The active site of dehydrogenase results from the contact of its two halves located in these two domains ([Fig. 25.5](#)).

Now I am going to discuss the noncontact (also called *allosteric*) interaction between active sites. Allosteric interactions between various binding and active sites, specifically in oligomeric proteins, play a crucial role in the control and integration of biochemical reactions. A “signal” about the state of one active site is transmitted to another site by means of a deformation of the protein globule that affects the recipient site.

Let us consider (in a strongly simplified form) the best-studied allosteric protein, hemoglobin. This protein is a tetramer, or rather, a complex of two α -chains and two similar to them β -chains ([Fig. 25.6A](#)). Its task is to *bind* oxygen in lungs (where it is plentiful), to *transport* it to muscles (where it is scanty) and to *pass* it to muscle myoglobin, which is a monomer protein similar to any of the four subunits of hemoglobin. The active site of myoglobin and of each α and β subunit of hemoglobin is heme, ie, a ring-shaped co-factor with an iron ion that can bind one O_2 molecule ([Fig. 25.6B](#)).

The successful action of hemoglobin as an oxygen carrier is determined by allosteric (in this case, concerted) interaction of its four hemes.

In the heme, an iron ion is fixed by four coordinate bonds $N\text{-Fe}^{2+}$. It also participates in one more bond of this kind to the closest histidine of hemoglobin. This happens to be histidine of the α -helix F. And Fe^{2+} can form yet another coordinate bond to O_2 (or to CO—which would cause carbon monoxide poisoning).

Analysis of the static structures of both myo- and hemoglobin showed that an oxygen faces a difficulty when approaching a heme, unless there is a simultaneous heat fluctuation of the conformations of a few heme-shielding side-groups ([Perutz, 1970](#)).

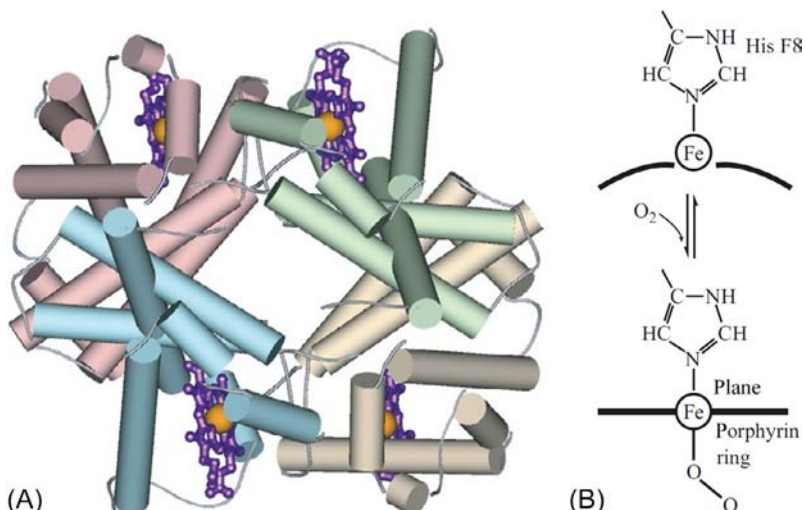


FIG. 25.6 (A) The hemoglobin molecule consists of two α - and two β -chains; each chain is colored differently; each chain forms many helices shown as cylinders and includes a heme shown as a violet wire model with an orange iron ion inside. (B) Scheme of oxygen binding to the hemoglobin's heme. Prior to binding O_2 , the iron ion (Fe^{2+}) is in a high-spin form with two outer electrons in different orbitals. This makes Fe^{2+} a bit too large to fit into the center of the heme's porphyrin ring, which is therefore somewhat bent. When O_2 is bound, the Fe^{2+} ion acquires the low-spin, more compact form, since the two outer electrons now have opposite spins and are in the same orbital. Now Fe^{2+} can enter the heme ring's center, and the ring acquires a flat form. The shown histidine of the α -helix F coordinates the iron ion. (B) Adapted from Stryer, L., 1995. Biochemistry, fourth ed. W.H. Freeman & Co., New York, with minor modifications.

When an oxygen approaches the heme and binds to its Fe^{2+} , the latter changes its spin form and, consequently, the electron envelope. Its diameter becomes a bit smaller, and it enters the center of the heme's porphyrin ring. Its slight displacement (by half an Angström, Å unit) causes a shift in the position of its coordinating histidine of the α -helix F.

This *electronic-conformational* interaction (implying a rapid change first in the electronic and then in the conformational state (Volkenstein, 1979; Rubin, 2000)) initiates a chain of conformational deformations in hemoglobin. The shift of histidine (through numerous small protein deformations) slightly changes the outline of the O_2 -bound subunit, and its contacts with three other subunits weaken. These subunits, still unbound to O_2 , begin to relax in their turn (obtaining the same outlines as a protein unaffected by interactions with neighbors and the same shifts of the inner atoms), so that their histidines begin to push the appropriate iron ions into the heme centers. Now oxygen binding to these irons is facilitated. As a result, one oxygen bound to hemoglobin provokes the binding of three more O_2 molecules; and, similarly, the loss of one oxygen provokes the loss of all others.

In parallel with oxygen binding and releasing, two more important reactions proceed in hemoglobin. These are also connected with allosteric conformational changes. When hemoglobin is in the O₂-free (“deoxy”) form, its subunits bind CO₂, mainly in a form of HCO₃⁻ (and using not the hemes but the N-termini of the chains) and H⁺ ions (using histidines of the C-terminal helices of subunits, which are close in space to their N-termini). When hemoglobin binds O₂ in lungs and changes to its “oxy” form, it loses these H⁺ (which is called the “Bohr effect”) and CO₂ molecules available to be breathed out.

It follows from the above that hemoglobin acts as a protein that binds several O₂ molecules *simultaneously*, and this is reflected by the nonlinear, S-shaped plot for the dependence of its (*tetrameric* protein) saturation with oxygen on the oxygen concentration (Fig. 25.7). As to myoglobin (*monomeric* protein), its O₂-saturation plot is free of the S-shaped sag.

Therefore, in the lungs where oxygen is plentiful, hemoglobin becomes oxygen-saturated. In tissues where the (venous) O₂ pressure is relatively low, the tetrameric hemoglobin *releases* O₂, while the monomeric myoglobin *still binds* it and passes it to the muscles (eg, to the muscles responsible for lung expansion and compression) to take part in oxidative reactions there.

In conclusion, I shall turn to *mechanochemical* functions of proteins.

To begin with, let's see how the protein kinesin works (I'll talk about one of its types, kinesin I). This dimeric protein transports mRNA, protein complexes,

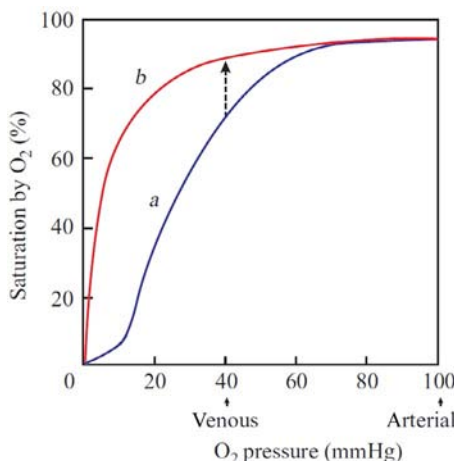


FIG. 25.7 Curves of oxygen saturation for tetrameric hemoglobin (a) and for monomeric myoglobin (b). The arterial pressure of oxygen corresponds to its binding in the lungs; the venous pressure corresponds to oxygen's passing from hemoglobin to myoglobin in muscles (which is shown by an arrow). The experimental curve of O₂-to-myoglobin binding corresponds to a first-order reaction. The experimental S-shaped curve of O₂-to-hemoglobin binding corresponds to a reaction of approximately the third-order (rather than to a fourth-order reaction, as indicated in the text for simplicity). (Adapted from Fersht, A., 1985. *Enzyme Structure and Mechanism*, second ed. W.H. Freeman, New York, with minor modifications.)

and so on, along the tubulin microtubules. By having digested one ATP molecule, it makes an 8 nm step from the “−” to “+” end of the microtubule; the whole working cycle of kinesin consists of two steps (Fig. 25.8).

Kinesin (as myosin, which we will consider afterwards) combines the “macroscopic” cycle of movements of its “heads” (actually serving as feet) with a “microscopic,” that is chemical, cycle of ATP cleavage.

During the “*microcycle*,” each of two heads (“motor domains”) of this dimeric protein can be (1) associated with ATP, (2) associated with ADP, or (3) remain “empty.”

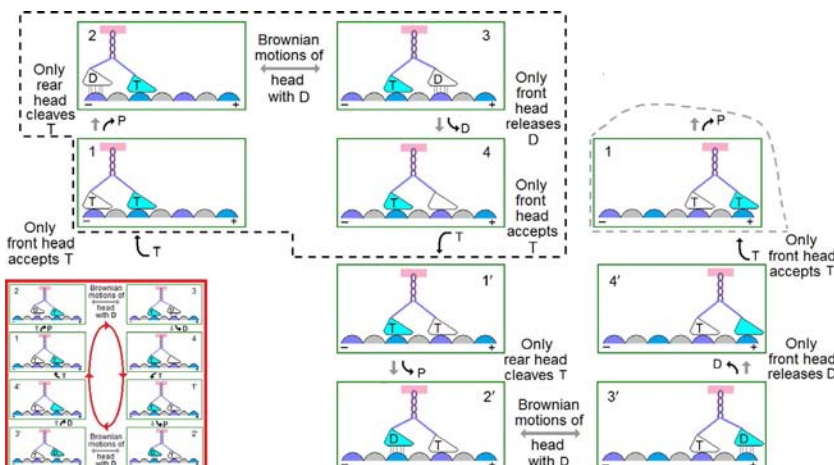


FIG. 25.8 Scheme of the movement of dimeric kinesin 1 along a tubulin microtubule (after Yildiz et al., 2008). The main figure shows the kinesin movement relative to the immobile microtubule. The insert (red frame in the bottom left corner) shows the same movement as a cycle: now the microtubule moves relative to kinesin. The tops of the tubulin globules (4 nm in diameter) are shown as hemispheres in the bottom of each panel. Rounded triangles (blue and white) show two heads of the dimeric kinesin; the double helix shows their common “neck.” The massive kinesin domains (responsible not for the movement but for cargo binding) and the cargo itself are shown only symbolically, as a very small (compared with their real size) pink rectangle above the neck. The thick lines show the “linkers” connecting the neck with the heads. Both kinesin heads are identical and attached to the microtubule in the same (relative to tubulin) orientation. The complete cycle of kinesin movement is shown. It consists of steps, each of which couples the “macrocycle” with the “microcycle.” Each gray arrow corresponds to one elementary “macrocycle” act of the kinesin head movement. Each black arrow corresponds to one elementary “microcycle” act of changing the state of the substrate ($T = \text{ATP}$, $D = \text{ADP}$, $P = \text{phosphate}$). Unidirectional arrows show the transitions that are virtually irreversible under existing intracellular concentrations of ATP, ADP, and phosphate. The easily reversible transition is shown by double arrows: this is diffusion of the head by $\approx 16 \text{ nm}$ (while the displacement of the kinesin neck is $\approx 8 \text{ nm}$). Heads with T and “empty” heads are strongly bound to the microtubule, heads with D are weakly bound to the microtubule (as shown by thin lines) and can detach from it. The “half-cycle” (states 1, 2, 3, and 4) that includes the movements and substrate exchanges made by one (white, in the figure) head is outlined in a black dashed line.

During the “*macrocycle*,” each kinesin head can have four positions. First, it can be either in the “rear” position (ie, behind the dimer’s “neck,” closer to the “–” end of the microtubule), or it can be in the “front” position (ie, before the dimer’s “neck,” closer to the “+” end of the microtubule). Second, in each of these two positions, the head can be either linked to the microtubule detached from it. The “rear” and “front” heads have slightly different conformations (because of different interactions with the linker differently positioned relatively to these heads), and therefore, they have different properties as regards to their interactions with ATP and ADP (Howard, 2000; Yildiz et al., 2008).

Note that a *directed cycle*, and hence, a *directed motion* is possible only when the number of states exceeds two (two states only allow oscillating back and forth).

Experimentally confirmed (Yildiz et al., 2008) conditions required for unidirectional movement of kinesin are: (1) ATP is accepted only by the head in “front” position; (2) ATP is cleaved only by the head in “rear” position; (3) ADP can be dissociated only by the head in “front” position; (4) the head with ADP loosely binds to tubulin (both when in the “rear” and “front” position), so that it can detach from tubulin; (5) the “empty” head and the head with ATP are strongly associated with tubulin and practically cannot be disconnected from it.

Thus, the kinesin dimer is constantly associated with the microtubule through at least its one head, while the other (when ADP-charged) can diffuse between the “rear” and “front” positions, but it can bind to the microtubule only when in the “front” position, where ADP can leave this head. Then this “front” head binds ATP, and cleavage of another ATP molecule (bound to another, the “rear” head, the only one capable of cleaving it) starts the new half-cycle; now this “rear” head is ready to make its move ... and so on

It is remarkable that the large-scale motion of kinesin (with all its cargo!) occurs through random Brownian motions between states 2 and 3, and it is directed only by the result of it (ie, by coming of the “Brownian ratchet” (Feynman et al., 1963) to state 3, where the kinesin head is in its “front” position): now the “pawl” is fixed, that is, ADP is released at the irreversible transition from state 3 to state 4.

Inner voice: Does mechanical motion require some kind of energy storage, like a system of elastic elements? You did not say a word about this!

Lecturer: The kinesin action is completely based on the Brownian motion and change of binding constants and catalytic properties of this molecule at different stages of the mechanochemical cycle shown in Fig. 25.8 and requires neither additional devices like elastic springs nor special “down-hill” transition pathways. The same is applicable to all other biological machines that I know (see Spirin and Finkelstein, 2011).

In this connection, it is not out of place mentioning that the “state $2 \leftrightarrow$ state 3” transition by diffusion is very fast: diffusion in water at a distance of ~ 10 nm takes ~ 1 μ s if kinesin with all its cargo is ~ 10 nm in diameter, and ~ 100 μ s if the diameter is as large as ~ 1 μ m (here I refer to results obtained at the end of [Lecture 8](#) and to Problems 8.8 and 24.2); this has to be compared with the kinesin working cycle that lasts much longer, ~ 1 s ([Yildiz et al., 2008](#)).

Now I will briefly describe the work of myosin, the protein which plays a key role in muscle contraction ([Fig. 25.9](#)).

We will consider the work of “myosin II,” working in the cross-striated muscles. Myosins of other types work essentially in the same way. Their work is similar to that of kinesin (and dynein, too), although with substantial variations in details.

The process of muscle contraction is satisfactorily described by the “swinging cross-bridge model.” It results from long-term studies by many groups and is based, specifically, on high-speed X-ray scattering from the contracting muscle, on electron microscopy of muscles, on X-ray crystallography of the myosin head in its different states, on neat single-molecular experiments, etc. ([Branden and Tooze, 1991, 1999; Howard, 2000; Rubin, 2000; Serdyuk et al., 2007](#)). These studies revealed the best part of the main stages of the muscle contraction process.

Like the kinesin head, the one of myosin couples the “macrocycle” with the “microcycle.”

In the “microcycle,” the myosin head can be (1) associated with ATP, or (2) associated with both ADP and phosphate, or (3) associated with ADP only, or (4) remain “empty.”

The free energy gained from ATP hydrolysis (15 kcal/mol at typical for muscles concentrations of ATP, $\sim 10^{-3}$ M, ADP, $\sim 10^{-5}$ M, and phosphate, $\sim 10^{-3}$ M) is spent on muscle contraction.

In the “macrocycle,” each myosin head can be either actin-bound (a+) or unbound (a-). In each of these states, the head can adopt either of two main conformations: the bent, or “45 degrees conformation” (R), and the straightened out (at 90 degrees about the myosin fiber), or “attacking” conformation (A). The R state has two substates: R', in which the cleft (connecting the catalytic to the actin binding site) is opened, and R'', where this cleft is closed ([Koubassova and Tsaturyan, 2011](#)). These states of the myosin head form a “macrocycle” ([Fig. 25.9E](#)): (R'', a+ \leftrightarrow R', a+) turns into (R'', a-), which turns into (A, a-), which turns into (A, a+), which turns into (R'', a+ \leftrightarrow R', a+), and so forth ([Howard, 2000; Koubassova and Tsaturyan, 2011](#)).

The coupling of “macrocycle” (conformational changes leading to the muscle contraction) and “microcycle” (ATP hydrolysis that supplies free-energy for

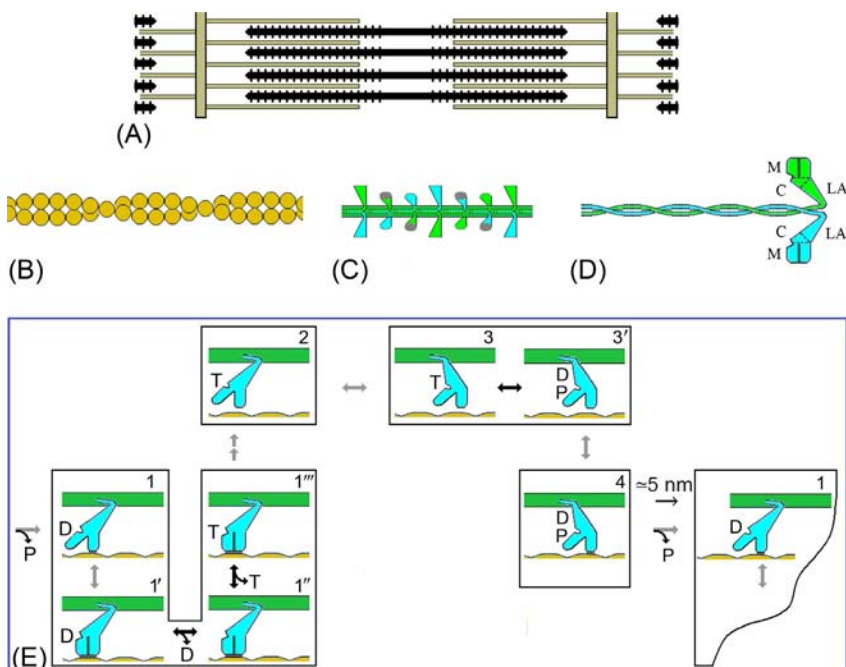


FIG. 25.9 (A) Scheme of the sarcomere, a structural unit of the muscle. Thick myosin filaments (with their heads sticking out) are placed between thin actin filaments attached to the sarcomere basal plates. The length of an actin filament is of about 1 μm . (B) Thin filament: a double-helix made of F-actin globules is shown; minor components of the filament (troponin, tropomyosin) are omitted. The actin polymerization needs ATP and Mg^{++} . Actin is able to bind myosin only at a sufficiently high concentration of calcium. (C) A thick filament made of myosin; one pair of the myosin heads is at a distance of 14.3 nm from another. (D) Schematic presentation of the myosin molecule consisting of two polypeptide chains. This molecule has two heads and a tail made of long double α -structural superhelix. The site of ATP (T) and ADP (D) binding is schematically shown as a small cleft in the myosin head comprising three domains (“motor,” M; “converter,” C; “lever arm,” LA). The myosin molecules form a single thread by sticking their tails together. (E) Mechanochemical cycle of the myosin head. The scheme shows the macroscopic states of myosin head and small ligands bound to it at each of the four main stages of this cycle. The myosin head is strongly bound to actin at stages 1', 1'', and 1''' (macroscopic state R' , a+) and 4 (A, a+), loosely at stages 4 (macroscopic state R'', a-) and 1 (macroscopic state R'' , a-), and not bound at stages 2 (macroscopic state R'', a-) and 3, 3' (macroscopic state A, a-). The head is bent at stages 1 (macroscopic state R'', a+), 1', 1'', 1''' (macroscopic state R', a+) and 2 (macroscopic state R'', a-), and straightened out at stages 3 (macroscopic state A, a-) and 4 (macroscopic state A, a+). At the transition from 1''' to 2 (ie, from R' to R'' conformation) the motor domain cleft opens, at the transition from 1 to 1' (ie, from R'' to R' conformation) the cleft closes. The cleft is always opened in the unbound (a-) head. The head changes its bend during the transition from stage 2 to stage 3 and from stage 4 to stage 1; in the latter case, the head is bound to actin, and therefore its bending is accompanied by a “power stroke” that shifts the myosin fiber along the actin fiber by ~ 5 nm. Transition to the next stage often consists of two subtransitions (this is depicted by a double arrow). The “macroscopic” subtransition is a change of either myosin conformation or its bridging to actin. The “microscopic” subtransition changes myosin binding to ATP or to the products of its hydrolysis (ADP and phosphate P). The order of these two elementary acts is not elucidated yet in many cases. For example, the loss of phosphate (P) can either precede or follow the “power stroke” during the transition from stage 4 to stage 1. The double-arrows: irreversible transitions; the single arrows: reversible transitions.

contraction) makes each “micro” step occur *only* at a certain “macro” state, with no unauthorized chemical reactions allowed.

The large-scale conformational changes coupled with alternation of the bound and unbound states lead to a kind of rowing action (which is a cycle: “oar behind in water—oar behind in air—oar in front in air—oar in front in water—oar behind in water—...,” cf. Fig. 25.9). This “rowing” moves the myosin filament along the actin filament like a boat being moved on water. This analogy should not take us too far, though. Usual rowing assumes continual pushing and pulling efforts. On the contrary, no stage of the myosin’s “microscopic rowing” assumes a continual effort. Each of them may occur by a Brownian motion that starts with a state with a higher free energy and ends with the state with a lower free energy.

Now it is necessary to get acquainted with another machine, F_1F_0 ATP synthase, which is very different from the “walking-machines” like kinesin and myosin. It is a rotary machine. Such machines, rotating one group of its subunits relative to another, are used to rotate the flagella or to synthesize ATP (Nelson and Cox, 2012).

F_0F_1 ATP synthase harnesses the free-energy from a proton gradient and thus uses the flux of ions across the membrane via the ATPase proton channel to drive the synthesis of ATP.

We shall consider the use of the proton flow to develop torque between the rotor and stator, but I have to say that if no proton gradient exists to drive ATP synthesis, F_0F_1 ATP synthase, which is a completely reversible machine, can perform the reverse reaction, ATP hydrolysis, to pump protons.

When the concentration of H^+ outside the cytoplasm is high, the motor is powered by free energy of the proton flow, which is passing through the rotor (subunit c_n , which is the H^+ turbine) and rotates it in the *counterclockwise* direction.

Inner voice: What prevents move in the opposite direction?

Lecturer: Look at Fig. 25.11, and specifically at its left-middle panel.

The c -subunit 2 is negatively charged (its H^+ escapes to the medium with a low H^+ concentration); the negative charge of the c -subunit 3 is neutralized with H^+ (which came from the H^+ -rich medium). Therefore, the turbine’s shift to the right (in the *counterclockwise* direction) is possible (it does not bring a net charge into the membrane), and the opposite shift that moves the net negative charge “ $-$ ” into the membrane (which is a medium of low permittivity) is forbidden. A series of directed shifts results in the directed rotation.

This direction is transmitted to the c_n -attached γ subunit, which is the eccentric shaft coming into the stator (see Fig. 25.10). This rotation of the shaft drives the operation of the chemical generator in the direction of ATP synthesis. The

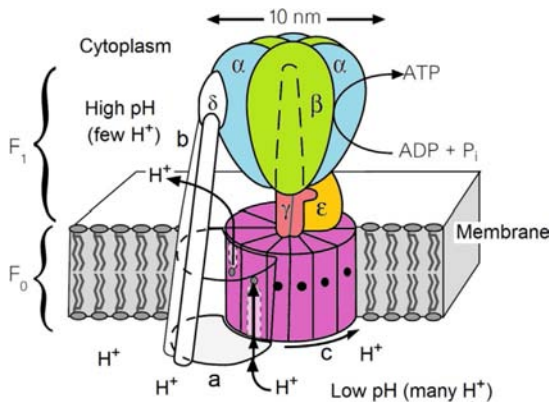


FIG. 25.10 General scheme of F_0F_1 ATP synthase (after Engelbrecht and Junge, 1997; Elston et al., 1998). The F_0F_1 ATP synthase consists of the cytoplasmic F_1 part (including three α , three β , γ , δ , and ϵ subunits) and the membrane F_0 part, which includes a monomeric subunit a , dimeric subunit b_2 , and n -meric subunit c_n (the number n is about 10–15 in different F_0F_1 ATP synthases). Subunits α , β , δ , a , b_2 form a “stator” (which is a chemical generator of ATP). The stator is fixed by the membrane. Subunits c_n , γ , and ϵ form a “rotor” (H^+ turbine) of F_0F_1 ATP synthase. The rotor rotates in the counterclockwise direction under the H^+ flow. Subunits with already X-ray-established structures are colored (after Junge et al., 2009). Cryo-electron microscopy images are available for the a subunit (consisting of membrane-spanning α -helices) and the b_2 subunit (Hakulinen et al., 2012). The proton channels lie at the interface between the a and c subunits. The dark spots are H^+ binding sites.

eccentric γ shaft, at some phase of rotation, allows bending of the β subunit (which thus forms an active site for the $ADP + P \leftrightarrow ATP$ reaction); at another phase of rotation, the eccentric γ shaft allows unbending of the β subunit and releases ATP (Oster and Wang, 1999). The H^+ turbine of the engine includes, in different F_0F_1 ATP synthases, a different number n of c subunits ($n = 10–15$, typically). Each c subunit carries one of H^+ and F_1 generator includes three β -subunits and thus ATPase active sites. Therefore, one complete rotation of the turbine transfers $n = 10–15$ of H^+ ions, for which price three ATP molecules are synthesized ($n/3 = 3–5$ of H^+ per ATP).

The ATP synthesis takes place when the proton gradient is high, so that synthesis of one ATP molecule can be paid by free-energy of transfer of these $n/3 = 3–5$ protons from the outer space to cytoplasm. In the opposite case, ATP hydrolysis pays for pumping of $n/3 = 3–5$ protons out of the cytoplasm.

X-ray analysis of the H^+ turbine (Pogoryelov et al., 2009; Preiss et al., 2010) has confirmed (see Fig. 25.12) the main items of schemes proposed by Elston et al. (1998) as early as in 1998 (see Figs. 25.10 and 25.11), together with the predicted location of the H^+ -binding site.

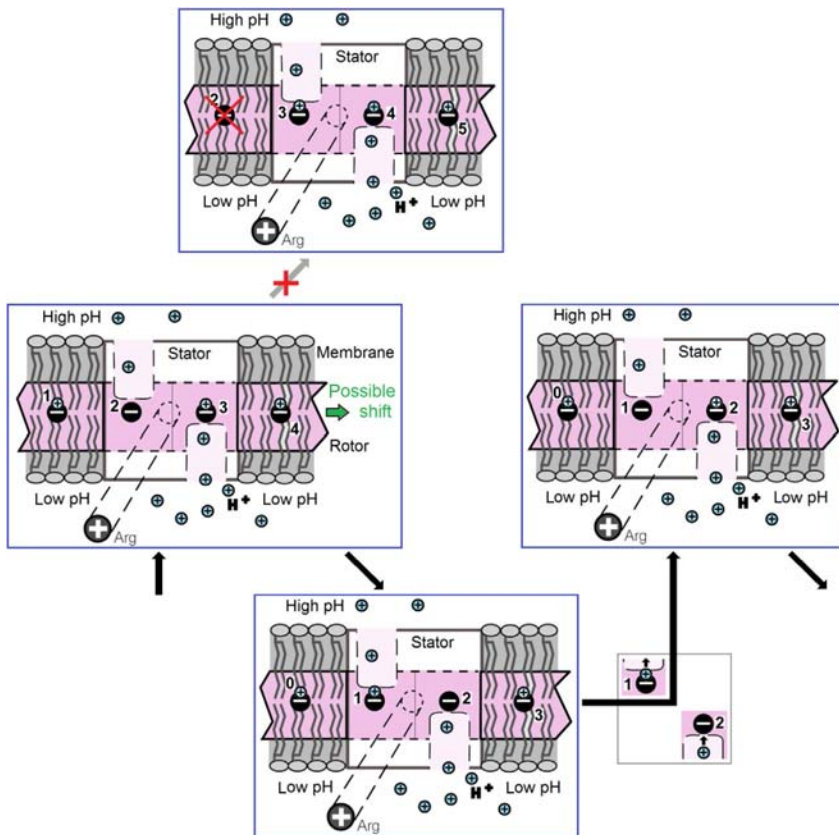


FIG. 25.11 Scheme of displacement of the H^+ turbine rotor by one c subunit (these subunits are colored pink and numbered). The left panel in the middle: the initial position. The negatively charged “–” site of the c subunit 3 is charged with H^+ through the “bottom” channel of the stator (more precisely, of its a subunit). This channel leads to the H^+ -rich outer space of low pH. The “–” site of the c subunit 2 is H^+ -free, as it is connected with the H^+ -poor cytoplasm by another (“upper”) stator’s channel (see Fig. 25.10). The “–” sites of the c subunits 1 and 4 are charged with H^+ and thus neutralized, so that the free-energy of their immersion into the membrane is low. H^+ cannot go directly from the site 3 to site 2, as the positively charged Arg prevents this. In principle, the Brownian motion of the rotor can move it either to the *right* (counterclockwise in Fig. 25.10) or *left*. However, the movement to the *left* is prohibited, as this brings (see upper panel) the naked “–” charge of site 2 into the membrane (medium with a low, relative to water, dielectric constant). The movement to the *right* is permitted, as this inserts into the membrane the electrically neutralized site 3 (see the bottom panel). Further, the site 2 is charged with H^+ from the outer space, and the site 1 loses its H^+ that goes to the cytoplasm (see the inset). This completes one step of the rotor displacement by one c subunit to the right (ie, counterclockwise in Fig. 25.10). (Reproduced from Elston, T., Wang, H., Oster, G., 1998. Energy transduction in ATP synthase. *Nature* 391, 510–513, with permission from Nature Publishing Group.)

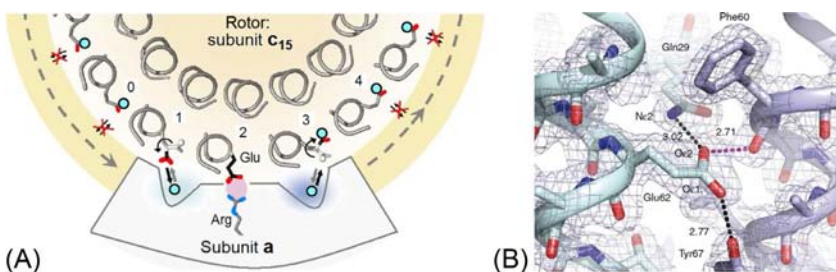


FIG. 25.12 (A) Scheme of the H⁺ turbine rotation according to the X-ray data. View along the axes of helices. Subunit a is depicted schematically, because its X-ray analysis has not yet been made. It is already known, however, that this subunit is a four-helix bundle (Hakulinen et al., 2012). (B) Ion binding site in the proton-locked conformation, with the electron density map contours. View perpendicular to the axes of helices. *Dashed lines* indicate the hydrogen bonding network around key Glu62 side chain. The position of the bound proton is in the middle of the *purple-colored dotted line* between Oe2 of Glu62 and the main chain carbonyl of Phe60. Distances are shown in Ångströms (Å). (The figures are adapted from the X-ray paper by Pogoryelov, D., Yıldız, Ö., Faraldo-Gómez, J.D., Meier, T., 2009. High-resolution structure of the rotor ring of a proton-dependent ATP synthase. *Nat. Struct. Mol. Biol.* 16, 1068–1073, with minor modifications, with permission from Nature Publishing Group.)

As a result of the work of the above-described protein machines, F₁F₀ ATP-synthase produces ATP, which is spent when kinesin walks along the microtubule or myosin walks along actin; then muscles contract, lungs pump the air, oxygen binds to hemoglobin and is handed over—via myoglobin—to muscles and other organs, and this is how we move, breathe, and live.

REFERENCES

- Branden, C., Tooze, J., 1991. Introduction to Protein Structure, first ed. Garland, New York (Chapter 10).
- Branden, C., Tooze, J., 1999. Introduction to Protein Structure, second ed. Garland Publ., Inc., New York (Chapters 8, 10, 11, 15).
- Elston, T., Wang, H., Oster, G., 1998. Energy transduction in ATP synthase. *Nature* 391, 510–513.
- Engelbrecht, S., Junge, W., 1997. ATP synthase: a tentative structural model. *FEBS Lett.* 414, 485–491.
- Enzyme Nomenclature, 1992. Academic Press, San Diego, CA. Available from <http://www.chem.qmul.ac.uk/iubmb/enzyme/index.html> and <http://www.chem.qmul.ac.uk/iubmb/enzyme/rules.html>.
- Fersht, A., 1985. Enzyme Structure and Mechanism, second ed. W.H. Freeman, New York (Chapters 1, 3, 7, 8, 10, 12).
- Fersht, A., 1999. Structure and Mechanism in Protein Science: A Guide to Enzyme Catalysis and Protein Folding. W. H. Freeman, New York (Chapters 1, 7, 10, 12, 13, 15, 16).
- Feynman, R., Leighton, R., Sands, M., 1963. The Feynman Lectures on Physics. Addison-Wesley Publishing Company, Inc., Reading, MA, vol. 1, (Chapter 46).
- Finkelstein, A.V., 1989. Is it possible to graft a new active site to the protein molecule? Biopolym. Cell 5, 89–93 (in Russian).

- Fischer, E., 1890. Über die optischen Isomeren des Traubenzuckers, der Gluconsäure und der Zuckersäure. *Ber. Dtsch. Chem. Ges.* 23, 2611–2624 (in German).
- Frauenfelder, H., 2010. *The Physics of Proteins. An Introduction to Biological Physics and Molecular Biophysics*. Springer, New York (Chapters 11–15).
- Hakulinen, J.K., Klyszejko, A.L., Hoffmann, J., et al., 2012. Structural study on the architecture of the bacterial ATP synthase F0 motor. *Proc. Natl. Acad. Sci. U. S. A.* 109, E2050–E2056. Available from: http://www.ncbi.nlm.nih.gov/pmc/articles/PMC3409797/bin/supp_109_30_E2050_index.html.
- Howard, J., 2000. *Mechanics of Motor Proteins and the Cytoskeleton*. Sinauer Associates, Sunderland, MA (Part III, Chapters 12–16).
- Junge, W., Sielaff, H., Engelbrecht, S., 2009. Torque generation and elastic power transmission in the rotary F0F1-ATPase. *Nature* 459, 364–370.
- Koshland Jr., D.E., 1994. The key-lock theory and the induced fit theory. *Angew. Chem. Int. Ed.* 33, 2375–2378.
- Koubassova, N.A., Tsaturyan, A.K., 2011. Molecular mechanism of actin-myosin motor in muscle. *Biochemistry (Mosc)* 76, 1484–1506.
- Nelson, D.L., Cox, M.M., 2012. *Lehninger Principles of Biochemistry*, sixth ed. W.H. Freeman, New York (Chapter 19).
- Nitta, K., Sugai, S., 1989. The evolution of lysozyme and alpha-lactalbumin. *Eur. J. Biochem.* 182, 111–118.
- Orengo, C.A., Michie, A.D., Jones, S., et al., 1997. CATH—a hierachic classification of protein domain structures. *Structure* 5, 1093–1108.
- Oster, G., Wang, H., 1999. ATP synthase: two motors, two fuels. *Structure* 7, R67–R72.
- Perutz, M.F., 1970. Stereochemistry of cooperative effects in haemoglobin. *Nature* 228, 726–734.
- Pogoryelov, D., Yildiz, Ö., Faraldo-Gómez, J.D., Meier, T., 2009. High-resolution structure of the rotor ring of a proton-dependent ATP synthase. *Nat. Struct. Mol. Biol.* 16, 1068–1073.
- Preiss, L., Yildiz, Ö., Hicks, D.B., Krulwich, T.A., Meier, T., 2010. A new type of proton coordination in an F0F1-ATP synthase rotor ring. *PLoS Biol.* 8.
- Rawlings, N.D., Barrett, A.J., 1995. Evolutionary families of metallopeptidases. *Methods Enzymol.* 248, 183–228.
- Rubin, A.B., 2000. *Biophysics* (in Russian), vol. 2. Publ. House ‘Universitet’, Moscow (Chapter XXV).
- Sasaki, G., Zepeda, S., Nakatsubo, S., et al., 2012. Quasi-liquid layers on ice crystal surfaces are made up of two different phases. *Proc. Natl. Acad. Sci. U. S. A.* 109, 1052–1055.
- Serdyuk, I.N., Zaccai, N.R., Zaccai, J., 2007. *Methods in Molecular Biophysics: Structure, Dynamics, Function*. Cambridge University Press, Cambridge (Chapter D6).
- Spirin, A.S., Finkelstein, A.V., 2011. The ribosome as a Brownian ratchet machine. In: Frank, J. (Ed.), In: *Molecular Machines in Biology*, Cambridge University Press, Cambridge, pp. 158–190.
- Sprang, S.R., 1997. G protein mechanisms: insights from structural analysis. *Annu. Rev. Biochem.* 66, 639–678.
- Thornton, J.M., Orengo, C.A., Todd, A.E., Pearl, F.M., 1999. Protein folds, functions and evolution. *J. Mol. Biol.* 293, 333–342.
- Ubbelohde, A.R., 1965. *Melting and Crystal Structure*. Clarendon Press, Oxford (Chapters 2, 11, 12, 14).
- Volkenstein, M.V., 1979. Electronic-conformational interactions in biopolymers. *Pure Appl. Chem.* 51, 801–829.
- Yildiz, A., Tomishige, M., Gennerich, A., Vale, R.D., 2008. Intramolecular strain coordinates kinesin stepping behavior along microtubules. *Cell* 134, 1030–1041.
- Young, R.D., Frauenfelder, H., Fenimore, P.W., 2011. Mössbauer effect in proteins. *Phys. Rev. Lett.* 107, 158102.

Appendices

Appendix A

Theory of Globule-Coil Transitions in Homopolymers

Here we will consider the simplest but fundamental model of the globule-coil transition in a homopolymer chain (Grosberg and Khokhlov 1994; Lifshitz et al. 1978). In this model many (N) equal monomers are connected by the chain, like beads. And we will compare it with the “cloud of monomers,” that is, with an aggregate of the same N monomers *unconnected* by the chain: this is the simplest model, used since van der Waals’ time (in the 19th century) to describe the gas–liquid transition (Fig. A.1). We will see that the polymer has no analog of separation into “liquid” and “gas” phases typical of the “cloud.”

Preliminary remark. I will assume that the monomers are attracted together (otherwise, it’s too dull: no dense phase will form, and that’s all), and that the strength of this attraction is temperature-independent, that is, that it is purely energetic in nature. The latter is often incorrect, since the monomers are floating in the solvent (recall the hydrophobic effect: it increases with temperature); but this allows us to find and consider all the basic scenarios of phase transitions in the simplest way. And later we can complicate the problem by adding the temperature dependence of the interactions and show at what temperature each of these scenarios can take place.

To begin with, I should like to give you the general idea and to explain in words why the “cloud” can have two phases and the polymer cannot, that is, why the polymer has to condense gradually. Then the same will be more rigorously shown in formulas.

What is the difference between the life of a monomer in the polymer and in the cloud? In the polymer it cannot go far away from its chain neighbor, while in the cloud it can go as far from any other monomer as the walls of the vessel permit.

Why do monomers form a dense phase, either liquid (if they are not connected by the chain) or globule (if otherwise)? Because they attract each other, and at low temperature, the attraction energy overcomes any tendency for the monomers to scatter and gain entropy: at low temperature, the role of entropy is small (recall: in the free energy $F = E - TS$ the energy E is compared with the entropy *multiplied* by the temperature). Overcomes always *but for* one case: when scattering leads to a virtually infinitely large entropy gain, that is, when the cloud of monomers is placed in a vast vessel. And just here the monomers have to choose between two

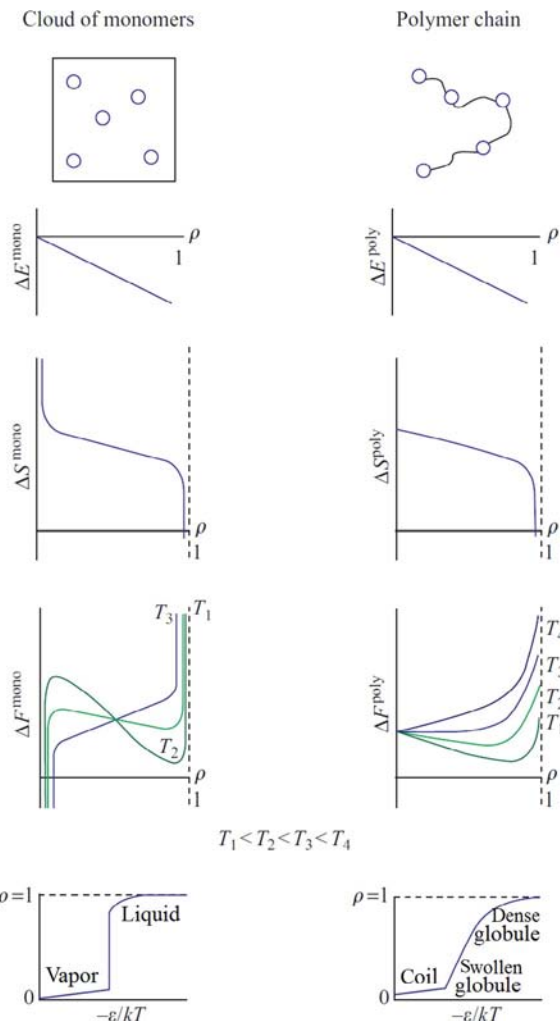


FIG. A.1 Schematic dependence of the monomer's energy ΔE , entropy ΔS , and free energy $\Delta F = \Delta E - T\Delta S$ on the density ρ for two systems: "cloud of monomers" and "polymer chain." The dependence of ΔF on ρ is shown for various temperatures T . A scheme of dependence of the density ρ on the monomer attraction energy (expressed in kT units) is shown in the auxiliary plot for each system (at the bottom). The plots refer to attracting monomers ($\varepsilon < 0$) and to a low (and constant) pressure: at very high, "supercritical" pressure the loose (with $\rho < 0.5$) states are absent.

phases: either to form a drop (low energy *but* low entropy as well) or to stay in a rarefied gas (negligible energy *but* a very high entropy).

The states of intermediate density (eg, of 10% or 50% of that of the drop) have a higher free energy (their entropy is not as large while their energy is not as low) and therefore are unstable. Thus, the stable state of the "cloud" at low

temperature can be either dense, or very rarefied, but not of an intermediate density. In other words, the “cloud” of monomers can exhibit an abrupt evaporation of the dense phase when the temperature rises.

This is what happens in the “cloud.” And what about the polymer? Here the situation is quite *different*, because a monomer cannot go far away from its chain neighbor even in the most diffuse coil. This means that the coil entropy cannot exceed a certain limit, and thus the entropy is not able (at low temperatures) to compete with the energy gained by compaction of the polymer. Thus, the polymer has no alternative: at low temperature its monomers cannot scatter, and it has to be a dense globule only, which means that (unlike the “cloud”) it cannot jump from the dense to the rare phase. Therefore, a change of conditions can cause only a gradual swelling (or compression) of the polymer globule rather than its abrupt “evaporation.”

Now, let us repeat the above in the language of equations.

Let us compare a “cloud” of N monomers confined within the volume V with a polymer of the same N monomers in the same volume V . Assuming that the monomers (of both the cloud and the polymer) are distributed over the volume more or less uniformly, let us add one monomer to each system and estimate the dependence of the free energy of the added monomer (ie, the *chemical potential* of the system) on the system’s density.

The chemical potential is appropriate for analysis of the co-existence of phases. The point is that the molecules pass from a phase with a higher chemical potential to a phase of a lower chemical potential: this decreases the total free energy, tending towards equilibrium. At equilibrium, the chemical potentials of molecules in both phases are equal. This means that an abrupt transition of one phase into another is possible only when *the same* chemical potential value refers to both phases, to both densities. On the contrary, if the chemical potential only increases (or only decreases) with increasing/decreasing density of the system, an abrupt phase transition is impossible.

It should be noted that phase stability requires an increasing chemical potential with increasing density of the system. Then penetration of each new particle to this phase is more and more difficult. This is the stable state: like a spring, the system increasingly resists the increasing impact. In the opposite case (if the chemical potential drops with increasing density), the system is unstable and does not resist occasional fluctuations that increase its density.

To summarize: the particular state of a system is determined by particular external conditions (ie, by the given volume or the given pressure), but the prerequisite for a possibility of a phase transition is the presence of two ascending (with density) branches of chemical potential values, and these two branches must have approximately equal chemical potential values, that is, they must be separated by a region where the chemical potential grows with increasing density of the system.

In exploring the chemical potential value, let us first consider the energy of the added monomer, or rather, that part of the energy which depends on the system’s density, that is, on the interactions of non-covalently bound monomers.

In both cases, the energy of the system (“cloud” or “polymer”) having the same density changes by the same value when a monomer is added. The change occurs because of the monomer’s interactions and is equal to

$$\Delta E = \epsilon\rho, \quad (\text{A.1})$$

where $\rho = N\omega/V$ is the system’s density, that is, the fraction of its volume V occupied by the N monomers having the volume ω each, and ϵ is the energy of interactions of this monomer at $\rho=1$, that is, in the most dense system ($\epsilon < 0$, since we have assumed that monomers are attracted together).

Thus, the added monomer’s energy behaves alike in both systems; but the added monomer’s entropy behaves very differently in the polymer as compared with the “cloud.”

The “cloud” leaves the volume V/N at the monomer’s disposal. However, since the volume $N\omega$ is already occupied by the monomers, the free volume at the monomer’s disposal in the “cloud” is

$$V_1^{\text{mono}} = (V - N\omega)/N = (V/N)(1 - \rho) = (\omega/\rho)(1 - \rho). \quad (\text{A.2})$$

Notice that this volume is infinitely large when the density ρ turns to zero. At the same time, the free volume at the monomer’s disposal in the polymer is

$$V_1^{\text{poly}} = W(1 - \rho); \quad (\text{A.3})$$

here, the volume Ω is limited by the monomer’s binding to the previous chain link, and the multiplier $(1 - \rho)$ shows, as above, that other monomers occupy the fraction ρ of the volume.

Then, the entropy change resulting from addition of a monomer to the “cloud” is

$$\Delta S^{\text{mono}} = k \ln [V_1^{\text{mono}}] = k \ln [(\omega/\rho)((1 - \rho))] \quad (\text{A.4})$$

while the entropy change resulting from addition of a monomer to the polymer is

$$\Delta S^{\text{poly}} = k \ln [V_1^{\text{poly}}] = k \ln [\Omega(1 - \rho)]. \quad (\text{A.5})$$

As the functions of the density ρ , ΔS^{mono} and ΔS^{poly} behave alike (see Fig. A.1) only as $\rho \rightarrow 1$ (where the term $\ln(1 - \rho)$ dominates in ΔS , so that both ΔS^{mono} and ΔS^{poly} decrease as $\rho \rightarrow 1$), but their behavior is *completely different* as $\rho \rightarrow 0$: ΔS^{poly} remains finite, while ΔS^{mono} grows infinitely because of the term ω/ρ .

Thus (see Fig. A.1), at low temperatures T , the chemical potential $\Delta F = \Delta E - T\Delta S$ of the “cloud” has two ascending branches, that is, two potentially stable regions divided by the first-order phase transition (rarefied gas at a low ρ , owing to the $-T\Delta S$ term, and liquid at a high ρ , owing to the ΔE term). And at high temperatures the “cloud” has only one ascending branch of ΔF value, that is, only one stable state (gas, owing to the $-T\Delta S$ term).

At the same time, the polymer entropy *does not* grow infinitely even as $\rho \rightarrow 0$, and here only *one* ascending branch of the ΔF value exists at all temperatures. At extremely low temperatures, or rather, at high $-\varepsilon/kT$ values, the origin of this branch corresponds to $\rho \approx 1$, that is, to a dense globular state. The temperature increase (or rather, the decrease in the $-\varepsilon/kT$ value) shifts the origin of the ascending branch towards lower densities ρ , and finally, the origin comes to the value $\rho = 0$ and stays there permanently (Fig. A.1). As you see, the chemical potential of the globule never has two ascending branches.

This means that the globule's expansion does not include a phase separation. And, since there is no phase separation, there is no first-order phase transition. It can be shown (this has been done by Lifshitz et al. 1978 and de Gennes 1979) that the *second*-order globule-to-coil phase transition occurs at $\rho \approx 0$ (or rather, at the coil state density $\rho \sim N^{-1/2}$), but this is beyond the scope of these lectures.

REFERENCES

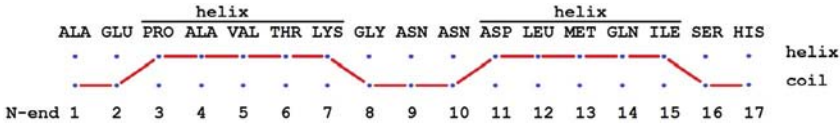
- de Gennes, P.-G., 1979. Scaling Concepts in Polymer Physics. Part A. Ithaka, London: Cornell University Press.
- Grosberg, A.Yu., Khokhlov, A.R., 1994. Statistical Physics of Macromolecules. NY: American Institute of Physics (Chapters 1, 2, 3, 7).
- Lifshitz, I.M., Grosberg, A. Yu., Khokhlov, A.R., 1978. Some problems of the statistical physics of polymer chains with volume interactions. Rev. Mod. Phys. 50, 683–713.

Appendix B

Theory of Helix-Coil Transitions in Homopolymers

Here we will consider the simplest but fundamental model of the helix-coil transition in a homopolymer chain.

Each monomer of this chain can be in one of two states: either “coil” or “helix.” A scheme



presents one of possible arrangements of helices in a short polypeptide chain as a path through a set of states.

The free energy of the coil of any length is zero by definition, and thus its statistical weight is 1. At the same time, the free energy of n -link helix formation from the coil is

$$\Delta F_\alpha = f_{\text{init}} + n \cdot f_{\text{el}}; \quad (\text{B.1})$$

the statistical weight of this helix is

$$\exp(-\Delta F_\alpha/kT) = \exp(-f_{\text{init}}/kT) \cdot [\exp(-f_{\text{el}}/kT)]^n = \sigma s^n. \quad (\text{B.2})$$

(here, we used designations $\sigma = \exp(-f_{\text{init}}/kT)$ and $s = \exp(-f_{\text{el}}/kT)$).

Strictly speaking, it should be $n \geq 3$ for α -helices (with their hydrogen bonds of the type 0–4, 1–5, etc.), but, given that α -helices are usually rather long, we, for simplicity, consider helices with all $n \geq 1$ (Schultz and Schirmer, 1979; Zimm and Bragg, 1959); for the more general case assuming that the minimal length of the helix may differ from 1, see Birstein and Ptitsyn (1966) and Flory (1969).

Calculation of the average helicity at given σ and s values is based on the Kramers–Wannier (1941) solution of the one-dimensional Ising (1925) problem.

We introduce two-component vectors $\vec{\mathbf{Q}}_i = (C_i, H_i)$, where C_i is the partition function of the chain of i links, the last of which is in the “coil” (c) state,

and H_i is the partition function of the chain, the last link of which is in the “helix” (h) state. In particular,

$$\vec{\mathbf{Q}}_1 = (1, \sigma s), \quad (\text{B.3})$$

$$\vec{\mathbf{Q}}_2 = (1 + \sigma s, \sigma s + \sigma s^2), \text{ etc}; \quad (\text{B.3a})$$

The value $Z_i = (C_i, H_i) \begin{pmatrix} 1 \\ 1 \end{pmatrix} \equiv C_i + H_i$ is the partition function of all 2^i conformation of the chain of i links.

It is easy to see that vectors $\vec{\mathbf{Q}}_{i-1}$ and $\vec{\mathbf{Q}}_i$ (with $i > 1$) are connected by a recursion

$$(C_{i-1}, H_{i-1}) \begin{pmatrix} 1 & \sigma s \\ 1 & s \end{pmatrix} = (C_i, H_i). \quad (\text{B.4})$$

Thus, the partition function of all 2^m possible conformations of the chain of m links is

$$Z_m = (1, \sigma s) \begin{pmatrix} 1 & \sigma s \\ 1 & s \end{pmatrix}^{m-1} \begin{pmatrix} 1 \\ 1 \end{pmatrix} \quad (\text{B.5})$$

To calculate this partition function for any m , we have to find eigenvalues λ_1, λ_2 of the matrix $\mathbf{U} = \begin{pmatrix} 1 & \sigma s \\ 1 & s \end{pmatrix}$. To do this, we use a well-known equation:

$$\text{Det} \begin{pmatrix} 1 - \lambda & \sigma s \\ 1 & s - \lambda \end{pmatrix} \equiv (1 - \lambda)(s - \lambda) - \sigma s = 0 \quad (\text{B.6})$$

and obtain

$$\begin{aligned} \lambda_1 &= 1 + \frac{s-1}{2} + \sqrt{\left(\frac{s-1}{2}\right)^2 + \sigma s}; \\ \lambda_2 &= 1 + \frac{s-1}{2} - \sqrt{\left(\frac{s-1}{2}\right)^2 + \sigma s}. \end{aligned} \quad (\text{B.7})$$

Then we calculate the matrix \mathbf{U} eigenvectors $\vec{\mathbf{A}}_1, \vec{\mathbf{A}}_2$ corresponding to the eigenvalues λ_1, λ_2 . The eigenvectors, which have an arbitrary length, can be taken in a form $\vec{\mathbf{A}}_1 = \begin{pmatrix} A_1 \\ 1 \end{pmatrix}, \vec{\mathbf{A}}_2 = \begin{pmatrix} A_2 \\ 1 \end{pmatrix}$. They are found from well-known equations $\begin{pmatrix} 1 - \lambda_k & \sigma s \\ 1 & s - \lambda_k \end{pmatrix} \begin{pmatrix} A_k \\ 1 \end{pmatrix} = 0$ (for $k = 1, 2$), that is, from

$$1 \cdot A_k + (s - \lambda_k) \cdot 1 = 0 \quad (\text{for } k = 1, 2). \quad \text{Thus, we obtain } \begin{pmatrix} A_1 \\ 1 \end{pmatrix} = \begin{pmatrix} \lambda_1 - s \\ 1 \end{pmatrix} \equiv \begin{pmatrix} 1 - \lambda_2 \\ 1 \end{pmatrix} \text{ and } \begin{pmatrix} A_2 \\ 1 \end{pmatrix} = \begin{pmatrix} \lambda_2 - s \\ 1 \end{pmatrix} \equiv \begin{pmatrix} 1 - \lambda_1 \\ 1 \end{pmatrix}.$$

The eigenvectors \vec{A}_1, \vec{A}_2 form a matrix $A = \begin{pmatrix} 1-\lambda_2 & 1-\lambda_1 \\ 1 & 1 \end{pmatrix}$, which can diagonalize the matrix U by transformation $A^{-1}UA = \begin{pmatrix} \lambda_1 & 0 \\ 0 & \lambda_2 \end{pmatrix}$; here, $A^{-1} = \frac{1}{\lambda_1 - \lambda_2} \begin{pmatrix} 1 & -1+\lambda_1 \\ 1 & 1-\lambda_2 \end{pmatrix}$. Now we can take the matrix U in a form $U = A \begin{pmatrix} \lambda_1 & 0 \\ 0 & \lambda_2 \end{pmatrix} A^{-1}$; since $U^2 = A \begin{pmatrix} \lambda_1 & 0 \\ 0 & \lambda_2 \end{pmatrix} A^{-1} A \begin{pmatrix} \lambda_1 & 0 \\ 0 & \lambda_2 \end{pmatrix}$, $A^{-1} = A \begin{pmatrix} \lambda_1 & 0 \\ 0 & \lambda_2 \end{pmatrix}^2 A^{-1}, \dots, U^n = A \begin{pmatrix} \lambda_1 & 0 \\ 0 & \lambda_2 \end{pmatrix}^n A^{-1}, \dots$, we have

$$\begin{aligned} Z_m &= (1, \sigma s) \begin{pmatrix} 1 & \sigma s \\ 1 & s \end{pmatrix}^{m-1} \begin{pmatrix} 1 \\ 1 \end{pmatrix} = (1, \sigma s) A \begin{pmatrix} \lambda_1 & 0 \\ 0 & \lambda_2 \end{pmatrix}^{m-1} A^{-1} \begin{pmatrix} 1 \\ 1 \end{pmatrix} \\ &= (1 - \lambda_2 + \sigma s, 1 - \lambda_1 + \sigma s) \begin{pmatrix} \lambda_1^{m-1} & 0 \\ 0 & \lambda_2^{m-1} \end{pmatrix} \frac{1}{\lambda_1 - \lambda_2} \begin{pmatrix} \lambda_1 \\ -\lambda_2 \end{pmatrix} \\ &= \frac{1}{\lambda_1 - \lambda_2} (\lambda_1^{m+1}(1 - \lambda_2) + \lambda_2^{m+1}(\lambda_1 - 1)). \end{aligned} \quad (\text{B.8})$$

(here we used the fact that $\sigma s = (\lambda_1 - 1)(1 - \lambda_2)$). It is seen that the magnitude of Z_m increases as $\sim \lambda_1^{m+1}$ (provided $\lambda_2 < \lambda_1$) when $m \rightarrow \infty$.

Since the partition function Z_m consists of summands which include the multiplier s as many times as many links in the helical state correspond to this summand, the value

$$\theta_m = \frac{1}{m} \cdot \frac{s}{Z_m} \cdot \frac{\partial Z_m}{\partial s} \equiv \frac{1}{m} \cdot \frac{\partial \ln Z_m}{\partial \ln s}, \quad (\text{B.9})$$

is the average degree of chain helicity is concerned.

It is easy to calculate that

$$\theta_m = \frac{\lambda_1 - 1}{\lambda_1 - \lambda_2} \cdot \frac{1 + \left(\frac{\lambda_2}{\lambda_1}\right)^{m+1} - \frac{2}{m} \cdot \frac{\lambda_2}{\lambda_1 - \lambda_2} \left[1 - \left(\frac{\lambda_2}{\lambda_1}\right)^m\right]}{1 + \frac{\lambda_1 - 1}{1 - \lambda_2} \left(\frac{\lambda_2}{\lambda_1}\right)^{m+1}}. \quad (\text{B.10})$$

When $(\lambda_2/\lambda_1)^m \ll 1$, then, for a sufficiently long chain, θ_m depends on the number m of the chain links as

$$\theta_{m \gg 1} \approx \frac{\lambda_1 - 1}{\lambda_1 - \lambda_2} \left(1 - \frac{2}{m} \cdot \frac{\lambda_2}{\lambda_1 - \lambda_2}\right) \quad (\text{B.11})$$

$$\left(\text{in particular, } \theta_{m \rightarrow \infty} = \frac{\lambda_1 - 1}{\lambda_1 - \lambda_2} = \frac{1}{2} \left[1 + \frac{s-1}{\sqrt{(s-1)^2 + 4\sigma s}}\right] \right).$$

For $s=1$ and $\sigma \ll 1$, we obtain

$$\theta_{m \gg 1} \approx \frac{1}{2} \left(1 - \frac{2}{m\sqrt{\sigma}} \right). \quad (\text{B.12})$$

This formula allows us to find the value of σ from the dependence of θ_m on m .

Finally, we can find the average number of helical regions in a very long chain. Since $Z_{m \gg 1} \approx (\lambda_1)^m$ and the partition function Z_m consists of summands which include the multiplier σ as many times as many helical (as well as coil!) regions correspond to this summand, the mean number of helical (and coil!) regions in a very long chain is

$$N_m = m \frac{\partial \ln \lambda_1}{\partial \ln \sigma} = \frac{m \cdot 2\sigma s}{(s+1) \sqrt{(s-1)^2 + 4\sigma s + (s-1)^2 + 4\sigma s}}. \quad (\text{B.13})$$

Therefore, with $s=1$, we obtain

$$\frac{N_m(s=1)}{m} = \frac{\sqrt{\sigma}}{2(1+\sqrt{\sigma})}, \quad (\text{B.14})$$

Consequently, with $s=1$, a helical (and a coil) region includes $\frac{1}{\sqrt{\sigma}} + 1$ chain links on the average.

REFERENCES

- Birshtein, T.M., Ptitsyn, O.B., 1996. Conformations of Macromolecules. NY: Interscience Publishers (Chapters 4, 9).
- Flory, P.J., 1969. Statistical Mechanics of Chain Molecules. NY: Interscience Publishers (Chapters 3, 7).
- Ising, E., 1925. Beitrag zur Theorie des Ferromagnetismus. Zeitschr. Phys. 31, 253–258.
- Kramers, H.A., Wannier, G.H., 1941. Statistics of the two-dimensional ferromagnet. Part I. Phys. Rev. 60, 252–262.
- Schulz, G.E., Schirmer, R.H., 1979 & 2013. Principles of Protein Structure. Appendix. NY: Springer.
- Zimm, B.H., Bragg, J.K., 1959. Theory of phase transition between helix and random coil in polypeptide chains. J. Chem. Phys. 31, 526–535.

Appendix C

Statistical Physics of One-Dimensional Systems and Dynamic Programming

STATISTICAL PHYSICS OF ONE-DIMENSIONAL SYSTEMS: EQUILIBRIUM DISTRIBUTION

Appendix B considered the helix-coil transition. The calculations were made for a homopolymer, and we were interested in the average degree of its helicity and some other average characteristics of the whole chain.

Now we shall consider a mathematical apparatus that can calculate the average degree of helicity for *any* link of a *heteropolymer* (Finkelstein, 1977) with an arbitrary sequence, and then generalize the results (Aho et al., 1979; Angel and Bellman, 1972; Finkelstein and Roytberg, 1993) to solve a variety of problems in statistical physics of inhomogeneous one-dimensional systems.

Among these, we will touch on the problem of searching for a structure corresponding to the minimum energy of the chain (which is called the “dynamic programming problem”).

Let us consider the helix-coil transition. Then, each link i of the chain can take only two conformations (later, we will get rid of this “only two” limitation): $q_i = q^{(1)}$ or $q_i = q^{(2)}$, where $q^{(1)}$ is “coil” and $q^{(2)}$ is “helix.”

It is easy to see that in the helix-coil transition problem, the energy of the given conformation q_1, \dots, q_m of an m -link chain has the form

$$E(q_1, \dots, q_m) = \sum_{i=1}^m \Phi_i(q_i) + \sum_{i=2}^m \Psi_i(q_{i-1}, q_i) \equiv \Phi_1(q_1) + \sum_{i=2}^m [\Psi_i(q_{i-1}, q_i) + \Phi_i(q_i)] \quad (\text{C.1})$$

where

$$\begin{aligned} \Phi_i(q^{(1)}) &\equiv 0, \\ \Phi_i(q^{(2)}) &= (f_{\text{init}})_i + (\cdot f_{\text{el}})_i, \end{aligned}$$

while

$$\begin{aligned}\Psi_i(q^{(1)}, q^{(1)}) &\equiv 0, \\ \Psi_i(q^{(1)}, q^{(2)}) &\equiv 0, \\ \Psi_i(q^{(2)}, q^{(1)}) &\equiv 0, \\ \Psi_i(q^{(2)}, q^{(2)}) &= -(f_{\text{init}})_I.\end{aligned}$$

One can see that the values $\Phi_1(q_1)$ form an array

$$\Phi_1(q_1 = q^{(1)}) = 0 \quad \Phi_1(q_1 = q^{(2)}) = (f_{\text{init}})_1 + (f_{\text{el}})_1$$

whose components correspond to logarithms of components of the vector $(1, \sigma s)$, and the values $\Psi_i(q_{i-1}, q_i) + \Phi_i(q_i)$ form an array

$$\begin{aligned}\Psi_i(q^{(1)}, q^{(1)}) + \Phi_i(q^{(1)}) &= 0 \quad \Psi_i(q^{(1)}, q^{(2)}) + \Phi_i(q^{(2)}) = (f_{\text{init}})_i + (f_{\text{el}})_i \\ \Psi_i(q^{(2)}, q^{(1)}) + \Phi_i(q^{(1)}) &= 0 \quad \Psi_i(q^{(2)}, q^{(2)}) + \Phi_i(q^{(2)}) = (f_{\text{el}})_i\end{aligned}$$

whose components correspond to logarithms of the components of matrix $\begin{pmatrix} 1 & \sigma s \\ 1 & s \end{pmatrix}$ (provided we used the same designations as in Appendix B: $\sigma = \exp(-f_{\text{init}}/kT)$ and $s = \exp(-f_{\text{el}}/kT)$).

In the homopolymer problem that has been considered in Appendix B, the values f_{init} and f_{el} (and therefore, σ and s) were the same for all units, but in a more general heteropolymer problem both $(f_{\text{init}})_i$ and $(f_{\text{el}})_i$ depend on the link i (on its chemical type and, probably, on the chemical type of surrounding links, as well).

The partition of the whole m -link chain is

$$\begin{aligned}Z_m &= \sum_{q_1} \dots \sum_{q_m} \exp[-E(q_1, \dots, q_m)/kT] \\ &\equiv \sum_{q_1} \dots \sum_{q_m} \exp[-\Phi_1(q_1)/kT] \cdot \prod_{i=2}^m \exp[-(\Psi_i(q_{i-1}, q_i) + \Phi_i(q_i))/kT]\end{aligned}\tag{C.2}$$

It consists of 2^m terms, but can be computed not only by their sequential addition (which would take time proportional to 2^m); it can be computed recurrently, in time proportional to m :

$$Z_m = (1, \sigma_1 s_1) \prod_{i=2}^m \begin{pmatrix} 1 & \sigma_i s_i \\ 1 & s_i \end{pmatrix} \begin{pmatrix} 1 \\ 1 \end{pmatrix};$$

here, $\sigma_i = \exp(-(f_{\text{init}})_i/kT)$ and $s_i = \exp(-(f_{\text{el}})_i/kT)$.

To make this computation efficiently, one can use two-component vectors $\vec{\mathbf{Q}}_i = [Q_i^{(1)}, Q_i^{(2)}]$ ($i=1, \dots, m$), where the value $Q_i^{(1)}$ is the partition function of the chain embracing links $1-i$, the link i being in the state $q^{(1)}$ = "coil", and $Q_i^{(2)}$ is the partition function of the same chain, the link i being in the state $q^{(2)}$ = "helix". Thus,

$$\vec{\mathbf{Q}}_1 = \left(\exp \left[-\Phi_1(q_1^{(1)})/kT \right], \exp \left[-\Phi_1(q_1^{(2)})/kT \right] \right), \quad (\text{C.3})$$

while vectors $\vec{\mathbf{Q}}_{i-1}$ and $\vec{\mathbf{Q}}_i$ ($1 < i \leq m$) are connected recursively:

$$\begin{aligned} Q_i^{(1)} &= \sum_q Q_{i-1}^{(q)} \cdot \exp \left[-(\Psi_i(q, q^{(1)}) + \Phi_i(q^{(1)})) / kT \right], \\ Q_i^{(2)} &= \sum_q Q_{i-1}^{(q)} \cdot \exp \left[-(\Psi_i(q, q^{(2)}) + \Phi_i(q^{(2)})) / kT \right], \end{aligned}, \quad (\text{C.4})$$

so that

$$Z_m = \sum_q Q_m^{(q)}. \quad (\text{C.5})$$

Now, one can introduce two-component vectors $\vec{\mathbf{R}}_i = [R_i^{(1)}, R_i^{(2)}]$ ($i=m, \dots, 1$). Here

$$\vec{\mathbf{R}}_m = (1, 1), \quad (\text{C.6})$$

while vectors $\vec{\mathbf{R}}_{m-1}, \dots, \vec{\mathbf{R}}_1$ are computed recursively:

$$\begin{aligned} R_{i-1}^{(1)} &= \sum_q \exp \left[-(\Psi_i(q^{(1)}, q) + \Phi_i(q)) / kT \right] \cdot R_i^{(q)}, \\ R_{i-1}^{(2)} &= \sum_q \exp \left[-(\Psi_i(q^{(2)}, q) + \Phi_i(q)) / kT \right] \cdot R_i^{(q)}, \end{aligned}, \quad (\text{C.7})$$

One can see that the value $Q_i^{(q)} \cdot R_i^{(q)}$ is statistical weight of the sum of all terms of the partition function Z_m , where a link i ($i=1, \dots, m$) is in the conformation q ($q=q^{(1)}, q^{(2)}$), so that the value

$$w_i(q_i) = Q_i^{(q)} \cdot R_i^{(q)} / Z_m \quad (\text{C.8})$$

is a probability to find, in the state of thermodynamic equilibrium, the link i in the conformation q .

The above formulas concern the simplest case, when each link i of the chain can take only two conformations, $q_i = q^{(1)}$ or $q_i = q^{(2)}$.

However, it is easy to generalize them to the case when each link can take k_i conformations, or states ($q_i = \{q^{(1)}, \dots, q^{(k_i)}\}$; k_i can be different for different links) (Finkelstein, 1977; Finkelstein and Roytberg, 1993). For example, in the "floating logs" model presented in Fig. 22.10, we used (Ptitsyn and Finkelstein, 1983) the following nine states:

Coil (loop)	β -strand side chain “down”	β -strand side chain “up”	α -helix N -end	α -helix side chain “down”	α -helix side chain “to right”	α -helix side chain “up”	α -helix side chain “to center”	α -helix C -end
$q^{(1)} = l$	$q^{(2)} = \beta\downarrow$	$q^{(3)} = \beta\uparrow$	$q^{(4)} = \alpha^N$	$q^{(5)} = \alpha\downarrow$	$q^{(6)} = \alpha\rightarrow$	$q^{(7)} = \alpha\uparrow$	$q^{(8)} = \alpha\leftarrow$	$q^{(9)} = \alpha^C$

A matrix for possible (+) and forbidden (0) transitions between these states looks as follows:

		$q_i^{(k)}$								
		l	$\beta\downarrow$	$\beta\uparrow$	α^N	$\alpha\downarrow$	$\alpha\rightarrow$	$\alpha\uparrow$	$\alpha\leftarrow$	α^C
$q_{i-1}^{(k)}$	l	+	+	+	+	0	0	0	0	0
	$\beta\downarrow$	+	0	+	+	0	0	0	0	0
	$\beta\uparrow$	+	+	0	+	0	0	0	0	0
	α^N	0	0	0	0	+	+	+	+	0
	$\alpha\downarrow$	0	0	0	0	0	+	0	0	+
	$\alpha\rightarrow$	0	0	0	0	0	0	+	0	+
	$\alpha\uparrow$	0	0	0	0	0	0	0	+	+
	$\alpha\leftarrow$	0	0	0	0	+	0	0	0	+
	α^C	+	+	+	0	0	0	0	0	0

I will allow myself not to present sequence-dependent values corresponding to various possible (+) transitions...

The above set of states (and transitions between them) looks rater complicated, but much more (hundreds!) states were used in the program “ALB” (Finkelstein, 1983) to describe various secondary structures, including antiparallel and parallel β -hairpins and β -sheets composed of such hairpins.

Vectors \vec{Q}_i , \vec{R}_i ($i=1, \dots, m$) have k_i components;

$$\vec{Q}_1 = \left(\exp \left[-\Phi_1(q_1^{(1)}) / kT \right], \dots, \exp \left[-\Phi_1(q_1^{(k_1)}) / kT \right] \right), \quad (\text{C.3a})$$

and components of vectors \vec{Q}_i ($i=2, \dots, m$) are recursively computed as

$$Q_i^{(q_i^{(k)})} = \sum_{q_{i-1}} Q_{i-1}^{(q_{i-1})} \cdot \exp \left[-\left(\Psi_i(q_{i-1}, q_i^{(k)}) + \Phi_i(q_i^{(k)}) \right) / kT \right] \quad (\text{C.4a})$$

(where $q_i^{(k)} = q_i^{(1)}, \dots, q_i^{(k_i)}$, $q_{i-1} = q_{i-1}^{(1)}, \dots, q_{i-1}^{(k_{i-1})}$), while

$$\vec{R}_m = (1, \dots, 1), \quad (\text{C.6a})$$

and components of vectors $\vec{\mathbf{R}}_{i-1}$ ($i = m, \dots, 2$) are recursively computed as

$$R_{i-1}^{(q_{i-1}^{(k)})} = \sum_{q_i} \exp \left[-\left(\Psi_i(q_{i-1}^{(k)}, q_i) + \Phi_i(q_i) \right) / kT \right] \cdot R_i^{(q_i)} \quad (\text{C.7a})$$

(where $q_{i-1}^{(k)} = q_{i-1}^{(1)}, \dots, q_{i-1}^{(k_{i-1})}$, $q_i = q_i^{(1)}, \dots, q_i^{(k_i)}$).

DYNAMIC PROGRAMMING: SEARCH FOR THE ENERGY MINIMUM

Let us now turn to the problem of finding the structure of the chain corresponding to the minimum of its energy, that is, the problem of *dynamic programming* (Aho et al., 1979; Angel and Bellman, 1972; Bellman, 2003).

The minimum of the chain energy is defined as:

$$E_{\min} = \min_{q_1} \dots \min_{q_m} \left[\Phi_1(q_1) + \sum_{i=2}^m (\Psi_i(q_{i-1}, q_i) + \Phi_i(q_i)) \right] \quad (\text{C.9})$$

It can also be computed without exhaustive enumeration of all 2^m compared (standing in []) terms, that is, recurrently, in time proportional to m .

To do this, one, as above, has to introduce k_i -component vectors $\vec{\mathbf{Q}}_i$, $\vec{\mathbf{R}}_i$ ($i = 1, \dots, m$; $q_i = \{q^{(1)}, \dots, q^{(k_i)}\}$; k_i , can be different for different links) (Bellman, 2003; Finkelstein and Roytberg, 1993). Here

$$\vec{\mathbf{Q}}_1 = \left(\Phi_1(q_1^{(1)}), \dots, \Phi_1(q_1^{(k_1)}) \right), \quad (\text{C.10})$$

and components of vectors $\vec{\mathbf{Q}}_i$ ($i = 2, \dots, m$) are recursively computed as

$$Q_i^{(q_i^{(k)})} = \min_{q_{i-1}} \left[Q_{i-1}^{(q_{i-1}^{(k)})} + \Psi_i(q_{i-1}, q_i^{(k)}) + \Phi_i(q_i^{(k)}) \right] \quad (\text{C.11})$$

(where $q_i^{(k)} = q_i^{(1)}, \dots, q_i^{(k)}$, $q_{i-1} = q_{i-1}^{(1)}, \dots, q_{i-1}^{(k_{i-1})}$). At each ($i = 2, \dots, m$) iteration step, one remembers an auxiliary “control” vector (Bellman, 2003)

$$\vec{\mathbf{R}}_i = \left(R_i(q_i^{(1)}), \dots, R_i(q_i^{(k_i)}) \right), \quad (\text{C.12})$$

where $R_i(q_i^{(k)}) = q_{i-1}^{\text{opt}K}$ is that q_{i-1} coordinate (or one—actually, arbitrary taken, see below—of those q_{i-1} coordinates), which minimizes $Q_i(q_i^{(k)})$ in (C.11).

As a result of iterations (C.11), one obtains the energy minimum

$$E_{\min} = \min_{q_m} \{Q_m(q_m)\} \quad (\text{C.13})$$

and the coordinate $q_m^{\text{opt}K}$ that corresponds to that q_m , which minimizes (C.13).

Now, having $q_m^{\text{opt}K}$ and the remembered set of support vectors $\vec{\mathbf{R}}_m, \vec{\mathbf{R}}_{m-1}, \dots, \vec{\mathbf{R}}_2$, one can find out the whole optimal (corresponding to the energy minimum E_{\min}) chain conformation $C^{\text{opt}} = \{q_1^{\text{opt}}, \dots, q_m^{\text{opt}}\}$:

$$q_m^{\text{opt}} = q_m^{\text{opt}K}; q_{m-1}^{\text{opt}} = R_m(q_m^{\text{opt}}), \dots, q_1^{\text{opt}} = R_2(q_2^{\text{opt}}). \quad (\text{C.14})$$

Note. There may be not one but several optimal (corresponding to the same E_{\min}) conformations of the chain. Then the choice of some of $R_i(q_i^{(k)}) = q_{i-1}^{\text{opt}K}$ and/or $q_m^{\text{opt}K}$ is ambiguous: the above described Bellman (2003) algorithm “randomly” finds *only one* of these conformations. This usually meets the engineering requirements but appears insufficient for natural science problems. Generalizations of Bellman dynamic programming algorithm to this case can be found in (Byers and Waterman, 1984; Finkelstein and Roytberg, 1993).

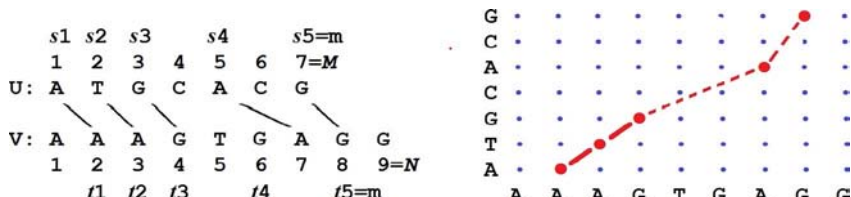
It can be seen that the algorithm for solving the problems of one-dimensional systems in statistical physics corresponds to the dynamic programming with replacements:

Statistical physics	Dynamic programming
Values $\exp(-\Phi_i/kT)$	Values Φ_i
Values $\exp[-\Psi_i/kT]$	values Ψ_i
Operations “summarize”	Operations “minimize”
Operations “multiply”	Operations “summarize”

For other generalizations of the dynamic programming method suitable for solving various problems, see Finkelstein and Roytberg (1993).

DYNAMIC PROGRAMMING AND SEARCH FOR OPTIMAL ALIGNMENT OF SEQUENCES

In molecular biology, the dynamic programming method is most often used when searching for homology of amino acid or nucleotide sequences (Needleman and Wunsch, 1970; Smith and Waterman, 1981). One compares two sequences: $U = a_1, a_2, \dots, a_M$ and $V = b_1, b_2, \dots, b_N$, where a_s and b_t are amino acid residues (or nucleotides). An alignment of sequences means the following: in the first pair of the alignment a_{s1} is set in correspondence with b_{t1} ; in the second pair a_{s2} is set in correspondence with b_{t2} , ..., in the last pair of the alignment a_{sM} is set in correspondence with b_{tM} (where $1 \leq s1 < s2 < \dots < sm \leq M$ and $1 \leq t1 < t2 < \dots < tm \leq N$). Two presentations of some alignment are shown here:



Correspondence of links a and b has a “weight” $\Phi(a,b)$. Transition from the correspondence a_s, b_t to the next correspondence $a_{s'}, b_{t'}$ has its weight $\Psi(s' - s, t' - t)$; usually, this weight has a form

$$\begin{aligned}\Psi(s' - s, t' - t) = & \Delta \cdot \theta(s' - s) + \sum_{J=s+1}^{s'-1} D(a_J) \\ & + \Delta \cdot q(t' - t) + \sum_{J=t+1}^{t'-1} D(b_J),\end{aligned}\quad (\text{C.15})$$

where $\theta(d) = 0$ at $d = 1$, $\theta(d) = 1$ at $d > 1$ ($d \leq 0$ is not possible, because $s < s'$ and $t < t'$, see above), and D is the weight of deleting the corresponding link from the alignment. The weight W of alignment $(a_{s1}, b_{t1}; a_{s2}, b_{t2}; \dots; a_{sm}, b_{tm})$ is the sum of weights of all correspondences and transitions in this alignment:

$$\begin{aligned}W(a_{s1}, b_{t1}; a_{s2}, b_{t2}; \dots; a_{sm}, b_{tm}) = & \Phi(a_{s1}, b_{t1}) \\ & + \sum_{i=2}^m [\Psi_i(s_i - s_{i-1}, t_i - t_{i-1}) + \Phi_i(a_{si}, b_{ti})].\end{aligned}\quad (\text{C.16})$$

The best alignment is the one that has the maximal weight W .

For maximization of W one can use the above given formalism of dynamic programming with replacement of q_i for correspondence (s_i, t_i) and formulas (C.11), (C.13) for formulas

$$Q(s', t') = -\min_{1 \leq i < t', 1 \leq j < s'} \{0, [Q(s, t) + \Psi(s' - s, t' - t)]\} + \Phi(s', t'), \quad (\text{C.11a})$$

$$W_{\min} = -\min_{1 \leq s \leq M, 1 \leq t \leq N} \{Q(s, t)\} \quad (\text{C.13a})$$

Working time of this algorithm is proportional to $(M \cdot N)^2$. A more complicated but faster working version of such an algorithm (its working time is proportional to $M \cdot N$) one can find in Smith and Waterman (1981). Without going into details, we note only that this fast algorithm uses not only the values $Q(s, t)$, corresponding to the best alignment of fragments $1 - s$ and $1 - t$ of U and V , but also auxiliary values $Q_U(s, t)$, $Q_V(s, t)$, $Q_{UV}(s, t)$. $Q_U(s, t)$ corresponds to the best alignment of fragments $1 - s$ and $1 - t' < t$ (links $t' + 1 - t$ being deleted from the alignment); $Q_V(s, t)$ corresponds to the best alignment of fragments $1 - s' < s$ and $1 - t$ (links $s' + 1 - s$ being deleted); $Q_{UV}(s, t)$ corresponds to the best alignment of fragments $1 - s' < s$ and $1 - t' < t$ (links $s' + 1 - s$ and $t' + 1 - t$ being deleted from the alignment).

REFERENCES

- Aho A., Hopcroft J., Ullman, J., 1976. The Design and Analysis of Computer Algorithms. Reading, MA: Addison-Wesley.
- Angel, E., Bellman, R., 1972. Dynamic Programming of a Partial Differential Equation. NY: Academic Press (Chapter 3).
- Bellman, R., 2003. Dynamic Programming. Mineola, NY: Dover Publications Inc (Chapters 1–3, 11).

- Birshtein, T.M., Ptitsyn, O.B., 1966. Conformations of Macromolecules. NY: Interscience Publishers (Chapters 4, 9).
- Byers, T., Waterman, M.S., 1984. Determining all optimal and near optimal solutions when solving shortest path problems by dynamic programming. Oper. Res. 32, 1381–1384.
- Finkelstein, A.V., 1977. Theory of protein molecule self-organisation. III. A calculating method for the probabilities of the secondary structure formation in an unfolded protein chain. Biopolymers 16, 525–529.
- Finkelstein, A.V., 1983. Program ALB for polypeptide and protein secondary structure calculation and prediction. Submitted to Brookhaven Protein Data Bank, Upton, NY, USA, and to EMBL Database, Heidelberg, FRG.
- Finkelstein, A.V., Roytberg, M.A., 1993. Computation of biopolymers: A general approach to different problems. BioSystems 30, 1–19.
- Needleman, S.B., Wunsch, C.D., 1970. A general method applicable to the search for similarities in the amino acid sequence of two proteins. J. Mol. Biol. 48, 443–453.
- Ptitsyn, O.B., Finkelstein, A.V., 1983. Theory of protein secondary structure and algorithm of its prediction. Biopolymers 22, 15–25.
- Smith, T.F., Waterman, M.S., 1981. Identification of common molecular subsequences. J. Mol. Biol. 147, 195–197.

Appendix D

Random Energy Model and Energy Gap in the Random Energy Model

In the theoretical physics studies of proteins, a so-called Random Energy Model, or simply REM is widely used. It describes statistical properties of energy spectra of complex systems in the simplest form. This model has been originally proposed by Derrida (1980, 1981) for the “disordered” physical systems such as spin glasses, and it was introduced to the physics of proteins by Bryngelson and Wolynes (1987, 1990). Its applicability to proteins was justified by Shakhnovich and Gutin (1989).

According to this model, the energy of one heteropolymer fold is statistically independent of that of another.

This assumption looks strange, but Shakhnovich and Gutin (1989) showed that it is valid for a dense globule, where transition from one chain fold to another requires so much altered intra-chain contacts, provided a variety of chemical units (chain monomers) is large.

The energy of each fold of a heteropolymer is determined by the primary structure of its chain and the system of contacts between the chain links. According to the random energy model, each chain fold i (which belongs to $M \gg 1$ of the possible globular folds) takes the energy E with a probability

$$P_i(E) = (2\pi\sigma_i^2)^{-1/2} \times \exp \left[-(E - \varepsilon_i)^2 / 2\sigma_i^2 \right], \quad (\text{D.1})$$

where ε_i is the average (over all primary structures) energy of the fold i , and σ_i is the average (over all primary structures) deviation of E from ε_i . In the simplest version of the random energy model it is assumed that all $\varepsilon_i = 0$ and all $\sigma_i = \sigma$ (ie, they are equal).

As a result, the expected density of the energy spectrum is:

$$w(E) = \sum_{i=1}^M P_i(E) = \frac{M}{\sqrt{2\pi\sigma^2}} \exp \left(-\frac{E^2}{2\sigma^2} \right). \quad (\text{D.2})$$

In this model, one can determine the energy E_C , typical of the lower edge of the energy spectrum, and the temperature T_C , characteristic of this edge.

$p_{E'} = \int_{-\infty}^{E'} P(E) dE$ is the “accumulated” probability that the energy E of one fold is below the level E' . The probability that the energies of all M folds lie above E' is $(1 - p_{E'})^M$. If $p_{E'} \ll 1$ (after all, we are interested in the lower edge of the spectrum), then $(1 - p_{E'})^M \approx \exp[-Mp_{E'}]$. Hence, when $-Mp_{E'} = \ln(\frac{1}{2})$, the chance that all chain folds simultaneously have energies greater than E' is $\frac{1}{2}$. Thus, the characteristic value of E_C can be found from the condition $p_{E_C} = (\ln 2)/M$. The value p_{E_C} is very small when $M \gg 1$. Therefore,

$$\begin{aligned} p_{E_C} &\equiv \int_{-\infty}^{E_C} P(E) dE = \int_{-\infty}^{E_C} (2\pi\sigma^2)^{-1/2} \exp[-E^2/2\sigma^2] dE \\ &= \int_{-\infty}^{E_C} (2\pi\sigma^2)^{-1/2} \exp\left\{-[(E - E_C) + E_C]^2/2\sigma^2\right\} dE \\ &= (2\pi\sigma^2)^{-1/2} \int_{-\infty}^0 \exp\left[-(x + E_C)^2/2\sigma^2\right] dx \\ &= (2\pi\sigma^2)^{-1/2} \exp[-E_C^2/2\sigma^2] \\ &\quad \int_{-\infty}^0 \exp[x(-E_C)/\sigma^2 - x^2/2\sigma^2] dx \end{aligned}$$

(where $x = E - E_C$). It is obvious that, because of a small p_{E_C} value, $E_C < 0$ and $E_C^2/\sigma^2 \gg 1$ (ie, $E_C/\sigma \ll -1$). Therefore, in that range of x , where the integrand (in the last expression) is not small [and where, consequently, $-1 \leq x(-E_C)/\sigma^2 \leq 0$, ie, $(x^2/\sigma^2)(E_C/\sigma)^2 \leq 1$, and hence, $x^2/\sigma^2 \leq (\sigma/E_C)^2 \ll 1$], the value of x^2/σ^2 can be neglected, and the integral is equal to $\sigma^2/(-E_C)$. As a result, we obtain

$$p_{E_C} \approx [2\pi(E_C^2/\sigma^2)]^{-1/2} \exp\{-E_C^2/2\sigma^2\}, \quad (\text{D.3})$$

from where

$$[2\pi(E_C^2/\sigma^2)]^{-1/2} \exp\{-E_C^2/2\sigma^2\} = (\ln 2)/M. \quad (\text{D.4})$$

If M is very large, the most significant terms of this equation are $\exp\{-E_C^2/2\sigma^2\}$ and M , so that we get

$$E_C \approx -\sigma(2 \ln M)^{1/2}. \quad (\text{D.5})$$

This is the energy that is typical of the lower edge of the energy spectrum of a random heteropolymer (and the middle of the spectrum, on the assumption that $\epsilon_i = 0$, corresponds to zero energy, while its upper edge to $|E_C|$).

Near the edge E_C , as seen from the preceding calculations, the probability p_E can be presented as $p_{E_C} \times \exp[(E - E_C)(-E_C/\sigma^2)]$. This means that “accumulated density” of the energy spectrum,

$$m_E = M p_E = (\ln 2) \times \exp [(E - E_C)(-E_C/s^2)],$$

is large enough already at a distance of $\sim \sigma^2/(-E_C)$ from the lower edge of the spectrum; this distance is small in comparison with the half-width $|E_C|$ of the spectrum. This allows using the Eq. (D.2) in the region $|E| \leq |E_C|$ to calculate the entropy of the system: $S(E) = k_B \ln[w(E)]$. Since $S(E)$ must turn to 0 at the edge $|E| = |E_C|$, then

$$S(E) = k_B (\ln M - E^2/2\sigma^2) = k_B (E_C^2 - E^2)/2\sigma^2. \quad (\text{D.6})$$

So, within the dense spectrum (at $|E| \leq |E_C|$) the spectrum's temperature is

$$T(E) = (dS/dE)^{-1} = -\sigma^2/k_B E, \quad (\text{D.7})$$

while

$$T_C = \sigma^2/(-k_B E_C) = [\sigma(2 \ln M)^{-1/2}] / k_B \quad (\text{D.8})$$

is the temperature corresponding to the lower edge of the energy spectrum (see Fig. 18.07), that is, the temperature of “freezing” the most stable folds of the considered random heteropolymer (also called the “glass transition temperature”). These folds have energy close to E_C .

The free energy of a random heteropolymer at temperature $T(E) \geq T_C$ is:

$$F(E) = E - T(E) \cdot S(E) = E + (E_C^2 - E^2)/2E. \quad (\text{D.9})$$

“ENERGY GAP” IN THE RANDOM ENERGY MODEL

Now let us address a “protein-like” heteropolymer where one of the chain folds (the “native fold”) is selected so that only its energy $E_C - |\Delta E|$ is below E_C , and the rest of the energy spectrum (see Fig. 18.07) is arranged like that of a random heteropolymer (Buchler and Goldstein, 1999; Finkelstein et al., 1995b).

Thus, the energy of the native fold is $E_N = E_C - |\Delta E|$, and its entropy it is 0 (because it is single); therefore, its free energy is equal to E_N at any temperature.

Thermodynamic equilibrium of the native and non-native folds occurs at such the energy E of non-native folds that corresponds to $F(E) = E_N$, that is,

$$E/2 + E_C^2/(2E) = E_N. \quad (\text{D.10})$$

Solution of the emerging equation $E^2 - 2E E_N + E_C^2 = 0$ is

$$E_1 = E_N + [E_N^2 - E_C^2]^{1/2} \quad (\text{D.11})$$

(the second root, $E_2 = E_N - [E_N^2 - E_C^2]^{1/2}$, has no physical sense, since it is less than the E_N , and at these energies there are no folds at all).

Consequently, the heat of melting is

$$\Delta H = E_1 - E_N = [E_N^2 - E_C^2]^{1/2} = |\Delta E|^{1/2} [|\Delta E| + |2E_C|]^{1/2}, \quad (\text{D.12})$$

the melting temperature is:

$$T_M = T(E_1) = \sigma^2 / (-k_B E_1) = (\sigma^2 / k_B) / [|E_C| + |\Delta E| - \Delta H], \quad (\text{D.13})$$

and the heat capacity jump at melting (from $C_N = dE_N/dT = 0$ to $C_{\text{denat}} = (dE/dT)|_{E=E_I} = (dT/dE)^{-1}|_{E=E_I}$) is $\Delta C_P = (dT/dE)^{-1}|_{E=E_I} = k_B E_1^2 / \sigma^2$,—or, considering the fact that $T_M \equiv T(E_1) = \sigma^2 / (-k_B E_1)$, it is

$$\Delta C_P = \sigma^2 / (k_B T_M^2). \quad (\text{D.14})$$

The last three equations relate all three parameters $|\Delta E|$, σ , $|E_C|$ of the “random energy model” to the three main parameters observed in protein melting (ΔH , T_M , ΔC_P), while the ratio $(2 \ln M)^{1/2} = |E_C| / \sigma$ [cm. (18.3.2)] allows evaluating M , the number of folds of the protein chain.

If $|\Delta E| \ll |E_C|$, the Eqs. (D.12) and (D.13) take a very simple form:

$$\Delta H \approx |2\Delta E/E_C|^{1/2} \cdot |E_C|, \quad (\text{D.15})$$

$$T_M \approx \{\sigma^2 / k_B\} / \{|E_C| - \Delta H\} = T_C / \{1 - \Delta H / |E_C|\}. \quad (\text{D.16})$$

Hence:

$$\sigma^2 = (k_B T_M^2) \Delta C_P, \quad (\text{D.17})$$

$$|E_C| = \Delta H + \Delta C_P T_M, \quad (\text{D.18})$$

$$|\Delta E| = \frac{1}{2} \Delta H / [1 + \Delta C_P T_M / \Delta H]. \quad (\text{D.19})$$

Addendum: The question arises as to whether we can use these equations to obtain the parameters M , σ , $|\Delta E|$ of that random energy model which corresponds to a protein whose main thermodynamic parameters mp (T_M , ΔH , ΔC_P) are known from the experiment.

Answer: Formally—yes. But, unfortunately, it cannot be done without introduction of further amendments, since the experimental thermodynamic parameters depend not only on reconstruction of chain folds (that are taken into account in the random energy model), but also on temperature-caused changes in hydrophobic and electrostatic interactions, which, without being implied in this model, contribute much to the measured values (in particular—to the value of ΔC_P , appearing in each of the Eqs. D.17–D.19).

Let us now determine the probability that one of the M chain folds has its energy below the $E_C - |\Delta E|$ (at a relatively small $|\Delta E|$), and the energies of the rest folds are above E_C .

The probability that *one given* fold has its energy below the $E_C - |\Delta E|$ (where the “energy gap” $|\Delta E|$ is much less than the spectrum half-width $|E_C|$) is

$$p_{E_C - |\Delta E|} \approx p_{E_C} \times \exp [(-|\Delta E|)(-E_C / \sigma^2)] = p_{E_C} \times \exp [-|\Delta E| / k_B T_C].$$

Thus, the probability that *some* of the M folds has energy below $E_C - |\Delta E|$, while the rest fold energies are above E_C , is

$$\begin{aligned}
 M \times p_{Ec - |\Delta E|} \times (1 - p_{Ec})^{M-1} &= M \times p_{Ec} \\
 &\quad \times \exp[-|\Delta E|/k_B T_C] \times (1 - p_{Ec})^{M-1} \\
 &\approx -\ln(\tfrac{1}{2}) \times \tfrac{1}{2} \\
 &\quad \times \exp[-|\Delta E|/k_B T_C] \\
 &\sim \exp[-|\Delta E|/k_B T_C]
 \end{aligned} \tag{D.20}$$

In conclusion: if the probability $P_i(E_C, 0, \sigma)$ corresponds to the case $\varepsilon_i = 0$ and $\sigma_i = \sigma$, then, for the case of $\varepsilon_i \neq 0$ and $\sigma_i = \sigma + \Delta\sigma_i$ for fold i (it is assumed that $\varepsilon_i, \Delta\sigma_i$ are small and $-E_C \gg \sigma$), we get:

$$\begin{aligned}
 P_i(E_C, \varepsilon_i, \sigma + \Delta\sigma_i) &= [2\pi(\sigma + \Delta\sigma_i)^2]^{-1/2} \times \exp[-(E_C - \varepsilon_i)^2/2(\sigma + \Delta\sigma_i)^2] \\
 &\approx P_i(E_C, 0, \sigma) \times \exp[-\varepsilon_i/k_B T_C - 0.5(\sigma \cdot \Delta\sigma_i)/(k_B T_C)^2]
 \end{aligned} \tag{D.21}$$

This “Boltzmann-like” distribution (Finkelstein et al., 1995a; Gutin et al., 1992) is applicable to statistics of protein architectures (see Lecture 16).

REFERENCES

- Bryngelson, J.D., Wolynes, P.G., 1987. Spin glasses and the statistical mechanics of protein folding. Proc. Natl. Acad. Sci. USA 84, 7524–7528.
- Bryngelson, J.D., Wolynes, P.G., 1990. A simple statistical field theory of heteropolymer collapse with application to protein folding. Biopolymers 30, 177–188.
- Buchler, N.E.G., Goldstein, R.A., 1999. Universal correlation between energy gap and foldability for the random energy model and lattice proteins. J. Chem. Phys. 111, 6599–6609.
- Derrida, B., 1980. Random energy model: limit of a family of disordered models. Phys. Rev. Lett. 45, 79–82.
- Derrida, B., 1981. The random energy model, an exactly solvable model of disordered systems. Phys. Rev. B 24, 2613–2626.
- Finkelstein, A.V., Badretdinov, A.Ya., Gutin, A.M., 1995a. Why do protein architectures have a Boltzmann-like statistics? Proteins 23, 142–150.
- Finkelstein, A.V., Gutin, A.M., Badretdinov, A.Ya., 1995b. Perfect temperature for protein structure prediction and folding. Proteins 23, 151–162.
- Gutin, A.M., Badretdinov, A.Ya., Finkelstein, A.V., 1992. Why is the statistics of protein structures Boltzmann-like? Mol. Biol. (in Russian) 26, 118–127.
- Shakhnovich, E.I., Gutin, A.M., 1989. Formation of unique structure in polypeptide-chains theoretical investigation with the aid of a replica approach. Biophys. Chem. 34, 187–199.

Appendix E

How to Use Stereo Drawings

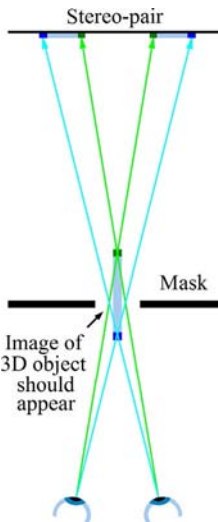
Protein is a three-dimensional (3D) object, and the two-dimensional (2D) image gives little understanding of its spatial structure. Fortunately, we can use the fact that each eye sees the object from a slightly different angle, and draw a “stereo-pair,” that is, a couple of pictures, one of which shows the object as it is seen by the right eye, and the other, by the left.

In the stereo illustrations, we will use *cross* stereo-pairs, where the image to be seen by the *right* eye is placed on the *left*, and the image to be seen by the *left* eye is placed on the *right*.

Besides of the *cross*-stereo images, people often use *direct* stereo images (where the image to be seen by the *right* eye is on the *right* and the image to be seen by the *left* eye is on the *left*). These look more “natural,” but their stereo effect is very sensitive to the distance between the eyes, and one usually needs special stereoscopic glasses to get a stereo effect using direct stereo images (only some special people, such as Alexey Murzin can do without the stereoscopes). The *cross*-stereo images require some practice, but thereafter no stereoscopic glasses are needed, and one can enjoy stereo pictures not only in book, but also at the computer screen or at the large screen where stereoscope glasses are useless.

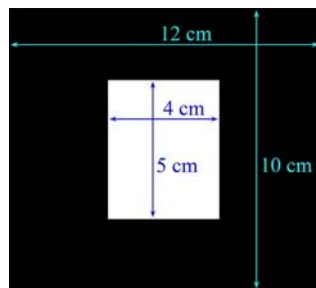
Therefore, I will teach you how to use cross-stereo illustrations

To have a stereo effect, cross your eyes and focus your *right* eye on the *left* part of the stereo-pair and your *left* eye on the *right* part of the stereo-pair, as it is shown in the diagram:



You have to look at the stereo drawing directly, keeping it at a distance of 40–50 cm.

At the beginning of training, you can use a cardboard mask with a hole:

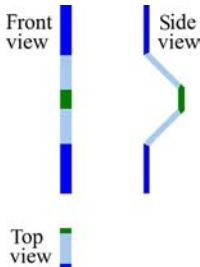


Put it at a distance of 15–20 cm from your face; it will allow your *right* eye to see only the *left* half of the stereo-pair, and your *left* eye will see only the *right* half of the stereo-pair; 15–20 cm is an approximate estimate of the distance; for the optimal—for you—position of the mask depends on the distance between your eyes and the distance to the stereo drawing.

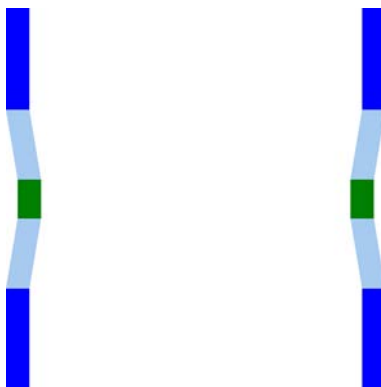
To find the optimal for you, position the mask, move it back and forth and rotate your head a little; try to see only the left half of the stereo-pair by your right eye (closing your left one), then only the right half of the stereo-pair by your left eye (closing your right one), and then open the both eyes and enjoy the stereo effect.

After 20–30 min of training you will be able to see the 3D image of the object protruding from the page.

Below is the object that I have chosen for training. It is a curved rod. Three projections of this rod are shown first:



and then the rod is presented as a stereo-pair.



Training in “stereovision” can be considered complete when you are sure to see the 3D image of the curved rod, even without the help of the mask. By the way, the experience gained will enable you to see the cross stereo-pairs not only in a book or journal, but on the big screen as well.

Problems With Solutions and Comments

All Science Is Either Physics or Stamp Collecting

Ernest Rutherford/John Desmond Bernal

The study of science suggests, in particular, problem solving. The lack of problems was a drawback of the first edition of this book. Now I have tried to fill this gap.

Since the book is designed for people with very different backgrounds, some of these problems may seem too complicated for some readers, and too elementary for others. “Too simple” problems were mostly inspired by e-mails from readers of previous editions of this book (who, being good specialists in one area of science, experienced difficulties in others). For the same reason, I gave fairly detailed solutions of some problems, even though they may seem unnecessary for the majority of readers.

The “too complicated” problems (and comments on them) complement the lectures, in fact. Some of them I’ve used as scaffoldings in my own studies. In addition, some problems are intended to supply a reader with useful qualitative or numerical estimates.

A.V. Finkelstein (2016)

BASIC CONSTANTS

Constant	Designation	Value	Unit
Planck’s constant	h	$\approx 6.626 \times 10^{-34}$	$\text{J s} \equiv \text{kg m}^2 \text{s}^{-1}$
Reduced Planck’s constant (or Dirac constant)	$\hbar = h/2\pi$	$\approx 1.054 \times 10^{-34}$	$\text{J s} \equiv \text{kg m}^2 \text{s}^{-1}$
Avogadro’s number	$N_A = \text{mole}$	6.022×10^{23}	–
Dalton	$\text{Da} = 1 \text{ g}/N_A$	1.661×10^{-27}	kg
		$1 \text{ g} = 6.022 \times 10^{23} \text{ Da}$	
Boltzmann’s constant	k_B or just k	1.381×10^{-23}	$\text{J K}^{-1} \equiv \text{m}^2 \text{ kg s}^{-2} \text{ K}^{-1}$

Gas constant	$R = (N_A/\text{mol})k_B$	8.314 =1.987	$\text{J K}^{-1} \text{ mol}^{-1}$ $\text{cal K}^{-1} \text{ mol}^{-1}$
Proton charge	e	1.602×10^{-19} $=4.803 \times 10^{-10}$	Coulombs Statcoulombs
Elementary unit of electrostatic interactions	$e^2/1 \text{ \AA}$	0.2307×10^{-20} =1389.3 =332.1 =14.40	kJ kJ mol^{-1} kcal mol^{-1} eV
Elementary unit of electric field potential	$e/1 \text{ \AA}$	14.40	V
Elementary unit of electric field strength	$e/1 \text{ \AA}^2$	14.40	$\text{V}/\text{\AA} \equiv 10^{10} \text{ V m}^{-1}$
		1 cal = 4.184 J 1 J = 0.239 cal 0°C = 273.15 K 1 eV = 1.602×10^{-19} J	

PROBLEM 2.1

There are the “left” and “right” amino acids. Is there “left” and “right” water? and ethanol? Why?

Solution

“Left” or “right” is exclusively the status of a molecule possessing the ground state that cannot be superposed with its mirror image by displacement and rotation in three dimensions.

A water molecule, H–O–H, consists of three atoms, which always are in one plane: they form a triangle. The mirror image of a planar body can be always superposed with it by overturning the plane. Thus, water cannot be “left” or “right.”

As to ethanol $\text{CH}_3\text{CH}_2\text{O}\text{H}$, its momentary configuration can differ from its mirror image, but its ground state cannot: the ground state and its mirror image (if they do not coincide at all) have equal energies, and their interconversion through rotation about the $-\text{C}-\text{C}-$, $-\text{C}-\text{O}-$ bonds takes a fraction of a nanosecond at room temperature. Thus, $\text{CH}_3\text{CH}_2\text{OH}$ cannot be “left” or “right” when observed for longer time.

But “heavy” ethanol $\text{CH}_3\text{CDH-O-H}$ has long-living “left” and “right” forms: its central C atom has covalent bonds with four all-different atoms (C, H, D, O), and transition of an atom from one bond to another requires a large activation energy and therefore takes virtually infinite time (just like interconversion of L and D forms of amino acids).

PROBLEM 2.2

Thermal vibrations excited at room temperature have frequencies below $\nu_T \approx 7 \times 10^{12} \text{ s}^{-1}$. What thermal vibrations are excited at -200°C ? at $+3000^\circ\text{C}$?

Solution

Limiting frequency of thermal vibrations follows from $h\nu_T \approx kT$, where T is the absolute temperature and h the Planck constant. The “room temperature” is 20 or 25°C ; the corresponding absolute temperature $T \approx 300 \text{ K}$; -200°C corresponds to $T \approx 73 \text{ K}$, that is, four times lower; $+3000^\circ\text{C}$ corresponds to $T \approx 3273 \text{ K}$, that is, about 11 times higher. Therefore, $\nu_T \approx 1.7 \times 10^{12} \text{ s}^{-1}$ at -200°C , and $\nu_T \approx 7.7 \times 10^{13} \text{ s}^{-1}$ at $+3000^\circ\text{C}$.

PROBLEM 2.3

Find the length of a light wave corresponding to the frequency of $\nu_T \approx 7 \times 10^{12} \text{ s}^{-1}$.

Solution

The light wave length is $\lambda_{\text{light}} = c/\nu$, where $c \approx 300,000 \text{ km s}^{-1}$ is the light speed. Thus, $\lambda_{\text{light},T} \approx [3 \times 10^8 \text{ m s}^{-1}] / [7 \times 10^{12} \text{ s}^{-1}] \approx 0.4 \times 10^{-4} \text{ m} = 40 \mu\text{m}$.

PROBLEM 2.4

Find the length of a sound wave in water that corresponds to the frequency of $\nu_T \approx 7 \times 10^{12} \text{ s}^{-1}$ (the sound speed in water is $u \approx 1500 \text{ m s}^{-1}$).

Solution

Formally, the corresponding sound wave length is $\lambda_{\text{sound},T} = u/\nu_T \approx [1500 \text{ m s}^{-1}] / [7 \times 10^{12} \text{ s}^{-1}] \approx 0.2 \times 10^{-9} \text{ m} = 2 \text{ \AA}$. However, such a sound wave is strongly damped because its length is close to interatomic distances.

PROBLEM 2.5

Find the quantum uncertainty in coordinate of a particle that experiences thermal vibration with a frequency of $\nu_T \approx 7 \times 10^{12} \text{ s}^{-1}$. The particle mass is (a) 1 Da (H atom), (b) 18 Da (water), (c) 100 Da (amino acid), (d) 10 kDa (protein domain).

Solution

According to the Heisenberg Principle, $m\Delta v\Delta x \sim \hbar$, where Δv , Δx are the quantum uncertainties in speed and coordinate. At vibration, the speed v changes from $+\omega A$ to $-\omega A$, where A is the vibration amplitude (so that the speed uncertainty $\Delta v = [\omega A - (-\omega A)]/2 = \omega A$), and the coordinate changes from $+A$ to $-A$ (so that the coordinate uncertainty $\Delta x = [A - (-A)]/2 = A$). Thus, $m(\omega\Delta x)\Delta x \approx \hbar$, and $\Delta x \sim (\hbar/m\omega)^{1/2} = [\hbar/(m \times 2\pi\nu)]^{1/2}$ (or, since $\hbar\omega \approx kT$, $\Delta x \sim \hbar/(mkT)^{1/2}$).

At $\nu_T \approx 7 \times 10^{12} \text{ s}^{-1}$ and $m = 1 \text{ Da} = 1.661 \times 10^{-27} \text{ kg}$, we have $\Delta x_T \approx 0.4 \text{ \AA}$; at $m = 18 \text{ Da}$, $\Delta x_T \approx 0.09 \text{ \AA}$; at $m = 100 \text{ Da}$, $\Delta x_T \approx 0.04 \text{ \AA}$; at $m = 10 \text{ kDa}$, $\Delta x_T \approx 0.004 \text{ \AA}$.

PROBLEM 3.1

Does van der Waals interaction depend on the inner or on the outer electrons?

Solution

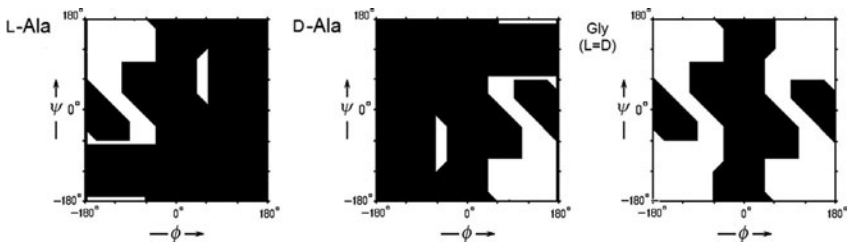
On the outer: their tie to their own nuclei is weaker, and therefore, they are more influenced by polarization produced by polarization of another atom.

PROBLEM 3.2

Recall the map of allowed ϕ , ψ angles of alanine L-Ala (Fig. 3.4). What does the map of allowed ϕ , ψ angles of D-Ala look like? And what about Gly (see Fig. 3.3)?

Solution

D-Ala is the mirror image of L-Ala; in the mirror, all rotation angles change their signs to the opposite. As to Gly, it coincides with its mirror image. Therefore:



PROBLEM 4.1

Why is the density of water lower than that of ice?

Solution

A water molecule has virtually the ball shape, but a ball has 12 immediate neighbors in the tight packing, while water has only four in ice (see Fig. 4.1).

PROBLEM 4.2

There are stories about the “dog caves” where small dogs suffocate, but a man can walk. This phenomenon is often explained as follows: heavy carbon dioxide (CO_2) emitted in the cave goes to its bottom, displaces lighter nitrogen and oxygen, and makes the “bottom” layer of air unfit for breathing. Is this the explanation correct?

Solution

Not quite. If the whole thing were static, the higher weight of CO_2 molecules would *not* have prevented them from spreading over the entire cave. According to the barometrical relationship, the density of gas consisting of molecules with a mass m decreases with the height h as $\exp(mgh/k_B T)$. For oxygen (O_2), it is $\exp(32 \text{ Da} \times gh/k_B T)$; for CO_2 , $\exp((16+32)\text{Da} \times gh/k_B T)$. If one does not feel a change in O_2 density in the cave (actually, up to a height of a few kilometers), one will not feel a change in CO_2 density as well. Thus, fatality of the “dog caves” is caused *not* by equilibrium distribution of CO_2 over the cave’s volume, but rather by kinetics of accumulation of CO_2 there. Apparently, in the “dog cave” CO_2 flows down to the bottom and stays there for a long time due to the slowness of diffusion and the lack of wind. However, if CO_2 ceases to arrive, diffusion will finally distribute it uniformly over the entire cave.

PROBLEM 5.1

What is the distance between H (or rather, H_3O) ions at pH 7? at pH 0?

Solution

At pH 0, the H^+ concentration is $1 \text{ mol L}^{-1} \approx [0.6 \times 10^{24} \text{ ions}] / [10^8 \text{ mm}]^3 = 0.6 \text{ ions per nm}^3 \approx 1 \text{ ion per } 1.7 \text{ nm}^3 \approx (1.2 \text{ nm})^3$.

Thus, $\approx 1.2 \text{ nm}$ is a typical H^+-H^+ distance at pH 0. At pH 7, the concentration is 10^7 -fold lower than at pH 0, and the distance is by $10^{7/3}$ times longer than at pH 0; it is equal to $\approx 260 \text{ nm}$.

PROBLEM 5.2

Let the ratio between concentrations of some molecule in water and an organic solvent is $X_{\text{in_water}}$: $X_{\text{in_org.solv.}} = 1:(5 \times 10^4)$ at 0°C , and $1:(10 \times 10^4)$ at 50°C .

Find the difference of chemical potentials μ in the free energy of interactions, ΔG , and its entropic, ΔS , and enthalpic, ΔH , constituents for the transfer of this molecule from water to the organic solvent.

Solution

$\Delta\mu \equiv 0$ at any temperature by definition of equilibrium conditions;

$\Delta G \equiv \Delta G_{\text{water} \rightarrow \text{org.solv.}} = RT \ln(X_{\text{in_water}} : X_{\text{in_org.solv.}})$, see Eq. (5.16);

$\Delta S = -d(\Delta G)/dT$, see Eq. (5.12); and

$$\Delta H = \Delta G + T\Delta S.$$

Thus:

$$\Delta G = RT \ln[1/(5 \times 10^4)] \approx (0.55 \text{ kcal mol}^{-1}) \cdot (-10.8) \approx -6.0 \text{ kcal mol}^{-1} \text{ at } 0^\circ\text{C}, \text{ ie, at } T = 273 \text{ K};$$

$$\Delta G = RT \ln[1/(10 \times 10^4)] \approx (0.65 \text{ kcal mol}^{-1}) \cdot (-11.5) \approx -7.5 \text{ kcal mol}^{-1} \text{ at } 50^\circ\text{C}, \text{ ie, at } T = 323 \text{ K};$$

$$\Delta G \approx -6.75 \text{ kcal mol}^{-1} \text{ in the center of the } 0\text{--}50^\circ\text{C interval, ie, at } 25^\circ\text{C};$$

$$\Delta S = -[(-7.5 \text{ kcal mol}^{-1}) - (-6.0 \text{ kcal mol}^{-1})]/50^\circ \approx 30 \text{ cal/(deg} \times \text{mol)} \text{ in the center of the } 0\text{--}50^\circ\text{C interval, ie, at } 25^\circ\text{C};$$

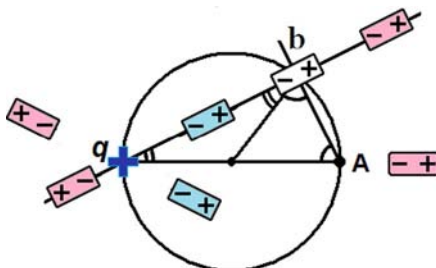
$$\Delta H \approx -6.75 \text{ kcal mol}^{-1} + 9 \text{ kcal mol}^{-1} \approx +2.25 \text{ kcal mol}^{-1} \text{ in the center of the } 0\text{--}50^\circ\text{C interval, ie, at } 25^\circ\text{C.}$$

PROBLEM 6.1

Charge q creates an electric field in some point A. Consider dipoles oriented by the charge q . What is the location of dipoles that *weaken* the potential of this charge-created field at point A? What is the location of dipoles that *reinforce* the potential of this charge-created field at point A?

Solution

Let us, for definiteness, assume that the charge q is positive (+). A dipole that weakens the potential created by $+q$ at point A (the pink dipole in the sketch below) has its “-” closer to A than its “+”; a dipole that reinforces this potential (light-blue in the sketch) has its “+” closer to A than its “-”; and a dipole perpendicular to the direction to A (white, in point b) does not change the potential at A.



According to the Thales' theorem of elementary geometry, if q , A and b are points on a circle where the line qA is a diameter of the circle, then the angle $\angle Abq$ is a right angle. Thus, if b is on the sphere with the diameter qA , the line qb (direction of the dipole) is perpendicular to the line ba (direction from b to A). This proves that the field created by $+q$ at point A is *reinforced* by dipoles located inside the sphere with the poles $+q$ and A , while it is *weakened* by dipoles lying outside this sphere.

PROBLEM 6.2

Let vacuum (medium with $\epsilon_1 = 1$) occupy half of the space, while metal, a conductor (a medium with $\epsilon_2 = \infty$) occupies the other half, the two being separated by a flat interface. Let a charge q be in vacuum, at the point "1" above the flat surface of the metal:

$$\frac{\text{Vacuum: } \epsilon_1=1}{\text{Metal: } \epsilon_2=\infty}$$

① q

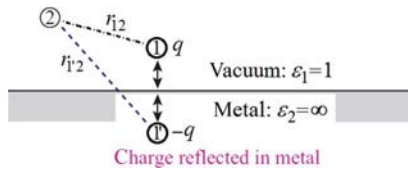
Find the electric field φ induced by this charge at an arbitrary point "2."

Solution

Potential of the resulting electric field is

$$\varphi = \begin{cases} \frac{q}{\epsilon_1 r_{12}} + \frac{-q}{\epsilon_1 r_{1'2}} & \text{in the "vacuum half-space"} \\ 0 & \text{in the "metal half-space": there is no field} \end{cases} \quad (6.2.1)$$

Here, $r_{12} = |\mathbf{r}_2 - \mathbf{r}_1|$, $r_{1'2} = |\mathbf{r}_2 - \mathbf{r}_{1'}|$, $\mathbf{r}_1, \mathbf{r}_2, \mathbf{r}_{1'}$ being coordinates of points 1, 2, $1'$, respectively; point $1'$ is the mirror image of point 1 in the face of the metal:



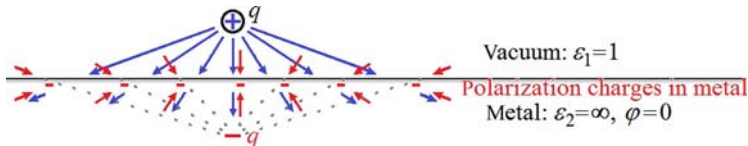
Comment

In the absence of metal, the field of charge q is:

$$\varphi = \frac{q}{\epsilon_1 r_{12}} \quad (6.2.2)$$

In the presence of metal, the metal's polarization charges produce the field which adds to the field of charge q . Inside the metal, the resulting field

is null: otherwise, free metal's charges would keep moving in the field until it was reduced to zero. Because the metal face is flat, the field of polarization charges *outside* the metal is mirror-symmetrical to the field produced by these charges *inside* it:



This scheme shows force lines of the field produced by the charge q in blue, and those produced by the polarization charges in red. The extrapolation of the "out-of-metal" force lines of these charges (the gray dotted lines) point to the sought-for mirror-image $-q$ of the charge q .

PROBLEM 6.3 (MORE DIFFICULT)

Let medium with permittivity ϵ_1 occupy half of the space, while medium with permittivity ϵ_2 occupy the other half, the two being separated by a flat interface. Let a charge q be in the first medium, at the point "1" above the flat surface.

Find the electric field φ induced by this charge at an arbitrary point "2."

Solution

Potential of the resulting electric field is

$$\varphi = \begin{cases} \frac{q}{\epsilon_1 r_{12}} + \frac{q'}{\epsilon_1 r_{1'2}} & \text{in the } \epsilon_1 \text{ half-space} \\ \frac{q''}{\epsilon_2 r_{12}} & \text{in the } \epsilon_2 \text{ half-space} \end{cases} \quad (6.3.1)$$

Here, $r_{12} = |\mathbf{r}_2 - \mathbf{r}_1|$, $r_{1'2} = |\mathbf{r}_2 - \mathbf{r}_{1'}|$, $\mathbf{r}_1, \mathbf{r}_2, \mathbf{r}_{1'}$ being coordinates of points 1, 2, $1'$, respectively; $q' = \frac{\epsilon_1 - \epsilon_2}{\epsilon_1 + \epsilon_2} q$; $q'' = \frac{2\epsilon_2}{\epsilon_1 + \epsilon_2} q$; point $1'$ is the mirror image of point 1 in the interface.

Comment

Solution of [Problem 6.2](#) shows us that one has to seek a solution for each half-space, and then to join them, and that the field in a given half-space is the sum of fields produced by real charges positioned in this half-space and imaginary charges positioned in the other half-space.

The method of reflections explained in solution of [Problem 6.2](#) shows where the imaginary charges should be positioned: in the first half-space, it is the

mirror-image point $1'$ of charge 1; in the other half-space, it is the point of charge 1. It remains only to find these charges, q' and q'' .

From Eq. (6.3.1) one can find the strength of electric fields operating in the “ ϵ_1 half-space” and “ ϵ_2 half-space”:

$$\mathbf{E}(\mathbf{r}_2) = -\frac{d\varphi}{d\mathbf{r}_2} = \begin{cases} \frac{q(\mathbf{r}_2 - \mathbf{r}_1)}{\epsilon_1 r_{12}^3} + \frac{q'(\mathbf{r}_2 - \mathbf{r}_{1'})}{\epsilon_1 r_{12}^3} & \text{in the "}\epsilon_1\text{ half-space"} \\ \frac{q''(\mathbf{r}_2 - \mathbf{r}_1)}{\epsilon_2 r_{12}^3} & \text{in the "}\epsilon_2\text{ half-space"} \end{cases} \quad (6.3.2)$$

The solutions are joined together at the interface of the two half-spaces on condition that the following two requirements (see any physics textbook):

(i) Continuity of the potential φ ; this results in equality

$$E_{||}(\mathbf{r}_2)_{\text{in space 1}} = E_{||}(\mathbf{r}_2)_{\text{in space 2}} \quad (6.3.3)$$

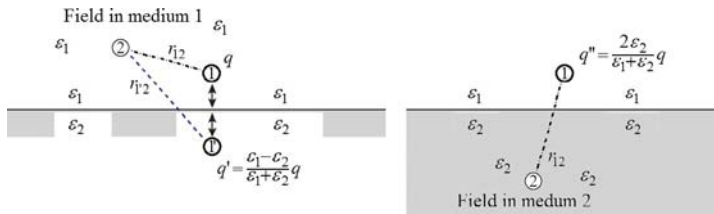
for the tangent (to the interface) constituents $E_{||}$ of electric field strengths.

(ii) The Gauss's law “the average flux of electric displacement field $\oint_S (\epsilon E)_{\perp} dS / 4\pi$ through any closed surface S is equal to the total charge q_{inside} enclosed by the surface.” This results in

$$\epsilon_1 E_{\perp}(\mathbf{r}_2)_{\text{in space 1}} = \epsilon_2 E_{\perp}(\mathbf{r}_2)_{\text{in space 2}} \quad (6.3.4)$$

for the perpendicular (to the interface) constituents E_{\perp} of electric field strength.

As a result, $q' = \frac{\epsilon_1 - \epsilon_2}{\epsilon_1 + \epsilon_2} q$; $q'' = \frac{2\epsilon_2}{\epsilon_1 + \epsilon_2} q$:

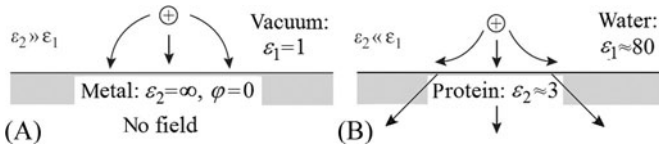


One can see that Eq. (6.3.1) with these q', q'' coincides with solution of Problem 6.2 at $\epsilon_2 = \infty$.

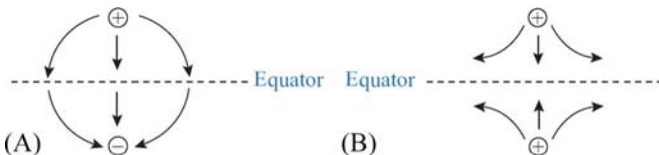
PROBLEM 6.4

Make a sketch of force lines for the field described by Eq. (6.3.1) with

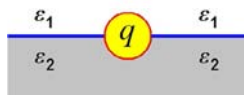
- (a) $\epsilon_1 \ll \epsilon_2$ (ie, for the charge in vacuum with $\epsilon_1 \approx 1$ near the surface of metal with $\epsilon_2 \approx \infty$);
- (b) $\epsilon_1 \gg \epsilon_2$ (ie, for the charge in water with $\epsilon_1 \approx 80$ near the surface of protein with $\epsilon_2 \approx 3$).

Solution

Compare with force lines of fields:

**PROBLEM 6.5**

Find electric field of charge q located at the interface between a media with permittivity ϵ_1 and a media with permittivity ϵ_2 .

**Solution**

Potential of the resulting electric field is:

$$\varphi = \frac{2}{\epsilon_1 + \epsilon_2} q \frac{1}{r_{12}} \quad (6.5.1)$$

where r_{12} is the distance from charge q located at the interface.

Comment

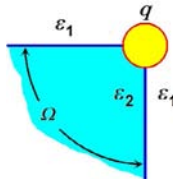
The result is obtained from Eq. (6.3.1) when the distance between charge q and the interface turns to zero. Then $r_{1'2} \rightarrow r_{12}$, potential in the “ ϵ_1 half-space”

$$\frac{q}{\epsilon_1 r_{12}} + \frac{q'}{\epsilon_1 r_{1'2}} \rightarrow \frac{q}{\epsilon_1 r_{12}} + \frac{q \frac{\epsilon_1 - \epsilon_2}{\epsilon_1 + \epsilon_2}}{\epsilon_1 r_{12}} = q \frac{2}{\epsilon_1 + \epsilon_2} \times \frac{1}{r_{12}}, \text{ and potential in the } \epsilon_2$$

$$\text{half-space"} \frac{q''}{\epsilon_2 r_{12}} = q \frac{2}{\epsilon_1 + \epsilon_2} \times \frac{1}{r_{12}}, \text{ as well.}$$

PROBLEM 6.6 (MORE DIFFICULT)

Find electric field of charge q located at the top of a cone with permittivity ϵ_2 in the media with permittivity ϵ_1 . The spherical angle of the cone is Ω .



Solution

$$\varphi(r_{12}) = \frac{1}{\epsilon_1 \left(1 - \frac{\Omega}{4\pi}\right) + \epsilon_2 \frac{\Omega}{4\pi}} \times \frac{q}{r_{12}}$$

Comment

Force lines corresponding to this potential go along the surface of the cone. Therefore, $E_\perp = 0$ at the both sides of the cone surface (so that Eq. (6.3.4) is automatically fulfilled). On the other hand, the integral $\oint_S (\epsilon E)_\perp dS / 4\pi$ (with $\mathbf{E}(\mathbf{r}_2) = -\frac{d\varphi}{d\mathbf{r}_2} = \frac{1}{\epsilon_1 \left(1 - \frac{\Omega}{4\pi}\right) + \epsilon_2 \frac{\Omega}{4\pi}} \times \frac{q}{r_{12}^3} \mathbf{r}_{12}$) taken over a sphere centered at the top of the cone is just equal to q , the total charge enclosed by this sphere, in accordance with the Gauss's law.

PROBLEM 6.7

Find the relationship between the enthalpy H and the free-energy G of interaction between charges in water. Permittivity ϵ of water strongly depends on temperature T : $\epsilon(T=273 \text{ K})=88$, and $\epsilon(T=373 \text{ K})=55$.

Solution

Since $G = H - TS$, then $H = G + TS$. Entropy $S = -dG/dT$, according to Eq. (5.12), so that

$$H = G - T(dG/dT) = G[1 - (T/G)(dG/dT)] = G[1 - d(\ln G)/d(\ln T)]$$

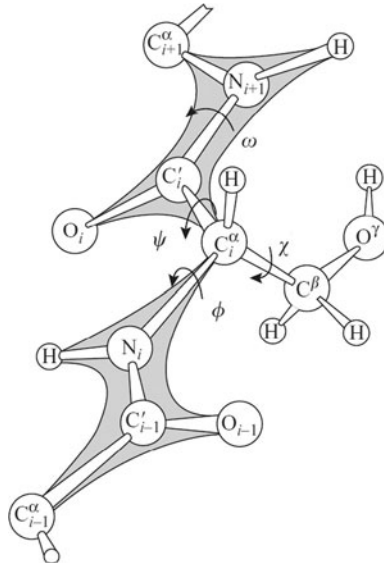
Since the free energy of interaction between charges is $G = qe/\epsilon r$, where q, e, r are temperature-independent, then $H = G[1 + d(\ln \epsilon)/d(\ln T)]$; this relationship is medium-independent, but the $d(\ln \epsilon)/d(\ln T)$ value depends on the

medium. If $\epsilon = \text{const}$ (as, eg, in vacuum), then $H = G$. But permittivity of water strongly depends on T . For water, the $d(\ln \epsilon)/d(\ln T)$ value can be estimated as $\{\ln[\epsilon(T=373 \text{ K})] - \ln[\epsilon(T=273 \text{ K})]\}/\{\ln[373 \text{ K}] - \ln[273 \text{ K}]\} = \ln[55/88]/\ln[373/273] = -0.47/0.31 \approx -1.5$. Thus, in water $1 + d(\ln \epsilon)/d(\ln T) \approx 1 - 1.5 \approx -0.5$, that is, $H = -0.5G$.

Thus, the water enthalpy is opposite in sign to the free energy, ie, here enthalpy *falls* (rather than rises, as it may seem intuitively!) when charges of the same sign approach one another (and the free energy increases, of course—but the resulting repulsion of charges is due *only* to entropy).

PROBLEM 7.1

What are the values of φ , ψ , ω , χ angles in this figure?



Solution

All these values are about 180° .

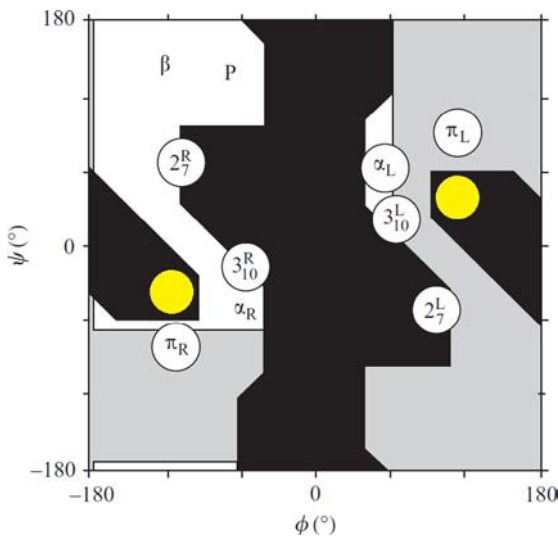
PROBLEM 7.2

Where is the β -bulge positioned at the Ramachandran plot?

Solution

Approximately as shown by yellow spots in this figure: close to conformation of helices where neighbor N–H bonds are directed to O-atoms which are very close

in space (see Fig. 7.5). This conformation is not forbidden only when two adjacent N–H groups form H-bonds with one and the same O atom.



PROBLEM 7.3

An increment by an amino acid residue in the contour length of a polypeptide chain is about 3.5 \AA ; the Kuhn segment (ie, the characteristic length after which the chain “forgets” its direction) in a polypeptide is 35 \AA long. What is the distance L between the ends of a polypeptide random coil?

Solution

$$L^2 = (3.5 \text{ \AA} \times 150) \times 35 \text{ \AA} = 18375.5 \text{ \AA}^2. \text{ Thus, } L \approx 136 \text{ \AA}.$$

PROBLEM 8.1

Find the average momentary kinetic and the average momentary potential energy, and corresponding heat capacities for a particle moving along one coordinate in a one-dimensional well with a potential $U = \frac{1}{2}Kx^2$; the temperature of the medium is T . Quantum effects are not considered.

Solution

In classical approximation: $\langle E_{\text{kinetic}} \rangle = kT/2$; $\langle E_{\text{potential}} \rangle = kT/2$.

According to the Boltzmann distribution, the averaging is made with a probability $w(E) = \exp\left(-\frac{E}{kT}\right) / \sum_e \exp\left(-\frac{\epsilon}{kT}\right)$. Thus:

1. For kinetic energy (which is equal to $\frac{mv^2}{2}$, where m is the mass and v the speed of the particle):

$$\begin{aligned}\langle E_{\text{kinetic}} \rangle &\equiv \left\langle \frac{mv^2}{2} \right\rangle = \int_{-\infty}^{+\infty} dv \left(\frac{mv^2}{2} \right) \exp \left(-\frac{mv^2}{2kT} \right) / \int_{-\infty}^{+\infty} dv \cdot \exp \left(-\frac{mv^2}{2kT} \right) \\ &= \frac{kT}{2} \int_{-\infty}^{+\infty} dx \cdot x^2 \cdot \exp \left(-\frac{x^2}{2} \right) / \int_{-\infty}^{+\infty} dx \cdot \exp \left(-\frac{x^2}{2} \right) = \frac{kT}{2}\end{aligned}$$

Here, we used a conventional transformation

$$\begin{aligned}\int_{-\infty}^{+\infty} dx \cdot x^2 \cdot \exp \left(-\frac{x^2}{2} \right) &\equiv \int_{-\infty}^{+\infty} d \frac{x^2}{2} \cdot x \cdot \exp \left(-\frac{x^2}{2} \right) \equiv \int_{-\infty}^{+\infty} -d \left[\exp \left(-\frac{x^2}{2} \right) \right] \\ &\cdot x \equiv \int_{-\infty}^{+\infty} -d \left[\exp \left(-\frac{x^2}{2} \right) \cdot x \right] + \int_{-\infty}^{+\infty} dx \cdot \exp \left(-\frac{x^2}{2} \right) \\ &= 0 + \int_{-\infty}^{+\infty} dx \cdot \exp \left(-\frac{x^2}{2} \right)\end{aligned}$$

2. For potential energy (which is equal to $\frac{Kx^2}{2}$):

$$\langle E_{\text{potential}} \rangle \equiv \left\langle \frac{Kx^2}{2} \right\rangle = \frac{\int_{-\infty}^{+\infty} dx \left(\frac{Kx^2}{2} \right) \exp \left(-\frac{Kx^2}{2kT} \right)}{\int_{-\infty}^{+\infty} dx \cdot \exp \left(-\frac{Kx^2}{2kT} \right)} = \frac{kT}{2}$$

Note that the total (kinetic + potential) average energy of an oscillator is kT .

3. Heat capacities, in both cases, are $\frac{d}{dT} \left(\frac{kT}{2} \right) = \frac{k}{2} = 0.69 \times 10^{-23} \text{ J K}^{-1} = 4.16 \text{ J K}^{-1} \text{ mol}^{-1} = 0.99 \text{ cal K}^{-1} \text{ mol}^{-1}$. The total (originating from an increase in both kinetic and potential energy) heat capacity of one elastic degree of freedom is $k \approx 2 \text{ cal K}^{-1} \text{ mol}^{-1}$.

Note also that both $\langle E_{\text{kinetic}} \rangle$ and $\langle E_{\text{potential}} \rangle$, being equal to $\frac{kT}{2}$ each, are independent of the mass m of the particle and the strength K of the potential.

However, it should be mentioned that the above solution relates to classical mechanics. Classical approximation is valid when $kT > \hbar\omega$, where $\omega = K/m$ is the oscillator frequency.

PROBLEM 8.2

Find the average momentary speed of a thermal movement of the following particles: (a) atom H ($m = 1 \text{ Da}$); (b) water molecule ($m = 18 \text{ Da}$); (c) small

protein ($m=10$ kDa); (d) large protein complex ($m=1000$ kDa); (e) for a cell ($m\sim 10^{12}$ Da). The temperature of the medium is $T=300$ K.

Solution

Having $\left\langle \frac{mv^2}{2} \right\rangle = \frac{kT}{2}$ for the movement along one coordinate, we have $\left\langle \frac{m(v_1^2 + v_2^2 + v_3^2)}{2} \right\rangle = \frac{3kT}{2}$ for the movement along all three coordinates in the 3D space. Thus, the average speed is $\bar{v} = \sqrt{3kT/m}$.

For $T=300$ K, $kT=(1.381 \times 10^{-23} \text{ m}^2 \text{ kg s}^{-2} \text{ K}^{-1}) \times 300\text{K} \approx 4.1 \times 10^{-21} (\text{m s})^{-2} \text{ kg}$.

For a particle with $m=1$ Da $= 1.661 \times 10^{-27}$ kg, $\bar{v} \approx \sqrt{\frac{3 \times 4.1 \times 10^{-21}}{1.7 \times 10^{-27}}} (\text{m s}^{-1}) \approx 2.7 \text{ km s}^{-1}$; for other particles, $\bar{v} \approx 2.7(\text{km s}^{-1})/\sqrt{\frac{m}{\text{Da}}}$. Thus, for a particle with $m=18$ Da: $\bar{v} \approx 640 \text{ m s}^{-1}$; for a particle with $m=10$ kDa: $\bar{v} \approx 27 \text{ m s}^{-1}$; for a particle with $m=1000$ kDa: $\bar{v} \approx 2.7 \text{ ms}^{-1}$; for a particle with $m \sim 10^{12}$ Da: $\bar{v} \approx 2.7 \text{ mm s}^{-1}$.

PROBLEM 8.3

Derive an equation for the coordinate entropy of ideal gas that has $N \gg 1$ equal particles in volume V .

Solution

$S=k_B \ln(V^N/N!)$, where $N! \equiv N \times (N-1) \times \dots \times 2 \times 1 \sim (N/e)^N$ according to the Stirling's approximation, which is valid for $N \gg 1$. Thus, $S \approx k_B N \times \ln(Ve/N)$.

PROBLEM 8.4

For ideal gas, derive the equation $PV=Nk_B T$ (where P is pressure, V is volume, T is temperature, $N \gg 1$ is number of molecules in the gas).

Solution

For any body, the change dF of the Helmholtz free energy $F=E-TS$ at a constant (provided by heat exchange with the medium) temperature is equal, by definition, to the work invested in the body. Pressure $P > 0$, also by definition, is the force acting at a unit area; on the surface area of σ the force $P\sigma$ acts. Compression, ie, a change in volume by $dV < 0$, corresponds to the shift of the surface at a distance $-dV/\sigma > 0$. This shift requires an investment of a work

$P\sigma \times (-dV/\sigma) = -PdV > 0$ in the body. Therefore, $dF = -PdV$, and thus, $(dF/dV)_{T=\text{const}} = -P$.

The free energy consists of kinetic and coordinate parts. The former only depends on speed of molecules, so that its increment to pressure is zero (at a constant temperature). Thus, $P = -(d(E^{\text{coord}} - TS^{\text{coord}})/dV)_{T=\text{const}} = Td(S^{\text{coord}})/dV_{T=\text{const}}$ (because $E^{\text{coord}} = 0$ for ideal gas), and $S^{\text{coord}} = k_B N \times \ln(Ve/N)$ according to [Problem 8.3](#). Thus, $P = Tk_B N/V$. Q.E.D.

PROBLEM 8.5

Derive an equation for the coordinate constituent of chemical potential of ideal gas that has $N \gg 1$ equal particles in volume V .

Solution

Coordinate constituent of Gibbs free energy is $G^{\text{coord}} = (E^{\text{coord}} + PV) - TS^{\text{coord}}$. For ideal gas $E^{\text{coord}} = 0$ and $PV = Nk_B T$ according to [Problem 8.4](#). $S^{\text{coord}} = k_B N \times \ln(Ve/N)$ according to [Problem 8.3](#). Thus, $G^{\text{coord}} = Nk_B T - Tk_B N \times \ln(Ve/N) = -Nk_B T \times \ln(V/N)$. Chemical potential is $\mu = G/N$.

Thus, the coordinate constituent of chemical potential is $\mu^{\text{coord}} = G^{\text{coord}}/N = -k_B T \times \ln(V/N)$.

Another variant:

Coordinate constituent of Helmholtz free energy is $F^{\text{coord}} = E^{\text{coord}} - TS^{\text{coord}}$. For ideal gas $E^{\text{coord}} = 0$ and $S^{\text{coord}} = k_B N \times \ln(Ve/N)$ according to [Problem 8.3](#). Chemical potential is $\mu = dF^{\text{coord}}/dN$.

Thus, the coordinate constituent of chemical potential is $\mu^{\text{coord}} = -k_B T \times \ln(V/N)$.

PROBLEM 8.6

What general form can be suggested for chemical potential of a molecule in solution where this molecule is present in a very low concentration?

Solution

$\mu = kT \ln[C] + \mu^0$, where $C \equiv N/V$ is concentration of the molecules in question (N being their number in volume V), and the concentration-independent term μ^0 depends on interaction of the molecule in question with the surrounding solvent and on temperature (thus including kinetic energy of the molecule and its surrounding).

PROBLEM 8.7

By how many times the 10 kcal mol⁻¹ increase in the height of the energy barrier slows down the process at 0°C? at 50°C? at 100°C?

Solution

By $\exp[-(10 \text{ kcal mol}^{-1})/RT]$ times, ie, $\approx 8 \times 10^7$ -fold at 0°C , $\approx 5 \times 10^6$ -fold at 50°C , $\approx 6 \times 10^5$ -fold at 100°C .

PROBLEM 8.8

Estimate the “mean free path” Δl_{kinet} typical of the friction-caused damping of thermal movement in water. Consider spherical particles with a diameter $D \approx 3 \text{ \AA}$ (\approx water), $D \approx 30 \text{ \AA}$ (\approx small protein), $D \approx 300 \text{ \AA}$ (\approx large protein complex). The density of each particle is assumed to be $\rho \approx 1.3 \text{ g cm}^{-3}$.

Solution

According to Eq. (8.24), the time typical of the friction-caused movement damping in water is $t_{\text{kinet}} \approx 10^{-15} \text{ s} (D/\text{\AA})^2$, where D is the particle’s diameter. Thus, $\Delta l_{\text{kinet}} \approx \bar{v} \times t_{\text{kinet}}$, where $\bar{v} \approx 2.7 (\text{km s}^{-1}) / \sqrt{m/D}$ is the speed of thermal movement of a particle with mass m (see Problem 8.2). The mass of a spherical particle

$$\text{with the diameter } D \text{ is } m = \frac{\pi}{6} \rho D^3 = \frac{\pi}{6} (1.3 \text{ g cm}^{-3}) D^3 = 0.41 \text{ Da} \cdot \left[\frac{D}{\text{\AA}} \right]^3.$$

Thus, $\Delta l_{\text{kinet}} \approx 0.042 \text{ \AA} \cdot \sqrt{\frac{D}{\text{\AA}}}$, and $\Delta l_{\text{kinet}} \approx 0.07 \text{ \AA}$ for a particle with $D \approx 3 \text{ \AA}$, $\approx 0.2 \text{ \AA}$ for a particle with $D \approx 30 \text{ \AA}$, 0.7 \AA for a particle with $D \approx 300 \text{ \AA}$.

PROBLEM 8.9

Consider diffusion in water with a viscosity of $\eta \approx 0.01 \text{ g cm}^{-1} \text{ s}^{-1}$ at 27°C . What time is necessary for (a) 10 nm, (b) 1 μm , and (c) 1 m displacement for: a water molecule with the diameter $D = 3 \text{ \AA}$; a small protein with $D = 30 \text{ \AA}$; a large protein complex with $D = 300 \text{ \AA}$.

Solution

According to Eq. (8.28), the square of diffusion displacement l_t of a particle in a liquid with viscosity η depends on the diffusion time t , the $k_B T$ value and the particle diameter D as $l_t^2 \approx t [2kT/\pi D\eta]$. (This equation is valid when l_t exceeds the friction-caused movement damping, which is always true when $l_t = 1000 \text{ \AA}$ and the particle’s diameter is $< 1 \text{ cm}$, see solution to Problem 8.8.)

Thus, diffusion time for the 10 nm distance in water is $\sim 0.12 \times 10^{-7} \text{ s}$ for the water molecule with $D = 3 \text{ \AA}$, $\sim 1.2 \times 10^{-7} \text{ s}$ for a small protein with $D = 30 \text{ \AA}$, $\sim 12 \times 10^{-7} \text{ s}$ for a large protein complex with $D = 300 \text{ \AA}$.

Diffusion time for the 1 μm distance in water is $\sim 0.12 \times 10^{-3} \text{ s}$ for the water molecule, $\sim 1.2 \times 10^{-3} \text{ s}$ for a small protein, $\sim 12 \times 10^{-3} \text{ s}$ for a large protein complex.

Diffusion time for the 1 m distance in water is $\sim 0.12 \times 10^9$ s (4 years) for the water molecule, $\sim 1.2 \times 10^9$ s (40 years) for a small protein, $\sim 12 \times 10^9$ s (400 years) for a large protein complex.

PROBLEM 8.10

Considering diffusion, we used Stokes' law and thus assumed that the flow around the diffusing particle is laminar. Is this assumption valid for the considered cases and objects?

Solution

Yes.

Explanation

It is known that the flow is laminar when the Reynolds number (Re) is not too high (look it up in the internet!). By definition, $Re = v\rho D/\eta$, where v is the fluid speed, ρ is the fluid density, η is the fluid viscosity, D is the object diameter, and purely laminar flow exists up to $Re = 10$ under this definition. Thus, the criterion is $v < 10\eta/(\rho D)$; it can be presented as $v < 10\eta/(\rho \times nm)/(D/nm)$. Having, for water, $\rho = 1 \text{ g cm}^{-3}$ and $\eta = 0.01 \text{ g cm}^{-1} \text{ s}^{-1}$, we obtain the criterion

$$v < 10^6 (\text{cm s}^{-1})/(D/nm)$$

For proteins and their complexes, $D/nm < 100$, and v does not exceed 10^4 (cm s^{-1}) at room temperature; for water and other small molecules, $D/nm < 1$, and v does not exceed 3×10^5 (cm s^{-1}). Thus, the criterion for laminar flow is met.

PROBLEM 8.11

Imagine that the “binding site” of some particle is a volume $w \approx 30 \text{ \AA}^3$, where some definite point A of this particle should get. Assume that the particle does not feel the proximity of the site until the point A is outside the volume w .

What time is necessary for the particle with the diameter $D = 30 \text{ \AA}$ to find this binding site by diffusion in the volume $V = 1 \mu\text{m}^3$ of water with viscosity $\eta \approx 0.01 \text{ g cm}^{-1} \text{ s}^{-1}$ at 27°C ?

Solution

Site search time: ~ 10 s.

Explanation

The simplest estimate is as follows. Since the particle does not feel the proximity of the site until the point A is outside the volume w , it needs to scan, by random diffusion, $\sim V/w$ ($\sim 3 \times 10^{-10}$ in our case) of such volumes to get to this site. The transition from one volume w to the next one requires displacement by a distance of $\sim w^{1/3} \approx 3 \text{ \AA}$. According to Eq. (8.28), the time of diffusion at such a distance is $t_1 \approx w^{2/3}/[2kT/\pi D\eta] \approx 1.2 \times 10^{-10} \text{ s}$ (see solution of Problem 8.9, taking into account that diffusion time is proportional to the square of diffusion distance). Thus, the total search time is $t \sim t_1[V/v_1] \approx 1.2 \times 10^{-10} \text{ s} \times 3 \times 10^{-10} \approx 4 \text{ s}$.

However, the above does not take into account that the particle can return and visit some volumes several times; but this effect is not significant: the mathematical expectation of coming to the initial point by an n -step random walk in 3D is proportional to $n^{-3/2}$ (according to the Flory formula for random loop closing), and the sum $\sum_{n=1}^{\infty} n^{-3/2} \approx 2.6$. Thus, each volume w on the diffusion pathway will be visited not once but about 2.6 times, and the resulting search time will increase accordingly: it will be $\sim 10 \text{ s}$ instead of $\sim 4 \text{ s}$; not a significant difference.

PROBLEM 8.12

Assume that H^+ instantly binds to COO^- approaching it at a distance where the electrostatic energy of the $\text{H}^+ \dots \text{COO}^-$ attraction exceeds kT .

How much time does the H^+ binding to COO^- take in water at pH 7 and 27°C ?

Solution

The binding time t is $\sim 10^{-3} \text{ s}$.

Explanation

Equation $t \sim V(\pi\eta/2kT)(D/w^{1/3})$ has been obtained in Problem 8.11, and we know that $t \sim 4 \text{ s}$ when $V = 1 \mu\text{m}^3$, $D = 30 \text{ \AA}$, $w^{1/3} \approx 3 \text{ \AA}$. So, now it remains only to estimate the values V (volume per particle), D (particle's diameter), $w^{1/3}$ (binding site's diameter) for the given problem.

The volume per H^+ at pH 7 is $V = 1/(10^{-7} \text{ mol L}^{-1}) = 10^7 \text{ L mol}^{-1} \approx 10^7 \times 10^{15} \mu\text{m}^3/6 \times 10^{23} \approx 1/60 \mu\text{m}^3$.

Since H^+ travels in water as $(\text{H}_3\text{O})^+$, the ion's diameter $D \sim 3 \text{ \AA}$.

Since H^+ "feels" COO^- at a distance r where $e^2/\epsilon r = kT$, then $r \approx 8 \text{ \AA}$ and $w^{1/3} \approx 16 \text{ \AA}$.

Thus, t is $\sim 10^{-3} \text{ s}$.

PROBLEM 9.1 (MORE DIFFICULT)

Suppose that a polymer consists of a large number of links, and the initiation time of some local structure in each of its links is t_{init} , which far exceeds the time τ required to involve yet another link in the already growing piece of structure (τ being independent of its size).

Find the characteristic time t_{str} required to involve the entire polymer in this structure.

Solution

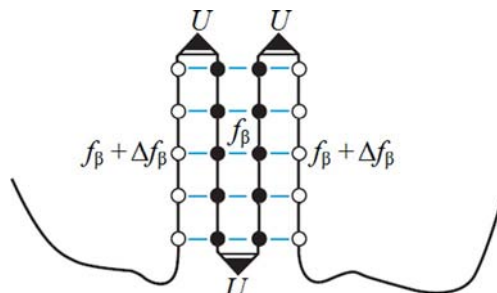
Characteristic time $t_{\text{str}} \approx 2(t_{\text{init}}\tau)^{1/2}$ for an infinitely long polymer.

Explanation

Let m be the average number of links forming a piece of structure initiated on some of its links. The time required to form such a piece is $t_m = t_{\text{init}}/m + \tau \cdot m$, because the fact that its initiation can occur in any of its links increases the rate of its initiation m -fold, while the subsequent addition of m links to this piece takes the time $\tau \cdot m$. This time is minimal for a piece of such size m_{opt} , that $dt_m/dm = 0$, that is, $-t_{\text{init}}/m^2 + \tau = 0$, so $m_{\text{opt}} = (t_{\text{init}}/\tau)^{1/2}$ and $t_m(m=m_{\text{opt}}) = 2(t_{\text{init}}\tau)^{1/2}$. The pieces comprising a larger or smaller number of links than m_{opt} take more time to form, so the optimal-size pieces will occupy the entire infinitely long polymer in a time of $\approx 2(t_{\text{init}}\tau)^{1/2}$.

PROBLEM 9.2

According to Eqs. (9.12) and (9.13), the free energy of the most stable β -sheet comprising M residues in m β -strands is $F(M,m) = Mf_\beta + 2(M/m)\Delta f_\beta + (m-1)U$,



where $f_\beta < 0$ is the free energy of a residue in the center of the β -sheet, $f_\beta + \Delta f_\beta > 0$ is the free energy of an edge β -strand residue, U is the free energy of a bend, and the optimal (for stability) number of β -strands is $m_{\text{opt}} = M^{1/2} (2\Delta f_\beta/U)^{1/2}$.

Assuming that Δf_β and M are big, that is, $\Delta f_\beta \gg -f_\beta$, $M\Delta f_\beta \gg U$, estimate the minimal size M_{\min} of a stable β -sheet, and then exclude the value f_β from the estimate of heights of the free energy barrier ($F^\ddagger = \frac{2U\Delta f_\beta}{(-f_\beta)}$, Eq. (9.11)) that hinders β -sheet formation.

Solution

$M_{\min} = 8f_\beta U / \Delta f_\beta^2$; therefore $f_\beta \approx -[8U\Delta f_\beta / M_{\min}]^{1/2} < 0$, so $F^\ddagger = \sqrt{U\Delta f_\beta / 2} \times \sqrt{M_{\min}}$. The latter shows that the barrier occurs due to the free energy loss at the β -sheet perimeter (which is proportional to \sqrt{M}).

PROBLEM 10.1

The average molecular weight of an amino acid residue is about 110 Da.

- (a) Estimate the average volume per amino acid residue, assuming that the density of protein is 1.3 g cm^{-3} .
- (b) What is the diameter of a globule of 150 amino acid residues?

Solution

(a) 140 \AA^3 ; (b) 34 \AA .

If ρ is protein density, and m is the average molecular weight of an amino acid residue, its volume $V = m/\rho = 110 \text{ g mol}^{-1}/1.3 \text{ g cm}^{-3} = [110 \text{ g}/(0.6 \times 10^{24})]/[1.3 \text{ g}/(10^{24} \text{ \AA}^3)] \approx 140 \text{ \AA}^3$.

The diameter of a globule of 150 amino acid residues is $D = (150 \times 140 \text{ \AA}^3 \times 6/\pi)^{1/3} \approx 34 \text{ \AA}$.

PROBLEM 10.2

Estimate the ratio of concentrations of H (or rather, H_3O) ions at pH 7 and charged amino acid residues in a solution where, like in the cell, the protein concentration is $\sim 10\%$ by weight.

Solution

1: 200,000.

If the protein content is $\sim 10\%$ by weight in solution, and the proportion of charged residues in the protein is $\sim 20\%$, then there are $\sim 20 \text{ g}$ of 100 Da residues in 1 L of solution, ie, their concentration is $\sim 0.2 \text{ mol L}^{-1}$, while concentration of H^+ is $10^{-7} \text{ mol L}^{-1}$ at pH 7.

PROBLEM 11.1

Which of the below given sequences is typical for an α -helical fibrous protein? for a β -structural fibrous protein? for collagen?

- (a) -Gly-Ala-Gly-Thr-Gly-Ala-Gly-Thr-Gly-Ala-
- (b) -Gly-Ala-Pro-Gly-Pro-Pro-Gly-Thr-Pro-Gly-Ala-Pro-Gly-Pro-Pro-
- (c) -Ala-Glu-Ser-Val-Gly-Lys-Asn-Ala-Glu-Ser-Gln-Gly-Arg-Gly-

Solution

- (a) β -Structural fibrous protein; period 2 for alternation of small Gly and larger residues:

-Gly-Ala-Gly-Thr-Gly-Ala-Gly-Thr-Gly-Ala-

- (b) Collagen; repeats of triplets of the Gly-X-Pro kind:

-Gly-Ala-Pro-Gly-Pro-Pro-Gly-Thr-Pro-Gly-Ala-Pro-Gly-
Pro-Pro-Gly-Pro-Pro-

- (c) α -Helical coiled-coil in fibrous protein; period $3.5 \times 2 = 7$ for alternation of hydrophobic (mostly small) and hydrophilic residues:

-Ala-Glu-Ser-Val-Gly-Lys-Asn-Ala-Glu-Ser-Gln-Gly-Arg⁺-Gly-

PROBLEM 12.1

- (a) Why do the typical membrane proteins look like either a bundle of α -helices extending from one side of the membrane to the other or like a β -cylinder extending from one side of the membrane to the other?
- (b) Can a β -sheet, not a β -barrel, lie within the lipid membrane?

Solution

- (a) Because structures of this type imply the absence of non-involved in hydrogen bonds H-bond donors and acceptors within the membrane: such “free” donors and acceptors cannot bind to water within the membrane, and therefore, the shortage of hydrogen bonds would reduce drastically the stability of the protein structure.
- (b) It is unlikely, since all edges of the β -sheet are not involved in H-bonding, and “free” donors and acceptors of H-bonds dramatically reduce the stability a β -sheet inside the membrane.

PROBLEM 12.2

Can a large irregular region be inside the membrane protein, just in the middle of its 3D structure?

Solution

It can, if the membrane protein has a wide, water-filled pore (see Fig. 12.5) where this irregular region is positioned.

PROBLEM 12.3

Suppose an electron which makes 10^{15} vibrations per second penetrates through the energy barrier of width L by tunneling within a millisecond. What time will it take the electron to penetrate through a twice thicker barrier of the same height?

Solution

The probability of electron penetration through a potential barrier of the given height by tunneling decreases exponentially with the width of this barrier. If an electron penetrates through an L -wide barrier in 0.001 s, the probability of its tunneling through the barrier during one oscillation (which takes 10^{-15} s) is 10^{-12} . Therefore, penetration through a barrier with the width $2L$ will take $10^{-15} \text{ s}/(10^{-12} \times 10^{-12}) = 10^9 \text{ s}$.

PROBLEM 12.4

How to experimentally distinguish tunneling penetration through an energy barrier from overcoming it by activation?

Solution

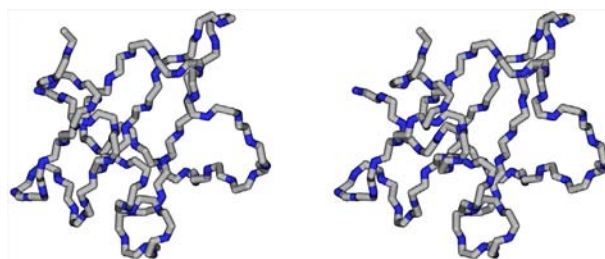
The time of penetration through a barrier by tunneling does not change with temperature, while overcoming it by activation exponentially depends on temperature (see Eq. (8.13)).

However, it should be noted that the exponential dependence of the overcoming time on $\Delta F^\# / RT$ (where $\Delta F^\#$ is the free energy of activation) does not necessarily mean that this time exponentially *decreases* with temperature, as it is often believed (and which is true in chemistry of small molecules): the enthalpy part of activation can be negative (and then the barrier is produced solely by entropy, as it happens, eg, in protein folding), and then the time of the process exponentially *increases* with temperature.

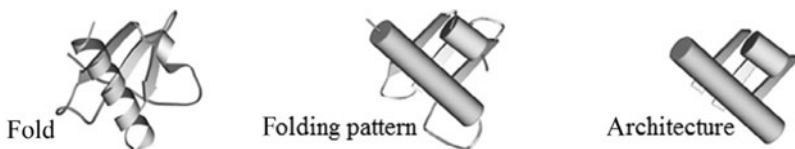
PROBLEM 13.1

The following stereo drawing shows the backbone of a small protein.

Single out secondary structures in it and then simplify the protein structure to the “fold,” then to the “folding pattern,” and finally to the “architecture” (ie, “stack of structural segments”).

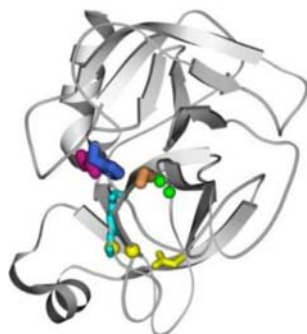


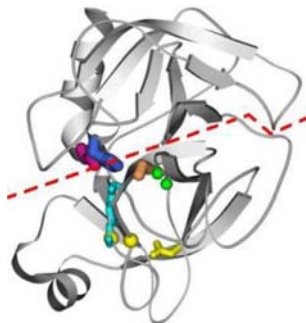
Solution



PROBLEM 13.2

Separate domains in this two-domain protein:



Solution

The separating surface has the minimal number of intersections with the protein backbone.

PROBLEM 14.1

The sequence of secondary structure segments (α and β) as appears to be $\beta\alpha\beta\alpha\beta\alpha\beta\alpha\beta$ in one domain, and $\beta\beta\alpha\beta\beta\beta\alpha\alpha\alpha\alpha$ in another. Which one of them belongs to the class of α/β proteins, and which to the class of $\alpha+\beta$ proteins?

Solution

α/β protein: $\beta\alpha\beta\alpha\beta\alpha\beta\alpha\beta$; $\alpha+\beta$ protein: $\beta\beta\alpha\beta\beta\beta\alpha\alpha\alpha\alpha$.

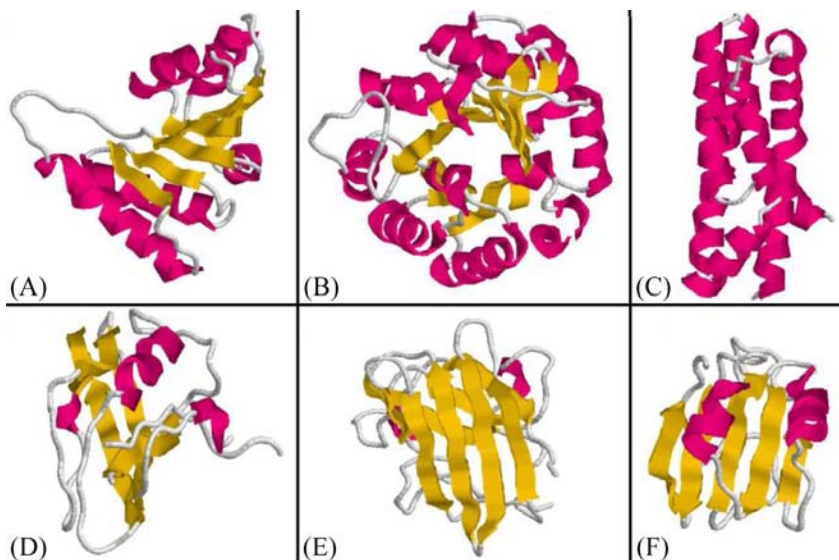
PROBLEM 15.1

Domains shown below belong to water-soluble globular proteins from four main classes (α , β , α/β , $\alpha+\beta$).

To what class does each of them belong?

Solution

- (a) α/β (Rossmann fold); (b) α/β barrel; (c) α bundle; (d) $\alpha+\beta$; (e) β ; (f) $\alpha+\beta$ ($\alpha\beta$ -plait).



PROBLEM 16.1

The *cis*- and *trans*- forms of proline continuously alternate in oligopeptides floating in water. The transition occurs in a second time range, and the experimentally measured ratio of these forms no such transition occurs: proline in a given position in the chain is either always *cis*-, or always *trans*-.

Evaluate the relationship between the *cis*- and *trans*-forms of proline that will be probably be observed in protein globules.

Solution

~1:10 in the order of magnitude (more precisely: protein statistics shows a proportion of $\approx 1:20$); statistics of elements of the native protein globules is similar to the Boltzmann statistics of these elements, taken separately at 300–400 K.

PROBLEM 17.1

Let the “independent melting unit” have two possible states, “0” (SOLID) and “1” (MOLTEN), each being able to bind a certain number of molecules A from solution. State “0” binds n_0 molecules A, and its free energy is $F_0 - n_0\mu_A$ (F_0 being its internal free energy, including that of binding to n_0 molecules A, and $-n_0\mu_A$ accounts for extraction of n_0 molecules A from solution where their

chemical potential is μ_A); state “1” binds $n_0 + \Delta n_A$ molecules A, and its free energy is $F_0 + \Delta F - (n_0 + \Delta n_A)\mu_A$.

Transition of the unit from state “0” to “1” occurs at a constant temperature T by increasing the concentration (and thus, the chemical potential μ_A) of molecules A.

Derive an analog of the van't Hoff criterion for this process.

Solution

Criterion of the “all-or-none” melting by a denaturant: the number of denaturant molecules A absorbed by the melting unit, $\Delta n_A = 4kT/\Delta\mu_A$, equals to $\Delta N_A/N_{\text{PROT}}$, the number of denaturant molecules absorbed by one protein molecule.

Explanation

At given μ_A , Boltzmann probabilities of states “0” and “1” are $P_0 = \frac{1}{1 + \exp\left(-\frac{\Delta F - \Delta n_A \mu_A}{kT}\right)}$ and $P_1 = 1 - P_0$. The value

$\frac{dP_0}{d\mu_A} = -P_0(1 - P_0) \frac{\Delta n_A}{kT}$ shows the rate of change of P_0 with changing μ_A (cf. Eqs. (17.1)–(17.5)). The maximal rate of change occurs at $P_0 = P_1 = \frac{1}{2}$; here, $\frac{dP_0}{d\mu_A} = -\frac{\Delta n_A}{4kT}$. On the other hand, $\frac{dP_0}{d\mu_A} = \frac{\Delta P_0}{\Delta\mu_A} = \frac{-1}{\Delta\mu_A}$, where $\Delta P_0 = -1$ and $\Delta\mu_A$ are changes in P_0 and μ_A values at the transition. Thus, $\Delta n_A \Delta\mu_A = 4kT$.

$\Delta\mu_A$ is known, since one knows at what concentration of A molecules the transition starts and ends. Δn_A is calculated from $\Delta n_A = 4kT/\Delta\mu_A$. Now one has to compare this Δn_A , the number of A molecules absorbed by the melting unit, to $\Delta N_A/N_{\text{PR}}$, the number of molecules A absorbed by one protein molecule (their number in solution being N_{PROT}); if these are equal, the transition is an “all-or-none” one. The number ΔN_A can be found from comparison of numbers of molecules A spent to increase μ_A by $\Delta\mu_A$ in the presence and absence of the protein. If “molecules A” are protons, this approach is called potentiometric titration.

PROBLEM 17.2

A protein undergoes an “all-or-none” melting at a temperature $T^* = 350$ K; the width of the melting range is $\Delta T = 7^\circ$.

What is the difference in the free energies ΔG , enthalpy ΔH and entropy ΔS between the denatured and native states at the melting temperature T^* ?

Solution

$\Delta G = 0$ by definition of the transition point, $\Delta H = 4k(T^*)^2/\Delta T = 4 \times (2 \text{ cal mol}^{-1} \text{ deg}^{-1} \times 350^\circ) \times (350^\circ/7^\circ) = 140 \text{ kcal mol}^{-1}$, $\Delta S = \Delta H/T^* = 140 \text{ kcal mol}^{-1}/350^\circ = 400 \text{ cal mol}^{-1} \text{ deg}^{-1}$.

PROBLEM 17.3

A protein catalyzes the chemical reaction producing $\delta E = 100 \text{ kcal mol}^{-1}$ per one reaction act. It is assumed that all this energy does not dissipate from the protein, and that the protein has 2000 internal elastic degrees of freedom.

What is the increase δT in temperature of this protein?

Solution

Heat capacity of one elastic degree of freedom is $k \approx 2 \text{ cal K}^{-1} \text{ mol}^{-1}$ (see Problem 8.1). Thus, the protein's heat capacity is $C = 2000k \approx 4 \text{ kcal K}^{-1} \text{ mol}^{-1}$ (which corresponds to a heat capacity of $0.4 \text{ cal K}^{-1} \text{ g}^{-1}$ for the protein of about 14 kDa shown in Fig. 17.2), and, since $C \cdot \delta T = \delta E$, then $\delta T \approx 25^\circ$ (if the energy does not dissipate!).

PROBLEM 17.4 (DIFFICULT)

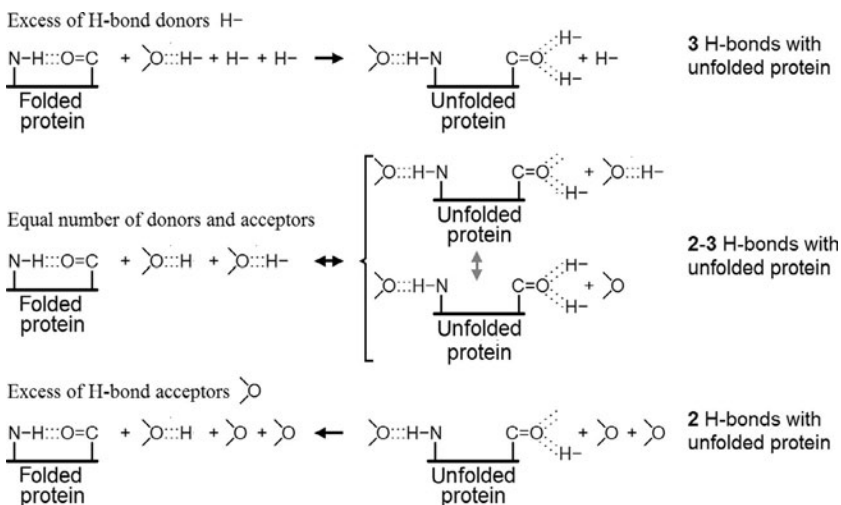
The commonly used protein denaturants, urea ($\text{NH}_2\text{—CO—NH}_2$) and guanidine hydrochloride ($[(\text{NH}_2)_3\text{C}]^+\text{Cl}^-$), have excess NH_2 groups, while many “renaturants” (substances which increase stability of protein structures), eg, Na_2SO_4 and (saccharides, have excess O atoms or OH groups).

Can you qualitatively explain this difference?

Solution

A peculiarity of H-bonding is that each H atom is able to form only one H-bond, and each O atom—two (see ice in Fig. 4.1). But, inside the secondary structure, the O-atom of C=O group has only one hydrogen bond. And the H-bonded secondary structure atoms, $\text{C=O}:::\text{H—N}$, lie on a straight line (and are often immersed in the globule), which hinders other bindings of the acceptor C=O to the H-bond donor of the solvent. However, when the $\text{C=O}:::\text{H—N}$ binding inside the protein is broken, the O atom of the C=O group can receive this additional H-bond.

Just this ability to attract an additional donor (not acceptor!) from the solvent leads to different action of the additional NH_2 groups (donors) and O atoms (acceptors) added to solution, as it is illustrated by a diagram below.



This is a rough qualitative explanation only. For a quantitative one, let us consider the following model. It assumes that the solution contains many H-bond donors H^- and acceptors O^- ; some of donors and acceptors are free, while others are H-bonded ($-O^-H^-$).

Each H-bond of the protein, being disrupted upon unfolding, attracts from solution two H-bond donors H^- and one acceptor O^- . To be attracted, these must be free from H-bonds in solution. Therefore, the attraction changes the free energy of the disrupted H-bond by

$$\Delta G = \Delta E_3 - (2\mu_{H^-} + \mu_{O^-}) \quad (17.4.1)$$

where ΔE_3 is the energy of formation of three H-bonds, while μ_{H^-} and μ_{O^-} are chemical potentials of the free donors and acceptors in solution.

The value ΔE_3 , being internal energy of the bonds, does not depend on concentration of free or H-bonded donors or acceptors.

The value $-(2\mu_{H^-} + \mu_{O^-})$ changes with concentrations of H^- and O^- . It can be presented as $-1.5(\mu_{H^-} + \mu_{O^-}) - 0.5(\mu_{H^-} - \mu_{O^-})$.

The value $\mu_{H^-} + \mu_{O^-}$ is equal to the chemical potential of an H-bonded dimer $-O^-H^-$. Since virtually all donors and acceptors are assumed to be in this form in solution, its chemical potential $\mu_{-O^-H^-}$ virtually does not depend on a small admixture of H^- and O^- . As a result of dynamic equilibrium between free (H^-, O^-) and H-bonded ($-O^-H^-$) donors and acceptors in solution, the sum of their chemical potentials must obey the equation $\mu_{H^-} + \mu_{O^-} = \mu_{-O^-H^-}$ (which corresponds to the old good law of mass action); that is, this sum virtually does not depend on a small admixture of H^- and O^- .

Chemical potentials of admixtures obey equations $\mu_{H^-} = kT \cdot \ln [C_{H^-}] + \mu_{H^-}^0$, $\mu_{O^-} = kT \cdot \ln [C_{O^-}] + \mu_{O^-}^0$ derived for dilute solutions (see [Problem 8.6](#)). Therefore, their difference is $\mu_{H^-} - \mu_{O^-} = kT \cdot \ln [C_{H^-}/C_{O^-}] + \text{const}$, where const virtually does not depend on concentration of H^- and O^- admixtures.

As a result, the attraction of H-bond donors and acceptors from solution changes the free energy of the disrupted protein H-bond by

$$\Delta G = -kT \cdot \ln [C_{\text{H}-}/C_{\text{O}-}] + \text{const}' \quad (17.4.2)$$

This equation shows that addition of extra donors (eg, NH₂ groups) to water solution decreases the free energy of a disrupted intra-protein H-bond (and thus, *destabilizes* its bonded state), while addition of extra acceptors (eg, O atoms) to water solution *stabilizes* this intra-protein H-bond to the same extent.

For a more detailed analysis, see Problems 17.6 and 17.7 in the last Russian edition of this book: Finkelstein, A.V., Ptitsyn, O.B., 2012. *Protein Physics. A Course of Lectures with Color and Stereoscopic Illustrations and Problems with Solutions*, 4th extended edition (in Russian). Publishing House “Universitet,” Moscow, but you will have to read it in Russian of course!

PROBLEM 18.1

Experiments on single-molecule protein denaturation by force are conducted as follows. One end of the molecule is chemically bound to the template, the other—to the cantilever of the atomic force microscope, and the cantilever-applied force unfolds the protein.

Estimate the force necessary to unfold the protein of 100 amino acid residues, the native state stability of which (as compared with the coil) is 10 kcal mol⁻¹. The observation time is not limited.

Solution

For protein unfolding, it is necessary to use work $A=10 \text{ kcal mol}^{-1}$. This work must be expended on the path ΔL equal to the difference between the linear dimensions of the extended coil and the protein globule, ie, $\Delta L \approx 350 \text{ \AA} - 40 \text{ \AA} \approx 300 \text{ \AA}$. The force $F=A/\Delta L$ (10 kcal mol^{-1})/ $300 \text{ \AA} \approx (42 \times 10^3 \text{ J/6} \times 10^{23})/(300 \times 10^{-10} \text{ m}) \approx 2 \times 10^{-12} \text{ N} = 2 \text{ pN}$.

PROBLEM 18.2

Suppose that the number of 3D folds that are in principle possible for chains consisting of N links is M , and these folds are assumed to be equal in terms of the opportunity to be optimal for at least some of the sequences (having the same compactness, secondary structure content, etc.).

What number K of the sorts of links allows the chain to have only one 3D structure with the minimal energy?

Solution

$$K \geq M^{1/N}$$

With K sorts of links, a chain of N links has K^N possible sequences. If $K^N < M$, and each sequence has only one optimal fold, these K^N optimal folds

cannot cover all the M possible folds (which are assumed to be equal in terms of opportunity to be optimal for at least some of the sequences). This contradiction shows that K^N must exceed M .

PROBLEM 19.1

A protein existing in water by 15° below its melting temperature is heated by 25° as a result of the chemical reaction that it has catalyzed. Will this protein melt?

Solution

No. To denature, a protein has to overcome a free energy barrier, and this takes at least microseconds (but rather seconds). But thermal energy will dissipate much faster, it takes picoseconds.

Explanation

In a given medium, heat flow is proportional to the temperature difference, gradient of temperature and the surface of the cooling object. For a 3D object, the latter is roughly proportional to its diameter (because this is the only parameter with the dimension of length in this Problem), while the temperature gradient is roughly inversely proportional to this diameter. Thus, at a given temperature difference between the body and the medium, the flow is proportional to the object's diameter, while the heat contained in the object is proportional to its volume, ie, its diameter cubed. As a result, the time necessary to lose this heat is proportional to the diameter squared.

Now, everybody knows that cooling of an egg in water takes about a minute (true: in water, this process is accelerated by convection; but convection does not change the rate of cooling by many orders of magnitude: in a very viscous porridge, cooling also takes minutes—check!). The egg has centimeters in diameter, a protein—nanometers, which makes a seven orders of magnitude difference. Thus, the time of cooling down of the protein (being proportional to the diameter squared) is by 14 orders of magnitude shorter than the time of cooling down of the egg: picoseconds instead of minutes. (By the way, it is close to the time of dissipation of kinetic energy, see Eq. (8.24), which is not a wonder.)

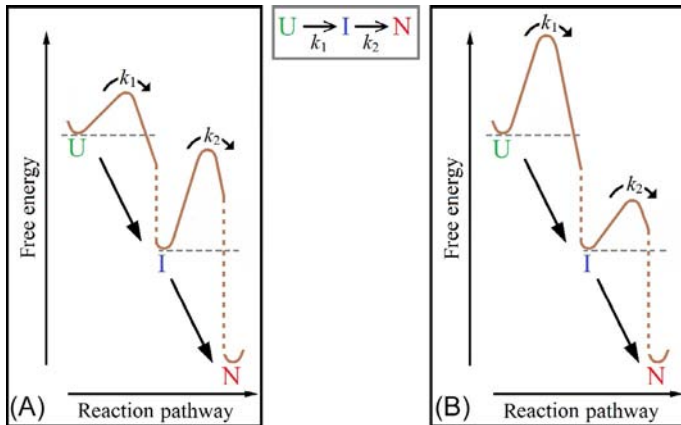
PROBLEM 20.1

Consider the irreversible three-state transition $U \rightarrow I \rightarrow N$ and outline the change of populations of states U , I , N when the rate constant k_1 for the $U \rightarrow I$ transition is

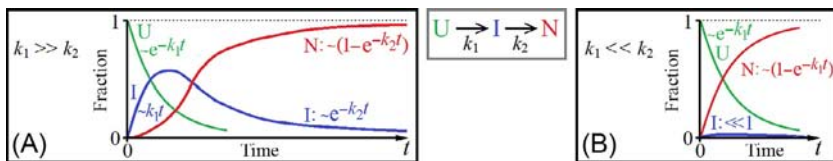
- (a) much *higher* than the rate constant k_2 for the $I \rightarrow N$ transition;
- (b) much *lower* than the rate constant k_2 for the $I \rightarrow N$ transition.

Solution

I would recommend to start solving such a problem with drafting a free-energy profile for the considered transition:



(here, the dashed lines symbolize an infinite—by definition—free energy decrease during the irreversible transition). Then the answer becomes obvious:



- (a) When $k_1 \gg k_2$: fast transition from U to I , and then slow transition from I to N ; in-between, state I accumulates. This process has two observable characteristic times: $1/k_1$ (fast decay of U and formation of I ; a small growth of N occurring during this period shows a quadratic dependence on time); and $1/k_2$ (slow formation of N from I which decays exponentially).
- (b) When $k_1 \ll k_2$: transition from U to I is accompanied by immediate transition from I to N ; thus, state I does not accumulate. This process has only one observable characteristic time: $1/k_1$. (For more details, see Nölting, B., 2010. *Protein Folding Kinetics: Biophysical Methods*. Springer, New York (Chapters 4 and 10)).

PROBLEM 20.2

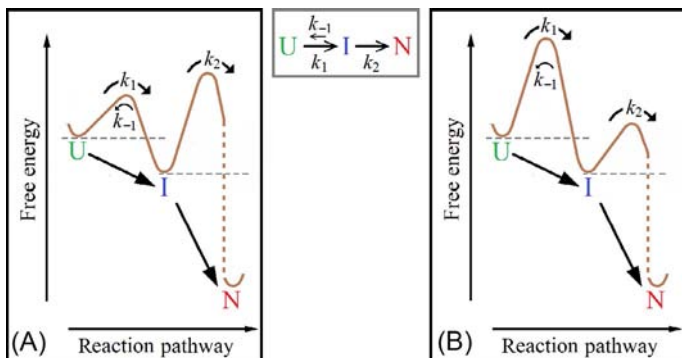
Consider the three-state transition $U \leftrightarrow I \rightarrow N$ (where the $I \rightarrow N$ transition is irreversible, while the $U \leftrightarrow I$ transition is reversible, and I is *more* stable than U , ie, the rate constant k_1 for the $U \rightarrow I$ transition is much *higher* than the rate

constant k_{-1} for the reverse $U \leftarrow I$ transition) and outline the change of populations of states U , I , N when the rate constant k_1 for the $U \rightarrow I$ transition is

- (a) much *higher* than the rate constant k_2 for the $I \rightarrow N$ transition;
- (b) much *lower* than the rate constant k_2 for the $I \rightarrow N$ transition.

Solution

Problem 20.1 is no more than the extreme case of this Problem (because irreversibility of the $U \rightarrow I$ transition in **Problem 20.1** implies that I is infinitely more stable than U):



Therefore, the answer to this Problem is essentially the same as the answer to **Problem 20.1**.

PROBLEM 20.3 (MORE DIFFICULT)

Consider the three-state transition $U \leftrightarrow I \rightarrow N$ (where the $I \rightarrow N$ transition is irreversible, while the $U \leftrightarrow I$ transition is reversible, and I is *less* stable than U , ie, the rate constant k_1 for the $U \rightarrow I$ transition is much *lower* than the rate constant k_{-1} for the reverse $U \leftarrow I$ transition) and outline the change of populations of states U , I , N when the rate constant k_1 for the $U \rightarrow I$ transition is

- (a) much *higher* than the rate constant k_2 for the $I \rightarrow N$ transition;
- (b) much *lower* than the rate constant k_2 for the $I \rightarrow N$ transition.

Solution

- (a) When $k_1 \gg k_2$, there is a fast transition from U to I (and even faster from U to I , since I is less stable than U), and a much slower transition from I to N . Thus, to the first approximation, we may consider a rapidly emerged Boltzmann distribution in the system $U \leftrightarrow I$. In this case,

$$(\text{Population of } U) \times k_1 = (\text{Population of } I) \times k_{-1}$$

where $k_{-1} \ll k_1$ is the rate constant of transition $I \rightarrow U$. Thus,

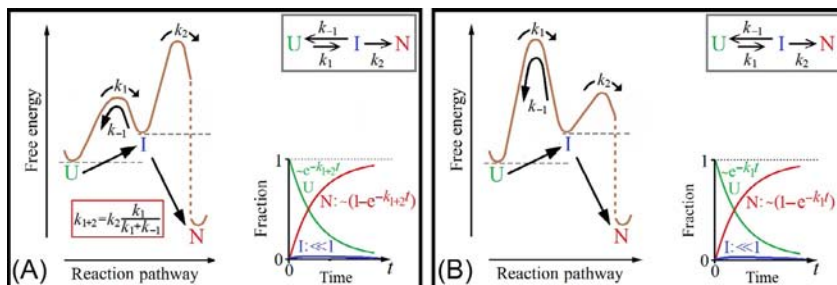
$$(\text{Population of } I) = (\text{Population of } U + \text{Population of } I) \times [k_1/(k_1 + k_{-1})]$$

and the rate of the flow over the last (the highest) free energy barrier is

$$\begin{aligned} (\text{Population of } I) \times k_2 &= (\text{Population of } U + \text{Population of } I) \\ &\quad \times [k_2 k_1 / (k_1 + k_{-1})] \end{aligned}$$

which means that $k_{1+2} = k_2 k_1 / (k_1 + k_{-1}) \approx k_2 - k_2 k_{-1} / k_1$ is the rate constant of the transition from $(U+I)$ to N .

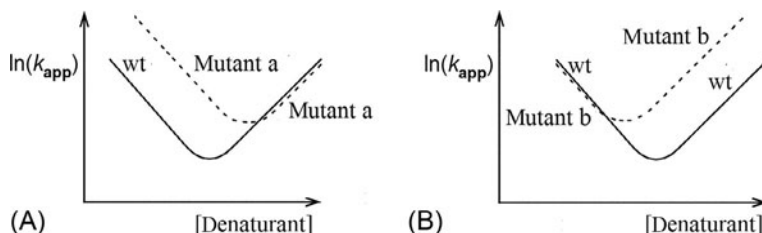
Thus, after a very short time of equilibration of U and I , the process is described by a single-exponential kinetics with the rate constant $k_{1+2} = k_2 k_1 / (k_1 + k_{-1})$, and the low-populated intermediate I is virtually invisible; see panel (a) in the scheme below. This process has only one observable characteristic time: $1/k_{1+2}$.



- (b) When $k_1 \ll k_2$, there is a slow transition from U to I (followed by a fast escape of molecules from I to N), which gives virtually the same kinetics as in the cases (b) in [Problems 20.1](#) and [20.2](#). This process also has only one observable characteristic time: $1/k_1$.

PROBLEM 20.4

Consider a protein where mutations of two different amino acid residues gave the chevron shifts relative to the “wild-type” (wt) chevron shown in the panels (a), (b), respectively.



What can we say about the involvement of these residues in the protein folding nucleus?

Solution

- (a) The shift of the chevron plot in “a” indicates a change in the folding rate (k_f) and no change in the folding rate (k_u) of the protein. Hence, the mutation affects stability of the folding nucleus, as well as stability of the native protein structure defined by the ratio k_f/k_u . So, the first residue is involved in the nucleus.
- (b) The opposite shift of the chevron plot in “b” indicates that the other residue is not involved in the nucleus.

PROBLEM 21.1

The protein undergoes an “all-or-none” transition from the unfolded to native state at room temperature; the rate of its folding is 3 s^{-1} , and the native state is more stable than the unfolded one by $7.5 \text{ kcal mol}^{-1}$.

- (a) What is the characteristic residence time of the protein (after folding) in the native state?
- (b) What is the characteristic residence time of the protein (after unfolding) in the unfolded state?
- (c) What does the folding-unfolding process look like in the given conditions, if we observe a single protein molecule for a long time?

Solution

- (a) About a day. If the native state is more stable than the unfolded one by $7.5 \text{ kcal mol}^{-1}$ at room temperature, protein unfolding is by $\exp[(7.5 \text{ kcal mol}^{-1})/(0.6 \text{ kcal mol}^{-1})] = 2.5 \times 10^5$ slower than folding. So, the unfolding rate is $(3 \text{ s}^{-1})/(2.5 \times 10^5) \approx 1/(83,000c)$: once a day.
- (b) About $1/(3 \text{ s}^{-1}) = 0.33 \text{ s}$.
- (c) ... about 0.3 s stay in the unfolded state—almost instantaneous folding—about a day stay in the folded state—almost instant unfolding—about 0.3 s stay in the unfolded state—almost instantaneous folding—...

PROBLEM 21.2 (MORE DIFFICULT)

The free energy of a cubic crystal emerging in solution is represented in a form

$$F = Mf + 6M^{2/3}\psi \quad (21.2.1)$$

where M is the number of molecules in the emerging crystal, f is the free energy of a molecule inside the crystal phase (as compared with that in the melt), ψ is the additional free energy of a molecule at the crystal surface.

Assuming, for simplicity, that the characteristic time τ of molecule joining to the growing crystal is independent of the crystal size or the shape of the surface—evaluate the characteristic time t_{init} of crystal initiation at a given

space point and connect the t_{init} estimate to the number of molecules M_{st} in a stable crystal of the minimal size. Obtain numerical evaluations at room temperature if $\tau = 10^{-11}$ s, $\psi = 0.3 \text{ kcal mol}^{-1}$, and (a) $f = -0.2 \text{ kcal mol}^{-1}$ or (b) $f = -0.1 \text{ kcal mol}^{-1}$.

Solution

From $F = Mf + 6M^{2/3}\psi = 0$, the minimal number of molecules in a stable crystal is $M_{\text{st}} = [6\psi/(-f)]^{3/2}$.

From $d(Mf + 6M^{2/3}\psi)/dM = 0$, the size of a critical nucleus of the crystal is $M_1 = [4\psi/(-f)]^{3/2} = 8/27 M_{\text{st}}$, and its free energy is $\Delta F^\# = 2\psi(M_1)^{2/3} = 8/9\psi(M_{\text{st}})^{2/3}$.

The characteristic time of crystal initiation at a given space point is

$$t_{\text{init}} = \tau \exp \left[+ \Delta F^\# / kT \right] = \tau \cdot \exp \left(\frac{8\psi}{9kT} M_{\text{st}}^{2/3} \right)$$

Numerical estimates at $T = 300 \text{ K}$ (ie, $kT = 0.6 \text{ kcal mol}^{-1}$), $\psi = 0.3 \text{ kcal mol}^{-1}$, $\tau = 10^{-11} \text{ s}$:

- (a) When $f = -0.2 \text{ kcal mol}^{-1}$, $M_{\text{st}} = 9^3 = 729$, $t_{\text{init}} = 10^{-11} \text{ s} \times \exp[4/9 \times 9^2] \sim 10^5 \text{ s}$, $t_{\text{trans}} = 10^{-11} \text{ s} \times \exp[2/9 \times 9^2] \sim 10^{-3} \text{ s}$.
- (b) When $f = -0.1 \text{ kcal mol}^{-1}$, $M_{\text{st}} = 18^3 = 5832$, $t_{\text{init}} = 10^{-11} \text{ s} \times \exp[4/9 \times 18^2] \sim 10^{52} \text{ s}$, $t_{\text{trans}} = 10^{-11} \text{ s} \times \exp[2/9 \times 18^2] \sim 10^{20} \text{ s}$.

The latter estimate shows that near the point of liquid-crystal equilibrium crystallization can occur actually only when there is some heterogeneity or impurity to facilitate it.

PROBLEM 22.1

Which of the below sequences is typical for an α -helical fibrous protein? for a β -structural fibrous protein? For a β -structural globular protein? For an irregular loop in a globular protein? for an intrinsically disordered protein? for collagen? For an α -helix in a membrane protein?

- (a) –Gly–Ala–Gly–Thr–Gly–Ala–Gly–Thr–Gly–Ala–
- (b) –Gly–Ala–Pro–Gly–Pro–Pro–Gly–Thr–Pro–Gly–Ala–Pro–Gly–Pro–Pro–
- (c) –Gly–Ala–Glu–Ser–Leu–Gly–Lys–Asn–Ala–Glu–Ser–Leu–Gly–Arg–Gly–Ala–Glu–
- (d) –Lys–Ser–Gly–Gly–Gly–Gly–Gly–Gly–Gly–Ser–Ser–
- (e) –Thr–Ala–Phe–Ser–Leu–Gly–Gly–Met–Leu–Ala–His–Leu–Ala–Gln–Gly–Ala–Asn–
- (f) –Gly–Thr–Val–Thr–Ile–Ala–Val–Thr–Gly–Ala–
- (g) –Gly–Met–Ala–Asp–Arg–Glu–Gln–Lys–Asn–Gln–Lys–Pro–Arg–Gly–

Solution

- (a) β -Structural fibrous protein; period 2 for alternation of small Gly and larger residues:

—Gly—Ala—Gly—Thr—Gly—Ala—Gly—Thr—Gly—Ala—

- (b) Collagen; repeats of triplets of the Gly—X—Pro kind:

—Gly—Ala—Pro—Gly—Pro—Pro—Gly—Thr—Pro—Gly—Ala—Pro—Gly—
Pro—Pro—

- (c) α -Helical coiled-coil in fibrous protein; period $3.5 \times 2 = 7$ for alternation of hydrophobic and hydrophilic residues (including many charged residues in positions 0–4, 0–3):

—Gly—Ala—Glu[—]—Ser—Leu—Gly—Lys⁺—Asn—Ala—Glu[—]—Ser—Leu—Gly—
Arg⁺—Gly—Ala—Glu[—]—

- (d) Intrinsically disordered protein; multiple repeat of a residue:

—Lys—Ser—Gly—Gly—Gly—Gly—Gly—Gly—Gly—Ser—Ser—

- (e) α -Helix in a membrane protein; period $3.5 \times 2 = 7$ for alternation of many hydrophobic and a few non-hydrophobic residues:

—Thr—Ala—Phe—Ser—Leu—Gly—Gly—Met—Leu—Ala—His—Leu—Ala—
Gln—Gly—Ala—Asn—

- (f) β -Structure in a globular protein; many branched and hydrophobic residues:

—Gly—Thr—Val—Thr—Ile—Ala—Val—Thr—Gly—Ala—

- (g) Irregular loop; does not have the above-mentioned peculiarities:

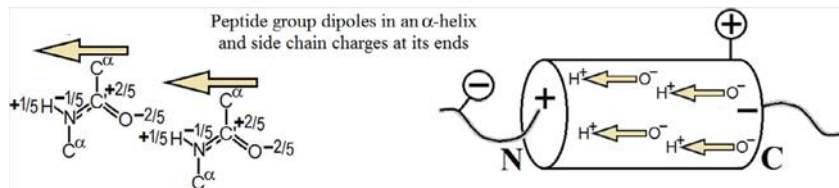
—Gly—Met—Ala—Asp—Arg—Glu—Gln—Lys—Asn—Gln—Lys—Pro—Arg—Gly—

PROBLEM 22.2

Estimate electrostatic interaction of charged side chains with ends of an α -helix in pure water and in 0.1 M solution of NaCl.

Solution

H, N, C' and O atoms of a peptide group have partial charges; therefore, the peptide group contains a dipole. In an α -helix all peptide dipoles moments point in the direction of the helix axis. The dipole moment of an individual peptide unit is about 3.46 Debye which equals $0.72 e \times \text{\AA}$ or $0.5 e \times 1.5 \text{\AA}$; 1.5 Å is the axial shift per residue in an α -helix. Inside the helix, all dipoles cancel out except for the C- and N-terminal ones. Thus, the N-terminus of the helix has a charge of $+0.5 e$, and the C-terminus a charge of $-0.5 e$.



The distance between the helix termini and the side chain charges of the neighbor amino acid residues is $\approx 5 \text{ \AA}$. Thus, the free energy of electrostatic interaction of charged side chains with the helix ends is $\approx 0.5 e \times 1 e/5 \text{ \AA} \approx 0.4 \text{ kcal mol}^{-1}$ in pure water, while in 0.1 M NaCl solution (with ionic strength $I = 0.1 \text{ M}$) the Debye–Hückel radius $D \approx \frac{3}{I^{1/2}} \text{ \AA} \approx 9 \text{ \AA}$, and the free energy of the “charged side chain-helix terminus” electrostatic interaction is $\approx 0.4 \text{ kcal mol}^{-1} \times \exp(-5 \text{ \AA}/9 \text{ \AA}) \approx 0.25 \text{ kcal mol}^{-1}$. (Actually, the energy may be somewhat higher due to reflection of the electric field from a helix of low permittivity, see Fig. 6.2, but consideration of this effect is out of the scope of this Problem.)

The electrostatics attracts negatively charged side chains to the N-terminus and repulses them from the C-terminus, while it attracts positively charged side chains to the C-terminus and repulses them from the N-terminus.

PROBLEM 23.1

Suppose that a protein structure prediction program contains errors in estimating the chain fold energies, and the errors are such that the probability to have an erroneous ΔE in the fold energy calculation obeys the Gaussian law: $P(\Delta E) = (2\pi\sigma^2)^{-1/2} \times \exp[-\Delta E^2/2\sigma^2]$, and the errors in calculation of energies of different folds are independent of one another.

Such a calculation perfectly distinguishes two structures whose actual energies differ by 10σ : a probability that calculations confuse the low- and high-energy structure is $\approx e^{-25} \approx 10^{-11}$.

Suppose now that we need to compare the energies of as many as $M \gg 1$ such structures and energy of one of them is by 10σ lower than that of all others.

At what number M the calculation will fail to single out the structure having the lowest actual energy?

Solution

Let the actual energy of the lowest-energy structure be 0, and the actual energy of each of the others be 10σ . The spectrum of calculated energies of $M - 1$ high-energy structures stretches (see Appendix D) from $\approx 10\sigma - \sigma(2 \ln M)^{1/2}$ to $\approx 10\sigma + \sigma(2 \ln M)^{1/2}$. If $10\sigma - \sigma(2 \ln M)^{1/2} \leq 0$, the calculated energy of at least one of the actually high-energy structures will appear below the calculated

energy of the actually lowest-energy structure. Thus, the critical value of M is obtained from the equation

$$10\sigma - \sigma(2 \ln M)^{1/2} = 0$$

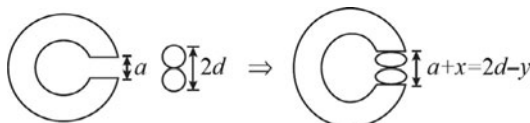
Result: $M > e^{50}$, the calculation fails to single out the structure having the lowest actual energy.

Because $e^{50} \approx 2^{70}$, while each amino acid residue has at least two possible conformations, the obtained estimate shows that calculations with the above described errors will cease revealing the actually most stable structure for the chain of more than 70 residues.

PROBLEM 24.1

Consider two molecules (having to form a chemical bond); suppose, they are drawn into the crevice (“active site”) of the protein at the expense of the absorption energy. In the scheme below, these molecules are shown as small balls having the diameter d , and the crevice has the initial width a . If $a < 2d$, the molecules are squeezed (which favors bond formation) and the crevice is widened. Both the protein and the molecules are assumed to be elastic (the balls only up to a certain extent, after which they form a chemical bond). Let the protein’s elasticity coefficient be k_{pr} , and the ball elasticity coefficient be k_{mol} .

The question is: what energy is spent to deform the balls (only this energy can be used to overcome the energy barrier that hinders spontaneous merging of the molecules), and what enzyme—soft or rigid—can concentrate more of the absorption energy on deformation of the molecules?



Solution

The crevice width grows from a to $a+x$ under the pressure from the balls. The height of the two-ball column shrinks from $2d$ to $2d-y=a+x$ under the pressure from the crevice; thus,

$$x+y=2d-a \quad (24.1.1)$$

According to Newton’s third law, the pressures to and from protein are equal; that is,

$$K_{pr}x=k_{mol}y \quad (24.1.2)$$

The absorption supplies energy to deform the molecules *and* protein. According to Hooke’s law, the energy spent on deformation of protein is $E_{pr}=k_{pr}x^2/2$, and the energy spent on deformation of the molecules is $E_{mol}=k_{mol}y^2/2$. Thus,

$$\begin{aligned} E_{\text{mol}}/E_{\text{pr}} &= (k_{\text{mol}}y^2/2)(k_{\text{pr}}x^2/2) = (1/2k_{\text{mol}})(k_{\text{mol}}y)^2/(1/2k_{\text{pr}})(k_{\text{pr}}x)^2 \\ &= k_{\text{pr}}/k_{\text{mol}} \end{aligned} \quad (24.1.3)$$

Thus, the energy is shared inversely to rigidity.

Obtaining x and y from Eqs. (24.1.1) and (24.1.2), we have:

$$E_{\text{mol}} = \frac{k_{\text{mol}}}{2} \times \left((2d - a) \frac{k_{\text{pr}}}{k_{\text{pr}} + k_{\text{mol}}} \right)^2 \quad (24.1.4)$$

Thus, if the protein is “soft” ($k_{\text{pr}} \ll k_{\text{mol}}$) the main energy is spent to deform it and it is useless in catalysis. Only a “rigid” protein (with $k_{\text{pr}} \gg k_{\text{mol}}$) can concentrate most of the absorption energy on deformation of molecules.

Thus, an efficient enzyme must be rigid.

PROBLEM 24.2

One act of enzymatic catalysis takes a microsecond or more. Can the energy released at substrate binding be stored for catalysis as kinetic energy of moving parts of the enzyme, for example, as the energy of its vibration?

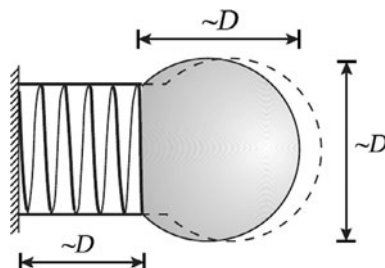
Solution

This is not possible.

One part of a protein moves about another in some viscous environment such as water or membrane. This movement is described by the usual equation

$$m(d^2x/dt^2) = F_{\text{frict}} + F_{\text{elast}} \quad (24.2.1)$$

Here m is the particle’s mass, d^2x/dt^2 is acceleration, F_{frict} is the force of friction, and F_{elast} is the elasticity force. The mass can be estimated as $m = \rho V$, where ρ is the particle’s density and V is its volume. The friction force $F_{\text{frict}} = -3\pi D\eta(dx/dt)$, or $\approx 10D\eta(dx/dt)$ according to Stokes’ law, where η is the viscosity of the medium, dx/dt is the particle’s velocity, and D is the particle’s diameter. The F_{elast} value can be estimated (from Hooke’s law) as $\approx -(ES/L)x$, where x is displacement from the equilibrium point, S is the cross-section of an elastic joint between two parts of the protein, L is the length of this joint, and E is the elasticity module. It is reasonable to assume, for the sake of simplicity, that all the linear dimensions are close (see the scheme below), so that $L \approx D$, $S \approx D^2$, $V \approx D^3$.



Eq. (24.2.1) determines two characteristic times.

One, the most important, we have already discussed in Lecture 8. This is t_{kinet} , the time of friction-caused damping of the movement. It can be estimated from the “kinetic” part of Eq. (24.2.1): $m(d^2x/dt^2) \approx -3\pi D\eta(dx/dt)$. The estimate is: $t_{\text{kinet}} = m/(3\pi D\eta) \approx 0.1\rho D^2/\eta$, since $m \approx \rho D^3$, and $3\pi \approx 10$. As $\rho \approx 1 \text{ g cm}^{-3}$ for all the molecules we deal with, and $\eta \approx 0.01 \text{ g cm}^{-1} \text{ s}^{-1}$ for water, $t_{\text{kinet}} \approx 10^{-13} \text{ s} \times (D/\text{nm})^2$, where (D/nm) is the particle’s diameter expressed in nanometers.

This means that the kinetic energy of a small part of protein ($D \approx 1 \text{ nm}$) dissipates in water within $\sim 10^{-13} \text{ s}$, and of a large protein ($D \approx 10 \text{ nm}$) in $\sim 10^{-11} \text{ s}$. In a more viscous environment, eg, in a membrane, the kinetic energy dissipation is proportionally faster.

Thus, kinetic energy cannot “survive” even a nanosecond!

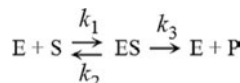
Another characteristic time is that of protein vibrations, t_{vibr} . Its value follows from the “oscillation” part of Eq. (24.2.1): $m(d^2x/dt^2) \approx EDx$: $t_{\text{vibr}} \approx (m/ED)^{1/2} \approx D(\rho/E)^{1/2}$. A value of the elasticity module typical for plastics, $E \sim 10^{10} \text{ g cm}^{-1} \text{ s}^{-2}$, can be taken for proteins. This gives $t_{\text{vibr}} \approx 10^{-12} \text{ s} \times (D/\text{nm})$.

Comparing $t_{\text{kinet}} \approx 0.1\rho D^2/\eta \approx 10^{-13} \text{ s} \times (D/\text{nm})^2$ to $t_{\text{vibr}} \approx D(\rho/E)^{1/2} \approx 10^{-12} \text{ s} \times (D/\text{nm})$, we see that oscillations are absolutely impossible for proteins with $D < 10 \text{ nm}$: they would be damped by friction before the first oscillation occurs even in water, not to mention more viscous environments like membrane.

This means that the energy released during substrate binding dissipates and converts into heat long before it can be of any use for catalysis.

PROBLEM 24.3

The simplest model of the enzymatic reaction kinetics (Michaelis-Menten model) interprets this reaction as a reversible formation of intermediate ES from the free substrate S and enzyme E, followed by irreversible conversion of S from ES into the product P that leaves the enzyme:



Find the dependence of the rate of the product P formation on the total concentration of the substrate $[S]_T \equiv [S] + [\text{ES}]$ and enzyme $[E]_T \equiv [E] + [\text{ES}]$ in solution. Assume that the substrate concentration is much higher than that of the enzyme.

Solution

In the stationary approximation (which is valid when $[\text{ES}] \ll [S]$),

$$d[\text{ES}]/dt = [\text{E}] \times [\text{S}]k_1 - [\text{ES}]k_2 - [\text{ES}]k_3 = 0 \quad (24.3.1)$$

Therefore,

$$[ES] = [E] \times [S]/K_M \quad (24.3.2)$$

where

$$K_M = (k_2 + k_3)/k_1 \quad (24.3.3)$$

is called the Michaelis constant.

Since the enzyme concentration is low, $[E] < [E]_T \ll [S]$, $[ES] \ll [S]$, and $[S] \approx [S]_T \equiv [S] + [ES]$, while $[E]$ may be substantially exceeded by $[E]_T \equiv [E] + [ES]$. Substituting $[E] \equiv [E]_T - [ES]$ in Eq. (24.3.2), one obtains $K_M[ES] = ([E]_T - [ES]) \cdot [S]_T$, and further

$$[ES] = [E]_T \times [S]_T / ([S]_T + K_M)$$

Finally, the rate of product formation is

$$d[P]/dt = [ES] \times k_3 = k_3 \times [E]_T \times [S]_T / ([S]_T + K_M) \quad (24.3.4)$$

Note that half of the enzyme is involved in the ES at $[S] = K_M$ and that $V_{\max} = k_3 \cdot [E]_T$ is the maximal rate of product formation which is achieved with the excess substrate, ie, when $[S]_T \gg K_M$.

PROBLEM 24.4

Derive an equation describing kinetics of the reaction described by the Michaelis-Menten model (Problem 24.3) assuming that $[E] \ll [S]_T$ and $[ES] \ll [S]_T \equiv [S] + [ES]$.

Solution

Since the sum of total concentrations of the product ($[P]$) and substrate ($[S]_T$) is constant, $[S]_T + [P] = [S]_0 = \text{const}$, so that $d[S]_T/dt = d[P]/dt$, Eq. (24.3.4) can be presented as

$$d[S]_T/dt = -V_{\max} \times [S]_T / ([S]_T + K_M) \quad (24.4.1)$$

where $V_{\max} = k_3 \cdot [E]_T$ and $K_M = (k_2 + k_3)/k_1$. This leads to

$$d[S]_T + K_M \times \ln([S]_T) = -V_{\max} \times dt$$

then to

$$[S]_T + K_M \times \ln([S]_T) = -V_{\max} \times t + \text{CONST}$$

and

$$[S]_T - [S]_0 + K_M \times \ln([S]_T/[S]_0) = -V_{\max} \times t$$

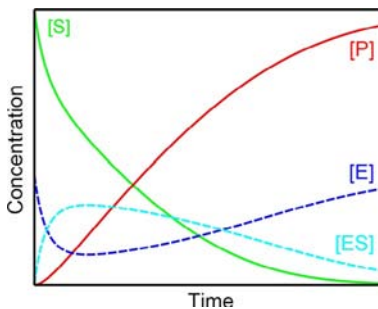
where $[S]_0 = [S]_T(t=0)$, and finally to

$$[\text{S}]_T/K_M + \ln([\text{S}]_T/[\text{S}]_0) = [\text{S}]_0/K_M - (V_{\max}/K_M) \times t \quad (24.4.2)$$

thus,

$$\frac{[\text{S}]_T}{[\text{S}]_0} \exp\left(\frac{[\text{S}]_T}{K_M}\right) = \exp\left(\frac{[\text{S}]_0 - V_{\max} \cdot t}{K_M}\right) \quad (24.4.2)$$

Below: a scheme of the change of $[\text{ES}] = \frac{\{E\}_T \{S\}_T}{\{S\}_T + K_M}$, $[\text{S}] = [\text{S}]_T - [\text{ES}]$, $[\text{E}] = [\text{E}]_T - [\text{ES}]$, $[\text{P}] = [\text{S}]_0 - [\text{S}]_T$ with time (taken from https://en.wikipedia.org/wiki/Michaelis-Menten_kinetics).



PROBLEM 25.1

What is the electric field strength at the surface of a multicharged ion like Zn^{2+} ?

Solution

According to Pauling, Zn^{2+} ionic radius is $r = 0.74 \text{ \AA}$. Thus, the electric field strength at its surface is $2e/r^2 = (2/0.74^2) \times e/(1 \text{ \AA}^2) \approx 4[e/(1 \text{ \AA})^2] = 50 \text{ V \AA}^{-1} = 5 \times 10^{11} \text{ V m}^{-1}$.

PROBLEM 25.2

The ATP dissociation constant in water is $K_{\text{diss}} = \frac{\{ADP\}[P]}{\{ATP\}_{\text{eq}}} = 5 \times 10^5 \text{ mol L}^{-1}$,

where the subscript eq denotes a concentration of ATP being in equilibrium with $[\text{ADP}]$ and $[\text{P}]$.

What is the free energy of ATP hydrolysis at physiological concentrations $[\text{ATP}]_{\text{phys}} \approx 10^{-3} \text{ mol L}^{-1}$, $[\text{ADP}]_{\text{phys}} \approx 10^{-5} \text{ mol L}^{-1}$, $[\text{P}]_{\text{phys}} \approx 10^{-3} \text{ mol L}^{-1}$?

At what ATP concentration with unchanged $[\text{ADP}]_{\text{phys}}$ and $[\text{P}]_{\text{phys}}$ the ATP decay turns into its synthesis?

Solution

At physiological concentrations of ATP, ADP, and P, $P \frac{[ADP]_{\text{phys}} [P]_{\text{phys}}}{[ATP]_{\text{phys}}} = 5 \times 10^{-5}$ mol L⁻¹. Thus, $[ATP]_{\text{phys}}$ by $5 \times 10^5 / 10^{-5} = 5 \times 10^{10}$ times exceeds the amount necessary for equilibrium. The corresponding free energy excess is $RT \cdot \ln(5 \times 10^{10}) \approx 25RT \approx 15 \text{ kcal mol}^{-1}$.

ATP decay turns into its synthesis when its concentration becomes 5×10^{10} times lower than the physiological one, that is, when $[ATP] \approx 10^{-3} \text{ mol L}^{-1} / 5 \times 10^{10} \approx 0.2 \times 10^{-13} \text{ mol L}^{-1}$.

PROBLEM 25.3

The myosin head hydrolyses ATP, and 50% of the obtained free energy (50% of 15 kcal mol⁻¹) is converted into the work of a muscle. Each cleavage leads to a power stroke resulting in a shift of the myosin fiber relative to actin by 5 nm.

Evaluate the force developed by the myosin head.

Solution

The myosin head develops the force $15 \text{ kcal mol}^{-1} \times 0.50 / 5 \text{ nm} = (15 \times 4.2 \times 10^3 \text{ J mol}^{-1} \times 0.50) / (5 \times 10^{-9} \text{ m}) \approx 6 \times 10^{12} \text{ N mol}^{-1} = 10^{-11} \text{ N}$.

Index

Note: Page numbers followed by *f* indicate figures, *t* indicate tables, and *np* indicate footnotes.

A

- Abzymes, 402–403
Actin, 158, 422, 423*f*, 424, 427
Activation of enzymes, 396, 402
Active sites, 11, 81, 146, 220, 373–374, 394, 406, 409–410, 417
Adenosine diphosphate (ADP), 420–422, 420*f*
Adenosine monophosphate (AMP), 168
Adenosine triphosphate (ATP), 3, 168–169, 420–422
Aggregation of proteins, 339–340, 343
Alanine
 α -helix, in, 131, 135, 187–188, 204–206, 235, 246–247*f*, 326, 332*f*, 355–357
 β -structure, in, 85, 86*f*, 130, 184, 187–188, 194, 210, 217, 221, 233, 276, 355–356, 358–359, 373, 379
 properties, 139, 140*t*
 Ramachandran plots, 31–34, 32*f*, 187
 in secondary structures, 141, 145
 and structure prediction, 349, 352–353, 360, 362
Albebetin, 379–381, 380–381*f*
Aligned packing in β -sheets, 187–189, 188*f*, 190*f*, 192, 192*f*
All-or-none transitions, 113–114, 113*f*, 256
 absence in helix-coil transitions, 76, 126–127, 127*f*, 129–130, 255*f*
 in denaturing of globular proteins, 268
 and energy gap, 324, 326, 342
 and two-state folding kinetics, 308–309, 314–315
Allosteric interactions, 417
 chameleon proteins, 285, 339
 α/β cylinders, 207
 $\alpha\beta$ -plaits, 210, 211*f*
 $\alpha+\beta$ proteins, 185, 204–205, 207*f*, 210–212, 211*f*, 390–392
 α/β proteins, 207, 208*f*, 210, 210–211*f*, 224, 412
 α -helical surfaces, and protein stability, 233–235
 α -helices
 in fibrous proteins, 85, 201, 205
 in globular proteins, 181, 182–183*f*, 184–185
 in membrane proteins, 5, 151
 in polypeptides, 128, 135–136
 rate of formation, 128
 α 2 interferon, 381
 α -keratin, 152
 α -lactalbumin, 218, 264–265*f*, 281*f*, 412
 α -proteins
 architecture, 185, 199, 412
 close packing in, 199, 204–205, 379
 structure, 210
Amino acids
 hybridization of electrons in peptide bonds, 19–20
 hydrophobicities, 61–64, 237
 residues, 3–5, 17, 19*f*, 24, 30–31, 33–37, 44–45, 61, 79, 85, 187, 222, 409
 sequences, 145, 186–187, 215, 221, 223, 228, 233, 248, 336, 342, 349, 350*f*, 353
L-Amino acids
 and secondary structure, 279
 and topology, 279
 and twist of β -sheets, 91*f*, 92, 193*f*, 204–205, 244–245, 244*f*
Aminoacyl-tRNA, 409, 410*f*
Amyloid aggregation, 160
Amyloids, 159, 339
Antibodies. *See* Immunoglobulins
Antigenic determinants, 392
Antiparallel β -structure
 in fibrous proteins, 85, 201, 205
 in globular proteins, 181, 182–183*f*, 184–185
 in immunoglobulins, 392, 394
Apomyoglobin, 261, 261*f*, 279, 282, 308
Arginine, 139, 140*t*
Asparagine, 139, 140*t*
Aspartic acid, 139, 140*t*

B

- Bacteriorhodopsin, 165–167, 167*f*, 411–412
Basic Local Alignment Search Tool (BLAST)
 program, 349, 350*f*
Benzene, 55, 61–64

- β - α - β unit, 208–209, 357–358, 357*f*
 β -bends, 90–92
 β -bulges, 92, 93*f*
 β -cylinder in α/β proteins, 207
 β -hairpins, 90–92, 130–133, 130*f*, 135, 165,
 192, 194, 194*f*, 210, 298–299, 358,
 379, 391*f*
 β -helix, 193–194
 β -prisms, 193–194, 217
 β -proteins, 185, 187, 187*f*, 194, 199, 211–212,
 217, 217*f*, 308
 β -sandwich, 159–160, 188–189, 190*f*, 192–193,
 194*f*
 β -sheets, 5, 90*f*, 135, 152, 184, 187, 188*f*, 189,
 191*f*, 193–194, 200*f*, 207, 221, 270–271,
 309*f*
 β -strand, 89, 89*f*, 91*f*, 131–132, 192, 195, 246*f*,
 355*f*, 370*f*, 416
 β -structure, 85, 86*f*, 130, 184, 187–188, 194,
 210, 217, 221, 233, 276, 355–356,
 358–359, 373, 379
 in DNA-binding, 389*f*, 390–392, 412
 features of, 151, 185, 185*f*
 in fibrous proteins, 85, 201, 205
 in globular proteins, 181, 182–183*f*, 184–185
 in immunoglobulins, 392, 394
 in membrane proteins, 5, 151
 and polymorphous transitions, 339
 rate of formation, 128
 surfaces, and protein stability, 67, 128, 233,
 239, 316–318, 317*f*
 β -turns, 90–92, 93*f*, 143*np*, 183*f*,
 355–358
Binding of natively disordered proteins, 55,
 253, 256, 343, 387–388
Binding of proteins, 253
Bioinformatics, 12–13, 352–353, 356–357,
 368–369, 372–374
Biosynthesis of proteins, 6–7, 156, 157*f*, 223,
 289–290, 293, 409
Bohr effect, 419
Boltzmann formula, 46, 242, 259
Boltzmann's constant, 46–47, 108
Bovine pancreatic trypsin inhibitor, 353, 353*f*,
 361*f*, 401, 401*f*
Brittle bone disease, 158
- C**
Calmodulin, 218–219, 222
cAMP. *See* Cyclic adenosine monophosphate
 (cAMP)
- Carboxypeptidase of thermolysin, 411
Catabolite activating protein (CAP), 189, 190*f*,
 389*f*
Catalysis, 3, 376, 387–388, 397–400, 403–404,
 413
Cell-free systems, protein folding in, 290, 291*f*
Central limit theorem, 240–241
Chameleon proteins, 285, 339
Chaperones, 178, 290, 294–296,
 303–304, 341
Charge on amino acid residue, 3–5, 17, 19*f*, 24,
 30–31, 33–37, 44–45, 61, 79, 85, 187,
 222, 409
Chelate bonds, 81
Chemical potential, 53–54, 56
Chlorophyll, 172*f*, 173–176, 174*f*, 411–412
Chymotrypsin, 10–11, 10*f*, 189, 191*f*, 395*f*,
 397–398, 398*f*, 401–402*f*, 405–406, 415
Chymotrypsinogen, 396–398, 398*f*
Circular dichroism (CD), 96, 97*f*, 254*f*, 263–265
Cis-conformations, 30–33
Cis-prolines, 24, 301
Class-architecturetopology-homology (CATH)
 classification of protein structures, 216, 216*f*,
 412
Clathrates, 60–61
Cleavage. *See* Proteolysis
Close packing in α -proteins, 199, 204–205, 379
Codons, 19*f*, 77, 139, 156, 293–294, 349, 375–376
Cofactors, 4, 9–10, 9*f*, 172*f*
Coil
 as denatured protein, 263, 270, 278, 280
 density of, 94–95
 rotational isomeric model of, 276, 278, 279*f*
 from unfolding of molten globules, 279,
 281–282, 300–301, 303, 313*f*, 334, 379
 volume of, 94–95
Coiled-coil helices, 152–153
Coil-globule transitions, 270–271
Coil-helix transitions, 131
Cold denaturing of globular proteins, 268
Collagen, 89–90, 155–158, 156–157*f*
Compact intermediates, 314–315
Conformation. *See also* Protein structure
 α -helices, 22
 changes in protein functions, 3, 8–10,
 185–186, 253, 343–344, 387, 409, 414
 jumps in, by side chains, 368
Co-operative transitions of globular proteins,
 254, 258
Coordinate bonds, 43, 79–81, 144, 411, 417
Co-translational folding, 291

- Covalent angles in peptides, 21–22, 33f
 Crowding, 294
 Crystals, hydrogen bonding in, 33f, 39, 61, 77, 79–81, 86, 155, 165, 426f
 Cyclic adenosine monophosphate (cAMP), 168–169, 389f
 Cyclohexane, 55–58, 56f, 61, 64f, 65, 237
 Cysteine, 79–80, 140f, 141
 Cytochrome, 9f, 10–11, 172f, 199, 200f, 254f, 350f
- D**
 Dali/FSSP classification of protein folds, 216
 Debye–Hückel effect, 77–78
 Defect-free structures, folding patterns in, 224
 Defects in structures, 221, 224, 226, 236
 Denaturing of globular proteins, 268
 Detailed balance law, 328
 Diffusion time, 119, 121
 Disulfide bonds. *See S–S bonds*
 Disulfide isomerase, 8, 79–80, 294
 DNA binding, 379, 388–392, 389f, 391f, 412, 415
 Double sieve effect, 409
 D steric forms, 17
 Dynamic programming, 368–369, 440, 443t, 444–445
- E**
 Efimov’s tree, 195, 195f, 217–218
 Elastase, 405–406, 415
 Elastin, 158
 Electron transfer in membrane proteins, 173, 174f, 175
 Electrostatic interactions, 30, 40, 67–68, 75, 77–79, 176
 Elongation of α -helices, 123–124, 129–132
 Energy
 and free energy, 45, 114, 131, 224, 275, 307–308, 325, 371–372, 422–424
 funnel, 325, 331f, 387
 gap, 243, 283–286, 283f, 324, 325f, 326, 334, 339–342, 450
 in globule-coil transitions, 269–270, 269f, 280, 432f
 and hydrophobicity, 51, 55, 57, 61, 63f, 65, 145, 153, 236–239, 278, 280, 352, 360, 409
 and protein folding, 13, 25, 160, 177–178, 215, 254, 285, 289, 323, 353, 367, 409
 and stability of globular protein structure, 212, 221
 in statistical mechanics, 342–343, 368–369
 Enthalpic catalysis, 399
 Enthalpy, 52. *See also Energy*
 Entropic catalysis, 399–400
 Entropy
 and free energy, 48, 55
 in globule-coil transitions, 269–270, 269f, 280, 432f
 and hydrophobicity, 51, 55, 57, 61, 63f, 65, 145, 153, 236–239, 278, 280, 352, 360, 409
 and protein folding, 13, 25, 160, 177–178, 215, 254, 285, 289, 323, 353, 367, 409
 and stability of globular proteins, 212, 221
 in statistical mechanics, 342–343, 368–369
 in thermodynamics, 13, 51, 54, 56f, 59f, 64f, 101, 105, 109, 258, 282–283, 301, 309, 323–326, 328
 of water molecules, 9–10, 33, 39–40, 43–45, 49, 57–61, 67–68, 71f, 74, 144–145, 184, 222, 256, 266f, 278, 354, 396, 411, 415
 Enzymatic catalysis, 3, 400, 404, 496
 Enzymatic peptide hydrolysis, 397–398, 397f, 399f
 Enzyme catalysis, 13
 Enzymes, 7–8, 11–13, 18, 75, 79, 158, 168–169, 219–220, 253, 284, 294–295, 376, 387–388, 396, 398–403, 409–411, 413, 415
 Ethanol, 41–42, 44, 55, 57, 416
 Eukaryotic proteins, 219, 297
 Evolution of proteins, 218–219
- F**
 Fermat’s last theorem of protein science, 298, 325
 Fibroin, 151–152, 156–158
 Fibrous proteins, 4–5, 7, 11, 85, 151, 220, 223, 223f
 First-order phase transitions, 112–113, 124, 132, 136, 256, 275, 317, 338–339, 342–343
 Folding domains, 333
 Folding intermediates, 298–301, 309, 319, 334–336, 340–341
 Folding of proteins. *See Protein folding*
 Folding patterns of proteins, 189, 208f, 224, 225f, 234f, 367
 Framework model of protein folding, 298–300, 299f

- Free energy, 45, 114, 131, 224, 275, 307–308, 325, 371–372, 422–424
 and β -structure formation, 130, 132, 134–136, 135f, 160, 269
 of bonding in α -helix, 85, 129, 129f, 131
 in charged side chains, 74, 144, 144f
 of closed loop in coils, 330–331, 335
 and entropy, 48, 55
 in enzymatic catalysis, 3, 400, 404
 of helix initiation and elongation, 123–124, 126–127, 127f
 and hydrophobicity, 51, 55, 57, 61, 63f, 65, 145, 153, 236–239, 278, 280, 352, 360, 409
 and permittivity, 30, 43, 67, 70, 73–75, 77–78
 in statistical mechanics, 342–343, 368–369
 in thermodynamics, 13, 51, 54, 56f, 59f, 64f, 101, 105, 109, 258, 282–283, 301, 309, 323–326, 328
 of transfer, of hydrophobic group, 64–65, 145, 235, 278–279, 356
 and transition state, 114, 115f, 133, 301, 309
 and transport of polar groups, 139, 141, 166, 227–228, 235, 276
 Free energy barrier, 111
 folding and unfolding sides, 257, 260, 312, 316, 317f, 328, 333–334, 333f, 342, 371–372
 Funnel, 208f, 209, 210f, 324–325, 325f, 338 landscapes, 324, 325f
- G**
 GDP. *See* Guanosine diphosphate (GDP)
 Gibbs free energy, 52, 54, 56f, 472
 Globins, 186–187, 199, 200f
 Globular proteins
 α -helices in, 156–157, 184–185, 185f
 architecture and functions, 4–5, 181, 182–183f
 denaturing (*see* Denaturing of globular proteins)
 folding of, 181, 185–186, 185f, 189
 hydrophobic core of, 184, 187–188, 188f
 sequences in, 185–187, 191
 stability of, 184
 structure, 181, 182–183f, 184
 Globule-coil transitions, 269–270, 269f, 280, 432f
 Glutamic acid, 140f, 151
 Glutamine, 140f, 151
 Glutathione, 79–80
 Glyceraldehyde-3-phosphate dehydrogenase, 416–417
- Glycine
 α -helix, in, 85–86
 in collagen, 89–90, 155, 156f, 158
 properties, 85, 92t
 and protein structure prediction, 349–350, 354, 369, 371, 373–374, 377, 494
 Ramachandran plots, 31–34, 32f, 187
- G-protein. *See* Guanine-binding protein (G-protein)
- Greek key configuration of β -sheets, 189, 190f, 192, 192f, 195–196, 195f, 224, 225f
- Green fluorescent protein, 246, 247f
- GTP. *See* Guanosine triphosphate (GTP)
- Guanine-binding protein (G-protein), 168–169, 168f, 413
- Guanosine diphosphate (GDP), 168–169
- Guanosine triphosphate (GTP), 168–169, 413
- H**
- Hardness of proteins, 10–12, 278, 387–388
- Heat shock, and protein folding, 294–296
- Heat shock protein 40 (Hsp40), 295
- Heat shock protein 60 (Hsp60), 295
- Heat shock protein 70 (Hsp70), 295
- Heisenberg's uncertainty principle, 20, 52, 176
- Helices lacking hydrogen bonds, 39, 44–45, 49, 58, 60–61, 87
- Helix as a long dipole, 87
- Helix-coil transition, 76, 126–127, 127f, 129–130, 255f
- Helix-turn-helix motif and DNA binding, 388, 389f, 390–392
- Helmholtz free energy, 52, 471–472
- Hemagglutinin, 235
- Hemerythrin, 9–11, 9f, 199, 200f, 201
- Hemoglobin, 4–6, 185, 218, 248, 417–419, 418–419f, 427
- Henry's law constant, 57
- Hexokinase, 415–416, 415f
- Histidine, 146, 378–379, 417–419, 418f
- HIV virus, 349, 350f
- HMMer program, 351–352
- Homology modeling, 352–353
- Homology of sequences, 349–351
- Hormone receptors, 168
- Hydrocarbon group-poor polypeptides, 5
- Hydrocarbons, 5, 55–57, 59–60, 63f, 64–65
- Hydrogen bonds
 and α -helices, 22
 and β -bulges, 92, 93f

and β -structure, 85, 86f, 130, 184, 187–188, 194, 210, 217, 221, 233, 276, 355–356, 358–359, 373, 379
and β -turns, 90–92, 93f, 143np, 183f, 355–358
and collagen, 89–90, 155–158, 156–157f
entropic in water environment, 80–81
in fibrous proteins, 85, 201, 205
in globular proteins, 181, 182–183f, 184–185
helices packing, 202
in membrane proteins, 5, 151
of proline, 23–24, 23f, 34, 127
within protein chain, 5, 11–12, 18, 22, 44–45, 49, 189, 219, 224, 233, 263, 373
Hydrolysis, 220, 396–398, 397f, 399f, 409, 425
Hydrophilic side chains, 144
Hydrophobic bond, 59f, 60
Hydrophobic effect, 12, 55, 61, 64–65, 145, 261–262
Hydrophobicity
 of amino acids, 61–64
 avoiding loss of H-bonds, 58–59, 243–244
 and core of proteins, 55, 236, 257, 379
 and entropy, 51, 55, 56f, 57, 61, 280
 of fibrous proteins, 201, 249
 of globular proteins, 4
 and group adhesion, 145, 359
 of membrane proteins, 223, 249, 373
 of protein chain, 278
 and protein structure prediction, 360
 temperature-dependent, 360
 thermodynamic parameters, 62t
 and thermodynamics, 51
Hysteresis, 111–112, 312, 313f

I

Ice, structure of, 39, 43
Imino acid, 34, 127, 139
Immunoglobulins, 218–219, 392
Inclusion bodies, and protein folding, 294
Induced fit, 415–416, 415f
Infrared spectroscopy of proteins, 98f, 263–265
Inhibitors, 298, 339–340, 349, 353f, 361f, 390–392, 401, 401–402f, 406, 409–410
Initiation of α -helices, 130–131
Insulin, 7–8, 159f
Interferon β , 362, 363f
Interleukin-8, 182f
Ionized side groups, 145, 146f
Isoleucine, 34, 140t, 410f
Isoleucine aminoacyl-tRNA, 409, 410f, 414

K

Key lock, 415
Kinesin, 419–422, 420f, 424, 427
Kinetic control of protein folding, 300–301, 333
Kinetics, 13, 101, 114–115, 115f, 117–118, 123, 130, 132, 135–136, 159f, 161f, 255, 260, 275, 283, 300f, 301, 307, 308f, 309, 312, 323, 414
Kinetics of transitions, 275

L

Lactate dehydrogenase, 416
Landau's theorem, 124
Leucine
 properties, 139, 140t
 side chain of, 34
Levinthal paradox, 297–298, 326–327, 329f
Limited set of protein folding patterns, 215
L-steric forms, 17
Luciferase, 290, 291f
Lysine
 properties, 140t
 side chain of, 158
Lysozyme, 158, 217f, 218, 226f, 310, 310f, 313f, 314, 333f, 412

M

Macroscopic evolution, 218–219
Mass action law, 76
Matrix proteins, 18, 152, 158
Meander configuration of β -sheets, 189–190f, 195
Mean free path, 120
Mechanisms of protein folding, 177–178, 178f, 298
Mechanochemical cycle, 421, 423f
Melting, 39, 43, 102, 111–112, 125–126, 157–158, 226–228, 247, 256, 258–261, 262f, 267–268, 275, 278, 281, 283–285, 283f, 311, 331, 353, 360
Melting temperature, 157–158, 227–228, 242, 247, 262f, 284–285, 360
Membrane proteins, 4, 11, 151, 156, 165, 168–170, 172, 177–178, 178f, 199, 201, 205, 223, 223f, 233, 249, 289, 294–295, 297, 303, 343, 372–373, 387, 412
Metalloproteases, 411
Metals, coordinate bonds of, 80–81, 411, 417
Methane, 42, 55
Methionine, 140t
Michaelis–Menten kinetics, 497

- Microscopic evolution, 218
 Microstates, 47, 49, 101–106, 105*f*, 108
 Microtubule, 3, 419–421, 420*f*, 427
 Misfolding, 158, 160, 334, 335*f*
 Mixed β -structures, 89*f*, 185, 207*f*
 Modeling of protein folding, 371
 Molten globule (MG)
 dry, 278
 wet, 278–279
 Multiple-blade propeller arrangement of
 β -proteins, 192
 Multi-state folding, 314–315, 320
 Multitude principle, 228, 233, 343–344
 Muscles, 3, 415–417, 419, 419*f*, 422–424,
 423*f*, 427
 Mutated proteins, 76, 315*f*, 316
 Mutations, 75*f*, 76–77, 158, 218, 239, 247–249,
 315*f*, 316–320, 342–343, 375–377, 377*f*,
 379, 392, 397, 409–410
 Myoglobin, 158, 199–201, 238, 282, 414, 417,
 419, 419*f*, 427
 Myosin, 5, 152–153, 420, 422, 423*f*, 424, 427
- N**
- NAD. *See* Nicotinamide adenine dinucleotide (NAD)
 Natively disordered proteins, 253, 256, 343,
 387–388, 415–416
 Native state of protein, 263
 Natural selection of protein folds, 239, 284, 320,
 343, 413
 Neuraminidase, 192–193, 193*f*
 Nicotinamide adenine dinucleotide (NAD),
 208*f*, 412, 416–417, 416*f*
 NMR. *See* Nuclear magnetic resonance (NMR)
 spectroscopy
 Non-covalent interactions, 5, 27, 242
 Nuclear magnetic resonance (NMR)
 spectroscopy, 4, 34–37, 96, 266–268,
 290–291
 Nucleus in protein folding, 302–303, 316–319,
 318*f*, 334–335
- O**
- One-dimensional systems, 368–369
 Optical excitation, 97–98
 Orientation of hydrogen bonds, 41
 Orthogonal packing, 187–189, 188*f*, 191*f*, 200/
 211*f*
 Osteogenesis, 158
 Oxalic acid, 74
 Oxyproline, 157–158
- P**
- Packing, 5–6, 59*f*, 145, 155*f*, 182*f*, 185–189,
 185*f*, 188*f*, 190–191*f*, 192, 199, 200–203*f*,
 201–202, 204–207, 221, 224, 226, 233,
 246*f*, 266*f*, 276, 277*f*, 279, 279*f*, 299–301,
 309, 337–338, 360, 372–373, 376–377,
 379. *See also* Protein folding
 Paired electrons, 27
 Palindromes in DNA, 388
 Papain, 405–406
 Parallel β -structures, 87, 93*f*, 160, 187–188,
 192–194, 207, 210–212, 217, 394
 Particulate media, 73
 Partition function, 101, 106–107
 Pauli exclusion principle, 27
 Pepsin, 189, 191*f*
 Peptides, 18, 24, 128, 158, 167, 296, 358*f*,
 378*f*
 Periodic sequences, 235
 Permittivity, 30, 42*f*, 43, 67–78, 72*f*, 144, 170
 pH, 6–7, 44, 74–76, 128, 139, 141, 145–146,
 146*f*, 160, 255*f*, 256, 358
 Phase co-existence
 stable in helix-coil transition, 127
 transient in protein folding, 275
 Phase diagram of protein, 280
 Phase transitions in statistical mechanics,
 342–343
 Phenylalanine, 140*t*, 401*f*
 Pheophytin, 172*f*, 173–176
 Φ -value analysis, 318*f*, 319, 320*f*
 pH-optimum of protein action, 75–76, 75*f*
 Photosynthetic reaction centre, 172–174, 172*f*,
 177, 411–412
 Physical selection of protein folds, 224, 249
 Planck's constant, 20–21, 52, 118, 176
 Polar groups, 139, 141, 144, 145*f*, 166, 170,
 233, 235, 265, 276, 379
 Polarization and surface charges, 40, 71
 Poly(Lys), 128, 160
 Polymer analog for globule-coil transitions, 269
 Polymers, proteins as, 276
 Polymorphous transitions, 339
 Polyproline helix, 89–90
 Porin, 169, 169*f*, 303
 Position-Specific Iterative Basic Local
 Alignment Search Tool (PSI-BLAST)
 program, 351–352
 Post-translational modifications, 7–8, 158
 Potential of rotation, 23–24*f*, 24
 Potentiometric titration, 128
 Pre-molten globule, 299*f*, 300, 319

- Primary structure, 5, 6*f*, 151–152, 153*f*, 155, 158, 219–220, 223, 233, 234*f*, 235, 242, 245–246, 392–393, 417
- Prion, 158–160, 159*f*
- Prokaryotic proteins, 219
- Proline and α -helix stability
in collagen, 89–90, 155, 157–158
conformation of, 34, 139–140, 144*f*, 155
properties, 140*t*
in protein folding, 127, 130
and protein structure prediction, 353–354
Ramachandran plots, 34
side chain of, 89–90, 139
- Prolyl peptide isomerase, 219
- Propane, 55
- Protein architectures, 5, 13, 210, 215, 226, 236, 343–344
- Protein chains, 4–6, 12–13, 18, 35*f*, 90, 92, 96, 159–160, 185, 224, 225*f*, 253–254, 256, 270–271, 291, 296–297, 325, 330*f*, 339, 342, 352–353, 367, 372–373
- Protein classes, 4–5, 210, 216, 390–392, 411*f*
- Protein Data Bank (PDB), 5, 36*f*, 165, 181, 367
- Protein design, 248–249, 374, 377–378, 380*f*
- Protein domains, 189, 216, 219–220, 367, 415–416
- Protein engineering, 11, 75, 77, 374–376, 375*f*, 381*f*, 398, 404
- Protein evolution, 220
- Protein folding
chaperones in, 295
of collagen, 156–158
folding patterns of, 224
in vitro, 290, 292–294, 296–297
in vivo, 290, 292–294
modeling, 371, 373
reversible nature of, 253, 257, 371–372, 387
unified mechanism of, 298
- Protein functions
and Napoleon's strategic principle, 413–414
- Protein globule. *See* Globular proteins
- Protein motors, 13, 420
- Protein statistics, 227–228, 238, 247, 338, 356, 360
explanation of, 247
- Protein structure
in crystals and in solution, 4, 29, 41
flexibility and binding, 21–22, 403
limited flexibility and functioning, 403
rigidity and functioning, 3, 226–227, 265
- Protein unfolding, 254*f*, 265, 316, 324, 328, 336
- Proteolysis, 7–8, 265, 267*f*, 380–381, 398*f*
- Proteomics, 12–13, 220, 352–353, 374
- PSI-BLAST program. *See* Position-Specific Iterative Basic Local Alignment Search Tool (PSI-BLAST) program
- Q**
- Quantum mechanics, 28–29, 107, 175–176
- Quantum tunnelling, 175–176
- Quasi-Boltzmann statistics of protein structures, 236
- Quasi-spherical polyhedron model of α -protein, 201–204, 202*f*
- Quaternary structures, 5–6
- Quinone, 172*f*, 173–174, 174*f*
- R**
- Ramachandran plots, 31–33, 32*f*
- Random energy model (REM), 448
- Random heteropolymers, 269, 271, 284
- Random sequences, 223–224, 233, 235–236, 240–241, 240*f*, 246–249, 285, 342–344
- Renaturation of globular proteins, 261*f*, 297
- Replication terminating protein (trp), 369, 369–370*f*
- Retinal, 166–167, 166–167*f*, 411–412
- Retinol-binding protein, 187–188, 189*f*, 193, 195*f*, 396
- Reynolds number, 474
- Ribosome, and protein synthesis, 220–221, 289
- Right-handed topology, 212*f*
- Rossmann fold, 207, 208*f*, 209–210, 210*f*, 246, 395*f*, 412, 417
- Rotation about covalent bonds, 22, 25
- Rotational isomerization of side chains, 276, 278, 279*f*
- Rotor motors, 424
- S**
- Secondary structures
in fibrous proteins, 151
in globular proteins, 224, 359
in membrane proteins, 151
in molten globule, 125
in polypeptides, 5–6, 45
prediction of, 360–361
- Second-order phase transitions, 112–113, 113*f*, 275
- Selectivity, 170, 171*f*, 253, 392, 394
- Selenocysteine, 19*f*, 139
- Self-organization of proteins, 7, 293.
See also Protein folding

Sequence alignment, 350–351, 351f, 373
 Serine, 18f, 140t, 151–152, 396–397, 399
 Serine proteases, 10–11, 10f, 319, 394, 395f,
 396–397, 402, 405f, 409–411, 410–411f
 Serpin, 285, 339–340, 340f
 Side chains of amino acids, 19f, 34, 139
 Specificity of enzymes, 284, 409–410
 Spontaneous protein folding, 293
 S–S bonds
 in fibroin, 152, 156–157
 and globule stability, 221, 239
 and protein folding, 292–293, 300–301
 Stability
 α -helices, 127, 135–136
 of globular proteins, 208–209, 233
 and protein folding, 319
 and protein structure prediction, 127,
 135–136
 Standard protein folds, 228
 Staphylococcus nuclease, structure, 211f
 Statistical mechanics, 342–343, 368–369
 Stepwise mechanism of protein folding, 325
 Stereochemistry of amino acid, 355–356
 Stereo drawings, 17, 90f
 L-Steric forms, 17
 Storage proteins, 3
 Structural classification of proteins (SCOP)
 classification, 216
 Structural genomics, 374
 Structural proteins, 3, 151, 158
 Subtilisin, 10f, 11, 410–411, 410–411f, 415
 Superoxide dismutase, 235
 Swelling of polymer globules, 270

T

T-cell receptors, 392
 Temperature, 6–8, 21, 27, 39, 51, 68, 101,
 124–125, 157–158, 177, 227–228, 239,
 253, 278, 291, 310, 340–341, 358, 380f, 414
 Tertiary structures, 6, 215, 342, 410
 Thermodynamics, 13, 51, 54, 56f, 59f, 64f, 101,
 105, 109, 258, 282–283, 301, 309,
 323–326, 328
 Thermodynamics of protein folding, 282
 Thermolysin, 202f, 405–406, 411
 Thermostat, 103–106, 109
 Threading method, 367–368, 370, 370f
 Three-dimensional structure prediction,
 349–350, 367, 373, 377
 Threonine, 34, 140t
 Tobacco mosaic virus, 9f, 199, 200f
 Trans-conformations, 24, 30–31

Transfer proteins, 3
 Transition state, 13, 115f, 118f, 129, 133–134,
 301–303, 308f, 309–310, 312–319, 313f,
 315f, 317–318f, 326, 333–334, 335f, 359,
 399–404, 400f, 403f, 413
 Transport selectivity in membrane proteins, 170
Trans-prolines, 24, 292, 294
 Trypsin, 195f, 298, 353f, 361f, 396–397,
 401–402f, 405–406, 410–412, 410–411f,
 415
 Trypsin inhibitor, 298, 353f, 361f, 401–402f
 Tryptophan, 140t, 141, 389–392, 390f
 Tryptophan repressor, 389–392, 390–391f, 415
 Tunnelling, 175–177, 175f
 Two-state folding of proteins, 308–309,
 314–315
 Tyrosine, 140t, 141, 404, 405f
 Tyrosyl-tRNA, 404, 405f

U

Unfolding of proteins. *See* Protein unfolding

V

Valine, 34, 140t
 van der Waals interaction, 28, 28f, 29t, 30,
 40–42, 65, 78, 89–90, 268, 394f, 403
 van't Hoff criterion, 238, 259–260
 Vibrations of covalent bonds and angles, 21
 Vitrifying temperature, 284

W

Water
 corpuscular structure, 68
 entropy of molecules, 45, 58, 80–81
 hydrocarbons in, 55–56, 60
 hydrogen bonding in, 33f, 39, 79
 and hydrophobic effect, 55, 61
 implicit water, 30
 orientation of molecules, 49, 71f, 73f
 partial charges, 39–40
 permittivity, 71, 73–74, 78–79
 properties, 39, 44
 and protein chains, 44
 as solvent, 39, 49, 51
 Water-soluble proteins, 5, 158, 173, 177–178,
 222, 297, 303, 373, 387
 What's good for General Motors is good for
 America, 32, 85, 139, 221, 239

Z

Zinc fingers, 379, 380f, 391f